

THE DESIGN AND SYNTHESIS OF NOVEL ANTIBIOFILM  
ANTIBIOTICS AND EFFORTS TOWARD THE TOTAL  
SYNTHESIS OF THE COMPLEX  
AMINOCYCLOPENTINOL  
PACTAMYCIN

by

Travis James Haussener

A dissertation submitted to the faculty of  
The University of Utah  
in partial fulfillment of the requirements for the degree of

Doctor of Philosophy

Department of Chemistry

The University of Utah

December 2016

Copyright © Travis James Haussener 2016

All Rights Reserved

# The University of Utah Graduate School

## STATEMENT OF DISSERTATION APPROVAL

The dissertation of Travis James Haussener  
has been approved by the following supervisory committee members:

<u>Ryan E. Looper</u>	, Chair	<u>8/19/2015</u> Date Approved
<u>Gary E. Keck</u>	, Member	<u>8/19/2015</u> Date Approved
<u>Jon D. Rainier</u>	, Member	<u>8/19/2015</u> Date Approved
<u>Bethany Anne Koehntop</u>	, Member	<u>8/19/2015</u> Date Approved
<u>Louis R. Barrows</u>	, Member	<u>8/19/2015</u> Date Approved

and by Cynthia J. Burrows, Chair/Dean of  
the Department/College/School of Chemistry

and by David B. Kieda, Dean of The Graduate School.

## **ABSTRACT**

Pactamycin was isolated in 1961 by the former UpJohn Company and to date is the most complex aminocyclopentanol known. This natural metabolite is decorated by six contiguous stereocenters, three of which are quaternary, with each position of the cyclopentane core functionalized. Biological testing has further revealed that pactamycin exhibits activity in every phylogenetic domain.

Pactamycin's activity arises from its ability to bind the E-site via a unique pi-stacking interaction within the ribosome which precludes protein synthesis and ultimately leads to cell death. Generating a less potent pharmacophore could lead to antineoplastic agents, antimalarials, and/or antibiotics due to the highly conserved nature of the ribosome. We have developed a short modular synthesis predicated upon producing analogs that perturb this pi-stacking network. From this sequence we have synthesized the highly complex oxygenated core of pactamycin using a diastereoselective epoxide-opening cascade reaction in 11 steps and in 4.2% overall yield. Our synthetic sequence further allows us to design analogs that contain the requisite di-aryl system by intercepting several advanced intermediates.

Pathogenic bacteria have been responsible for countless infections and deaths. Clinicians and researchers alike have developed effective management strategies for these infections with the implementation of antibiotics and sterility measures. However, the community is facing a new problem with higher incidences of bacterial resistance.



Additionally, certain pathogenic colonies can aggregate together and begin to produce a protective coating known as a biofilm, consisting of amino acids, polysaccharides, and deoxyribonucleic acid (DNA) which safeguards them from perturbation by temperature, salinity, pH, and most importantly antibiotics.

Biofilms have emerged as a new target for infection control. However, killing the bacteria associated with the biofilm does not always remove the protective film. The resulting nutrient-rich environment provides a surface for additional bacteria to proliferate on. We realized that in order to develop an effective antibiofilm antibiotic, the compound must act in dual-fold manner, both killing the bacteria and dispersing the associated extracellular biofilm matrix.

We recognized membrane-active antibiotics like daptomycin as a useful platform for developing our library. Adding various known polyamino-motif biofilm dispersants to these membrane active mimics provided a unique combination which allowed our compounds to be active against both planktonic bacteria as well as biofilm-forming species. These polyamine-functionalized scaffolds were effective at clearing biofilms generated by multiple species of bacteria. To date, the modular construction of these antibiofilm antibiotics has allowed us to produce a comprehensive library of over 200 active compounds. Furthermore, our efforts have resulted in the generation of several lead compounds that are noncytotoxic, nonhemolytic, yet retain competent bactericidal and antibiofilm activity.

*To my parents who taught me the true definition of hard work*

## TABLE OF CONTENTS

ABSTRACT .....	iii
LIST OF TABLES .....	ix
LIST OF FIGURES .....	xi
Chapters	
1. EFFORTS TOWARD THE TOTAL SYNTHESIS OF PACTAMYCIN USING A UNIQUE EPOXIDE OPENING CASCADE REACTION.....	1
1.1 Background .....	1
1.2 Isobe's Partial Synthesis of Pac .....	3
1.3 Knapp's Partial Synthesis of Pac .....	4
1.4 Johnson's Partial Synthesis of Pac.....	6
1.5 Hanessian's Total Synthesis of Pac .....	7
1.6 Johnson's Total Synthesis of Pac.....	10
1.7 Looper's Partial Synthesis of Pac .....	11
1.8 Analog Studies .....	17
1.9 Future Aims .....	18
1.10 Supporting Information.....	39
1.10.1 General Experimental Conditions .....	39
1.10.2. Experimental Procedures .....	40
1.10.3 Representative <sup>1</sup> H NMR and <sup>13</sup> C NMR.....	52
1.11 References .....	61
2. INITIAL STUDIES TOWARD GENERATING ANTIBIOFILM ANTIBIOTICS ..	64
2.1 Background .....	64
2.2 Common Current Antibiotics Structures and Functions.....	65
2.2.1 β-lactam Antibiotics .....	65
2.2.2 Quinolines and Fluoroquinolones .....	66
2.2.3 Tetracyclines .....	67
2.2.4 Macrolides .....	68
2.2.5 Lipopeptides, Defensins, and Defensin Mimics.....	69
2.3 The Biofilm Phenotype .....	69
2.3.1 Biofilms in Industry.....	71
2.3.2 Biofilms in Medical Devices .....	72

2.3.3 Chronic Infections Related to Biofilm .....	73
2.4 Finding a Cellular Target for the Biofilm Phenotype .....	75
2.5 Design and Synthesis of Novel Antibiofilm Biocides .....	77
2.5.1 Squalamine .....	77
2.5.2 The Ceragenin's .....	78
2.5.3 Looper's Initial Design Concept .....	80
2.6 Looper's First Generation Biocide Synthesis.....	80
2.7 Conclusion and Future Aims .....	83
2.8 Supporting Information .....	95
2.8.1 General Experimental Conditions.....	95
2.8.2 Missing Experimental Data.....	97
2.8.3 Experimental Procedures .....	97
2.8.4 Representative <sup>1</sup> H NMR and <sup>13</sup> C NMR .....	103
2.9 References .....	113
 3. SYNTHESIS OF N'N'' ALKYL AND DIALKYL POLYAMINES WITH RESPECT TO THEIR APPLICATION IN THE SYNTHESIS OF CZ-01 COMPOUNDS.....	117
3.1 Background .....	117
3.2 DFMO: An Inhibitor of Ornithine Decarboxylase.....	119
3.3 AMD 3100 .....	120
3.4 N1,N11-diethylnorspermine .....	122
3.5 Synthesis of Unnatural Polyamines .....	123
3.5.1 Woster and Casero's Synthesis of Unnatural Spermine Derivatives ..	123
3.5.2 Bergeron's Synthesis of Unnatural Spermidine Derivatives.....	124
3.5.3 Uriac and Sinbandhit's Resin Based Synthesis of Nospermidine Derivatives.....	125
3.6 Preliminary Studies .....	125
3.7 Looper's Synthesis of Alkyl Polyamine Derivatives.....	126
3.8 Conclusion and Future Aims .....	130
3.9 Supporting Information.....	142
3.9.1 General Experimental Conditions .....	142
3.9.2 Polyamine Naming .....	143
3.9.3 Experimental Procedures.....	143
3.9.4 Representative <sup>1</sup> H NMR and <sup>13</sup> C NMR.....	156
3.10 References .....	187
 4. ADVANCED MEDICINAL CHEMISTRY PROFILE OF INITIAL CZ-01 ANTIBIOFILM ANTIBIOTIC ANALOGS.....	191
4.1 Background .....	191
4.2 Looper's Second Generation Biocide synthesis .....	192
4.2.1 Initial Suzuki sp <sup>2</sup> -sp <sup>2</sup> Cross Coupling.....	192
4.2.2 Dimethyl 5-hydroxyisophthalate as a Precursor to Ethereal Derivatives.....	193
4.2.3 Side-Chain Adjustment on Preexisting Scaffolds .....	194

4.2.4 Additional Side-Chain Modifications in Order to Alleviate Cytotoxicity .....	199
4.2.5 Modification of the <b>CZ-01-099</b> Scaffold .....	199
4.2.6 Synthesis and Activity of Analogs from an Advanced Side-Chain Library .....	200
4.2.7 Use of $\alpha$ -helix Mimetics as a Source for CZ-Compound Structural Diversity .....	201
4.3 Biological Studies on <b>CZ-01-099</b> .....	203
4.4 In vivo Pharmacokinetic Studies and Reselection of Lead Compounds .....	205
4.5 Conclusion and Future Aims .....	206
4.6 Supporting Information .....	236
4.6.1 General Experimental Conditions .....	236
4.6.2 Missing Experimental Data .....	237
4.6.3 ISO 10993 Assay .....	238
4.6.4 Experimental Procedures .....	238
4.6.5 Representative $^1\text{H}$ NMR and $^{13}\text{C}$ NMR .....	303
4.7 References .....	397

## LIST OF TABLES

### Tables

1.1	Attempted condition used to achieve the N-H insertion .....	20
2.1	CDC analysis of current microbial threats .....	84
2.2	The in vitro activity of the initial single side-chain CZ series as MICs against MRSA.....	84
2.3	The in vitro activity of the bis and tris polyamine CZ series as MICs against MRSA.....	85
3.1	Batch Variability Data for CZ-01-086 .....	132
4.1	The in vitro activity of the initial second generation CZ series as MICs against Gram-positive MRSA and Gram-negative <i>Pseudomonas aeruginosa</i> .....	209
4.2	The in vitro activity of the substituted phenoxy second generation CZ series as MICs against Gram-positive MRSA and Gram-negative <i>Pseudomonas aeruginosa</i> .....	209
4.3	Batch Variability Data for CZ-01-086 .....	210
4.4	The in vitro activity, of the substituted alkylated-norspermidine CZ series using [1,1'-biphenyl]-3,5-dicarbaldehyde, as MICs against Gram-positive MRSA and Gram-negative <i>Pseudomonas aeruginosa</i> .....	210
4.5	The in vitro activity, of the substituted alkylated-norspermidine CZ series using isophthalaldehyde, as MICs against Gram-positive MRSA and Gram-negative <i>Pseudomonas aeruginosa</i> .....	210
4.6	The in vitro activity, of the amino-etheral CZ-series, as MICs against Gram-positive MRSA and Gram-negative <i>Pseudomonas aeruginosa</i> .....	211
4.7	The in vitro activity, of the substituted norspermidine etheral CZ-series, as MICs against Gram-positive MRSA and Gram-negative <i>Pseudomonas aeruginosa</i> .....	211
4.8	The in vitro activity, of the substituted tris norspermidine CZ-series, as MICs against Gram-positive MRSA and Gram-negative <i>Pseudomonas aeruginosa</i> .....	211

4.9 The in vitro activity, of the substituted urea CZ-series, as MICs against Gram positive MRSA and Gram negative <i>Pseudomonas aeruginosa</i> .....	211
4.10 The in vitro activity, of the modified <b>CZ-01-099</b> analogs, as MICs against Gram-positive MRSA and Gram-negative <i>Pseudomonas aeruginosa</i> .....	212
4.11 The in vitro activity, of the altered norspermidine side chain CZ-series, as MICs against Gram-positive MRSA and Gram-negative <i>Pseudomonas aeruginosa</i> .....	212
4.12 The in vitro activity, of the altered norspermidine side chain CZ-series with respect to <b>CZ-01-099</b> , as MICs against Gram-positive MRSA and Gram-negative <i>Pseudomonas aeruginosa</i> .....	212
4.13 The in vitro activity, of the dialdehyde terphenyl CZ-series, as MICs against Gram-positive MRSA and Gram-negative <i>Pseudomonas aeruginosa</i> .....	213
4.14 The in vitro activity, of the trialdehyde terphenyl CZ-series, as MICs against Gram-positive MRSA and Gram-negative <i>Pseudomonas aeruginosa</i> .....	213
4.15 The in vitro activity, of the pyrimidine terphenyl CZ-series, as MICs against Gram-positive MRSA and Gram-negative <i>Pseudomonas aeruginosa</i> .....	213
4.16 The in vitro activity, of the <i>tert</i> -butyl terphenyl CZ-series, as MICs against Gram-positive MRSA and Gram-negative <i>Pseudomonas aeruginosa</i> .....	213

## LIST OF FIGURES

### Figures

1.1	The structure of pac .....	20
1.2	Crystallographic analysis of pac's pi-stacking interaction in the ribosome from a species of <i>Thermus thermophiles</i> .....	20
1.3	(a) Biosynthetic analogs of pac synthesized by the Mahmud laboratory with potent antimalarial activity (b) Natural products structurally related to pac .....	21
1.4	Confirmed X-ray structure of sulfamoyl ester <b>95</b> with the epoxide up, in line with N1 .....	21
1.5	Confirmed X-ray structure of azide <b>110</b> with the azide in line with N1 .....	22
1.6	Specific analogs intercepted from synthesis of <b>120</b> .....	22
2.1	The structures of various members of the $\beta$ -lactam family of antibiotics .....	85
2.2	The structure of 1 <sup>st</sup> , 2 <sup>nd</sup> , 3 <sup>rd</sup> , and 4 <sup>th</sup> generation quinolone antibiotics .....	85
2.3	Several representative examples from the tetracycline class of antibiotics .....	86
2.4	Several representative examples from the macrolide class of antibiotics .....	86
2.5	The lipopeptides daptomycin and colistin .....	87
2.6	Artistic representation of the five stages of biofilm formation from the planktonic phenotype (1) to biofilm development (2 and 3) to a fully mature, multiple species biofilm (4) to biofilm dispersal (5) .....	88
2.7	Artistic representation of antibiotic treatment of a mature single species biofilm; cell death results but the biofilm remains as a site for another round of maturation .....	89
2.8	The structure of squalamine isolated from the dogfish shark ( <i>Squalus acanthias</i> ) ....	89
2.9	Initial synthetic design for developing a membrane active amphiphilic molecule ....	90



2.10 The single side-chain CZ compounds .....	90
2.11 The bis and tris substituted CZ compounds with a variety of cationic polyamine side chains .....	91
2.12 Biofilms of <i>Alcanivorax borkumensis</i> grown for 48 h on galvanized steel and then: either left untreated or treated for 2 h with <b>CZ-01-25</b> .....	92
2.13 Qualitative biofilm dispersal by <b>CZ-01-25</b> .....	92
3.1 Select naturally occurring polyamines .....	133
3.2 Select examples of polyamines used in medical and industrial applications .....	133
3.3 Comparative MBIC analysis shown by Clardy and Losick .....	133
3.4 Representative polyamines from the AMD-series .....	134
3.5 Select analogs with the norspermidine and alkyl norspermidine side-chain .....	134
3.6 The structure of biocide CZ-01-086, synthesized with isobutyl norspermidine .....	135
3.7 Attempted reductive aminations to produce the desired mono-alkylated amine .....	135
3.8 Attempted alkylations to produce the desired mono-alkylated amine .....	135
3.9 Alkylated hydrobromide salts .....	136
3.10 Fully functionalized norspermidine derivatives .....	137
3.11 Dialkylated derivatives shown to demonstrate the versatility of this strategy .....	138
4.1 Initial second generation CZ-compounds made via the Suzuki coupling with a variety of $sp^2$ boronic acids, followed by Boc-norspermidine reductive amination .....	214
4.2 Etheral CZ compounds constructed from dimethyl 5-hydroxyisophthalate .....	215
4.3 1D $^1H$ NMR of <b>CZ-01-086</b> .....	215
4.4 Representative TLC of <b>CZ-01-086</b> .....	216
4.5 Structure profile of the initial alkylated-norspermidine analogs with a single phenyl ring at the 5-position .....	217
4.6 Structure profile of the initial alkylated-norspermidine analogs with isophthalaldehyde as the precursor .....	218

4.7 Amino-ethereal derivatives with the amended 5-position with side-chain modifications .....	219
4.8 Alkylated phenoxy derivatives with requisite norspermidine side-chain .....	219
4.9 Alkylated tris-norspermidine analogs .....	220
4.10 Terminally functionalized urea analogs with tris-counterpart or the cyclohexyl methyl ether .....	221
4.11 Truncated CZ-01-099 analogs both of which contain the <i>i</i> -butyl alkylated side-chain.....	221
4.12 Additional alkylated iterations on the norspermidine side-chains .....	222
4.13 Alkylated norspermidine mono-phenyl and bi-phenyl analogs .....	222
4.14 Tris-alkylated norspermidine bi-phenyl analogs based off of <b>CZ-01-099</b> .....	223
4.15 The structure of brilacidin .....	223
4.16 Two representative examples of Hamilton's terphenyl protein-protein inhibitors ..	224
4.17 Initial terphenyl CZ-compounds with modulated norspermidine side-chain.....	225
4.18 The structures of the CZ-compounds generated from the terphenyl trialdehyde with modulated norspermidine side-chain .....	226
4.19 Structures of the pyrimidine analogs with modulated norspermidine side-chain and internal pyrimidine nitrogens .....	226
4.20 Structures of the <i>tert</i> -butyl terphenyl analogs with modulated norpsermidine side-chain .....	227
4.21 Cultured MRSA on chrome-agar plates from pig 3 of the topical wound model .....	228
4.22 Qualitative biofilm dispersion data of <b>CZ-01-099</b> in conjunction with gluatraldhyde and vancomycin .....	228
4.23 Desired structural investigation of older ether scaffolds with new norspermidine derivatives .....	229
4.24 (a) Desired aldehydes used for additional SAR studies (b) Desired <b>CZ-01-114</b> analogs resultant from alternative side chains .....	230

# CHAPTER 1

## SYNTHETIC EFFORTS TOWARD THE TOTAL SYNTHESIS OF PACTAMYCIN USING A UNIQUE EPOXIDE OPENING CASCADE REACTION

### 1.1 Background

Pactamycin (pac) was isolated by scientists at the former Upjohn Company in 1961 from a fermentation broth of *Streptomyces pactum* var. *pactum*.<sup>1</sup> Initial structural investigation was accomplished using chemical degradation in 1970 which provided evidence for the trans C4-C5 diol and cis C1-C2 amines; the structure of pac was further verified by X-ray crystallographic analysis in 1972, which revealed and established the correct structure and absolute stereochemistry (Figure 1.1).<sup>2</sup> In biological tests, pac was found to have activity against every phylogenetic domain (archaea, eukaryota, bacteria). Nanomolar cytotoxicity was observed in eukaryotic cells (KB,  $IC_{50}$  = 5.3 nM; MCR-5,  $IC_{50}$  = 53 nM; HCT116  $IC_{50}$   $\approx$  100 nM).<sup>3,4</sup> Pac has also shown activity against both Gram-positive and Gram-negative bacteria and recently was shown active against *Plasmodium falciparum* ( $IC_{50}$  = 14.0 nM) and *Trypanosoma brucei* ( $IC_{50}$  = 7.0 nM).<sup>3</sup>

Elegant X-ray crystallographic studies have determined pac to be an inhibitor of the highly conserved ribosomal E-site, the third and final binding site for t-RNA during protein synthesis. Bound mRNA occupies the pocket shown below (Figure 1.2a) interacting

with ribosomal domains H28, H23b, H24a, and the c-terminus of protein S7. However, when pac is involved, it can also bind to the E-site facilitated through the pi-stacking of the two aromatic subunits (Figure 1.2b), mimicking two nucleotides, which subsequently prevents mRNA from entering (Figure 1.2c). This strong interaction prevents mRNA from entering the E-site which then causes an inhibition in protein synthesis and eventually leads to cell death.<sup>5, 6, 7</sup>

Due to its broad spectrum activity, owing to the highly conserved nature of the E-site it was once thought the development of pac as an efficacious drug candidate was severely limited. However, recent, studies published by the Mahmud group demonstrated that biosynthetic analogs of pac specifically **TM-025 (2)** and **TM-026 (3)** (Figure 1.3a) have diminished eukaryotic cytotoxicity while retaining activity against both chloroquine resistant and chloroquine sensitive *Plasmodium falciparum*.<sup>4</sup> Related natural products 7-deoxypactamycin (**4**)<sup>8</sup> and jogyamycin (**5**) (Figure 1.3b) show similar structural changes albeit with increased eukaryotic cytotoxicity.<sup>9</sup> These studies did not investigate the mechanism of action and therefore did not confirm that these analogs were binding the E-site of the ribosome. However, they did provide evidence that small structural changes to the scaffold of this highly complex aminocyclopentanol can result in dramatic shifts in biological data.

Architecturally, pac is an exceptionally complex molecule, decorated by three quaternary centers, six contiguous stereocenters, and a cyclopentane core with every position functionalized. In addition, it contains a salicylate, a urea, an aniline, a 1,2-diol, and a 1,2-trans diamine (Figure 1.1). To date, no aminocyclopentanol has been discovered which possesses a more complex structure.

Pac's intriguing and unique structure along with its interesting biological profile has attracted several partial and total syntheses'. Chronologically, the Isobe group was the first to report a partial synthesis in 2005 culminating with a unique Pauson-Khand reaction to produce the cyclopentane core of pac.<sup>10</sup> The Knapp group carried out a stereoselective partial synthesis in 2007 using a tethered-nitrogen Michael addition to functionalize their cyclopentane core.<sup>11</sup> In 2011, pac finally succumbed to total synthesis, 50 years after discovery, by the Hannessian group in which Hanessian was able to carefully introduce the functional groups present on pac through a modular process starting from L-threonine.<sup>12</sup> Alternate semisyntheses were published in 2012 by Looper<sup>13</sup> and Johnson.<sup>14</sup> In 2013, Johnson further demonstrated his interest by publishing the shortest linear synthetic sequence to pac in 15 steps with overall yield of 1.9% through which C1, C2, C3, C4, C5, and C7 (Figure 1.1) were all prepared simultaneously by an enantioselective Mannich reaction.<sup>15</sup>

## 1.2 Isobe's Partial Synthesis of Pac

The Isobe group was the first to publish chemistry en route to pac. Their synthesis used a Pauson Khand reaction, developed by their group, to assemble the five-membered cyclopentane ring present in the natural product.<sup>16</sup> Starting from diacetone D-glucose **6**, oxidation of the free alcohol followed by a Wittig/reduction sequence produced the allylic alcohol **7** (Scheme 1.1). Attachment of a labile allylic trichloroacetimidate produced **8**. A subsequent Overman rearrangement afforded **9** as a single product whose structure was confirmed by two-dimensional NMR analysis. Ozonolysis of **9** and nucleophilic addition with methylmagnesium bromide yielded secondary alcohol **10**.<sup>10</sup>

At this point the C7 configuration was inverted to the stereochemistry present in the

natural product through an Albright and Goldman oxidation followed by a Luche reduction to afford alcohol **11** (Scheme 1.2). Treatment of **11** with 1,8-diazabicycloundec-7-ene (DBU) provided the corresponding oxazolidinone **12**. Following benzyl amine formation selective deprotection and deoxygenation of the terminal acetonide gave the allyl-acetonide **14**. The remaining internal acetonide was hydrolyzed with TFA to afford the corresponding hemi-acetal. Reduction and oxidative cleavage gave the hydroxyl aldehyde **15**.<sup>10</sup>

TMS-acetylide mediated alkynylation yielded the enyne **16** (Scheme 1.3) ready for the key Pauson-Khand reaction. Unfortunately, attempts at treating enyne **16** with  $\text{Co}_2(\text{CO})_8$  resulted in an inseparable mixture of diastereomers. To their satisfaction, treatment of the crude material **17** with acetic anhydride produced the diacetate **18** as the major product which was easily separated by column chromatography. Isobe concluded his synthesis with formation of the parent five-membered ring. Highlighted by a very efficacious Pauson-Khand reaction, the Isobe group developed a unique route to the core of pac from diacetone-D-glucose. The final tricycle **18** possessed all the necessary functionalities for further functionalization.<sup>10</sup>

Isobe was able to construct the core cyclopentane of pac in 20 steps from diacetone D-glucose. Using a unique Pauson-Khand reaction, the final product possessed the requisite chemical information for introduction of the remaining functional groups present on pac.<sup>10</sup>

### 1.3 Knapp's Partial Synthesis of Pac

In 2007, the Knapp group was able to synthesize a complex oxygenated intermediate en route to pac. Their synthetic sequence used a number of stereoelectronic tactics for modifying the cyclopentane core. Starting from commercially available 2-methyl-2-

cyclopenten-1-one **19**, an enantioselective Corey-Bakshi-Shibata (CBS) reduction afforded the alcohol **20** (Scheme 1.4). Silyl protection with TBS produced the silyl ether **21** which was immediately converted to the diol **22** with an osmium-promoted dihydroxylation. Subsequent Swern oxidation of the unprotected secondary alcohol gave the highly functionalized  $\alpha$ -hydroxy-ketone **23** in four trivial steps from **19**. A Wittig reaction on the pendent ketone **23** produced olefin **24**. Peroxy acid oxidation with *m*-CPBA afforded epoxide **25**. In a two-step sequence of isomerization (via base-mediated epoxide opening to produce diol **26**) followed by benzoylation they were able to produce the benzoylated olefin **27**.<sup>11</sup>

With the ene-protected-triol **27** in hand, stereoselective epoxidation would properly introduce the requisite stereochemistry at C4. To this end, selective silyl group protection of the tertiary alcohol followed by selective deprotection afforded the diol **29** (Scheme 1.5). Further peroxy acid oxidation delivered epoxide **30** appropriately via the Hanbest interaction with O1. Epoxide **30** was then oxidized under mild basic conditions to produce the corresponding  $\alpha$ - $\beta$  unsaturated ketone **31**. The epoxide ring was opened during this synthetic step to produce the tertiary alcohol at C4. Delivering the nitrogen to C3 was accomplished via a tethered 1,4 addition of 2-nitrobenzenesulfonylisocyanate to enone **31** which produced oxazolidinone **32** as a single stereoisomer. Installation of the final methine carbon on C1 was accomplished via a vinyl-triflate-mediated palladium coupling. To generate the precursor, ketone **32** was converted to the vinyl triflate **33**, with the addition of the hindered phosphazane base 2-*tert*-Butylimino-2-diethylamino-1,3-dimethylperhydro-1,3,2-diazaphosphorine (BEMP). Palladium-assisted coupling of triflate **33** with ethyl 2-(tri-*n*-butylstannyl)vinyl ether produced enol ether **34**. Acid

hydrolysis of enol ether **34** generated the final oxygenated core **35**.<sup>11</sup>

Knapp prepared his final oxygenated compound in 16 overall steps from a nonchiral starting material using the well precededent Corey-Bakshi-Shibata (CBS) reduction to impart chirality.<sup>11</sup>

#### 1.4 Johnson's Partial Synthesis of Pac

Johnson's partial synthesis envisaged using an advanced acyclic intermediate to generate stereochemistry through a modified enantioselective Tsuji-Trost allylation. The cyclopentane ring was then to be constructed by a late stage methasis. Starting from methylacetoacetate **36**, diazo transfer with *p*-acetamidobenzenesulfonyl azide afforded the corresponding diazo-keto-ester **37** (Scheme 1.6). A Rh-catalyzed N-H insertion further installed the dimethyl urea on C1 to yield urea **38**. Given the low pKa of the  $\alpha$ -carbon, Johnson could now install the allyl group through modified Tsuji-Trost conditions developed by Ito and coworkers. Initially the synthetic design relied on forming the racemate of the urea but optimization adopted an enantioselective allylation whereby the allyl group was installed to construct keto-ester **39** with an *er* of 92:8. Treatment of the pendant ketone with L-selectride, followed by TBSOTf afforded methyl ester **40**.<sup>14</sup>

Conversion of the methyl ester to the methyl ketone **41** was accomplished using TMSCH<sub>2</sub>Li. It should be noted that, although simple in design, this reaction was unsuccessful under standard conditions (MeMgBr, MeLi, Cp<sub>2</sub>TiMe<sub>2</sub>) due to the presence of the adjacent quaternary center, we too had similar problems in producing our methyl ketone **90** via this method (see Section 1.7). Activation of ketone **41** with CeCl<sub>3</sub> followed by isopropenyl Grignard addition smoothly provided the olefin **42**. Grubbs second generation catalyst was employed to form the cyclopentane core **43**. Unfortunately, once



the final ring was constructed, nOesy analysis revealed inverted stereochemistry at C5, again demonstrating the challenges of this highly congested pentacycle (Scheme 1.7).<sup>14</sup>

Given the C5 stereocenter is constructed by two nucleophilic additions (TMSCH<sub>2</sub>Li addition followed by isopropenyl Grignard), Johnson's group was able to reverse the order of these reactions and deliver the correct stereochemical product. In this regard, from methyl ester **40** DIBAL-H reduction followed by DMP oxidation provided aldehyde **44**. Addition of (3-hydroxyprop-1-en-2-yl)lithium produced the corresponding diol **45**. The primary alcohol was then selectively silylated, followed by DMP oxidation of the remaining free alcohol to afford the unsaturated enone **46**. Following the same sequence of reactions as above (methyl Grignard/Grubbs II metathesis) Johnson was able to generate his advanced cyclopentane ring **48** with proper stereochemistry at the C5 position, confirmed via NOESY analysis (Scheme 1.8).<sup>14</sup>

With the correct epimer in hand OsO<sub>4</sub> catalyzed dihydroxylation of olefin **48** provided diol **49**. Swern oxidation of the pendant secondary alcohol afforded the  $\alpha$ -hydroxy-ketone **50** which was further protected with excess 2,2-dimethoxypropane to afford the highly substituted bis-dioxolane **51** (Scheme 1.9).<sup>14</sup>

Johnson's semisynthesis, in parallel with Knapp, used nonchiral starting materials which were later functionalized. Using an enantioselective Tsuji-Trost reaction Johnson was able to report the synthesis of a highly functionalized intermediate en route to pac.<sup>14</sup>

### 1.5 Hanessian's Total Synthesis of Pac

Finally in 2011, after 50 years, pac succumbed to total synthesis by the Hanessian group. Hanessian's strategy was to relay stereochemistry around the cyclopentane ring using the chirality of L-threonine as a starting point. The utility of this natural amino acid

is evidenced by the stereochemical information at C1, C2, C7, and C8 mirrored on *pac*. After careful construction of the cyclopentane core around L-threonine the Hanessian group was able to adjust a variety of functional groups to meet *pac*'s stereochemical requirements.<sup>12</sup>

Starting from L-threonine **52** a three-step sequence provided them the oxazoline **53**. Subsequent alkylation with O-TBDPS-2-hydroxymethyl acrolein followed by silylation of the pendant alcohol afforded the allylic diol **54**. Reduction of the benzyl ester with DIBAL-H and then subsequent methyl Grignard addition provided alcohol **55**, which was immediately exposed to Swern oxidation conditions to produce methyl-ketone **56**. Ozonolysis of the olefin provided the ketone which was subjected to a Mukaiyama-type intramolecular aldol condensation to provide the diol **57**. B-elimination of the activated alcohol at C4 provided the enone **58** which was appropriately set for functionalization at C2, C3, C4 (Scheme 1.10).<sup>12</sup>

With the cyclopentane ring now intact, base induced epoxidation smoothly provided the epoxide **59** as a single diastereomer. Reduction of the C2 ketone using Luche conditions delivered the alcohol **60**. The alcohol **60** was activated to the triflate ester which was secured for inversion via *tert*-butyl ammonium azide substitution to yield azide **61**. Silyl deprotection, followed by periodate oxidation produced the azido-ketone **62**. The proper stereochemical information was installed on C5 by methyl Grignard addition to produce tertiary alcohol **63**. Deprotection of the primary alcohol was accomplished with tetrabutylammonium fluoride (TBAF) and upon epoxide activation with Zn(OTf)<sub>2</sub> the stereochemistry at C4 was inverted to yield triol **64**. The acetate group that was inadvertently added was replaced with TBDPSCl to afford silyl ether **65**. The resultant diol

was then converted to the endocyclic epoxide by triflic anhydride mediated activation to yield the epoxy-azide **66**. With the help of X-ray crystallographic analysis all the stereocenters on the epoxy-cyclopentane **66** were confirmed (Scheme 1.11).<sup>12</sup>

The addition of a mild Lewis acid to epoxide **66** in the presence of 3-(prop-1-en-2-yl)aniline produced the azido-masked trans-diamine **67** (Scheme 1.12). In final preparation for the natural compound, the oxazoline was opened with 2N HCl to afford the benzoyl protected alcohol **68**. Sequential removal of the silyl ether followed by treatment with 2,2-dimethoxypropane produced the requisite acetonide **69**. The dimethyl-urea was to be an easily installed functional group, however addition of *N,N*-dimethylcarbamoyl chloride to the amine on C1 (not shown) only produced oxazoline **67**. Formation of the urea was accomplished using a careful set of conditions whereby the reactive amine was first converted to isocyanate in the presence of diphosgene and subsequently reacted with dimethylamine to afford urea **70**. Conversion of the benzoyl group to the secondary alcohol was carried out by addition of DIBAL-H, followed by Johnson-Lemieux oxidative cleavage of the remaining olefin, and acetonide deprotection to yield the azido-triol **71**. The functionalized ester **72** was procured by the treatment of primary alcohol on C9 with cyanomethyl 2-hydroxy-6-methylbenzoate. The remaining azide on C2 was converted to the amine in the presence of Lindlar's catalyst generating **pac** in 29 linear steps and overall 3.0% yield (Scheme 1.12).<sup>12</sup>

Hanessian's work demonstrates the challenges to functionalize such a sterically and electronically congested molecule. Synthetic construction of this complex aminocyclopentanol will allow for targeted SAR studies in order to develop less toxic biologically active congeners.<sup>12</sup>

## 1.6 Johnson's Total Synthesis of Pac

Johnson's efforts toward the complex aminocyclopentanol culminated in 2013. The Johnson group recognized the utility of pac in 2012 but were unable to complete their synthesis from the initial route. Johnson's alternative approach detailed below is the shortest total synthesis to date, and is accomplished in 15 total steps.<sup>15</sup>

Starting from the achiral diketo-urea **73**, addition of the cinnamaldehyde imine **74** under Lewis acid control with cinchonidine produced the highly functionalized Mannich adduct **75** in a 98:2 enantiomeric ratio (Scheme 1.12). The utility of this single step was demonstrated by the fact that the product possessed all 5 carbons present in the pac core and contained the "difficult to install" (as observed in Hanessian's synthesis) dimethyl urea.<sup>12</sup> Addition of lithium tri(*tert*-butoxy)aluminum hydride produced the corresponding hydroxyketone which was silylated affording silyl-ether **76**. Enolate formation was accomplished with lithium diisopropylamide, which was subsequently added to formaldehyde to yield alcohol **77**. Olefin ozonolysis procured the functionalized keto-aldehyde **78** for an intramolecular aldol condensation. Sodium methoxide addition formed the 5-membered cyclopentene core **79** (Scheme 1.13).<sup>15</sup>

With the cyclopentenone **79** in hand nucleophilic epoxidation afforded the epoxy alcohol which was silylated with the robust *tert*-butyldiphenylsilyl (TBDPS) group to yield silyl ether **80** (Scheme 1.14). Methyl Grignard addition to the pendant ketone provided the tertiary alcohol **81** at C5 in excellent diastereoselectivity. Upon the addition of a mild Lewis acid, the C3-C4 epoxide was opened with 1-(3-aminophenyl)ethan-1-one to produce the masked diamine **82**. TBAF deprotection of the pendant silylether garnered the free primary alcohol **83**. Johnson was able to secure the final aryl ester using the same conditions

elucidated by Hanessian to construct di-aryl **84**. Treatment of carbamate **84** with palladium on carbon produced the final amine, and thus the formation of pac in 15 total steps with an overall 1.9% yield.<sup>15</sup>

The Johnson group retains the shortest and second total synthesis to date. Their ingenuity allowed construction of pac in 15 steps starting from a unique enantioselective Mannich reaction. Once more, Johnson's synthesis demonstrates the necessity in achieving this complex aminocyclopentanol in short sequence for analog development.<sup>15</sup>

### 1.7 Looper's Partial Synthesis of Pac

Our synthetic assault on pac was predicated upon the development of novel analogs which modify pac's pi-stacking interactions (Scheme 1.15). Similarly to Hanessian<sup>12</sup> we found L-threonine to be a useful chiral synthon containing the chemical information at C1, C5, and C7. From L-threonine we could quickly access the alkylated oxazoline methyl ester **85**. Cyclization of **85** would allow for construction of the functionalized cyclopentene **86**. With the cyclopentene in hand the aldehyde on C4 would act as a handle for introduction of an aryl ring. We felt the alternate aryl ring on C3 could be introduced via a metal catalyzed N-H insertion on **87**, or through the subsequent substitution (after an olefin  $\alpha$ -halogenation) on halide **88**. Either method would provide the requisite bi-aryl system for analog development and potential bioactivity. Further analysis suggested that with this method we also have the desired chemical information to proceed forward with the synthesis of the natural product.

Starting from L-threonine **52** we first generated the methyl ester, which was then added to methyl benzimidate hydrochloride in refluxing CH<sub>2</sub>Cl<sub>2</sub> to produce oxazoline **89** (Scheme 1.16).<sup>17</sup>

With the oxazoline-methyl ester **89** introduction of C2, C3, and C4 could be accomplished through a carefully controlled alkylation. Alkylation at C1 with 1-bromo-5-pentene under standard conditions, however, provided a complex mixture of products. After several failed attempts at alkylation we discovered that rather than the desired alkylation, the oxazoline was undergoing  $\beta$ -elimination to afford the linear protonated product **87** (Scheme 1.17). We reasoned this undesired product was being formed because our electrophile was not strong enough.

Exchanging the bromide for the iodide provided 1-iodo-5-pentene.<sup>18</sup> Subjecting the newly formed iodo-pentene to our conditions, resulted in roughly a 3:1 ratio of an inseparable mixture of diastereomers, along with a significant amount of the  $\beta$ -eliminated product **90**. We attributed these unwanted byproducts to two reaction attributes: 1) a poorly available nucleophile and 2) unfavorable temperature increases during both enolate formation and electrophile addition. To circumvent these problems, we focused on solvation of the lithium counterion with the addition of HMPA after LDA formation. In conjunction, we also lowered the temperature by submerging the reaction vessel in a MeOH/N<sub>2</sub> (-85 °C) bath instead of dry ice/acetone (-78 °C). Carefully monitoring the temperature via an internal thermocouple after each addition ensured the temperature was between -82 and -85 °C, and cleanly yielded the alkylated product **85** as a single diastereomer in good yield (Scheme 1.18).<sup>19</sup>

Next, we directed our attention to forming the methyl ketone from the methyl ester in a two-step process using Weinreb's amide.<sup>20</sup> Both Hanessian and Johnson were unable to perform this sequence using the Weinreb amidation and instead resorted to additional steps (See Schemes 1.8 and 1.10). Although this process is well documented in the literature, the

steric bulk adjacent to the methyl ester made this transformation difficult as evidenced by both Hanessian's and Johnson's stepwise method.<sup>21</sup>

Given the proximity of the quaternary center adjacent to the methyl ester we were also fearful of having to resort to this sequence. We first attempted to introduce the methyl ketone via a two-step process, forming the Weinreb amide and then converting it to the ketone via methyl Grignard addition (Scheme 1.19). However, this sequence was unreliable due to low yields a consequence of the adjacent quaternary center. In an attempt to take advantage of the poor reactivity due to the adjacent quaternary center, we next tried to add a single equivalent of methyl Grignard in hopes that the steric bulk of the newly formed tetrahedral intermediate would prevent further addition and provide the methyl ketone **93**. Unfortunately, this reaction proved to be unproductive resulting in starting material recovery.

A report by Grabowski and coworkers which documented a similar problem, was circumvented by slurrying the N,O-dimethylhydroxylamine and methyl ester together first for 5 min before adding an excess of methyl Grignard.<sup>22</sup> We found these amended conditions worked well with our substrate, which afforded the methyl ketone **93** in an 82% yield in a single step process (Scheme 1.20).

With the successful installation of C2, C3, and C4 and methyl addition we turned our attention to the formation of the cyclopentane core. The aldehyde was formed through oxidative cleavage of the alkene which provided **94** (Scheme 1.21). Reductive workup of the molozonide was initially attempted with dimethyl sulfide (DMS), but was amended to the use of triphenylphosphine. We found the DMS did not possess the required nucleophilicity to reduce the molozonide but rather chromatographic and NMR analysis

revealed that we had isolated this unstable byproduct. An intramolecular aldol reaction was initiated with the addition of SiO<sub>2</sub> and Hünigs base at elevated temperature to provide the cyclopentene **86** in good yield. These conditions, although simplistic, were serendipitously discovered when a basified column was run on the precursor aldehyde **94**, which generated the cyclized product **86** in situ.

We now required a suitable method to functionalize C2 and C3. Reduction of the aldehyde afforded the alcohol **95** which was followed by epoxidation of the C4-C5 olefin to provide the epoxide **96** as a single diastereomer in good yield (Scheme 1.22). We then turned our attention to a nitrene insertion reaction which could be directed from the pendant alcohol onto C3.<sup>23</sup> Upon thorough examination of the reaction, we felt that a cascade sequence could install both nitrogens at C3 and C2 (Scheme 1.23). Deprotonation of the primary alcohol with sodium hydride followed by addition of sulfamoyl chloride provided the corresponding sulfamoyl amide **97**. The diastereoselectivity of the above reaction sequence was based primarily on the configuration of the C4 stereocenter which was determined explicitly by X-ray crystallography (Figure 1.4).

With the sulfamoyl group properly installed a series of conditions were selected based on chemistry by both DuBois<sup>24</sup> and He.<sup>25</sup> Unfortunately, the nitrene insertion was never successful which we attributed partly to the poor solubility of the sulfamoyl ester **95** (Table 1.1). Thorough evaluation of the reaction sequence led us to attempt this transformation with the carbamate **97** instead, which again proved to be unsuccessful (Table 1.1).

Establishing conditions to properly functionalize C3 proved to be difficult. A report by Iwashita and coworkers showed a select example of brominating the alpha position of an unfunctionalized  $\alpha$ - $\beta$  unsaturated ester.<sup>26</sup> We felt this chemistry could be applied to our



ene-aldehyde to produce the corresponding brominated derivative. Therefore, olefin **86** was subjected to halogenation conditions using NBS which provided the subsequent bromo-aldehyde **106** in modest yield (Scheme 1.24). To the best of our knowledge this is the only  $\alpha$ -bromination on an  $\alpha$ - $\beta$  unsaturated aldehyde present in the literature.<sup>13</sup> After optimization of these reaction conditions it was found that dichloromethane could be substituted for carbon tetrachloride as a cheaper and more readily available solvent. An exogenous base, in this case  $K_2CO_3$ , also helped prevent unwanted side reactions by removing any preformed HBr. Furthermore, bromine was chosen as the bromine radical source, over *n*-bromosuccinimide, as it provided the most consistent yields. Unfortunately, the stereochemistry of C3 was unknown and further functionalization was necessary to produce a derivative that could be analyzed by crystallographic or spectroscopic means.

The bromide was displaced with sodium azide, aldehyde reduction with sodium borohydride produced the corresponding azido-alcohol **107**. Hydrolysis of the oxazoline in 2N HCl produced the corresponding benzoate. The free amine was then protected with PMBzCl to produce amide **108**. Peroxy acid oxidation of the olefin, following a similar protocol to that developed earlier in our failed nitrene chemistry, produced the epoxide **109**. We felt the stereochemistry at C4/C5 was the same as the sulfamyl epoxide **97** as a similar epoxidation protocol was followed.

In order to properly install the anti-diol at C4 and C5 a cascade reaction was envisioned whereby the epoxide on C4/C5 would be opened through an intramolecular process by the pendant carbonate group on O7 (Scheme 1.25).<sup>27</sup> This could further alleviate any problems associated with the incorrect stereocenter present on C7 which would be inverted upon cyclization (originally the C7 stereocenter was to be inverted by classical methods).

Lanthanum triflate was chosen as our Lewis acid catalyst, as it was mild and readily available. Unfortunately, addition of lanthanum resulted in only recovered starting material. Use of  $\text{BF}_3 \cdot \text{OEt}_2$  as the Lewis acid, resulted in the formation of **110**. Structural analysis, was hindered by a side product **111** which arose from migration of the benzoyl group. Global hydrolysis of the mixture of esters **110** and **111** with LiOH afforded **112**, which proved to be crystalline. From the triol **112** we were able to establish the absolute structure of our cyclized product by X-ray crystallography. We confirmed that the stereochemistry at C7 was indeed inverted to represent that of the natural product, and the cyclization provided the diol as anticipated (Figure 1.5). However, further analysis revealed that the azide on C3 was in fact the opposite of what was required for pac (Scheme 1.26).

In order to circumvent the improper C3 stereochemistry, we investigated chemistry whereby the stereocenter at C3 could be doubly inverted. After several failed attempts, largely due to substrate decomposition when using hydroxide as a nucleophile, we turned to a milder oxygen nucleophile. Sodium acetate was chosen and cleanly afforded the C3 alcohols **113** and **114** under solvolysis conditions. The intermediate acetates were presumably cleaved during the reaction. Spectral analysis revealed a  $^3J$  splitting pattern for **113** which was identical to that of the corresponding azide **107**. On the other hand, the other diastereomer, **114**, lacked the same splitting pattern as the azide but was consistent with the  $^3J$  splitting of the initial bromide **106** indicating it retained the same stereochemistry as the starting bromide (Scheme 1.27).

Given our ability to clearly identify the stereoisomers at C3, we sought a way to stereoselectively introduce an oxygen nucleophile. Sodium benzoate proved to be a good

alternative to acetate as it gave exclusively one diastereomer. Reduction of both ester and aldehyde provided diol **116** (Scheme 1.28). The oxazoline was hydrolyzed via the same conditions used before to provide the corresponding free amine, which was subjected to PMBz protection with PMBzCl to afford the anisole ester **117**. As before, epoxidation provided **118** as a single diastereomer. Performing the key epoxide opening cascade reaction was smoothly accomplished by the addition of  $\text{BF}_3 \cdot \text{OEt}_2$ . Further addition of benzoic acid led to the acyl transfer which provided **119** as a single isomer in 90% yield. Oxidation of the remaining secondary alcohol was accomplished with the addition of (2,2,6,6-Tetramethylpiperidin-1-yl)oxyl (TEMPO) and bis-acetoxy iodobenzene (BAIB) to produce the ketone **120**.

The synthesis delineated above represents another powerful sequence in pursuing aminocyclopentanols. Although our synthesis is unfinished, obtaining analogs that perturb the pi-stacking framework, responsible for pactamycin's potent activity, should be synthetically accessible from bromide **106** as well as ketone **120**. Our synthesis introduced the trans-C4-C5-diol, and established the correct stereochemistry at C1, C4, C5, and C7. We have also demonstrated an unprecedented  $\alpha$ -bromination on an ene-aldehyde which assisted in the synthesis of the final ketone **120**. The utility of our epoxide opening cascade as well as the  $\alpha$ -bromination could be exploited to produce analogs with varying substitution patterns at C4, C5, and C3 and could further help in the development of a clinically viable compound.

## 1.8 Analog Studies

In order to pursue potential therapeutic leads we intercepted a number of functionalized intermediates to determine if they had biological activity based on whole cell MIC (MRSA)

and enzymatic assays (rabbit reticulocyte protein synthesis). We selected intermediates based on the similarity to pac's pi-stacking mechanism of action. In light of this, we focused on compounds with at least one pendant aryl ring and contained the requisite cyclopentane core. The compounds selected were further decorated with various functional groups which could complement binding.

Three advanced intermediates met these criteria and are shown below (Figure 1.6). Unfortunately, the compounds tested lack any viable MIC against MRSA ( $>64 \mu\text{g/mL}$ ) as well as any inhibition in protein synthesis. It is likely that the analogs generated do not meet the conformational parameters of the ribosome and thereby are inactive when tested. However, iterations on current analogs and other intermediates may produce a more viable and active compound.

## 1.9 Future Aims

In 12 steps, a significant portion of the highly complex amino cyclopentanol has been synthesized. Possible routes to synthesize the natural product are outlined below (Scheme 1.29). Starting from the ketone  $\alpha$ -halogenation followed by azide displacement should produce the requisite nitrogen on C2 to afford azide **124**. Although stereochemistry would be difficult to control in this transformation, the incorrect isomer could be converted to the proper one in a short sequence (not shown). From the azido-ketone **124** removal of the oxazoline and dimethyl urea introduction, following Hanessian's elegant protocols, should produce the azido-triol **125**. The final ketone could then be reductively aminated with 3-(prop-1-en-2-yl)aniline and finally azide reduction would provide the natural product.

Given the parallels between Hanessian's synthesis and ours we also have the opportunity to intercept a number of his intermediates.<sup>12</sup> Starting from the advanced ketone

using  $\alpha$ -halogenation followed by azide displacement should produce the requisite nitrogen on C2 to afford azide **124** again (Scheme 1.30). Reductive amination with 3-(prop-1-en-2-yl)aniline would provide the masked diamine **126**, which with the exception of the robust TBDPS group on the oxygen at C9, is identical to Hanessian's amine **67**.

Although the synthesis of pac has yet to be elucidated by the Looper group the highlights of our synthesis include a novel epoxide opening cascade reaction and a short synthetic sequence that allows for modularity in designing the desired di-aryl pi stacking systems responsible for biological activity.

Table 1.1: Attempted conditions used to achieve the N-H insertion

Compound	Catalyst	Additive	Solvent	Temperature	Outcome
<b>95</b>	Rh <sub>2</sub> (Oct) <sub>4</sub>	BAIB, MgO	CH <sub>2</sub> Cl <sub>2</sub>	rt - 40 °C	NR
<b>95</b>	Rh <sub>2</sub> (esp) <sub>2</sub>	BAIB, MgO	CH <sub>2</sub> Cl <sub>2</sub>	rt - 40 °C	NR
<b>95</b>	Rh <sub>2</sub> (OAc) <sub>4</sub>	BAIB, MgO	DCE	80 °C	NR
<b>95</b>	Rh <sub>2</sub> (OAc) <sub>4</sub>	BAIB, MgO	CH <sub>2</sub> Cl <sub>2</sub>	rt - 40 °C	NR
<b>97</b>	AgNO <sub>3</sub>	BAIB, <i>t</i> -butripy	CH <sub>3</sub> CN	80 °C	NR

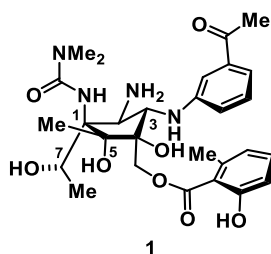


Figure 1.1: The structure of pac

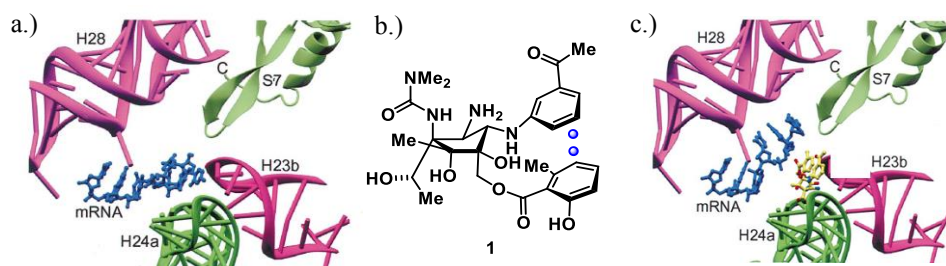


Figure 1.2: Crystallographic analysis of pac's pi-stacking interaction in the 30s subunit of the ribosome from a species of *Thermus thermophilus* used with the permission of Venkatraman Ramakrishnan

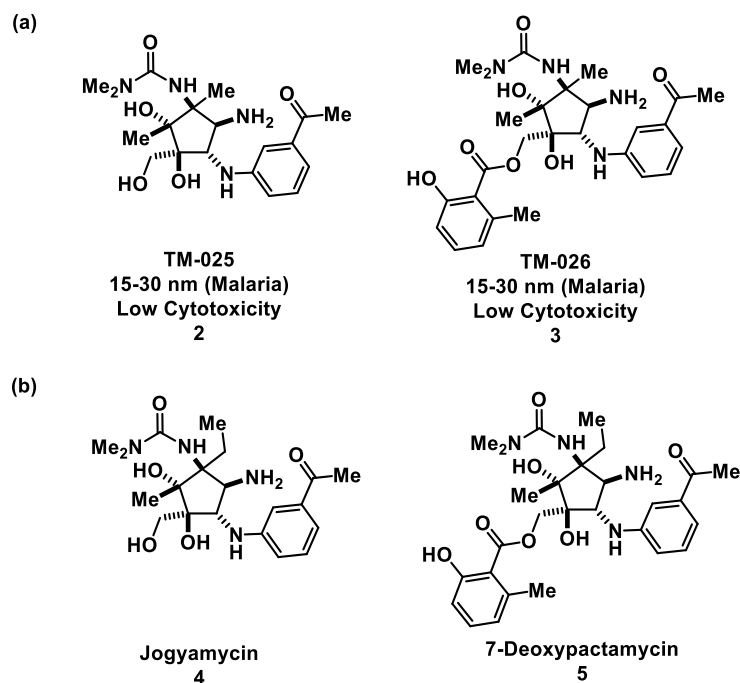


Figure 1.3: (a) Biosynthetic analogs of pac synthesized by the Mahmud laboratory with potent antimalarial activity (b) Natural products structurally related to pac

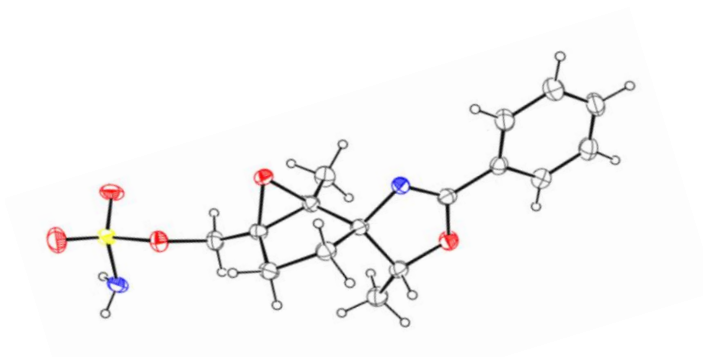


Figure 1.4: Confirmed X-ray structure of sulfamoyl ester **97** with the epoxide up, in line with N1

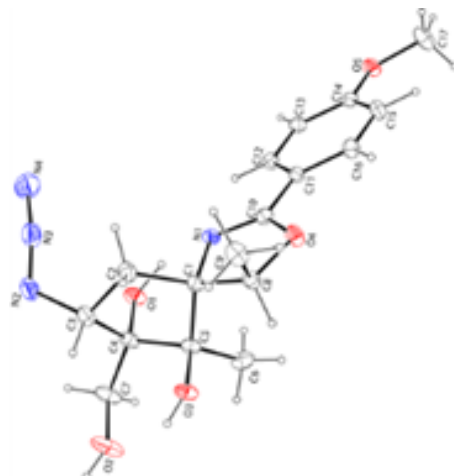


Figure 1.5: Confirmed X-ray structure of azide **112** with the azide in line with N1

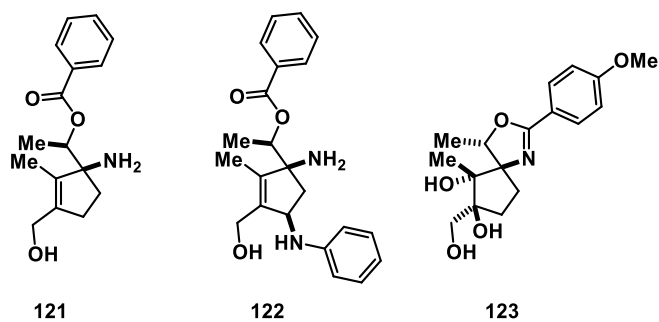
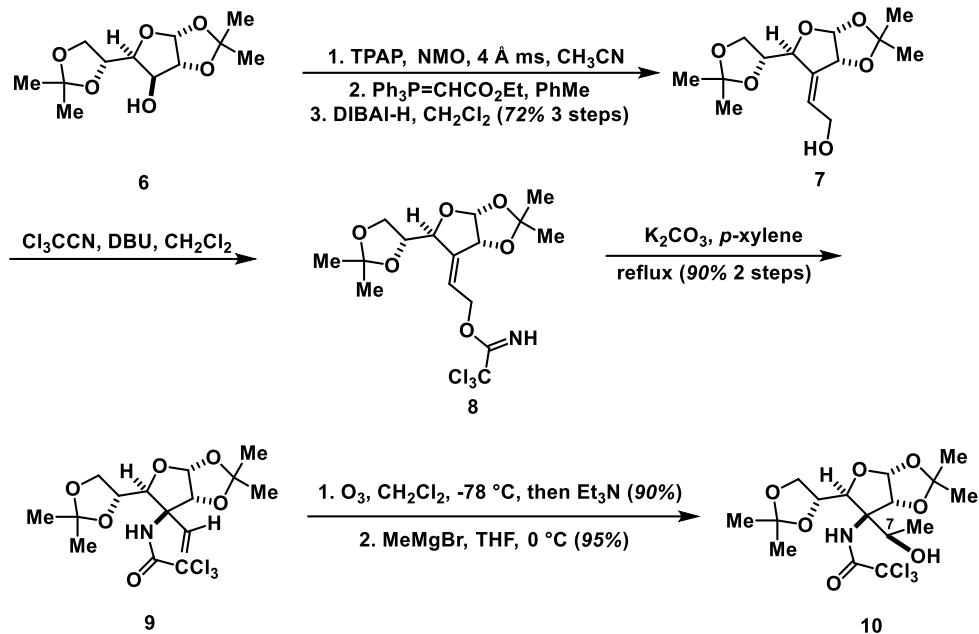
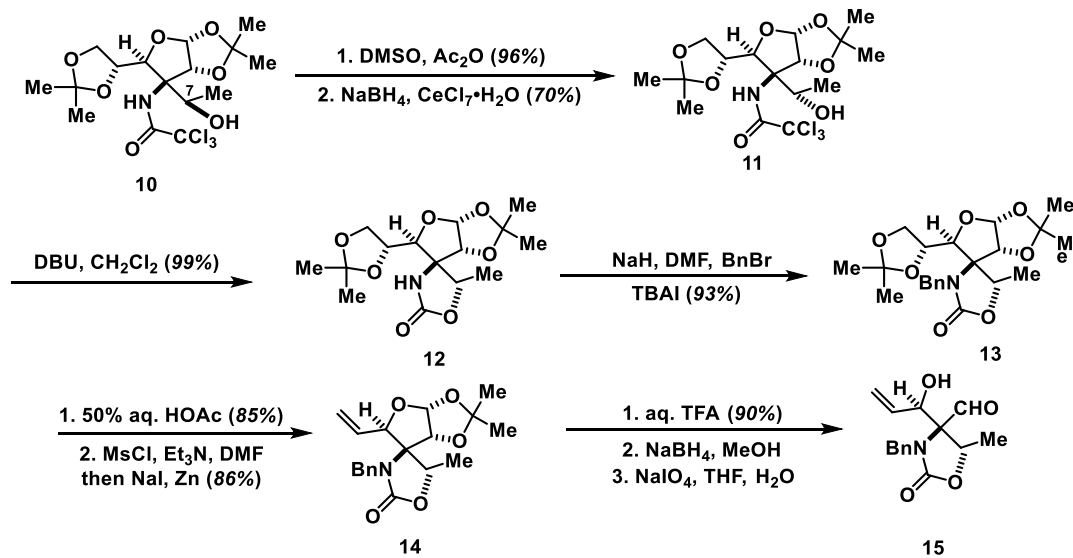


Figure 1.6: Specific analogs intercepted from the synthesis of **120**

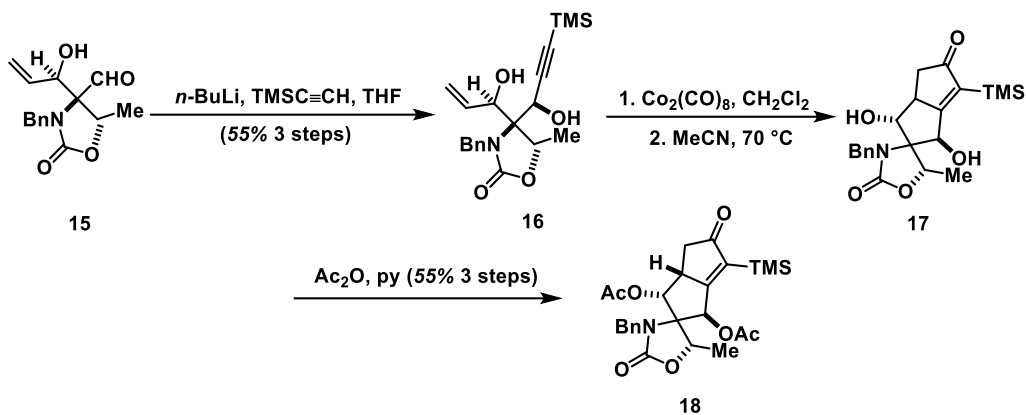




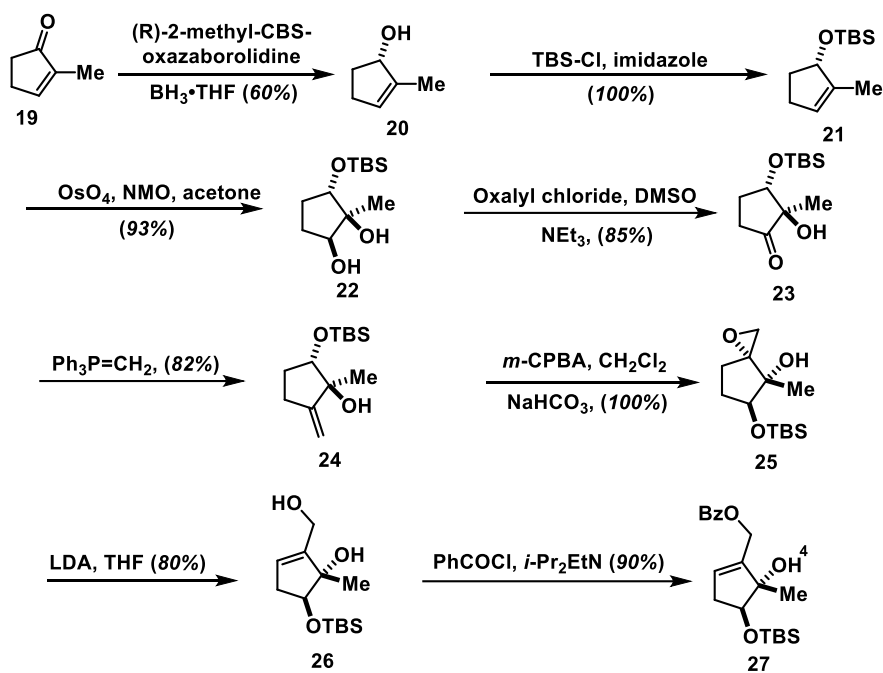
Scheme 1.1: Isobe's synthesis of the advanced trichloroacetamide



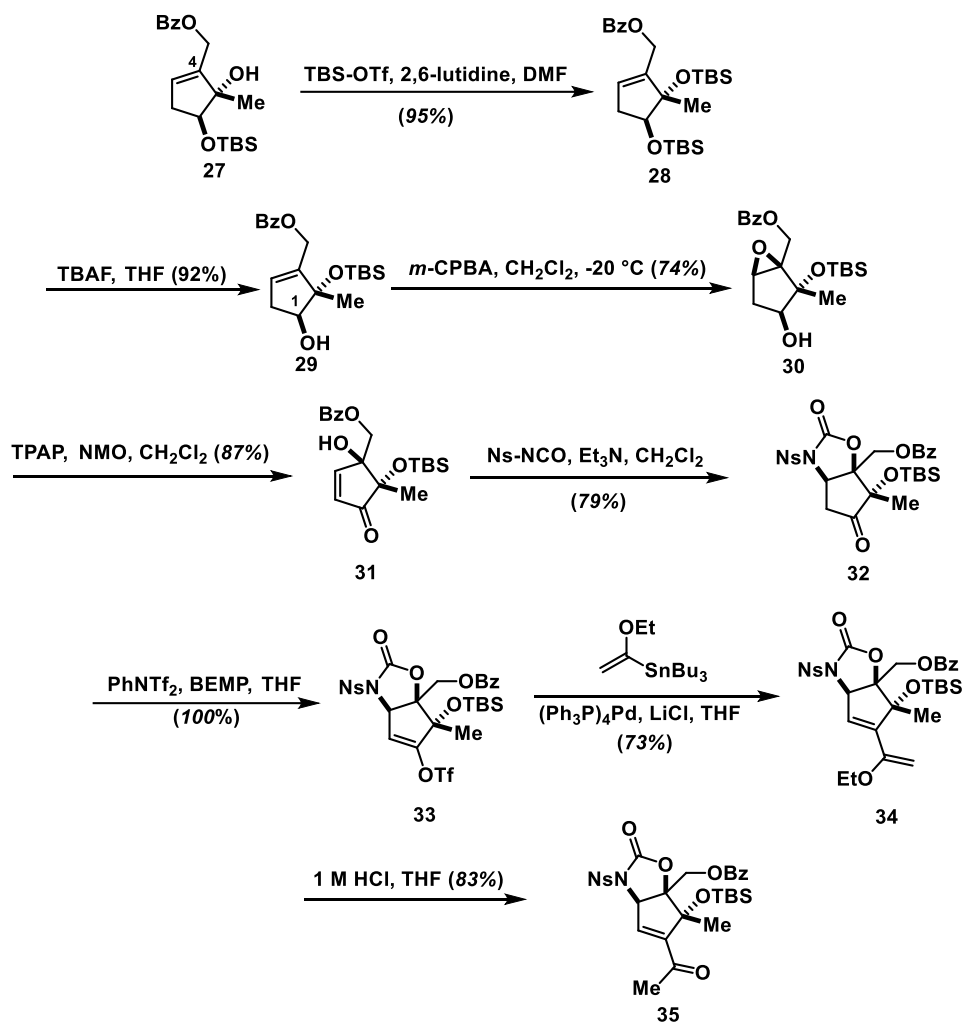
Scheme 1.2: Construction of the pendant alkene



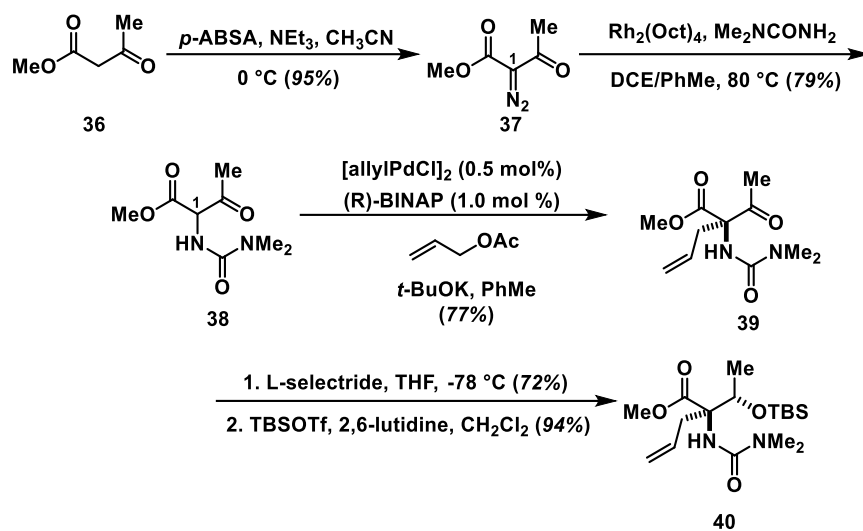
Scheme 1.3: Construction of the final pentacycle via the key Pauson-Khand reaction



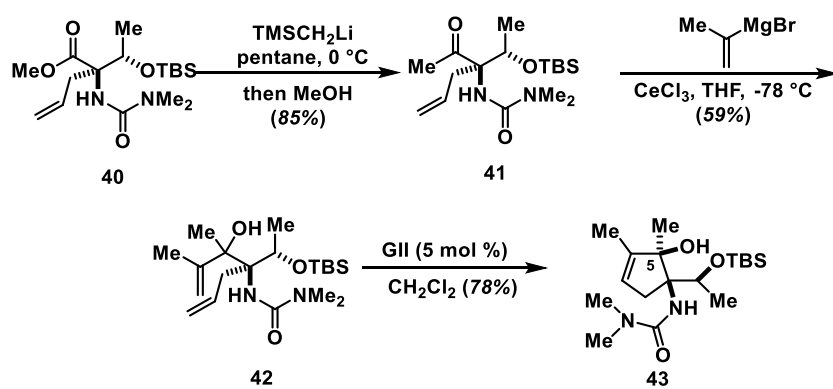
Scheme 1.4: Construction of the advanced benzylated olefin from 2-methyl-2-cyclopenten-1-one



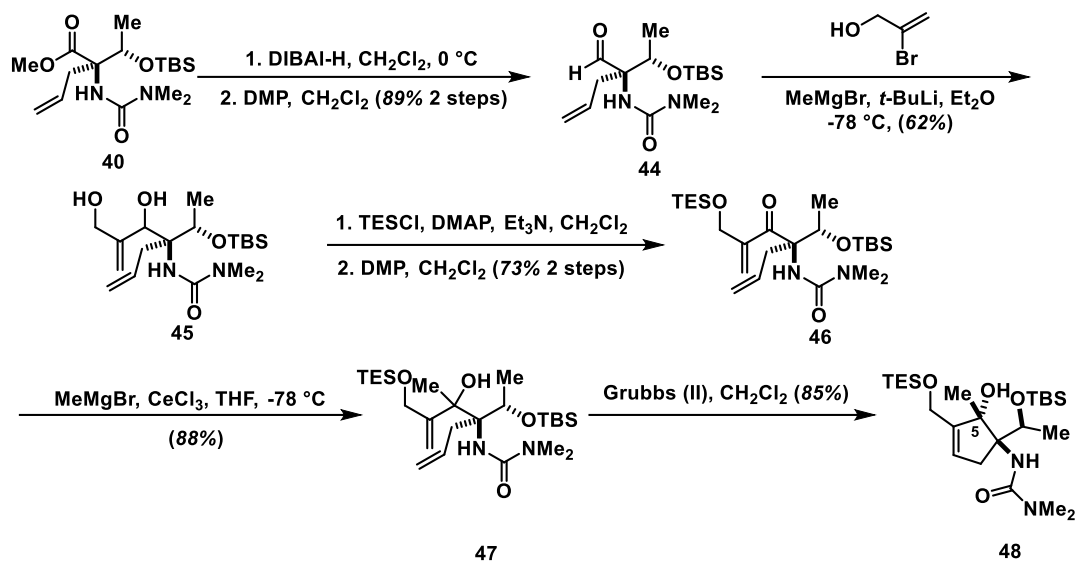
Scheme 1.5: Knapp's preparation of the final functionalized pentacycle



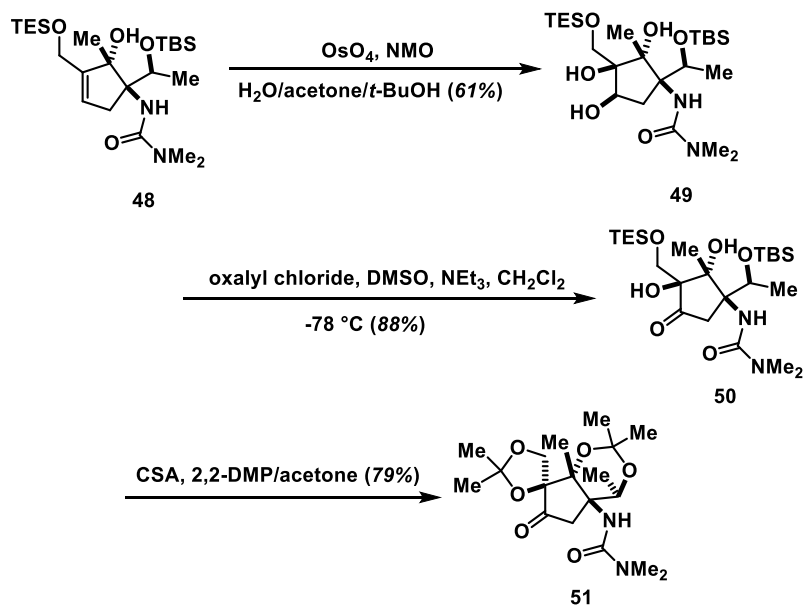
Scheme 1.6: Synthesis of the advanced acyclic urea



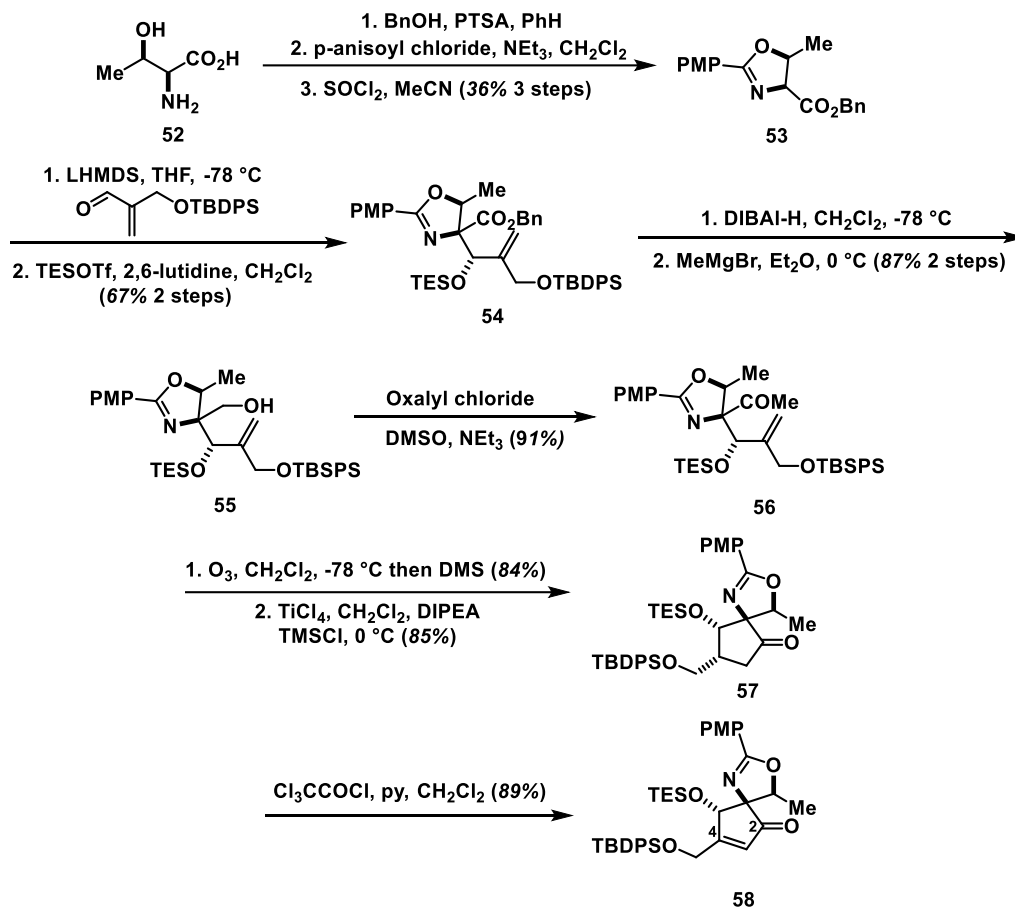
Scheme 1.7: Synthesis of the core pentacycle with the incorrect stereoisomer at C5



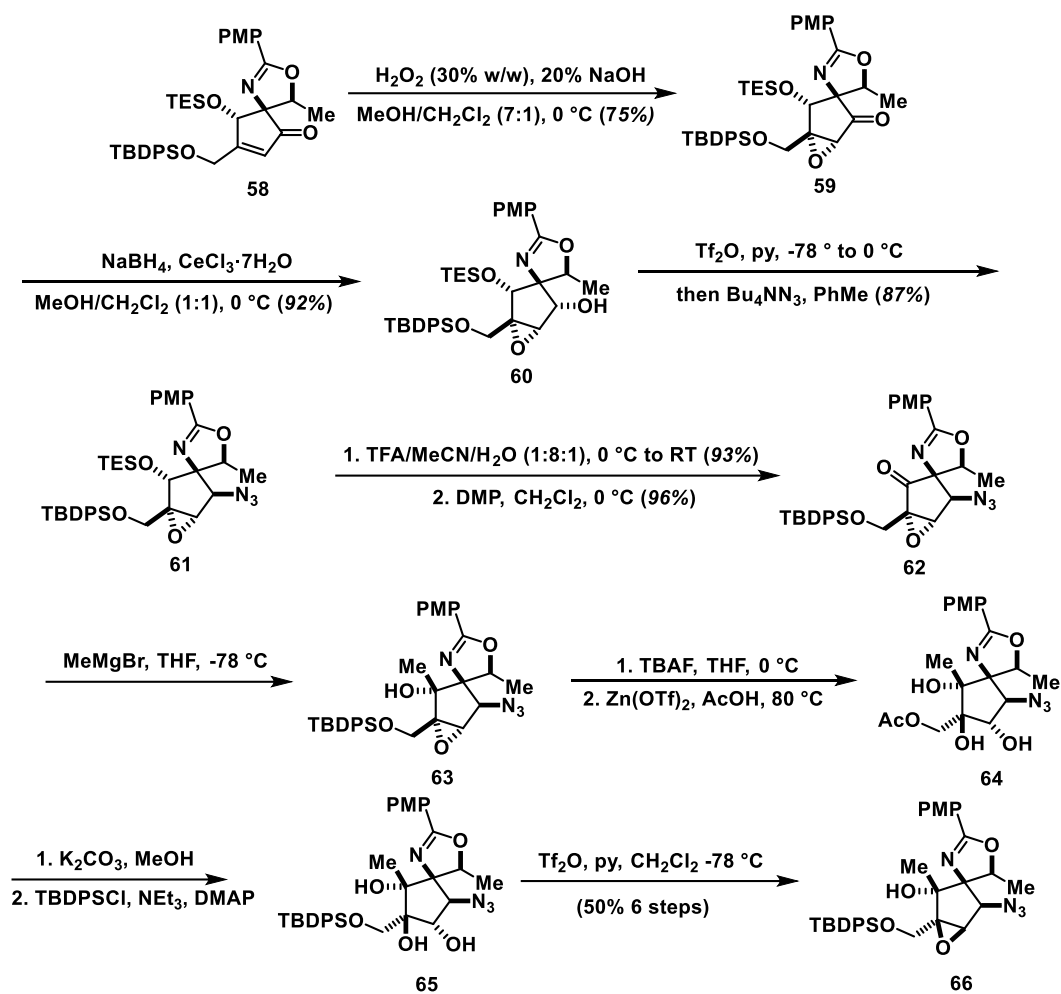
Scheme 1.8: Construction of the key pentacycle with the correct stereochemistry at C5



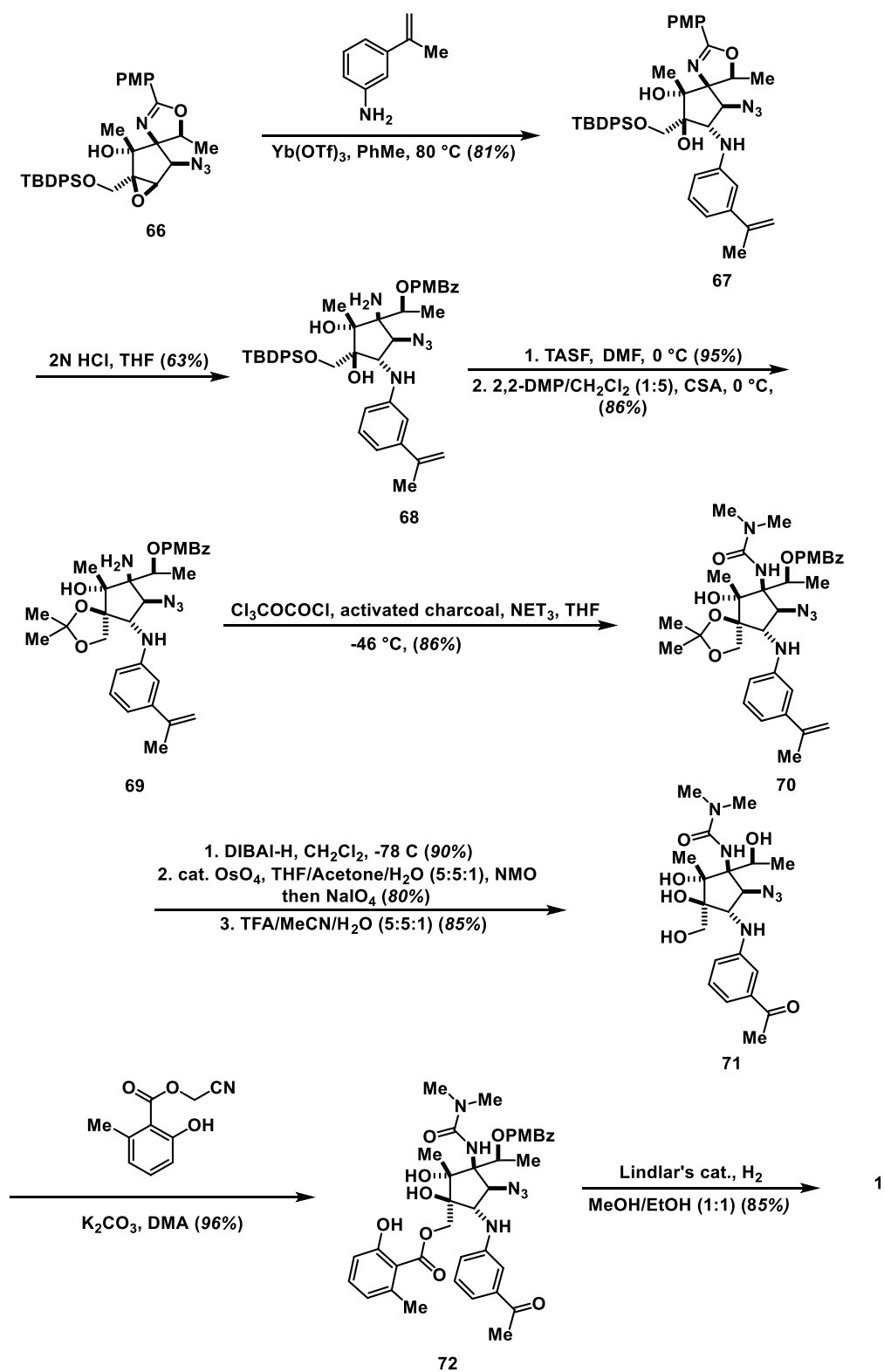
Scheme 1.9: Functionalization of the cyclopentane core



Scheme 1.10: Construction of the oxazoline protected cyclopentenone

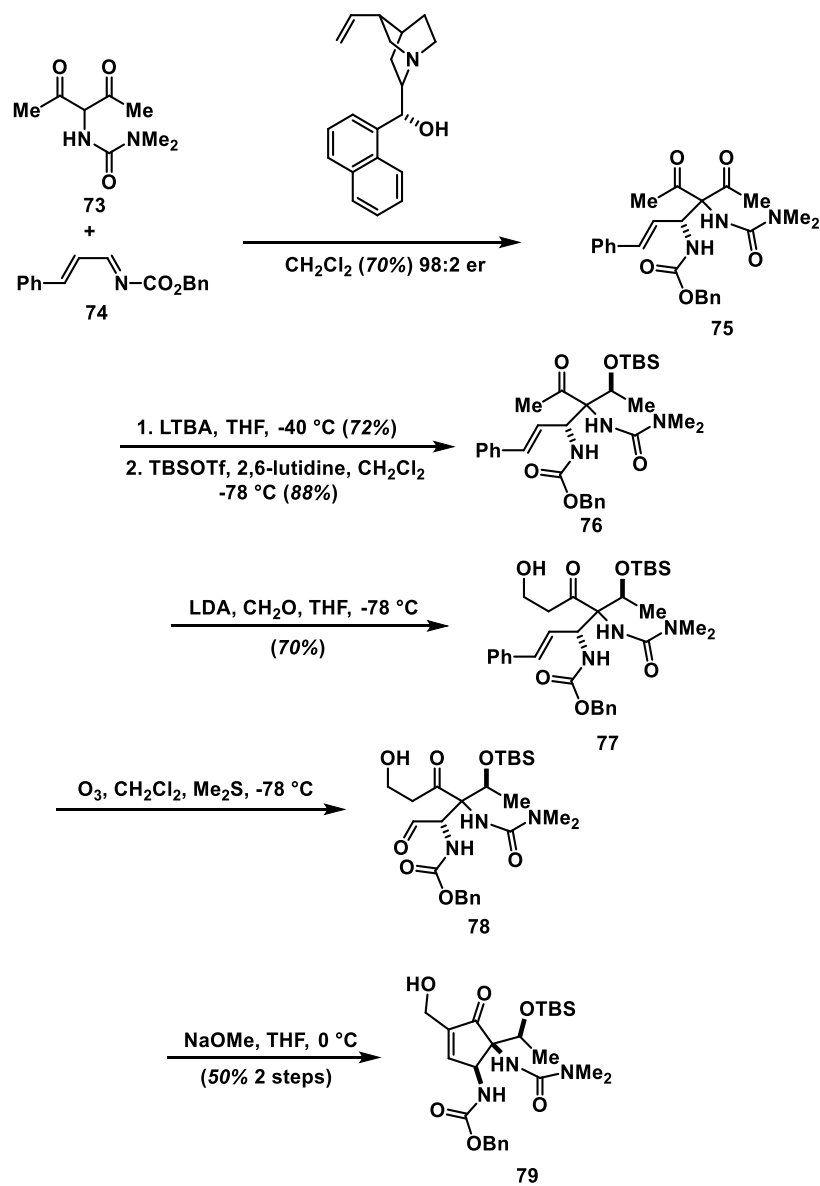


Scheme 1.11: Synthesis of Hanessian's key epoxy-azide

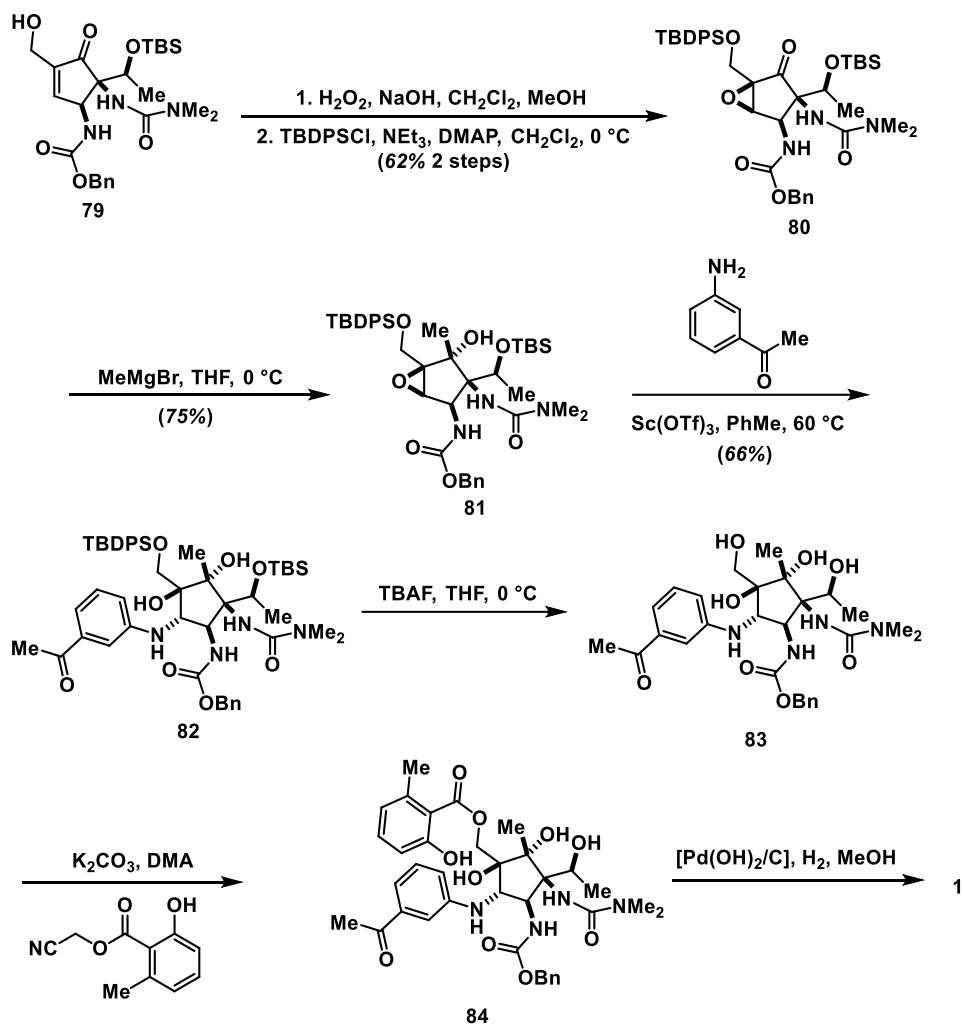


Scheme 1.12: Preparation of the final natural product pac

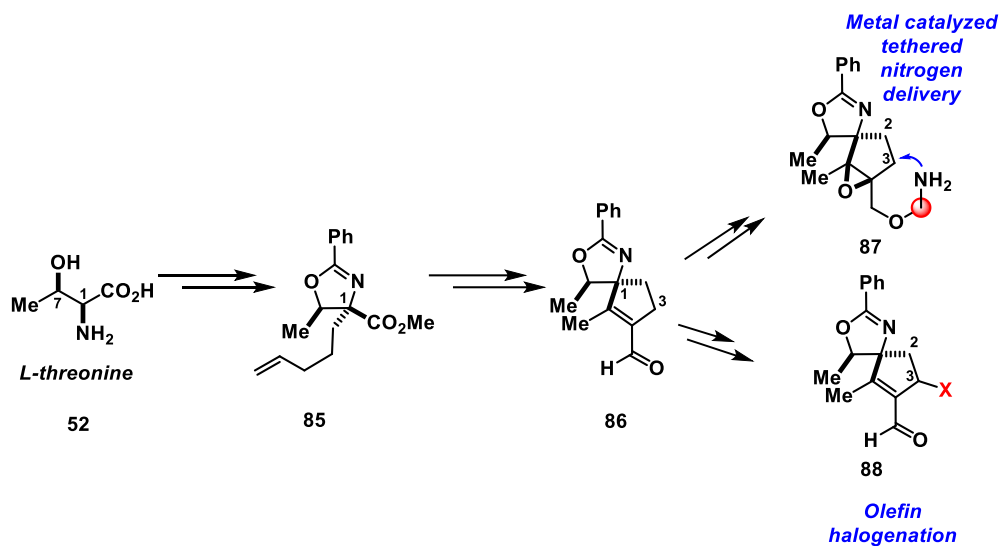




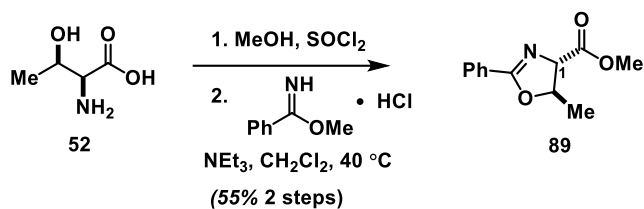
Scheme 1.13: Johnson's synthesis of the advanced pentacycle via a highly advantageous Mannich reaction



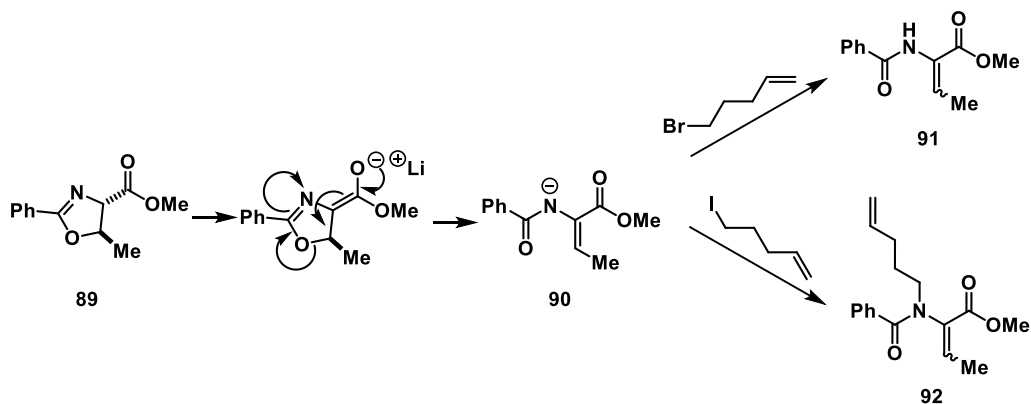
Scheme 1.14: Johnson's final steps to produce pac



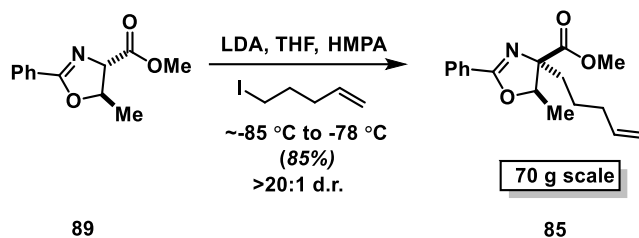
Scheme 1.15: Approach to functionalizing C3 and C4 from L-threonine



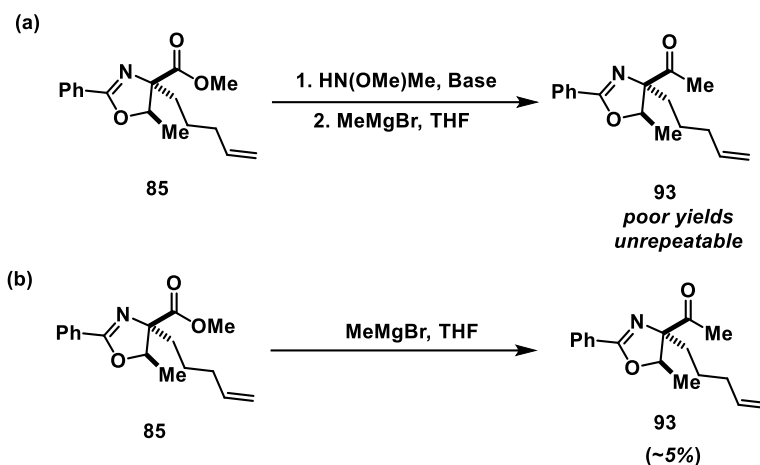
Scheme 1.16: Formation of the parent oxazoline



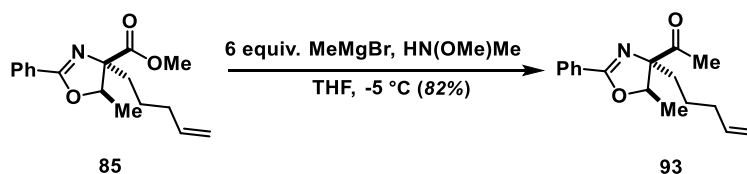
Scheme 1.17: β-elimination of the oxazoline produces unwanted byproducts



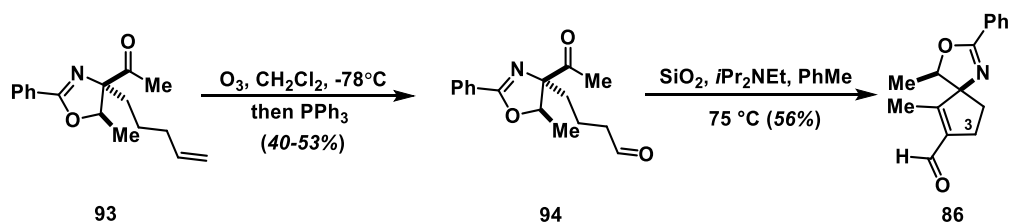
Scheme 1.18: Successful alkylation of the oxazoline



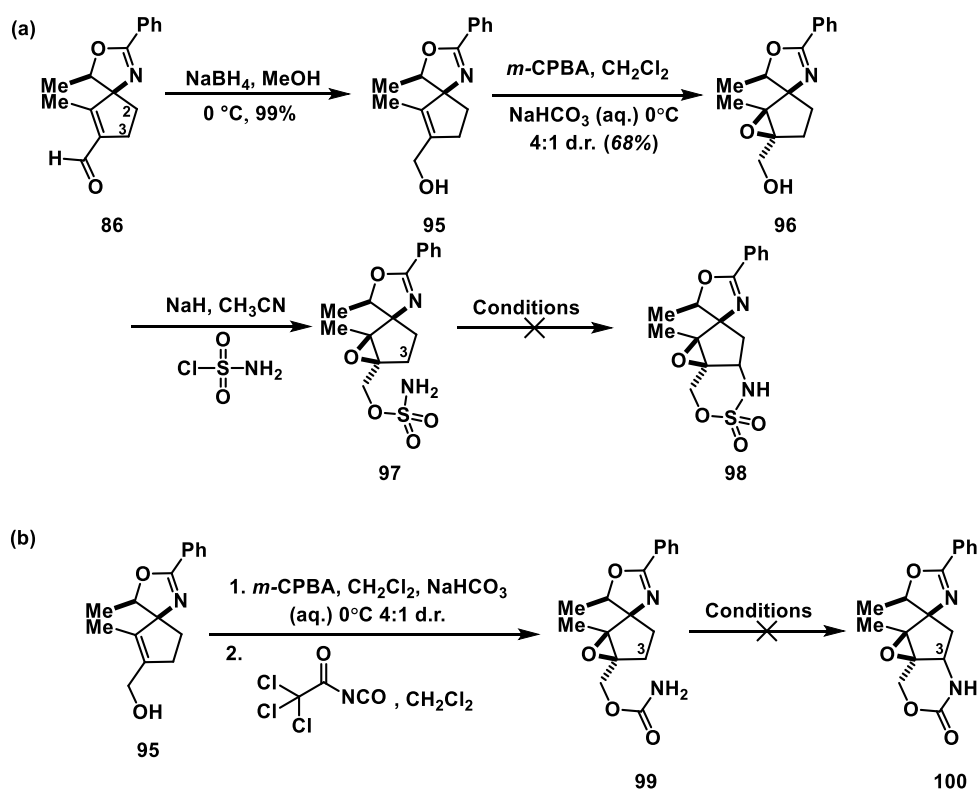
Scheme 1.19: Unsuccessful attempts at generating the methyl ketone



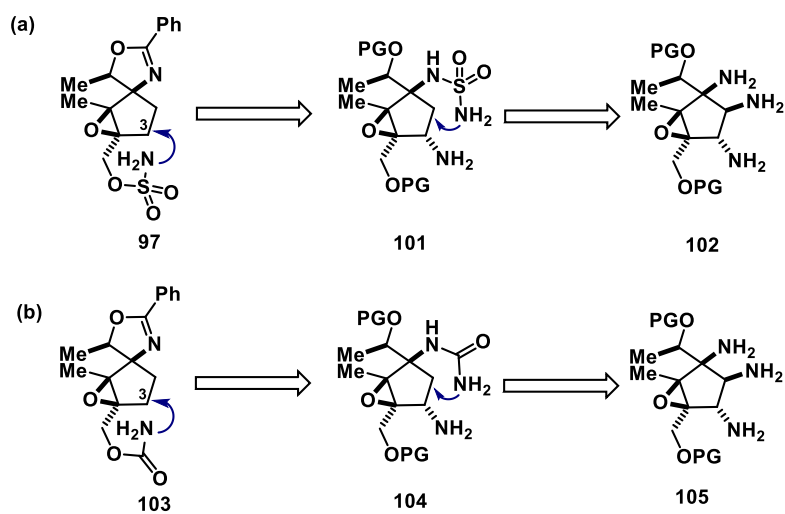
Scheme 1.20: Successful use of Grabowiski's Weinreb amidation to produce the methyl ketone in a single step



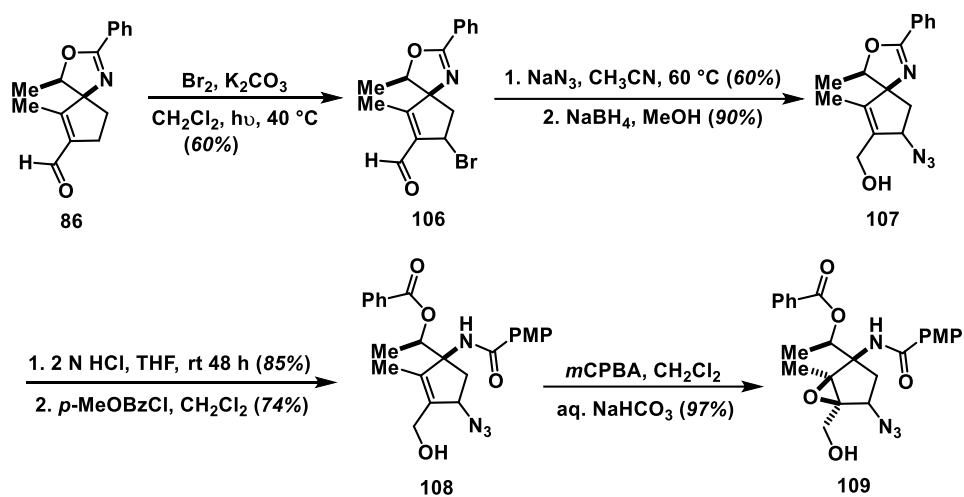
Scheme 1.21: Construction of the cyclopentene core



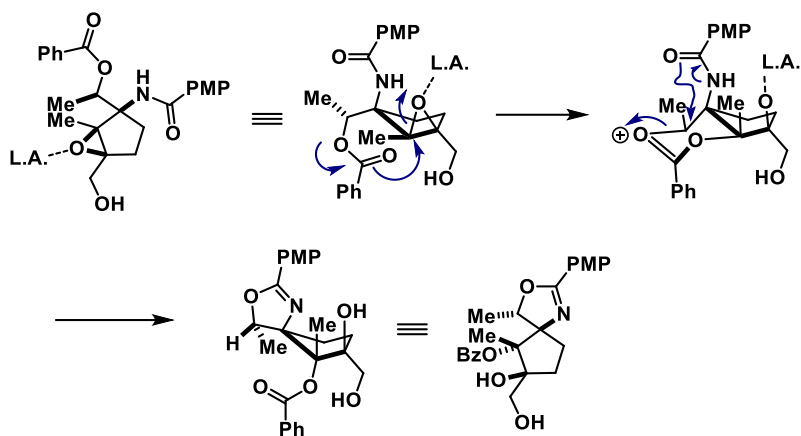
Scheme 1.22: Synthesis of the N-H insertion precursor (a) sulfamate ester (b) carbamate



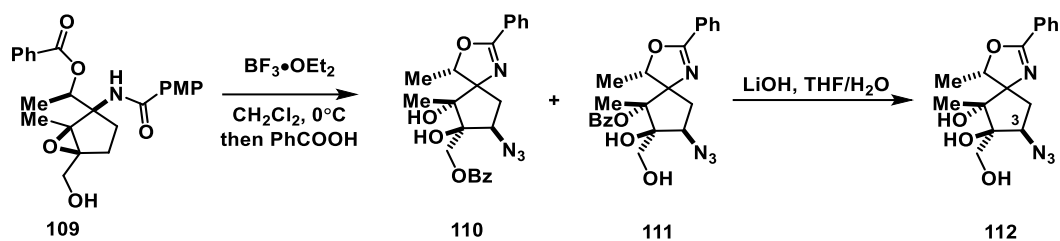
Scheme 1.23: General design of the tethered N-H insertion sequences



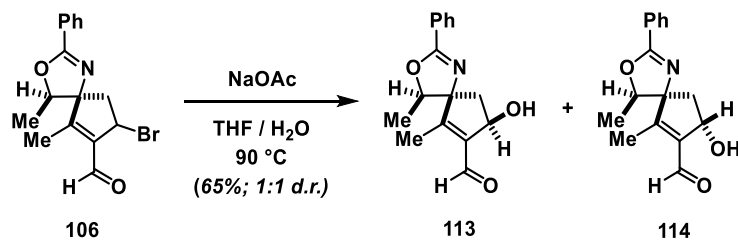
Scheme 1.24: Synthesis of the azido epoxide

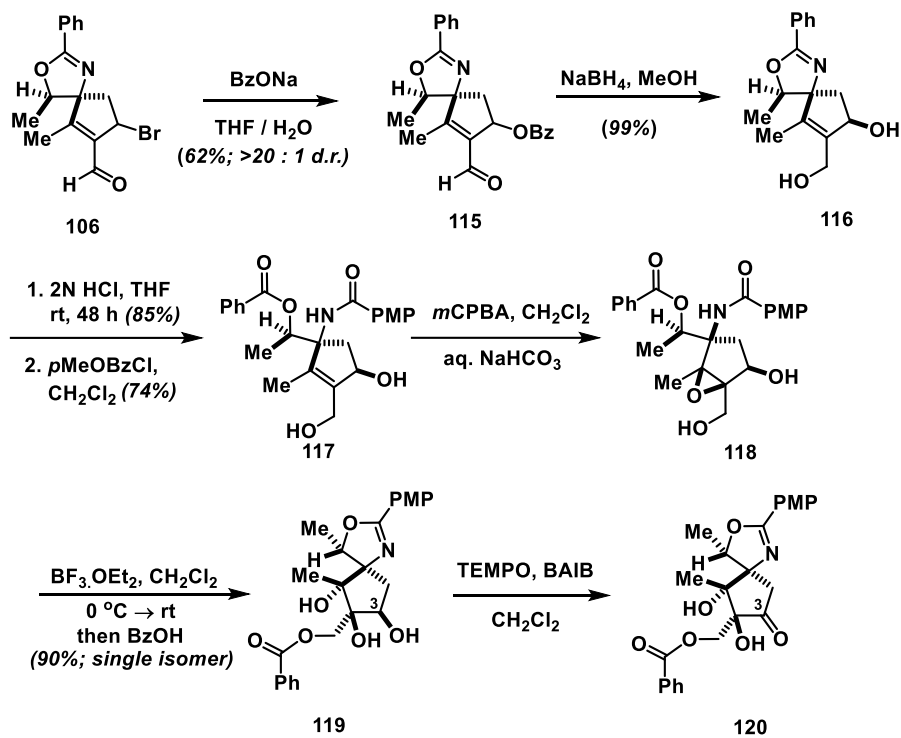


Scheme 1.25: Epoxide opening cascade design

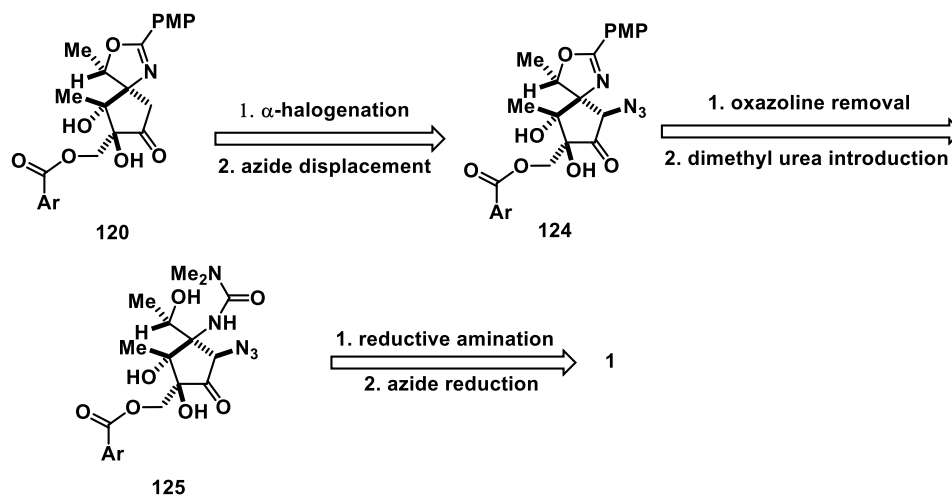


Scheme 1.26: Synthesis of the key triol with the improper stereochemistry at the C3 azide

Scheme 1.27: Solvolysis of bromide **106**

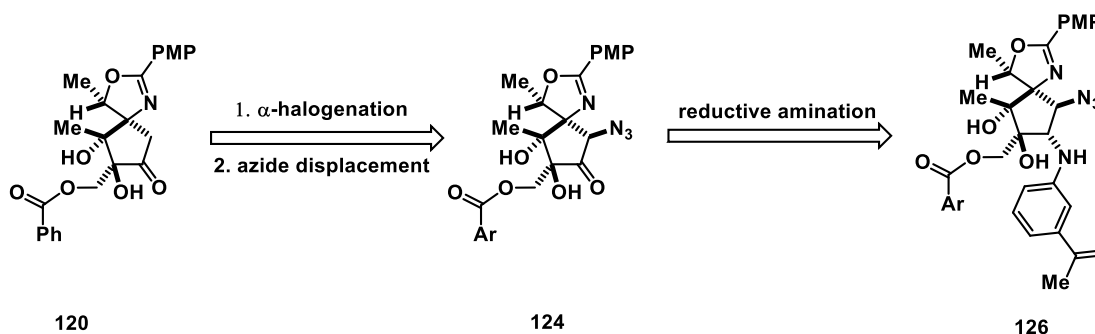


Scheme 1.28: Key cascade sequence imparting the correct stereochemistry



Scheme 1.29: Remaining proposed forward synthesis





Scheme 1.30: Proposed formal synthesis to achieve Hanessian's advanced masked diamine **67**

## 1.10 Supporting Information

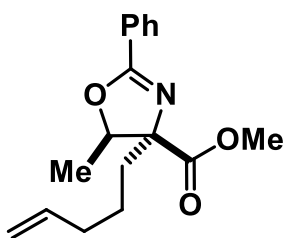
### 1.10.1 General Experimental Conditions

Unless otherwise noted, materials were obtained from commercial sources and used without purification; otherwise, materials were purified according to *Purification of Laboratory Chemicals*.<sup>28</sup> All reactions requiring anhydrous conditions were performed under a positive pressure of nitrogen using flame-dried glassware. Diisopropylamine, triethylamine ( $\text{NEt}_3$ ), and *N,N*-diisopropylethylamine (Hünig's Base) were distilled from  $\text{CaH}_2$  immediately prior to use. Dichloromethane ( $\text{CH}_2\text{Cl}_2$ ), tetrahydrofuran (THF), toluene, and acetonitrile ( $\text{CH}_3\text{CN}$ ) were degassed with nitrogen and passed through a solvent purification system (Innovative Technologies Pure Solv). Methanol (MeOH) was distilled over magnesium prior to its usage. *m*-CPBA was used as purchased (77% wt) with 4-chlorobenzoic acid and  $\text{H}_2\text{O}$  impurities. HMPA is considered to be very toxic and should be handled with great care when used.

Yields were calculated for material judged homogeneous by thin-layer chromatography and  $^1\text{H}$  NMR. Thin-layer chromatography was performed on silica plates eluting with the solvents indicated and visualized by a 254nm UV lamp. Flash column chromatography was

performed with slurry-packed silica gel with solvents indicated in glass columns.  $^1\text{H}$  NMR spectra were recorded at 500 MHz as indicated. The chemical shifts ( $\delta$ ) of proton resonances are reported relative to the deuterated solvent peak: 7.26 for  $\text{CDCl}_3$  and 4.87 for  $\text{H}_2\text{O}$  in  $\text{CD}_3\text{OD}$ , using the following format: chemical shift [multiplicity (s = singlet, d = doublet, t = triplet, q = quartet, m = multiplet, app = apparent), coupling constant(s) (J in Hz), integral].  $^{13}\text{C}$  NMR spectra were recorded at 125 MHz. The chemical shifts of carbon resonances are reported relative to the deuterated solvent peak: 77.3 (center line) for  $\text{CDCl}_3$  and 49.0 (center line) for  $\text{CD}_3\text{OD}$ . Infrared spectra were recorded on a Nicolet 380-FT IR spectrometer fitted with a Smart Orbit sample system. All absorptions are reported in  $\text{cm}^{-1}$  relative to polystyrene. Mass spectra were obtained by ESI/APCI for LRMS or ESI/APCI-TOF for HRMS. Melting points were recorded on a Fisher-Johns melting point apparatus using a digital thermocouple to determine temperature. Optical rotations were obtained at ambient temperature on a Perkin Elmer Model 343 polarimeter ( $\text{Na}_\text{D}$  line) using a microcell with a 1 decimeter path length.

#### 1.10.2 Experimental Procedures

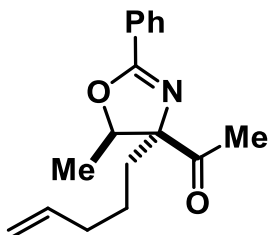


**(4R,5R)-methyl**

**5-methyl-4-(pent-4-en-1-yl)-2-phenyl-4,5-dihydrooxazole-4-**

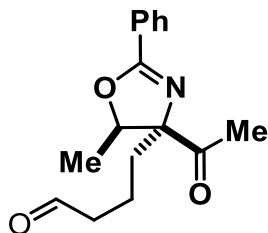
**carboxylate:** To a freshly distilled solution of diisopropylamine (57.0 mL, 0.410 mol, 1.45 equiv.) in THF (2 L) at  $-78^\circ\text{C}$  (dry ice/acetone) in a 3 L three neck roundbottomed flask containing a magnetic stir bar equipped with a thermocouple under a stream of  $\text{N}_2$  was

added *n*BuLi (157.0 mL, 2.5M in THF, 0.390 mol, 1.4 equiv.). Following complete addition the reaction was taken out of the cold bath and warmed for 30 min or until the reaction temperature rose to 0°C. The reaction was then cooled back to -78°C and HMPA (200.0 mL, 1.120 mol, 4 equiv.) was added to the solution quickly. The solution was further cooled to -85 °C (liq. N<sub>2</sub>/MeOH) and oxazoline **6** (61.2 g, 0.279 mol, 1 equiv.) was added dropwise over a period of 35 min. The reaction temperature was monitored by a thermocouple and never rose above -80 °C and never below -90 °C. The solution was then warmed to -78 °C and 5-iodo-1-pentene (109.0 g, 0.560 mol, 2 equiv.) was added over a period of 30 min making sure the temperature never rose above -70 °C. The reaction was allowed to warm to rt over a period of 24h. The solvent was removed under reduced pressure. The crude material was dissolved in CH<sub>2</sub>Cl<sub>2</sub> (500 mL) and washed with sat. LiCl (3 x 500 mL) to yield analytically pure **7** (56.85 g, 71%) as a light yellow oil. *R*<sub>f</sub> = 0.61 (50% ethyl acetate/hexanes).  $[\alpha]^{20}_{\text{D}} = +37.4$  (*c* = 0.7, CH<sub>2</sub>Cl<sub>2</sub>). <sup>1</sup>H NMR (500 MHz, CDCl<sub>3</sub>): 7.99 (d, *J* = 7.5 Hz, 2H), 7.48 (t, *J* = 7.5 Hz, 1H), 7.41 (t, *J* = 7.0 Hz, 2H), 5.77 (dddd, *J* = 7.0, 7.0, 10.0, 17.0 Hz, 1H), 5.02-4.92 (m, 2H), 4.58 (q, *J* = 7.0 Hz, 1H), 3.75 (s, 3H), 2.14-2.05 (m, 3H), 1.76-1.62 (m, 2H), 1.46-1.36 (m, 1H), 1.32 (d, *J* = 6.5 Hz, 3H) ppm. <sup>13</sup>C NMR (CDCl<sub>3</sub>, 125 MHz): 172.6, 164.3, 138.5, 131.8, 128.7, 128.5, 127.8, 115.0, 83.2, 81.0, 52.3, 39.1, 33.9, 23.4, 17.1 ppm. IR (neat): 2949 (w), 1731, 1646, 1449, 1283, 1148 (all s) cm<sup>-1</sup>. HRMS (ESI) calculated for C<sub>17</sub>H<sub>22</sub>NO<sub>3</sub> *m/z* 288.1600 (M+H), Obsd. 288.1590.



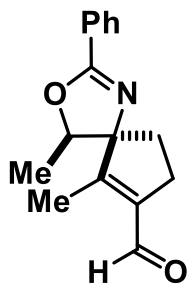
**1-((4R,5R)-5-methyl-4-(pent-4-en-1-yl)-2-phenyl-4,5-dihydrooxazol-4-yl)ethanone:**

To a 1 L round bottomed flask containing a magnetic stir bar, oxazoline **7** (10.0 g, 34.8 mmol, 1 equiv.) in a solution of THF (350 mL) and equipped with a thermocouple under a stream of N<sub>2</sub> was added N,O-dimethylhydroxylamine hydrochloride (5.10 g, 52.2 mmol, 1.5 equiv.). The solution was stirred for 5 min until the solids were finely slurried. The solution was further cooled to -5 °C (Acetone/ice/dry ice) and MeMgBr (64.0ml, 3M in THF, 192.0 mmol, 5.5 equiv.) was added at rate where the temperature never rose above 0 °C. The reaction was left to warm to rt and stirred until TLC analysis showed complete consumption of the starting material. The excess MeMgBr was quenched with sat. NH<sub>4</sub>Cl. The crude reaction mixture was then extracted with Et<sub>2</sub>O (100 ml x 2). The organic layer was dried with Na<sub>2</sub>SO<sub>4</sub> and concentrated under reduced pressure. Purification of the product was accomplished using flash chromatography eluting with 10% ethyl acetate/hexanes. The fractions containing product were concentrated under reduced pressure to give the methyl ketone **8** (7.80 g, 82%) as a light yellow oil.  $R_f$  = 0.66 (50% ethyl acetate/hexanes).  $[\alpha]_D^{20}$  = +43.2 ( $c$  = 0.3, CH<sub>2</sub>Cl<sub>2</sub>). <sup>1</sup>H NMR (500 MHz, CDCl<sub>3</sub>): 8.01(d,  $J$  = 7.0 Hz, 2H), 7.51 (t,  $J$  = 7.5 Hz, 1H), 7.46 (t,  $J$  = 7.5 Hz, 2H), 5.75 (dddd,  $J$  = 7.0, 7.0, 10.0, 17.0 Hz, 1H), 5.00-4.91 (m, 2H), 4.58 (q,  $J$  = 6.5 Hz, 1H), 2.28 (s, 3H), 2.16-1.94 (m, 3H), 1.68-1.55 (m, 2H), 1.36-1.28 (m, 1H), 1.25 (d,  $J$  = 6.5 Hz, 3H) ppm. <sup>13</sup>C NMR (125 MHz, CDCl<sub>3</sub>): 218.5, 164.1, 138.5, 131.8, 128.6, 128.0, 115.0, 84.5, 83.5, 39.1, 34.1, 30.4, 23.1, 17.3 ppm. IR (neat): 2940 (w), 1710 (s), 1644 (s), 1450 (m), 1352 (m), 1150 (s) cm<sup>-1</sup>. <sup>1</sup>. HRMS (ESI) calculated for C<sub>17</sub>H<sub>21</sub>NO<sub>2</sub>Na  $m/z$  294.1470 (M+Na), Obsd. 294.1451.



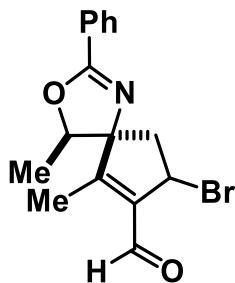
**4-((4R,5R)-4-acetyl-5-methyl-2-phenyl-4,5-dihydrooxazol-4-yl)butanal:** A 250 mL flask, open to the atmosphere, was charged with methyl ketone **8** (9.4 g, 34.8 mmol, 1 equiv.) and ethyl acetate (175 mL) and cooled to  $-78^{\circ}\text{C}$ . Excess  $\text{O}_3$  was then bubbled through the solution until a faint blue color was observed. The reaction was subsequently purged of excess  $\text{O}_3$  by bubbling  $\text{N}_2$  through the solution. When the blue color disappeared  $\text{N}_2$  was bubbled through for an additional 10 min. The reaction was then placed under  $\text{N}_2$ , a magnetic stir bar added, and  $\text{PPh}_3$  (18.2 g, 69.7 mmol, 2 equiv.) added in a single portion. The reaction was allowed to warm to rt and further heated to reflux for 8h. The solvent was removed under reduced pressure. Purification of the product was accomplished using flash chromatography eluting with 10% ethyl acetate/hexanes. The fractions containing product were concentrated under reduced pressure to give aldehyde (7.02 g, 79%) as a light yellow oil. For fear of instability the product was stored in benzene at  $-80^{\circ}\text{C}$  until used.  $R_f = 0.57$  (50% ethyl acetate/hexanes).  $[\alpha]_D^{20} = +25.8$  ( $c = 1.8$ ,  $\text{CH}_2\text{Cl}_2$ ).  $^1\text{H}$  NMR (500 MHz,  $\text{CDCl}_3$ ): 9.73 (t,  $J = 3$  Hz, 1H), 8.00 (d,  $J = 7.0$  Hz, 2H), 7.52 (tt,  $J = 7.0$  Hz, 1H), 7.48 (t,  $J = 7.0$  Hz, 2H), 4.59 (q,  $J = 6.5$  Hz, 1H), 2.45 (td,  $J = 1.5, 7.5$  Hz, 2H), 2.28 (s, 1H), 2.03 (ddd,  $J = 4.5, 4.5, 18$  Hz, 1H), 1.91-1.84 (m, 1H), 1.65 (td,  $J = 4, 11.5$  Hz, 1H), 1.59-1.52 (m, 1H), 1.26 (d,  $J = 7.0$  Hz, 3H) ppm.  $^{13}\text{C}$  NMR (125 MHz,  $\text{CDCl}_3$ ): 212.1, 202.2, 164.6, 132.0, 128.6, 127.8, 84.3, 83.7, 44.1, 38.5, 30.4, 17.2, 16.7 ppm. IR (neat): 1708 (s), 1644 (s), 1450 (m), 1352 (m), 1063 (s)  $\text{cm}^{-1}$ . HRMS (ESI) calculated for  $\text{C}_{17}\text{H}_{21}\text{NO}_2\text{Na}$   $m/z$  294.1470 ( $\text{M}+\text{Na}$ ), Obsd. 294.1451. HRMS (ESI) calculated for  $\text{C}_{16}\text{H}_{19}\text{NO}_3\text{Na}$   $m/z$

296.1263 (M+Na), Obsd. 296.1266.



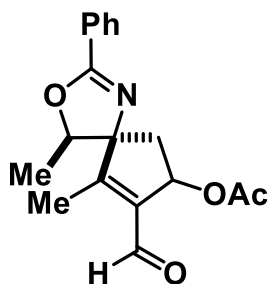
**(4R,5S)-4,6-dimethyl-2-phenyl-3-oxa-1-azaspiro[4.4]nona-1,6-diene-7-carbaldehyde:**

To a 250 mL flask containing keto aldehyde (7.50 g, 27.9 mmol, 1.0 equiv.) in toluene (200 mL) was added SiO<sub>2</sub> (1.70 g, 28.3 mmol, 1 equiv.). The solution was stirred for 5 min followed by the addition of freshly distilled diisopropylethylamine (19.4 mL, 111.6 mmol, 4 equiv.). The reaction was then heated to 75°C for 48 h or until TLC analysis showed complete consumption of the starting material. The solvent was removed under reduced pressure to yield a yellow slurry which was filtered through a plug of celite with dichloromethane to remove any excess silica. The filtrate was concentrated *in vacuo* and the resultant solid was recrystallized from *i*-PrOH to yield the cyclopentane **9** (6.04 g, 85%) as a light yellow solid. *R*<sub>f</sub> = 0.58 (50% ethyl acetate/hexanes). mp. 87-89°C.  $[\alpha]_D^{20} = -151.2$  (*c* = 0.3, CH<sub>2</sub>Cl<sub>2</sub>). <sup>1</sup>H NMR (500 MHz, CDCl<sub>3</sub>): 10.07 (s, 1H), 7.98 (d, *J* = 7.5 Hz, 2H), 7.50 (t, *J* = 7.5 Hz, 1H), 7.41 (t, *J* = 7.5 Hz, 2H), 4.64 (q, *J* = 6.5 Hz, 1H), 2.69-2.64 (m, 1H), 2.52-2.41 (m, 2H), 2.06 (t, *J* = 2.0 Hz, 3H), 2.00-1.95 (m, 1H), 1.38 (d, *J* = 6.5 Hz, 3H) ppm. <sup>13</sup>C NMR (125 MHz, CDCl<sub>3</sub>): 189.2, 164.7, 159.5, 140.0, 132.0, 128.6, 127.6, 87.5, 85.6, 37.2, 27.4, 16.0, 12.3 ppm. IR (neat): 1667 (s), 1635 (s), 1285 (w), 1059 (m), 1012 (w) cm<sup>-1</sup>. HRMS (ESI) calculated for C<sub>16</sub>H<sub>18</sub>NO<sub>2</sub> *m/z* 256.1338 (M+H), Obsd. 256.1334.



**(4R,5S)-8-bromo-4,6-dimethyl-2-phenyl-3-oxa-1-azaspiro[4.4]nona-1,6-diene-7-**

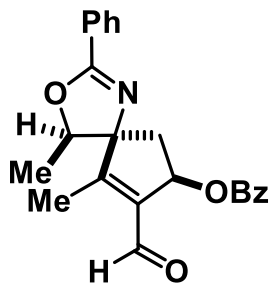
**carbaldehyde:** To a 100 mL flask equipped with a magnetic stirring bar under a stream N<sub>2</sub> containing cyclopentene **9** (1.10 g, 4.31 mmol, 1 equiv.) in a solution of CH<sub>2</sub>Cl<sub>2</sub> (65 mL) was added K<sub>2</sub>CO<sub>3</sub> (253 mg, 2.5 mmol, 4equiv.). Bromine (3.7 g, 21.0 mmol, 5 equiv.) was added to the solution followed by AIBN (35 mg, 0.2 mmol, .05 equiv.). The reaction was then heated to 40 °C until NMR showed 50-80% consumption of the starting material. The excess bromine was quenched with aq. Na<sub>2</sub>S<sub>2</sub>O<sub>3</sub> (50 mL) and extracted with CH<sub>2</sub>Cl<sub>2</sub> (2 x 100 mL). The combined organics were dried with Na<sub>2</sub>SO<sub>4</sub>. The solvent was removed under reduced pressure and the mixture was purified using flash chromatography eluting with 10% Ethyl acetate/hexanes. **9** would co-elute with the product **10** and any attempt to run the reaction for longer times would result in substantial decomposition. As such, a mixture of the bromide and starting material were carried forward to the next reaction. R<sub>f</sub> = 0.58 (50% ethyl acetate/hexanes).



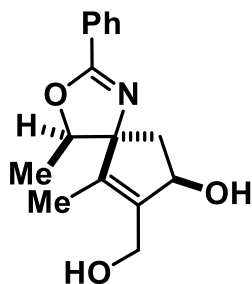
**(4R,5S,7R)-8-formyl-4,9-dimethyl-2-phenyl-3-oxa-1-azaspiro[4.4]nona-1,8-dien-7-yl-acetate (16) and (4R,5S,7S)-8-formyl-4,9-dimethyl-2-phenyl-3-oxa-1-**

**azaspiro[4.4]nona-1,8-dien-7-yl-acetate:** A 100 mL flask was charged with a solution of bromo aldehyde **10** (90mg, .27 mmol, 1 equiv.) which contained ~40% of the aldehyde **9** in THF (5 mL). Sodium acetate (710mg, 8.6 mmol, 32 equiv.), and H<sub>2</sub>O (1 mL) were then added and the reaction was stirred for 8 h at reflux. The solvent was evaporated *in vacuo*. Purification of the product was accomplished using flash chromatography eluting with 5% ethyl acetate/hexanes followed by 10% ethyl acetate/hexanes. The fractions containing product were concentrated under reduced pressure to give acetates **16** (29 mg, 35%) and **17** (25 mg, 30%) as yellow oils. (**16**):  $R_f = .13$  (50% Ethyl acetate/Hexanes).  $[\alpha]^{20}_D = -98.2$  ( $c = 0.6$ , CH<sub>2</sub>Cl<sub>2</sub>). <sup>1</sup>H NMR (500 MHz, CDCl<sub>3</sub>): 10.07 (s, 1H), 7.99 (d,  $J = 7.5$  Hz, 2H), 7.53 (t,  $J = 7$  Hz, 1H), 7.44 (t,  $J = 7.5$  Hz, 2H), 5.09 (t,  $J = 6$  Hz, 1H), 4.63 (q,  $J = 7$  Hz, 1H), 2.48 (dd,  $J = 6.5, 13.5$  Hz, 1H), 2.37 (dd,  $J = 7, 13.5$  Hz, 1H), 2.09 (s, 3H), 1.32 (d,  $J = 7$  Hz, 3H) ppm. <sup>13</sup>C NMR (125 MHz, CDCl<sub>3</sub>): 190.4, 165.1, 161.7, 140.7, 132.2, 128.7, 128.6, 127.4, 85.5, 84.0, 72.5, 46.5, 15.3, 12.5 ppm. IR (neat): 3383 (bs), 2935 (w), 1674 (s), 1637 (s), 1287 (w), 1059 (m) cm<sup>-1</sup>. HRMS (ESI) (**17**):  $R_f = .20$  (50% Ethyl acetate/Hexanes).  $[\alpha]^{20}_D = -84.1$  ( $c = 0.7$ , CH<sub>2</sub>Cl<sub>2</sub>). <sup>1</sup>H NMR (500 MHz, CDCl<sub>3</sub>): 10.07 (s, 1H), 7.98 (d,  $J = 7.5$  Hz, 2H), 7.52 (t,  $J = 6.5$  Hz, 1H), 7.44 (t,  $J = 7.5$  Hz, 2H), 5.14 (d,  $J = 7.5$  Hz, 1H), 4.74 (d,  $J = 6.5$  Hz, 1H), 2.79 (q,  $J = 7.0$  Hz, 1H), 2.09 (s, 3H), 1.90 (d,  $J = 14.5$  Hz, 1H), 1.51 (d,  $J = 7.0$  Hz, 3H) ppm. <sup>13</sup>C NMR (125 MHz, CDCl<sub>3</sub>): 189.8, 165.5, 162.3, 141.3, 132.1, 128.7, 128.6, 127.5, 86.4, 86.1, 72.1, 45.8, 14.8, 12.4 ppm. IR (neat): 3368 (bs), 2933 (w), 1671 (s), 1638 (s), 1281 (w), 1095 (w), 1059 (w) cm<sup>-1</sup>.



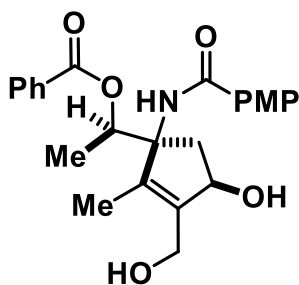


**(4R,5S,7R)-8-formyl-4,9-dimethyl-2-phenyl-3-oxa-1-azaspiro[4.4]nona-1,8-dien-7-yl benzoate:** A 100 mL flask was charged with a solution of bromo aldehyde **10** (83mg, .25 mmol, 1 equiv.) which contained ~40% of the aldehyde **9** in THF (5 mL). Sodium benzoate (710mg, 5.0 mmol, 20 equiv.), K<sub>2</sub>CO<sub>3</sub> (140mg, 0.9 mmol, 4 equiv.), and H<sub>2</sub>O (1 mL) were then added and the reaction was stirred for 12 h. The solvent was evaporated *in vacuo*. Purification of the product was accomplished using flash chromatography eluting with 5% ethyl acetate/hexanes. The fractions containing product were concentrated under reduced pressure to give benzoate ester **18** (54 mg, 58%) as a white solid.  $R_f = .60$  (50% Ethyl acetate/Hexanes). mp 47-50 °C.  $[\alpha]^{20}_D = -23.1$  ( $c = 1.3$ , CH<sub>2</sub>Cl<sub>2</sub>). <sup>1</sup>H NMR (500 MHz, CDCl<sub>3</sub>): 10.06 (s, 1H), 8.03 - 7.99 (m, 4H), 7.56 - 7.52 (m, 2H), 7.46 - 7.41 (m, 4H), 6.27 (t,  $J = 6.0$  Hz, 1H), 4.68 (q,  $J = 6.5$  Hz, 1H), 2.69 - 2.61 (m, 2H), 2.16 (d,  $J = 1.5$  Hz, 3H), 1.39 (d,  $J = 6.5$  Hz, 3H) ppm. <sup>13</sup>C NMR (125 MHz, CDCl<sub>3</sub>): 188.1, 166.5, 165.4, 161.9, 137.2, 133.3, 132.3, 130.3, 130.0, 128.8, 128.7, 128.6, 127.3, 95.0, 85.7, 84.7, 74.4, 45.3, 15.0, 13.0 ppm. IR (neat): 1715 (s), 1679 (s), 1636 (s), 1450 (w), 1272 (s), 1111 (s), 1096 (m) cm<sup>-1</sup>. HRMS (ESI) calculated for C<sub>23</sub>H<sub>22</sub>NO<sub>4</sub>  $m/z$  376.1549 (M+H), Obsd. 376.1563.



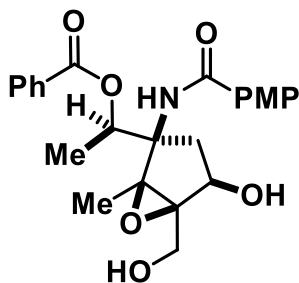
**(4R,5S,7R)-8-(hydroxymethyl)-4,9-dimethyl-2-phenyl-3-oxa-1-azaspiro[4.4]nona-**

**1,8-dien-7-ol:** A 50 mL flask was charged with **18** (29 mg, .07 mmol, 1 equiv.) and placed under N<sub>2</sub>. THF (5 mL) was then added and the solution cooled to 0 °C. LiAlH<sub>4</sub> (15 mg, .40 mmol, 5 equiv.) was then added in small portions and the reaction stirred for 1h. The reaction was quenched by Fieser's method and concentrated. The resultant material was purified by column chromatography eluting with a solution of 4% methanol in dichloromethane. The fractions containing product were concentrated to yield **19** (23 mg, 90%) as an off white solid. R<sub>f</sub> = 0.5 (10% MeOH/CH<sub>2</sub>Cl<sub>2</sub>). mp 123-126 °C. [ $\alpha$ ]<sub>D</sub><sup>20</sup> = -70.0 (c= .2, CH<sub>2</sub>Cl<sub>2</sub>). <sup>1</sup>H NMR (500 MHz, CDCl<sub>3</sub>): 7.96 (d, *J* = 8.0 Hz, 2H), 7.50 (t, *J* = 7.0 Hz, 1H), 7.42, (t, *J* = 7.5 Hz, 2H), 4.52 (q, *J* = 6.5 Hz, 1H), 4.45 (1/2ABq, *J* = 12.5 Hz, 1H), 4.32 (1/2ABq, *J* = 12.5 Hz, 1H), 3.36 (bs, 2H), 1.63 (s, 3H), 1.32 (d, *J* = 7.0 Hz, 3H) ppm. <sup>13</sup>C NMR (125 MHz, CDCl<sub>3</sub>): 164.0, 141.2, 138.1, 131.9, 128.7, 128.5, 127.7, 85.1, 83.8, 76.0, 58.6, 47.8, 14.7, 11.8 ppm. IR (neat): 3224 (bs), 2935 (w), 1632 (s), 1450 (w), 1321 (w), 1295 (w) 1280 (w), 1057 (s), 1014 (m) cm<sup>-1</sup>.

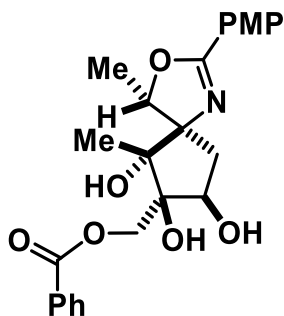


**PMBz Protected Amine:** A 50 mL flask was charged with diol **19** (40 mg, .15 mmol, 1 equiv.) and THF (6 mL). 2N HCl (6 mL) was then added and the reaction was stirred for 3 d. The reaction mixture was quenched with sat. NaHCO<sub>3</sub> (20 mL) and extracted with ethyl acetate (3 x 25 mL). The organics were combined and dried with Na<sub>2</sub>SO<sub>4</sub> and concentrated under reduced pressure to yield the free amine. A 25 mL round bottomed flask was charged

with a solution of the crude amine from above (30 mg, 0.10 mmol, 1 equiv.) in  $\text{CH}_2\text{Cl}_2$  (5 mL). Para-methoxybenzoyl chloride (26 mg, 0.15 mmol, 1.5 equiv.) was then added and the reaction stirred for 3 h. The reaction was diluted with  $\text{CH}_2\text{Cl}_2$  (25 mL) transferred to a separatory funnel and washed with 1N NaOH (25 mL). The aqueous layer was extracted again with  $\text{CH}_2\text{Cl}_2$  (2 x 10 mL). The organics were combined, dried with  $\text{Na}_2\text{SO}_4$ , and concentrated under reduced pressure. Purification of the product was accomplished using flash chromatography eluting with 50% ethyl acetate/hexanes followed by 100% ethyl acetate. The fractions containing product were concentrated under reduced pressure to give PMBz protected amine **20** (30 mg, 48% from diol **19**) as a white solid.  $R_f = 0.07$  (5% MeOH/ $\text{CH}_2\text{Cl}_2$ ). mp 173 - 175 °C.  $[\alpha]_D^{20} = -40.0$  ( $c = 0.5$ ,  $\text{CH}_2\text{Cl}_2$ ).  $^1\text{H}$  NMR (500 MHz,  $\text{CDCl}_3$ ): 8.03 - 8.02 (m, 2H), 7.65 - 7.61 (m, 3H), 7.49 (t,  $J = 7.5$  Hz, 2H), 7.00 (s, 1H), 6.87 (d,  $J = 9.0$  Hz, 2H), 5.44 (q,  $J = 6.5$  Hz, 1H), 4.82 (d,  $J = 7.0$  Hz, 1H), 4.54 (1/2 ABq,  $J = 13.0$  Hz, 1H), 4.35 (1/2 ABq,  $J = 13.0$  Hz, 1H), 3.82 (s, 3H), 2.62 (dd,  $J = 8.0, 15.0$  Hz, 1H), 2.34 (d,  $J = 15.5$  Hz, 1H), 1.74 (s, 3H), 1.33 (d,  $J = 6.5$  Hz, 3H) ppm.  $^{13}\text{C}$  NMR (125 MHz,  $\text{CDCl}_3$ ): 167.1, 166.8, 162.8, 143.1, 134.7, 134.1, 129.9, 129.6, 129.0, 128.9, 126.7, 114.2, 76.0, 74.8, 71.8, 59.1, 55.7, 45.6, 15.2, 11.3 ppm. IR (neat): 3306 (bs), 1716 (s), 1647 (m), 1606 (s), 1257 (s), 1176 (w) 1069 (w)  $\text{cm}^{-1}$ . HRMS (ESI) calculated for  $\text{C}_{24}\text{H}_{27}\text{NO}_6\text{Na}$   $m/z$  448.1736 (M+Na), Obsd. 448.1745.

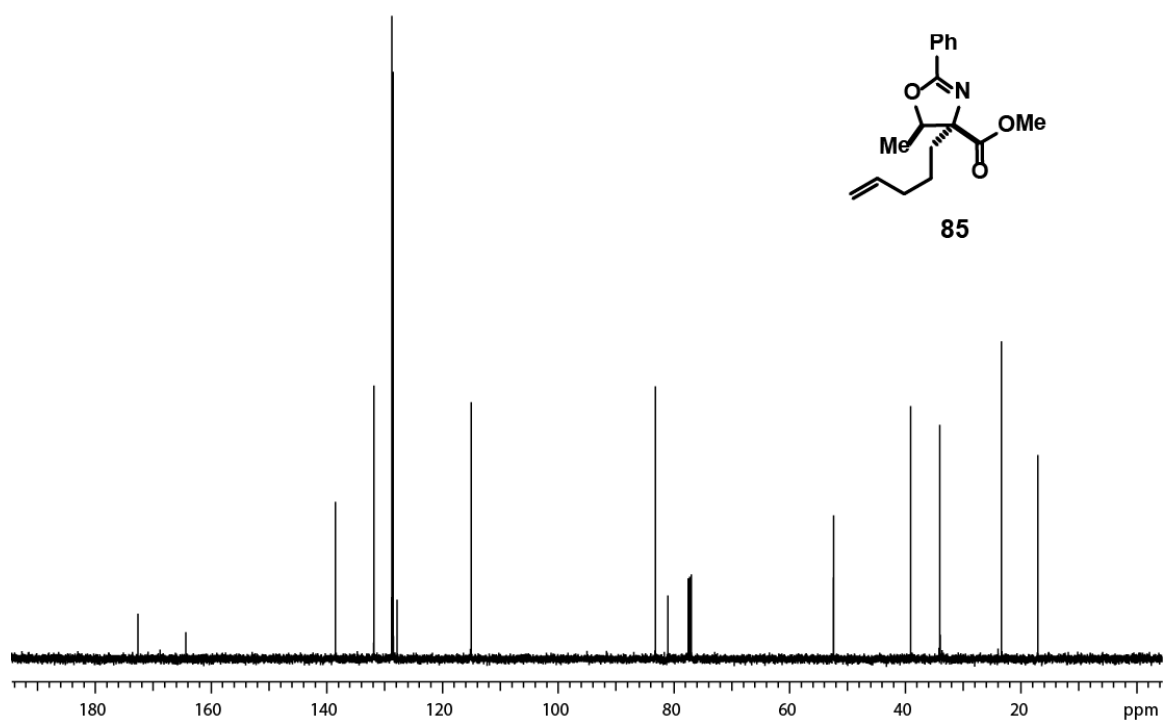
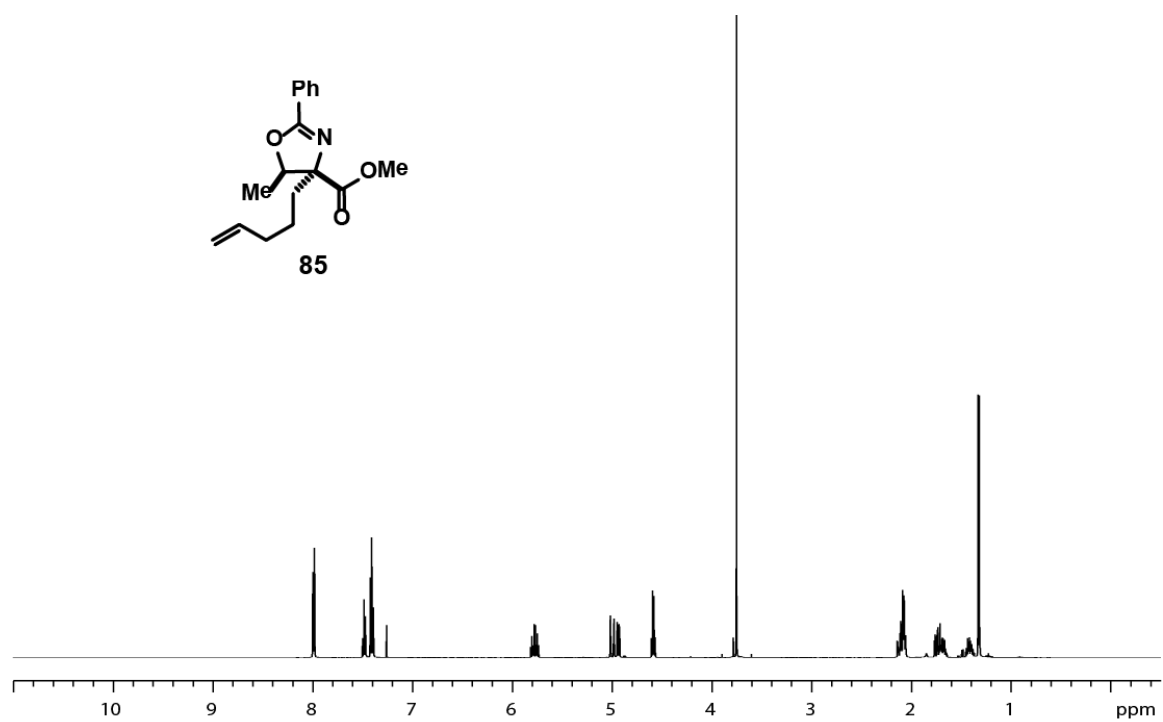


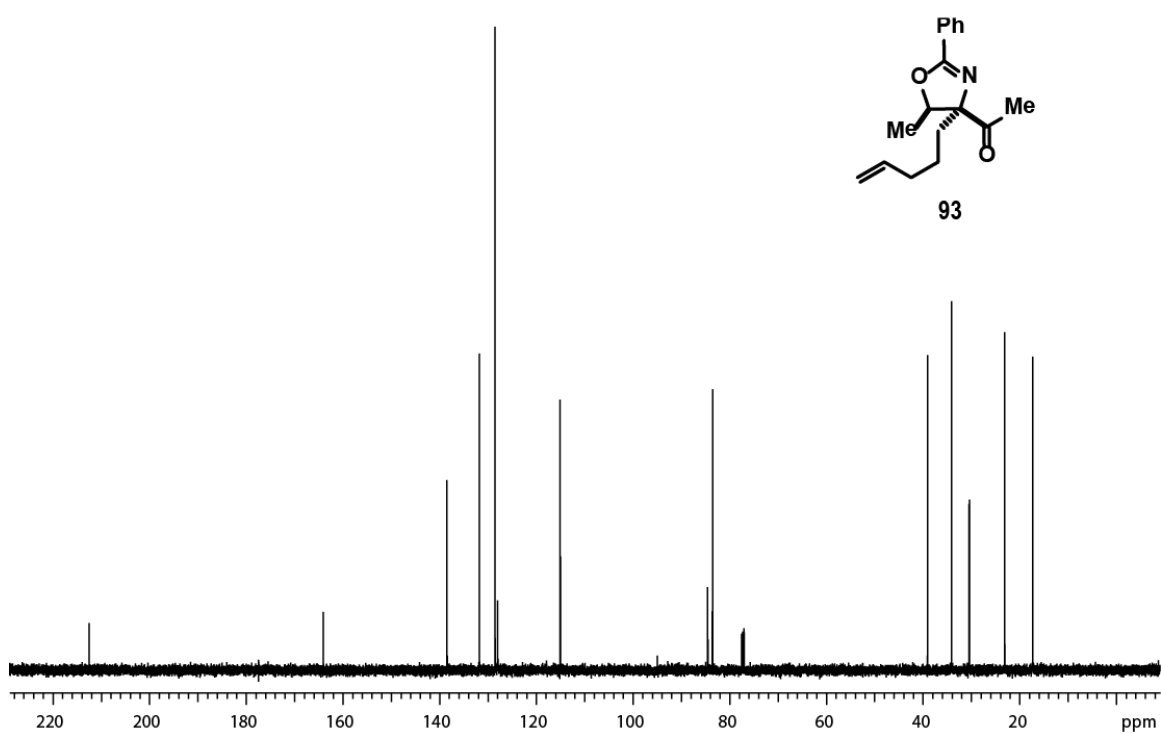
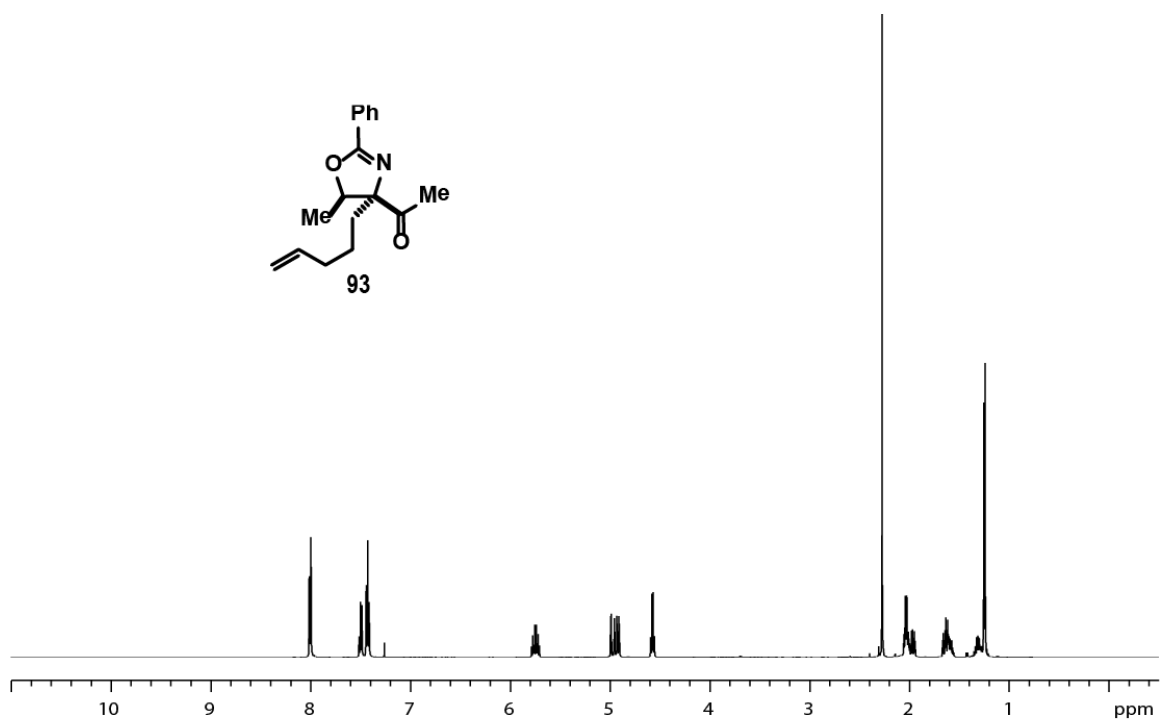
**Epoxide:** A 25 mL round bottomed flask was charged with the PMBz protected amine **20** (20 mg, 50  $\mu$ mol, 1 equiv.) and CH<sub>2</sub>Cl<sub>2</sub> (2 mL). *m*-CPBA (21 mg, 90  $\mu$ mol, 2 equiv.) was then added in a single portion along with sat. NaHCO<sub>3</sub> (2 mL). The reaction was stirred for 3 h and then diluted with CH<sub>2</sub>Cl<sub>2</sub> (25 mL), transferred to a separatory funnel and washed with H<sub>2</sub>O (1 x 25 mL). The organics were dried with Na<sub>2</sub>SO<sub>4</sub> and concentrated under reduced pressure. Purification of the product was accomplished using flash chromatography eluting with 50% ethyl acetate/hexanes followed by 100% ethyl acetate. The fractions containing product were concentrated under reduced pressure to give the epoxide **21** (15 mg, 75%) as a clear oil.  $R_f$  = 0.44 (2% MeOH/CH<sub>2</sub>Cl<sub>2</sub>).  $[\alpha]^{20}_D = -0.18$  ( $c=0.5$ , CH<sub>2</sub>Cl<sub>2</sub>). <sup>1</sup>H NMR (500 MHz, CD<sub>3</sub>OD): 8.02 (d,  $J$  = 6.5 Hz, d), 7.90 (bd,  $J$  = 29.0 Hz, 1H), 7.70 - 7.67 (m, 2H), 7.62 - 7.58 (m, 1H), 7.49 - 7.46 (m, 3H), 6.94 - 6.90 (m, 2H), 6.42 (q,  $J$  = 6.5 Hz, 1H), 4.63 (t,  $J$  = 8.0 Hz, 1H), 3.99 (1/2 ABq,  $J$  = 12.0 Hz, 1H), 3.82 (s, 3H), 3.45 (1/2 ABq,  $J$  = 12 Hz, 1H), 2.76 (dd,  $J$  = 8.0, 13.5 Hz, 1H) 1.71 (dd,  $J$  = 7.5, 14.0 Hz, 1H), 1.69 (s, 3H), 1.38 (d,  $J$  = 6.5 Hz, 3H) ppm. <sup>13</sup>C NMR (125 MHz, CD<sub>3</sub>OD): 170.9, 167.1, 163.9, 134.3, 133.0, 131.6, 130.7, 130.4, 129.6, 128.6, 114.6, 73.2, 71.8, 70.6, 68.5, 58.4, 55.9, 39.7, 22.1, 15.8, 13.6 ppm. IR (neat): 3369 (bs), 1716 (s), 1606 (s), 1503 (s), 1257 (s), 1177 (w), 1069 (w) cm<sup>-1</sup>. HRMS (ESI) calculated for C<sub>24</sub>H<sub>27</sub>NO<sub>7</sub>Na  $m/z$  464.1685 (M+Na), Obsd. 464.1697.

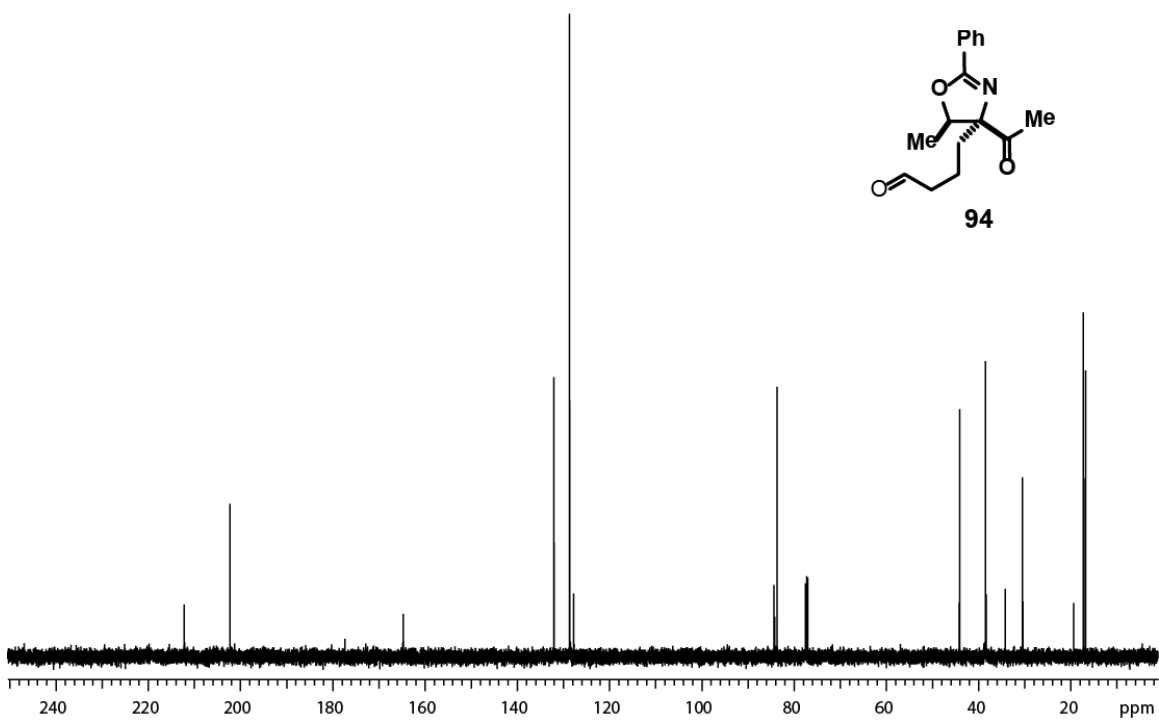
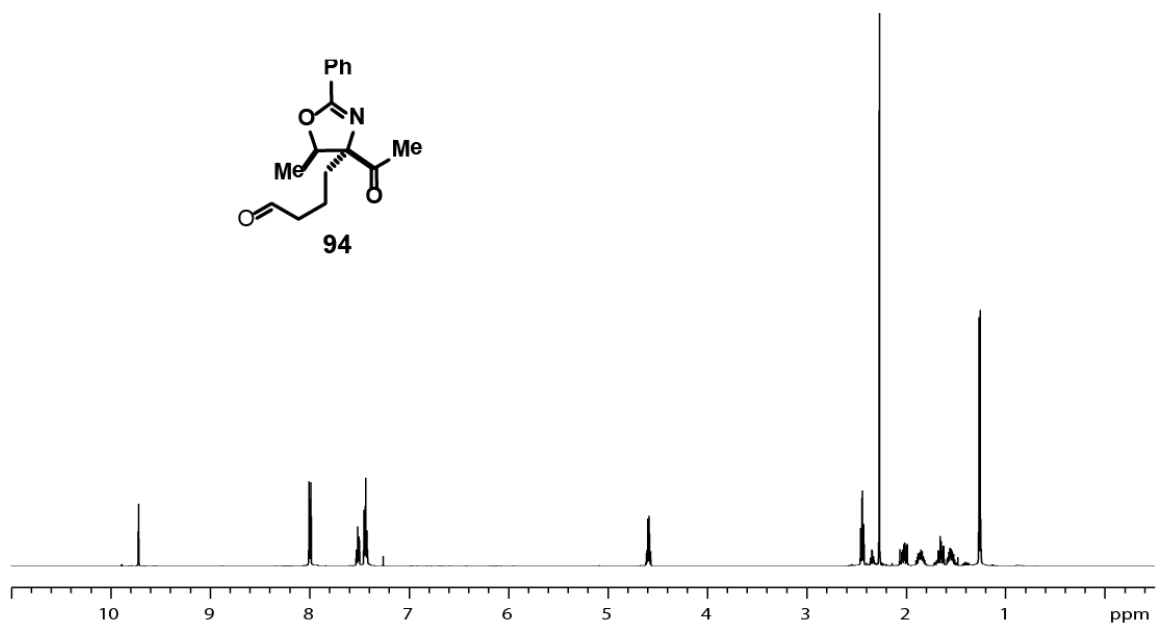


**Triol:** A 50 mL flask was charged with the epoxide **21** (15 mg, 0.03 mmol, 1 equiv.) and CH<sub>2</sub>Cl<sub>2</sub>. The flask was cooled to 0 °C and BF<sub>3</sub>•OEt<sub>2</sub> (12 mg, 0.09 mmol, 3 equiv.) was added. After stirring for 1 h, benzoic acid (37 mg, 0.30 mmol, 10 equiv.) was added and the reaction was left to stir for an additional 3 h. The mixture was transferred to a separatory funnel and washed with 10% NaOH (3 x 20 mL). The organic layer was dried over Na<sub>2</sub>SO<sub>4</sub> and concentrated *in vacuo*. Purification of the product was accomplished using flash chromatography eluting with 2% MeOH/CH<sub>2</sub>Cl<sub>2</sub>. The fractions containing product were concentrated under reduced pressure to give triol **22** (12 mg, 90%) as a clear oil. R<sub>f</sub> = .47 (4% MeOH/CH<sub>2</sub>Cl<sub>2</sub>). [ $\alpha$ ]<sup>20</sup><sub>D</sub> = + 10.0 (c0.3, MeOH). <sup>1</sup>H NMR (500 MHz, CD<sub>3</sub>OD): 8.09 - 8.07 (m, 2H), 7.85 - 7.83 (m, 2H), 7.61 - 7.57 (m, 1H), 7.49 - 7.45 (m, 2H), 6.99 - 6.97 (m, 2H), 4.91 (q, *J* = 6.5 Hz, 1H), 4.59 (1/2 ABq, *J* = 7.5 Hz, 1H), 4.50 (1/2 ABq, *J* = 11.5 Hz, 1H), 4.31 (dd, *J* = 4, 10 Hz, 1H), 3.84 (s, 3H), 2.72 (dd, *J* = 9.5, 14 Hz, 1H), 1.64 (dd, *J* = 4.5, 15 Hz, 1H), 1.37 (d, *J* = 6.5 Hz, 3H) ppm. <sup>13</sup>C NMR (CD<sub>3</sub>OD, 125 MHz): 168.3, 164.1, 162.7, 134.2, 131.6, 131.0, 130.7, 129.5, 120.7, 114.9, 84.4, 84.4, 83.9, 79.9, 74.3, 66.8, 55.9, 40.8, 18.6, 16.9 ppm. IR (neat): 3361 (bs), 2926 (w), 1718 (w), 1645 (s), 1275 (s), 1100 (s), 1028 (w) cm<sup>-1</sup>. HRMS (ESI) calculated for C<sub>24</sub>H<sub>27</sub>NO<sub>7</sub>Na *m/z* 464.1685 (M+Na), Obsd. 464.1695.

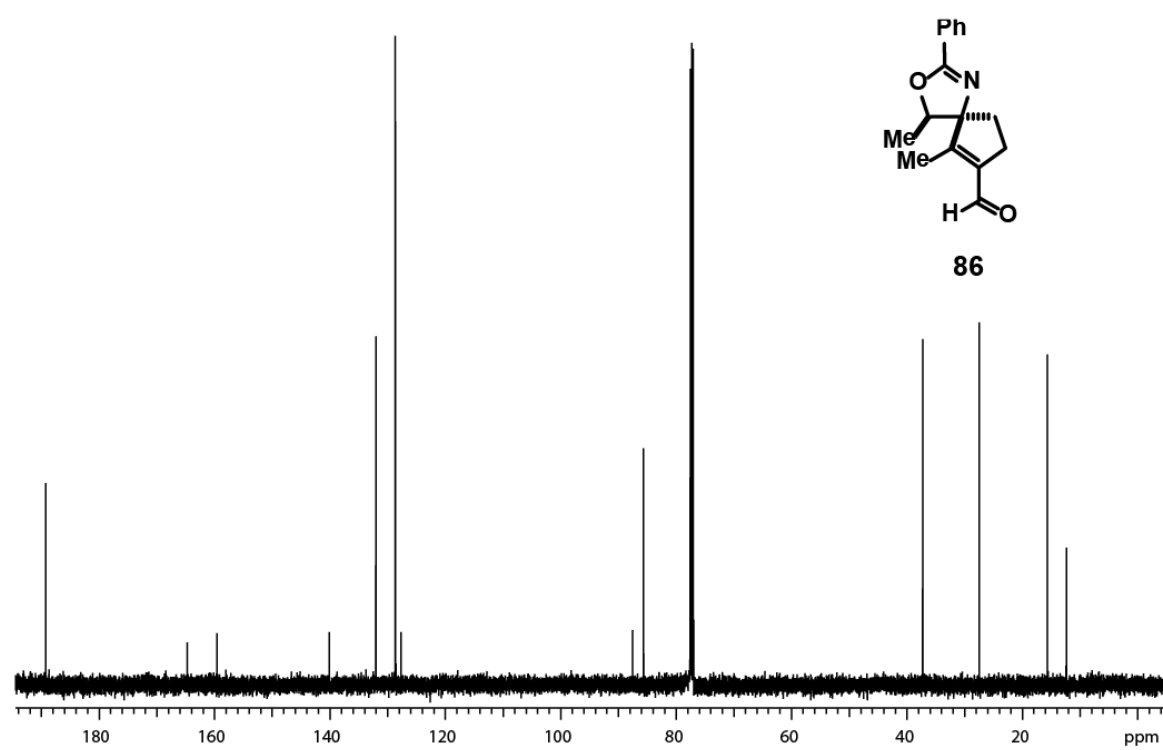
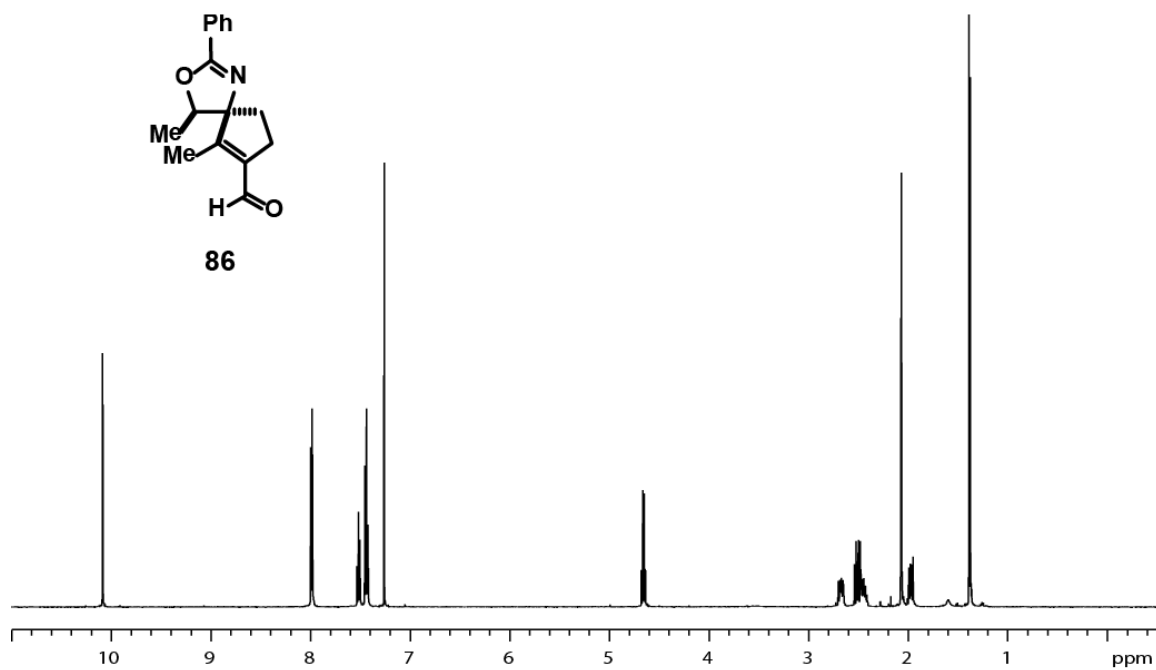
1.10.3 Representative  $^1\text{H}$  NMR and  $^{13}\text{C}$  NMR

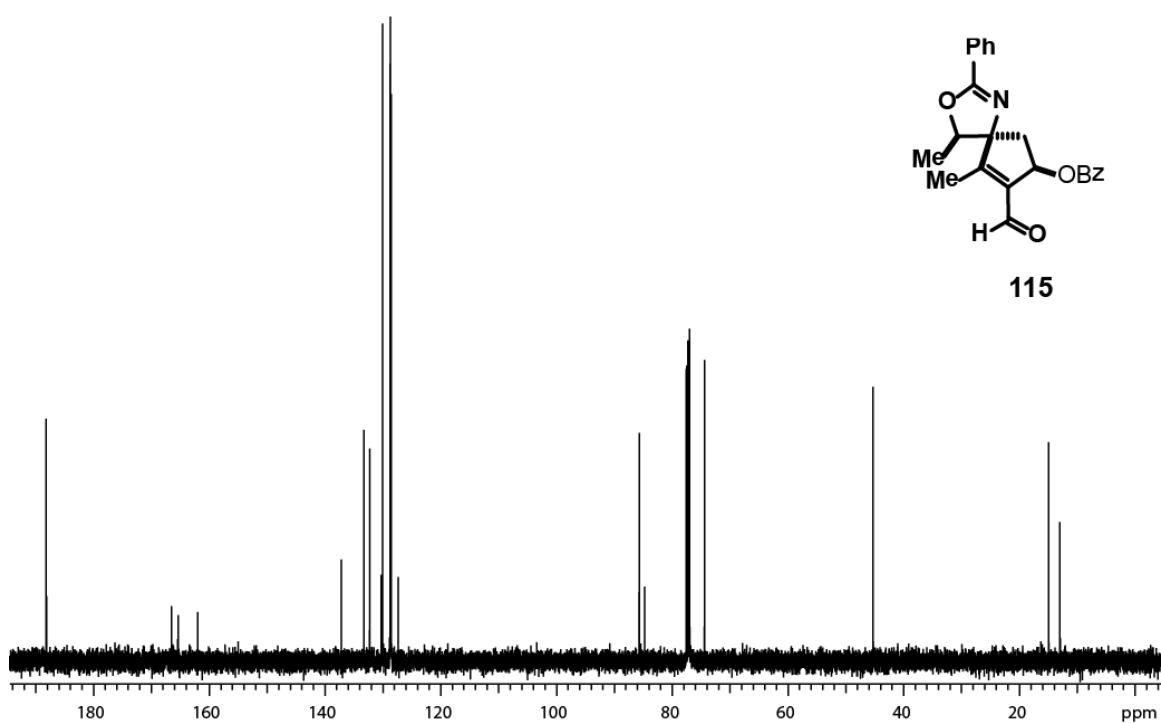
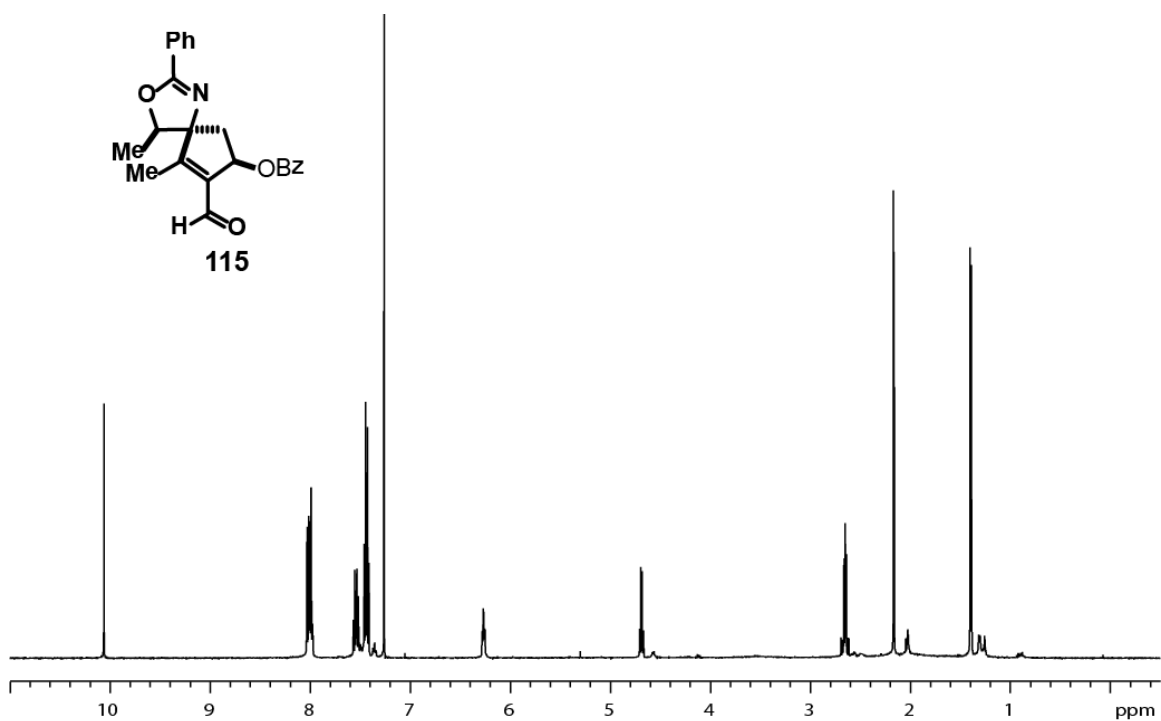


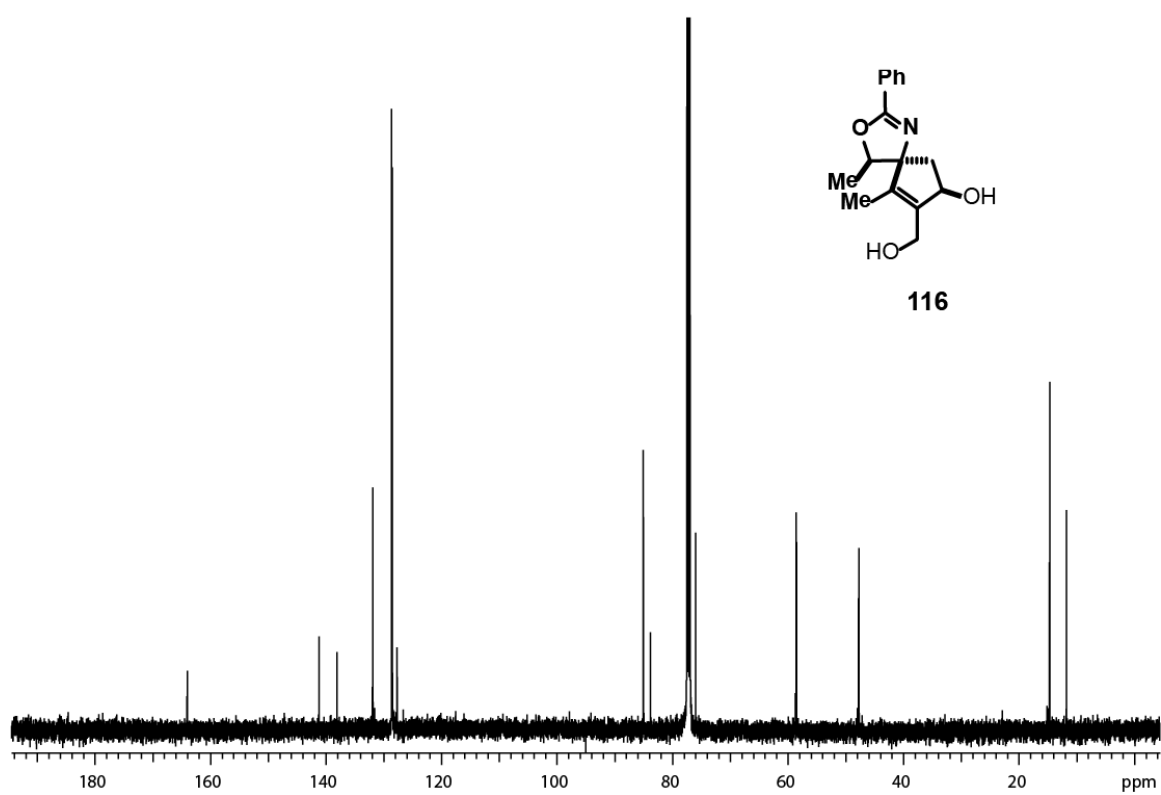
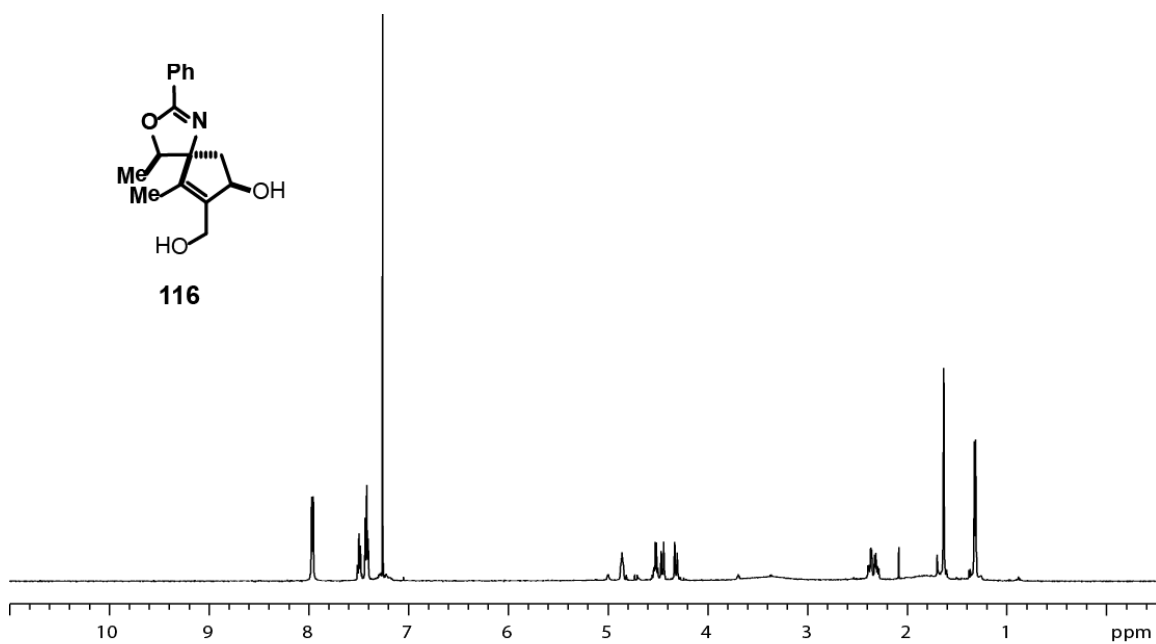


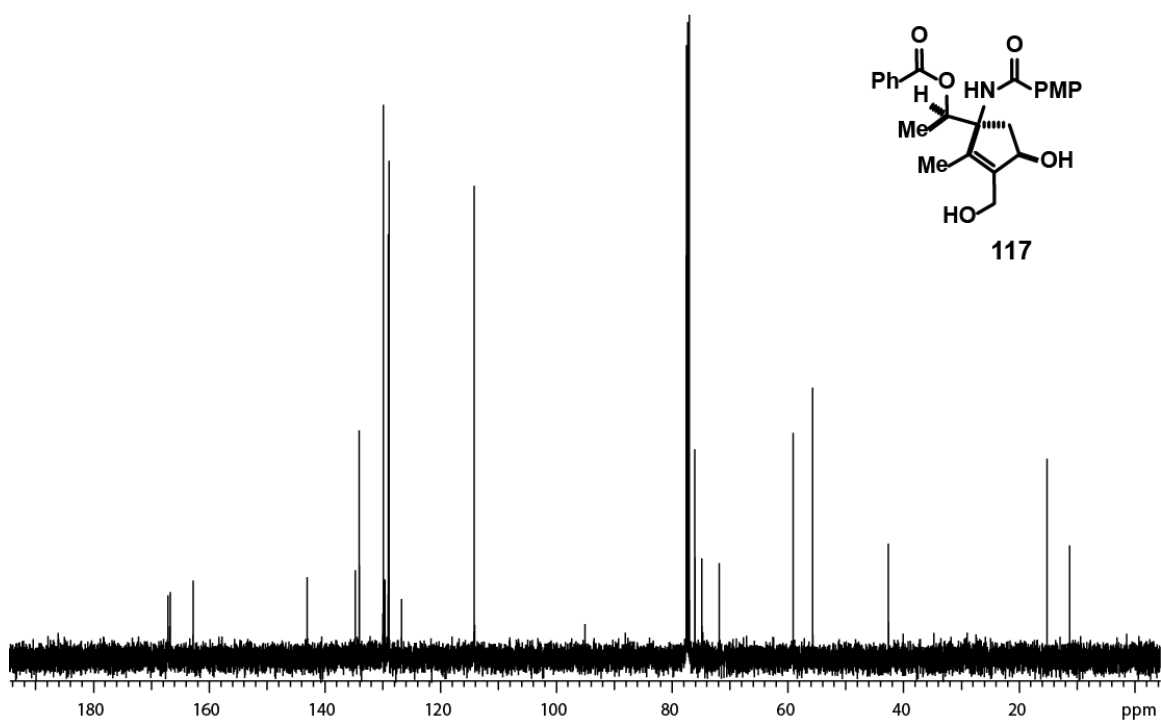
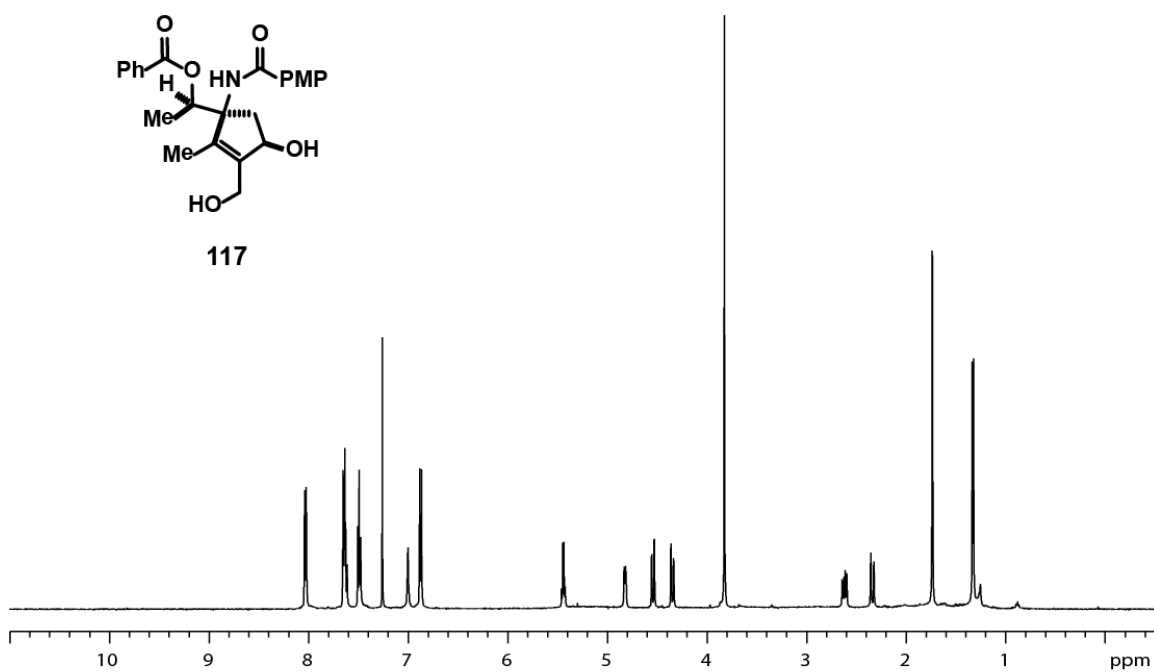


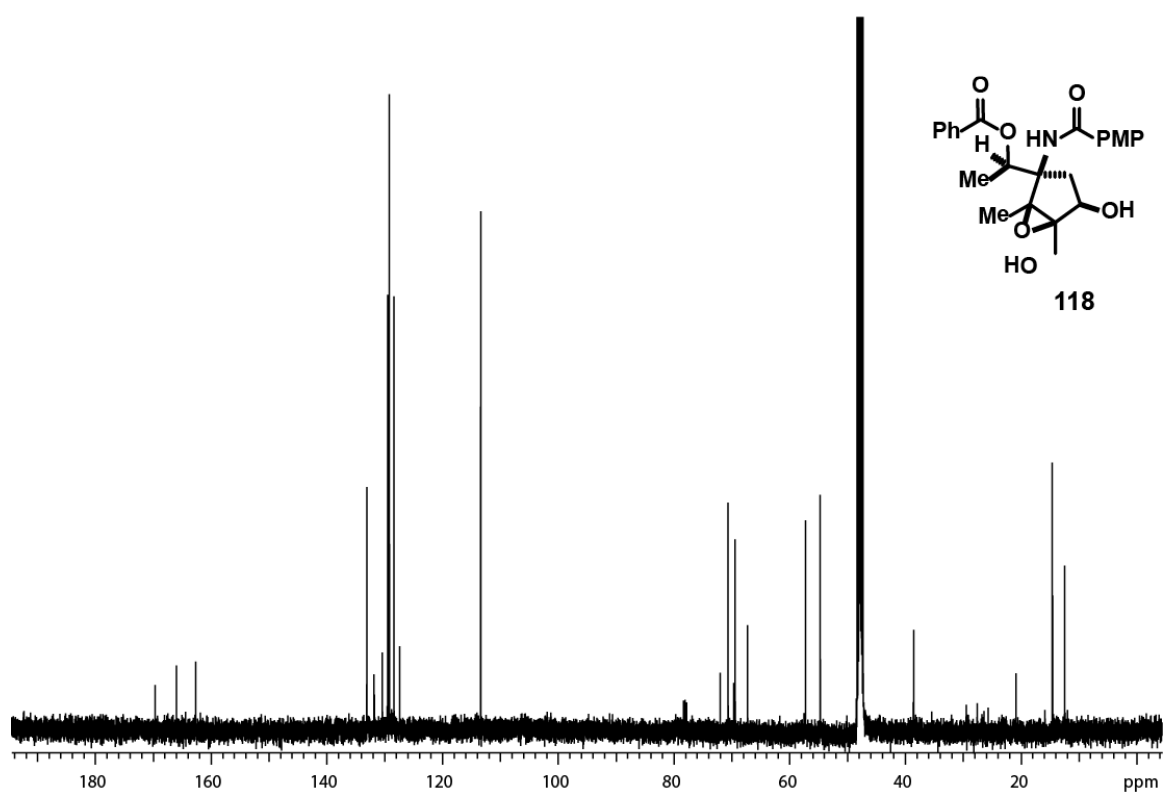
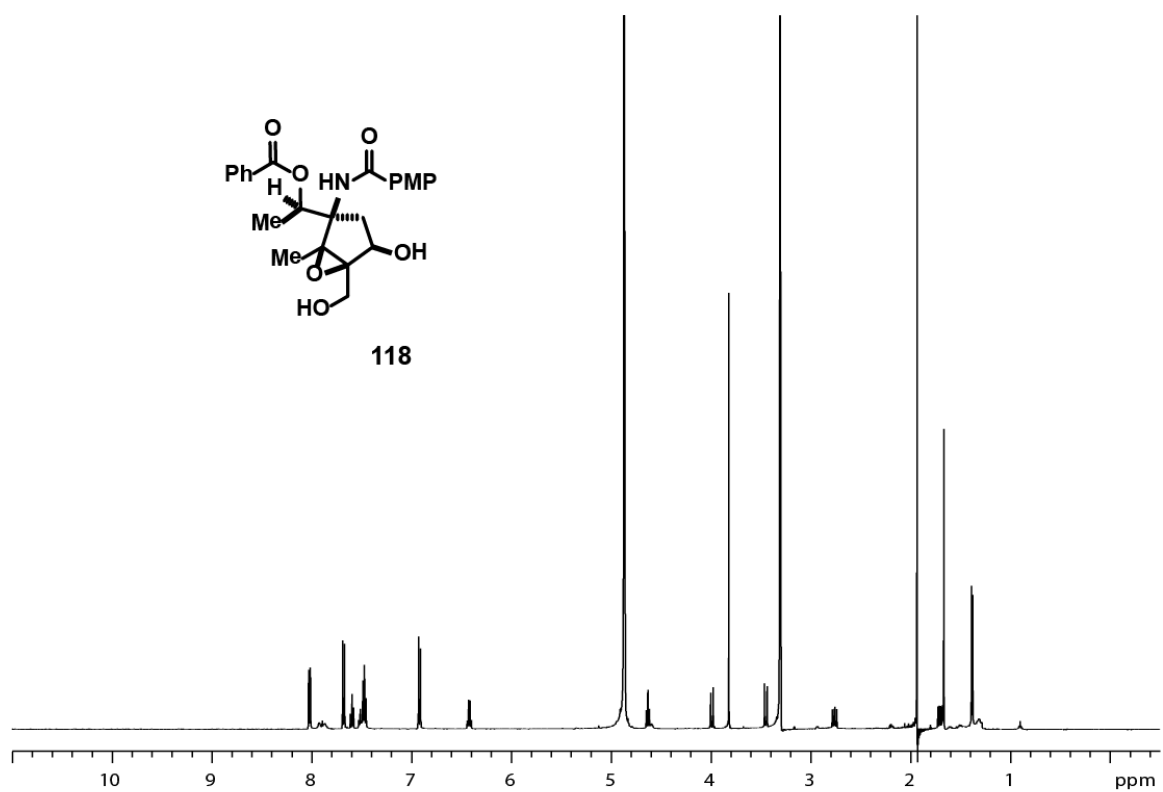


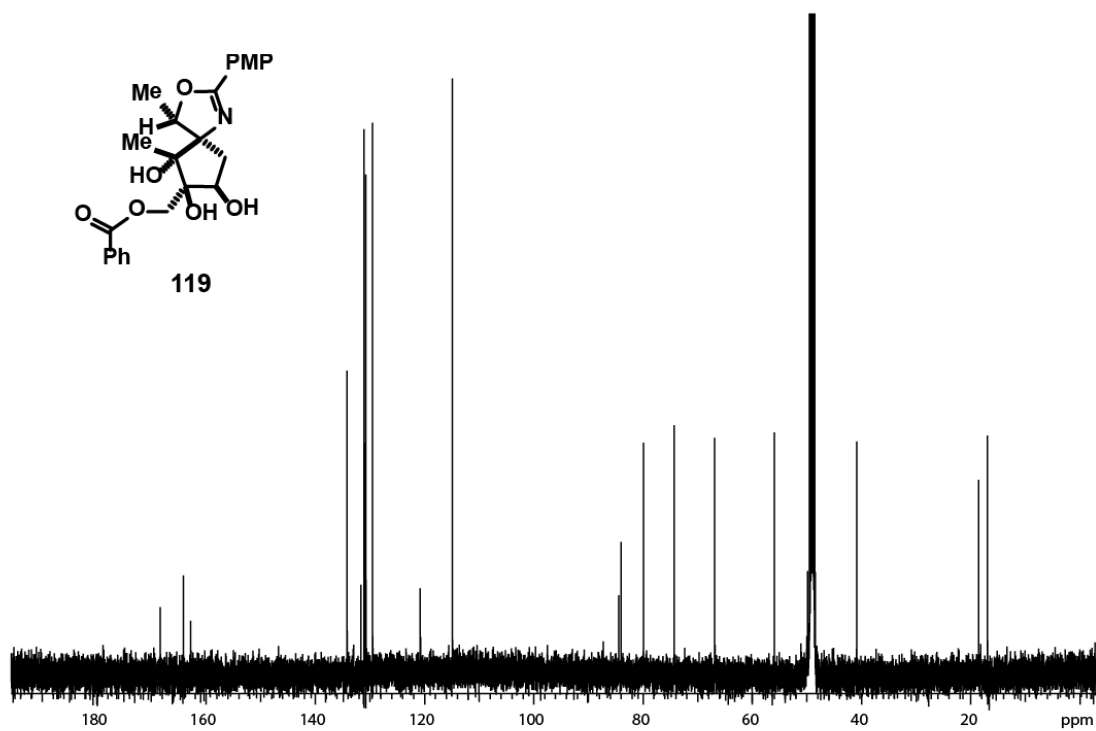
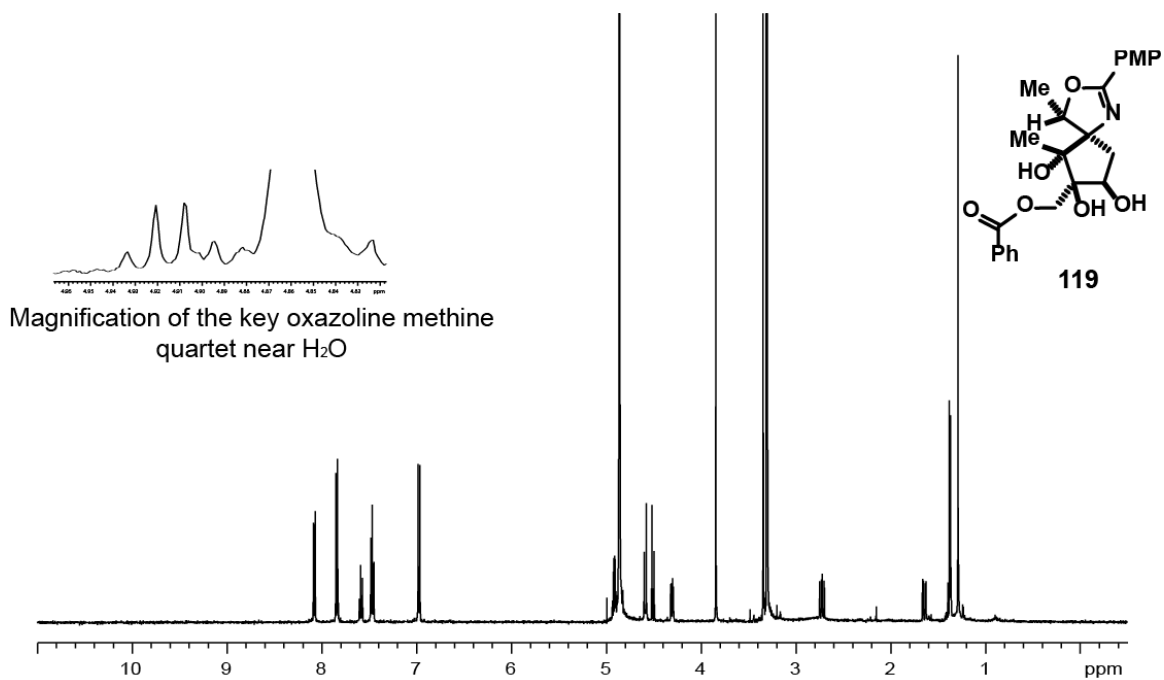












### 1.11 References

1. Argoudelis, A. D.; Jahnke, H. K.; Fox, J. A. Pactamycin, a New Antitumor Antibiotic. II. Isolation and Characterization. *Antimicrob. Agents Chemother.* **1962**, 191-197.
2. Duchamp, D. J. In *Abstracts*, American Crystallographic Association Winter Meeting, Albuquerque, NM, April 3-7, 1972; American Crystallographic Association: Buffalo, NY, 1972; 23.
3. Otogourol, K.; Iwatsuki, M.; Ishiyama, A.; Namatame, M.; Nishihara-Tukashima, A.; Shibahara, S.; Kondo, S.; Yamada, H.; Omura, S. Promising Lead Compounds for Novel Antiprotozoals. *J. Antibiot.* **2010**, *63*, 381-384.
4. Lu, W.; Roongsawang, N.; Mahmud, T. Biosynthetic Studies and Genetic Engineering of Pactamycin Analogs with Improved Selectivity Toward Malarial Parasites. *Chem. Biol.* **2011**, *18*, 425-431.
5. Carter, A. P.; Clemons, W. M., Jr.; Brodersen, D. E.; Morgan-Warren, R. J.; Wimberly, B. T.; Ramakrishnan, V. Functional Insights from the Structure of the 30S Ribosomal Subunit and its Interactions with Antibiotics. *Nature* **2000**, *407*, 340-348.
6. Mankin, A. S. J. Pactamycin Resistance Mutations in Functional Sites of 16 S rRNA. *Mol. Biol.* **1997**, *274*, 8-15.
7. Brodersen, D. E.; Clemons, W. M., Jr.; Carter, A. P.; Morgan-Warren, R. J.; Wimberly, B. T.; Ramakrishnan, V. The Structural Basis for the Action of the Antibiotics Tetracycline, Pactamycin, and Hygromycin B on the 30S Ribosomal Subunit. *Cell* **2000**, *103*, 1143-1154.
8. Dobashi, K.; Isshiki, K.; Sawa, T.; Obata, T.; Hamada, M.; Naganawa, H.; Takita, T.; Takeuchi, T.; Umezawa, H.; Bei, H. S. 8''-Hydroxypactamycin and 7-deoxypactamycin, New Members of the Pactamycin Group. *J. Antibiot.* **1986**, *39*, 1779-1783.
9. Iwatsuki, M.; Nishihara-Tsukashima, A.; Ishiyama, A.; Namatame, M.; Watanabe, Y.; Handasah, S.; Pranamuda, H.; Marwoto, B.; Matsumoto, A.; Takahashi, Y.; Otoguro, K.; Omura, S. Jogyamycin, a New Antiprotozoal Aminocyclopentitol Antibiotic, Produced by *Streptomyces* sp. a-WM-JG- 16.2. *J. Antibiot.* **2012**, *65*, 169-171.
10. Tsujimoto, T.; Nishikawa, T.; Urabe, T.; Isobe, M. Synthesis of Functionalized Cyclopentane for Pactamycin, a Potent Antitumor Antibiotic. *Synlett.* **2005**, *3*, 433-436.
11. Knapp, S.; Younong, Y. Synthesis of the Oxygenated Pactamycin Core. *Org. Lett.* **2007**, *9*, 1359-1362.
12. Hanessian, S.; Vakiti, R. R.; Dorich, S.; Banerjee, S.; Lecomte, F.; DelValle, J. R.; Zhang, J.; Deschênes-Simard, B. Total Synthesis of Pactamycin. *Angew. Chem. Int. Ed.*

**2011**, *50*, 3497-3500.

13. Haussener, T. J.; Looper, R. E. Access to the Pactamycin Core via an Epoxide Opening Cascade. *Org. Lett.* **2012**, *14*, 3632-3635.

14. Malinowski, J. T.; McCarver, S. J.; Johnson, J. S. Diastereocontrolled Construction of Pactamycin's Complex Ureido Triol Functional Array. *Org. Lett.* **2012**, *14*, 2878-2881.

15. Malinowski, J. T.; Sharpe, R. J.; Johnson, J. S. Enantioselective Synthesis of Pactamycin, a Complex Antitumor Antibiotic. *Science* **2013**, *340*, 180-182.

16. For a comprehensive Pauson-Khand review see: Pauson, P. L. The Khand Reaction: A Convenient and General Route to a Wide Range of Cyclopentenone Derivatives. *Tetrahedron* **1985**, *41*, 5855-5860.

17. Aït-Haddou, H.; Hoarau, O.; Cramailère, D.; Pezet, F.; Daren, J.; Balavoine, G. G. A. New Dihydroxy Bis(Oxazoline) Ligands for the Palladium-Catalyzed Asymmetric Allylic Alkylation: Experimental Investigations of the Origin of the Reversal of the Enantioselectivity. *Chem.; Eur. J.* **2004**, *10*, 699-707.

18. For the synthesis of 5-iodo-pentene from 5-bromo-pentene, see: Shi, B.; Hawryluk, N. A.; Snider, B. B. Formal Synthesis of (±)-Guanacastepene A. *J. Org. Chem.* **2003**, *68*, 1030-1042.

19. Reddy, L. R.; Fournier, J.; Subba Reddy, B. V.; Corey, E. J. An Efficient, Stereocontrolled Synthesis of a Potent Omuralide–Salinosporin Hybrid for Selective Proteasome Inhibition. *J. Am. Chem. Soc.* **2005**, *127*, 8974-8976.

20. Nahm, S.; Weinreb, S. M. N-methoxy-N-methylamides as Effective Acylating Agents. *Tetrahedron Lett.* **1981**, *22*, 3815-3818.

21. For a review see: Sibi, M. P. Chemistry of N-methoxy-N-methylamides Application in Synthesis. A Review. *Org. Prep. Proc. Intl.* **1993**, *25*, 15-40.

22. Williams, J. M.; Jobson, R. B.; Nobuyoshi, Y.; Marchesini, G.; Dolling, U.; Grabowski, E. J. A New General Method for Preparation of N-methoxy-N-methylamides. Application in Direct Conversion of an Ester to a Ketone. *Tetrahedron. Lett.* **1995**, *36*, 5461-5464.

23. For select reviews see: (a) Li, Z.; He, C. Recent Advances in Silver-Catalyzed Nitrene, Carbene, and Silylene-Transfer Reactions. *Eur. J. Org. Chem.* **2006**, 4313-4322. (b) Davies, H. M. L.; Manning, J. R. Catalytic C-H Functionalization by Metal Carbenoid and Nitrenoid Insertion. *Nature*, **2008**, *451*, 417-424.

24. Espino, C. G.; Fiori, K. W.; Kim, M.; Du Bois, J. Expanding the Scope of C–H Amination through Catalyst Design. *J. Am. Chem. Soc.* **2004**, *126*, 15378-15379.



25. Cui, Y.; He, C. A Silver-Catalyzed Intramolecular Amidation of Saturated C-H Bonds. *Angew. Chem. Int. Ed.* **2004**, *43*, 4210-4212.
26. Hattori, K.; Kido, Y.; Yamamoto, H.; Ishida, J.; Iwashita, A.; Mihara, K. Rational Design of Conformationally Restricted Quinazolinone Inhibitors of Poly(ADP-ribose)polymerase. *Bioorg. Med. Chem. Lett.* **2007**, *17*, 5577-5581.
27. For selected epoxide cascade reactions, see: (a) Vilotijevic, I.; Jamison, T. F. Epoxide-Opening Cascades in the Synthesis of Polycyclic Polyether Natural Products. *Angew. Chem., Int. Ed.* **2009**, *48*, 5250-5281. (b) Feng, X.; Shu, L.; Shi, Y. Complete Conversion of Racemic Enol Ester Epoxides into Optically Active  $\alpha$ -Acyloxy Ketones. *J. Am. Chem. Soc.* **1999**, *121*, 11002-11003. (c) Molander, G. A.; Pozo Losada, C. D. Sequenced Reactions with Samarium(II) Iodide. Domino Epoxide Ring-Opening/Ketyl Olefin Coupling Reactions. *J. Org. Chem.* **1997**, *62*, 2935-2943. (d) Minami, A.; Migita, A.; Inada, D.; Hotta, K.; Watanabe, K.; Oguri, H.; Oikawa, H. Enzymatic Epoxide-Opening Cascades Catalyzed by a Pair of Epoxide Hydrolases in the Ionophore Polyether Biosynthesis. *Org. Lett.* **2011**, *13*, 1638.
28. Amarego, W. L. F.; Chai, C. L. L. *Purification of Laboratory Chemicals*. 6th ed.; Elsevier Inc.: Burlington, MA, 2009.

## **CHAPTER 2**

### **INITIAL STUDIES TOWARD GENERATING ANTIBIOFILM ANTIBIOTICS**

#### **2.1 Background**

In 1928 Alexander Fleming contaminated a *Staphylococcus* bacteria colony growing in a petri dish. This contamination resulted in the serendipitous discovery of the first observed bacterial zones of inhibition, thus sparking the advent of antibiotics.<sup>1</sup> Antibiotics have been one of the most significant advances in medicine in the 20<sup>th</sup> century and their rich history continues to date. The introduction of these antibiotics, however, placed pressure on bacteria to develop resistance to them. With antibiotic use rising and drug development slowing, bacterial infections because of resistance has become increasingly difficult to treat over the past 20 years.<sup>2</sup>

The United States Centers for Disease Control and Prevention (CDC) estimates that every year approximately 2 million people in the United States contract a severe infection from drug-resistant bacteria, and that over 23,000 deaths are a direct result of these antibiotic-resistant infections.<sup>2</sup>

Numerous reports that outline the current threats of antibiotic resistance have been published by the CDC and other health agencies. This list includes, a number of species in the categories of urgent and serious threats (Table 2.1), due to their; “clinical impact, incidence, 10-year projection of incidence, economic impact, transmissibility, availability

of effective antibiotics, barriers to prevention.” Although the “golden age” of antibiotic discovery has passed, clinicians are in dire need of new antibiotic platforms to treat ever evolving bacterial species.<sup>2</sup>

## **2.2 Common Current Antibiotic Structures and Functions**

Many of the above bacterial species have a limited window of treatment. The antibiotics prescribed to treat these infections are still effective, albeit to a narrow degree. Several key antibiotic scaffolds are outlined below as both historical and clinical examples.

### *2.2.1 $\beta$ -lactam Antibiotics*

The  $\beta$ -lactam antibiotics represent one of the largest known classes of antibiotics. Originally this class was occupied by the penicillins. Over time however, research led to development of the cephalosporin  $\beta$ -lactams followed by countless others including monocyclic  $\beta$ -lactams, carbapenems, carbacephems, oxapenams, and oxacephems (Figure 2.1).<sup>3,4</sup> Their namesake  $\beta$ -lactam functional group is linked to a variety of side chain functionalities in their molecular structure.

Their mode of action relies on the inhibition of DD-transpeptidases, a series of penicillin-binding proteins (PBPs). This irreversible inhibition of PBP's leads to the prevention of cross-linking newly formed peptidoglycans (polymeric mixture that forms the bacteria cell wall) thereby arresting the bacterial cell wall synthesis resulting in cell death.<sup>4</sup>

Unfortunately, given the selective pressure present over the last 75 years bacteria have evolved a number of ways to evade this mechanism of action. First and foremost, a significant number of resistant bacteria species now possess  $\beta$ -lactamase enzymes capable

of cleaving the  $\beta$ -lactam ring before it forms the covalent bond to PBP, rendering it ineffective. One method of combating this problem is the introduction of  $\beta$ -lactamase inhibitors like clavulanic acid, in conjunction with other  $\beta$ -lactam antibiotics. The inhibition of  $\beta$ -lactamase effectively allows standard of care  $\beta$ -lactams to function appropriately. However, this resensitization is still a challenging problem and even with the introduction of a suicide inhibitor like clavulanic acid; bacteria have evolved to up-regulate the amount of  $\beta$ -lactamase enzymes present, thereby overwhelming the clavulanic acid inside the cell and rendering any antibiotics ineffective.<sup>4</sup>

Significant alteration in the primary structure of PBPs has also led to resistant strains of bacteria. The most comprehensive example of this phenomena is the *mecA*(gene) present in Methicillin-resistant *Staphylococcus aureus* (MRSA). The *mecA* gene prevents the  $\beta$ -lactam structure of penicillin and penicillin-like antibiotics from binding to the PBPs. The prevention of these interactions allows resistant strains to freely proliferate in the presence of a number of  $\beta$ -lactam antibiotics.<sup>4</sup>

### 2.2.2 Quinolones and Fluoroquinolones

The quinolones and fluoroquinolones are another important class of administered antibiotics. They consist of a quinolone framework structurally decorated by various substitution patterns on N1 and off of the aromatic ring. The first generation drugs like Nalidixic acid do not possess the aromatic fluoro substitution on position 6 as shown in Figure 2.2. Addition of a fluoro group in second generation analogs like ciprofloxacin resulted in a 100-fold enhancement of MIC values and is now a common addition to the chemical scaffold.<sup>5</sup>

The quinolone class of antibiotics work by selectively binding to either topoisomerase

II (1<sup>st</sup> and 2<sup>nd</sup> generation compounds like Nalidixic Acid and Ciprofloxacin) or topoisomerase IV (3<sup>rd</sup> and 4<sup>th</sup> generation compounds like Levofloxacin and Gatifloxacin) in bacteria, while sparing the mammalian counterparts of these enzymes. The inhibition of either of these enzymes eventually disrupts cell replication by preventing the alleviation of overcoiled DNA, leading to cell death.<sup>5</sup>

Even given their unique mechanism of action, a significant amount of resistance has developed for this scaffold. One of the most prevalent ways for bacteria to remove the unwanted bactericide is through efflux, whereby the drug is removed via multidrug-resistant efflux systems. These active transporters are responsible for exclusion of unwanted cellular drug contents yielding a loss in clinical efficacy.<sup>5</sup> Moreover, the emergence of resistance is also associated with mechanisms that alter the active sites of both topoisomerase II and IV. This reduction in the binding affinity of the quinolones renders them ineffective.<sup>5</sup>

### 2.2.3 Tetracyclines

The tetracyclines represent another large class of commonly prescribed antibiotics. These broad spectrum polyketides were isolated from a *Streptomyces* genus and all contain various functional group modulation on a tetracyclic core, several examples are shown in Figure 2.3.<sup>6</sup>

The tetracyclines act by inhibiting bacteria protein synthesis. Tetracycline bound to the A-site of the ribosomal 30S subunit prevents aminoacyl t-RNA association, effectively halting protein synthesis, resulting in cell death.<sup>6</sup>

Once again, resistance has occurred through a variety of mechanisms. Both Gram-negative and Gram-positive resistant species possess the efflux proteins to export any

intracellular tetracycline out of the cell, thereby reducing the effective concentration and preventing it from binding the A-site of the ribosome. Although a number of the tetracyclines (i.e., glycylcycline and minocycline) are still impervious to the efflux proteins, laboratory studies have managed to produce resistant strains quite readily and it is only a matter of time before they present themselves clinically.<sup>6</sup>

Both Gram-negative and Gram-positive strains have also developed nine ribosomal protection proteins which effectively prevent tetracycline binding to the ribosome. Moreover these ribosomal protection proteins are less specific for the drug itself and more specific for the active site targeted, and thus generate a much broader range of resistance.<sup>6</sup>

#### 2.2.4 Macrolides

The macrolide antibiotics are another key group of protein synthesis inhibitors. They are typically characterized by a large macrocyclic lactone decorated by one or more deoxy sugars attached to the parent ring (Figure 2.4). This compound class is mainly represented by metabolites isolated from the *Streptomyces* sp. In contrast to the tetracyclines, macrolides bind to the 23s component of the large ribosomal subunit (50S) thus preventing elongation.<sup>7</sup>

Site-specific methylations in the active site preclude macrolide binding, and in most cases are the most relevant resistance mechanism. These methylations reduce the drug's efficacy, and unfortunately in most cases this resistance mechanism is broad spectrum and encompasses a number of macrolides.<sup>7</sup> Furthermore, Gram-negative bacteria are capable of producing a transport system to remove any unwanted material in the cellular contents, again rendering the drugs ineffective.

### 2.2.5 Lipopeptides, Defensins, and Defensin Mimics

As resistance becomes more prevalent, the requirement for different antibiotic scaffolds is more urgent. In recent years, the lipopeptides like daptomycin and colistin (Figure 2.5) have met these demands. These semisynthetic secondary metabolites work by either binding the exopolysaccharide of the bacterial outer membrane of Gram-negative strains, or binding the lipid-rich membrane in Gram-positive strains. This amphipathic interaction causes cellular leaching and rapid cell death. The novelty of these compounds has also precluded their over-usage in agricultural, industrial and clinical setting and garnered fewer amounts of confirmed resistance. More importantly, the unique mechanism of action possessed by these compounds has also been shown to limit resistance.<sup>8</sup>

Further analysis reveals that the unique mechanism of the lipopeptides resembles the defensin antimicrobial peptides. These small peptides are  $\beta$ -sheet rich, highly cationic (via lysine and arginine residues), and contain six disulphide-linked cysteine residues. More importantly, these antimicrobial peptides are present in mammalian cells (thus at physiological concentrations are nontoxic) and confer very little known resistance. A nontoxic “defensin-mimic” like the lipopeptides demonstrates the ability of the pharmaceutical community to develop new and efficacious antibiotics.<sup>8</sup>

Unfortunately, these semisynthetic bioanalogs are difficult to make, expensive, and susceptible to proteolytic degradation. Moreover performing relevant SAR studies on the complex molecules is complicated by their synthesis.<sup>8</sup>

## 2.3 The Biofilm Phenotype

The abundant use of preexisting antibiotics have triggered an evolutionary response by bacteria to develop resistance mechanisms. In addition, bacteria are able to defend

themselves by existing primarily in a polymeric matrix-enclosed system more commonly referred to as a biofilm. The observation of biofilm forming bacteria was first reported over 70 years ago by Zobell.<sup>9, 10</sup> Scientists first studied bacteria from planktonic or freely floating arrangements. However, bacteria rarely exist in this form, and are more commonly involved in complex metabolic, structural, and chemical communities.<sup>11, 12</sup>

Biofilm bacteria are found on almost every natural and man-made surface and act as a direct method to protect themselves from the ever-changing environment they inhabit.<sup>11</sup> Costerton observed biofilms in stream water in the late 1970's identifying them by their encasement in "slime" which anchored the bacteria to the bed surface they lived on.<sup>13</sup>

The complex life cycle of a biofilm begins with attraction to a biological or nonbiological surface via weak Van der Waals interactions (Figure 2.6-1). These weak interactions lead to more prevalent and stronger associations between the bacteria and the surface. Expansion begins when microcolonies occupy the newly formed space via replication of the initial attached bacteria (Figure 2.6-2,3). As the microcolonies replicate, macrocolonies begin to form and secrete a vast amount of nutrients (including water, sugars, and proteins) that enrich the structure and ensure proper maturation of the biofilm (Figure 2.6-4).<sup>11, 14</sup> This phenotype safeguards the bacteria from external stimuli including temperature, salt content, antibiotic content, toxic molecules, and the mammalian immune system. When the bacteria have saturated the environment they are in, cell signaling pathways disperse the biofilm causing disaggregation, allowing the bacteria to go out and find a new hospitable environment (Figure 2.6-5). Cohabitation of the biofilm is possible, a phenomena which typically begins with two independent colonies coalescing to form one entity.<sup>15</sup> So called "mixed-species" biofilms have been observed in the lungs of patients



with CF as well as in the oral cavity of patients with dental plaque.<sup>16</sup>

The biofilm phenotype is a ubiquitous living structure present on natural and unnatural surfaces. Its widespread incidence can be very detrimental in industry and healthcare and has been implicated in several disease states.

### *2.3.1 Biofilms in Industry*

Biofilm formation in industrial settings result in billions of dollars (the complexities of these industrial processes prevent an accurate cost analysis) in damages a year through destructive process collectively referred to as biofouling which occurs primarily in oil pipelines, ship hulls, steel and paper production, the food and beverage industry, water desalination and water treatment plants.<sup>11a, 17, 18</sup> The aqueous environment of many piping and cooling systems serve as an excellent staging area for biofilm growth. These sources are typically fed with fresh, nutrient rich, temperate water; variables that promote biofilm formation and growth. Unfortunately, even with biocidal agents and the implantation of antifouling processes, the inhibition of these unwanted biofilms is only temporary. Even in the absolute best case scenarios, that is, use of an antifouling surface, high degree of biocide administration, and mechanical debridement of the surface, only several years of biofilm free growth are guaranteed.<sup>18</sup> Further data has shown that killing the bacteria that reside in the biofilm without removing the outer matrix (EPS) results in an optimum medium for the next round of biofilm growth. As shown in Figure 2.7, a chemical biocide is administered to a mature biofilm. The biocide causes the biofilm to die; however, its structural components remain, which can then serve as nutrient rich source for the next biofilm to build upon.<sup>18</sup>

In oil piping systems, biofilm aerobic respiratory activity can lead to cathodic and

anodic regions, which promote electron flow and eventually leads to destruction of the metal surface. To further complicate the problem of biofouling the presence of iron and sulfate reducing species can also lead to the degradation of the steel used in pipelines.<sup>19</sup>

Paper production can also be stunted by bacterial growth. Again the high throughput of clean, nutrient-rich water results in optimal conditions for biofilm formation. Biofouling in this environment can often lead to clogged filters, sheet breaks, and holes in the paper.<sup>20</sup>

In order to amend these unwanted effects industries have turned to using toxic biocidal agents, like glutaraldehyde for treatment.<sup>21</sup> Typically any alternative less toxic approaches, that is, dispersants, enzymes, and altering water composition are ineffective.<sup>18</sup> The unwanted effects of biofilms in industrial media demand the need for novel more effective treatment methods.

### *2.3.2 Biofilm in Medical Devices*

Invasive medical devices, such as catheters, intratracheal tubes, central vein lines, and peritoneal dialysis catheters, have advanced the standard of care in the modern clinical setting. However, introduction of a foreign object into the body can be met with severe reactions. Not only is the body trying to suppress these foreign objects via an autoimmune response, these objects can also serve as host for biofilm formation and development. According to a 1987 report by Costerton, biofilms were found in the following devices: wound drainage tubes, sutures, hemodialysis buttons, intraarterial and intravenous catheters, Hickman and silastic cardiac catheters, Swann-Ganz pulmonary artery catheters, urinary catheters, ureteral stents, biliary stents, penile prostheses, prosthetic hip joints, endotracheal tubes, intrauterine contraceptive devices (IUDs), transparent dressing, hemasite access devices, cardiac pacemakers, mechanical heart valves, and Dacron grafting

systems. In most cases no pathogenic infection was associated with the presence of the biofilm. This auspicious consequence, however, suggests that the presence of the biofilm phenotype is not only undetectable by the body's own host-defense system but also the administration of antibiotics associated with surgical intervention is ineffective at destroying these macrocolonies. These sites of growth can also lead to subsequent manifestation of dormant bacteria, leading to a chronic pathogenesis.<sup>11b</sup>

The inherent microstructure of plastic lends itself as to biofilm growth. Various medical devices, including endotracheal tubes have microsurfaces that promote biofilm growth.<sup>22</sup> These engineered surfaces contain a vast amount of troughs and crests which provide an ideal environment for the biofilm to not only reside, but also one which it is protected in.<sup>22</sup> The severity of this problem was amplified by the introduction of needleless infusion systems, which were implemented in the late 90's to curtail the transmission of blood-bourne pathogens including HIV and hepatitis B (previously large bore hollow stainless steel hypodermic needles were used).<sup>23</sup> These needleless connections, though safer for healthcare professionals, have been implicated in several pathogenic outbreaks.<sup>23</sup>

In order to solve this problem devices can be coated or impregnated with bactericidal agents like chlorohexidene or rifampin.<sup>24</sup> Again however, the administration of these agents will only curtail infections rates on a short term.

### *2.3.3 Chronic Infections Related to Biofilm*

Clinicians have developed a number of successful methods for treating acute bacterial infections. Acute bacterial infections are characterized by rapid onset, swelling and redness at the site of infection, and can be treated by a standard antibiotic regimen. The lack of persistence of these infections is directly related to the planktonic, nonaggregated state the

bacteria are in, making them susceptible (albeit depending on their resistance level and how quickly the infection has been detected) to modern antibiotics.<sup>25</sup>

A chronic infection on the other hand, is often marked by slower progression and is difficult, if not impossible, to treat with standard antibiotics. Often, the bacteria responsible for infection are observed in a dormant, aggregated state. The bacteria responsible for these infections can result in pneumonia in cystic fibrosis patients, chronic wounds, catheter and implant associated infections and chronic otitis media (infections of the inner ear).<sup>25</sup> Given the characteristics of chronic infections the scientific community has suggested that these hard to treat bacteria are living in a biofilm or biofilm-like state.

Cystic fibrosis (CF) is an inherited autosomal recessive disease affecting one out of every 20,000 people.<sup>26</sup> The cause of CF was recognized in 1989 as mutations in both copies of the gene that encodes for the protein cystic fibrosis transmembrane conductance regulator (CFTR). The ineffective CFTR results in an ion imbalance leading to excessive dehydration of bodily fluids causing sweat, digestive fluids, and mucous to thicken. Most CF patients maintain a reasonable quality of life by extensive antibiotic treatment, commonly via inhalative Tobramycin therapy.<sup>27</sup> Despite an effective and rigorous antibiotic program, persons with CF eventually lose their life due to excessive chronic lung infections and complications thereof. The constant strain put on the lung tissues through multiple pathogenic *P. aeruginosa* infections as well as administration of large amounts of antibiotics eventually leads to tissue destruction by the body's own immune system. Given the conditions of CF, it is firmly believed that the resultant difficult to treat *P. aeruginosa* infections are caused primarily by biofilms.<sup>25, 26</sup>

Costerton first observed biofilms in CF patients in 1980. The electron micrograph of a

thin section of alveolar material contained cells of *P. aeruginosa* and what Costerton referred to as “microcolonies...enveloped in a fibrous anionic matrix”.<sup>28</sup> Further work by Davies and coworkers found evidence of clusters of *P. aeruginosa* enveloped in a thick matrix. Davies was also able to identify two significant quorum sensing signals which were in consonance with laboratory biofilm isolates.<sup>29</sup>

With the detrimental effects of biofilms in CF patients it is not surprising that biofilms are also observed in other chronic infections. An increasing amount of the general populace is stricken by diabetes and heart disease. The poor cardiovascular bloodflow as well as the myriad of other physiological complications associated with these disease states can lead to chronic infections via unnoticed wounds and/or general unhealed lacerations. Although these wounds are referred to as chronic, resultant from their delayed repair and healing, they have been shown to contain a significant amount of biofilm bacteria. Again the presence *P. aeruginosa* has led a number of researchers and clinicians to conclude that the delayed response of heavy antibiotic treatment coupled with persistent wounds are due to biofilms clearly associated with these disease states.<sup>30</sup> Furthermore, when *P. aeruginosa* is found in the chronic wound, studies have shown the wound to be larger in area compared to other examples lacking *P. aeruginosa*.<sup>31</sup>

Given the relevance of the above clinical infections, drug design must not only include planktonic data but also move toward a design that addresses biofilm forming species. In doing so, the risk for developing chronic biofilm infections may be mitigated.

## **2.4 Finding a Cellular Target for the Biofilm Phenotype**

Quorum sensing is the mechanism by which bacteria can communicate with each other through signaling molecules in relation to population density. The maturation of a biofilm

induces a number of quorum sensing factors which are bacterially produced. These quorum sensing signals tell the bacteria to go out in search of nutrients, new habitable zones, and thus prevent the accumulation of waste products in the biofilm. When these signals are released they effectively cause the biofilm to disassemble through several mechanisms, including: terminating the synthesis of the extracellular polymeric substance (EPS) matrix, breaking down the matrix itself, or disrupting the noncovalent surface adhesion interactions which keep the biofilm anchored to its surface.<sup>32</sup>

Given the above criteria, these biofilm disassembly methods could be used as targets for biofilm dispersal. Moreover, the unique design of a biocidal agent that could influence dispersal as well as act as an antibiotic would be highly valued due to the detrimental association of biofilms in various media as shown above.

Losick and Clardy have reported success in this arena, by developing polyamine compounds that can disperse *Bacillus subtilis*, and *Staphylococcus aureus* biofilms. They found several polyamines to be highly interactive with the exopolysaccharide subunit of the biofilm causing its degradation. Clardy and Losick show that 25  $\mu\text{M}$  norspermidine, prior to inoculation, inhibits biofilm formation without disrupting planktonic growth. Further analysis shows that spermidine (one extra methylene unit) is inactive at concentrations  $< 2 \text{ mM}$  while the four-nitrogen counterpart of norspermidine, norspermine is active at  $\sim 50 \text{ }\mu\text{M}$ . The authors speculate these results are due to the highly interactive nature of norspermidine (and other 3 carbon conjugates) with the EPS causing a weakness in the biofilm secondary structure and ultimately biofilm dispersal. However, the seminal works of Losick and Clardy have been disputed several times in the community, and presently it is unknown whether these polyamines act as biofilm disruptors at the

concentrations reported.<sup>33, 34, 35</sup>

The groups of Wall and Michael, as well as Berg, have reported antibiofilm activity by norspermidine, however, they reported norspermidine to be 10 times less potent than the data reported by Losick and Clardy.<sup>35</sup> Unfortunately, it is unknown at this time which data is in agreement with the biological activity of these polyamino compounds norspermidine and norspermine.

Due to the sensitivity and reproducibility of the biofilm dispersion data presented above there is a need for additional tests to provide a more conclusive analysis as to what effect norspermidine and other polyamines have on biofilm production, assembly, and disassembly.

## **2.5 Design and Synthesis of Novel Antibiofilm Antibiotics**

Given the generalized structure of the defensins and the lipopeptide (defensin-like) antibiotics (highly polar cationic tails attached to a nonpolar body) we sought to develop an antimicrobial that was cheap, easy to make, and highly potent against bacteria. Several compound classes in the literature further rigidified our hypothesis for structure requirements as they possessed the requisite information to properly mimic the lipopeptides and defensins. Furthermore, a number of these compounds contained a polyamine subunit which we felt could invoke antibiofilm characteristics in agreement with Clardy and Losicks original data.<sup>34</sup>

### **2.5.1 Squalamine**

Squalamine (Figure 2.8) is a potent secondary metabolite found in the dogfish shark (*Squalus acanthias*). Squalamine displays potent Gram-negative and Gram-positive

activity, as well as antiprotozoa effects.<sup>36</sup> Additionally, this aminosterol has been investigated as an anticancer therapeutic for its ability to inhibit angiogenesis in several mouse cancer models.<sup>37</sup>

When tested, squalamine displayed potent bactericidal activity. Gram-positive strains like *Staphylococcus aureus* showed MIC values of 1-2 µg/mL, while Gram-negative strains like *E. coli* and *Pseudomonas aeruginosa* showed MIC values of 1-2 µg/mL and 4-8 µg/mL, respectively.<sup>36</sup>

Given the structure of squalamine, we can deduce that the steroidal core provides the hydrophobic bulk for the molecule while the polyamine tail gives cationic character. Furthermore, given Losick and Clardy's finding, the pendant polyamine (spermidine) may also provide some effect on biofilm antifouling. Although in their examples norspermidine (1 methylene unit shorter) was much more effective.<sup>33, 34</sup>

### 2.5.2 The Ceragenins

The ceragenins or cationic steroidal antimicrobials (CSAs) are a class of steroidal compounds developed in Paul Savage's lab at Brigham Young University. The CSAs were developed as a complement and mimic of the ever expanding group of lipopeptides. Use of synthetic small molecules instead of large polypeptides has a number of benefits as the ceragenin's have no proteolytically cleavable side chains and are obtained from commercially available chemical stock thereby eliminating any biosynthesis. Originally termed as CSA, the Savage group opted to name their molecules ceragenin's to avoid any stigma associated with the steroid name.<sup>38</sup>

The mechanism of action of these molecules is similar to the lipopeptides, as the compounds show strong association for lipid A, in Gram-negative models, leading to



membrane depolarization and ultimately cell death. In Gram-positive bacteria the ceragenin's have been shown to bind to the phospholipids present in the cell membrane causing cellular leakage and eventually death. Both membranes are rich in negatively charged side-chains (teichoic acid for Gram-positive and lipid A for Gram-negative) and thus the association of the cationic ceragenin causes pores leading to cell death.<sup>38</sup>

Synthetically (Scheme 2.1), the ceragenins were prepared from cholic acid methyl ester (**1**). Starting from **1**, a hydride reduction of the methyl ester followed by trityl chloride protection of the pendent alcohol afforded the protected sterol. Subsequent tris-allylation of the secondary alcohols produced **2**. Hydroboration was accomplished with 9-BBN after which the resultant alcohols were mesylated to provide **3**. Subsequent azide displacement produced tris-azide **4**. With the tris-azide in hand, the trityl group was removed and the resulting alcohol was activated again with mesyl chloride to yield the mesylate **5**. Displacement of the activated alcohol with octylamine afforded the desired amine **6**. To generate the desired ceragenin CSA-13, reduction of the remaining tris-azide was accomplished with  $\text{LiAlH}_4$ .<sup>38</sup>

In their development of the Ceragenin's, the Savage group was able to procure several effective bactericides. CSA-13, for example, shows potent activity against resistant strains of *Staphylococcus aureus* with an MIC of 4  $\mu\text{g/mL}$ . Further potency data has revealed CSA-13 to be active against protozoa including *Leishmania major* ( $\text{LD}_{50} = 4.9 \mu\text{m}$ ) and *Trypanosoma cruzi* ( $\text{LD}_{50} = 9.0 \mu\text{m}$ ). The synthetic flexibility, novel mechanism of action, and lack of proteolytic cleavage make the ceragenins an effective class of antimicrobial compounds. Future research in this compound class may produce clinically significant antibiotics.<sup>38</sup>

### 2.5.3 *Looper's Initial Design Concept*

The above examples showcase an underrepresented class of molecules which have broad spectrum activity, are chemically accessible, and more importantly are noncytotoxic against mammalian cells. Further, their unique mechanism of action makes these peptide membrane-active mimics immune to resistance. These steroidal biocides are governed by a simple principle, highly cationic tails are localized on a hydrophobic backbone but lack the cleavable amide linkages present in peptide-based antibiotics both natural and synthetic. We felt several adjustments could be made in order to expand on this dogma.

First, a simplified synthetic approach would not only provide more applicable structural modularity, but would also favor analog design (Figure 2.9). Second, Clardy and Losick have shown various polyamines to have antibiofilm activity (see above).<sup>33, 34</sup> Given the structure of squalamine (Figure 2.8), we hypothesize that potential antibiofilm activity could be observed through polyamine design on a hydrophobic scaffold. With these criteria in mind, we constructed a number of compounds in a concise synthetic sequence which would allow for modularity aimed at SAR studies.

Although elegant in design, Savage's work lacked modularity and synthetic accessibility, this is demonstrated in the lengthy synthesis of CSA-13 shown in Scheme 2.1.<sup>38</sup> If the steroidal core was simplified to a smaller, less complex, hydrophobic backbone, the synthetic sequence would be significantly shortened.

## 2.6 **Looper's First Generation Biocide Synthesis**

We felt that the Wieland-Miescher ketone (**7**) provided us with the requisite chemical information to support this process as it met three of the criteria: 1) the ketone was cheap and readily available, 2) the carbonyl functional groups allowed for facile synthetic

adjustments, and 3) the three dimensional structure of the bicycle should be similar to that of the steroidal backbone. Starting from racemic Wieland-Miescher ketone (**7**) hydrogenation of the olefin followed by reduction of the pendant ketones afforded the diol **8**. From **8**, alkylation with allyl bromide provided diene **10**. Unfortunately, the allylation required harsh conditions to produce **10** and was low yielding. Also, the remaining S<sub>N</sub>2 displacement of the mesylate **11** by nitrogen-nucleophiles required very forcing conditions and never produced the desired product **12** (Schemes 2.2 and 2.3).

Since the Wieland-Miescher ketone approach was unsuccessful in our hands, we turned our attention to even simpler backbones. Using the idea of tethering a cationic tail to a nonpolar body, benzyl halides were chosen as initial starting materials. We synthesized compounds (Figure 2.10) using a displacement reaction with the respective benzyl halide and mono-Boc protected diamine and triamines to generate a series analogs with a single side chain (Scheme 2.4). We quickly discovered that reductive amination of the requisite aldehyde was a cheaper approach compared to the displacement of a benzyl halide and we adjusted our synthesis to utilize aldehyde starting materials (Scheme 2.5).

Based on the MICs of **CZ-01-003** through **CZ-01-016** (Table 2.2), the single side-chain compounds showed limited activity with values ranging from 100 to 1300 µg/mL. However, these compounds supported our initial rational design and we felt that the simplest and fastest approach to increasing activity would be to add another polyamine side chain (Scheme 2.6). This was facilitated through the use of isophthalaldehyde, a starting material that is readily accessible and inexpensive. A significant increase in potency resulted, as shown in the differences between **CZ-01-007** (>800 µg/mL) and **CZ-01-025** (20 µg/mL) as well as **CZ-01-004** (1300 µg/mL) and **CZ-01-012** (100 µg/mL). Our SAR

studies were strengthened by the addition of several other functional groups to our series, including internal and external amides, **CZ-01-040** and **CZ-01-027** respectively (Figure 2.11). As well as the tri-methyl conjugate **CZ-01-019**.

We were able to gather further empirical biofilm data based on SEM analysis of biofilms grown on galvanized steel coupons. **CZ-01-025** was the first lead in this series, selected due to its bactericide and antibiofilm properties. As shown in Figure 2.12 biofilms of *Alcanivorax borkumensis* were grown on galvanized steel for 48 h and left untreated (positive control). The masses of growth can be seen at both 200x and 1000x magnification. When these colonies were treated with **CZ-01-025** for 2 h, and a significant reduction in biofilm is observed (rightmost image) again at both 200x and 1000x magnification. This experiential data gave us evidence that not only was **CZ-01-025** active in planktonic media but also in the biofilm phenotype and **CZ-01-025** was responsible for both biofilm dispersal and bacterial kill.

Again, we were able to observe this trend when biofilm were grown in a CDC reactor and treated with **CZ-01-25**. As shown in Figure 2.13, the biofilm was sustained in the water but after application of our compound very fine fragments were observed. These fragments are indicative of biofilm dispersal.<sup>39</sup> These data, albeit qualitative, clearly show proof of concept to our compound design.

We further elected to use a tri-aldehyde starting material to produce compounds containing three side-chains. Although benzene-1,3,5-tricarbaldehyde had to be purchased from a specialty chemical supplier, its derivatives again showed a similar increase in potency as the alteration from one side chain to two. As shown in Table 2.3, **CZ-01-52** had an MIC of 4.5  $\mu\text{g/mL}$  while its bis-counterpart had an MIC of 20  $\mu\text{g/mL}$ , similarly **CZ-01-**

**32** had an MIC of 50  $\mu\text{g/mL}$  whereas the doubly aminated derivative **CZ-01-12** had an MIC of 100  $\mu\text{g/mL}$ . Again, this trend indicated that first, more cationic character had a direct influence on activity, and the norspermidine derivatives were the most potent compounds of the group. Several other side chains were used in conjugation with benzene-1,3,5-tricarbaldehyde including *N*<sup>1</sup>,*N*<sup>1</sup>-dimethylpropane-1,3-diamine (**CZ-01-46**), Boc-norspermidine (**CZ-01-54**), and nospermine (**CZ-01-57**), and again their initial MICs were higher than **CZ-01-52**.

## 2.7 Conclusion and Future Aims

The first generation series, shown above, provided proof for our initial concept design where a simple phenyl ring acted as the hydrophobic backbone and a variety of polyamines were selected as the cationic tail(s). With our synthetic method we were able to provide a set of carefully constructed compounds in two steps displaying both potent MICs and antibiofilm activity. We were able to further conclude norspermidine was the most potent side-chain used in analog development and the linkage of it to a hydrophobic backbone delivered compounds with antibiofilm properties. The modularity of this first generation synthesis was limited by what aldehydes were commercially available, and in order to pursue a broader SAR analysis we were pressed to find alternative sources of aldehydes through chemical synthesis.

Table 2.1: CDC analysis of current microbial threats

Bacterium	CDC Threat Classification
<i>Clostridium Difficile</i> (CDIFF)	Biggest Threat
Carbapenem-Resistant Enterobacteriaceae	Biggest Threat
<i>Neisseria gonorrhoeae</i>	Biggest Threat
Multidrug resistant (MDR) <i>Acinetobacter</i>	Serious Threat
MDR <i>Pseudomonas Aeruginosa</i>	Serious Threat
Methicillin-Resistant <i>Staphylococcus Aureus</i> (MRSA)	Serious Threat
Drug-Resistant Tuberculosis	Serious Threat
Drug-Resistant Non-Typhoidal <i>Salmonella</i>	Serious Threat
Drug-Resistant <i>Shigella</i>	Serious Threat
Extended Spectrum Enterobacteriaceae (ESBL)	Serious Threat

Table 2.2: The in vitro activity of the initial single side-chain CZ series as MICs against MRSA

Cmpd	MIC ( $\mu\text{g/mL}$ )
<b>CZ-01-003</b>	700
<b>CZ-01-004</b>	1300
<b>CZ-01-005</b>	100
<b>CZ-01-006</b>	>100
<b>CZ-01-007</b>	>800
<b>CZ-01-009</b>	1300
<b>CZ-01-011</b>	>200
<b>CZ-01-013</b>	No data available
<b>CZ-01-016</b>	1100

Table 2.3: The in vitro activity of the bis and tris polyamine CZ series as MICs against MRSA

Cmpd	MIC ( $\mu\text{g/mL}$ )
<b>CZ-01-012</b>	100
<b>CZ-01-019</b>	100
<b>CZ-01-021</b>	50
<b>CZ-01-025</b>	20
<b>CZ-01-027</b>	>100
<b>CZ-01-032</b>	50
<b>CZ-01-033</b>	50
<b>CZ-01-040</b>	>400
<b>CZ-01-046</b>	No data available
<b>CZ-01-052</b>	4.5
<b>CZ-01-053</b>	10
<b>CZ-01-054</b>	5
<b>CZ-01-057</b>	10

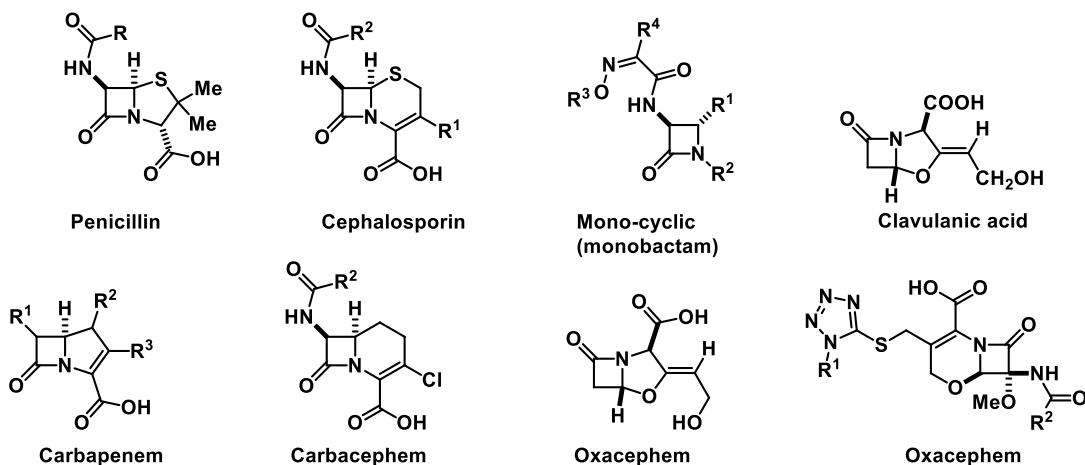


Figure 2.1: The structures of various members of the  $\beta$ -lactam family of antibiotics

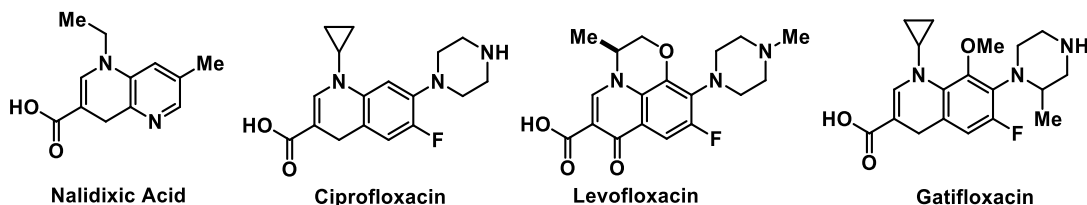


Figure 2.2: The structures of 1<sup>st</sup>, 2<sup>nd</sup>, 3<sup>rd</sup>, and 4<sup>th</sup> generation quinolone antibiotics

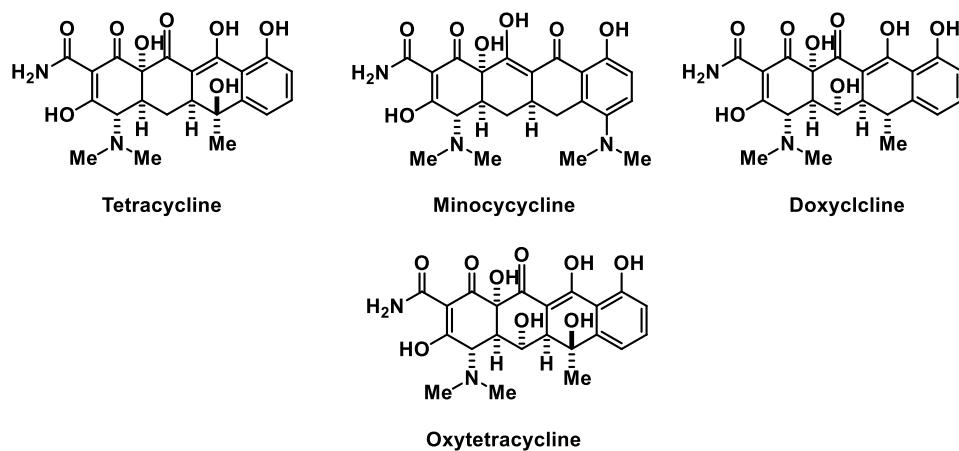


Figure 2.3: Several representative examples from the tetracycline class of antibiotics

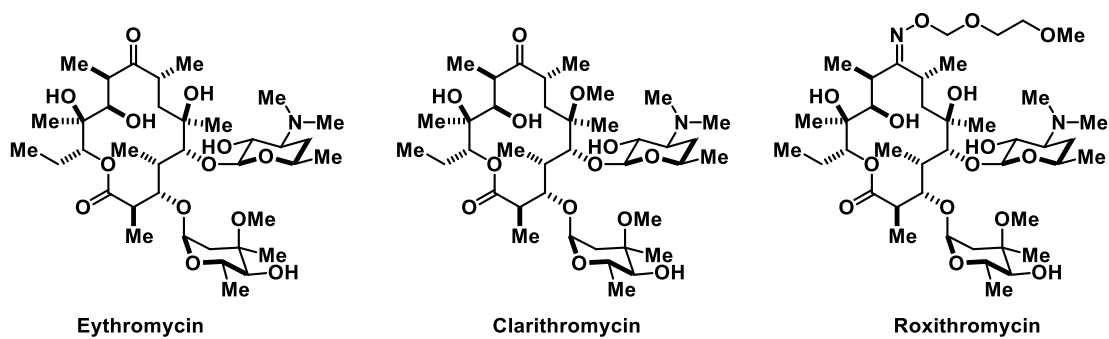


Figure 2.4: Several representative examples from the macrolide class of antibiotics



Figure 2.5: The lipopeptides daptomycin and colistin

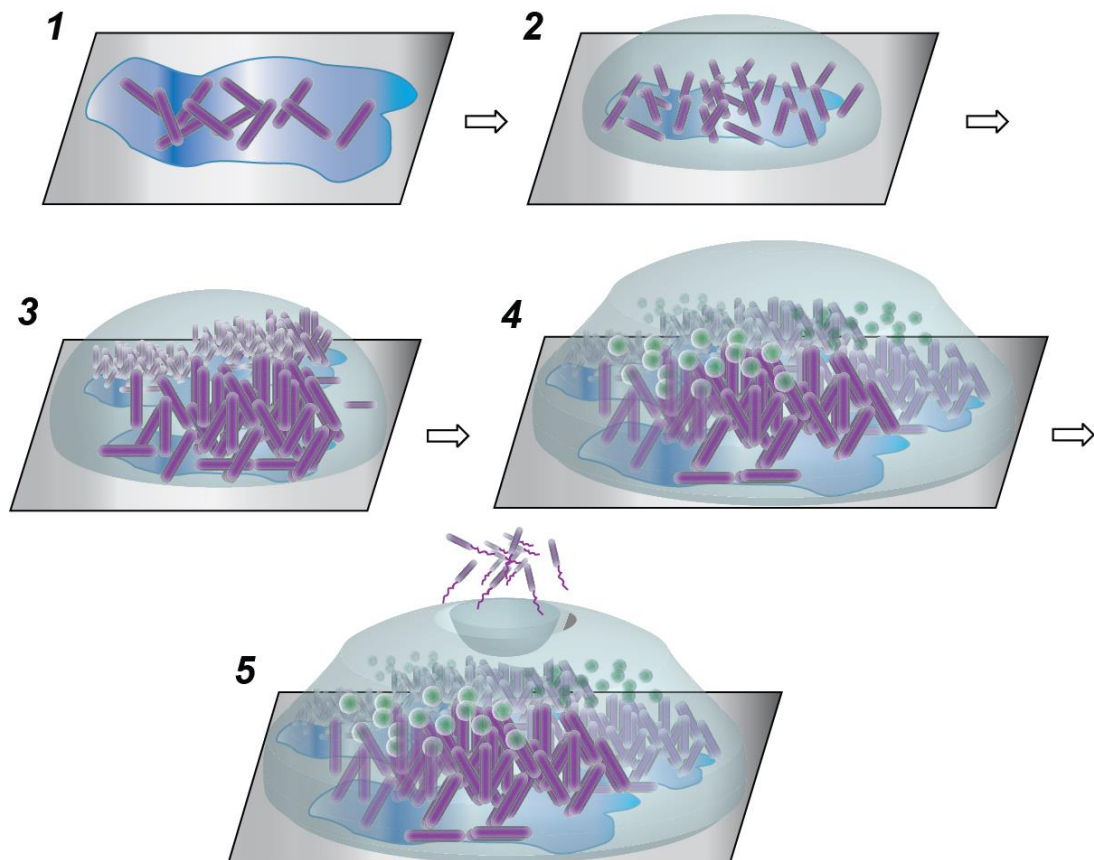


Figure 2.6: Artistic representation of the five stages of biofilm formation from the planktonic phenotype (1) to biofilm EPS (hemispherical outer coating) development (2 and 3) to a fully mature, multiple species biofilm (4) to biofilm dispersal (5)

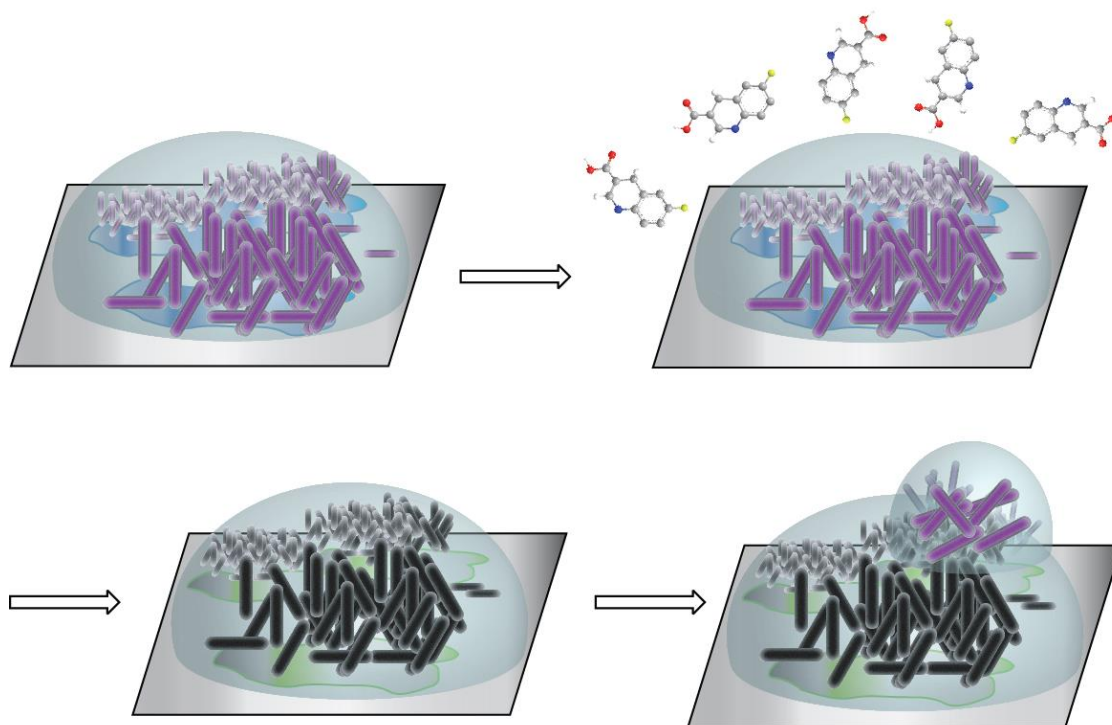


Figure 2.7: Artistic representation of antibiotic treatment of a mature single species biofilm; cell death results but the biofilm remains as a site for another round of maturation

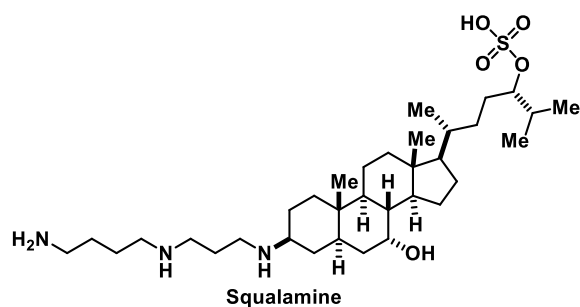


Figure 2.8: The structure of squalamine isolated from the dogfish shark (*Squalus acanthias*)

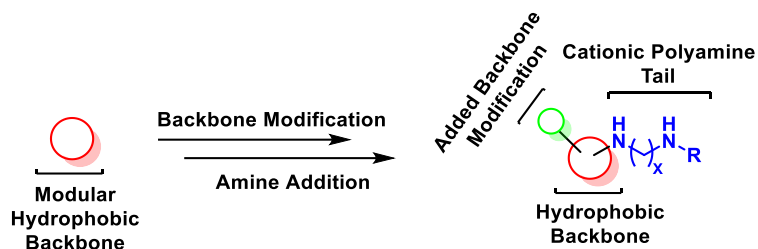


Figure 2.9: Initial synthetic design for developing a membrane active amphiphilic molecule

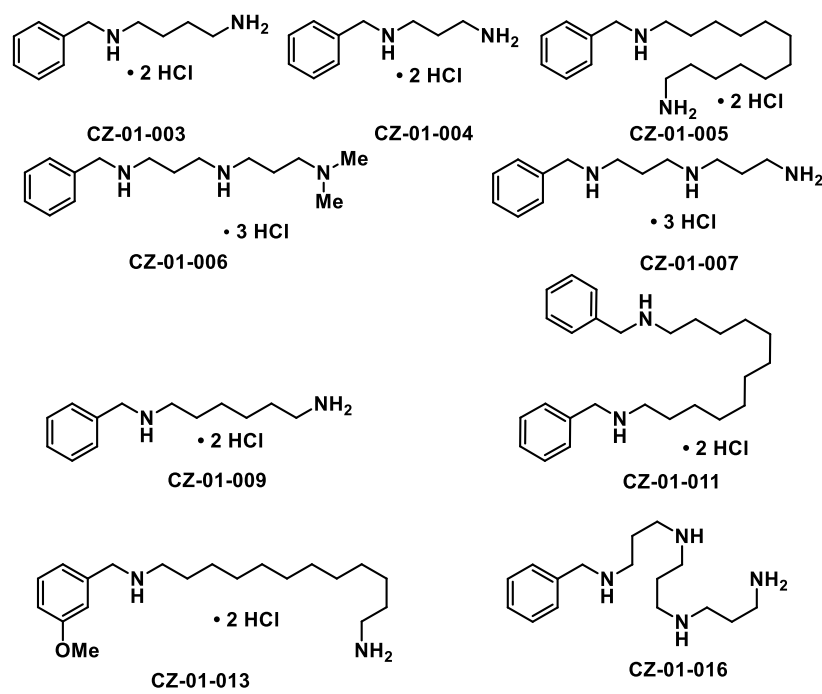


Figure 2.10: The single side-chain CZ compounds

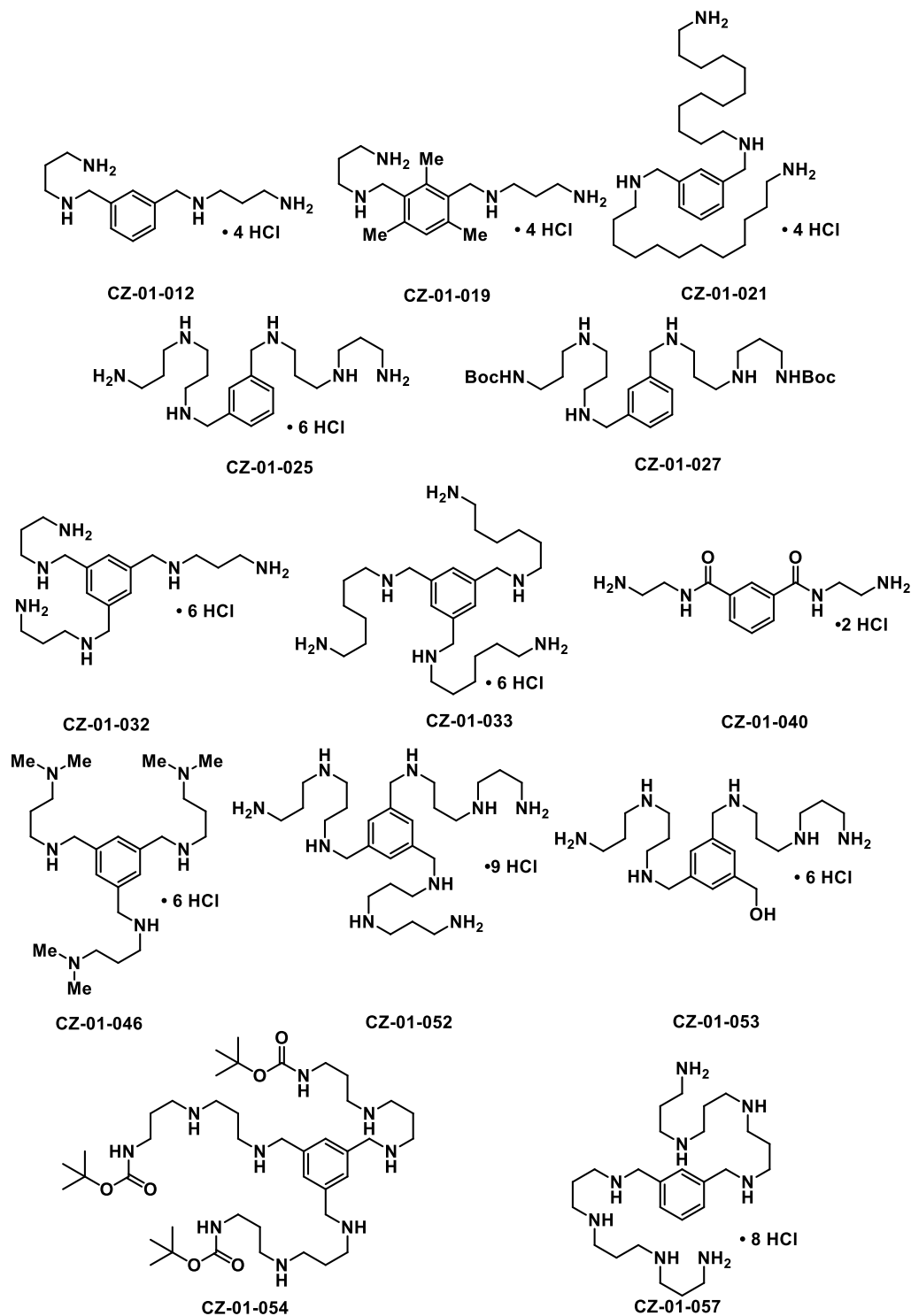


Figure 2.11: The bis and tris substituted CZ compounds with a variety of cationic polyamine side chains

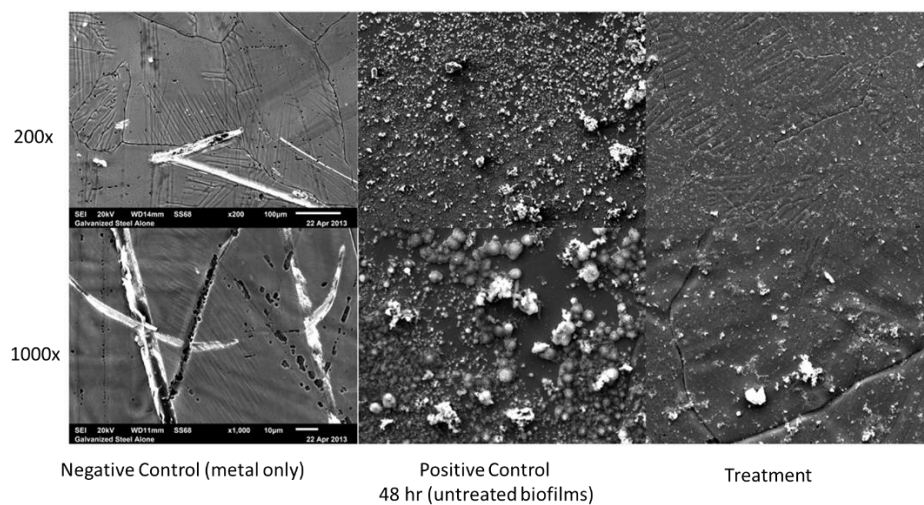


Figure 2.12: Biofilms of *Alcanivorax borkumensis* grown for 48 h on galvanized steel and then: either left untreated or treated for 2 h with **CZ-01-25**

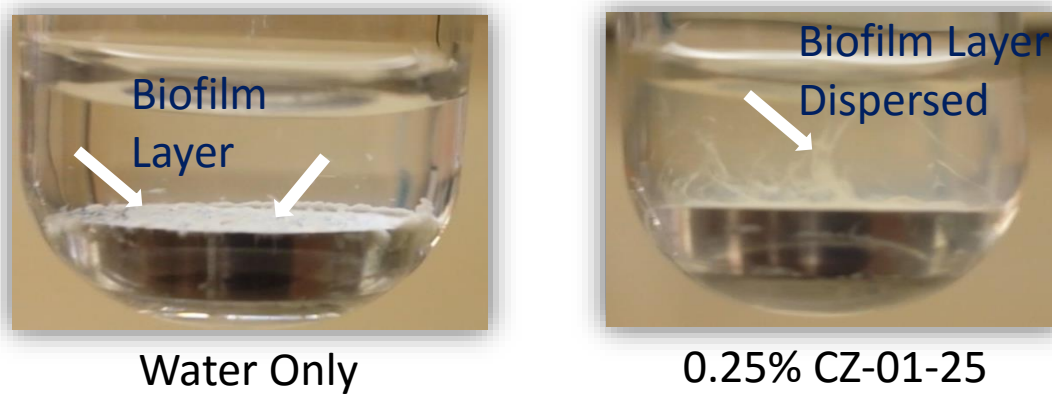
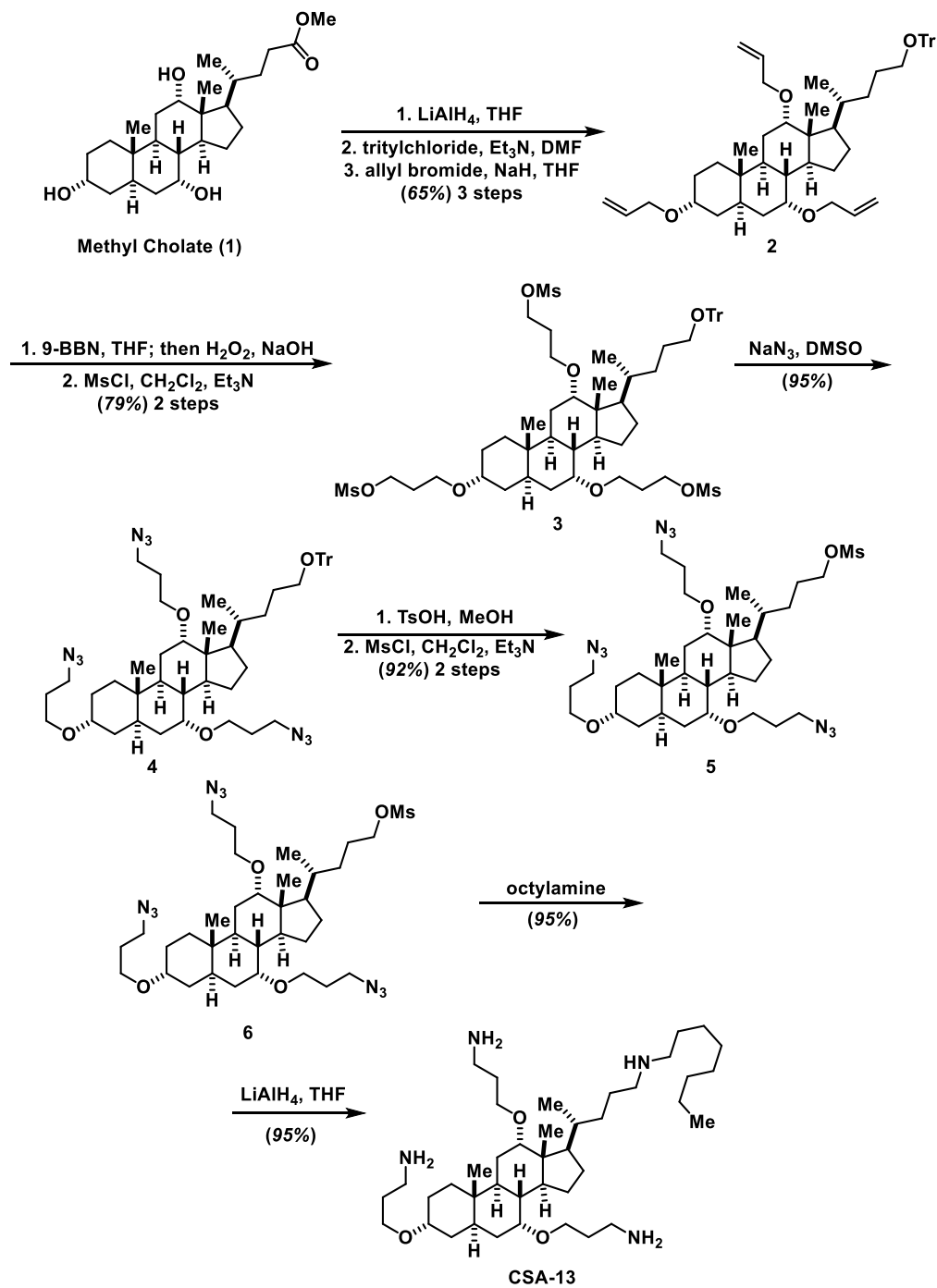
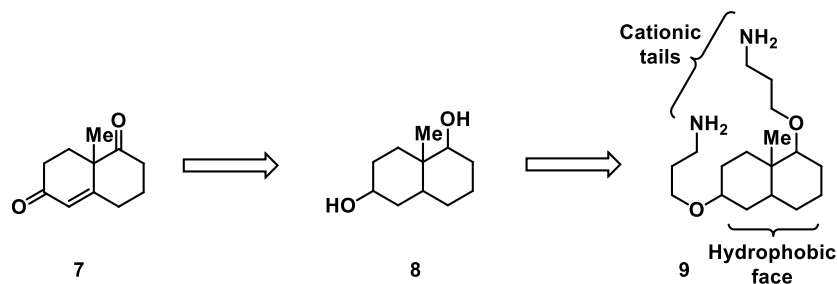


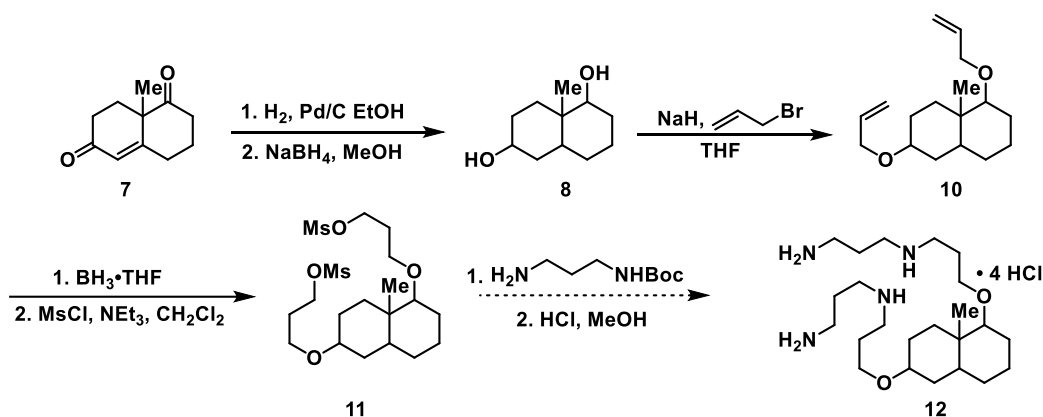
Figure 2.13: Qualitative biofilm dispersal by **CZ-01-25**



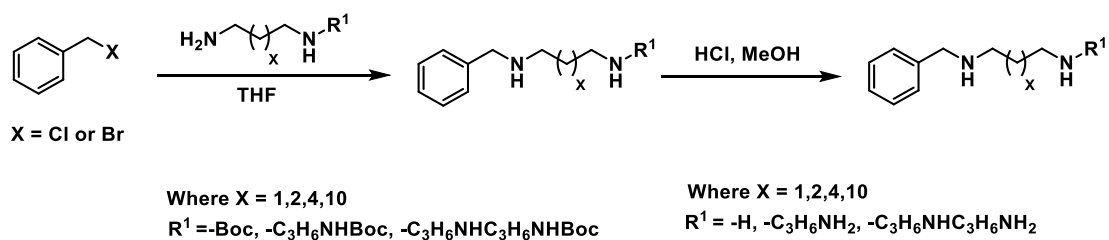
Scheme 2.1: The preparation of Ceragin (CSA-13) from methyl cholate



Scheme 2.2: Synthetic analysis of making amphipathic antimicrobials from the Wieland-Miescher ketone

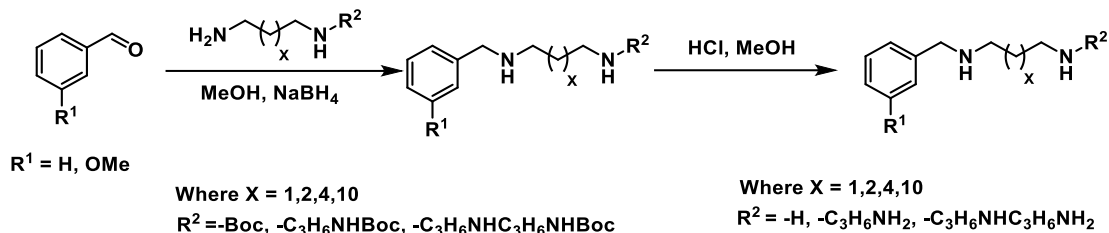


Scheme 2.3: Synthetic attempts to make a polycationic amino-bicycle from the Wieland-Miescher ketone

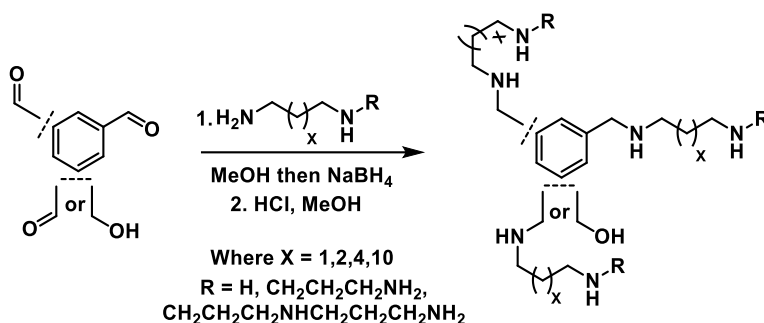


Scheme 2.4: Synthetic analysis for mono-polyamine compounds from the respective benzyl-halide





Scheme 2.5: Synthetic analysis for mono-polyamine compounds from the respective aldehyde



Scheme 2.6: Synthetic analysis for the bi- and tri-substituted phenyl CZ compounds

## 2.8 Supporting Information

### 2.8.1 General Experimental Conditions

Unless otherwise noted, materials were obtained from commercial sources and used without purification; otherwise, materials were purified according to Purification of Laboratory Chemicals.<sup>40</sup> All reactions requiring anhydrous conditions were performed under a positive pressure of nitrogen using flame-dried glassware. Methanol (MeOH) was distilled over magnesium prior to its usage. Diaminopropane is highly toxic and should be handled with great care. Any volatile polyamine synthesized should also be regarded as toxic and should be handled with care and always stored under  $\text{N}_2$  due to reactivity with  $\text{O}_2$  and  $\text{CO}_2$ . Yields were calculated for material judged homogeneous by thin-layer chromatography and  $^1\text{H}$  NMR. Thin-layer chromatography was performed on silica plates

eluting with the solvents indicated and visualized by a 254nm UV lamp. Flash column chromatography was performed with slurry-packed silica gel with solvents indicated in glass columns. Both the solvent system used for TLC and column chromatography needs to be made fresh upon usage due to the volatile nature of  $\text{NH}_3$  in  $\text{H}_2\text{O}$ .  $^1\text{H}$ NMR spectra were recorded at 500 or 300 MHz as indicated. The chemical shifts ( $\delta$ ) of proton resonances are reported relative to the deuterated solvent peak: 4.79 ppm for  $\text{H}_2\text{O}$  using the following format: chemical shift [multiplicity (s = singlet, d = doublet, dd = doublet of doublets, t = triplet, q = quartet, pent = pentet, hex = hextet, sept = septet, oct = octet, non = nonet m = multiplet), coupling constant(s) (J in Hz), integral].  $^{13}\text{C}$  NMR spectra were recorded at 125 MHz. Mass spectra were obtained by ESI/APCI for LRMS. Material purity was quantified with a Thermo scientific Ultimate 3000 LC system. Certain carbon experiments conducted with the VXR500 MHz NMR contain an artifact peak between 170.0-174.0 ppm, which has been confirmed by the facility administrator.

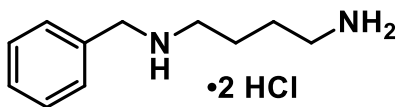
Efficacy profiles of CZ-01-XXX against planktonic MRSA were determined using the microdilution minimum inhibitory concentration (MIC) and minimum bactericidal concentration (MBC) assays defined by Clinical and Laboratory Standards Institute (CLSI) in the M26-A guideline. For comparison, efficacy profiles were also determined in parallel for vancomycin. In short, to perform MIC analysis, several colonies of freshly-cultured MRSA or *P. aeruginosa* from blood agar were used to adjust a 0.5 McFarland standard (equated to  $\sim 7.5 \times 10^8$  colony forming units (CFU)/mL) in phosphate buffered saline (PBS; Fisher Scientific, catalog # BP399-1). Bacteria were diluted 1:100 in a glass test tube. In a 96-well plate, columns 2-11 were filled with cation adjusted Mueller Hinton broth (CAMHB; Fisher Scientific, catalog #B12322), antibiotic solution and MRSA as per the

protocol. In order to fill the wells, liquids were poured into sterile dispensing reservoirs (Fisher Scientific, catalog #07-200-127) then pipetted using a multichannel pipet. This process gave a concentration range of antibiotic from 128  $\mu\text{g/mL}$  in column 2 to 0.25  $\mu\text{g/mL}$  in column 11. A 96-well plate was covered with a plastic plate cover and incubated at 37° C for 24 h after which time the plate was read. The lowest concentration of antibiotic with no growth (no pellet formation) of bacteria was defined as the MIC.

### 2.8.2 Missing Experimental Data

Some examples included in the formal report were omitted for clarity, as these compounds were synthesized only once and handed off to our biological counterpart without full compound characterization. Furthermore, we felt the biological data related to these samples did not warrant any additional pursuit.

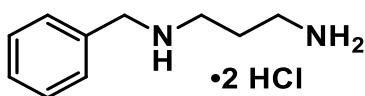
### 2.9.3 Experimental Procedures



**CZ-01-003: *N*<sup>1</sup>-benzylbutane-1,4-diamine, hydrochloride salt:** To a solution of benzaldehyde (0.50 g, 4.72 mmol, 1.0 equiv.) in MeOH (10 mL) was added *tert*-butyl (4-aminobutyl)carbamate (0.88 g, 4.72 mmol, 1.0 equiv.) and the reaction was left to stir for 16 h. Sodium borohydride (0.71 g, 18.88 mmol, 4 equiv.) was then added portion wise and the reaction mixture was left to stir for an additional 1 h. The excess MeOH was evaporated and the crude solid was partitioned between EtOAc (50 mL) and 10% NaOH (mL). The aqueous layer was then back extracted with EtOAc (1 x 50 mL) dried over Na<sub>2</sub>SO<sub>4</sub> and evaporated to afford the crude free base which was carried forward without further

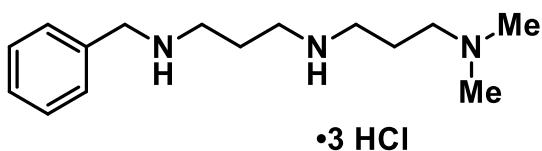
purification. The crude free base was acidified with HCl in MeOH (50 mL) and then placed at 0 °C for 1 h to precipitate. The corresponding precipitate was filtered and dried to afford the HCl salt as a white solid (48%).  $^1\text{H}$  NMR (500 MHz,  $\text{D}_2\text{O}$ )  $\delta$  7.52 (s, 5H), 4.26 (s, 2H), 3.15 (t,  $J = 8$  Hz, 2H), 3.07 (t,  $J = 7.5$  Hz, 2H), 1.86-1.74 (m, 4H).  $^{13}\text{C}$  NMR (125 MHz,  $\text{D}_2\text{O}$ ) 130.6, 129.9, 129.7, 129.2, 51.0, 46.3, 38.8, 23.9, 22.7. LRMS calculated for  $\text{C}_{11}\text{H}_{18}\text{N}_2$   $m/z$  179.1  $[\text{M}+\text{H}]^+$ , Obsd. 179.2.

The following examples were prepared similar to **CZ-01-003**:

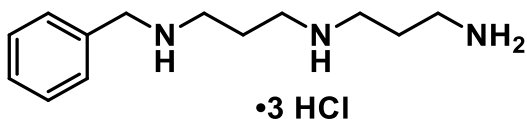


**CZ-01-004:  $N^1$ -Benzylpropane-1,3-diamine, hydrochloride salt:**

$^1\text{H}$  NMR (500 MHz,  $\text{D}_2\text{O}$ )  $\delta$  7.49 (quint,  $J = 3$  Hz, 5H), 4.26 (s, 2H), 3.17 (t,  $J = 8$  Hz, 2H), 3.07 (t,  $J = 8$  Hz, 2H), 2.09 (quint,  $J = 7.5$  Hz, 2H).  $^{13}\text{C}$  NMR (125 MHz,  $\text{D}_2\text{O}$ )  $\delta$  130.6, 129.9, 129.8, 129.4, 51.4, 44.1, 36.7, 23.9. LRMS calculated for  $\text{C}_{10}\text{H}_{16}\text{N}_2$   $m/z$  165.2  $[\text{M}+\text{H}]^+$ , Obsd. 165.4.

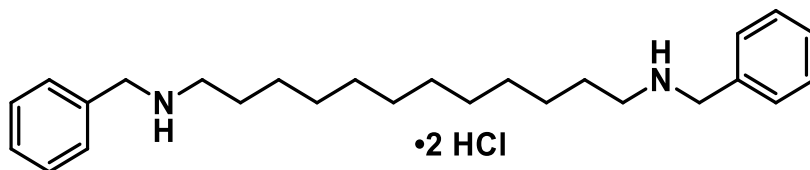


**CZ-01-006:  $N^1$ -(3-(Benzylamino)propyl)- $N^3,N^3$ -dimethylpropane-1,3-diamine, hydrochloride salt:**  $^1\text{H}$  NMR (500 MHz,  $\text{D}_2\text{O}$ )  $\delta$  7.41 (s, 5H), 4.18 (s, 2H), 3.20-3.08 (m, 8 H), 2.83 (s, 6H), 2.15-2.03 (m, 4H).  $^{13}\text{C}$  NMR (125 MHz,  $\text{D}_2\text{O}$ ) 131.0, 130.5, 130.4, 129.9, 54.8, 51.8, 45.3, 45.1, 44.5, 43.5, 23.2, 21.8.

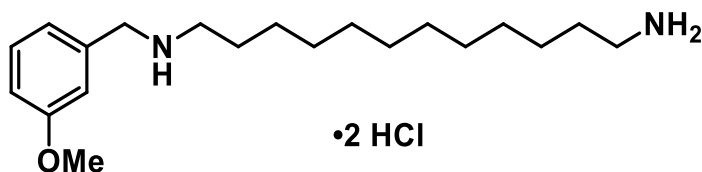


**CZ-01-007: *N*<sup>1</sup>-(3-Aminopropyl)-*N*<sup>3</sup>-benzylpropane-1,3-diamine, hydrochloride salt:**

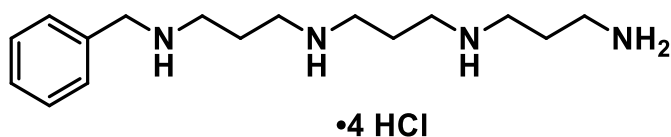
<sup>1</sup>H NMR (500 MHz, D<sub>2</sub>O) δ 7.49 (s, 5H), 4.25 (s, 2H), 3.20-3.15 (m, 6H), 3.11 (t, *J* = 8 Hz, 2H), 2.17-2.07 (m, 4H). <sup>13</sup>C NMR (125 MHz, D<sub>2</sub>O) δ 130.3, 129.8, 129.7, 129.2, 51.2, 44.6, 44.6, 43.8, 36.5, 23.7, 22.6. LRMS calculated for C<sub>13</sub>H<sub>23</sub>N<sub>3</sub> m/z 222.2 [M+H]<sup>+</sup>, Obsd. 222.2.

**CZ-01-011: *N*<sup>1</sup>,*N*<sup>12</sup>-Dibenzyl dodecane-1,12-diamine, hydrochloride salt:**

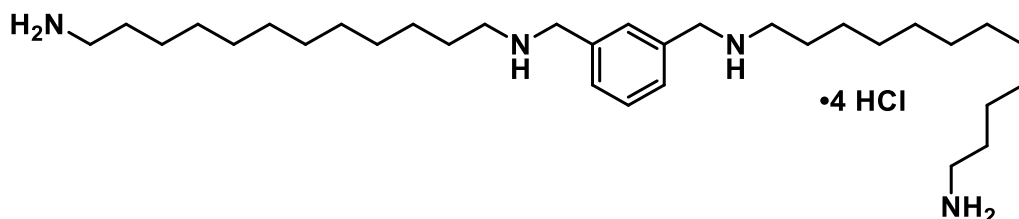
<sup>1</sup>H NMR (500 MHz, D<sub>2</sub>O + CD<sub>3</sub>OD) δ 7.53 (s, 10H), 4.24 (s, 4H), 3.04 (t, *J* = 8.5 Hz, 4H), 1.77-1.70 (m, 4H), 1.42-1.28 (m, 16 H). <sup>13</sup>C NMR (125 MHz, D<sub>2</sub>O + CD<sub>3</sub>OD) δ 131.0, 129.8, 129.6, 129.3, 50.9, 47.0, 29.2, 29.1, 28.7, 26.2, 25.7.

**CZ-01-013: *N*<sup>1</sup>-(3-Methoxybenzyl)dodecane-1,12-diamine, hydrochloride salt:**

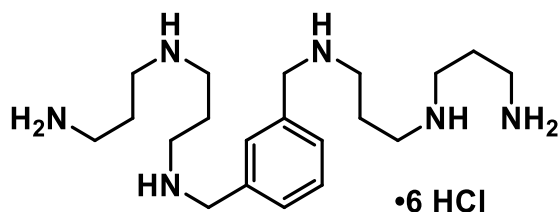
<sup>1</sup>H NMR (500 MHz, D<sub>2</sub>O) δ 7.40 (t, *J* = 8.0 Hz, 1H), 7.06 (s, 1H), 7.05 (s, 1H), 7.03 (s, 1H), 4.16 (s, 2H), 3.82 (s, 3H), 3.00-2.93 (m, 4H), 1.66-1.58 (m, 4H), 1.32-1.22 (m, 16H). <sup>13</sup>C NMR (125 MHz, D<sub>2</sub>O) δ 158.4, 131.5, 129.8, 121.6, 114.5, 114.3, 54.7, 49.8, 46.1, 38.7, 27.8, 27.7, 27.4, 25.9, 24.8, 24.5.



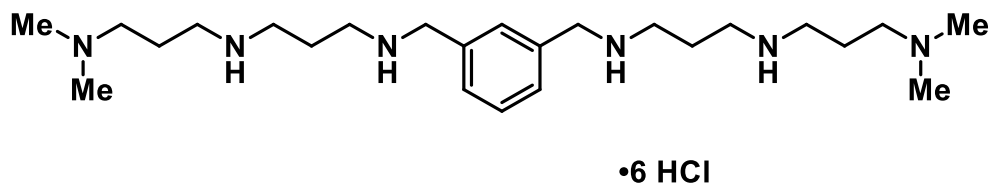
**CZ-01-016:** *N*<sup>1</sup>-(3-Aminopropyl)-*N*<sup>3</sup>-(3-(benzylamino)propyl)propane-1,3-diamine, hydrochloride salt: <sup>1</sup>H NMR (500 MHz, D<sub>2</sub>O) δ 7.49 (s, 5H), 4.27 (s, 2H), 3.51-3.49 (m, 6H), 3.27-3.14 (m, 6H), 3.12 (t, *J* = 8.0 Hz, 2H), 2.21-2.10 (m, 4H). <sup>13</sup>C NMR (125 MHz, D<sub>2</sub>O) δ 130.5, 130.0, 130.0, 129.5, 51.4, 45.3, 45.2, 43.9, 43.2, 36.6, 27.8, 23.9, 22.8.



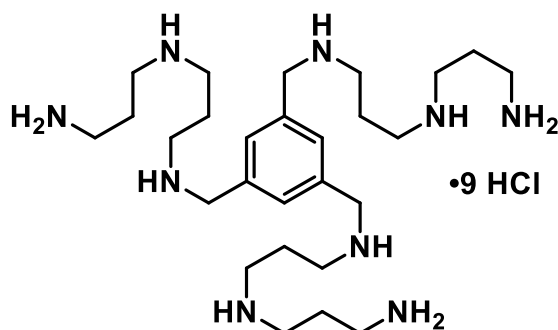
**CZ-01-021:** *N*<sup>1</sup>,*N*<sup>1'</sup>-(1,3-Phenylenebis(methylene))bis(dodecane-1,12-diamine), hydrochloride salt: <sup>1</sup>H NMR (500 MHz, D<sub>2</sub>O) δ 7.65 (s, 3H), 4.36 (s, 4H), 3.11 (t, *J* = 8.0 Hz, 4H), 3.06 (t, *J* = 7.5 Hz, 4H), 1.77-1.68 (m, 8H), 1.47-1.33 (m, 32H). <sup>13</sup>C NMR (125 MHz, D<sub>2</sub>O) δ 130.4, 129.9, 129.7, 128.9, 49.0, 45.6, 38.2, 27.3, 27.3, 27.2, 27.1, 26.9, 26.8, 25.4, 24.4, 24.3, 24.0. Calculated for C<sub>32</sub>H<sub>62</sub>N<sub>4</sub> m/z 503.5 [M+H]<sup>+</sup>, Obsd.503.5.



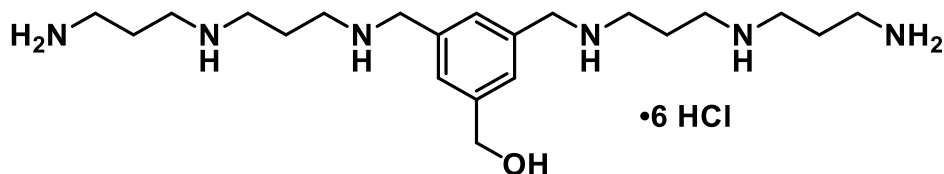
**CZ-01-025:** *N*<sup>1</sup>,*N*<sup>1'</sup>-(1,3-phenylenebis(methylene))bis(*N*<sup>3</sup>-(3-aminopropyl)propane-1,3-diamine), hydrochloride salt: <sup>1</sup>H NMR (500 MHz, D<sub>2</sub>O) δ ppm 7.62 (s, 4H), 4.36 (s, 4H), 3.28-3.21 (m, 12H), 3.15 (t, *J* = 8.0 Hz, 4H), 2.23-2.11 (m, 8H). <sup>13</sup>C NMR (125 MHz, D<sub>2</sub>O) 131.4, 131.3, 131.1, 130.2, 50.8, 44.7, 44.6, 44.1, 36.5, 23.6, 22.6. Calculated for C<sub>20</sub>H<sub>40</sub>N<sub>6</sub> m/z 365.3 [M+H]<sup>+</sup>, Obsd. 365.3.



**CZ-01-043:** *N*<sup>1</sup>,*N*<sup>1'</sup>-(((1,3-Phenylenebis(methylene))bis(azanediyl))bis(propane-3,1-diyl))bis(*N*<sup>3</sup>,*N*<sup>3</sup>-dimethylpropane-1,3-diamine), hydrochloride salt: <sup>1</sup>H NMR (500 MHz, D<sub>2</sub>O) δ 7.57 (s, 4H), 4.31 (s, 4H), 3.28-3.14 (m, 16H), 2.91 (s, 12H), 2.20-2.10 (m, 8H). <sup>13</sup>C NMR (125 MHz, D<sub>2</sub>O) δ 132.1, 131.9, 131.8, 130.9, 54.8, 51.5, 45.3, 45.1, 44.8, 43.5, 23.3, 21.9.

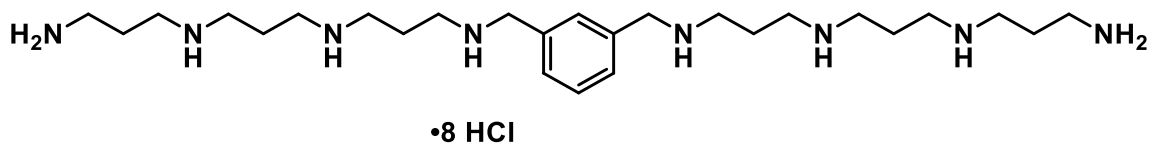


**CZ-01-052:** *N*<sup>1</sup>,*N*<sup>1'</sup>,*N*<sup>1''</sup>-(benzene-1,3,5-triyltris(methylene))tris(*N*<sup>3</sup>-(3-aminopropyl)propane-1,3-diamine), hydrochloride salt: <sup>1</sup>H NMR (500 MHz, D<sub>2</sub>O) δ 7.74 (s, 3H), 4.41 (s, 6H), 3.30 (t, *J* = 7.5 Hz, 6H), 3.24 (q, *J* = 9.0 Hz, 12H), 3.16 (t, *J* = 8.0 Hz, 6H), 2.26-2.12 (m, 12H). <sup>13</sup>C NMR (125 MHz, D<sub>2</sub>O) δ 132.7, 132.6, 50.5, 44.7, 44.6, 44.3, 36.5, 23.7, 22.7. LRMS calculated for C<sub>27</sub>H<sub>57</sub>N<sub>9</sub> *m/z* 508.5 [M+H]<sup>+</sup>, Obsd.508.5.



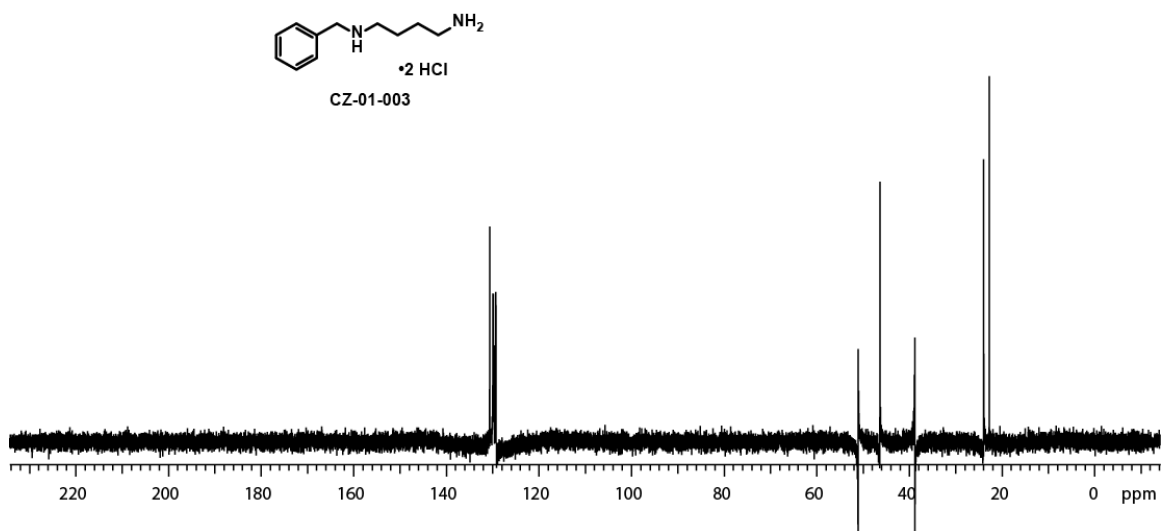
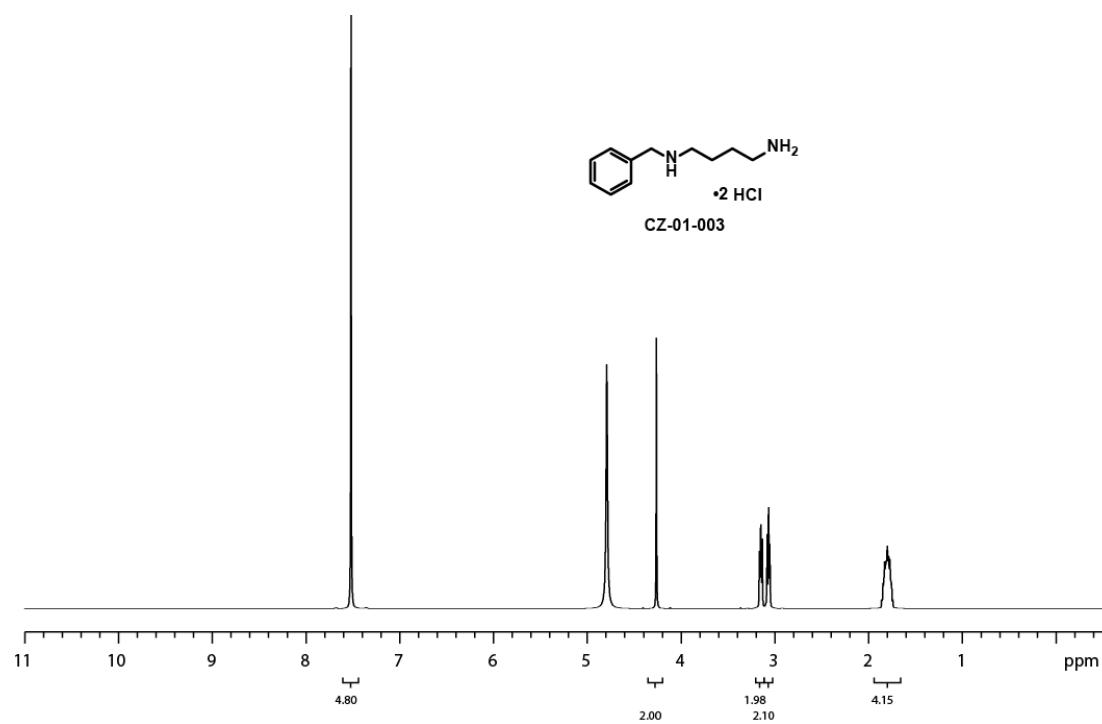
**CZ-01-053: (3,5-Bis(((3-((3-aminopropyl)amino)propyl)amino)methyl)phenyl)**

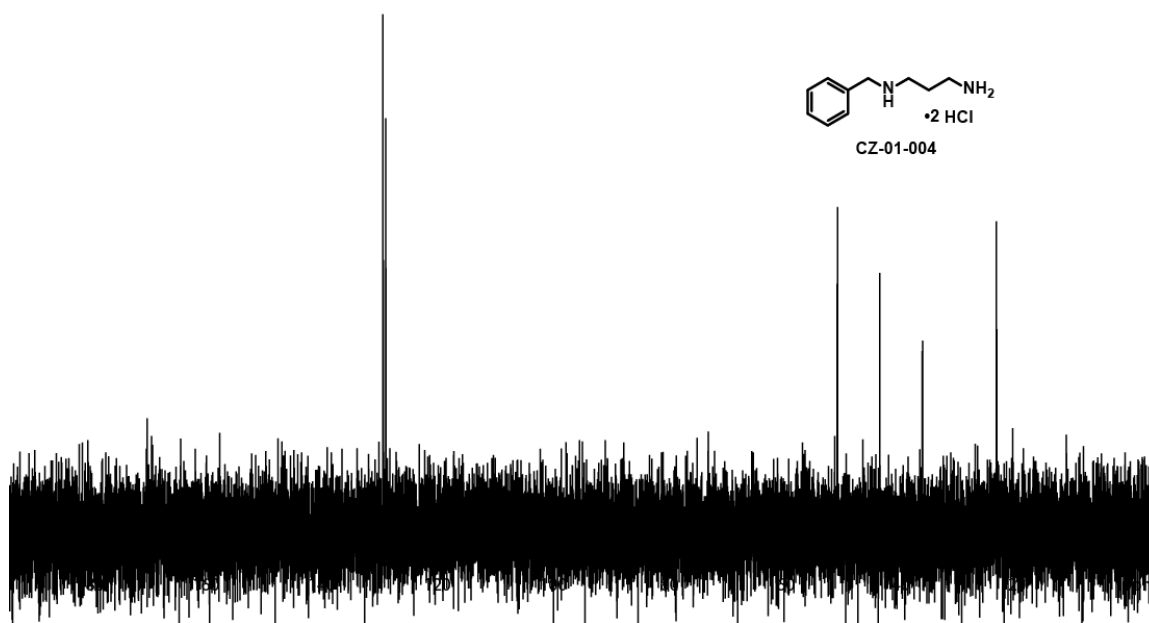
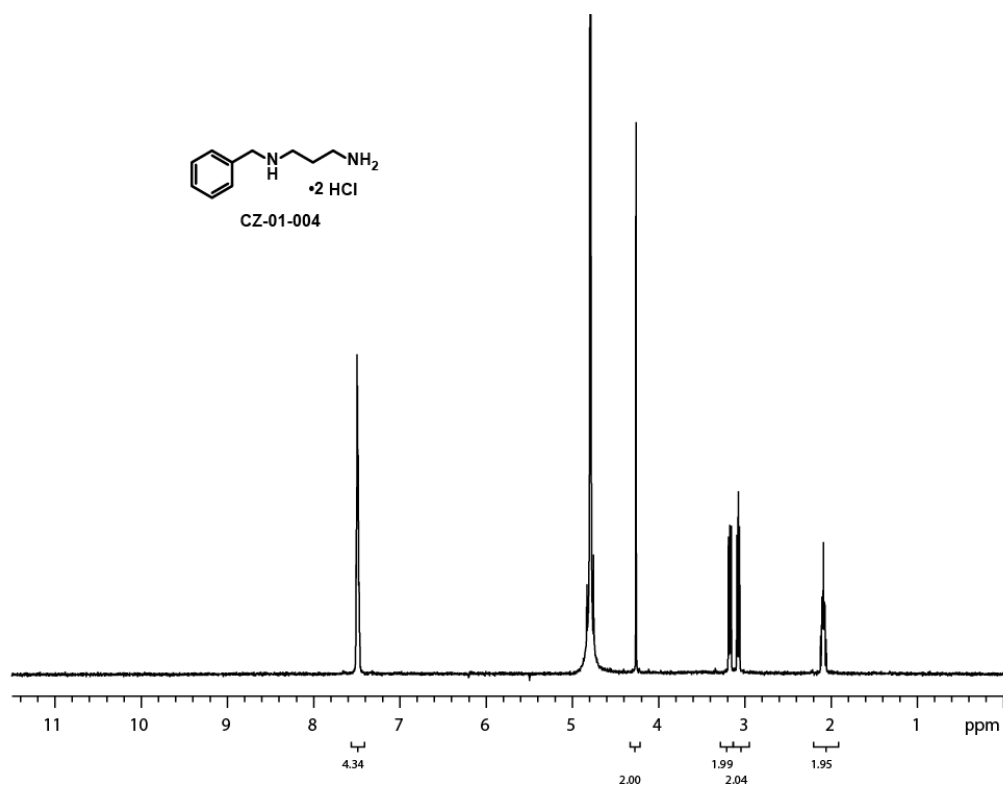
**methanol, hydrochloride salt:**  $^1\text{H}$  NMR (500 MHz,  $\text{D}_2\text{O}$ )  $\delta$  7.57 (s, 2H), 7.55 (s, 1H), 4.72 (s, 2H), 4.35 (s, 4H), 3.26-3.19 (m, 12H), 3.13 (t,  $J = 7.5$  Hz, 4H), 2.21-2.09 (m, 8H).  $^{13}\text{C}$  NMR (125 MHz,  $\text{D}_2\text{O}$ )  $\delta$  142.8, 132.0, 130.7, 130.0, 63.2, 51.0, 44.9, 44.8, 44.4, 36.7, 23.9, 22.9.

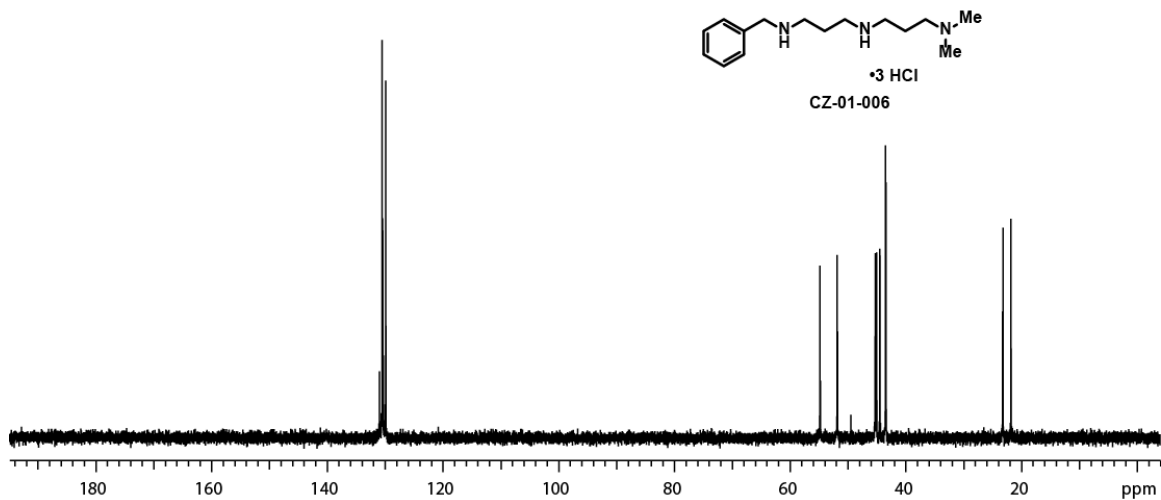
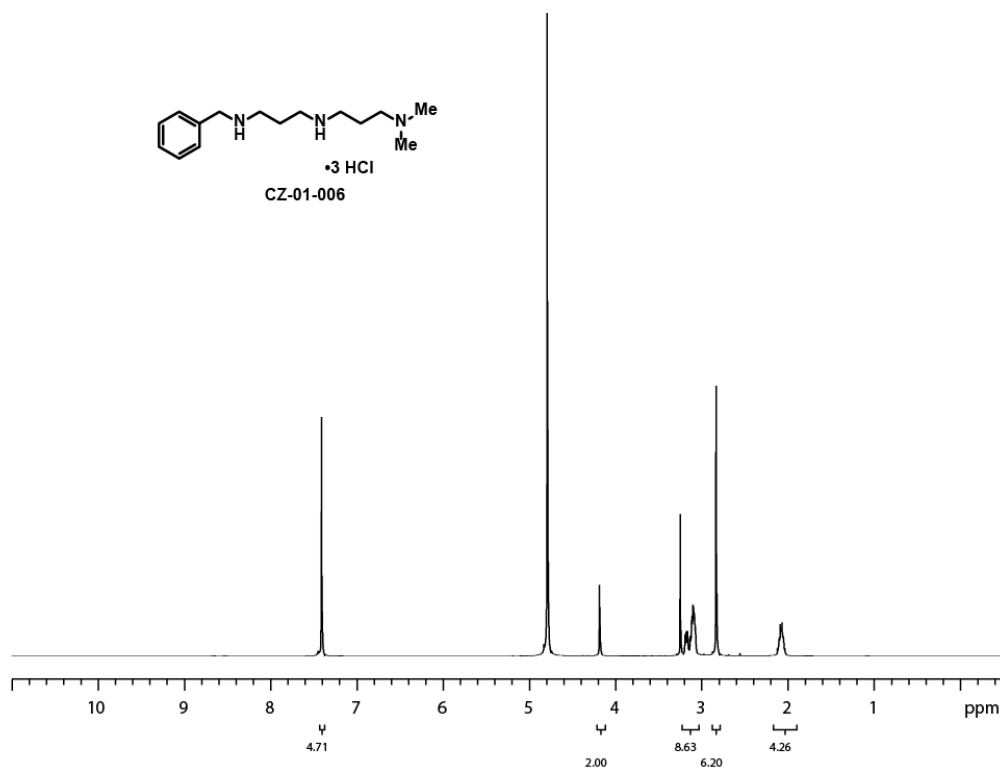


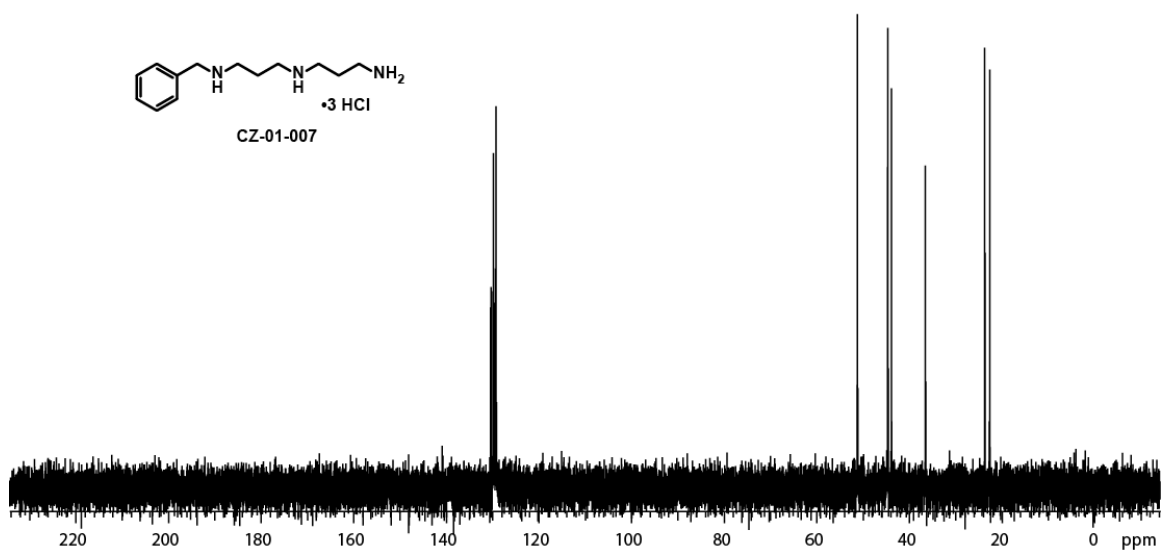
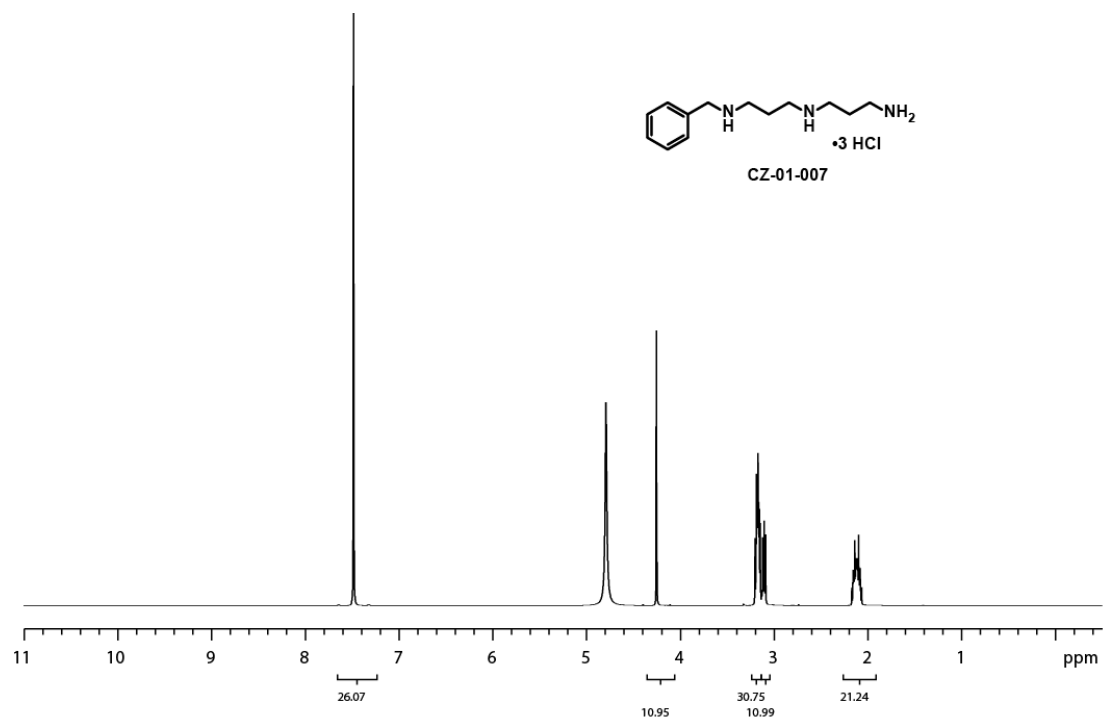
**CZ-01-057:**  $N^1, N^{1'}\text{-(1,3-Phenylenebis(methylene))bis}(N^3\text{-(3-((3-aminopropyl)amino)propyl)propane-1,3-diamine})$ , **hydrochloride salt:** LRMS calculated for  $\text{C}_{26}\text{H}_{54}\text{N}_8$   $m/z$  479.4  $[\text{M}+\text{H}]^+$ , Obsd.479.4.

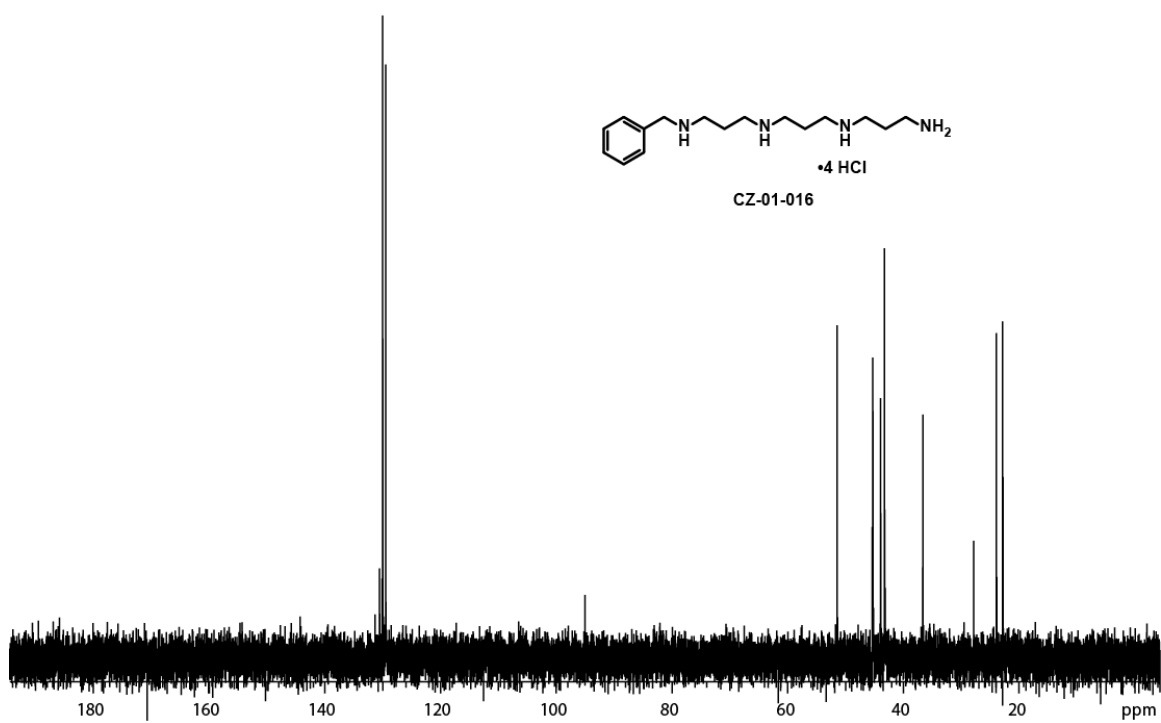
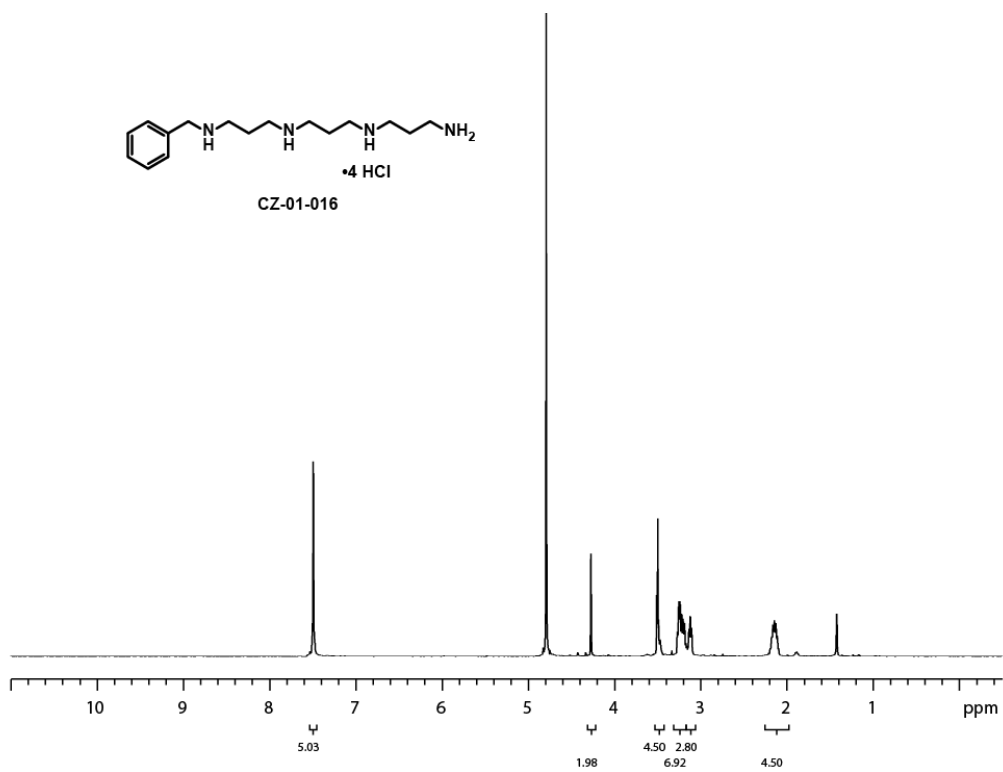


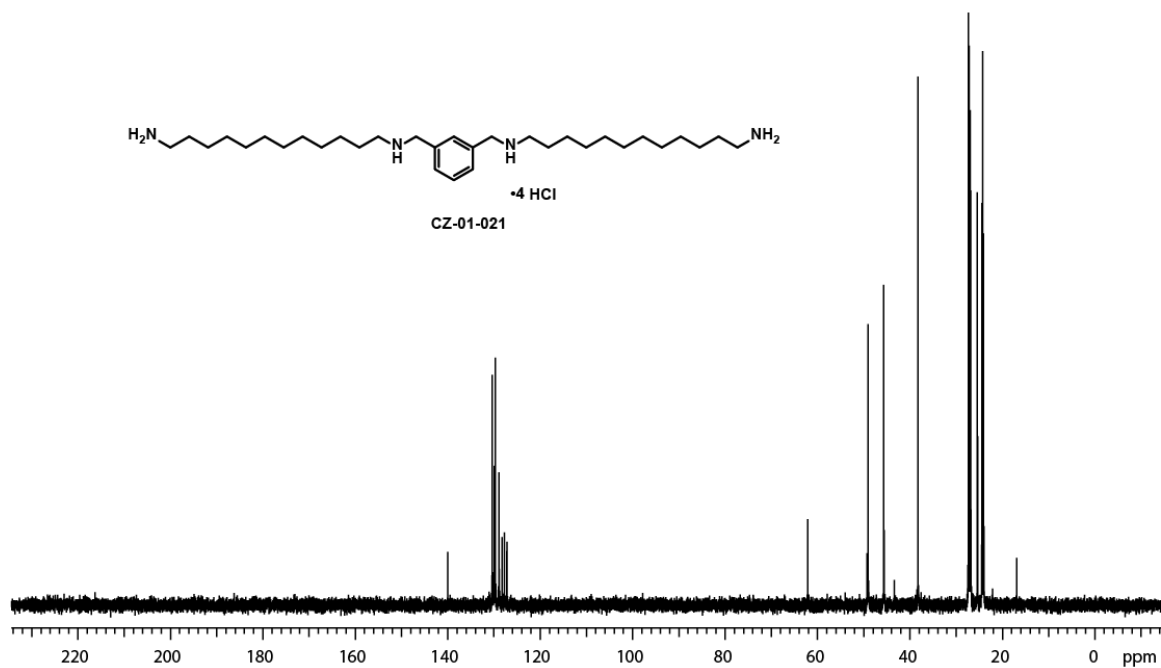
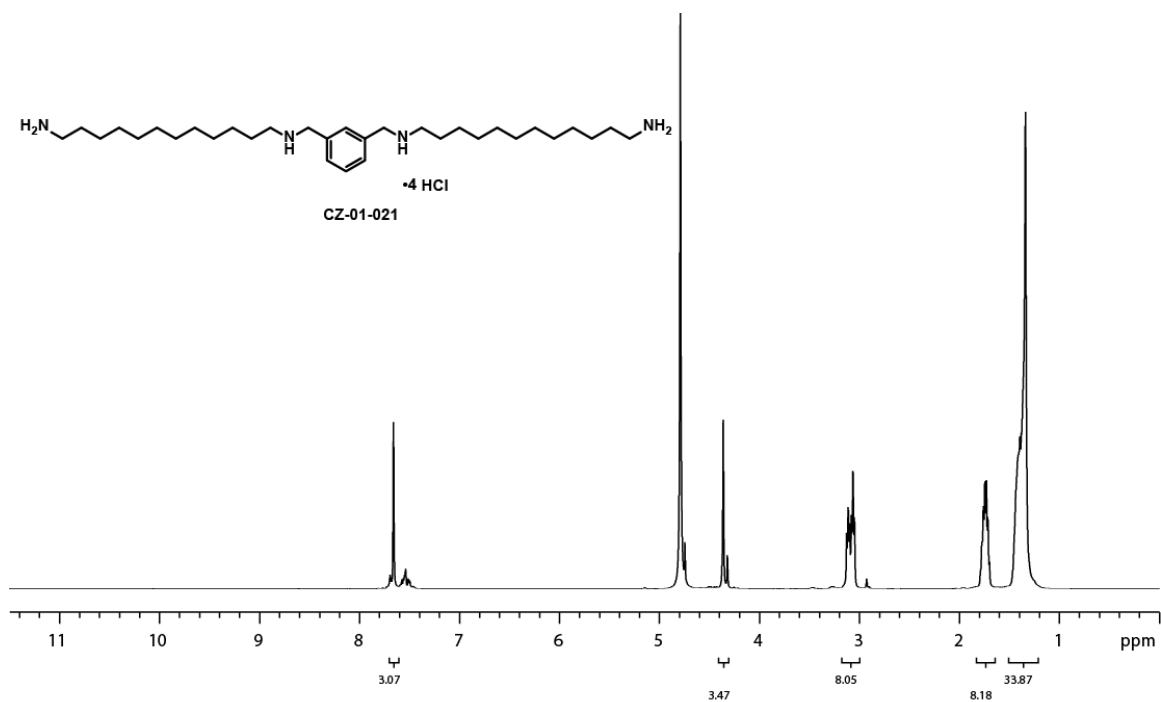
2.8.4 Representative  $^1\text{H}$  NMR and  $^{13}\text{C}$  NMR

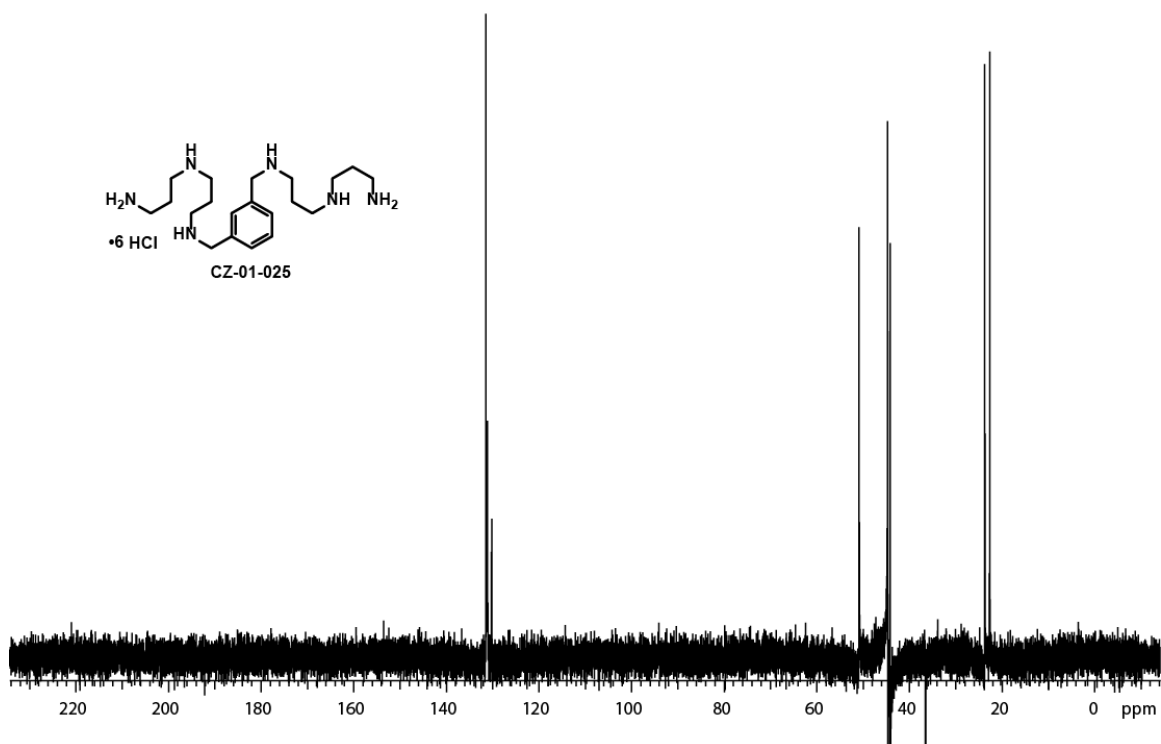
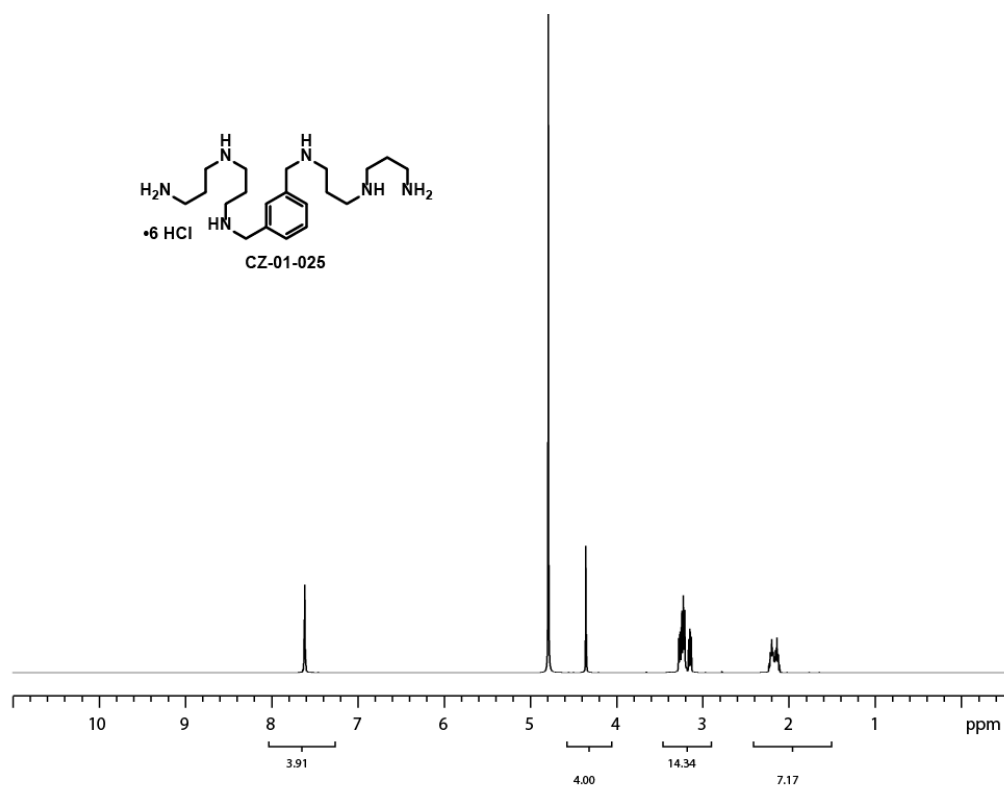


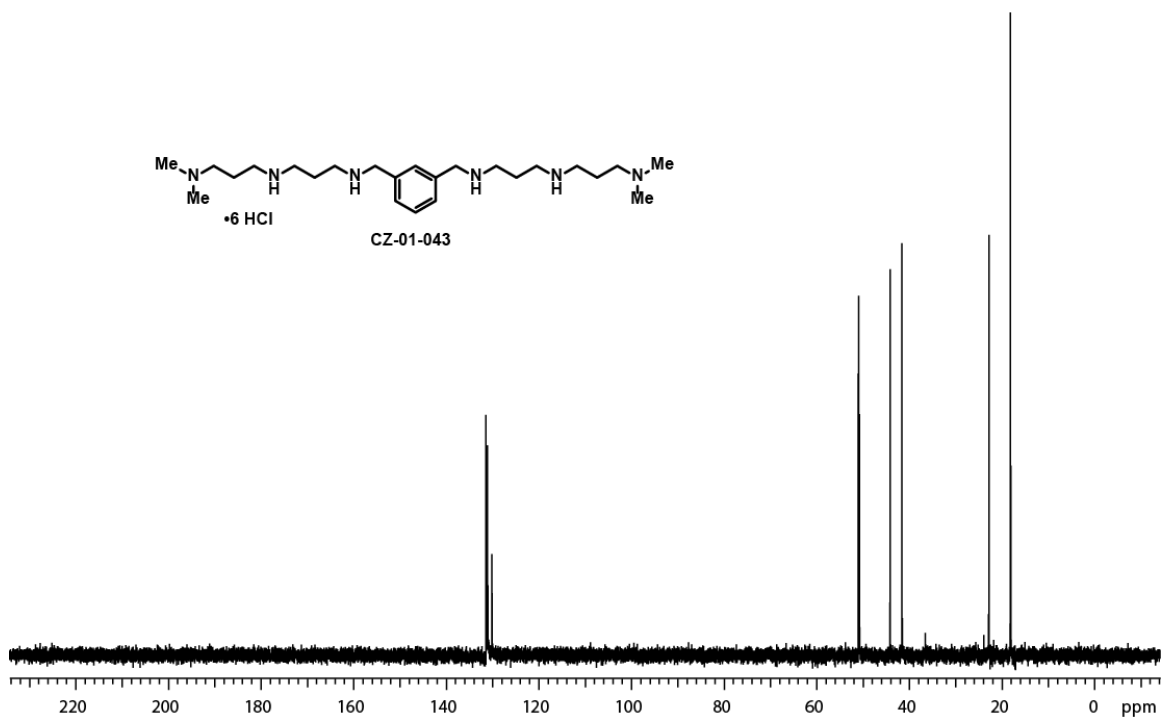
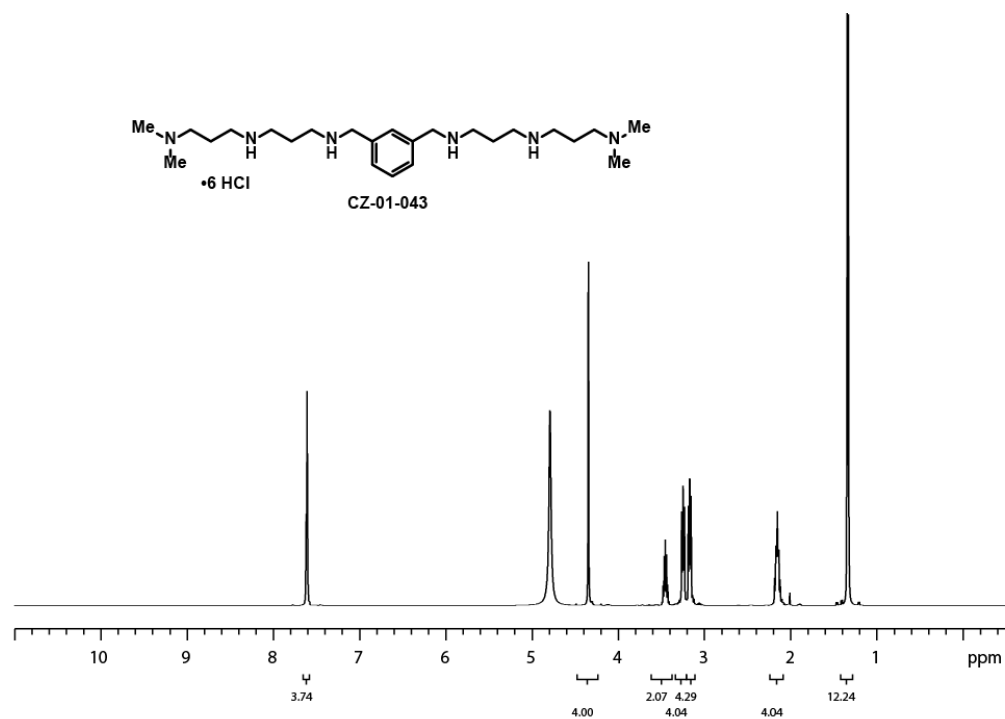




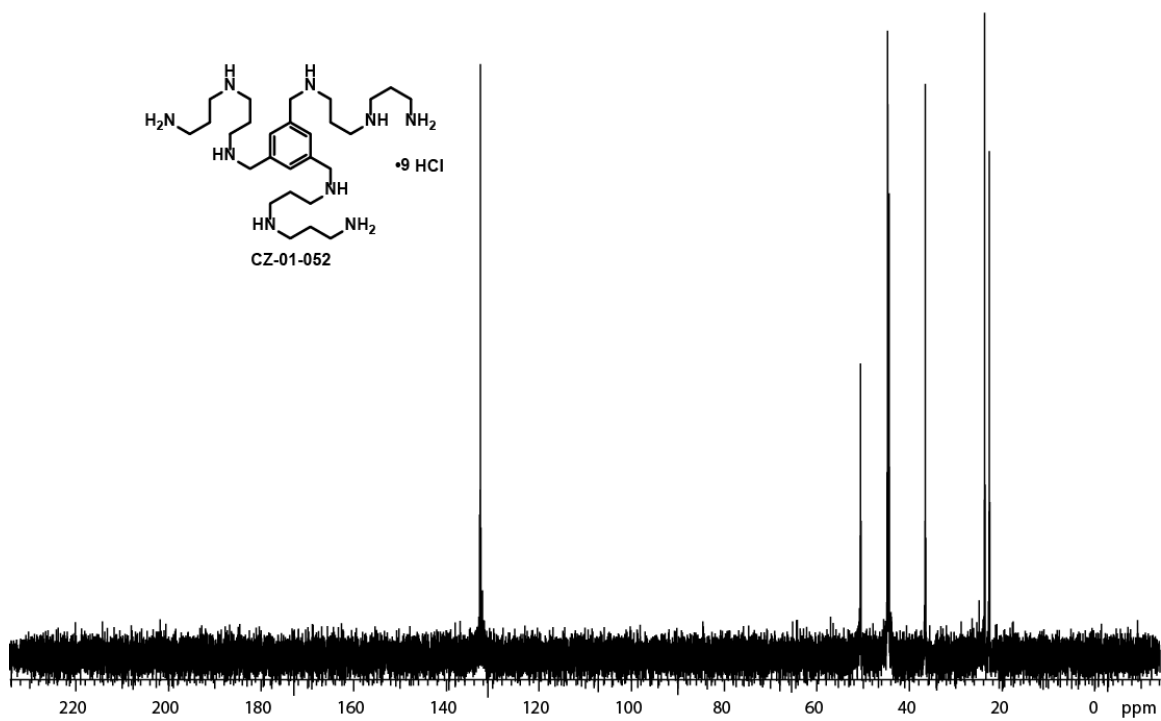
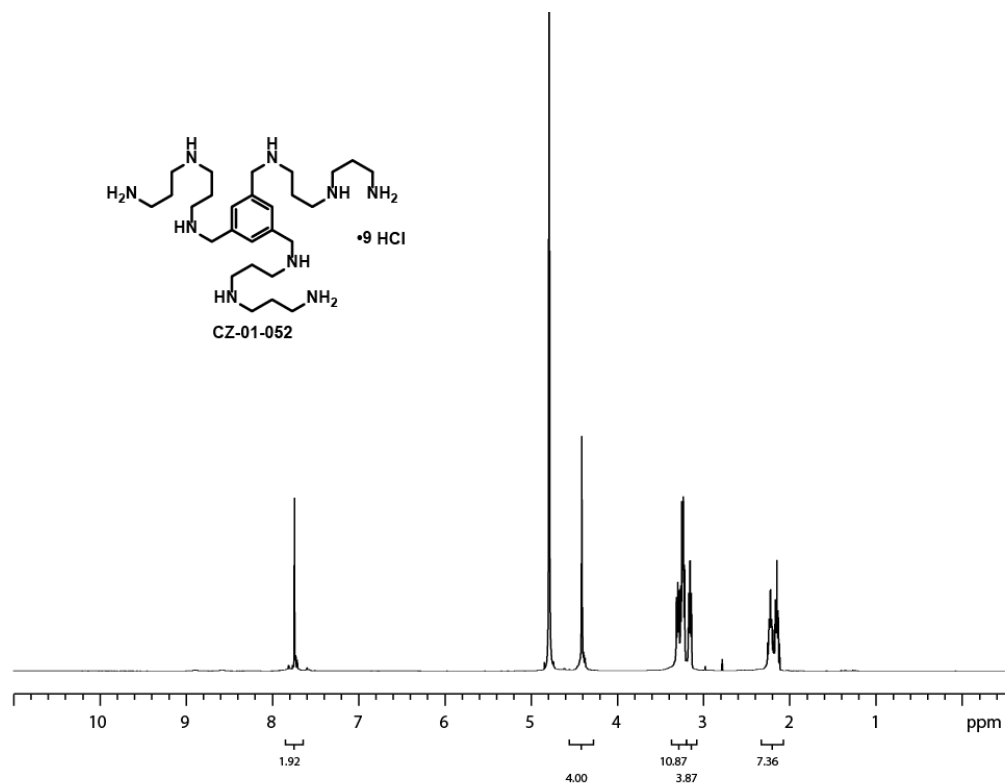


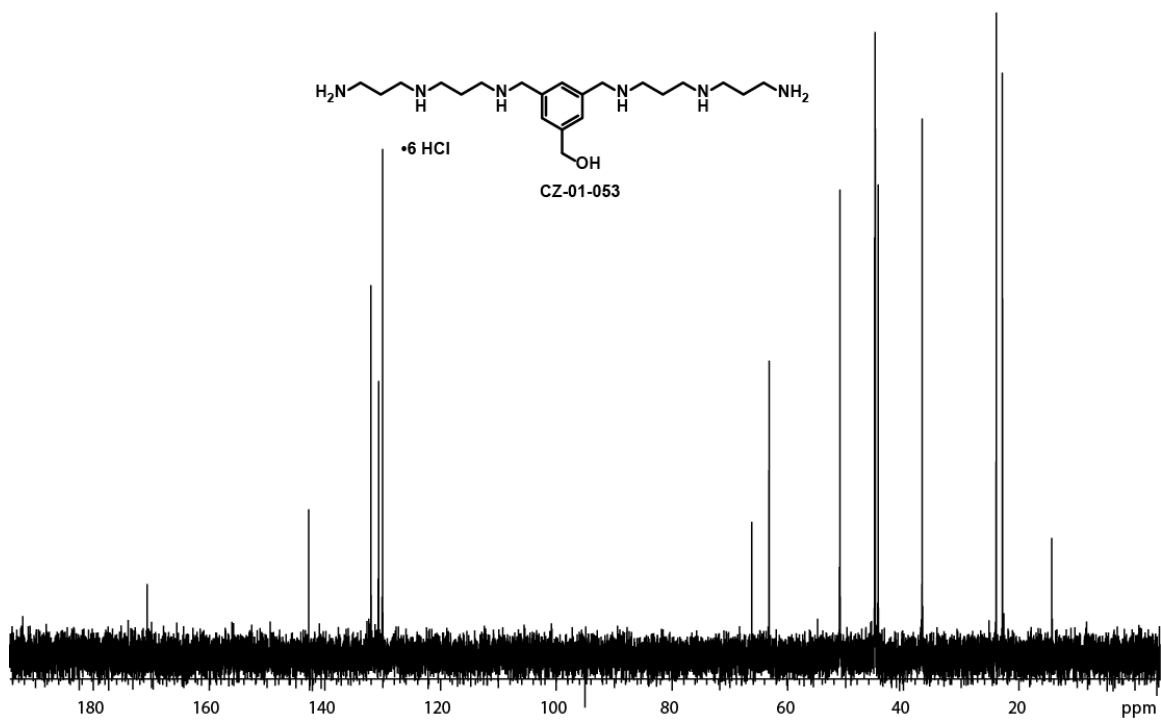
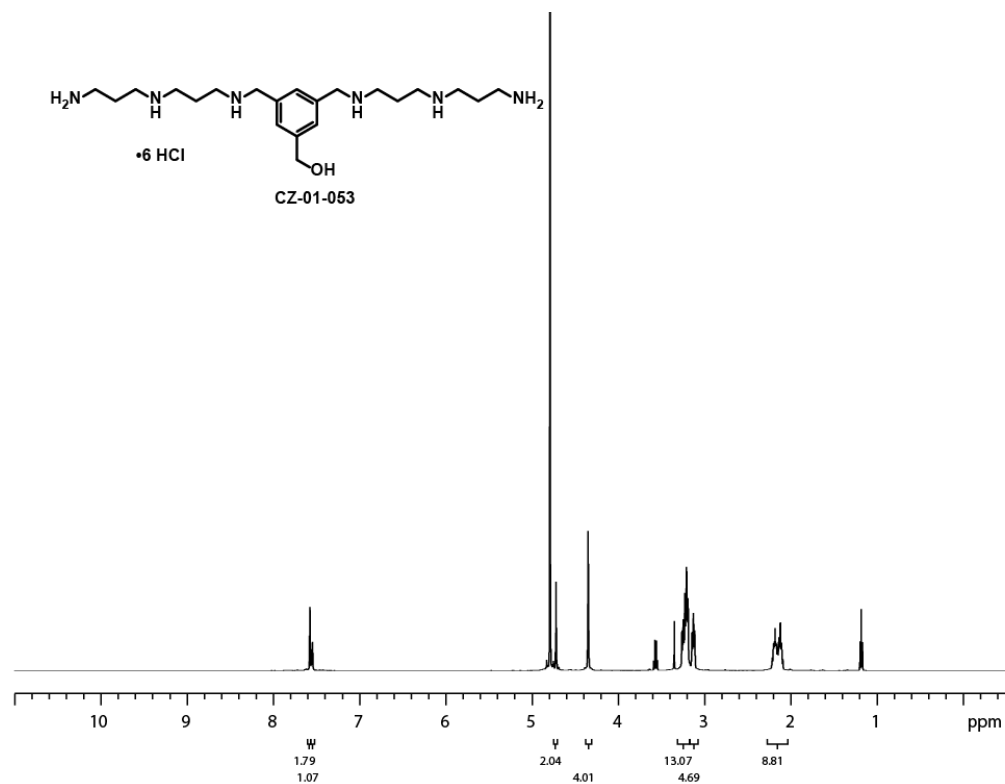












## 2.9 References

1. Goldsworthy, P. D.; McFarlane, A. C. Howard Florey, Alexander Fleming and the Fairy Tale of Penicillin. *Med. J. Aust.* **2002**, *176*, 176-178.
2. For comprehensive reports see: (a) *Antibiotic Resistance Threats in the United States, 2013*; U.S. Department of Health and Human Services, Centers for Disease Control and Prevention: Atlanta, GA, 2013. (b) *Antimicrobial Resistance Surveillance in Europe 2013*; European Centre for Disease Prevention and Control: Stockholm, Sweden, 2013.
3. Walsh, C. T. Where Will New Antibiotics Come From? *Nat. Rev. Microbiol.* **2003**, *1*, 65-70.
4. For an extensive up to date review see: Fisher, J. F.; Meroueh, S. O.; Mobashery, S. Bacterial Resistance to  $\beta$ -Lactam Antibiotics: Compelling Opportunism, Compelling Opportunity. *Chem. Rev.* **2005**, *105*, 395-424.
5. For an extensive up to date review see: Scholar, E. M. Fluoroquinolones: Past, Present and Future of a Novel Group of Antibacterial Agents. *Am. J. Pharm. Educ.* **2003**, *66*, 164-172.
6. For an extensive up to date review see: Chopra, I.; Roberts, M. Tetracycline Antibiotics: Mode of Action, Applications, Molecular Biology, and Epidemiology of Bacterial Resistance. *Microbiol. Mol. Biol. Rev.* **2001**, *65*, 232-260.
7. For an extensive up to date review see: Zuckerman, J. M. Macrolides and ketolides: azithromycin, clarithromycin, telithromycin. *Infect. Dis. Clin. N. Am.* **2004**, *18*, 621-649.
8. For extensive up to date reviews see: (a) Pirri, G.; Giuliani, A.; Nicoletto, S. F.; Pizzuto, L.; Rinaldi, A. C. Lipopeptides as Anti-infectives: a Practical Perspective. *Cent. Eur. J. Biol.* **2009**, *4*, 258-273. (b) Straus, S. K.; Hancock, R. E. W. Mode of Action of the New Antibiotic for Gram-positive Pathogens Daptomycin: Comparison with Cationic Antimicrobial Peptides and Lipopeptides. *Biochim. Biophys. Acta.* **2006**, *1758*, 1215-1223.
9. Zobell, C. E. The Influence of Solid Surface upon the Physiological Activities of Bacteria in Seawater. *J. Bacteriol.* **1937**, *33*, 86.
10. Zobell, C. E. The Effect of Solid Surfaces upon Bacterial Activity. *J. Bacteriol.* **1943**, *46*, 39-56.
11. For comprehensive reviews see: (a) Dufour, D.; Leung, V.; Lévesque, C. M. Bacterial Biofilm: Structure, Function, and Antimicrobial Resistance. *Endod. Topics* **2012**, *22*, 2-16. (b) Costerton, J. W.; Cheng, K. J.; Geesey, G. G.; Ladd, T. I.; Nickel, J. C.; Dasgupta, M.; Marrie, T. J. Bacterial Biofilms in Nature and Disease. *Ann. Rev. Microbiol.* **1987**, *41*, 435-464.

12. For general information about biofilms see: Center for Biofilm Engineering. Center for Biofilm Engineering: Biofilm Research and Education Relevant to Industry, Health, and the Environment. <https://www.biofilm.montana.edu/> (accessed Apr 25, 2015).
13. Geesey, G. G.; Richardson, W. T.; Yeomans, H. G.; Irvin, R. T.; Costerton, J. W. Microscopic Examination of Natural Sessile Bacterial Populations from an Alpine Stream. *Can. J. Microbio.* **1977**, *23*, 1733-1736.
14. Marshall, K. C.; Stout, R.; Mitchell, R. Mechanisms of the Initial Events in the Sorption of Marine Bacteria to Surfaces. *J. Gell. Microbiol.* **1971**, *68*, 337-348.
15. Rickard, A. H.; Palmer, R. J. Autoinducer 2: A Concentration-dependent Signal for Mutualistic Bacterial Biofilm Growth. *Mol. Microbiol.* **2006**, *60*, 1446-1456.
16. For a comprehensive review on mixed species biofilms see: Elias, S.; Banin, E. Multi-species Biofilms: Living with Friendly Neighbors. *FEMS Microbiol. Rev.* **2012**, *36*, 990-1004.
17. Beech, I. B.; Sunner J. A.; Hiraoka, K. Microbe-surface Interactions in Biofouling and Biocorrosion Processes. *Int. Microbiol.* **2005**, *8*, 157-168.
18. For a comprehensive review on industrial biofouling see: Flemming, H. C. Microbial Biofouling: Unsolved Problems, Insufficient Approaches, and Possible Solutions. *Biofilm Highlights* **2011**, *5*, 81-110.
19. Neria-González, I.; Wang, E. T.; Ramírez, F.; Romero, J. M.; Hernández-Rodríguez, C. Characterization of Bacterial Community Associated to Biofilms of Corroded Oil Pipelines from the Southeast of Mexico. *Anaerobe* **2006**, *12*, 122-133.
20. Klahre, J.; Flemming H. C. Monitoring of Biofouling in Papermill Water Systems. *Wat. Res.* **2000**, *34*, 3657-3665.
21. McGinley, H. R. *Glutaraldehyde Uses and Counterfeits*; Dow Chemical Company: Midland, MI, 2012; 30-32.
22. May, R. M.; Hoffman, M. G.; Sogo, M. J.; Parker, A. E.; O'Toole, G. A.; Brennan, A. B.; Reddy, S. T. Micro-patterned Surfaces Reduce Bacterial Colonization and Biofilm Formation in vitro: Potential for Enhancing Endotracheal Tube Designs. *Clin. Transl. Med.* **2014**, *3*, 1-9.
23. Donlan, R. M.; Murga, R.; Bell, M.; Toscano, C. M.; Carr, J. H.; Novicki, T. J.; Zuckerman, C.; Corey, L. C.; Miller, J. M. Protocol for Detection of Biofilms on Needleless Connectors Attached to Central Venous Catheters. *J. Clin. Microbiol.* **2001**, *39*, 750-753.
24. For select examples see: (a) Maki, D. G.; Stolz, S. M.; Wheeler, S.; Mermel L. A.

Prevention of Central Venous Catheter-related Bloodstream Infection by use of an Antiseptic-impregnated Catheter. A Randomized, Controlled Trial. *Ann. Intern. Med.* **1997**, *127*, 257-266. (b) Raad, I.; Darouiche, R.; Hachem, R.; Mansouri, M.; Bodey, G. P. The Broad-spectrum Activity and Efficacy of Catheters Coated with Minocycline and Rifampin. *J. Infect. Dis.* **1996**, *173*, 418-424.

25. Costerton, J. W.; Stewart, P. S.; Greenberg, E. P.; Bacterial Biofilms: A Common Cause of Persistent Infections. *Science* **1999**, *284*, 1318-1322.

26. For an extensive review on Cystic Fibrosis see: Rowe, S. M.; Miller, S.; Sorscher, E. J. Cystic Fibrosis. *N. Engl. J. Med.* **2005**, *252*, 1992-2001.

27. Flume, P. A.; Mogayzel, P. J.; Robinson, K. A.; Goss, C. H.; Rosenblatt, R. L.; Kuhn, R. J.; Marshall, B. C. Cystic Fibrosis Pulmonary Guidelines. *Am. J. Respir. Crit. Care Med.* **2009**, *180*, 802-808.

28. Lam, J.; Chan, R. Lam, K.; Costerton, J. W. Production of Mucoïd Microcolonies by *Pseudomonas aeruginosa* Within Infected Lungs in Cystic Fibrosis. *Infect. Immun.* **1980**, *28*, 546-556.

29. Davies, D. G.; Parsek, M. R.; Pearson, J. P.; Iglewski, B. H.; Costerton, J. W.; Greenberg, E. P. The Involvement of Cell-to Cell Signals in the Development of a Bacterial Biofilm. *Science* **1998**, *280*, 295-298.

30. James, G. A.; Swogger, E.; Wolcott, R.; Pulcini, E. D.; Secor, P.; Sestrich, J. Biofilms in Chronic Wounds. *Wound Repair Regen.* **2008**, *16*, 37-44.

31. Madsen, S. M.; Westh, H.; Danielsen, L.; Rosdahl, V. T. Bacterial Colonization and Healing of Venous Leg Ulcers. *APMIS* **1996**, *104*, 895-899.

32. For a review on quorum sensing see: Waters, C. M.; Bassler, B. L. Quorum Sensing: Cell-to-cell Communication in Bacteria. *Annu. Rev. Cell Dev. Biol.* **2005**, *21*, 319-346.

33. Kolodkin-Gal, I.; Cao, S.; Böttcher, T.; Kolter, R.; Clardy, J.; Losick, R. A Self-produced Trigger for Biofilm Disassembly that Targets Exopolysaccharide. *Cell* **2012**, *149*, 684-692.

34. Böttcher, T.; Kolodkin-Gal, I.; Kolter, R.; Losick, R.; Clardy, J. Synthesis and Activity of Biomimetic Biofilm Disruptors. *J. Am. Chem. Soc.* **2013**, *135*, 2927-2930.

35. Hobley, L.; Kim, S. H.; Maezato, Y.; Wyllie, S.; Fairlamb, A. H.; Stanley-Wall, N. R.; Michael, A. J. Norspermidine is Not a Self-produced Trigger for Biofilm Disassembly. *Cell* **2014**, *156*, 844-854.

36. Moore, K. S.; Wehrl, S.; Roder, H.; Rogers, M.; Forrest Jr., J. N.; McCrimmon, D.; Zasloff, M. Squalamine: An Aminosterol Antibiotic from the Shark. *Proc. Natl. Acad. Sci.*

**1993**, 90, 1354-1358.

37. Hao, D.; Hammond, L. A.; Eckhardt, S. G.; Patnaik, A.; Takimoto, C. H.; Schwartz, G. H.; Goetz, A. D.; Tolcher, A. W.; McCreery, H. A.; Mamun, K.; Williams, J. I.; Holroyd, K. J.; Rowinsky, E. K. A Phase I and Pharmacokinetic Study of Squalamine, an Aminosterol Angiogenesis Inhibitor. *Clin. Cancer. Res.* **2003**, 9, 2465-2471.

38. For select examples see: (a) Li, C.; Budge, L. P.; Driscoll, C. D.; Willardson, B. M.; Allman, G. W.; Savage, P. B. Incremental Conversion of Outer-Membrane Permeabilizers into Potent Antibiotics for Gram-negative Bacteria. *J. Am. Chem. Soc.* **1999**, 121, 931-940. (b) Lai, X.; Feng, Y.; Pollard, J.; Chin, J. N.; Rybak, M. J.; Bucki, R.; Epand, R. F.; Epand, R. M.; Savage, P. B. Ceragenins: Cholic Acid-based Mimics of Antimicrobial Peptides. *Acc. Chem. Res.* **2006**, 41, 1233-1240. (c) Ding, B.; Taotofa, U.; Orsak, T.; Chadwell, M.; Savage, P. B. Synthesis and Characterization of Peptide-cationic Steroid Antibiotic Conjugates. *Org. Lett.* **2004**, 6, 3433-3436.

39. Déziel, E.; Comeau, Y.; Villemur, R. Initiation of Biofilm Formation by *Pseudomonas aeruginosa* 57RP Correlates with Emergence of Hyperpiliated and Highly Adherent Phenotypic Variants Deficient in Swimming, Swarming, and Twitching Motilities. *J. Bacteriol.* **2001**, 183, 1195-1204.

40. Amarego, W. L. F.; Chai, C. L. L. *Purification of Laboratory Chemicals*. 6th ed.; Elsevier Inc.: Burlington, MA, 2009.

**CHAPTER 3**

**SYNTHESIS OF *N,N'* ALKYL AND DIALKYL POLYAMINES**

**WITH RESPECT TO THEIR APPLICATION**

**IN THE SYNTHESIS OF**

**CZ-01 COMPOUNDS**

**3.1 Background**

Polyamines are an important class of organic molecules that contain two or more amine functional groups. The polyamines spermidine, spermine, and putrescine (Figure 3.1) play an intrinsic role by regulating growth and cellular differentiation.<sup>1</sup> It is not surprising that upon addition of these polyamines in vitro, a variety of cellular responses are elicited as these highly cationic molecules are very promiscuous, binding with nucleic acids, proteins, and phospholipids.<sup>2</sup>

For years, polyamines have served as clinically relevant molecules and are currently being evaluated for use as chemotherapeutics,<sup>3</sup> antimalarials,<sup>4</sup> biomimetics,<sup>5</sup> pesticides,<sup>6</sup> and antihuman immunodeficiency virus (HIV) retrovirals (Figure 3.2).<sup>7</sup> Norspermidine, for example, has been shown to have significant antiproliferative activity against a number of cancer cell lines, not limited to L1210 leukemia, 3LL carcinoma, and EL4 lymphoma.<sup>8</sup> Further investigation has revealed several alkyl-polyamine analogs are effective anti-neoplastic agents. In particular, *N*<sup>1</sup>,*N*<sup>11</sup>-diethylnorspermine was selected to proceed forward in Phase IIa clinical trials for metastatic breast cancer.<sup>9</sup>

As a ubiquitous source of polyamines, eukaryotic cells have been studied extensively to determine the role of polyamines in malignant disease. Elevated levels of polyamines have been observed in patients suffering from leukaemias, melanomas, adenocarcinomas and lymphomas. Further diagnostic studies have shown that patients in remission had a clinically comparable polyamine concentration to normal individuals. Additionally, when patients suffered from a tumor recurrence, polyamine levels once again became elevated<sup>10</sup>.

Russell and Snyder first observed a connection between increased polyamine synthesis and cellular growth in 1968. They reported that with high levels of ornithine decarboxylase (ODC), the enzyme responsible for forming the polyamine putrescine (1,4 diamino butane) from ornithine, tumor production increased and growth of tissues including rat liver and chick embryo were observed.<sup>11</sup> In addition, there are a number of exogenous chemical promoters of ODC, including UV light and asbestos; these agents are often implicated in carcinogenesis.<sup>12</sup>

Given the above phenomena one can conclude that there is a link between polyamines and cancer. Further investigation of polyamine adducts could have beneficial therapeutic results.

Polyamines are vital for prokaryotic function as well. Recently, polyamines have been shown to be important in siderophore biosynthesis, swarming, and biofilm formation. Clardy and Losick were able to demonstrate that norspermidine could disrupt biofilm formation in *Bacillus subtilis*; yet minimal changes in the polyamine structure increased the minimum biofilm inhibitory concentration (MBIC) 10-100 fold.<sup>13</sup> This difference was most apparent in the decrease in MBIC by changing the norspermidine to spermidine which features one extra methylene (Figure 3.3).



Polyamines are ubiquitous molecules involved in cellular processes in both prokaryotes and eukaryotes. The current polyamine compounds on the market and in the pipeline have had impacts on drug discovery in the past 60 years and continue to show promise as clinically active compounds.

### **3.2 DFMO: An Inhibitor of Ornithine Decarboxylase**

The link between heightened levels of polyamine content leading to excessive cellular proliferation has been presented in the literature for over 40 years. Researchers used this phenomenon to develop a series of ODC inhibitors in the late 1970's at the Merrell Research Institute. At the time, this research was developed in efforts to produce novel, viable treatments for cancer and other diseases. The molecule DFMO (Figure 3.2) was prepared by Merrell shortly thereafter.<sup>14</sup>

The molecule DFMO has had the most noteworthy impact on polyamine research in the past 5 decades. Although clinically DFMO has failed to advance as an anticancer agent, its ability to inhibit ornithine decarboxylase (ODC) makes it unique. Over time, DFMO has found successful clinical uses as both an antiprotozoal drug and as an active agent in reducing excessive facial hair growth on women.<sup>15</sup>

DFMO and other ODC inhibitors have been reported to prevent tumor formation and growth in experimental models of breast, colon, bladder, and skin carcinogenesis.<sup>16</sup> One clinical breast cancer study showed that increased ODC activity is loosely linked with decreased survival rates.<sup>16</sup> Furthermore, a number of studies have shown that high levels of ODC activity are observed in several forms of colonic polyps. When left untreated, these unwanted cellular growths can develop into colorectal cancer.<sup>17</sup>

Given their role in cellular processes, ODC activity and polyamine formation has been

implicated in a number of carcinogenic polyp cases. In 1993, Gerner and coworkers identified a link between ODC activity and colon cancer. When ODC activity and polyamine content was examined in 48 benign polyps and 18 malignant colorectal cancers (five of which were malignant polyps), they found that these growths had elevated ODC activity.<sup>17</sup>

Unfortunately, initial clinical studies on DFMO yielded several side effects including abdominal pain, diarrhea, moderate anemia, and thrombocytopenia.<sup>18</sup> Shortly thereafter, American biologist Cyrus Bacchi tested DFMO in a murine trypanosomiasis model and found that DFMO cured *Trypanosoma brucei* without any related acute mouse toxicity.<sup>19</sup> Further clinical trials supported these early results, and in 1990, DFMO was approved for its use in the treatment of African sleeping sickness. Currently, DFMO is the only treatment for Melarsoprol resistant strains.<sup>20,21</sup>

### 3.3 AMD 3100

The polyamine AMD 3100 (Figure 3.2) was first developed by AnorMED and subsequently bought by Genzyme. It is more commonly referred to as Plerixafor. AMD 3100 was initially valued as an anti-HIV drug but since has been evaluated as an immunostimulant after patients receive heavy doses of chemotherapy.<sup>22</sup>

In 1985, several polyoxometalates (spherical polyanionic compounds with strong metal affinity) were developed to treat HIV by inhibiting cell replication through inhibition of reverse transcriptase.<sup>23</sup> These compounds had an extremely promising in vitro profile, but were never pursued clinically due to their administration protocols (systemic IV). However, a number of researchers recognized large organo-porphyrins and porphyrin like compounds also represented a diverse and underrepresented class of metal coordination

complexes and could be designed to have a similar mechanism of action as the polyoxometalates. The cyclams were chosen as a starting point, given the cyclic arrangement of 4 nitrogen atoms and their known affinity for metal ions. Synthetic manipulations were made on a series of cyclam like compounds, including JMS1657 and JMS2763, and structure activity relationships led De Clercq to produce AMD3100 (chronologically labeled as JM3100 as shown in Figure 3.4) which displayed an excellent in vitro profile ( $EC_{50}$  against HIV-1(III<sub>B</sub>) = 3 nM).<sup>22, 23</sup>

Unlike most polyamines AMD3100 can be prepared readily from commercially available cyclam **1**. Phosphonation of three of the four nitrogens afforded the phosphorotriamide **2** (Scheme 3.1). The protected cyclam **2** was bis-alkylated with 1,4-bis(bromomethyl)benzene to produce the protected AMD3100 (**3**). Hydrolysis with 3M HCl then completed the synthesis yielding the HCl salt of AMD3100 in a three-step one-pot sequence with good yields.<sup>24</sup>

Despite its promising in vitro profile, AMD3100 was eventually withdrawn from HIV testing due to unforeseen problems that led test subjects to develop cardiac disturbances, including rhythm disorders in Phase I trials. Shortly thereafter, subsequent testing revealed that AMD3100 was a potent CXCR4 receptor antagonist. This discovery led to the development of AMD3100 as an effective recruitment therapy for hematopoietic stem cells. Consequently, AMD3100 could be used to mobilize hematopoietic stem cells from the bone marrow to the bloodstream after a patient received high-dose myeloablative chemotherapy (method of cancer treatment used to kill cells in the bone marrow).<sup>22</sup>

The new indication led AMD3100 to another round of clinical trials whereby a more promising in vivo profile was uncovered. AMD3100 was approved for the above therapy

in 2008 and is currently used for treating patients undergoing this form of chemotherapy.<sup>22</sup>

Given the structure of the polyamine compounds synthetically prepared by the Looper group (Chapters 2 and 4) it is worth noting some of the pharmacokinetic data for AMD3100. The original clinical study on this molecule showed adverse cardiac effects, however, when the dose was limited (40-320  $\mu\text{g/kg}$ ) in the haemotopoietic stem cell trial no reports of cardiac arrhythmias were noted.<sup>22</sup> The active pharmaceutical ingredient (API) is cleared at a rate of 4.9 L/h and has a half-life of 3.7-4.7 h. Further analysis revealed that the peak plasma concentration is 750-1020 ng/mL and the time required to reach peak levels is approximately 1 h. AMD3100 represents a unique class of polycationic molecules which are bioavailable with an adequate half-life. Given its unique structure and limited toxicity, AMD3100 represents precedence for the Looper group polyamines as they are carried forward for animal studies.<sup>25</sup>

### 3.4 $N^1,N^{11}$ -diethylnorspermine

The polyamine  $N^1,N^{11}$ -diethylnorspermine (Figure 3.2) has shown a great deal of promise as an active chemotherapeutic agent. Given the rich polyamine pool intrinsic to cellular growth, cellular mimics like  $N^1,N^{11}$ -diethylnorspermine may hold the key to impeding cell proliferation. These unnatural polyamines amass inside the cell and decrease the amount of natural polyamines in the cell cycle. This cellular imbalance prevents cell growth and differentiation and eventually leads to cell death.<sup>1b</sup>

When tested clinically,  $N^1,N^{11}$ -diethylnorspermine was found to have limited toxicity, in dogs at doses of 12.5, 25, and 50 mg/kg. Phase I human trials determined IV doses of 25 mg/m<sup>2</sup>/day to be safe after five consecutive dosing days. Furthermore, the maximum tolerated dose was found to be 185 mg/m<sup>2</sup>/day.<sup>26</sup> When the drug was administered in a

preliminary phase II clinical trial, the in vivo phase I toxicological data were validated at the doses administered but no significant efficacy was seen in a 16 person metastatic breast cancer cohort.<sup>9</sup>

Despite its setbacks,  $N^1,N^{11}$ -diethylnorspermine shows very promising in vitro activity and a good toxicological profile. Further adjustment of the chemical via structure activity relationship studies could provide a more potent and equally safe compound, despite its regression in clinical trials.

### 3.5 Synthesis of Unnatural Polyamines

Despite their trivial structure, functionalization of any of these polyamines is synthetically challenging. Literature searches have revealed several ways to amend this problem, however, to the best of our knowledge, methods to produce these synthetically modified polyamines are limited and typically protecting group intensive as well as impractical for large scale synthesis as they require multiple column chromatography steps for purification.

#### 3.5.1 *Woster and Casero's Synthesis of Unnatural Spermine*

##### *Derivatives*

Woster, Casero, and coworkers published an exhaustive protecting group strategy to address this problem while constructing norspermine analogs in 1993. Although their synthesis demonstrates the tenacity to tackle a challenging problem, they are heavily reliant on classical protection and deprotection strategies and limited to purifying intermediates via column chromatography as shown in Scheme 3.2. Starting from diaminopropane **4**, a selective reductive amination based on precedent by Bergeron afforded the mono-benzyl

amine **5**.<sup>27</sup> Protection of **5** produced the corresponding mesityl diamine **6**. Nucleophilic addition of the secondary amine onto 3-bromo-propyl-phthalimide yielded the fully protected triamine **7**, which was subsequently used later in the synthesis. Woster and Casero were able to bring in their next piece in a convergent fashion. Starting from ethanaminium chloride **8**, mesityl protection afforded the sulfone **9**. Alkylation with 1,3 diiodopropane subsequently produced the iodinated alkyl amine **10**. Adding **10** to their previously constructed triamine **7** they were able to afford fully protected tetraamine **11**. Hydrogenation conditions removed the benzyl group to yield the phthalimide **12**. Furnishing the newly formed free amine with another mesityl group afforded **13**. Final removal of the phthalimide with hydrazine produced the fully protected tetraamine **14** whereby only the terminal nitrogen was reactive.<sup>28</sup>

### 3.5.2 Bergeron's Synthesis of Unnatural Spermidine Derivatives

In order to make *N*<sup>1</sup>-ethyl-spermidine **20** Raymond Bergeron at the University of Florida adopted similar chemistry to that of Woster and Casero. Starting from propylamine **15**, mesityl protection produced the protected primary amine **16**. Treatment of the amino-sulfone with 1,4-dibromobutane afforded the alkylated protected amine **17**. Again, adopting a convergent approach this alkylated derivative was used after formation of the protected diamine **18** from diaminopropane **4**. Combining sulfones **18** with **17** under displacement conditions produced the fully protected spermidine derivative **19** which was further deprotected upon acidolysis to afford ethyl spermidine **20** (Scheme 3.3).<sup>29</sup>

### 3.5.3 Uriac and Sinbandhit's Resin Based Synthesis of Norspermidine Derivatives

The groups of Uriac and Sinbandhit used resin chemistry to overcome some of the protecting group problems present in the previous examples. Starting from the Wang resin carbonate **21**, mono-Boc-norspermidine (using a three-step procedure) addition mediated the release of 4-nitro phenol to produce the carbamate **22**. Addition of dansyl chloride provided the fully functionalized polyamine **23**, which was then activated for solid support release. Acid-mediated removal of the carbamate resin as well cleavage of the Boc-protecting group cleanly afforded the mono-alkylated polyamine **24** (Scheme 3.4).<sup>30</sup>

The above examples represent clear indications that a protecting group-free synthesis with minimal synthetic steps would be valuable for making various polyamine analogs. Also avoiding chromatographic purification would be highly advantageous in order to reach industrial process scale.

## 3.6 Preliminary studies

We initially investigated norspermidine as a useful bactericidal agent for treatment of biofilm forming bacteria. Upon our investigation, we found that norspermidine and several other polyamines alone are inactive against most Gram-negative and Gram-positive planktonic strains of bacteria; although they disrupted biofilm formation as Clardy had shown.<sup>13</sup> However, upon attachment of these polyamines to a core structure we were able to significantly increase potency of our bactericidal compounds in both planktonic and biofilm bacteria with dual-fold activity, killing, and dispersing the biofilm (for more information see Chapters 2 and 4).

This phenomena led us to envision a series of bactericidal compounds which could be

utilized in treatment of biofilm related infections (see Chapters 2 and 4). Initial structure activity relationship studies showed that norspermidine attached to a linker molecule, in our case [1,1'-biphenyl]-3,5-dicarbaldehyde or [1,1'-biphenyl]-3,3',5-tricarbaldehyde, had promising activity. The increase in potency was generally tied to an increase in backbone hydrophobicity, so we were led to further modulate the polarity of the side chain. As such, a general decrease in the side chain polarity was met with a further increase in potency and decrease in cytotoxicity (Figure 3.5).

Furthermore, we felt that the primary terminal amine was a metabolic liability, and thus, we turned our attention to a series of alkyl-norspermidines and alkyl-polyamines like those present in  $N^1$ ,  $N^{11}$  diethylnorspermine to avoid these problems.

### 3.7 Looper's Synthesis of Alkyl Polyamine Derivatives

When tested, in initial SAR studies, the CZ-analogs with norspermidine as the side-chain consistently had the lowest MIC. In order to add more hydrophobicity and modularity to our CZ-compounds and remove the unwanted terminal primary amine, a series of terminally alkylated polyamines were envisioned (for naming see Supporting Information). With the precedence outlined above, we felt the synthesis of these compounds, however, would be difficult. Moreover, given that the strategy involved selectively altering one nitrogen on a substrate with three nearly chemically equivalent amines, purification would be inadequate at providing large quantities of research grade material. Initially a Boc-protection of norspermidine **25** was employed in order to protect the terminal primary amine. Excess norspermidine prevented overprotection and yielded the Boc-norspermidine **26** in moderate yields and moderate purity (Scheme 3.5). The excess norspermidine could then be removed by water upon workup. However, upon TLC analysis three distinct spots



could be seen (implicitly assigned as di-Boc-norspermidine, mono-Boc-norspermidine, and norspermidine).  $^1\text{H}$  NMR analysis of this mixture, on the other hand, was only sensitive enough to display the desired product, mono-Boc-norspermidine. Later studies confirmed this fact, and spiking samples with excess byproducts afforded indistinguishable results relative to pure material. This crude material, however, was carried forward in order to produce the final compound.

Following a reductive amination of **26**, we were able to achieve our alkyl norspermidines side chains which required further column purification. Drastic fluctuations in our biological assays led us to the conclusion that, although our final CZ-compounds were empirically pure by NMR, we lacked both the synthetic means and analytical data to provide pure compound consistently. This is exemplified in Table 3.1, whereby the individual batches of **CZ-01-086** (Figure 3.6) yielded significant differences in MIC values ranging from sub-micromolar (batch 1) to greater than 25  $\mu\text{g/mL}$  (batch 9) against planktonic MRSA.

We felt that the adjustment of the above method could benefit us in both reaction purity and reduction of side products as well as aid in the production novel polyamino compounds. With a substantial increase in purity, validation of our biological data could then be assured. Given the low cost and availability of norspermidine, several attempts were made at adjusting the previous strategy to afford analytically pure material.

Given that the structure of norspermidine contains only two primary nitrogens we rationalized that a controlled reductive amination could produce the desired product with a limited amount of side products (Figure 3.7). Fractional vacuum distillation could then be employed to remove any unwanted materials as the di-isobutyl norspermidine derivative

would have a significantly higher boiling point than its mono-isobutyl counterpart. When attempted this strategy was unsuccessful. Qualitative TLC analysis consistently displayed a number of byproducts in roughly equal amounts.

Exploration of reaction conditions as well as various electrophilic alkyl groups proved to be inconsequential (Figure 3.8). After attempting to synthesize the desired product with norspermidine and any number of alkyl halogens, a number of byproducts were observed both by NMR and TLC. Adjustment of molarity, reaction temperature, and molar equivalents was unsuccessful at affording the desired product. We believed that in both cases (alkylation via halide electrophiles and reductive amination) the symmetric terminal amines were competing to produce a mixture of bis-alkyl-norspermidine, mono-alkyl-norspermidine, and unreacted norspermidine and small amounts of other impurities.

We turned our attention to a linear approach in which each amine was introduced selectively, negating the chance of any excess reactivity taking place. 3-amino-1-propanol was chosen as a useful starting material for this process as it met three criteria: 1) the reagent was cheap and readily available in large quantities (>20 kg), 2) the amine group could be synthetically manipulated without effecting the alcohol functionality on the chain. 3) the hydroxyl group acted as a leaving group synthon whereby it could be activated to the bromide, sulfate, or tosylate for displacement.

After screening conditions we found a reductive amination of the pendent amine to the alkylated derivative would provide us with our alkyl amino alcohol. This process is limited in the sense that a reductive amination must be used to provide us with pure material. A borohydride reduction carried out in water then produced the desired alkyl amine (Figure 3.9).

Activation of the alcohol was first attempted via sulfonate formation. Although successful, the sulfonate was inactive to our amine nucleophile in the next step under standard and elevated temperatures.<sup>31</sup> Adjustment of the alcohol to another suitable leaving group was achieved through bromination with HBr. The excess water/HBr was then distilled off to afford the crude HBr salt which was recrystallized with MeOH/ether or *i*-PrOH to yield white crystalline material.<sup>32</sup> The scope of this method is shown in Figure 3.7 where a variety of bromide salts were synthesized. Branched and unbranched alkyl systems were used, as well as cyclic and phenyl substituents. If desired this synthesis can work on a variety of amino-alcohols, as both two-carbon and three-carbon derivatives were produced.

From the alkylated HBr salt, the substrate was now equipped for the final introduction of the remaining diamine. We felt addition of 1,3-diaminopropane to the salt would produce the desired norspermidine derivative under carefully controlled reaction conditions. We expected the addition of low molar equivalents of 1,3 diaminopropane and/or elevated temperatures would produce unwanted byproducts as was observed by TLC when this reaction sequence was performed. To circumvent this problems excess (10-20 equivalents) of 1,3 diaminopropane were used. This worked two-fold, in providing enough base to deprotonate the HBr acid salt, and to severely limit any unwanted formation of any dialkylated norspermidine. The remaining 1,3-diaminopropane was then easily removed by a water wash and vacuum distillation. Vacuum distillation was further employed to purify the final product.

With a successful strategy in hand we chose to make a variety of polyamine derivatives (consisting mostly of the norspermidine backbone) which could be further employed for

SAR studies (Figure 3.10). Functionalities ranged from butyl to octyl and included a variety of substituted alkyl derivatives. The diamines were varied to include 1,4-diaminobutane in order to generate the respective spermidine analogs **42** and **51**.

To further exemplify the utility of this strategy, we subjected a number of our newly formed norspermidine derivatives to a second round of reductive amination (Figure 3.11). Both alkyl and aromatic functional aldehydes were chosen. The compounds produced had very little bactericidal activity, but nonetheless demonstrate the effectiveness of this process.

### 3.8 Conclusion and Future Aims

With the above method we have generated an effective way to functionalize these tri-amine derivatives and are no longer restricted by unsuccessful protecting group strategies and inefficient reaction conditions. Our synthesis is amenable to a number of side chains and can be completed on large scale (>100 g) with the only purification method being distillation and/or recrystallization.

The difficulty of synthetically deriving these polyamino compounds in high purity is evidenced by the examples shown above (Section 3.5). Although the manipulation of these compounds seemed trivial, they impart a great deal of synthetic forethought. In our pursuit of a large scale synthesis of these alkylated polyamines minor impurities caused variations in the MIC of the final product. The synthesis derived from this mitigated these impurities, used simple starting materials, and allowed for facile purification by either distillation and/or recrystallization. Although the alkylations of amines by substitution reactions on alkyl halides are notorious for yielding multiple products and poor yields, we have found our method to be selective for the formation of mono-alkylated products and any

dialkylated species are purified upon distillation.

Expansion of this chemistry is of great importance to producing more analogs and narrowing down pertinent structure activity relationships. We would further like to explore chemistry through several avenues in order to rationally design more functionalized molecules.

Functionalization of the diethylmalonate system would be a useful tool to expand and investigate novel systems with different substitution patterns (Scheme 3.6). Starting from diethylmalonate, simple di-enolization followed by nucleophilic addition would produce the mono (not shown) and dialkylated products. Reduction of the pendant esters followed by an activation/substitution sequence should afford the uniquely substituted diaminopropane compound which could be further employed in our current chemistry.

We realized that our modular approach was somewhat limited in the aldehyde used during the initial reductive amination. Literature searches have exposed a limited supply of readily available aldehydes, which has significantly hindered SAR studies. A side chain synthesis whereby we could tune the functionality of any group terminus as well as adjust the overall length could be used in synthesizing a number of analogs. A brief look through the literature has led us to chemistry done by the Hrabálek group shown in Scheme 3.7.<sup>33</sup> With this in mind, we can modulate our above synthetic route to bring in aldehydes of varying chain lengths and terminal substitution patterns. Scheme 3.7 exemplifies this as an *n*-membered lactone is converted to the corresponding sodium salt. The terminal bromide is then replaced with a variety of alkyl Grignard's reagents, followed by the oxidation to produce the fully functionalized aldehyde.

The motuporamines are a small class of polyamine natural products. These polyamines

have shown promising anti-invasive and antiangiogenic activity.<sup>34</sup> Given their simple structure and biological profile we feel a facile synthesis using the methods described above could deliver these compounds in a short synthetic sequence.

Starting from the amino alcohol, conditions facilitating intramolecular alkylation would produce the desired 13-membered ring. Using the bromination chemistry described above would yield the HBr salt, which upon treatment with 1,3-diaminopropane would afford the natural product, motuporamine A (Scheme 3.8).

The above examples represent important underexplored problems which the Looper lab would like to address in the future. Further amendment of our “side-chain” chemistry has the potential to provide more active and safer antimicrobial compounds. The chemistry we have developed has allowed us to access a significant number of norspermidine and polyamine analogs in a linear sequence with the abolishment of column chromatography. These reactions can be completed on kg-scale and are clean, efficient, and high yielding.

Table 3.1: Batch Variability Data for **CZ-01-086**

<b>CZ-01-086</b> Batch	MIC ( $\mu\text{g}/\text{mL}$ )
1	0.9
2	15
3	13
4	>15
5	<1
6	6
7	>12
8	>16
9	>25

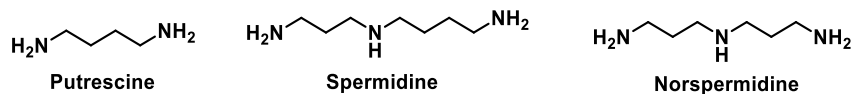


Figure 3.1: Select naturally occurring polyamines

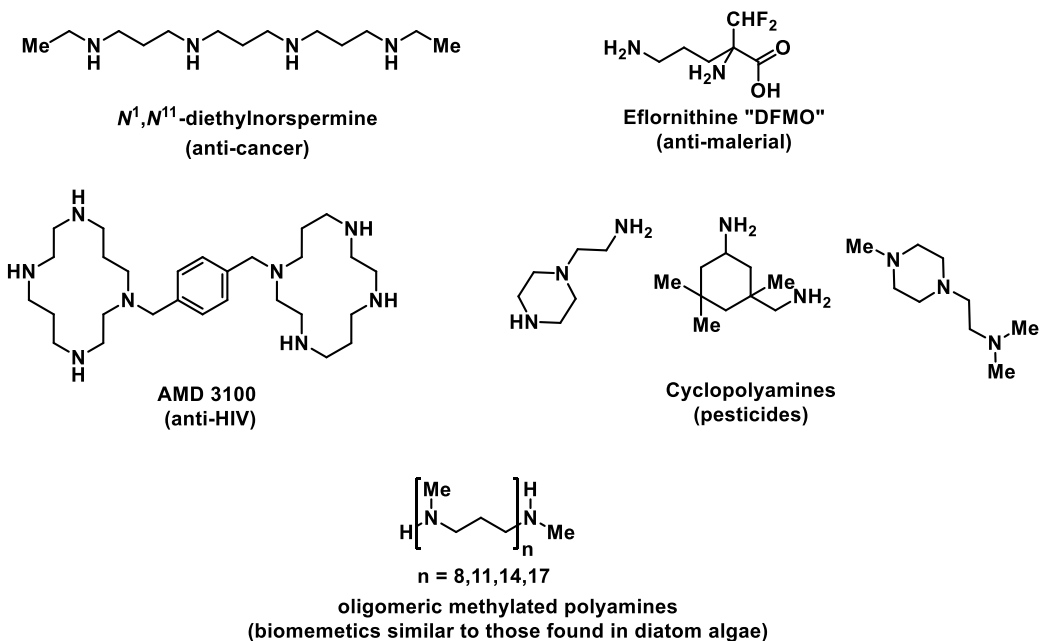


Figure 3.2: Select examples of polyamines used in medical and industrial applications

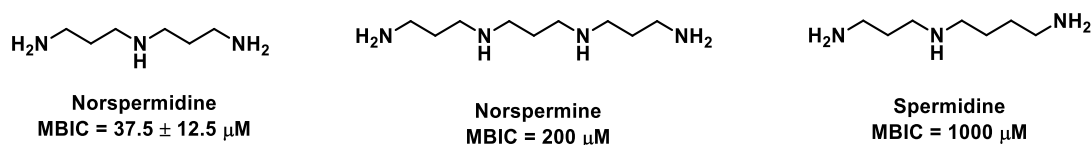


Figure 3.3: Comparative MBIC analysis shown by Clardy and Losick

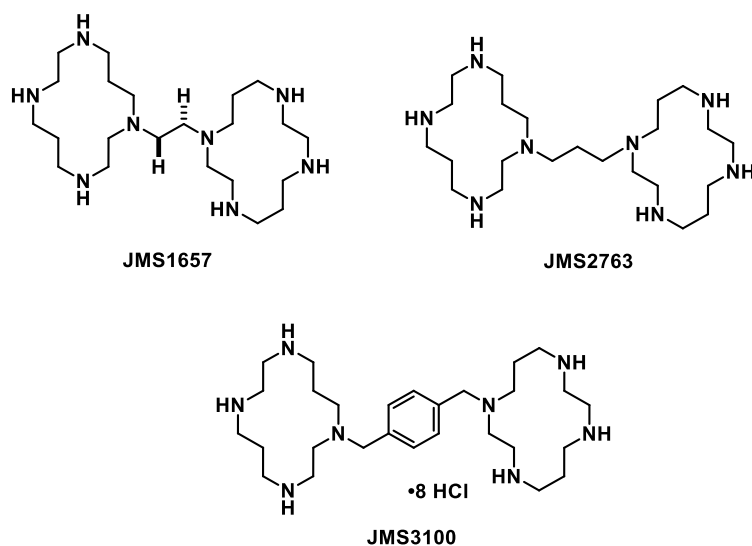


Figure 3.4: Representative polyamines from the AMD-series

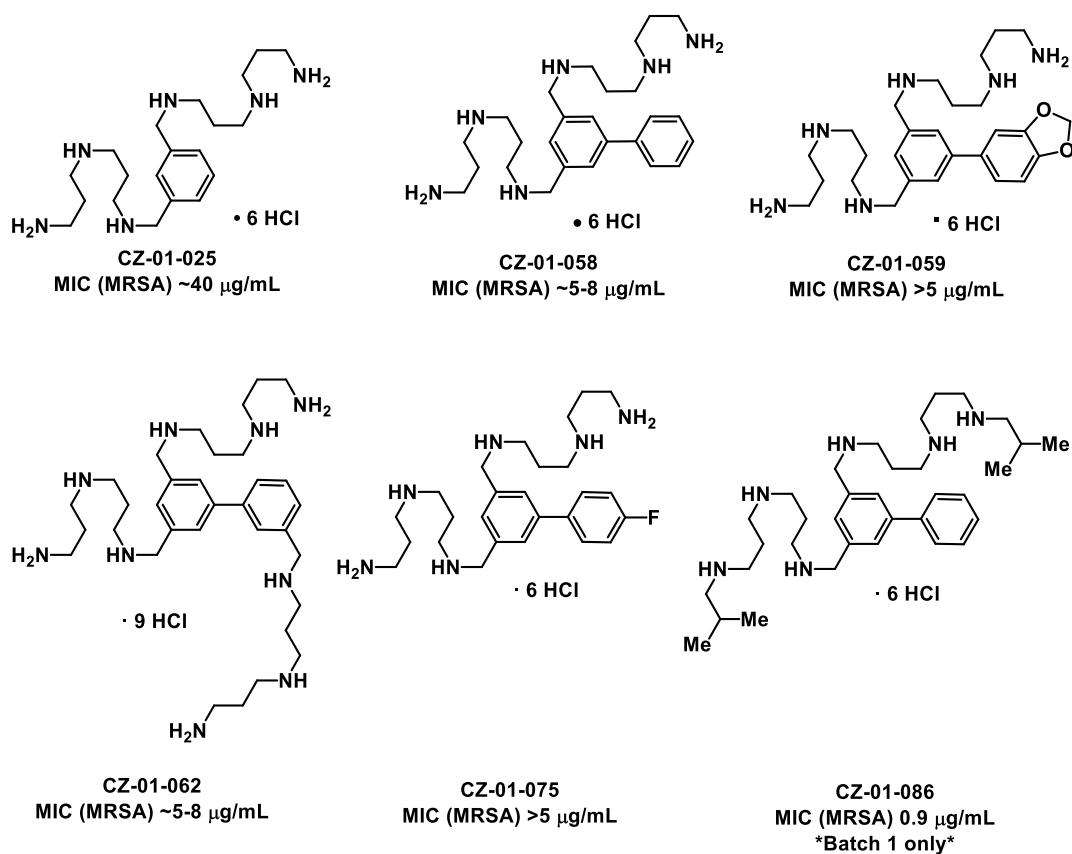


Figure 3.5: Select analogs with the norspermidine and alkyl norspermidine side-chain



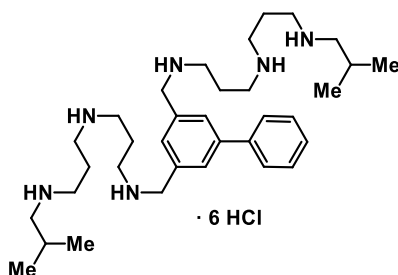


Figure 3.6: The structure of biocide **CZ-01-086**, synthesized with isobutyl norspermidine

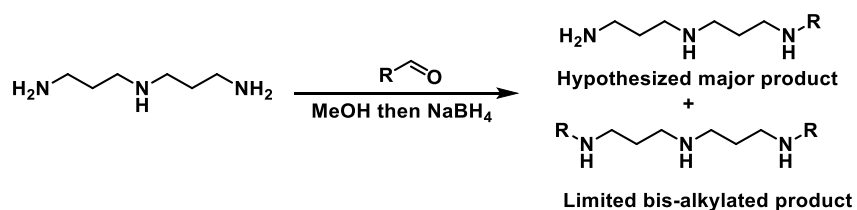


Figure 3.7: Attempted reductive aminations to produce the desired mono-alkylated amine

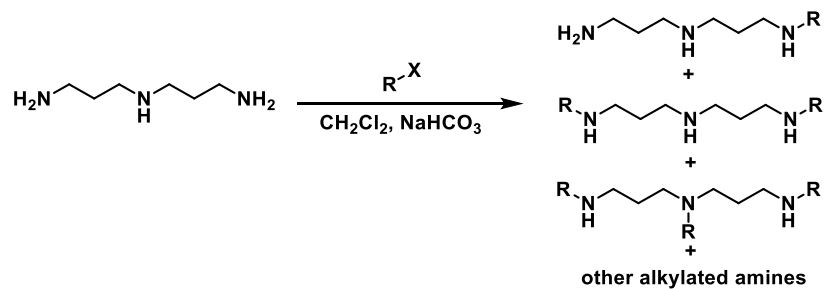


Figure 3.8: Attempted alkylations to produce the desired mono-alkylated amine

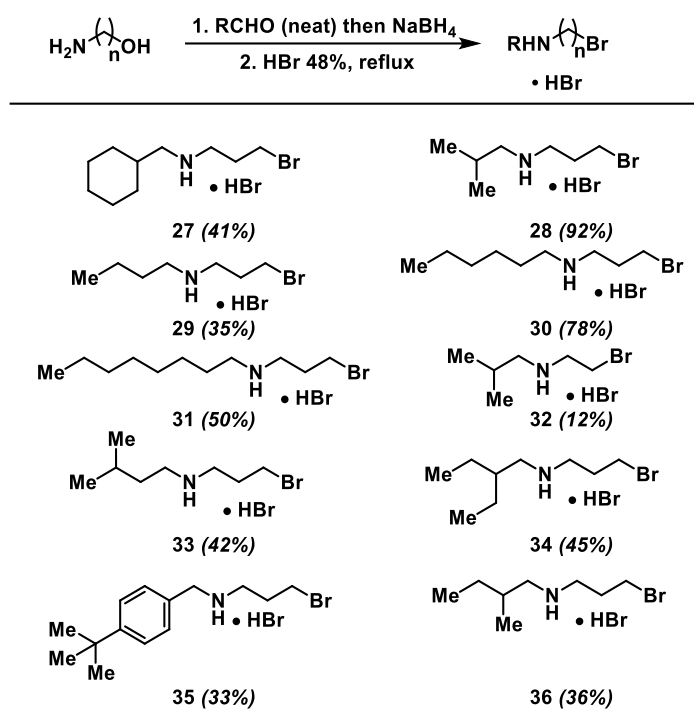


Figure 3.9: Alkylated hydrobromide salts

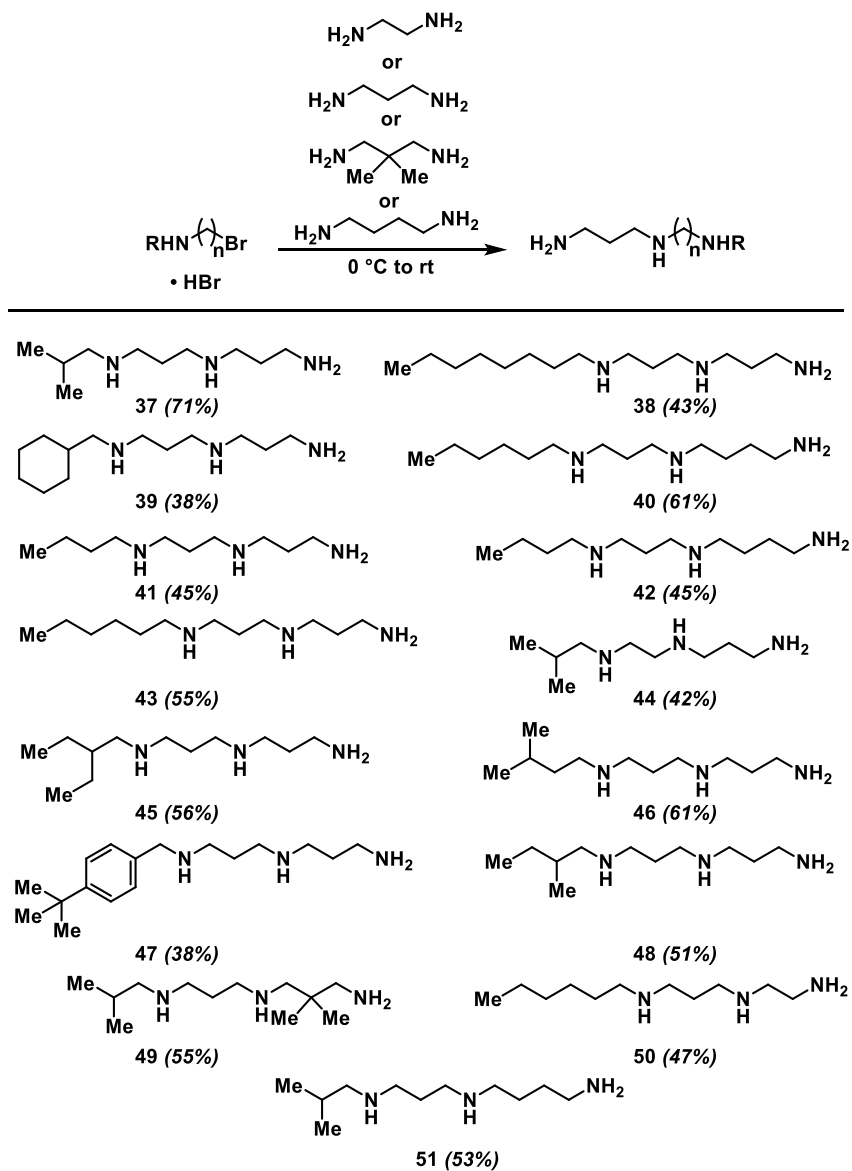


Figure 3.10: Fully functionalized norspermidine derivatives

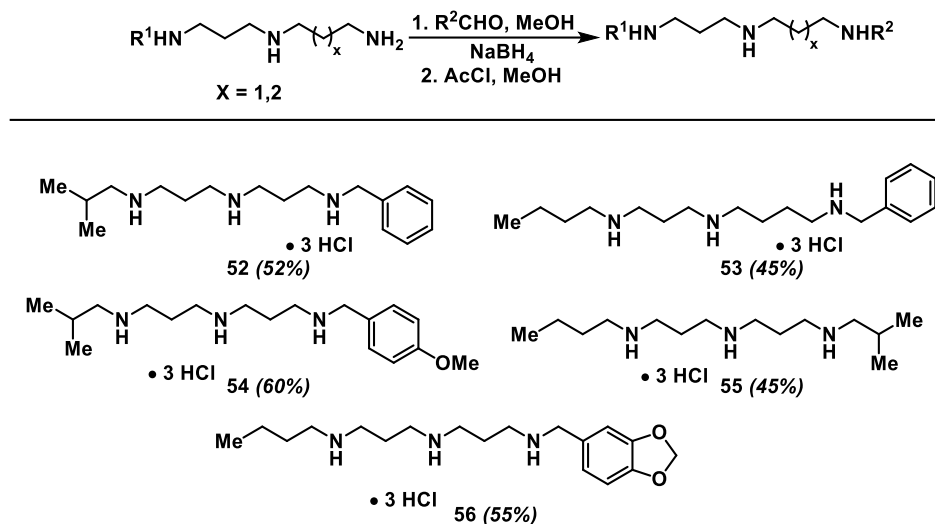
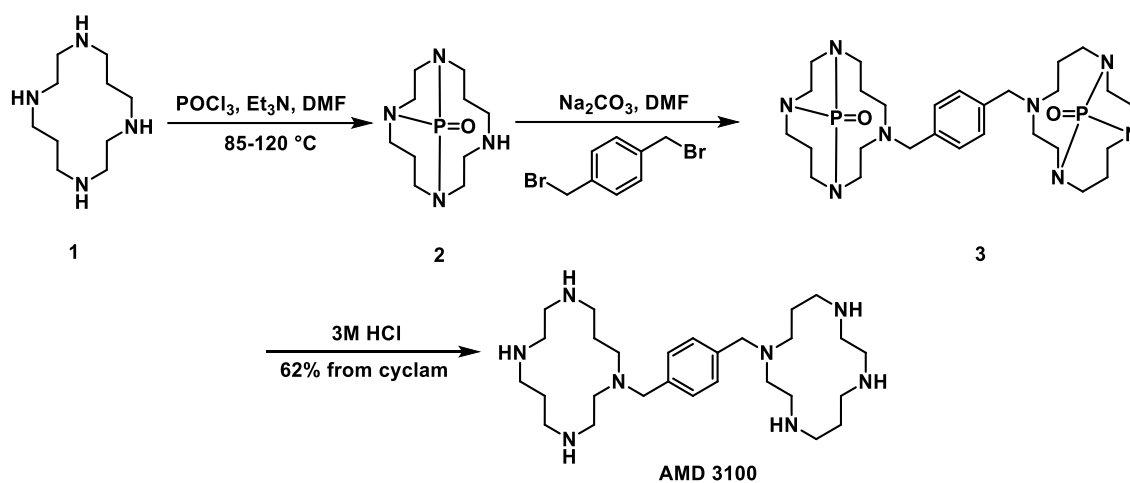
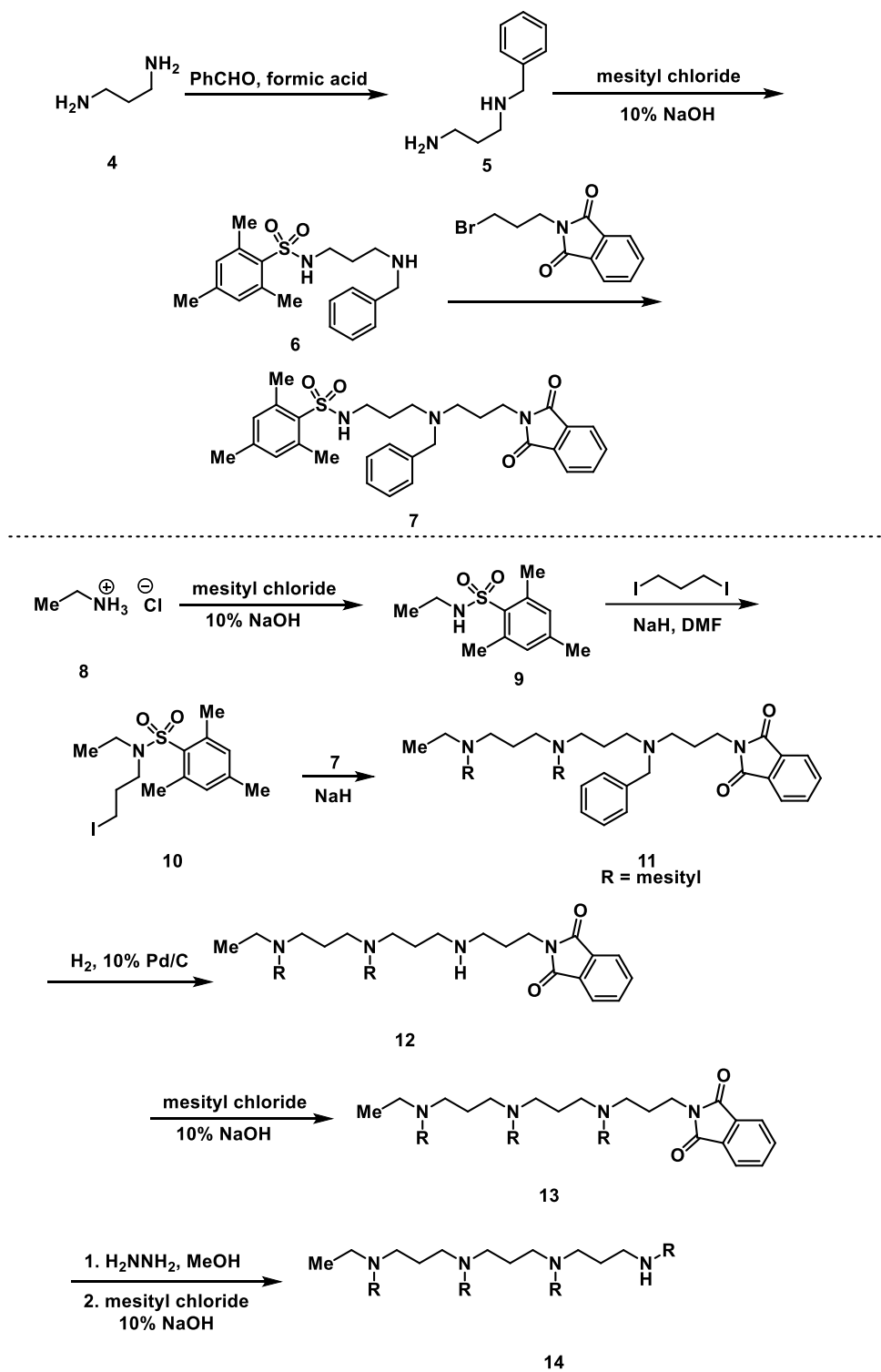


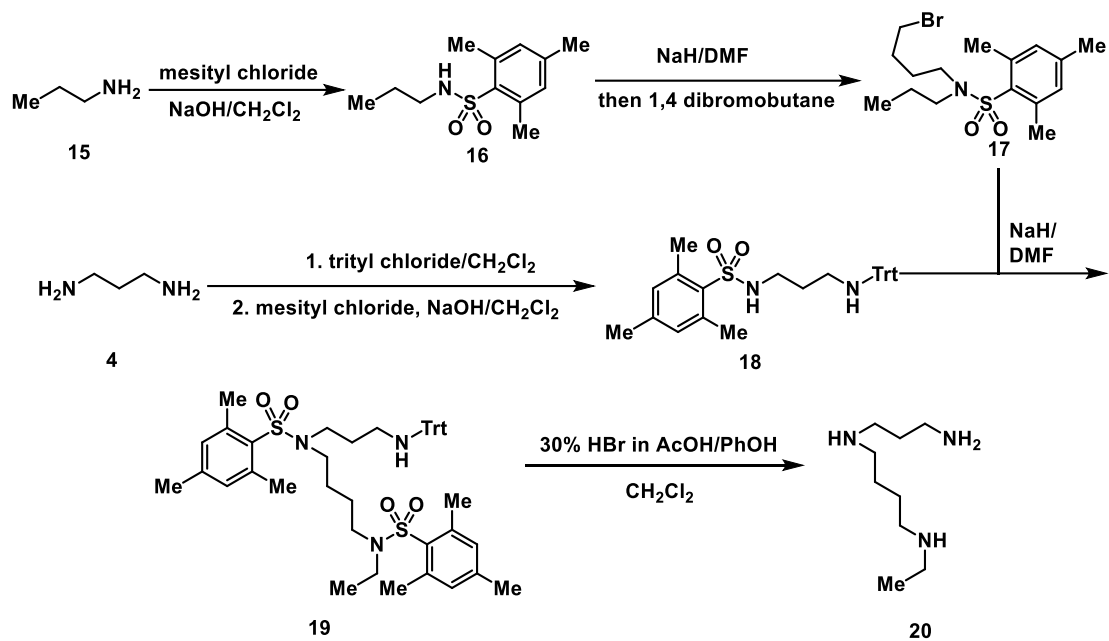
Figure 3.11: Dialkylated derivatives shown to demonstrate the versatility of this strategy



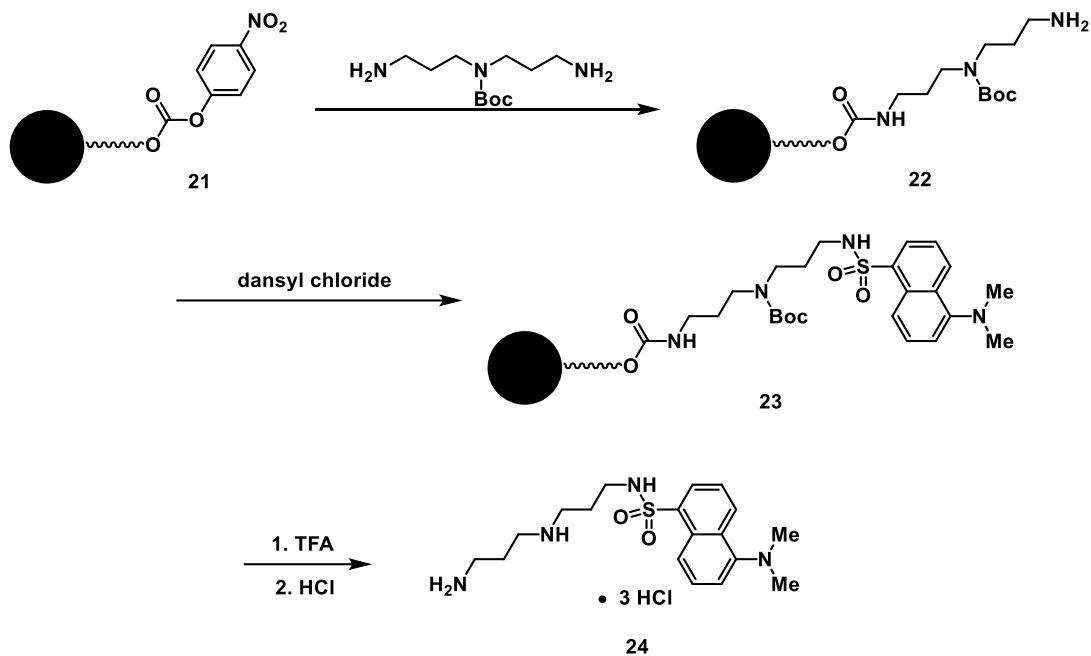
Scheme 3.1: The synthesis of AMD3100 (Plerixafor)



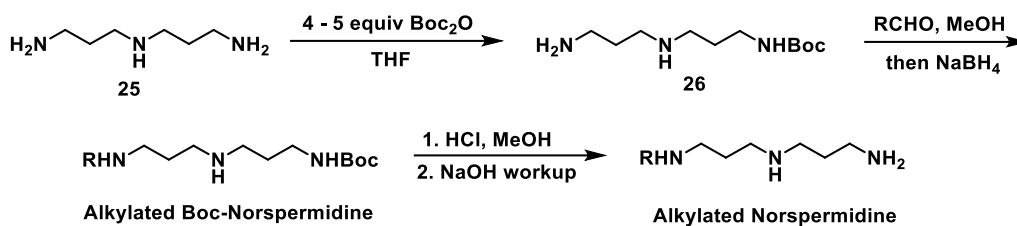
Scheme 3.2: Woster and Casero's alkylated norspermine synthesis



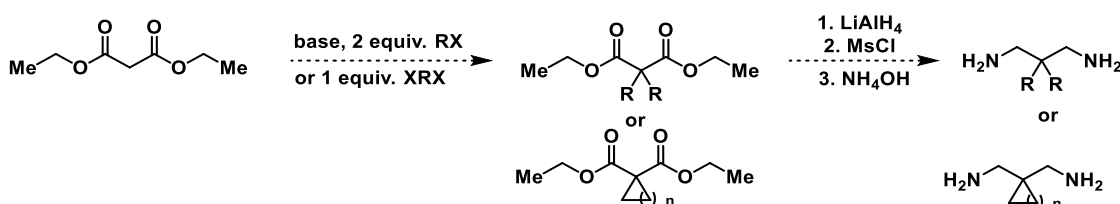
Scheme 3.3: Bergeon's unnatural norspermidine synthesis



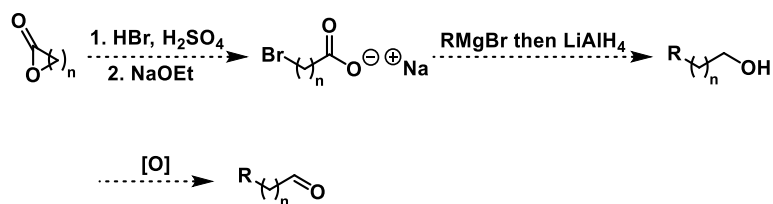
Scheme 3.4: Uriac and Sinbandhit's solid phase polyamine synthesis



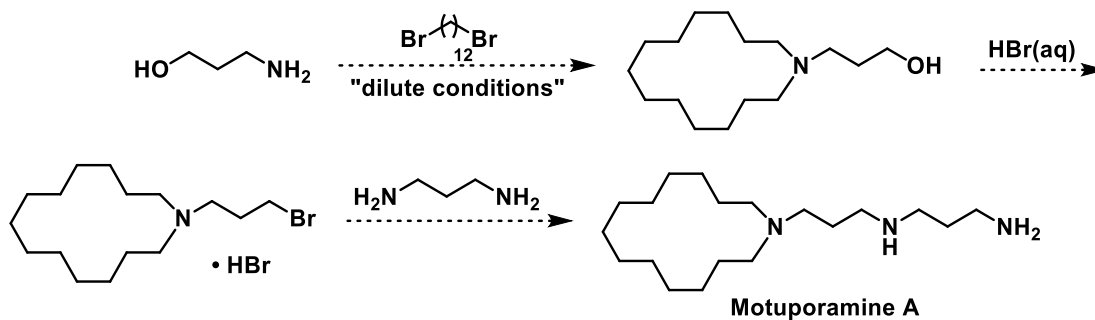
Scheme 3.5: Looper's initial design for alkylated norspermidine



Scheme 3.6: Using diethylmalonate as a precursor for unique substitution patterns on a diamino propane scaffold



Scheme 3.7: Conversion of a variety of lactones to desired long chained alkyl aldehydes



Scheme 3.8: Using Looper's method to achieve Motuporamine A

### 3.9 Supporting Information

#### 3.9.1 General Experimental Conditions

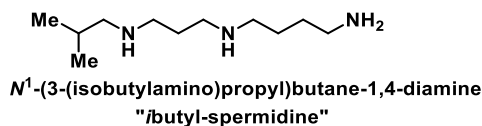
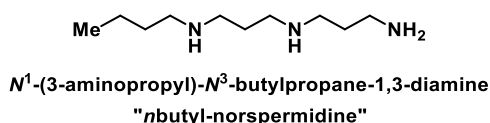
Unless otherwise noted, materials were obtained from commercial sources and used without purification; otherwise, materials were purified according to *Purification of Laboratory Chemicals*.<sup>35</sup> All reactions requiring anhydrous conditions were performed under a positive pressure of nitrogen using flame-dried glassware. Methanol (MeOH) was distilled over magnesium prior to its usage. Diaminopropane is highly toxic and should be handled with great care. Any volatile polyamine synthesized should also be regarded as toxic and should be handled with care and always stored under N<sub>2</sub> due to reactivity with O<sub>2</sub> and CO<sub>2</sub>. Distillations were carried out under reduced pressure with a sodium bicarbonate (NaHCO<sub>3</sub>) scrubber for distillations involving HBr and a citric acid scrubber for any distillations involving amines. Yields were calculated for material judged homogeneous by thin-layer chromatography and <sup>1</sup>H NMR. Thin-layer chromatography was performed on silica plates eluting with the solvents indicated and visualized by a 254nm UV lamp or permanganate stain. <sup>1</sup>HNMR spectra were recorded at 500 or 300 MHz as indicated. The chemical shifts (δ) of proton resonances are reported relative to the deuterated solvent peak: 7.26 ppm for CDCl<sub>3</sub> and 4.79 ppm for H<sub>2</sub>O using the following format: chemical shift [multiplicity (s = singlet, d = doublet, dd = doublet of doublets, t = triplet, q = quartet, pent = pentet, hex = hextet, sept = septet, oct = octet, non = nonet m = multiplet), coupling constant(s) (J in Hz), integral]. <sup>13</sup>C NMR spectra were recorded at 125 MHz. The chemical shifts of carbon resonances are reported relative to the deuterated solvent peak: 77.0 (first line) for CDCl<sub>3</sub>. Mass spectra were obtained by ESI/APCI for LRMS or ESI/APCI-TOF for HRMS. Certain carbon experiments conducted with the



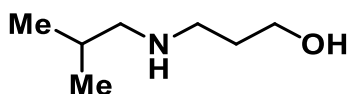
VXR500 MHz NMR contain an artifact peak between 170.0-174.0 ppm, which has been confirmed by the facility administrator.

### 3.9.2 Polyamine Naming

In the laboratory the utility of naming compounds based on the designated IUPAC system is sometimes impractical. We choose a simplified naming system for the polyamine side chains we synthesized, based on the principle that we were only interested in terminally substituted derivatives. Hence most derivatives were named as “the side-chain present” then the polyamine. For example *N*<sup>1</sup>-(3-aminopropyl)-*N*<sup>3</sup>-butylpropane-1,3-diamine the butylated analog would be simplified to *n*-butyl-norspermidine this same principle applies to *N*<sup>1</sup>-(3-(isobutylamino)propyl)butane-1,4-diamine which again by our naming system would be *i*-butyl-spermidine and so on.



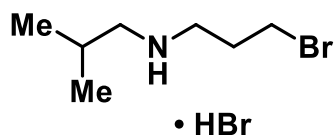
### 3.9.3 Experimental Procedures



**3-(isobutylamino)propan-1-ol:** 3-Amino-1-propanol (35.4 g, 0.58 mol, 1 equiv.) was placed in a round bottomed flask. The solution was cooled to 0 °C (ice/water) and isobutyraldehyde (41.8 g, 0.58 mol, 1 equiv.) was added over the span of 20 min. The reaction was left to warm and stirred for 8 h. Sodium borohydride (11.0 g, .29 mol, .5 equiv.) in water (100 mL) was added slowly to the reaction mixture. After bubbling had ceased the solution was extracted with EtOAc (2 x 200 mL), dried over Na<sub>2</sub>SO<sub>4</sub>, filtered,

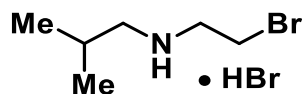
and concentrated under reduced pressure to afford the amino-alcohol as a yellow oil (65.8 g, 97%).  $^1\text{H}$  NMR (300 MHz,  $\text{CDCl}_3$ )  $\delta$  ppm 3.79 (t,  $J = 5.1$  Hz, 2H), 2.84 (t,  $J = 5.7$  Hz, 2H), 2.40 (d,  $J = 6.6$  Hz, 2H), 1.70-1.62 (m, 3H), 0.88 (d,  $J = 6.9$  Hz, 6H).  $^{13}\text{C}$  NMR (125 MHz,  $\text{CDCl}_3$ )  $\delta$  ppm 65.0, 58.2, 50.7, 30.8, 28.6, 21.0.

The other 5 substituted amino alcohols were used without further purification. If desired vacuum distillation can be performed on the substituted amino alcohol to ensure purity.

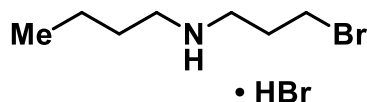


**3-bromo-*N*-isobutylpropan-1-amine, hydrobromide salt:** 3-(Isobutylamino)propan-1-ol (46.0 g, 0.39 mol, 1 equiv.) was placed in a round bottomed flask and cooled to 0 °C (ice/water) to this was carefully added HBr (294 mL in  $\text{H}_2\text{O}$ ). The reaction mixture was heated to reflux for 16 h. The remaining HBr in  $\text{H}_2\text{O}$  was distilled off at 110 °C to provide the crude material as a brown solid which was recrystallized from MeOH/ $\text{Et}_2\text{O}$  or *i*-PrOH to afford the pure HBr salt as white crystals (47.9 g, 45% 2<sup>nd</sup> time 92%, 3<sup>rd</sup> time 85% from 3-Amino-1-propanol).  $^1\text{H}$  NMR (500 MHz,  $\text{D}_2\text{O}$ )  $\delta$  ppm 3.54 (t,  $J = 6.5$  Hz, 2H), 3.21 (t,  $J = 8.0$  Hz, 2H), 2.92 (d,  $J = 7.0$  Hz, 2H), 2.30-2.23 (m, 2H), 2.02 (sept,  $J = 7.0$  Hz, 1H), 0.99 (d,  $J = 6.5$  Hz, 6H).  $^{13}\text{C}$  NMR (125 MHz,  $\text{D}_2\text{O}$ ) 55.0, 46.9, 30.0, 28.5, 25.8, 19.4. HRMS (ESI) calculated for  $\text{C}_7\text{H}_{16}\text{BrN}$   $m/z$  194.0544 ( $\text{M}+\text{H}$ ), Obsd. 194.0546.

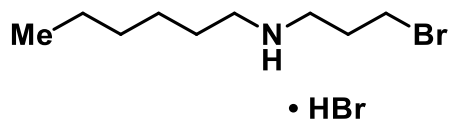
The following compounds were prepared similar to 3-bromo-*N*-isobutylpropan-1-amine, hydrobromide salt:



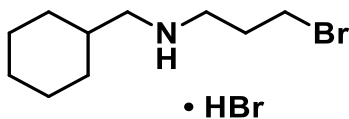
**N-(2-bromoethyl)-2-methylpropan-1-amine, hydrobromide salt:**  $^1\text{H}$  NMR (500 MHz,  $\text{D}_2\text{O}$ )  $\delta$  ppm 3.73 (t,  $J = 6.0$  Hz, 2H), 3.55 (t,  $J = 6.0$  Hz, 2H), 2.98 (d,  $J = 7.5$  Hz, 2H), 2.06 (non,  $J = 7.0$  Hz, 1H), 1.01 (d,  $J = 6.5$  Hz, 6H).  $^{13}\text{C}$  NMR (125 MHz,  $\text{D}_2\text{O}$ ) 54.6, 48.9, 25.9, 25.5, 19.3. HRMS (ESI) calculated for  $\text{C}_6\text{H}_{14}\text{BrN}$   $m/z$  180.0388 (M+H), Obsd. 180.0394. Yield (12% from 3-Amino-1-propanol).



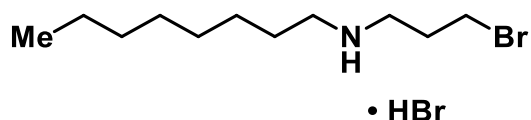
**N-(3-bromopropyl)butan-1-amine, hydrobromide salt:**  $^1\text{H}$  NMR (500 MHz,  $\text{D}_2\text{O}$ )  $\delta$  ppm 3.55 (t,  $J = 6.5$  Hz, 2H), 3.22 (t,  $J = 8.0$  Hz, 2H), 3.07 (t,  $J = 7.5$  Hz, 2H), 2.29-2.23 (m, 2H), 1.70-1.64 (m, 2H), 1.39 (hex,  $J = 7.5$  Hz, 2H), 0.93 (t,  $J = 7.5$  Hz, 3H).  $^{13}\text{C}$  NMR (125 MHz,  $\text{CDCl}_3$ )  $\delta$  ppm 48.2, 46.8, 29.8, 28.6, 27.8, 20.1, 13.6. HRMS (ESI) calculated for  $\text{C}_7\text{H}_{16}\text{BrN}$   $m/z$  194.0544 (M+H), Obsd. 194.0546. Yield (22% from 3-Amino-1-propanol).



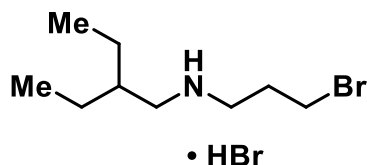
**N-(3-bromopropyl)hexan-1-amine, hydrobromide salt:**  $^1\text{H}$  NMR (500 MHz,  $\text{D}_2\text{O}$ )  $\delta$  ppm 3.51 (t,  $J = 6.0$  Hz, 2H), 3.18 (t,  $J = 7.0$  Hz, 2H), 3.03 (t,  $J = 7.5$  Hz, 2H), 2.23 (pent,  $J = 6.5$  Hz, 2H), 1.65 (pent,  $J = 8.0$  Hz, 2H), 1.36-1.27 (m, 6H), 0.84 (t,  $J = 7.0$  Hz, 3H).  $^{13}\text{C}$  NMR (125 MHz,  $\text{D}_2\text{O}$ )  $\delta$  ppm 48.0, 46.2, 30.6, 29.7, 28.5, 25.6, 25.5, 21.9, 13.4. HRMS (ESI) calculated for  $\text{C}_9\text{H}_{20}\text{BrN}$   $m/z$  222.0857 (M+H), Obsd. 222.0862. Yield (53% from 3-Amino-1-propanol).



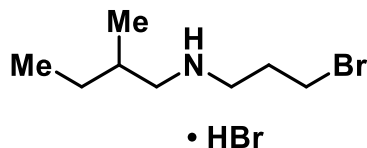
**3-bromo-*N*-(cyclohexylmethyl)propan-1-amine, hydrobromide salt:**  $^1\text{H}$  NMR (500 MHz,  $\text{D}_2\text{O}$ )  $\delta$  ppm 3.54 (t,  $J = 6.0$  Hz, 2H), 3.20 (t,  $J = 7.5$  Hz, 2H), 2.92 (d,  $J = 7.0$  Hz, 2H), 2.28-2.23 (m, 2H), 1.74-1.64 (m, 6H), 1.30-1.13 (m, 3H), 1.04-0.97 (m, 2H).  $^{13}\text{C}$  NMR (125 MHz,  $\text{CDCl}_3$ )  $\delta$  ppm 54.2, 47.3, 34.5, 30.9, 29.9, 28.4, 25.8, 25.3. HRMS (ESI) calculated for  $\text{C}_{10}\text{H}_{20}\text{BrN}$   $m/z$  234.0857 ( $\text{M}+\text{H}$ ), Obsd. 234.0862. Yield (41% from 3-Amino-1-propanol).



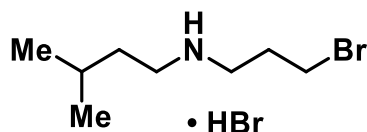
***N*-(3-bromopropyl)octan-1-amine, hydrobromide salt:**  $^1\text{H}$  NMR (500 MHz,  $\text{D}_2\text{O}$ )  $\delta$  ppm 3.53 (t,  $J = 6.0$  Hz, 2H), 3.20 (t,  $J = 7.5$  Hz, 2H), 3.05 (t,  $J = 8.0$  Hz, 2H), 2.27-2.22 (m, 2H), 1.67 (pent,  $J = 7.0$  Hz, 2H), 1.38-1.27 (m, 10H), 0.85 (t,  $J = 7.0$  Hz, 3H).  $^{13}\text{C}$  NMR (125 MHz,  $\text{CDCl}_3$ )  $\delta$  ppm 48.3, 46.6, 31.7, 29.8, 29.1, 29.0, 28.6, 26.8, 25.8, 22.6, 14.1. HRMS (ESI) calculated for  $\text{C}_{11}\text{H}_{24}\text{BrN}$   $m/z$  250.1170 ( $\text{M}+\text{H}$ ), Obsd. 250.1176. Yield (21% from 3-Amino-1-propanol).



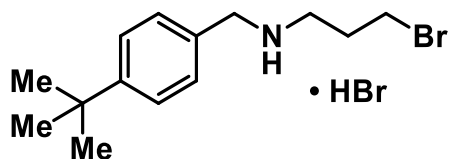
***N*-(3-bromopropyl)-2-ethylbutan-1-amine, hydrobromide salt:**  $^1\text{H}$  NMR (500 MHz,  $\text{D}_2\text{O}$ )  $\delta$  ppm 3.53 (t,  $J = 6.0$  Hz, 2H), 3.21 (t,  $J = 7.5$  Hz, 2H), 3.00 (d,  $J = 7.0$  Hz, 2H), 2.29-2.23 (m, 2H), 1.66 (sept,  $J = 7.0$  Hz, 1H), 1.39 (p,  $J = 7.0$  Hz, 4H), 0.87 (t,  $J = 7.0$  Hz, 6H).  $^{13}\text{C}$  NMR (125 MHz,  $\text{D}_2\text{O}$ )  $\delta$  ppm 50.8, 46.8, 37.6, 29.6, 28.1, 22.4, 9.4. HRMS (ESI) calculated for  $\text{C}_9\text{H}_{20}\text{BrN}$   $m/z$  222.0857 ( $\text{M}+\text{H}$ ), Obsd. 222.0856. Yield (45% from 3-Amino-1-propanol).



***N*-(3-bromopropyl)-2-methylbutan-1-amine, hydrobromide salt:**  $^1\text{H}$  NMR (500 MHz,  $\text{D}_2\text{O}$ )  $\delta$  ppm 3.51 (t,  $J = 6.0$  Hz, 2H), 3.18 (t,  $J = 7.0$  Hz, 2H), 3.00 (dd,  $J = 6.5, 12$  Hz, 1H), 2.86 (dd,  $J = 8.0, 12.5$  Hz, 1H), 2.26-2.21 (m, 2H), 1.78 (oct,  $J = 7.0$  Hz, 1H), 1.43-1.35 (m, 1H), 1.25-1.17 (m, 1H), 0.94 (d,  $J = 6.5$  Hz, 3H), 0.86 (t,  $J = 7.5$  Hz, 3H).  $^{13}\text{C}$  NMR (125 MHz,  $\text{D}_2\text{O}$ )  $\delta$  ppm 53.3, 46.7, 31.7, 29.7, 28.2, 26.2, 16.1, 10.1. HRMS (ESI) calculated for  $\text{C}_8\text{H}_{18}\text{BrN}$   $m/z$  208.0701 ( $\text{M}+\text{H}$ ), Obsd. 208.0703. Yield (36% from 3-Amino-1-propanol).



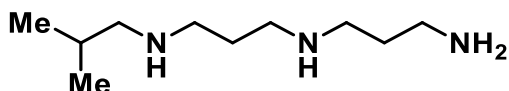
***N*-(3-bromopropyl)-3-methylbutan-1-amine, hydrobromide salt:**  $^1\text{H}$  NMR (500 MHz,  $\text{D}_2\text{O}$ )  $\delta$  ppm 3.54 (t,  $J = 6.5$  Hz, 2H), 3.20 (t,  $J = 8.0$  Hz, 2H), 3.08 (t,  $J = 8.0$  Hz, 2H), 2.27-2.22 (m, 2H), 1.66 (non,  $J = 6.5$  Hz, 1H), 1.58-1.54 (m, 2H), 0.91 (d,  $J = 7.0$  Hz, 6H).  $^{13}\text{C}$  NMR (125 MHz,  $\text{D}_2\text{O}$ )  $\delta$  ppm 46.5, 46.3, 34.4, 29.9, 28.6, 25.4, 21.6. HRMS (ESI) calculated for  $\text{C}_8\text{H}_{18}\text{BrN}$   $m/z$  208.0701 ( $\text{M}+\text{H}$ ), Obsd. 208.0705. Yield (42% from 3-Amino-1-propanol).



**3-bromo-*N*-(4-(*tert*-butyl)benzyl)propan-1-amine, hydrobromide salt:**  $^1\text{H}$  NMR (500 MHz,  $\text{D}_2\text{O}$ )  $\delta$  ppm 7.54 (d,  $J = 8.5$  Hz, 2H), 7.41 (d,  $J = 7.5$  Hz, 2H), 4.20 (s, 2H), 3.66 (t,  $J = 5.5$  Hz, 2H), 3.12 (t,  $J = 7.5$  Hz, 2H), 1.91 (pent,  $J = 6.5$  Hz, 2H), 1.27 (s, 9H).  $^{13}\text{C}$

NMR (125 MHz, D<sub>2</sub>O)  $\delta$  ppm 153.3, 129.7, 127.7, 126.2, 58.9, 50.5, 44.6, 34.1, 30.4, 27.8.

HRMS (ESI) calculated for C<sub>14</sub>H<sub>22</sub>BrN  $m/z$  284.1014 (M+H), Obsd. 284.1017. Yield (33% from 3-Amino-1-propanol)

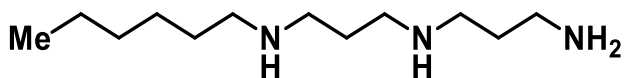


***N*<sup>1</sup>-(3-aminopropyl)-*N*<sup>3</sup>-isobutylpropane-1,3-diamine (Iso-butyl norspermidine):** A

round bottomed flask was charged with 1,3 diaminopropane (61.8 g, 0.83 mol, 10 equiv.), cooled to 0 °C (ice/water) and to this solution was added 3-bromo-*N*-isobutylpropan-1-amine hydrobromide salt (15.5 g, 0.08 mol, 1 equiv.) portionwise over the span of 1.5 h.

The reaction mixture was left to warm and stirred for 12-16 h. Excess 1,3 diaminopropane was removed under reduced pressure, and the remaining semisolid was taken up in 5% NaOH (100 mL) and extracted with 85:15 CHCl<sub>3</sub>/*i*-PrOH (5 x 100 mL), dried over Na<sub>2</sub>SO<sub>4</sub>, filtered, and concentrated under reduced pressure. Purification was accomplished by fractional distillation (oil bath set at 210 °C, distillate collected at 110 °C) to afford pure *N*<sup>1</sup>-(3-aminopropyl)-*N*<sup>3</sup>-isobutylpropane-1,3-diamine as a clear oil (7.4 g, 50%, best 71%).

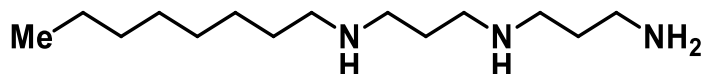
<sup>1</sup>H NMR (300 MHz, CDCl<sub>3</sub>)  $\delta$  ppm 2.76 (t, *J* = 6.9 Hz, 2H), 2.70-2.63 (m, 6H), 2.39 (d, *J* = 6.9 Hz, 2H), 1.80-1.59 (m, 5H), 1.49 (bs, 4H), 0.89 (d, *J* = 6.6 Hz, 6H). <sup>13</sup>C NMR (125 MHz, CDCl<sub>3</sub>)  $\delta$  ppm 58.4, 49.0, 48.9, 48.2, 40.8, 34.2, 30.7, 28.5, 20.9. HRMS (ESI) calculated for C<sub>10</sub>H<sub>25</sub>N<sub>3</sub>  $m/z$  188.2127 (M+H), Obsd. 188.2123.



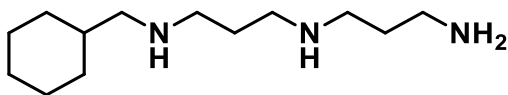
***N*<sup>1</sup>-(3-aminopropyl)-*N*<sup>3</sup>-hexylpropane-1,3-diamine (Hexyl norspermidine):** <sup>1</sup>H NMR

(500 MHz, CDCl<sub>3</sub>)  $\delta$  ppm 2.75 (t, *J* = 7.0 Hz, 2H), 2.65 (td, *J* = 2.5 Hz, 7.0 Hz, 6H), 2.57 (t, *J* = 7.5 Hz, 2H), 1.69-1.59 (m, 4H), 1.47-1.43 (m, 2H), 1.32-1.22 (m, 6H), 1.13 (bs, 4H),

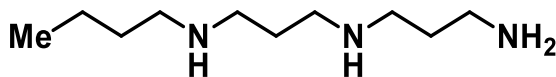
0.87 (t,  $J = 6.5$  Hz, 3H).  $^{13}\text{C}$  NMR (125 MHz,  $\text{CDCl}_3$ )  $\delta$  ppm 50.3, 48.9, 48.8, 48.1, 40.8, 33.7, 32.0, 30.2, 27.3, 22.8, 14.3. HRMS (ESI) calculated for  $\text{C}_{12}\text{H}_{29}\text{N}_3$   $m/z$  216.2440 (M+H), Obsd. 216.2443. Yield (55%, 12.74 g).



**$N^1$ -(3-aminopropyl)- $N^3$ -octylpropane-1,3-diamine (Octyl norspermidine):**  $^1\text{H}$  NMR (500 MHz,  $\text{CDCl}_3$ )  $\delta$  ppm 2.75 (t,  $J = 7.0$  Hz, 2H), 2.66 (t,  $J = 7.0$  Hz, 6H), 2.57 (t,  $J = 7.5$  Hz, 2H), 1.69-1.60 (m, 4H), 1.49-1.42 (m, 2H), 1.27 (s, 10H), 1.04 (bs, 4H), 0.87 (t,  $J = 6.5$  Hz, 3H).  $^{13}\text{C}$  NMR (125 MHz,  $\text{CDCl}_3$ ) 50.1, 48.7, 48.6, 47.9, 40.5, 33.6, 31.8, 30.1, 30.0, 29.5, 29.2, 27.4, 22.6, 14.1. HRMS (ESI) calculated for  $\text{C}_{14}\text{H}_{33}\text{N}_3$   $m/z$  244.2753 (M+H), Obsd. 244.2756. Yield (43%, 6.70 g).

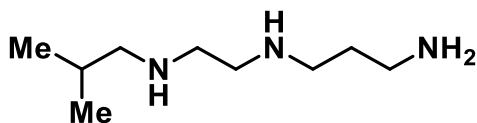


**$N^1$ -(3-aminopropyl)- $N^3$ -(cyclohexylmethyl)propane-1,3-diamine (cyclohexylmethyl norspermidine):**  $^1\text{H}$  NMR (500 MHz,  $\text{CDCl}_3$ )  $\delta$  ppm 2.75 (t,  $J = 7.0$  Hz, 2H), 2.66-2.61 (m, 6H), 2.40 (d,  $J = 7.0$  Hz, 2H), 1.72-1.59 (m, 9H), 1.47-1.38 (m, 1H), 1.27-1.03 (m, 7H), 0.91-0.84 (m, 2H).  $^{13}\text{C}$  NMR (125 MHz,  $\text{CDCl}_3$ )  $\delta$  ppm 57.2, 49.0, 48.2, 40.8, 38.2, 34.2, 31.7, 30.7, 26.9, 26.3. HRMS (ESI) calculated for  $\text{C}_{13}\text{H}_{29}\text{N}_3$   $m/z$  228.2440 (M+H), Obsd. 228.2439. Yield (38%, 3.43 g).

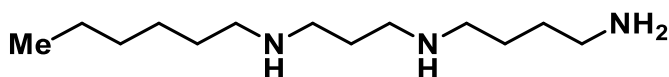


**$N^1$ -(3-aminopropyl)- $N^3$ -butylpropane-1,3-diamine (*n*-butyl-norspermidine):**  $^1\text{H}$  NMR (500 MHz,  $\text{CDCl}_3$ )  $\delta$  ppm 2.64-2.46 (m, 10H), 1.56-1.49 (m, 4H), 1.37-1.30 (m, 2H), 1.27-1.18 (m, 6H), 0.81-0.77 (m, 3H).  $^{13}\text{C}$  NMR (125 MHz,  $\text{CDCl}_3$ )  $\delta$  ppm 50.1, 48.9, 48.8,

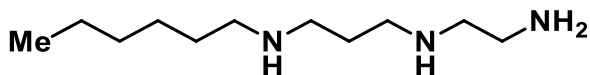
48.1, 40.8, 34.2, 32.5, 30.7, 20.7, 14.0. HRMS (ESI) calculated for  $C_{10}H_{25}N_3$   $m/z$  188.2127 (M+H), Obsd. 188.2126. Yield (45%, 7.01 g).



***N*<sup>1</sup>-(2-(isobutylamino)ethyl)propane-1,3-diamine:**  $^1H$  NMR (500 MHz,  $CDCl_3$ )  $\delta$  ppm 2.71 (t,  $J = 7.0$  Hz, 2H), 2.64 (s, 4H), 2.62 (t,  $J = 7.0$  Hz, 2H), 2.33 (d,  $J = 7.0$  Hz, 2H), 1.97 (bs, 4H), 1.66 (sept,  $J = 6.5$  Hz, 1H), 1.58 (pent,  $J = 7.0$  Hz, 2H), 0.82 (d,  $J = 6.5$  Hz, 6H).  $^{13}C$  NMR (125 MHz,  $CDCl_3$ )  $\delta$  ppm 58.1, 49.5, 49.4, 47.9, 40.6, 33.4, 28.4, 20.8. HRMS (ESI) calculated for  $C_9H_{23}N_3$   $m/z$  174.1970 (M+H), Obsd. 174.1977. Yield (42%, 4.04 g).

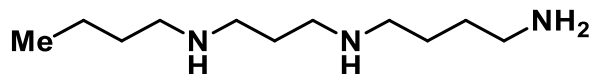


***N*<sup>1</sup>-(3-(hexylamino)propyl)butane-1,4-diamine (Hexyl spermidine):**  $^1H$  NMR (500 MHz,  $CDCl_3$ )  $\delta$ : 2.80 (bs, 4H), 2.65-2.50 (m, 10H), 1.65-1.59 (m, 2H), 1.46-1.38 (m, 6H), 1.25-1.17 (m, 6H), 0.81 (t,  $J = 7.0$  Hz, 3H).  $^{13}C$  NMR (125 MHz,  $CDCl_3$ )  $\delta$  ppm 50.2, 49.9, 48.6, 42.0, 31.9, 31.3, 30.2, 30.1, 27.4, 27.2, 22.7, 14.2. HRMS (ESI) calculated for  $C_{13}H_{31}N_3$   $m/z$  230.2596 (M+H), Obsd. 230.2601. Yield (51%, 4.54 g).

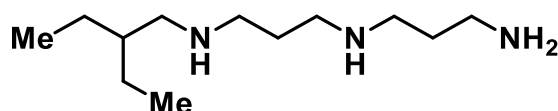


***N*<sup>1</sup>-(2-aminoethyl)-*N*<sup>3</sup>-hexylpropane-1,3-diamine:**  $^1H$  NMR (500 MHz,  $CDCl_3$ )  $\delta$ : 2.68 (t,  $J = 6.0$  Hz, 2H), 2.58-2.54 (m, 6H), 2.47 (t,  $J = 7.0$  Hz, 2H), 1.57 (pent,  $J = 7.0$  Hz, 2H), 1.39-1.31 (m, 2H), 1.22-1.07 (m, 10H), 0.77 (t,  $J = 7.5$  Hz, 3H).  $^{13}C$  NMR (125 MHz,  $CDCl_3$ )  $\delta$  ppm 52.7, 50.2, 48.6, 48.4, 41.8, 31.8, 30.5, 30.2, 27.1, 22.6, 14.1. HRMS (ESI) calculated for  $C_{11}H_{27}N_3$   $m/z$  202.2283 (M+H), Obsd. 202.2291. Yield (47%, 3.23 g).

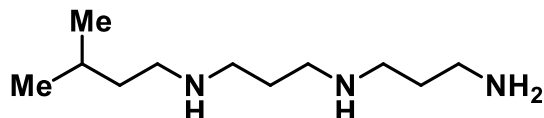




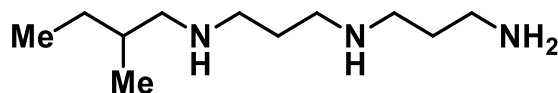
***N*<sup>1</sup>-(3-(butylamino)propyl)butane-1,4-diamine (Butyl spermidine):** <sup>1</sup>H NMR (300 MHz, CDCl<sub>3</sub>) δ: 2.67-2.51 (m, 10H), 1.62 (pent, *J* = 7.2 Hz, 2H), 1.52-1.34 (m, 6H), 1.30 (pent, *J* = 7.2 Hz, 2H), 0.98 (bs, 4H), 0.86 (t, *J* = 7.2 Hz, 3H). <sup>13</sup>C NMR (75 MHz, CDCl<sub>3</sub>) δ ppm 50.2, 50.1, 48.8, 48.8, 42.4, 32.5, 31.9, 30.8, 27.7, 20.7, 14.2. HRMS (ESI) calculated for C<sub>11</sub>H<sub>27</sub>N<sub>3</sub> *m/z* 202.2283 (M+H), Obsd. 201.2284. Yield (48%, 5.28 g).



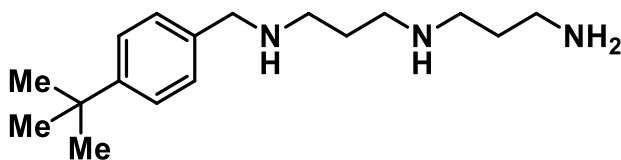
***N*<sup>1</sup>-(3-aminopropyl)-*N*<sup>3</sup>-(2-ethylbutyl)propane-1,3-diamine (Gem-diethylnorspermidine):** <sup>1</sup>H NMR (300 MHz, CDCl<sub>3</sub>) δ ppm 2.64 (t, *J* = 6.9 Hz, 2H), 2.58-2.51 (m, 6H), 2.36 (d, *J* = 5.4 Hz, 2H), 1.53 (sept, *J* = 6.6 Hz, 4H), 1.25-1.15 (m, 5H), 0.97 (bs, 4H), 0.74 (t, *J* = 6.9 Hz, 6H). <sup>13</sup>C NMR (75 MHz, CDCl<sub>3</sub>) δ ppm 53.1, 49.1, 49.0, 48.1, 41.0, 40.7, 34.2, 30.5, 24.2, 11.1. HRMS (ESI) calculated for C<sub>12</sub>H<sub>29</sub>N<sub>3</sub> *m/z* 216.2440 (M+H), Obsd. 216.2439. Yield (56%, 11.92 g).



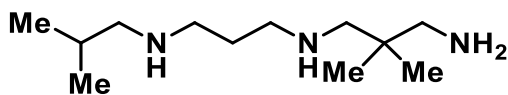
***N*<sup>1</sup>-(3-aminopropyl)-*N*<sup>3</sup>-isopentylpropane-1,3-diamine (Iso-amyl norspermidine):** 2.75 (t, *J* = 6.5 Hz, 2H), 2.66 (t, *J* = 12.0 Hz, 6H), 2.58 (t, *J* = 13.0 Hz, 2H), 1.72-1.55 (m, 5H), 1.39-1.32 (m, 6H), 0.88 (d, *J* = 11.0 Hz, 6H). <sup>13</sup>C NMR (125 MHz, CDCl<sub>3</sub>) δ ppm 48.7, 48.2, 47.9, 40.5, 39.2, 33.9, 30.4, 26.1, 22.6. HRMS (ESI) calculated for C<sub>11</sub>H<sub>27</sub>N<sub>3</sub> *m/z* 202.2283 (M+H), Obsd. 202.2283. Yield (61%, 16.89 g).



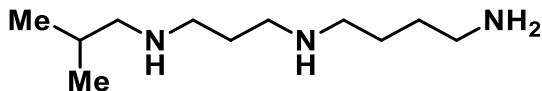
***N*<sup>1</sup>-(3-aminopropyl)-*N*<sup>3</sup>-(2-methylbutyl)propane-1,3-diamine:** <sup>1</sup>H NMR (500 MHz, CDCl<sub>3</sub>) δ ppm 2.71 (t, *J* = 7.0 Hz, 2H), 2.63-2.58 (m, 6H), 2.46 (dd, *J* = 6.0, 11.5 Hz, 1H), 2.31 (dd, *J* = 7.5, 12.0 Hz, 1H), 1.65-1.55 (m, 4H), 1.51-1.42 (m, 1H), 1.39-1.30 (m, 1H), 1.12-1.05 (m, 5H), 0.85-0.82 (m, 6H). <sup>13</sup>C NMR (125 MHz, CDCl<sub>3</sub>) δ ppm 56.5, 49.0, 48.1, 40.7, 34.9, 34.2, 30.6, 27.7, 17.8, 11.5. HRMS (ESI) calculated for C<sub>11</sub>H<sub>27</sub>N<sub>3</sub> *m/z* 202.2283 (M+H), Obsd. 202.2287. Yield (51%, 10.06 g).



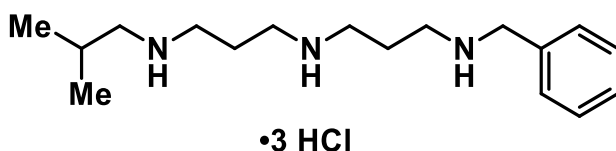
***N*<sup>1</sup>-(3-aminopropyl)-*N*<sup>3</sup>-(4-(*tert*-butyl)benzyl)propane-1,3-diamine (*Tert*-butyl-benzyl norspermidine):** <sup>1</sup>H NMR (500 MHz, CDCl<sub>3</sub>) δ ppm 7.34 (d, *J* = 8.0 Hz, 2H), 7.23 (d, *J* = 8.0 Hz, 2H), 3.74 (s, 2H), 2.75 (t, *J* = 7.0 Hz, 2H), 2.71-2.64 (m, 6H), 1.70 (pent, *J* = 7.0 Hz, 2H), 1.62 (pent, *J* = 7.0 Hz, 2H), 1.43 (bs, 4H), 1.31 (s, 9H). <sup>13</sup>C NMR (125 MHz, CDCl<sub>3</sub>) δ ppm 149.8, 137.2, 127.9, 125.3, 53.6, 48.4, 47.8, 47.7, 40.2, 34.5, 32.8, 31.4, 29.9. LRMS calculated for C<sub>17</sub>H<sub>31</sub>N<sub>3</sub> *m/z* 278.2596 [M+H]<sup>+</sup>, Obsd. 278.2594. Yield (38%, 5.16 g).



***N*<sup>1</sup>-(3-(isobutylamino)propyl)-2,2-dimethylpropane-1,3-diamine:** <sup>1</sup>H NMR (500 MHz, CDCl<sub>3</sub>) δ ppm 2.63 (t, *J* = 7.0 Hz, 4H), 2.50 (s, 2H), 2.39-2.37 (m, 4H), 1.77-1.62 (m, 3H), 1.02 (bs, 4H), 0.88 (d, *J* = 7.0 Hz, 6H), 0.84 (s, 6H). <sup>13</sup>C NMR (125 MHz, CDCl<sub>3</sub>) δ ppm 59.1, 58.5, 51.7, 49.9, 49.0, 35.6, 30.5, 28.5, 23.9, 20.9. HRMS (ESI) calculated for C<sub>12</sub>H<sub>29</sub>N<sub>3</sub> *m/z* 216.2440 (M+H), Obsd. 216.2444. Yield (55%, 8.60 g).



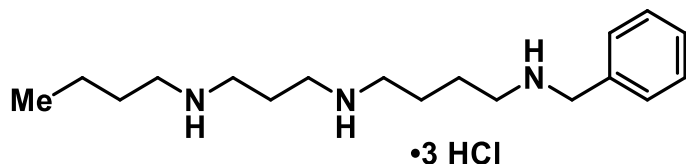
***N*<sup>1</sup>-(3-(isobutylamino)propyl)butane-1,4-diamine (Iso-butyl spermidine):** <sup>1</sup>H NMR (500 MHz, CDCl<sub>3</sub>) δ ppm 2.66-2.54 (m, 8H), 2.35-2.33 (m, 2H), 1.70-1.59 (m, 3H), 1.49-1.40 (m, 4H), 0.98 (bs, 4H), 0.85-0.83 (m, 6H). <sup>13</sup>C NMR (125 MHz, CDCl<sub>3</sub>) δ ppm 58.4, 50.1, 48.9, 48.9, 42.4, 31.9, 30.6, 28.4, 27.7, 20.8. HRMS (ESI) calculated for C<sub>11</sub>H<sub>27</sub>N<sub>3</sub> m/z 202.2283 (M+H), Obsd. 202.2284. Yield (53%, 7.95 g).



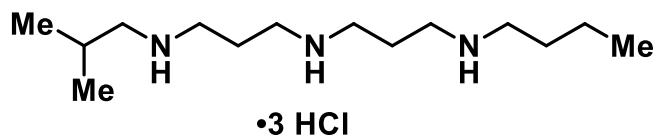
***N*<sup>1</sup>-benzyl-*N*<sup>3</sup>-(3-(isobutylamino)propyl)propane-1,3-diamine, hydrochloride salt:** Benzaldehyde (0.16 g, 1.56 mmol, 1 equiv.) was added dropwise to a cooled solution (0 °C) of isobutyl-norspermdine (0.29 g, 1.56 mmol, 1 equiv.) in MeOH (5 mL) and the reaction was left to stir for 16 h. Sodium borohydride (.24 g, 6.24 mmol, 4 equiv.) was then added portionwise and the reaction mixture was left to stir for an additional 1 h. The excess MeOH was evaporated and the crude solid was partitioned between EtOAc (50 mL) and 10% NaOH (1 x 50 mL). The aqueous layer was then back extracted with EtOAc (1 x 50 mL) dried over Na<sub>2</sub>SO<sub>4</sub> and evaporated to afford the crude free base which was carried forward without further purification. The crude free base was acidified with HCl in MeOH (50 mL) and then placed at 0 °C for 1 h to precipitate. The corresponding precipitate was filtered and dried to afford the pure HCl salt as a white solid (52%). <sup>1</sup>H NMR (500 MHz, D<sub>2</sub>O) δ ppm 7.51 (s, 5 H), 4.28 (s, 2H), 3.23-3.14 (m, 8H), 2.93 (d, *J* = 6.5 Hz, 2H), 2.19-2.12 (m, 4H), 2.02 (sept, *J* = 6.5 Hz, 1H), 1.00 (d, *J* = 7.0 Hz, 6H). <sup>13</sup>C NMR (125 MHz, D<sub>2</sub>O) δ ppm 130.6, 130.1, 130.0, 129.5, 55.1, 51.4, 45.0, 44.9, 44.8, 44.0, 25.8, 22.8, 22.7,

19.3. Yield (52%, 0.31 g).

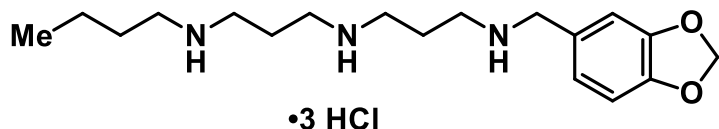
The following examples were prepared similar to *N*<sup>1</sup>-(benzo[d][1,3]dioxol-5-ylmethyl)-*N*<sup>3</sup>-(3-(butylamino)propyl)propane-1,3-diamine, chloride salt:



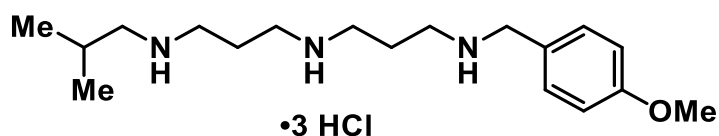
***N*<sup>1</sup>-benzyl-*N*<sup>3</sup>-(3-(butylamino)propyl)propane-1,3-diamine, hydrochloride salt:** <sup>1</sup>H NMR (500 MHz, D<sub>2</sub>O) δ ppm 7.52-7.49 (m, 5H), 4.28 (s, 2H), 3.22-3.13 (m, 8H), 3.07 (t, *J* = 7.5 Hz, 4H), 2.18-2.09 (m, 4H), 1.66 (pent, *J* = 7.5 Hz, 2H), 1.39 (hex, *J* = 7.5 Hz, 2H), 0.93 (t, *J* = 7.0 Hz, 3H). <sup>13</sup>C NMR (125 MHz, D<sub>2</sub>O) δ ppm 130.5, 130.0, 130.0, 129.5, 51.4, 47.8, 44.8, 44.8, 44.4, 44.0, 27.7, 22.8, 19.3, 12.9. HRMS (ESI) calculated for C<sub>18</sub>H<sub>33</sub>N<sub>3</sub> *m/z* 292.2753 (M+H), Obsd. 292.2753. Yield (45%, 0.82 g).



***N*<sup>1</sup>-butyl-*N*<sup>3</sup>-(3-(isobutylamino)propyl)propane-1,3-diamine, hydrochloride salt:** <sup>1</sup>H NMR (500 MHz, D<sub>2</sub>O) δ ppm 3.19-3.13 (m, 8H), 3.06 (t, *J* = 7.5 Hz, 2H), 2.92 (d, *J* = 7.5 Hz, 2H), 2.16-2.08 (m, 4H), 2.01 (sept, *J* = 7.0 Hz, 1H), 1.65 (pent, *J* = 7.5 Hz, 2H), 1.38 (hex, *J* = 7.0 Hz, 2H), 0.98 (d, *J* = 6.5 Hz, 6H), 0.91 (t, *J* = 8.0 Hz, 3H). <sup>13</sup>C NMR (125 MHz, D<sub>2</sub>O) δ ppm 55.1, 47.8, 44.9, 44.8, 44.4, 27.7, 25.8, 22.8, 22.7, 19.3, 19.2, 12.9. HRMS (ESI) calculated for C<sub>14</sub>H<sub>33</sub>N<sub>3</sub> *m/z* 244.2753 (M+H), Obsd. 244.2750. Yield (45%, 0.24 g).

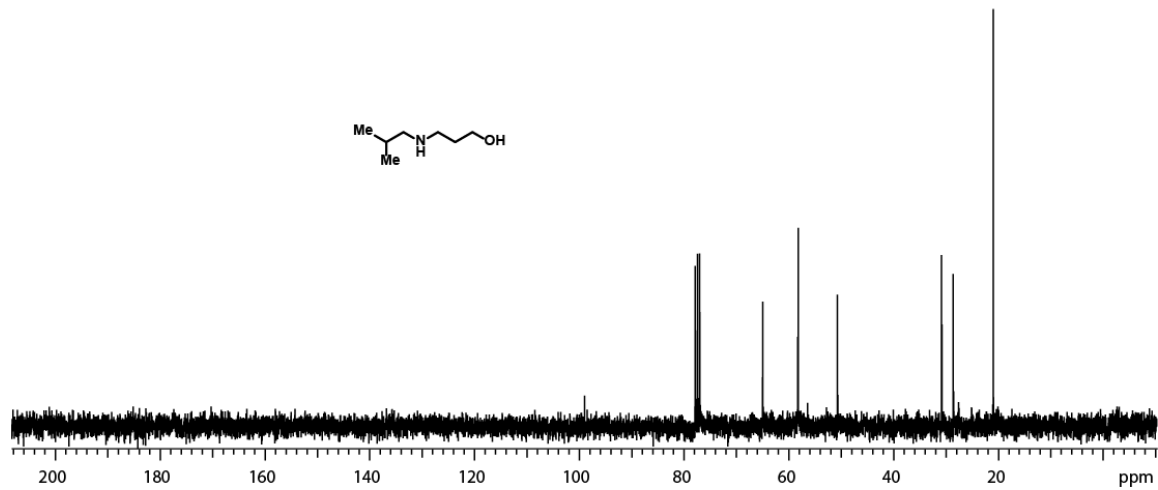
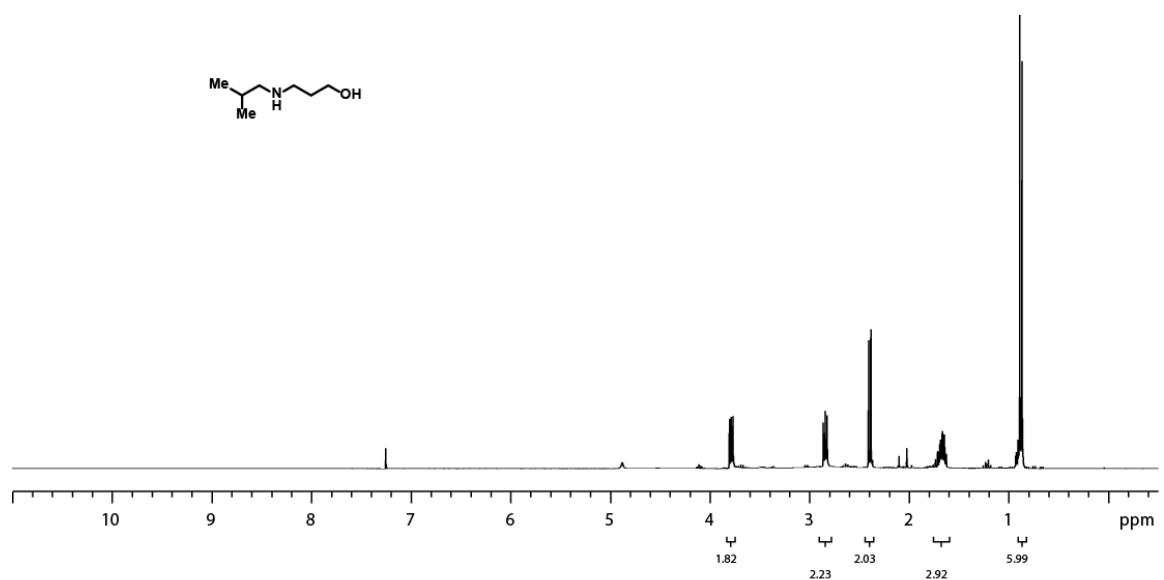


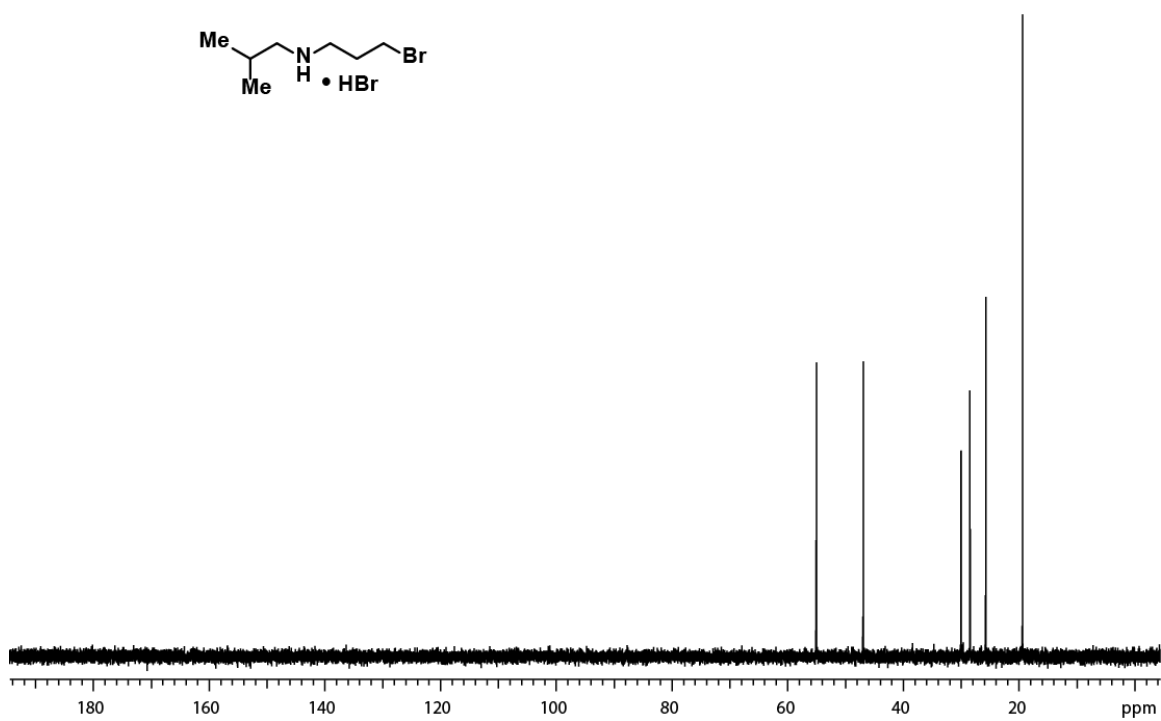
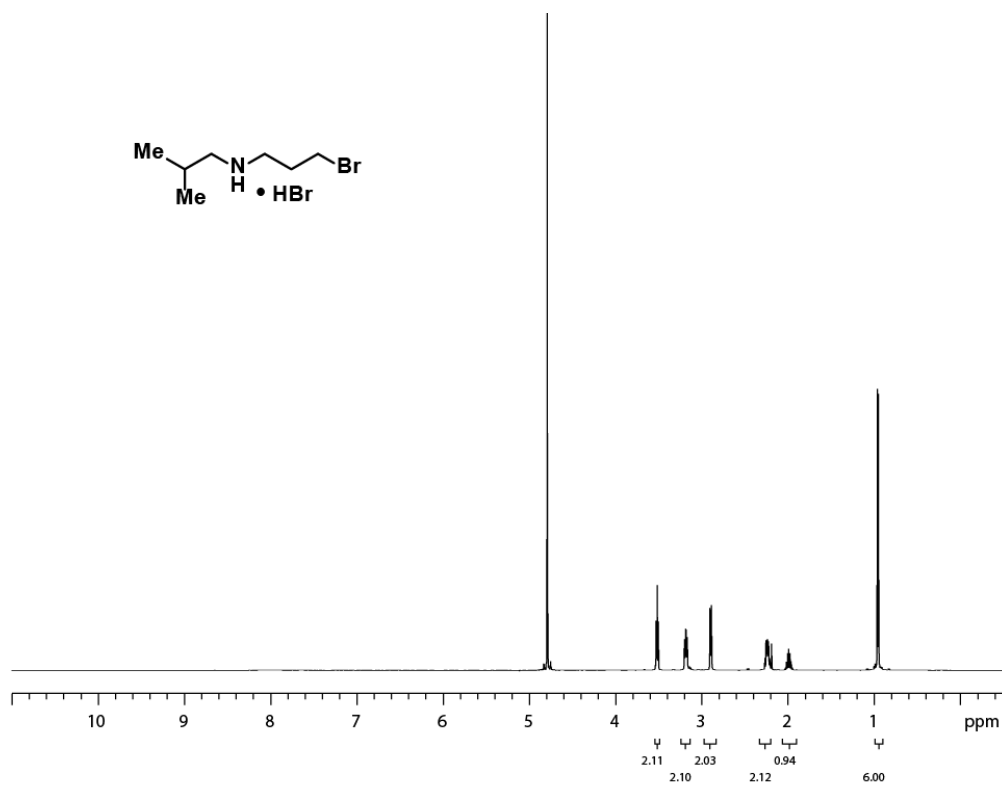
***N*<sup>1</sup>-(benzo[d][1,3]dioxol-5-ylmethyl)-*N*<sup>3</sup>-(3-(butylamino)propyl)propane-1,3-diamine, hydrochloride salt:** <sup>1</sup>H NMR (500 MHz, D<sub>2</sub>O) δ ppm 6.98-6.92 (m, 3H), 6.00 (s, 2H), 4.16 (s, 2H), 3.17-3.11 (m, 8H), 3.05 (t, *J* = 7.0 Hz, 2H), 2.15-2.08 (m, 4H), 1.64 (pent, *J* = 7.5 Hz, 2H), 1.37 (hex, *J* = 7.0 Hz, 2H), 0.90 (t, *J* = 7.5 Hz, 3H). <sup>13</sup>C NMR (125 MHz, D<sub>2</sub>O) δ ppm 148.4, 147.9, 124.4, 124.2, 110.1, 109.1, 108.1, 51.2, 47.8, 44.8, 44.8, 43.8, 27.7m 22.9, 19.3, 12.9. HRMS (ESI) calculated for C<sub>18</sub>H<sub>31</sub>N<sub>3</sub>O<sub>2</sub> m/z 322.2511 (M+H), Obsd. 322.2494. Yield (55%, 0.17 g).

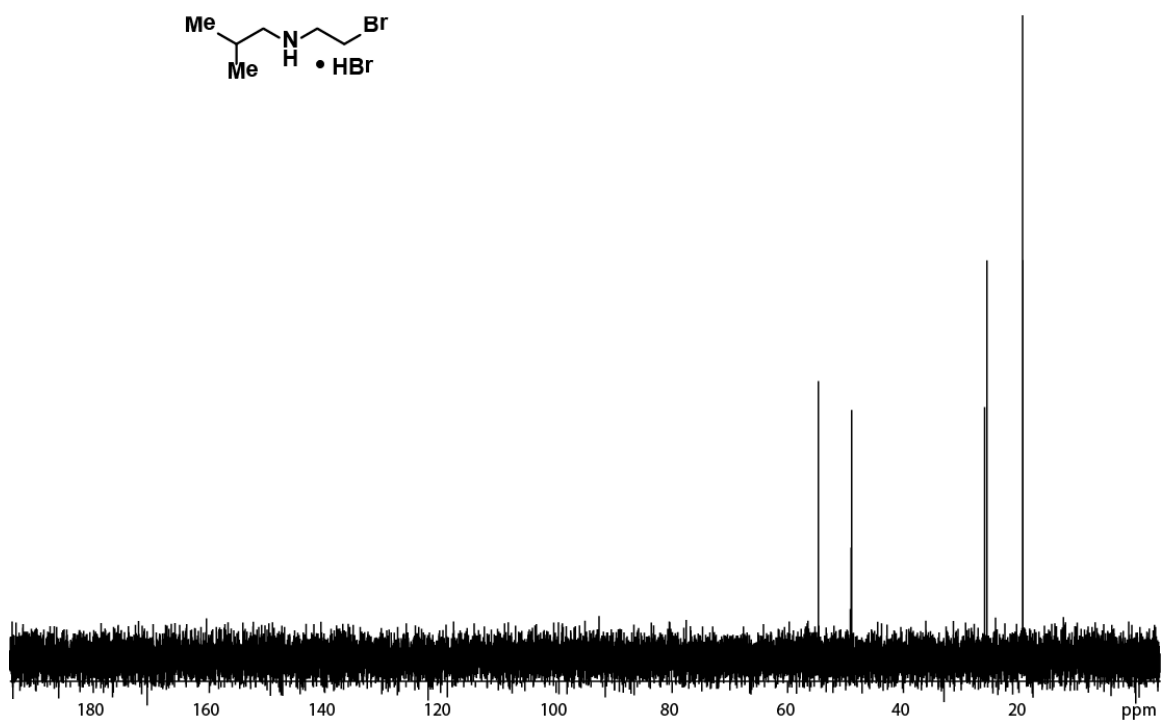
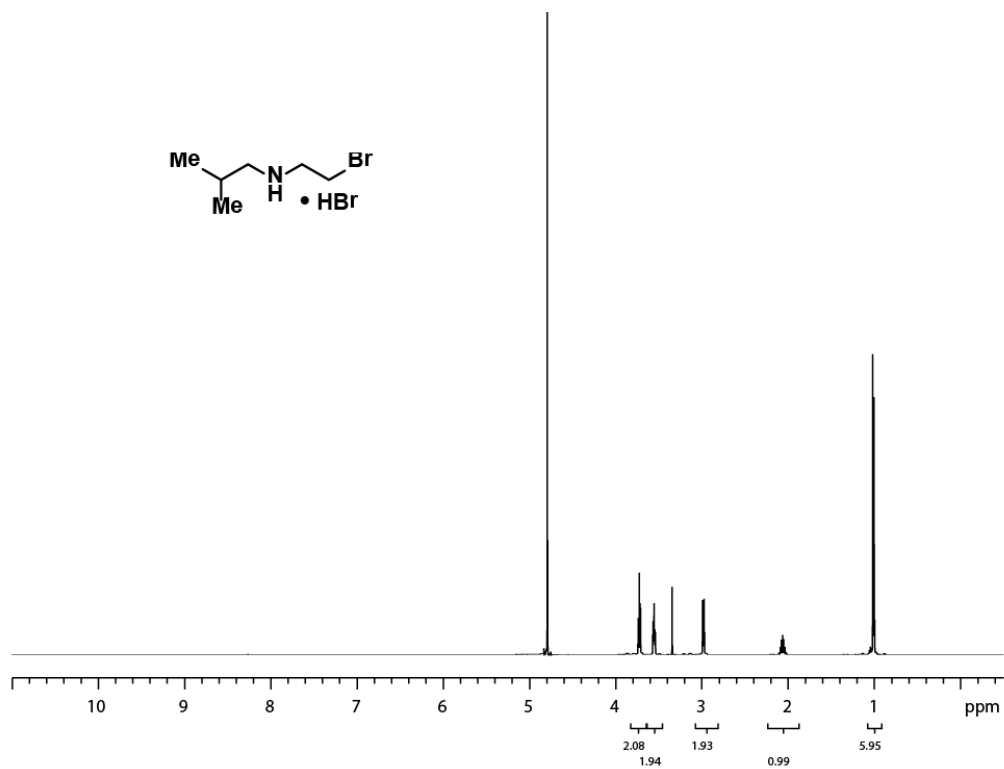


***N*<sup>1</sup>-isobutyl-*N*<sup>3</sup>-(3-((4-methoxybenzyl)amino)propyl)propane-1,3-diamine, hydrochloride salt:** <sup>1</sup>H NMR (500 MHz, D<sub>2</sub>O) δ ppm 7.44 (d, *J* = 8.0 Hz, 2H), 7.05 (d, *J* = 9.0 Hz, 2H), 4.22 (s, 2H), 3.84 (s, 3H), 3.19-3.14 (m, 8H), 2.93 (d, *J* = 7.0 Hz, 2H), 2.18-2.11 (m, 4H), 2.02 (sept, *J* = 7.0 Hz, 1H), 1.00 (d, *J* = 7.0 Hz, 6H). <sup>13</sup>C NMR (125 MHz, D<sub>2</sub>O) δ ppm 160.0, 131.8, 123.0, 114.8, 55.6, 55.1, 50.9, 45.0, 44.8, 43.8, 25.8, 22.8, 22.7, 19.3. HRMS (ESI) calculated for C<sub>18</sub>H<sub>33</sub>N<sub>3</sub>O m/z 308.2702 (M+H), Obsd. 308.2702. Yield (60%, 0.58 g).

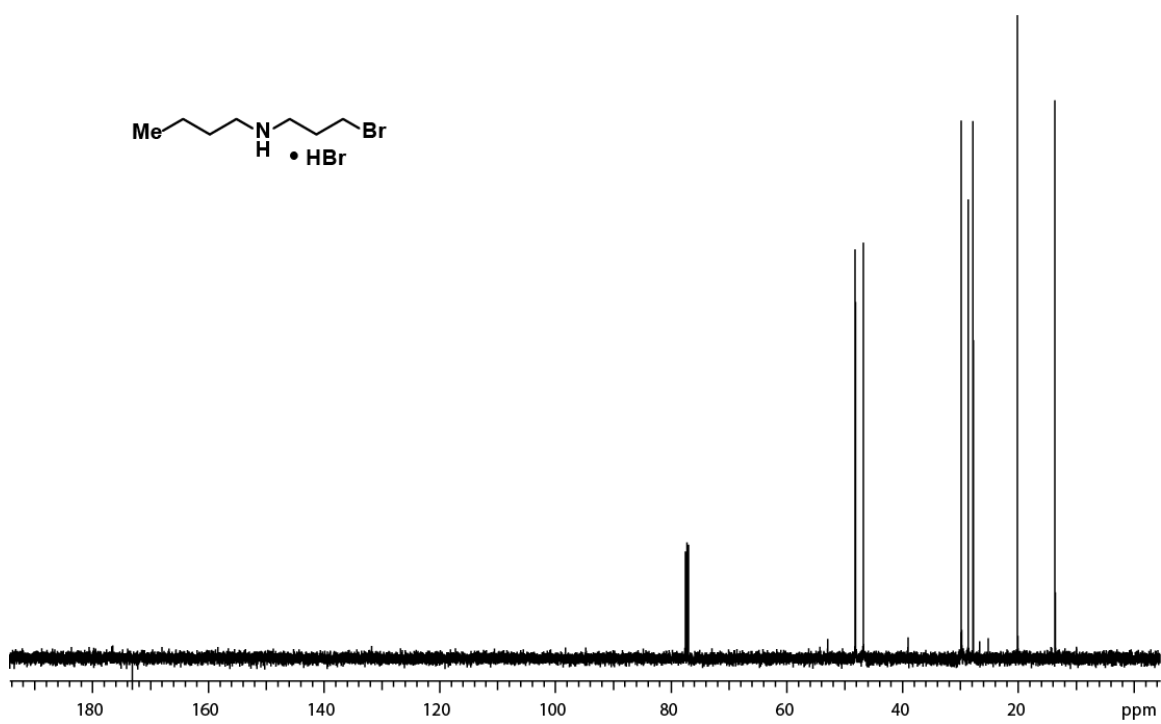
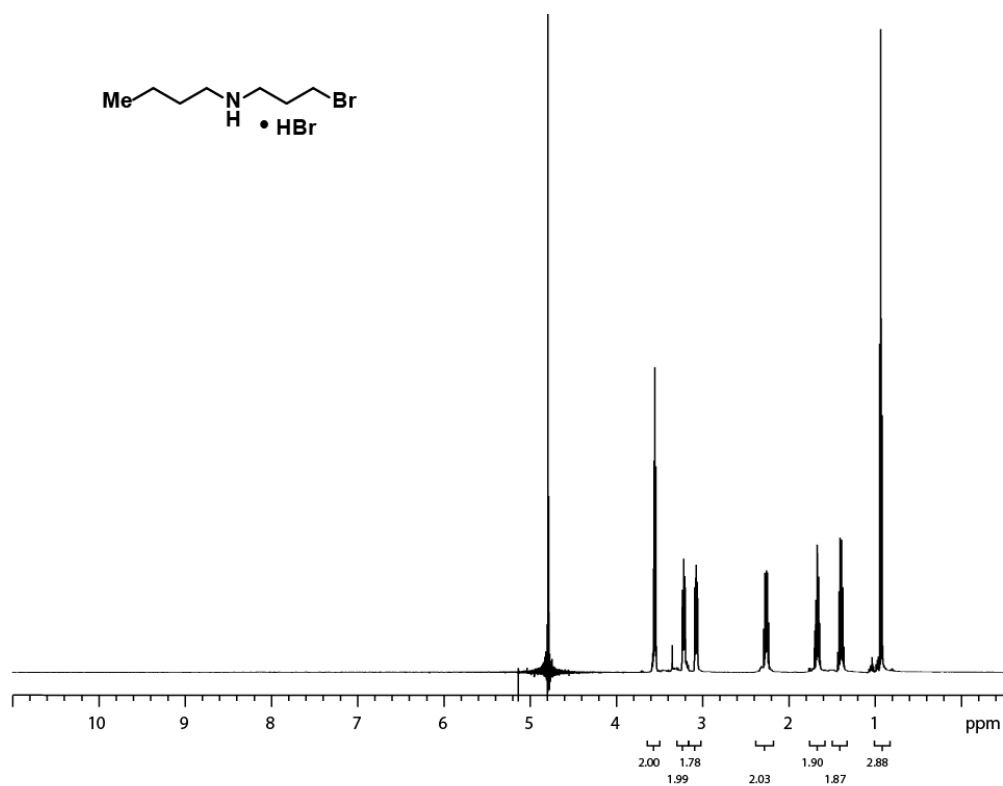
### 3.9.4 Representative $^1\text{H}$ NMR and $^{13}\text{C}$ NMR

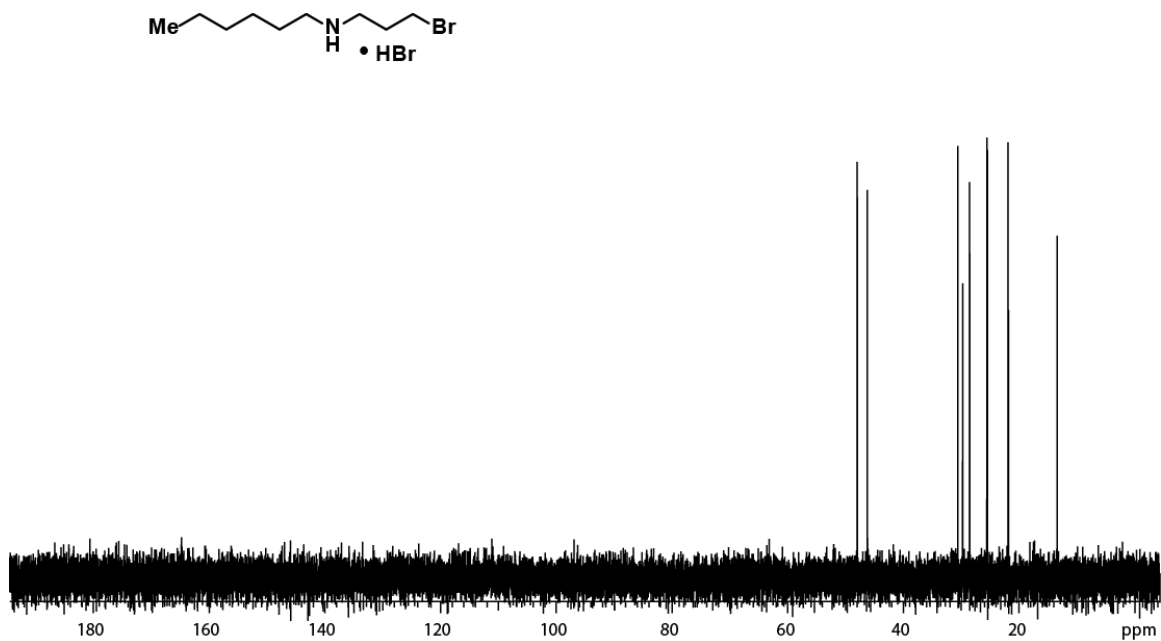
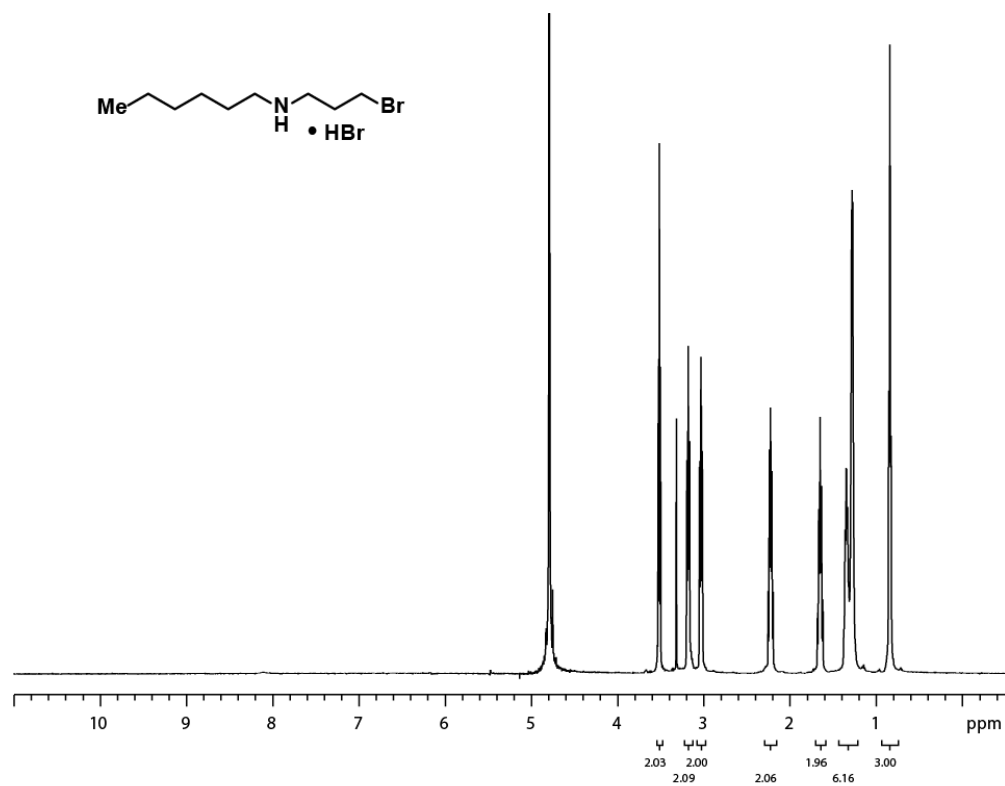


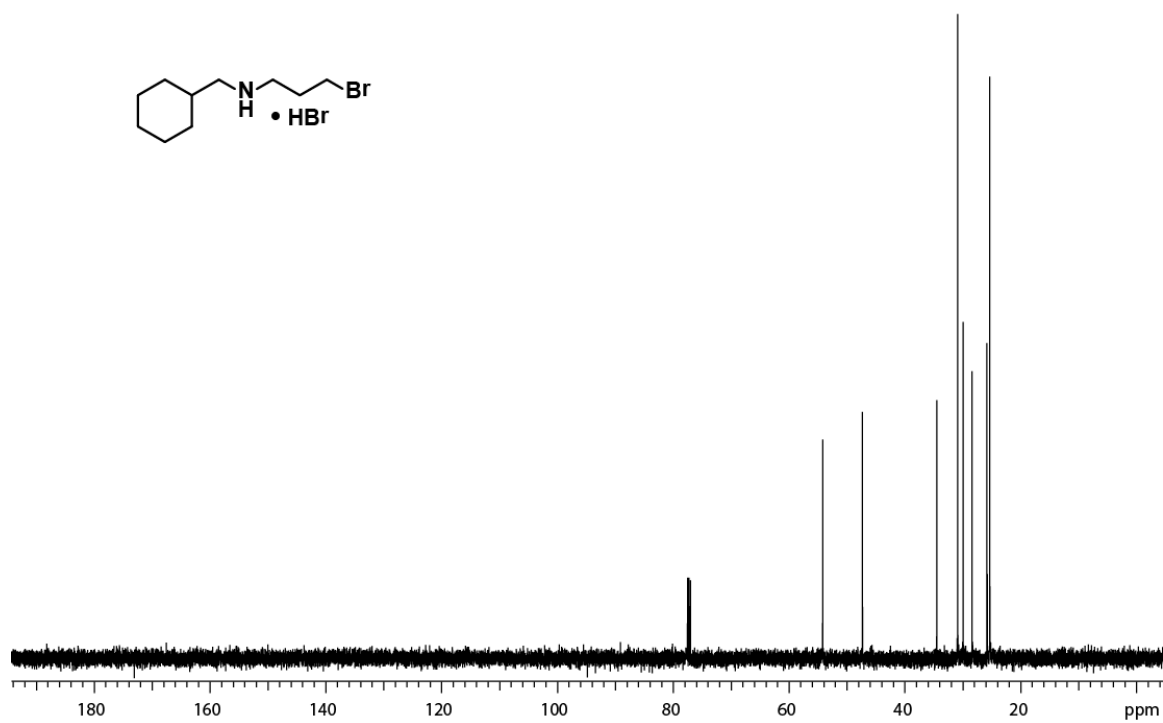
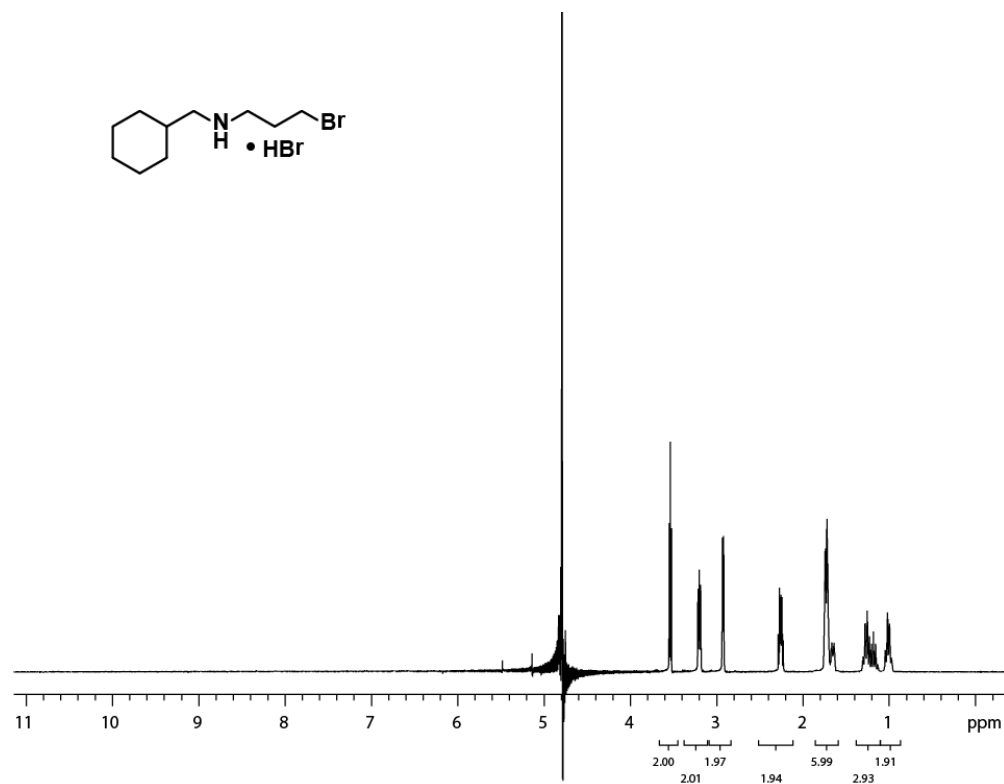


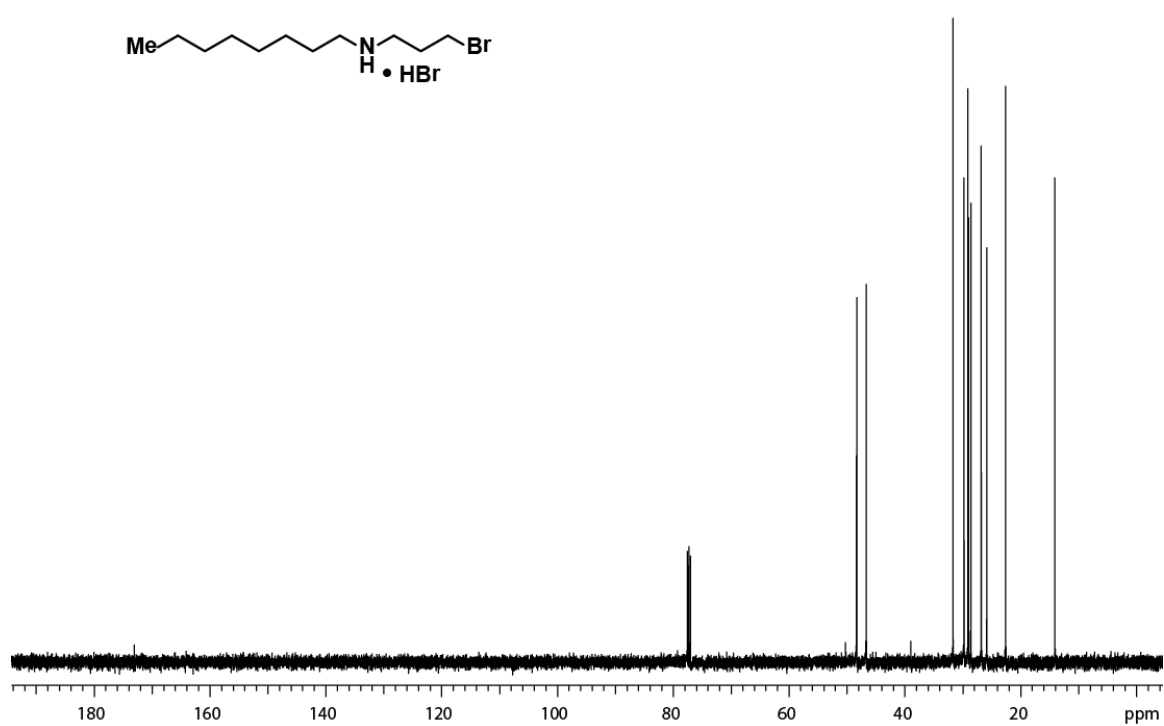
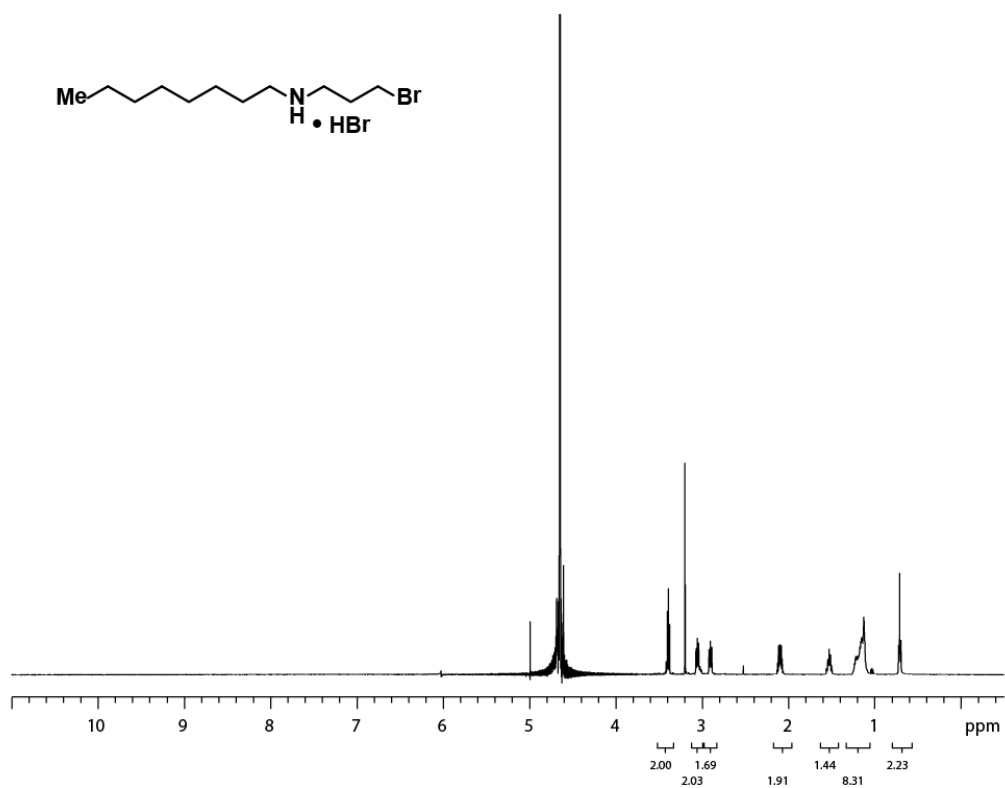


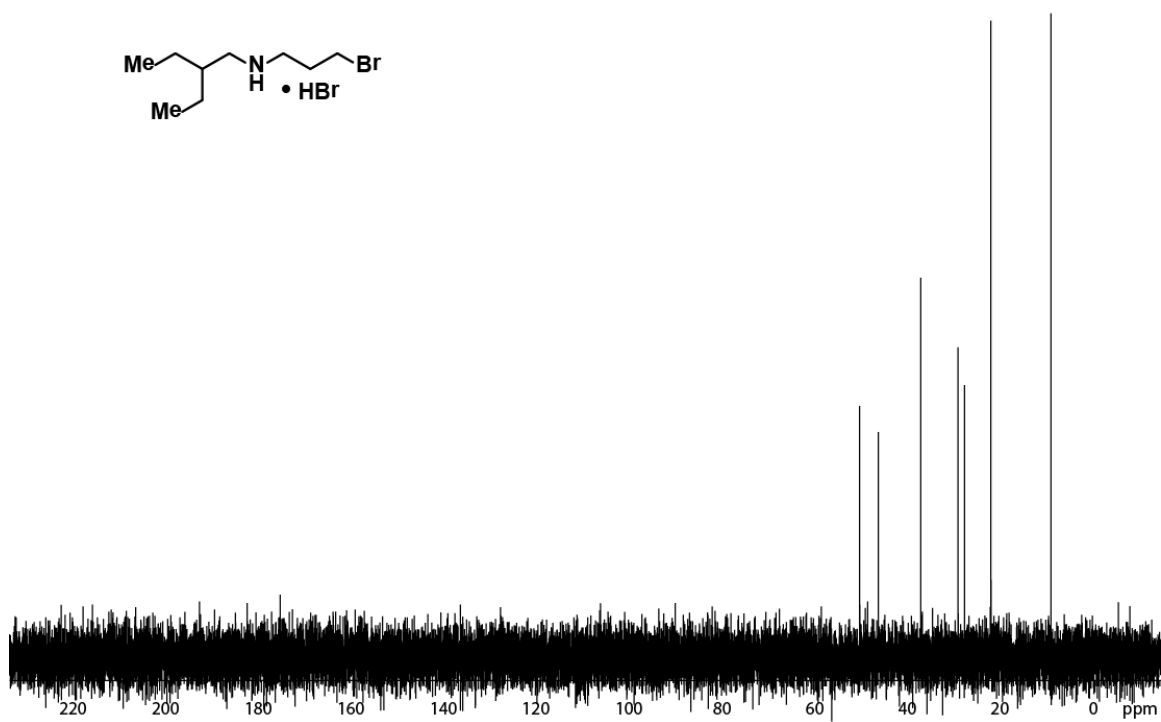
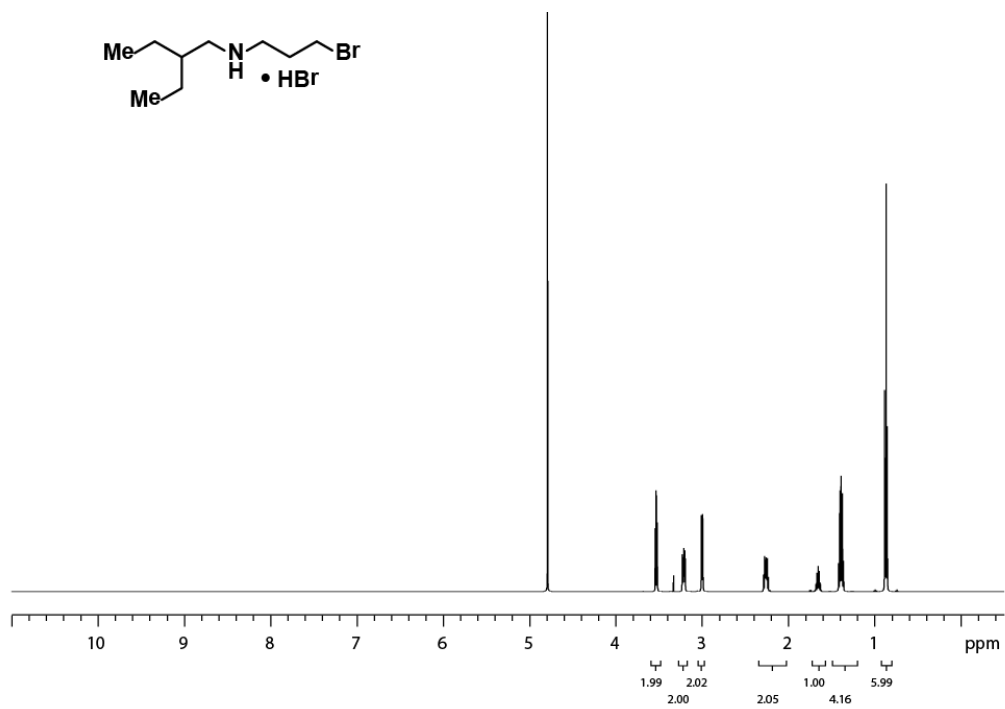


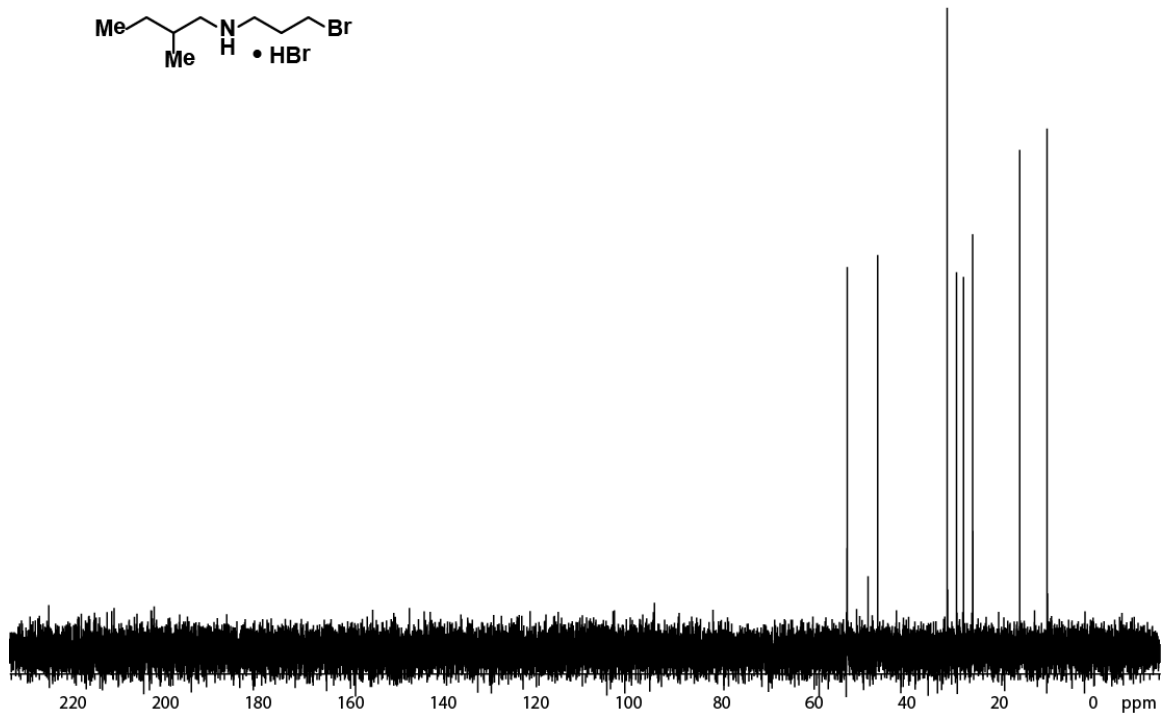
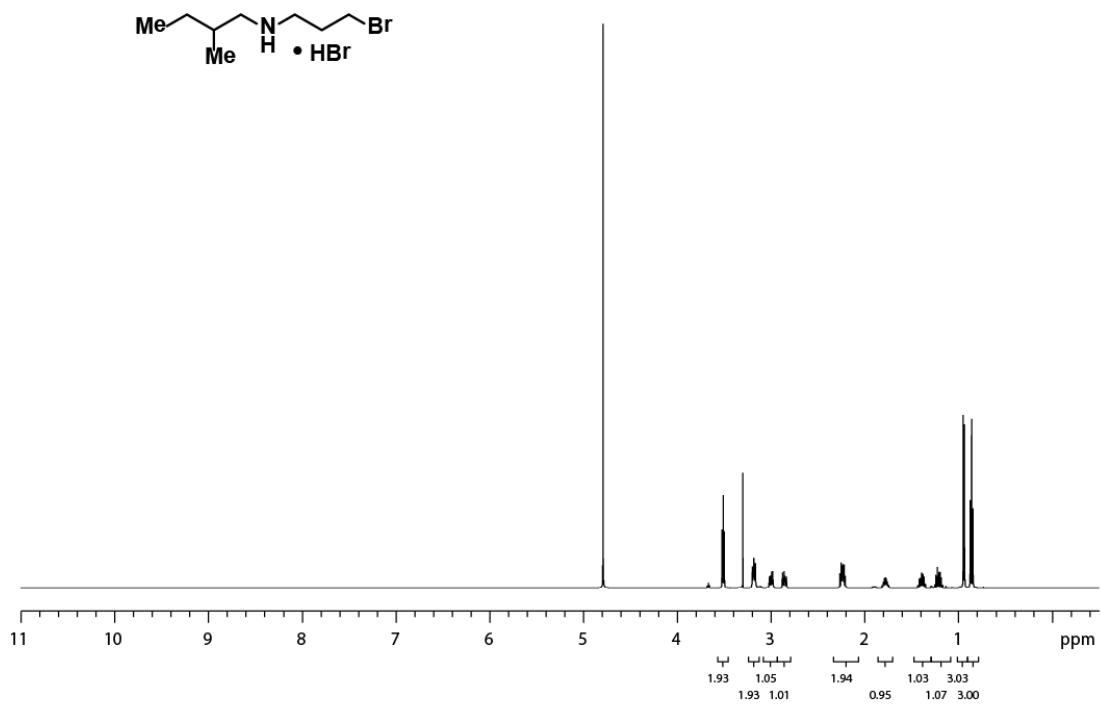


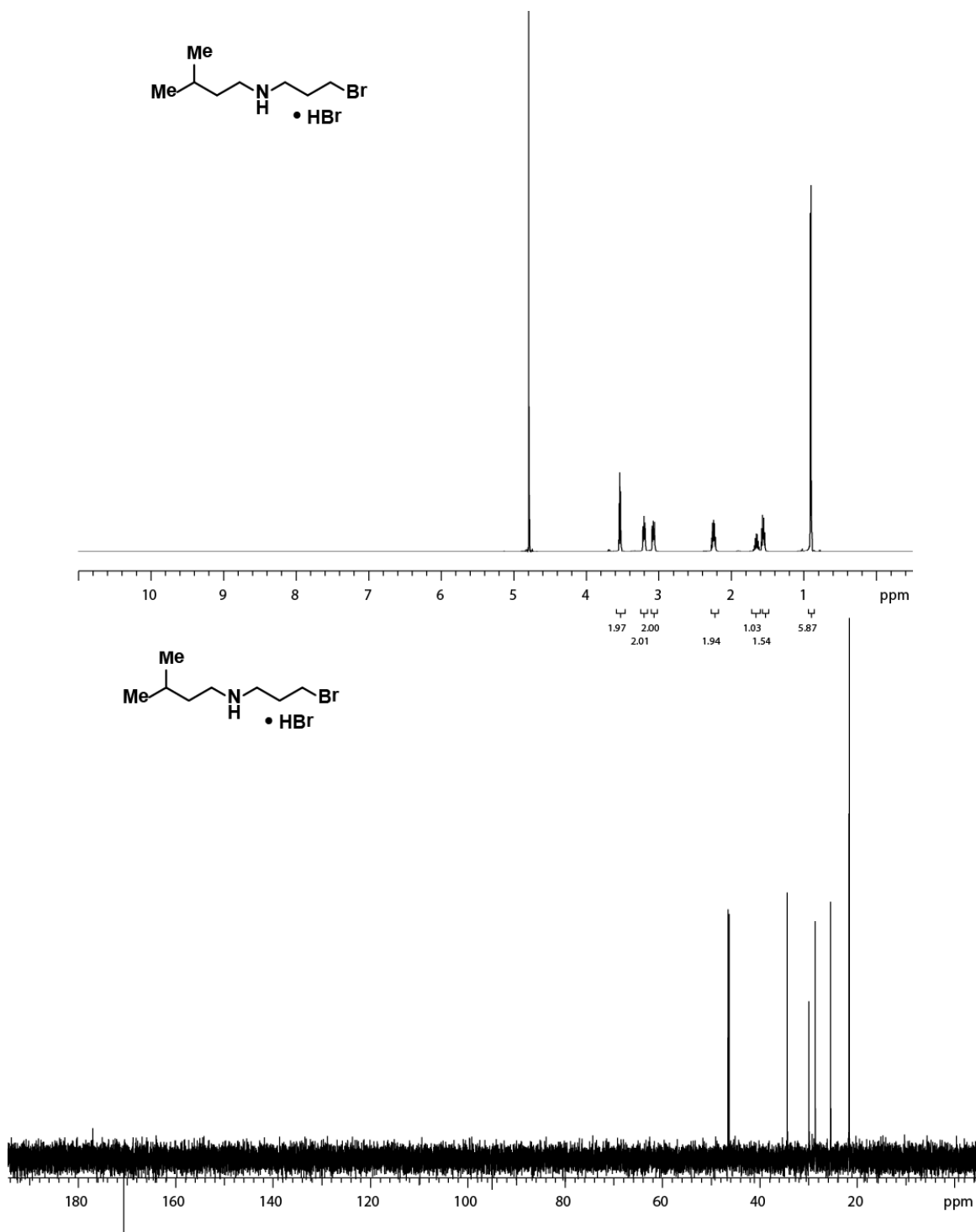


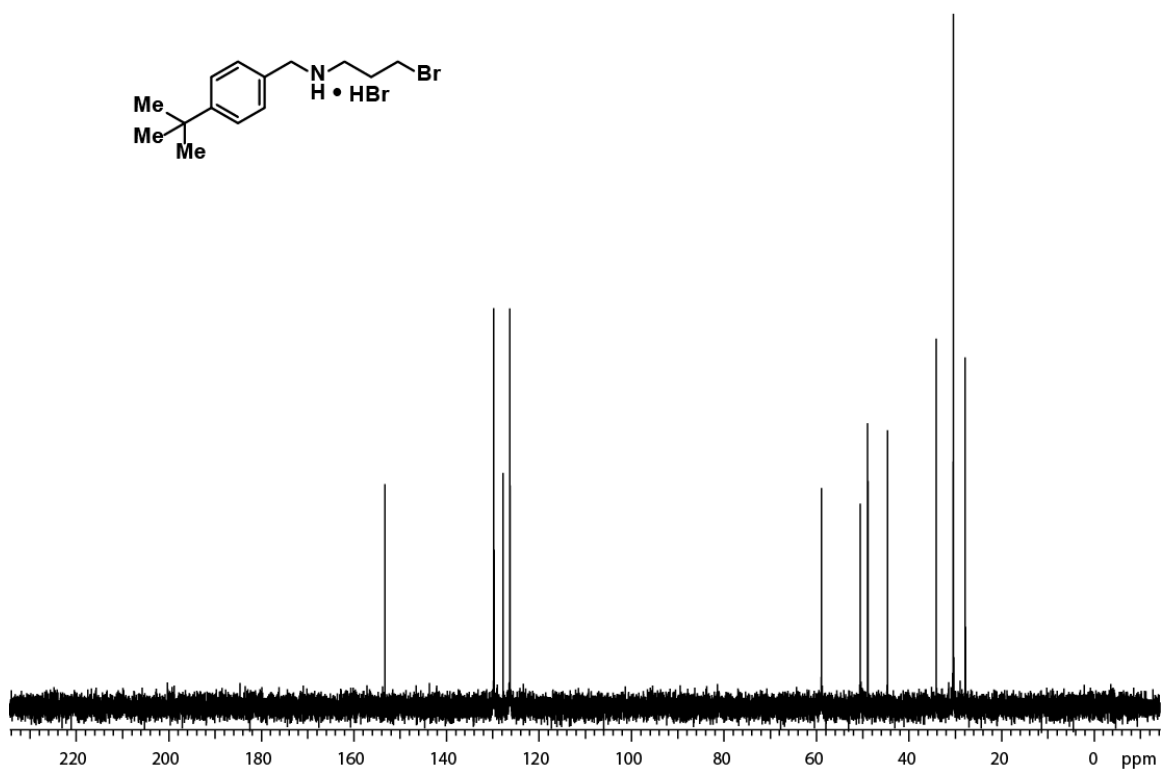
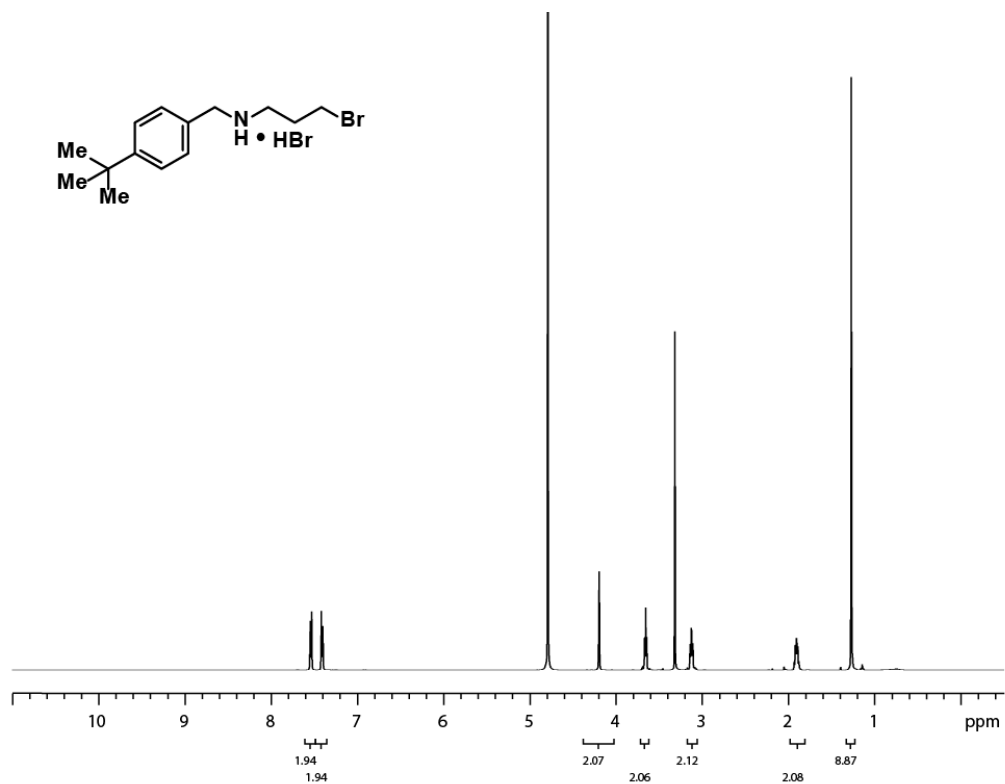




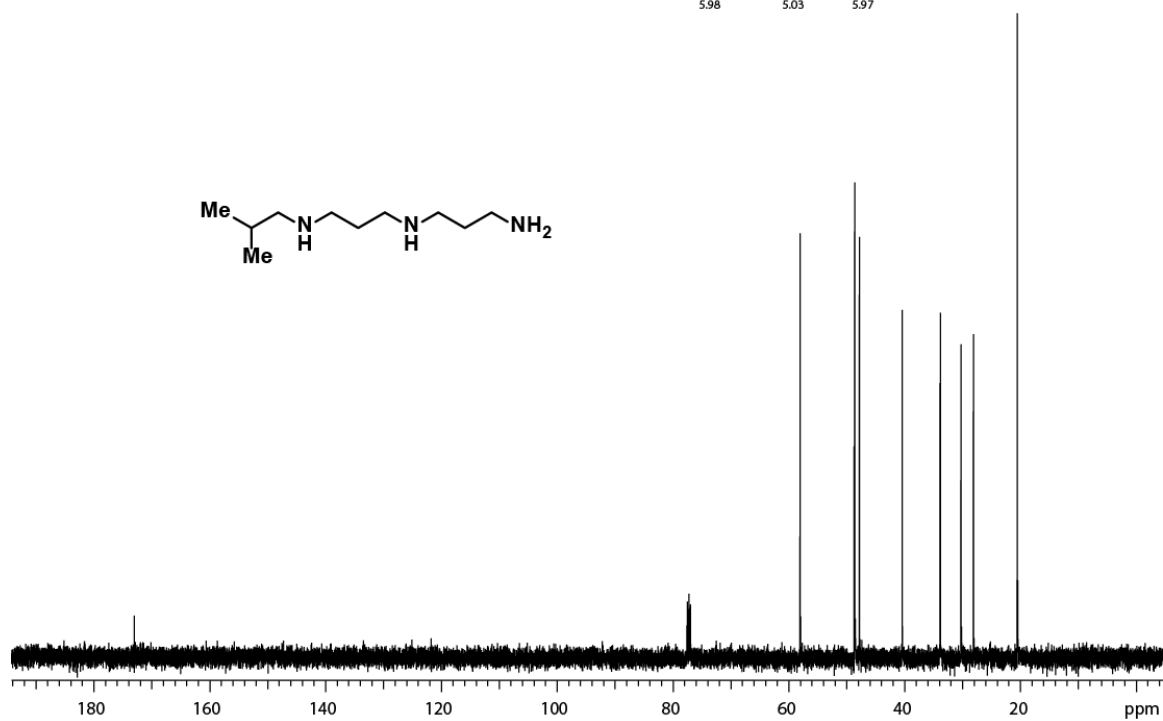
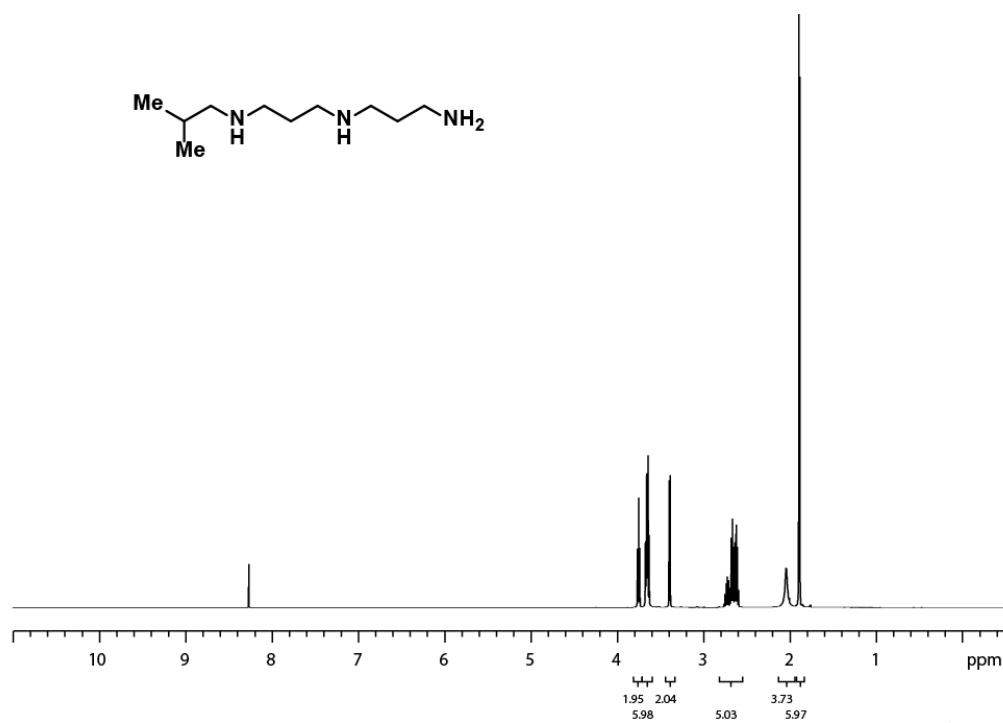


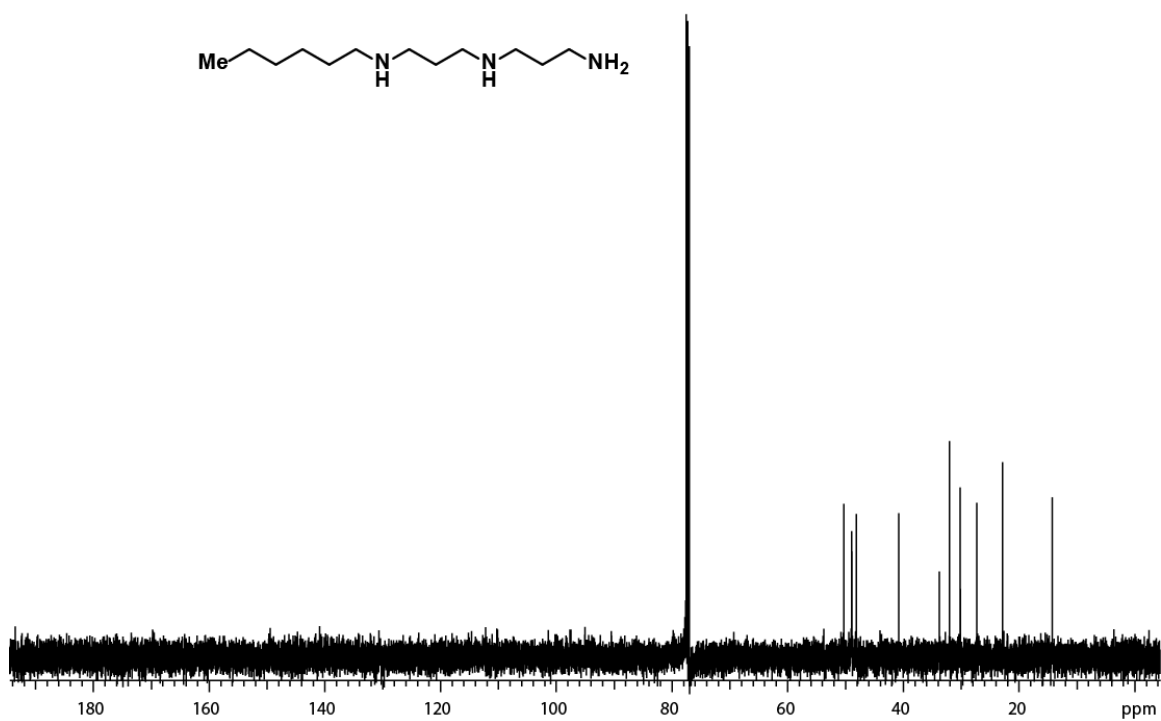
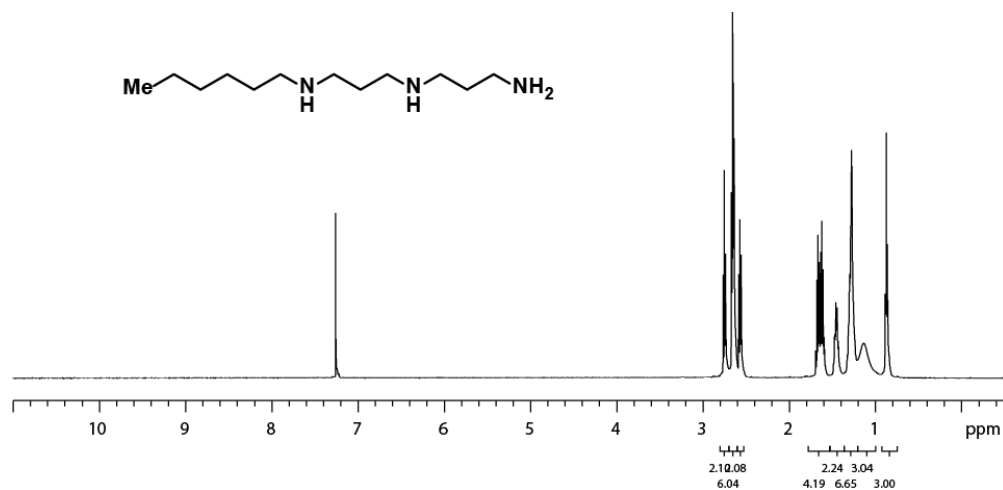


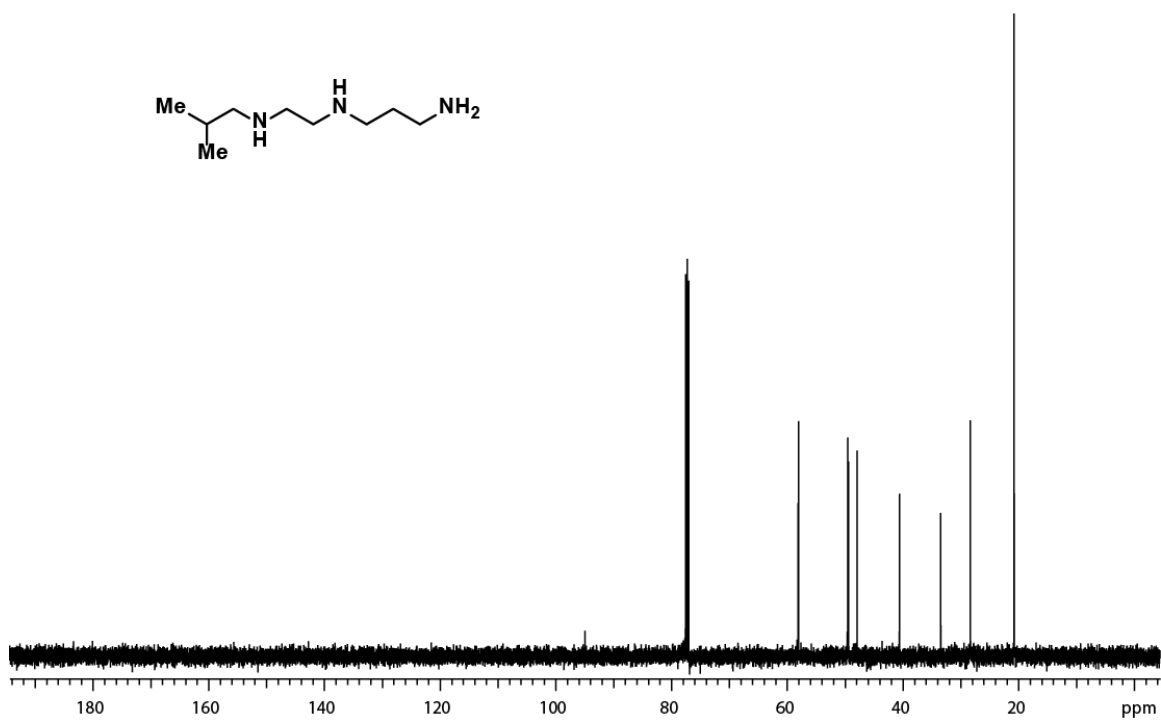
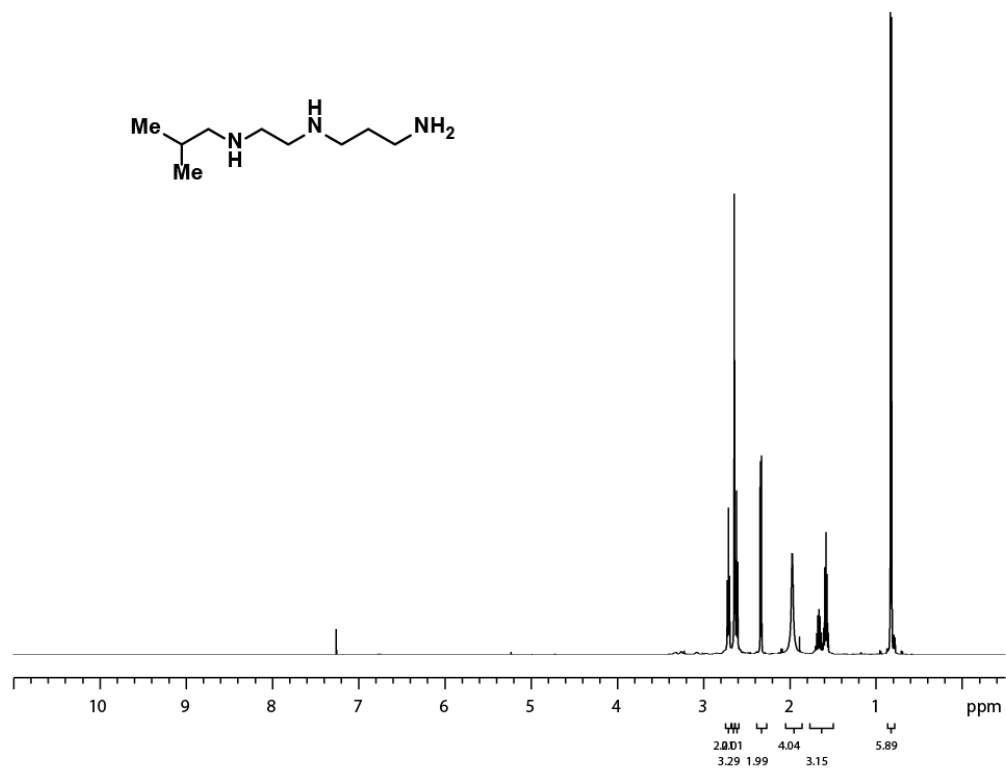


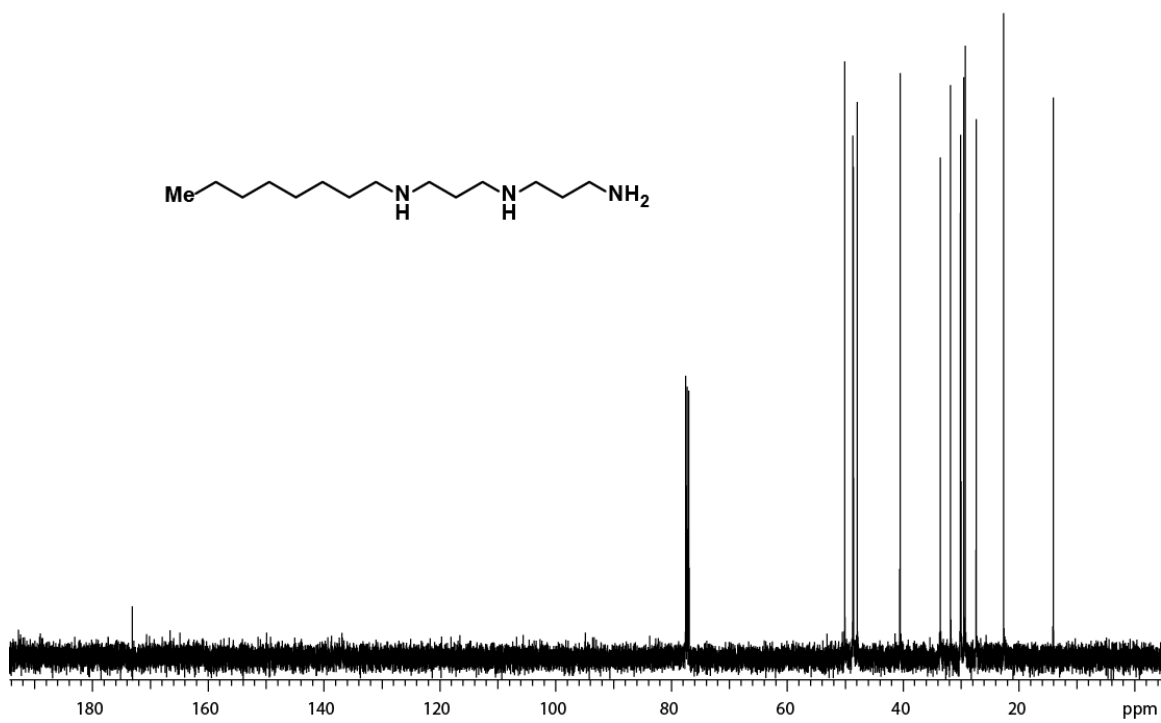
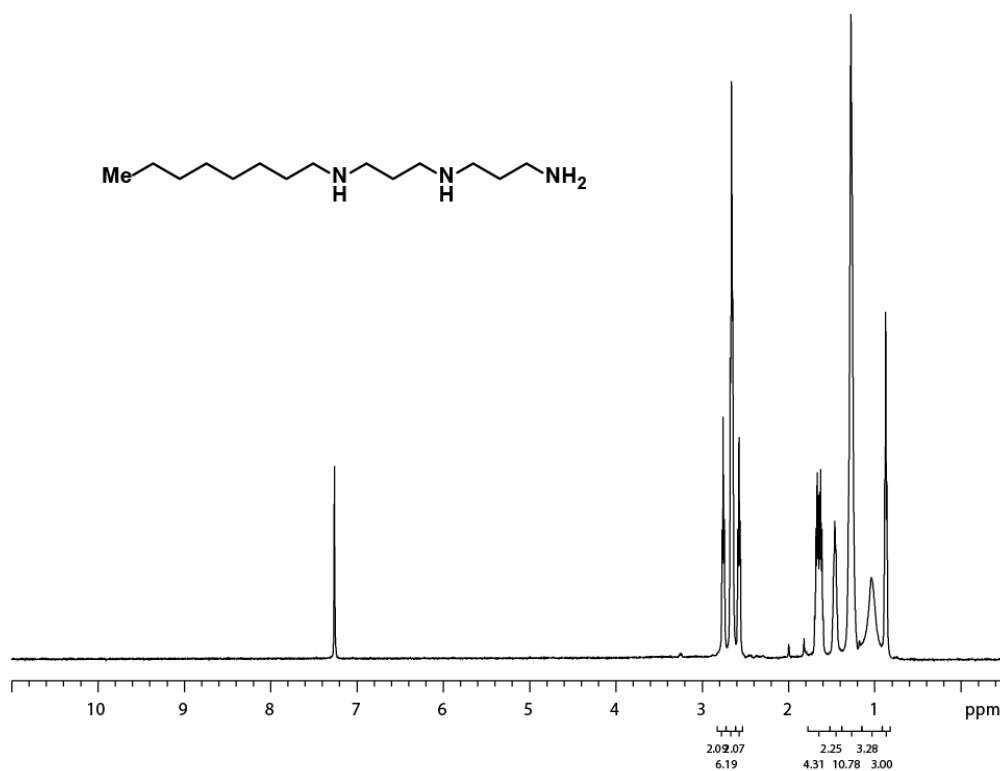


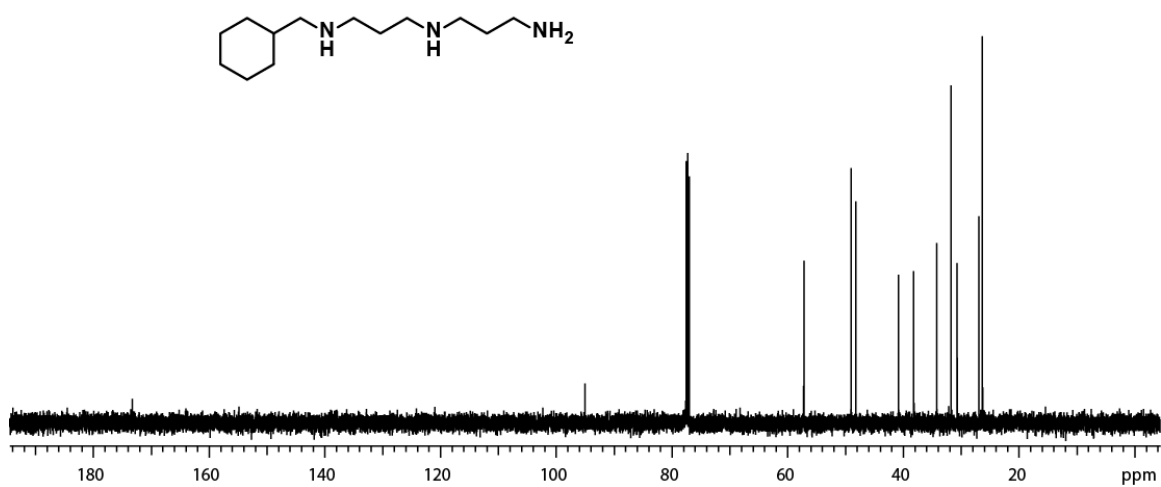
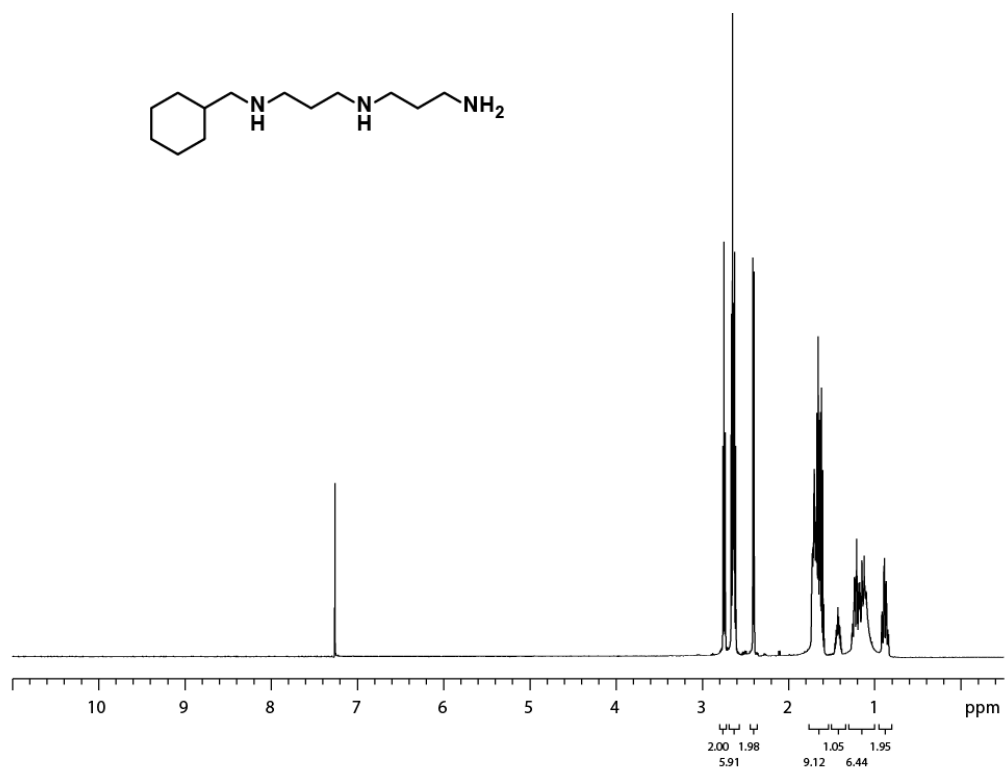


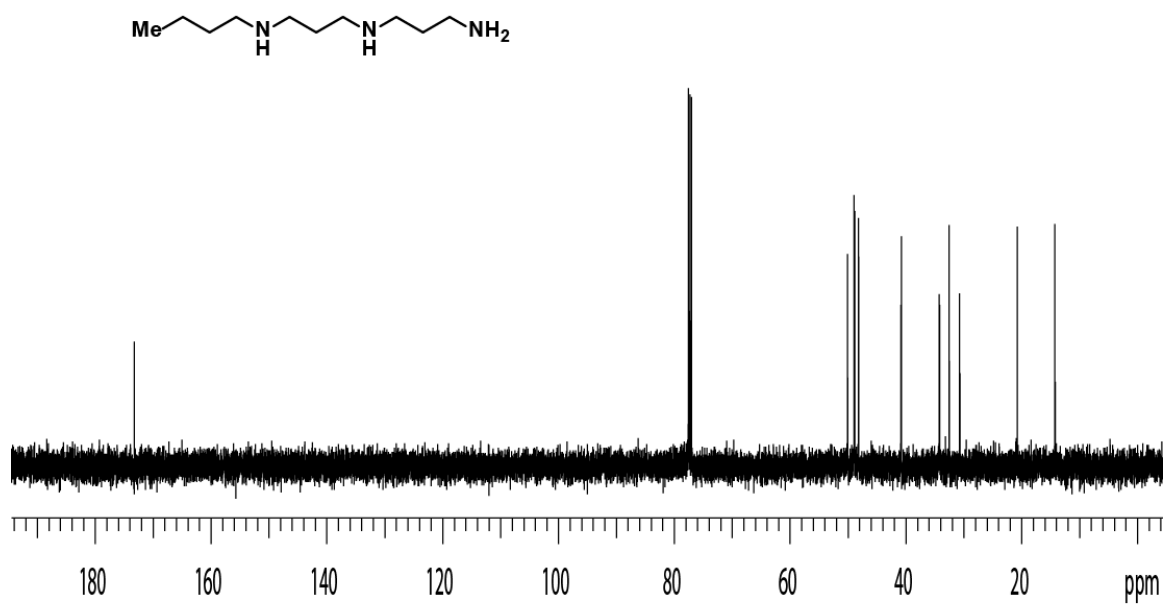
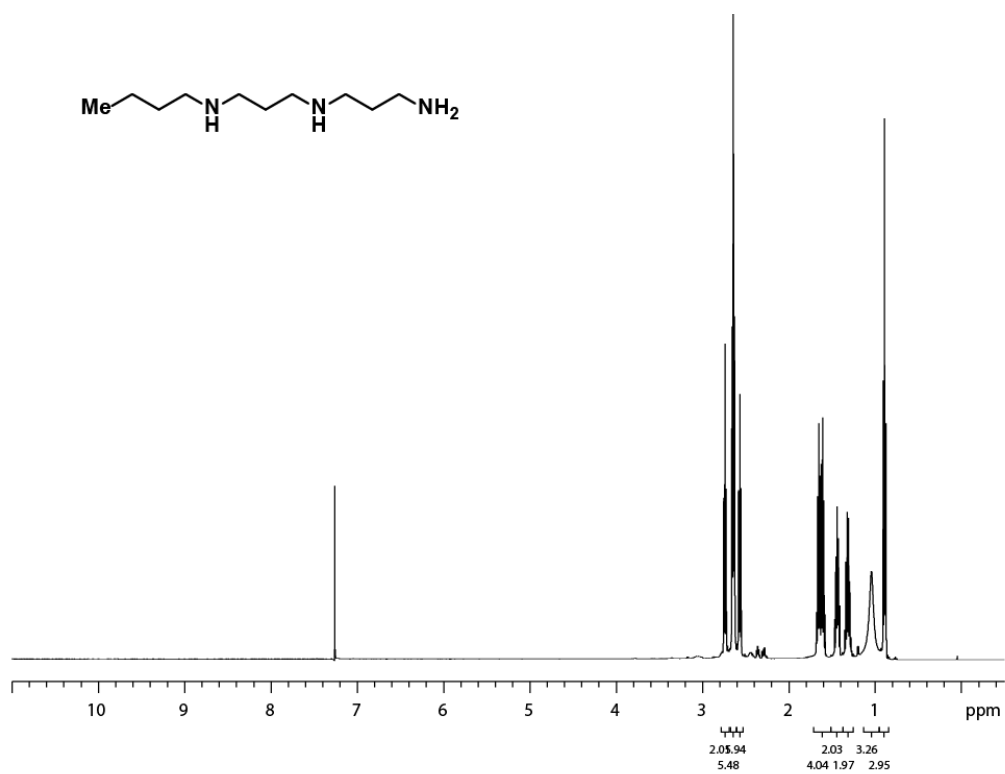


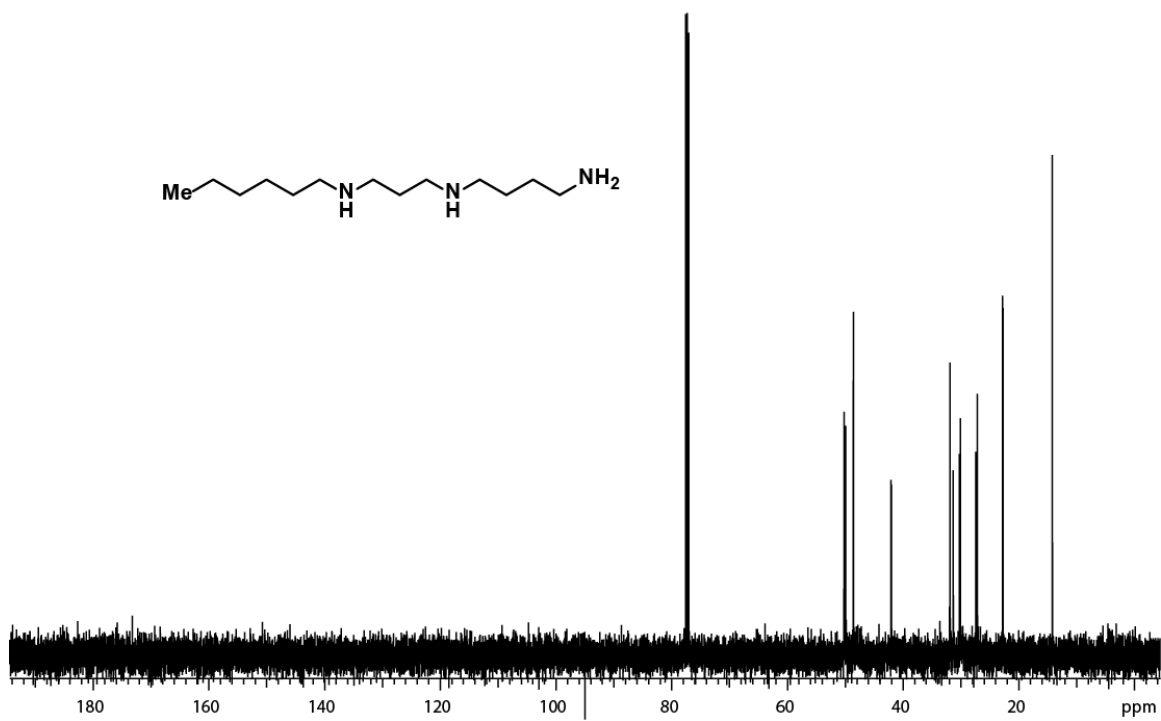
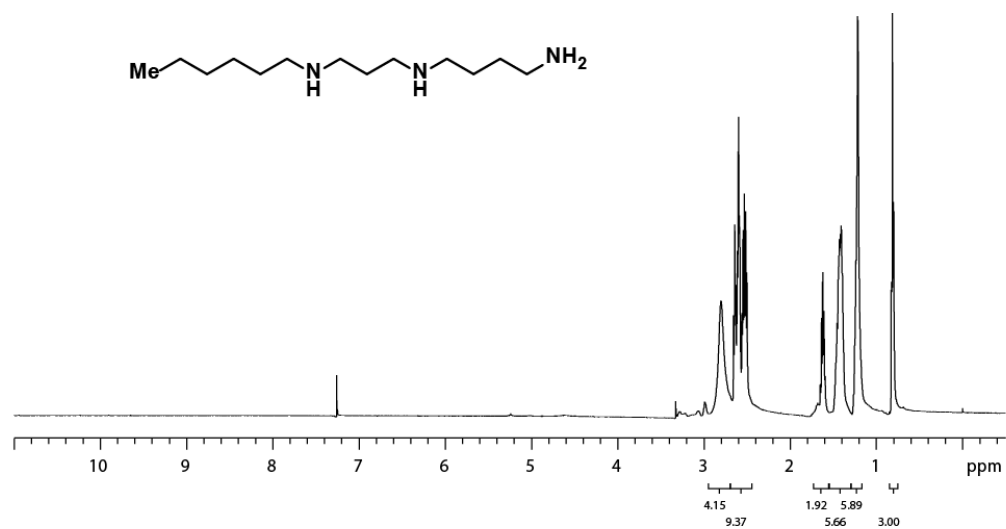


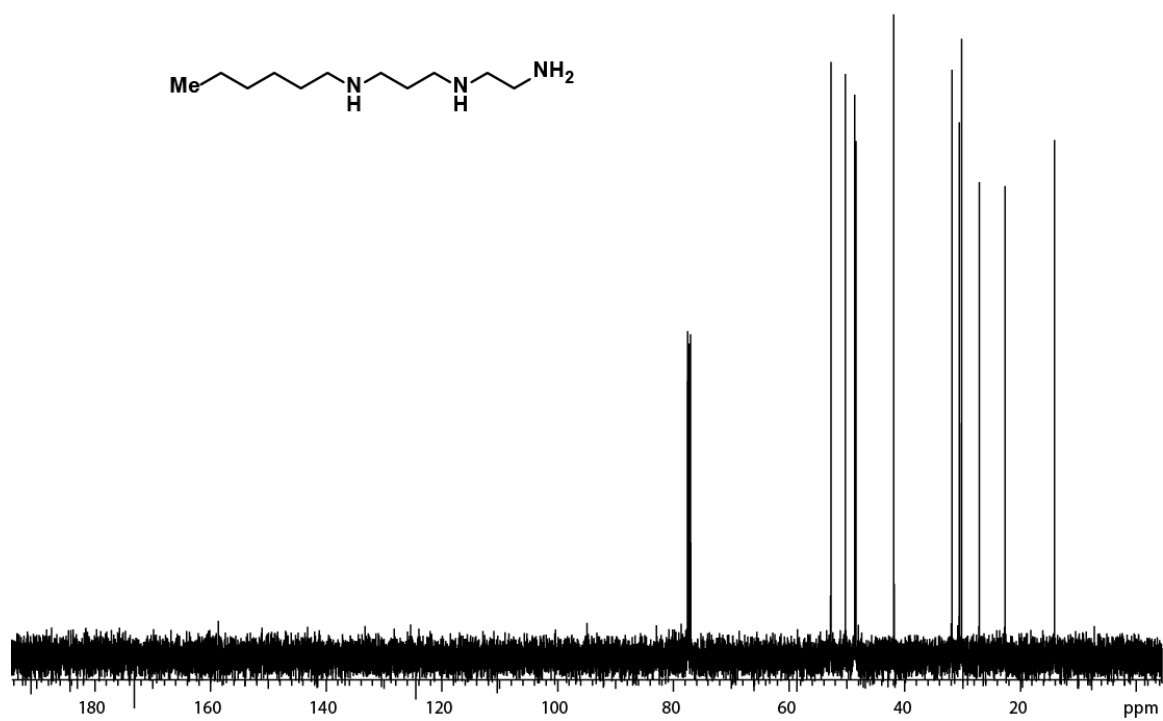
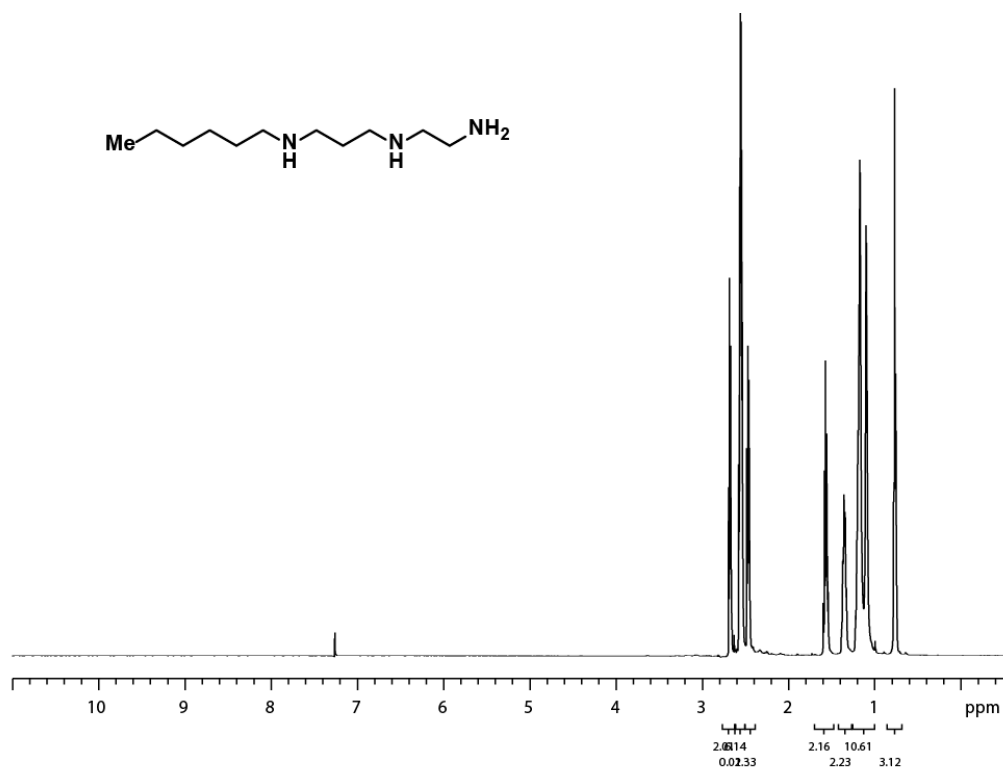




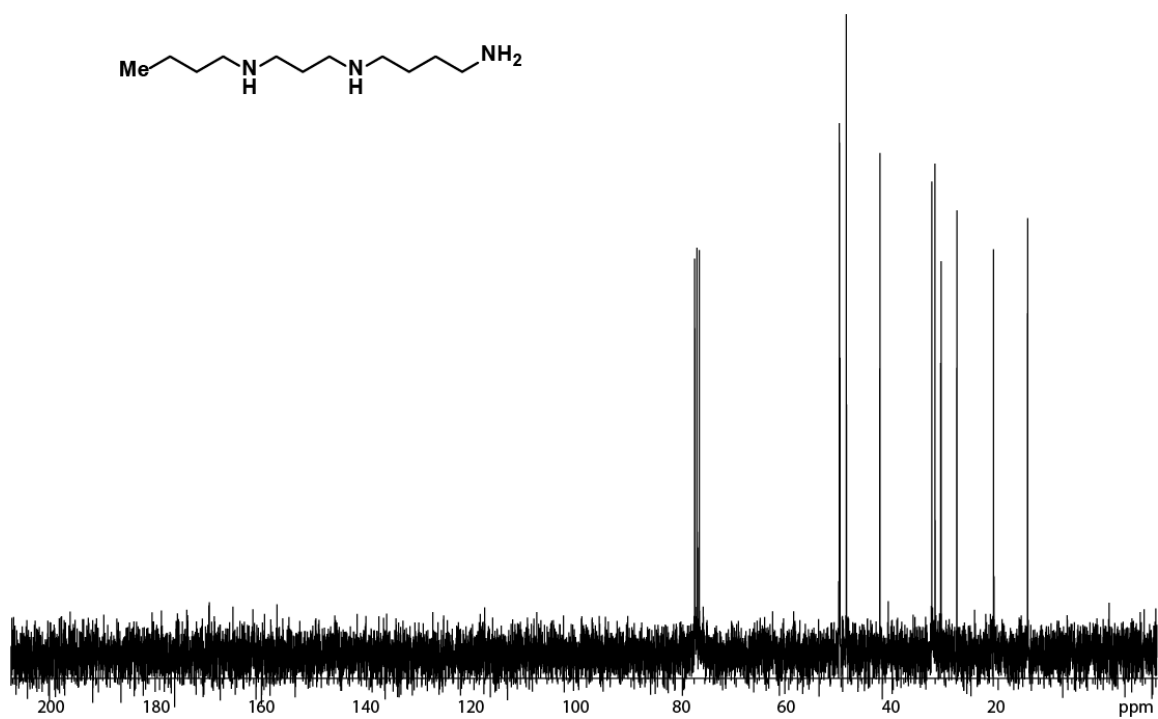
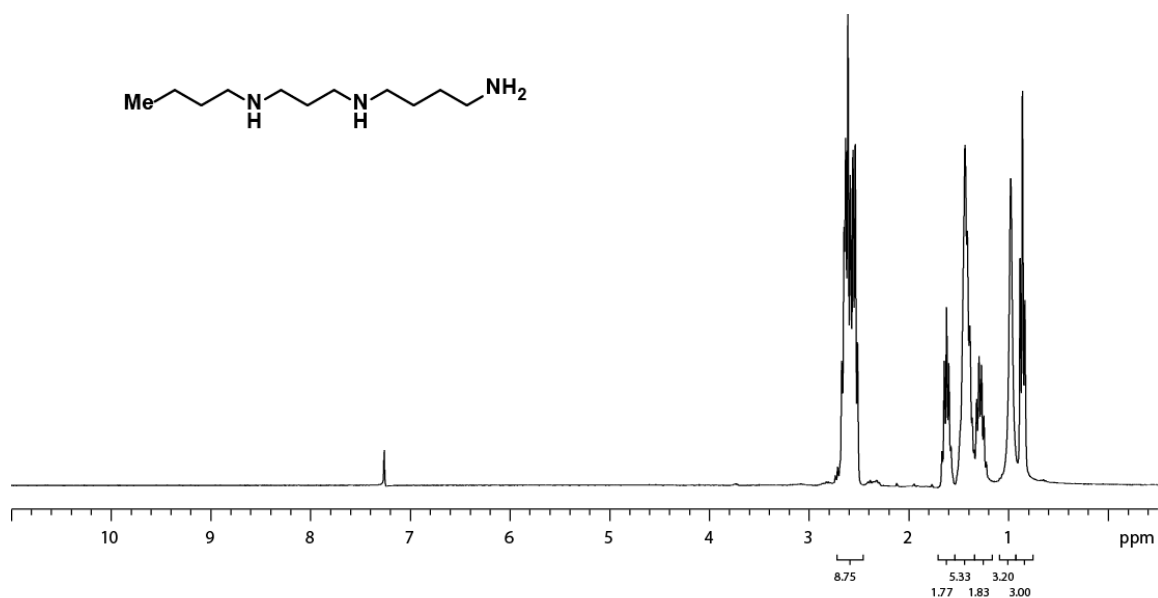


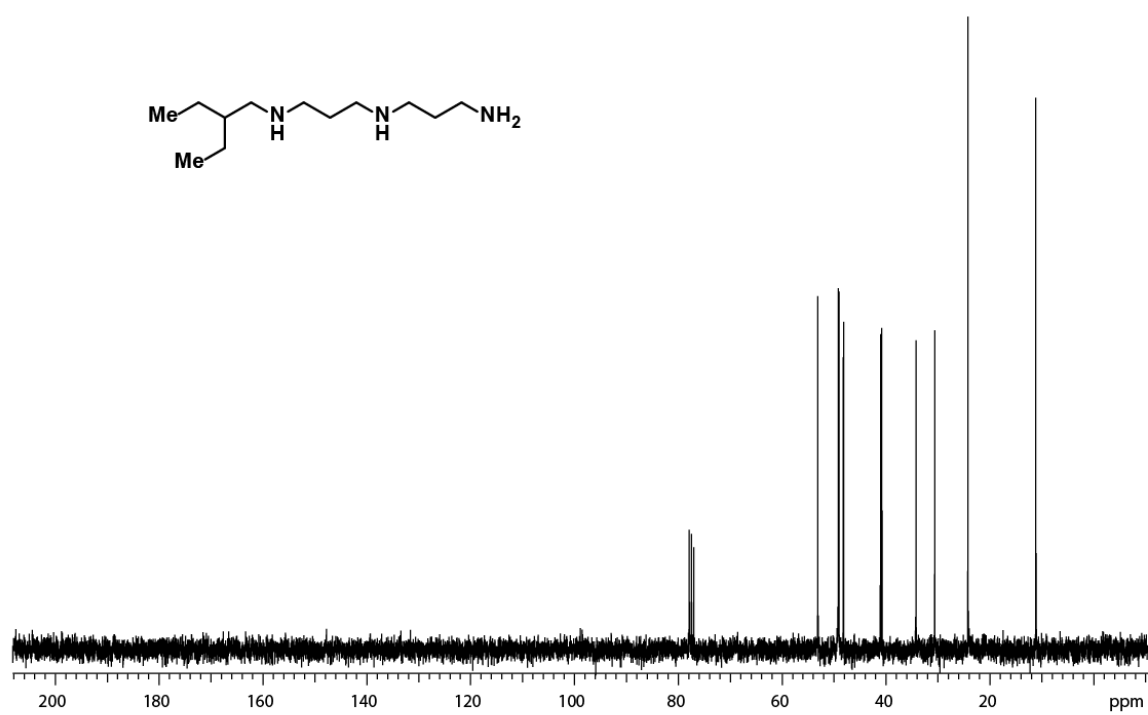
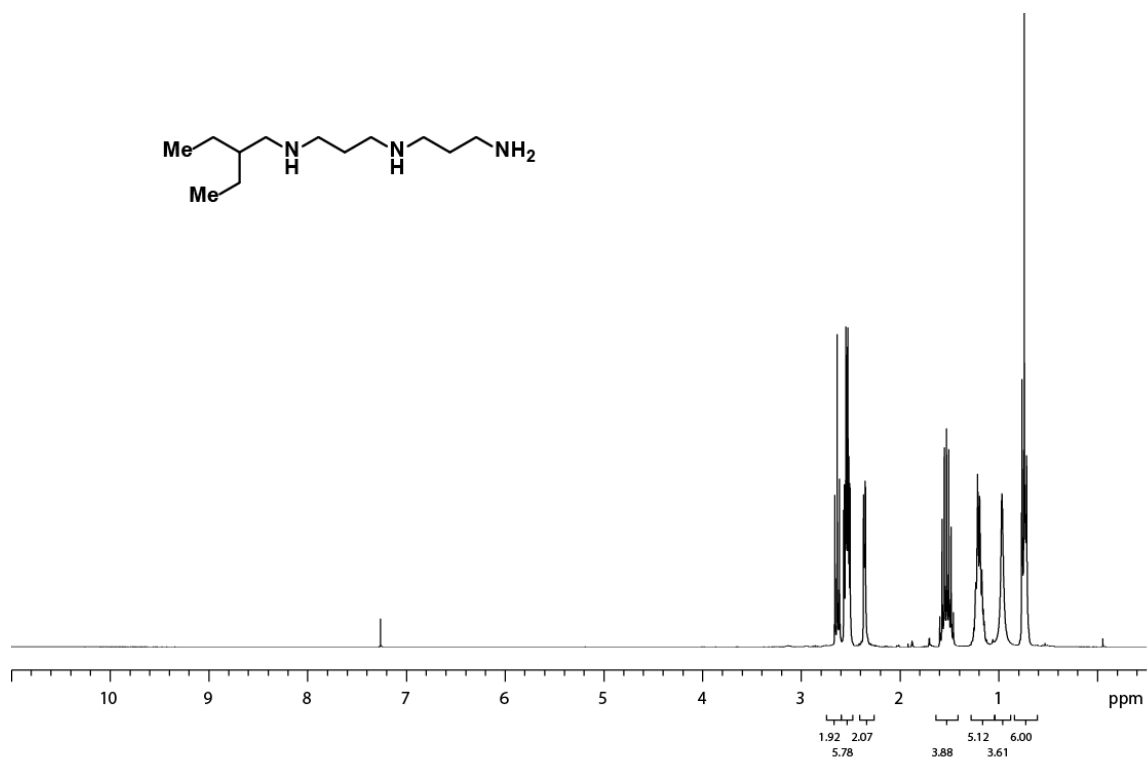


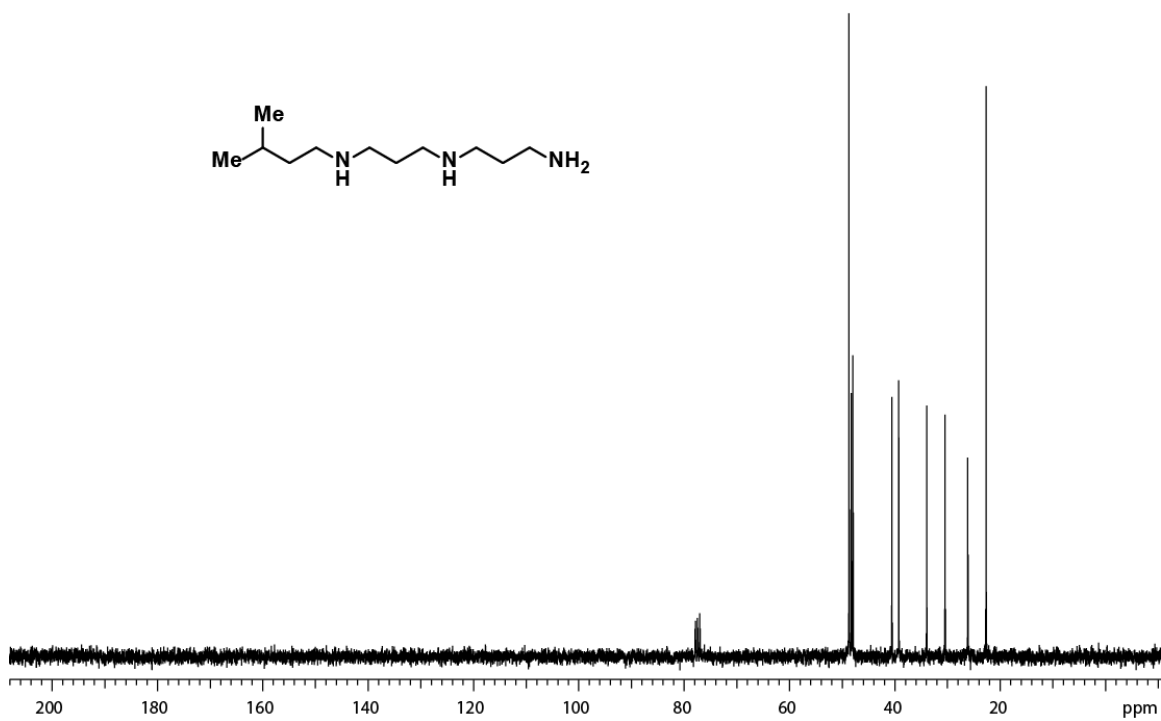
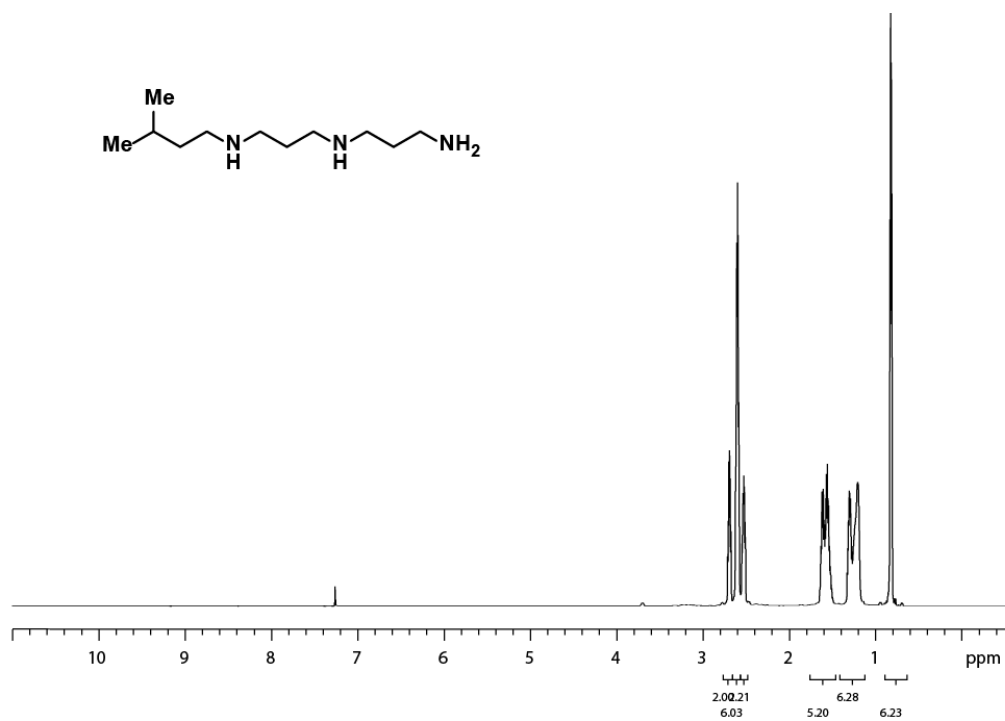


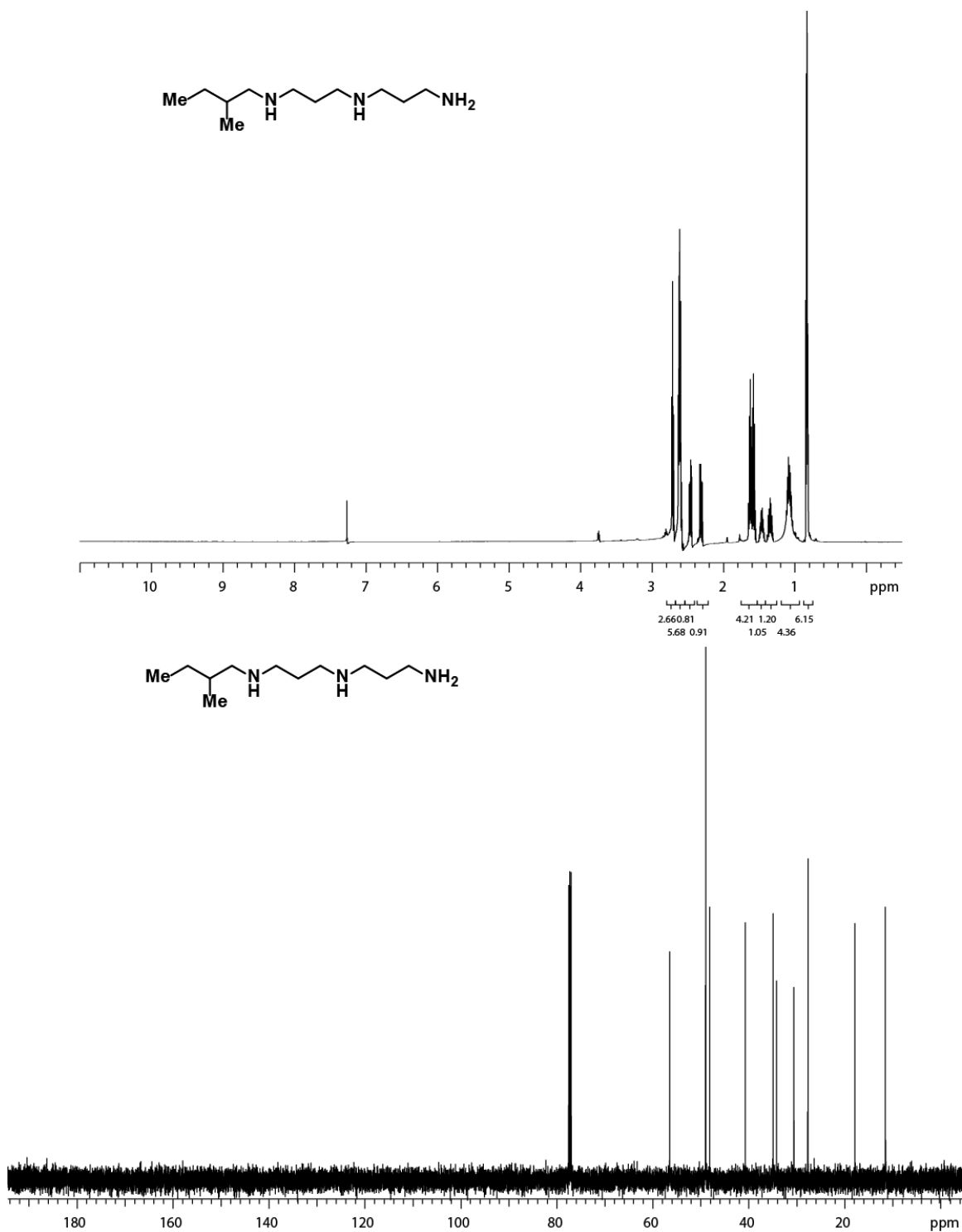


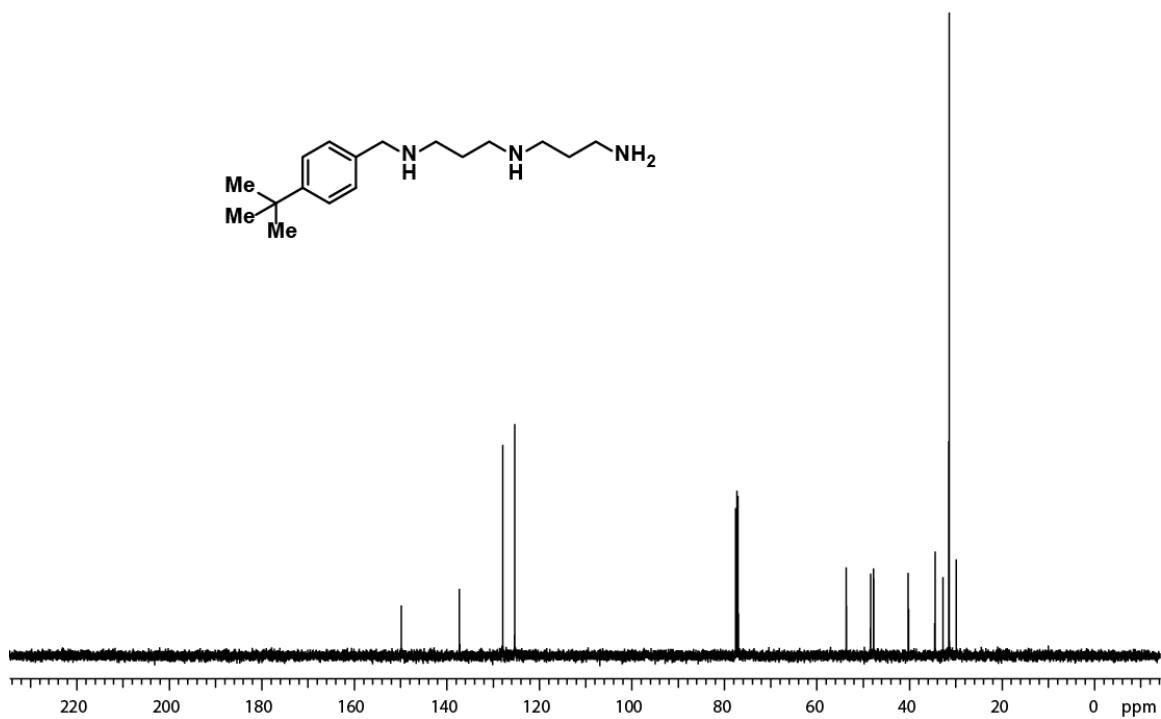
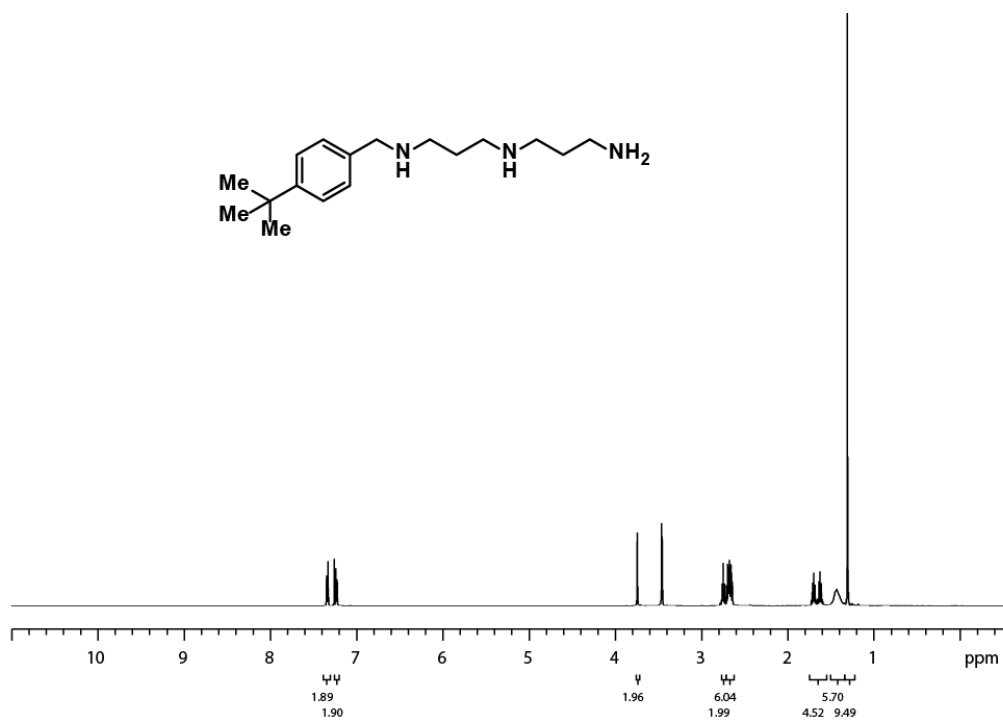


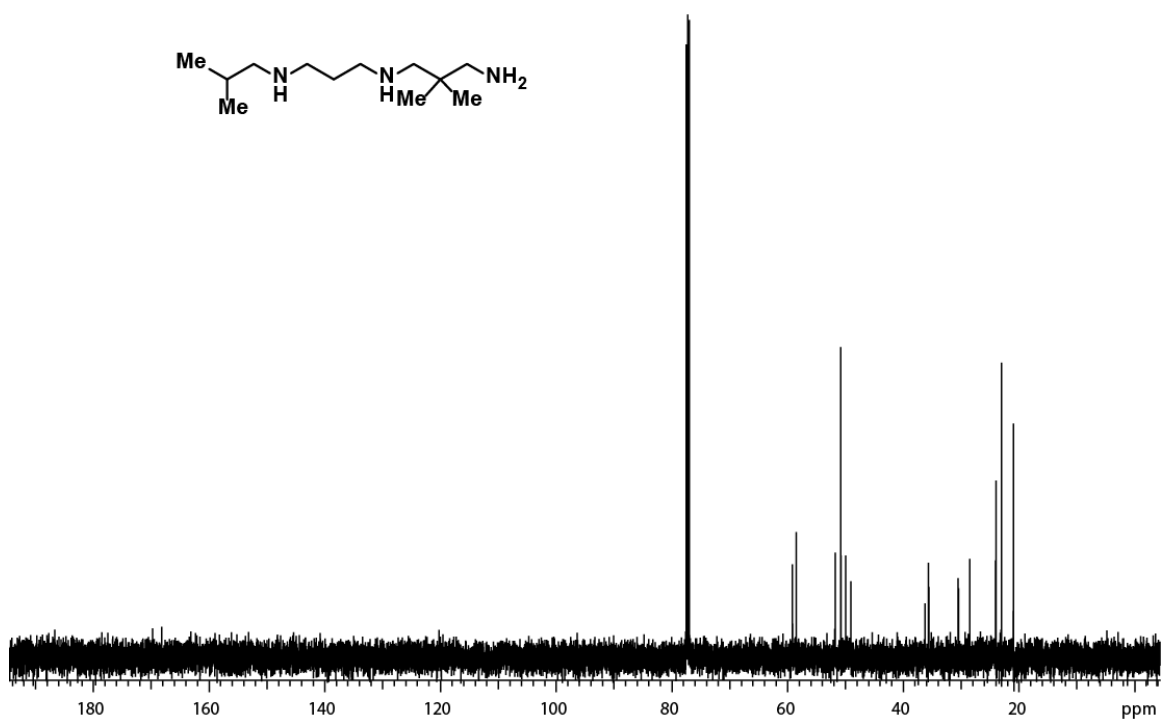
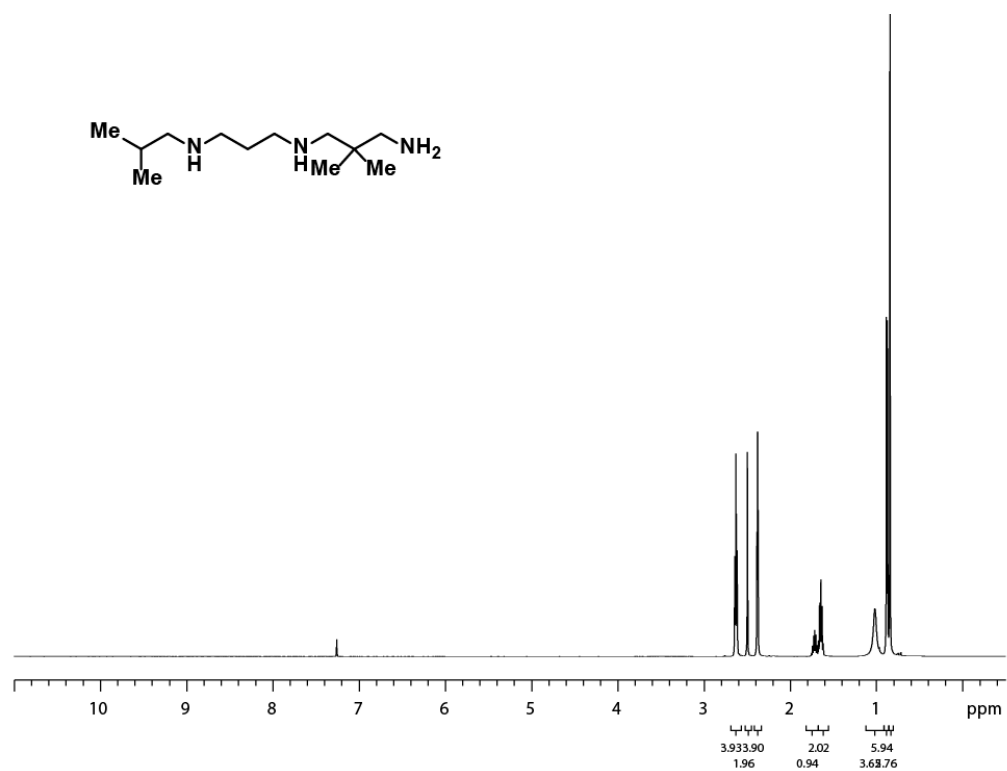


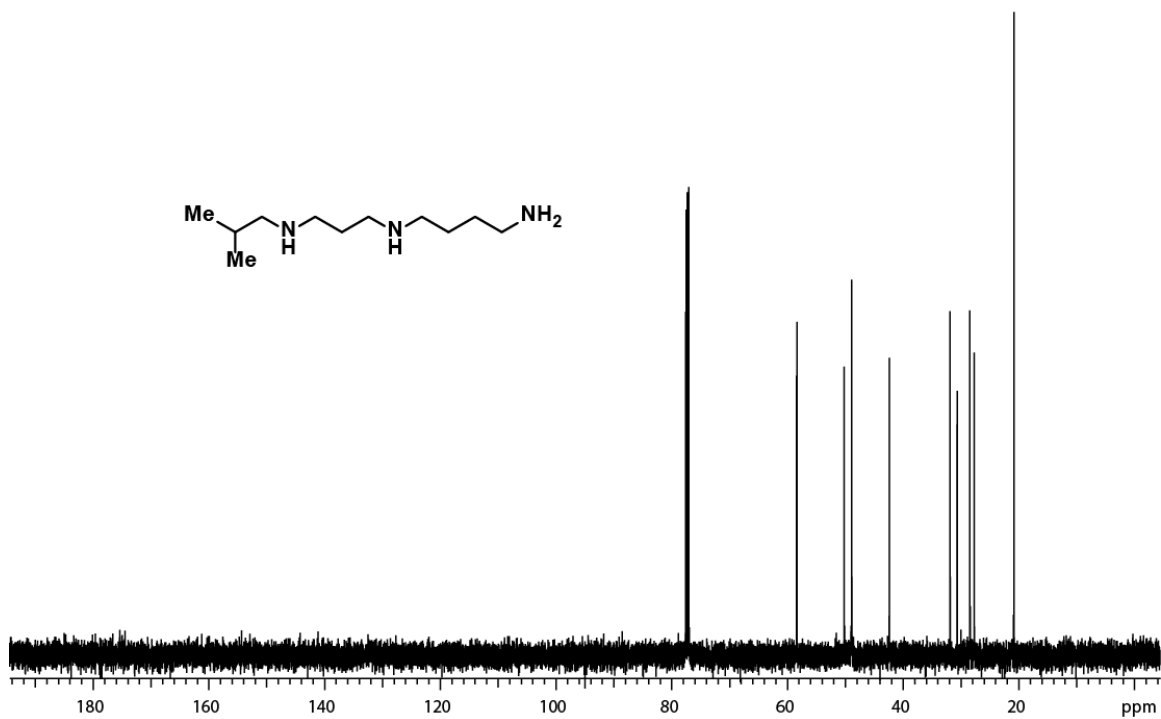
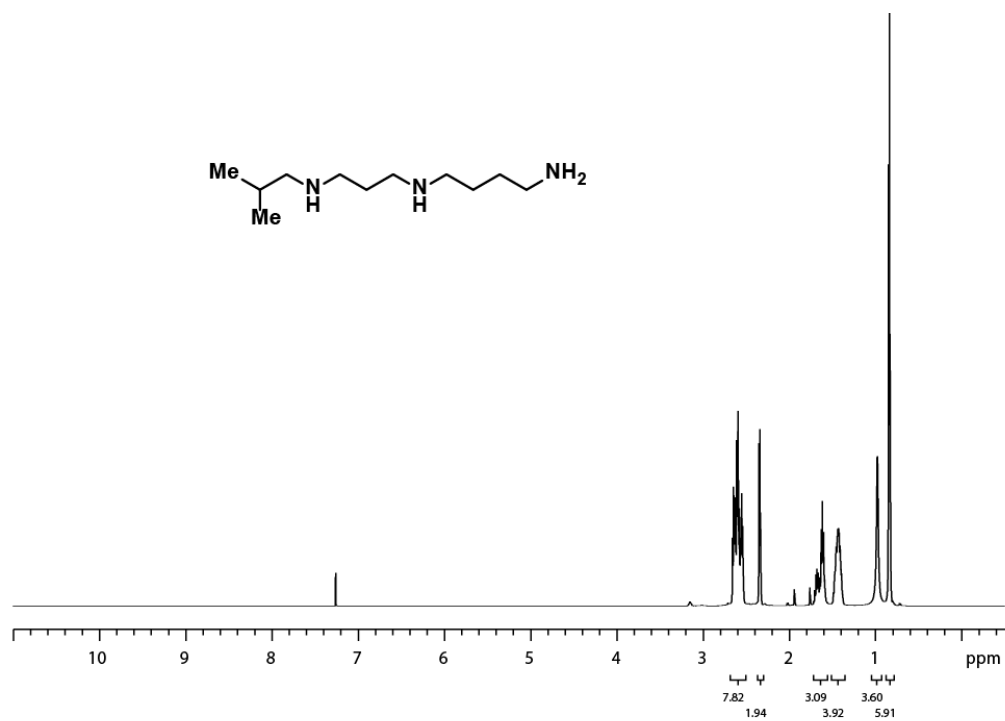


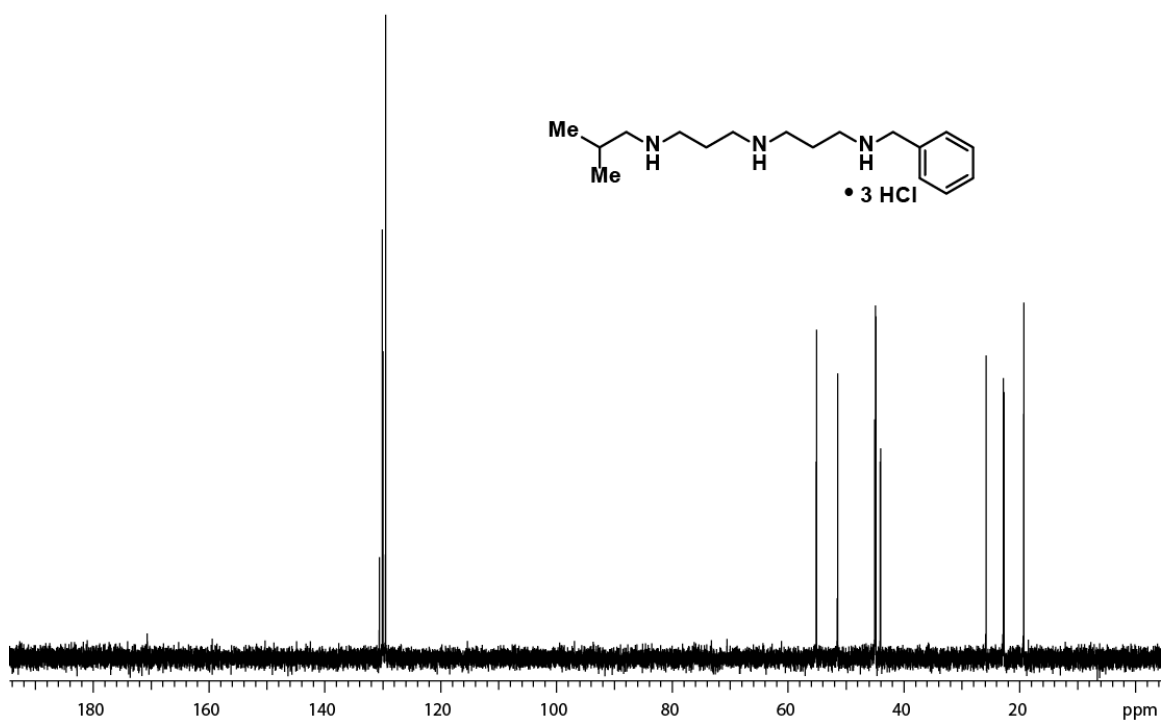
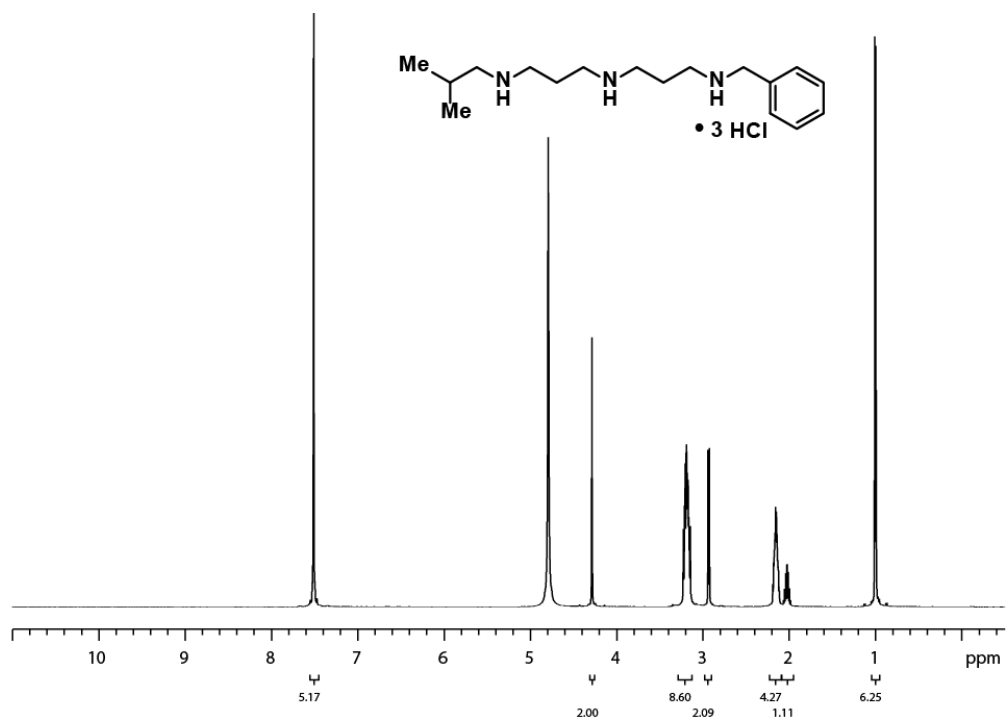




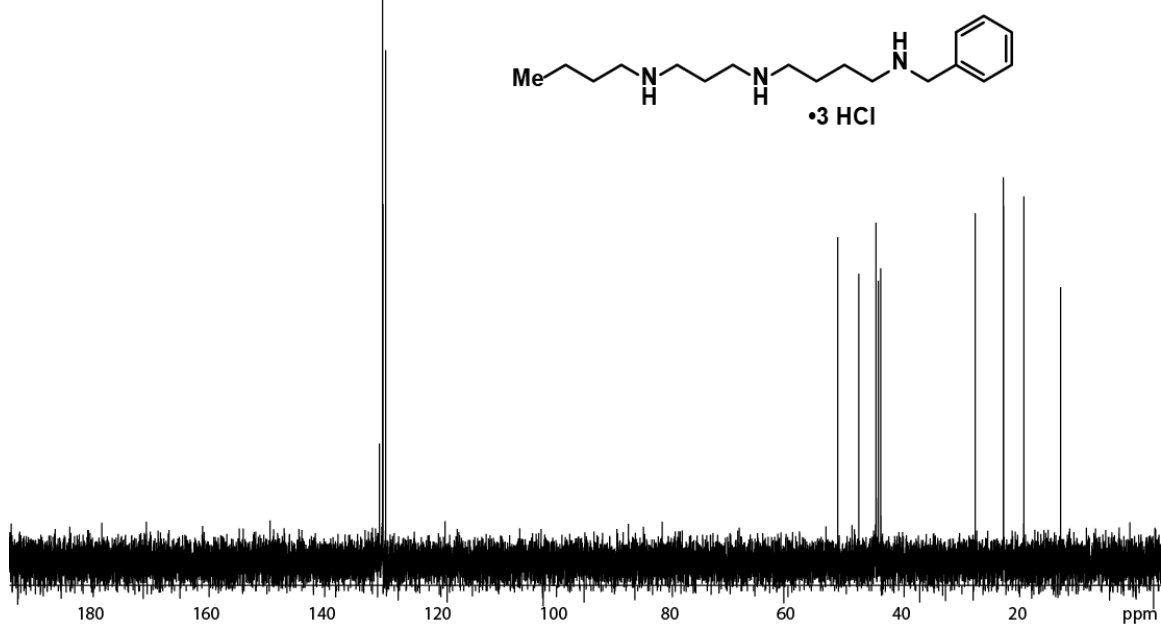
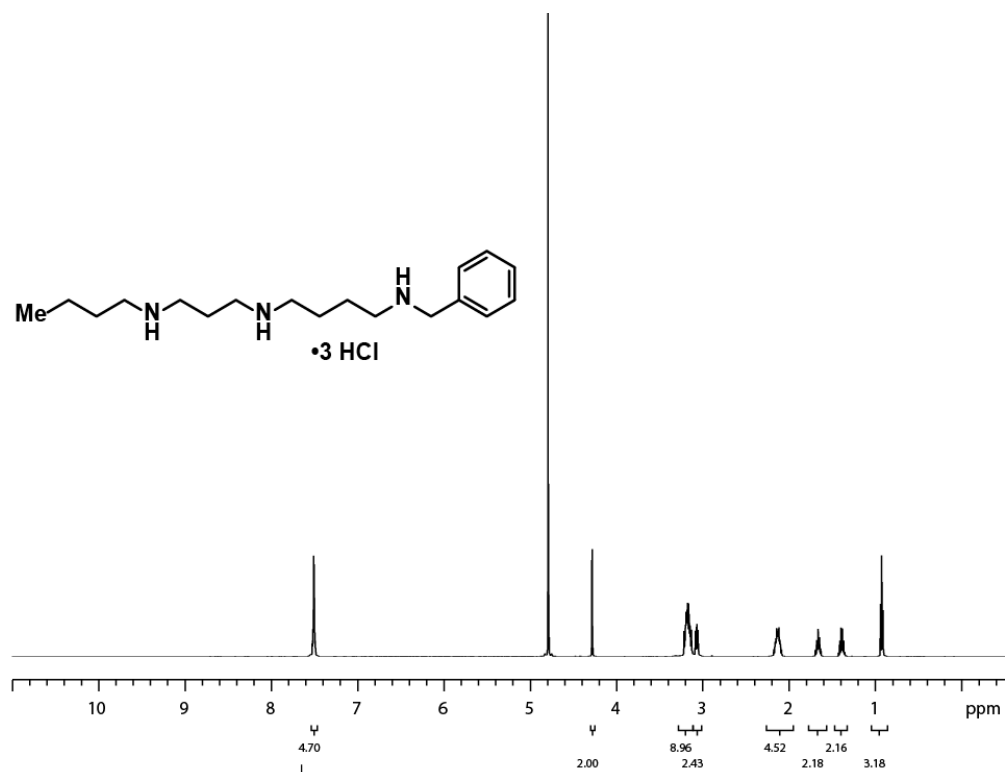


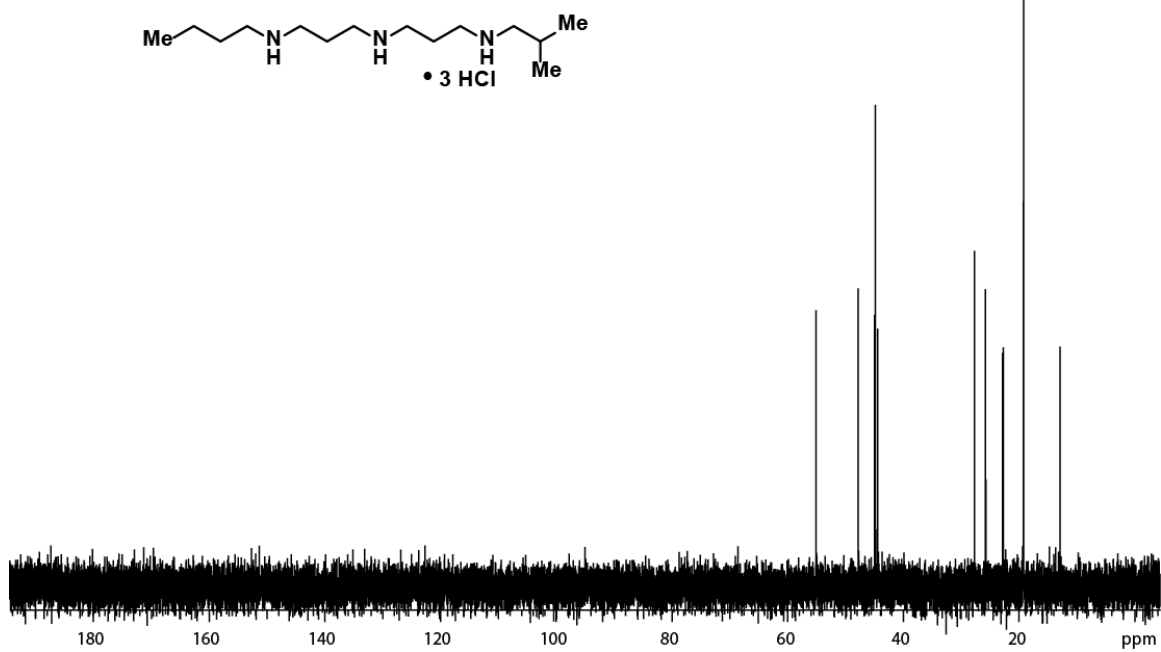
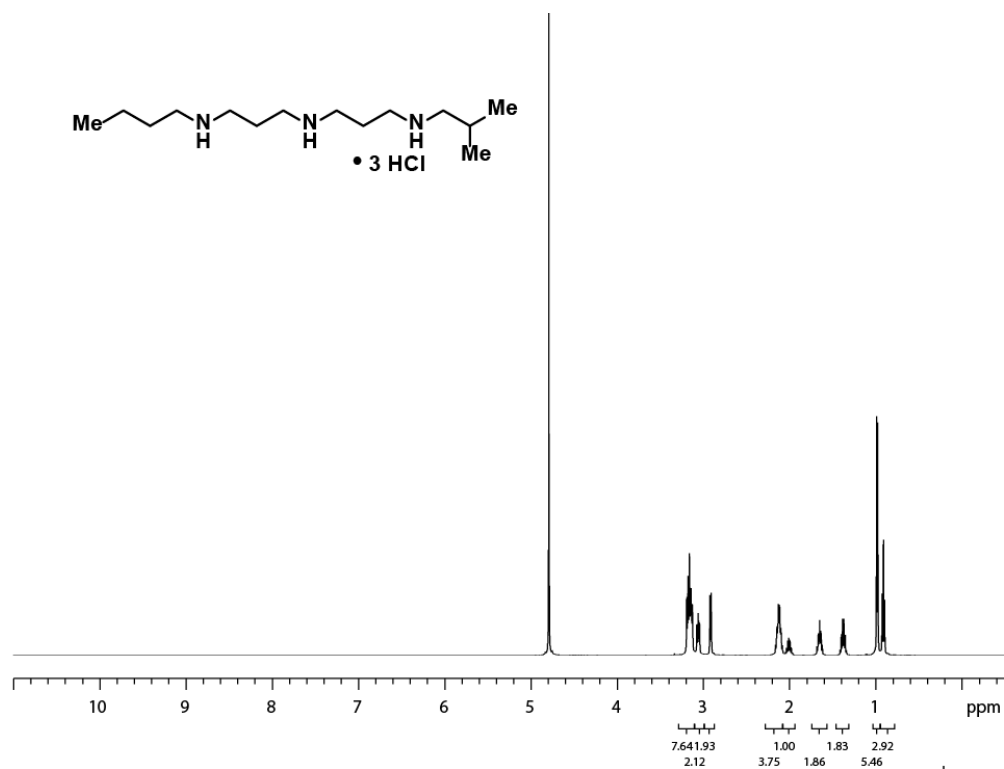


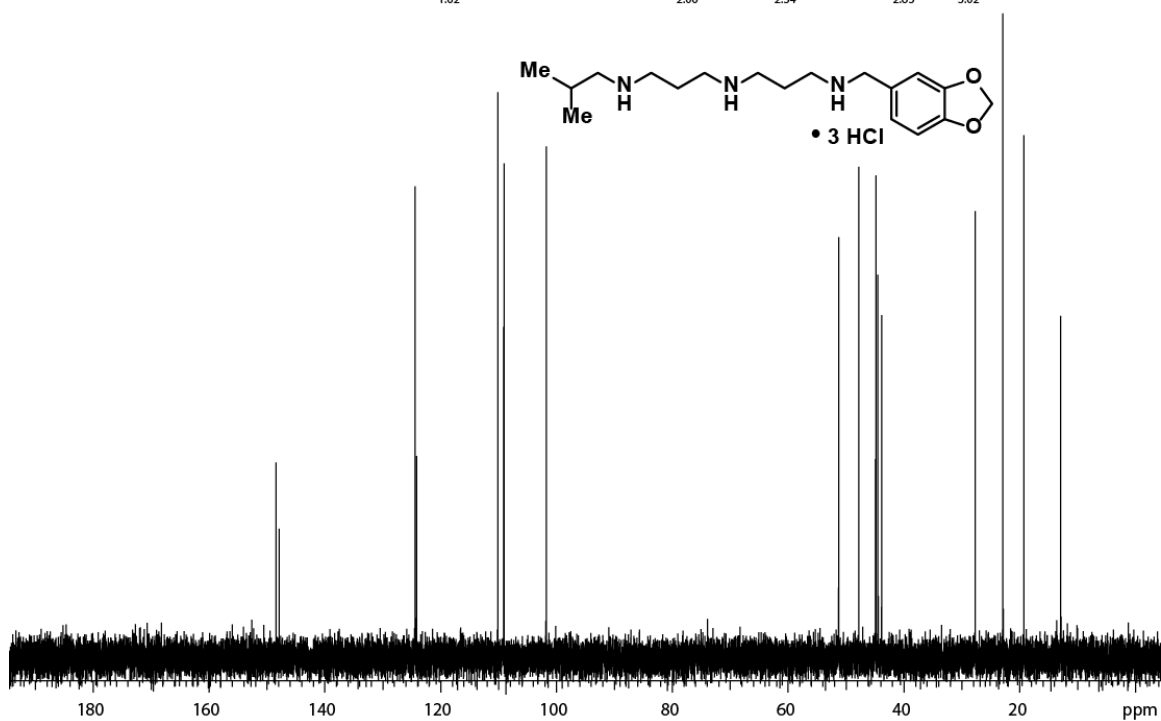
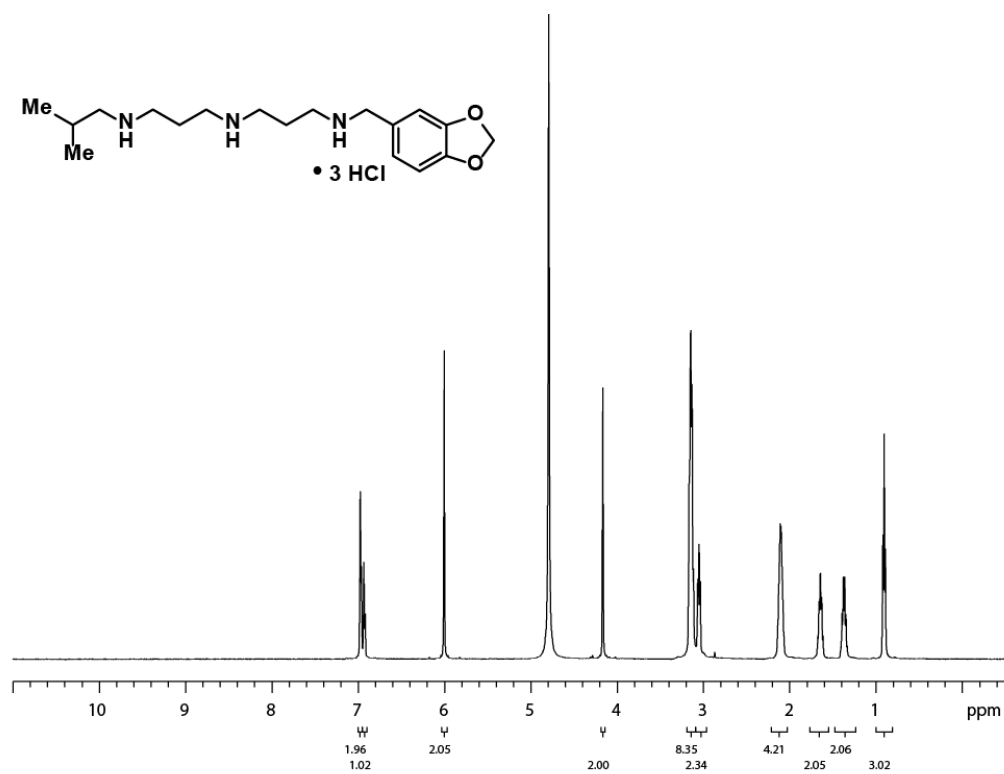


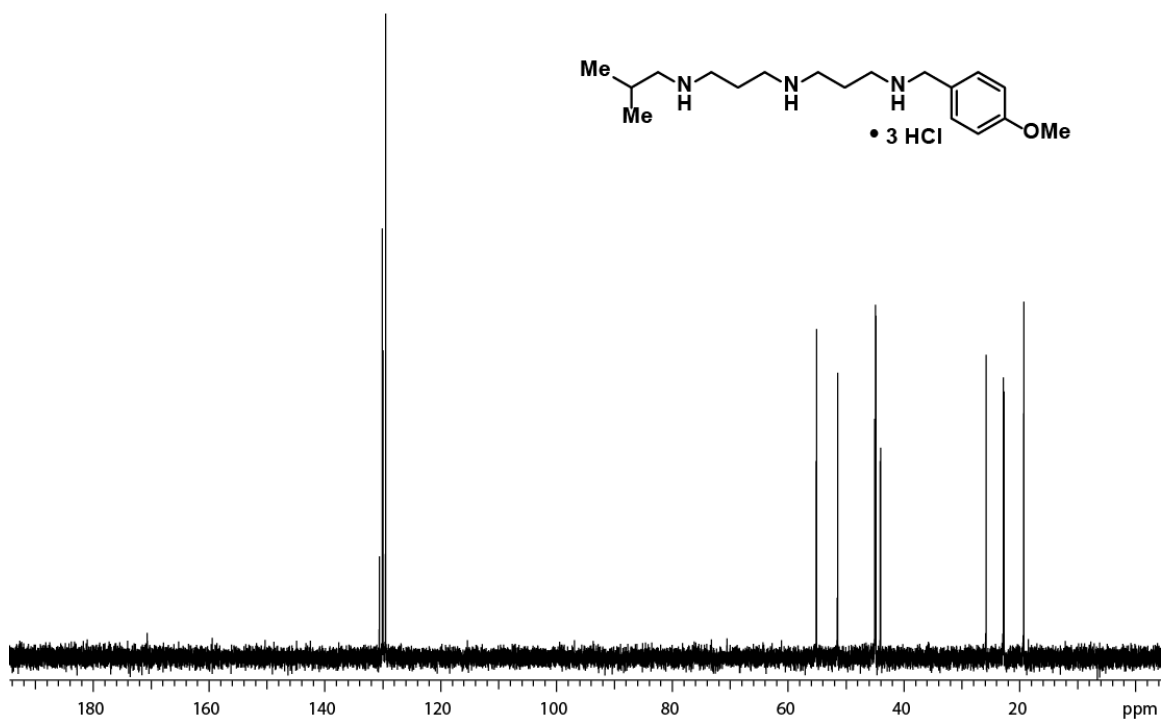
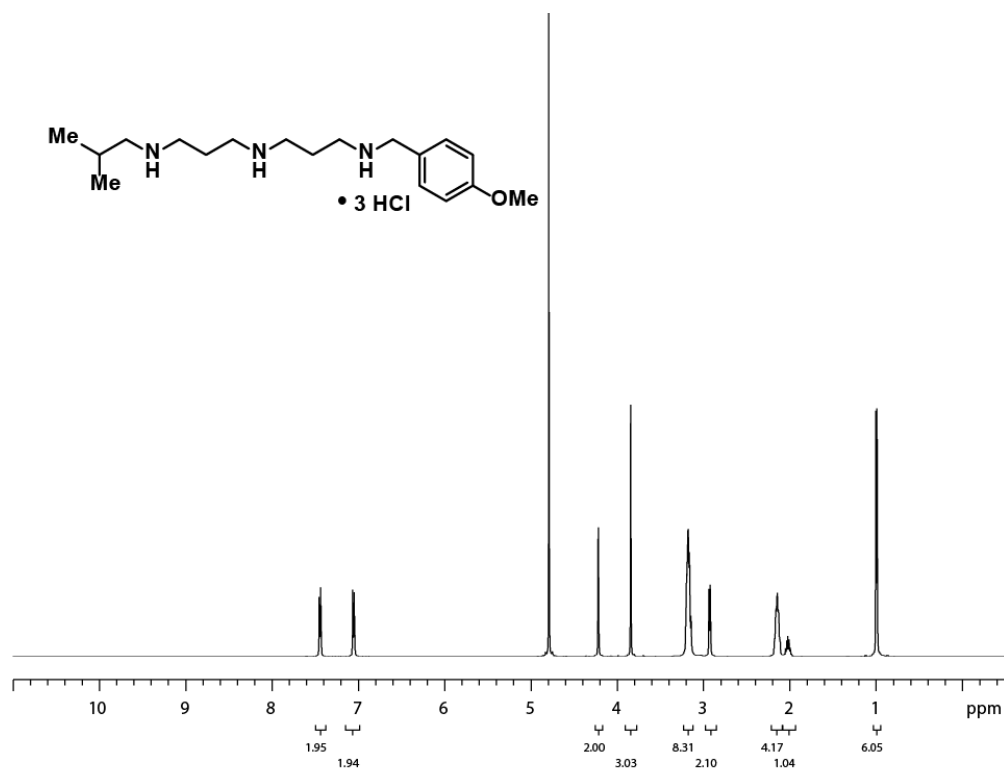












### 3.10 References

1. For reviews see: (a) Bachrach, U.; Heimer, Y. M. *The Physiology of Polyamines*; CRC Press: Boca Raton, FL, 2000. (b) Woster, P.; Casero, R. *Polyamine Drug Discovery*; RSC Publishing: Cambridge, U.K., 2012. (c) Gerner, E. W.; Meyskens Jr, F. L. Polyamines and Cancer: Old Molecules, New Understanding. *Nat. Rev. Cancer* **2004**, *4*, 781-792.
2. Pegg, A. E. Polyamine Metabolism and Its Importance in Neoplastic Growth and as a Target for Chemotherapy. *Cancer Res.* **1988**, *48*, 759-774.
3. For select examples see: (a) N'soukpoe-Kossi, C. N.; Ouameur, A. A.; Thomas, T.; Shirahata, A.; Thomas T. J.; Tajmir-Riahi, H. A. DNA Interaction with Antitumor Polyamine Analogues: A Comparison with Biogenic Polyamines. *Biomacromolecules* **2008**, *9*, 2712-2718. (b) Muth, A.; Madan, M.; Archer, J. J.; Ocampo, N.; Rodriguez, L.; Phanstiel, O. J. Polyamine Transport Inhibitors: Design, Synthesis, and Combination Therapies with Difluoromethylornithine. *Med. Chem.* **2014**, *57*, 348-363. (c) Boncher, T.; Bi, X.; Varghese, S.; Casero, R. A.; Woster, P.M. Revival of 2-(difluoromethyl)ornithine (DFMO), an Inhibitor of Polyamine Biosynthesis, as a Cancer Chemopreventive Agent. *Biochem. Soc. Trans.* **2007**, *35*, 356-363.
4. Choomuenwai, V.; Schwartz, B. D.; Beattie, K. D.; Andrews, K. T.; Khokhar, S.; Davis, R. A. The Discovery, Synthesis and Antimalarial Evaluation of Natural Product-based Polyamine Alkaloids. *Tetrahedron Lett.* **2013**, *54*, 5188-5191.
5. Yuan, J.; Jin, R. Polyamine@silica Hybrid Nanogress: Biomimetic Fabrication, Structure Characterization and Surface Functionalization. *J. Mater. Chem.* **2011**, *21*, 10720-10729.
6. Bowe, S.; Hixson, A.; Xu, W. Compositions Containing Identical Polyamine Salts of Mixed Anionic Pesticides. U.S. Patent WO2012059494 A1, May 10, 2012.
7. For select examples see: (a) Hatse, S.; Princen, K.; Clercq, E. D.; Rosenkilde, M. M.; Schwartz, T. W.; Hernandez-Abad, P. E.; Skerlj, R. T.; Bridger, G. J.; Schols, D. AMD3465, a Monomacrocyclic CXCR4 Antagonist and Potent HIV Entry Inhibitor. *Biochem. Pharmacol.* **2005**, *70*, 752-761. (b) Moret, V.; Dereudre-Bosquet, N.; Clayette, P.; Laras, Y.; Pietrancosta, N.; Rolland, A.; Weck, C.; Marc, S.; Kraus, J. Synthesis and Anti-HIV Properties of New Hydroxyquinoline-polyamine Conjugates on Cells Infected by HIV-1 LAV and HIV-1 BaL Viral Strains. *Bioorg. Med. Chem. Lett.* **2006**, *16*, 5988-5992. (c) Dessolin, J.; Galea, P.; Vlieghe, P.; Chermann, J.; Kraus, J. New Bicyclam-AZT Conjugates: Design, Synthesis, Anti-HIV Evaluation, and Their Interaction with CXCR-4 Coreceptor *J. Med. Chem.* **1999**, *42*, 229-241.
8. Prakash, N. J.; Bowlin, T. L.; Davis, G. F.; Sunkara, P. S.; Sjoerdsma, A. Antitumor Activity of Norspermidine, a Structural Homologue of the Natural Polyamine Spermidine. *Anticancer Res.* **1988**, *8*, 563-568.

9. Wolff, A. C.; Armstrong, D. K.; Fetting, J. H.; Carducci, K.; Riley, C. D.; Bender, J. F.; Casero, R. A. Davidson, N. E. A Phase II study of the polyamine analog N1,N11-diethylnorspermine (DENSpm) daily for five days every 21 days in patients with previously treated metastatic breast cancer. *Clin. Cancer Res.* **2003**, *9*, 5922-5928.
10. Wallace, H. M.; Fraser, A. V. Polyamine analogues as anticancer drugs. *Biochem. Soc. Trans. Pt. 2* **2003**, *31*, 393-396.
11. Russell, D.; Snyder, S. H. Amine Synthesis in Rapidly Growing Tissues: Ornithine Decarboxylase Activity in Regenerating Rat Liver, Chick Embryo, and Various Tumors. *Proc. Natl. Acad. Sci.* **1968**, *60*, 1420-1427.
12. O'Brien, T. G.; Simsiman, R. C.; Boutwell, R. K. Induction of the polyamine-biosynthetic enzymes in mouse epidermis by tumor-promoting agents. *Cancer Res.* **1975**, *35*, 1662-1670.
13. (a) Gal-Kolodkin, I.; Cao, S.; Chai, L.; Böttcher, T.; Kolter, R.; Clardy, J.; Losick, R. A Self-Produced Trigger for Biofilm Disassembly that Targets Exopolysaccharide. *Cell* **2012**, *149*, 684-692. (b) Böttcher, T.; Gal-Kolodkin, I.; Kolter, R.; Losick, R.; Clardy, J. Synthesis and Activity of Biomimetic Biofilm Disruptors. *J. Am. Chem. Soc.* **2013**, *135*, 2927-2930.
14. Pohjanpelto, P., and Raina, A. Identification of a Growth Factor Produced by Human Fibroblasts in vitro as Putrescine. *Nature New Biol.* **1972**, *235*, 247-249.
15. For a comprehensive review see: Meyskens Jr., F. L.; Gerner, E. W. Development of Difluoromethylornithine (DFMO) as a Chemoprevention Agent. *Clin. Cancer Res.* **1999**, *5*, 945-951.
16. Manni, A., Mauger, D., Gimotty, P., and Badger, B. Prognostic Influence on Survival of Increased Ornithine Decarboxylase Activity in Human Breast Cancer. *Clin. Cancer Res.* **1996**, *2*, 1901-1906.
17. Hixson, L. J.; Garewal, H. S.; McGee, D. L.; Sloan, D.; Fennerty, B.; Sampliner, R. E.; Gerner, E. W. Ornithine Decarboxylase and Polyamines in Colorectal Neoplasia and Mucosa. *Cancer Epidemiol. Biomarkers Prev.* **1993**, *2*, 369-374.
18. Meyskens, F. L.; Kingsley, E. M.; Glattke, T.; Loescher, L.; Booth, A. A Phase II Study of  $\alpha$ -Difluoromethylornithine (DFMO) for the Treatment of Metastatic Melanoma. *Invest. New Drugs* **1986**, *4*, 257-262.
19. Bacchi, C. J.; Nathan, H. C.; Hutner, S. H.; McCann, P. P.; Sjoerdsma, A. Polyamine Metabolism: a Potential Therapeutic Target in Trypanosomes. *Science* **1980**, *210*, 332-334.
20. Nightingale S. L. Drug for sleeping sickness approved. *JAMA* **1991**, *265*, 1229.

21. Steverding, D. The Development of Drugs for Treatment of Sleeping Sickness: a Historical Review. *Parasit. Vectors* **2010**, *3*, 1-9.
22. For a comprehensive review see: Clercq, E. D. The Bicyclam AMD3100 Story. *Nat. Rev. Drug Discov.* **2003**, *2*, 581-587.
23. De Clercq, E. Antiviral Metal Complexes. *Metal-Based Drugs* **1997**, *4*, 173-192.
24. Liu, K. K-C.; Sakya, S. M.; O'Donnell, C. J.; Flick, A. C.; Li, J. Synthetic Approaches to the New 2009 Drugs. *Bioorg. and Med. Chem.* **2011**, *19*, 136-154.
25. Wagstaff, A. J. Plerixafor, in Patients with Non-Hodgkin's Lymphoma or Multiple Myeloma. *Drugs* **2009**, *69*, 319-326.
26. Hahm, H. A.; Ettinger, D. S.; Bowling, K. Hoker, B.; Chen, T. L.; Zabelina, Y.; Casero Jr., R. A. Phase I Study of  $N^1,N^{11}$ -Diethylnorspermine in Patients with Non-Small Cell Lung Cancer. *Clin. Cancer Res.* **2002**, *8*, 684-690.
27. Bergeron, R. J.; Garlich, J. R.; Stolowich, N. J. Reagents for the Stepwise Functionalization of Spermidine, Homospermidine and Bis(3-aminopropyl)amine. *J. Org. Chem.* **1984**, *49*, 2997-3001.
28. Saab, N. H.; West, E. E.; Bieszk, N. C.; Preuss, C. V.; Mank, A. R.; Casero, R. A. Jr.; Woster, P. M. Synthesis and evaluation of unsymmetrically substituted polyamine analogues as modulators of human spermidine/spermine-N1-acetyltransferase (SSAT) and as potential antitumor agents. *J. Med. Chem.* **1993**, *36*, 2998-3004.
29. Bergeron, R. J.; Neims, A. H.; McManis, J. S.; Hawthorne, T. R.; Vinson, J. R. T.; Bortell, R.; Ingeno, M. J. Synthetic Polyamine Analogues as Antineoplastics. *J. Med. Chem.* **1988**, *31*, 1183-1190.
30. Renault, S. C.; Tomasi, S.; Sinbandhit, S.; Blagbrough, I. S.; Uriac, P. Solid-phase Organic Synthesis of Unnatural Polyamine Analogues Bearing a Dansyl or Acridine Moiety. *Pharm. Pharmacol. Commun.* **1999**, *5*, 151-157.
31. Heine, H. W.; Greiner, R. W.; Boote, M. A.; Brown, B. A. The Synthesis and Alkaline Decomposition of  $\gamma$ -Aminopropylsulfuric Acid. *J. Am. Chem. Soc.* **1953**, *75*, 2505-2506.
32. Prabhakaran, E. N. Templates for Nucleation and Propagation of Peptide Secondary Structure. U.S. Patent 2010/0228004 A1, Sept. 9, 2010.
33. Klimentová, J.; Kosák, P.; Vávrová, K.; Holas, T.; Hrabálek. Influence of Terminal Branching on the Transdermal Permeation-Enhancing Activity in Fatty Alcohols and Acids. *Bioorg. Med. Chem.* **2006**, *14*, 7681-7687.
34. Williams, D. E.; Craig, K. S.; Patrick, B.; McHardy, L. M.; van Soest, R.; Roberge, M.;

Andersen, R. Motuporamines, Anti-Invasion and Anti-Angiogenic Alkaloids from the Marine Sponge *Xestospongia exigua* (Kirkpatrick): Isolation, Structure Elucidation, Analogue Synthesis, and Conformational Analysis. *J. Org. Chem.* **2002**, *67*, 245-258.

35. Amarego, W. L. F.; Chai, C. L. L. *Purification of Laboratory Chemicals*. 6th ed.; Elsevier Inc.: Burlington, MA, 2009.



## CHAPTER 4

### ADVANCED MEDICINAL CHEMISTRY PROFILE OF INITIAL CZ-01 ANTIBIOFILM ANTIBIOTIC ANALOGS

#### 4.1 Background

Looper's first generation polyamine biocides were simple in design with little modularity built into their scaffolds (see Chapter 2). Typically, a known aldehyde was reductively aminated to produce the final product in a single step (Scheme 4.1). While the facile delivery of large amounts of compound is a benefit of these first generation analogs, their potency was not comparable to marketed antibiotics. Structure activity relationship studies were also limited by the aldehydes and amines that were commercially available (Scheme 4.1).

Furthermore, initial studies assessed viability through qualitative evaluation of biofilm deconstruction after being subjected to the **CZ-01** series. In order to have a traditional drug discovery program, however, we turned our attention to more quantitative results. To this end, the newly designed molecules focused primarily on the MICs of both Gram-positive (MRSA) and Gram-negative (*P. aeruginosa*) strains where biofilm dispersal was considered a secondary indication of our compounds efficacy.

To address SAR limitations, literature searches led us to 5-bromo-isophthalaldehyde **2**, which is easily prepared (see supporting information) from the precursor

isophthalaldehyde (Scheme 4.2).<sup>1</sup> More importantly, isophthalaldehyde **1**, as shown in Chapter 2, is readily available and cheap (500g for \$216). We felt that the halogen substitution on the 5-position would be a synthetic handle for derivatization via both Buchwald-Hartwig and Suzuki cross coupling reactions.<sup>2,3</sup>

## 4.2 Looper's Second Generation Biocide Synthesis

In order to explore structure activity relationship studies we began our second generation synthesis by reacting isophthalaldehyde and NBS in sulfuric acid. Elevated temperatures provided the product upon crystallization. With the 5-bromo-isophthalaldehyde in hand we could investigate a variety of cross coupling reactions, and further pursue other structural optimizations with these initial target hits.

### 4.2.1 Initial Suzuki $sp^2$ - $sp^2$ Cross Coupling

First generation SAR studies led us to conclude that norspermidine was the most potent side-chain to date and thus was the polyamine linker used in our initial second generation studies. Given the breadth of boronic acids commercially available, we initially focused on Suzuki reactions to generate diversified analogs. Treatment of 5-bromo-isophthalaldehyde **2** with a substituted-phenylboronic acid, palladium tetrakis triphenylphosphine, and cesium carbonate in toluene/EtOH/H<sub>2</sub>O produced the aldehyde **3** in a 45-80% yield as white crystalline material. Boc-norspermidine (for non-IUPAC naming see Supporting Information) was employed in the reductive amination of our newly formed dialdehyde. Methanolic HCl acidification not only cleaved the Boc-groups but also provided the final material **4** as the HCl salt (Scheme 4.2).

The library of compounds synthesized using this method is shown below (Figure 4.1).

Compounds range from ethereal-phenyl-boronic acids to formyl-phenyl-boronic acids but are limited to  $sp^2$  hybridized boronic acids (Figure 4.1). Attempts at using  $sp^3$  adducts resulted in recovered starting material. Further analog design via Buchwald-Hartwig couplings was unfortunately unsuccessful. Attempts at modifying the Buchwald-Hartwig procedure including; ligand selection, solvent degassing, and amine selection was unproductive as we tried to make both the pyrimidine derivative **5** as well as the morpholino aldehyde **6** (Scheme 4.3).

The 2<sup>nd</sup> generation analogs developed were on average more potent than our 1<sup>st</sup> generation analogs (Table 4.1). **CZ-01-058**, **CZ-01-62**, **CZ-01-65** and **CZ-01-66** all had MICs less than 10  $\mu\text{g/mL}$  against MRSA. These data suggested that the more hydrophobic backbones were beneficial for compound efficacy, and more structural adjustments in relation to hydrophobicity would be pertinent for studying bioactivity.

#### *4.2.2 Dimethyl 5-hydroxyisophthalate as a Precursor to Ethereal*

##### *Derivatives*

In addition to exploring cross coupling reactions, we also evaluated another starting material, dimethyl 5-hydroxyisophthalate **7**, which could be modified at the 5-position of the phenyl ring to distribute hydrophobicity. A series of aldehydes were synthesized whereby, first the 5-oxy-position was alkylated to produce the substituted ether **8**, and then the pendant esters were converted to the aldehydes **9** in a two-step reduction/oxidation sequence (Scheme 4.4). The oxidation was first carried out with PCC but was amended to use  $\text{MnO}_2$  for ease of workup and purification. Further treatment of the newly formed aldehyde with Boc-norspermidine, followed by acidification afforded the polyamino ether **10**. The analogs constructed from this series are shown below (Figure 4.2).

The ether series gave promising biological data. **CZ-01-81** for example, had an MIC of 5  $\mu\text{g/mL}$  against MRSA. **CZ-01-095** as well, has an MIC of 10  $\mu\text{g/mL}$  (Table 4.2).

Based on these initial results, we realized that the hydrophobicity of our compounds played an important factor in determining efficacy. For example **CZ-01-81** was potent against both Gram-positive and Gram-negative bacterial strains with MICs of 5  $\mu\text{g/mL}$  and 8.5  $\mu\text{g/mL}$ , respectively (Table 4.2), and contained the most nonpolar tail (2-ethylhexyl).

#### 4.2.3 Side-Chain Adjustment on Preexisting Scaffolds

We turned our attention to the adjustment of our polyamine side-chain to improve the hydrophobic character of these compounds. Starting from Boc-norspermidine **11**, the addition of butyl iodide produced *n*-butyl-norspermidine **12**, upon a acidification/basification/column purification sequence (Scheme 4.5a). With **12** in hand the reductive amination of [1,1'-biphenyl]-3,5-dicarbaldehyde **13** afforded **CZ-01-083** (Scheme 4.5b). Initial biological data for **CZ-01-083** was promising with an MIC value against MRSA of 5  $\mu\text{g/mL}$ . Further construction of nonpolar side-chains led us to the isobutylated norspermidine derivative (isobutyl-norspermidine). Using the same method as above, reductive amination of [1,1'-biphenyl]-3,5-dicarbaldehyde produced **CZ-01-086**. Again preliminary test MIC results for **CZ-01-086** were favorable (MIC MRSA = 0.9  $\mu\text{g/mL}$ ).

Unfortunately, the second batch of **CZ-01-086** was drastically different by MIC, with a value of 15  $\mu\text{g/mL}$ . In order to verify our biological data we remade the material and developed an alternate route (Scheme 4.5c). The alternate route benefited us as it was more modular in design and allowed for the construction of analogs in a quick and efficient fashion whereby the freebase of **CZ-01-058** was reductively aminated with an aldehyde,

in this case isobutyraldehyde, to afford **CZ-01-086** after acidification. This batch had a much higher MIC than what was initially reported. We felt that significant variables in the reaction conditions were attributed to some, if not all, of our inconsistent biological data.

Unbeknownst to us, these reactions were quite impure and the discrepancies in our biological data were a direct result of this (Table 4.3).  $^1\text{H}$  and  $^{13}\text{C}$  NMR analysis had been the principal analytical technique used to assess the purity of the **CZ-01** series. As shown below (Figure 4.3), the NMR spectrum of **CZ-01-086** was pristine, and moreover, we felt any impurities were negligible in producing drastic biological effects. Qualitative analysis by TLC (Figure 4.4) however, provided empirical evidence that our **CZ-01** series compounds were impure as numerous compound spots were observed. Moreover, NMR spectroscopy was not sensitive enough to pick up minute impurities (<5%), and our compounds, more than likely, contained various <5% impurities. The active CZ compound was then only 60-80% pure, but nondiscernable (from pure material) by NMR analysis.

The first principle cause of these impurities was reasoned to be the contaminants from the side-chain. A linear approach to our norspermidine derivatives would mitigate any impurities present and further validate our biological data. Starting from 3-amino-1-propanol **14** a reductive amination produced the alkylated amine **15** (Scheme 4.6). Treating the pendant alcohol with aqueous HBr afforded the brominated acid salt **16**, which could be recrystallized from *i*-PrOH or MeOH/Et<sub>2</sub>O. Construction of the substituted norspermidine derivative was accomplished by the addition of the newly formed acid salt to neat diaminopropane (8-10 equiv). Vacuum distillation afforded pure material **17**. The scope of this sequence can be seen in Chapter 3.

With the assistance of Paul Sebahar, Ph.D., we were able to design conditions that

appropriately purified these compounds to a level of 85-95%. Specifically, column chromatography with a unique mobile phase ( $\text{CH}_2\text{Cl}_2$ , MeOH,  $\text{NH}_4\text{OH}$ , 250:16:1) was able to separate impurities and the **CZ-01** compounds. With this in mind, we were able to amend our synthesis to not only provide research grade material, but also were now able to modulate the side-chain. Unfortunately, LC-MS was unproductive for determining compound purity due to the high polar character of these hexa- and nona-HCl salts.

With an efficient and scalable process now in hand, we augmented our series with a great deal of synthetic breadth (Figure 4.5). Given the relative success of **CZ-01-086** we amended this series to include compounds from the initial scope of reaction shown in Chapter 3. Furthermore, no Boc-protection was necessary as the initial aldehyde would primarily react with the only primary amine present on norspermidine, and any unwanted material was purified by chromatographic means. The biological activity of these analogs shows promising data with **CZ-01-114** and **CZ-01-118** both having low MICs ( $\sim 1 \mu\text{g/mL}$ ) against MRSA (Table 4.4).

Given the cheap cost and availability of isophthalaldehyde, it was apparent that the newly developed substituted norspermidine side-chain chemistry should be applied to this series as well. Starting from isophthalaldehyde, reductive amination with a number of the alkylated norspermidine side-chains produced the series shown below (Figure 4.6). The compounds **CZ-01-097**, **CZ-01-100**, and **CZ-01-158** had adequate MICs against both Gram-positive and Gram-negative strains (Table 4.5). This was attributed to the hydrophobicity of the side-chain as was suggested by our previous SAR studies. We felt it was imperative to ascertain preliminary efficacy data on compounds with promising biological profiles (MICs  $< 5 \mu\text{g/mL}$  for MRSA  $< 30 \mu\text{g/mL}$  for *P. aeruginosa*). **CZ-01-**

**100** was tested for cell lysis in an ISO 10993 L929 assay (see Supporting Information). Unfortunately, **CZ-01-100** exhibited excessive cell lysis at 12.5  $\mu\text{g/mL}$ , which would prohibit its use in humans due to cytotoxicity. Furthermore, data suggested that cytotoxicity is correlated to Gram-negative activity, which we believe is due to the increased hydrophobicity of these molecules which exhibit more broad-spectrum activity.

The substituted norspermidine side-chain synthesis yielded large amounts of substituted amino bromides **16** which we felt were worthy of using as electrophiles with dimethyl 5-hydroxyisophthalate **7**. A select series of the phenoxy derivatives were made (Figure 4.7). At first, we had tried the direct alkylation with a roughly 1:1 ratio of electrophile bromide to nucleophile 3,5-bis(methoxycarbonyl)phenolate. Unfortunately all attempts were unsuccessful at affording the desired amino-alkylated product (Scheme 4.7). We felt the required free amine was too reactive. A Boc-protection was subsequently employed to produce the desired bromo-alkylated carbamate which then was used as a successful electrophile to yield the CZ-compound in four known steps (Scheme 4.7).

This combinatorial process is valued for its modularity, and a significant number of analogs could be synthesized in a short sequence (for biological data see Table 4.6). However, we chose to focus on a particular subset as they were the strongest lead compounds at the time. These include both hexyl, *i*-butyl, and octyl analogs (Figure 4.7).

In order to satisfy any missing data in our SAR studies it was imperative that we use the substituted norspermidine derivatives for the parent-ether series as well (Scheme 4.4). Several CZ-compounds were synthesized primarily using 5-(cyclohexylmethoxy)isophthalaldehyde as the starting material (Figure 4.8). Again, a significant increase in potency was observed with the octyl-norspermidine analog (Table

4.7). The remaining analogs though viable, against Gram-positive strains, showed little to no activity against Gram-negative bacteria.

Concurrently, we began to construct systems with three aldehydes like those used to make **CZ-01-062**, **CZ-01-065**, **CZ-01-066**, and **CZ-01-069**. With our amended side-chain, in a combinatorial process, several analogs were made by treating the desired trialdehyde with three equivalents of our alkylated norspermidine (Figure 4.9). These tris-derivatives again saw an increase in potency in comparison with their bis-counterparts (Table 4.8). More importantly, **CZ-01-128** had a clinically relevant MIC (3.5 µg/mL) against Gram-negative bacteria *P. aeruginosa*. Further analysis revealed that **CZ-01-099** had passed cytotoxicity testing, on the ISO10993 L929 cytotoxicity assay, at concentrations of 1000 µg/mL (not causing cell death), meaning its therapeutic window for Gram-positive bacteria was roughly 500 times MIC. Unfortunately, the octyl counterpart **CZ-01-128** failed at every dilution level down to 12.5 µg/mL. This result reinforced our skepticism of the utility of the octyl-norspermidine side-chain, as it more than likely possessed inherent cytotoxicity, potentially due to its hydrophobicity.

The above data points allowed us to draw several conclusions about our second generation compounds: 1) typically a greater clogp (hydrophobicity) often afforded increased potency, 2) the longer alkyl chains (often associated with greater clogp) typically resulted in a higher cytotoxicity. From here SAR studies were modified to: 1) increase potency levels on both Gram-positive and Gram-negative strains primarily MRSA and *P. aeruginosa* respectively and 2) reduce cytotoxicity in the ISO10993 L929 assay. Given that the cytotoxicity of **CZ-01-099** was negligible, there was an opportunistic window to develop both a more potent and safer CZ-analog. A number of analogs were synthesized



to meet our demands.

#### 4.2.4 Additional Side-Chain Modifications in Order to Alleviate Cytotoxicity

In order to amend the cytotoxicity issues, additional modifications of the side-chain were made. We started with urea functional groups which were made from the corresponding amino-bromide and isocyanate (Scheme 4.8). The cytotoxicity of the respective analogs from this series could be mitigated by transformation of the terminal amine to the urea, while the additional hydrophobicity could still be employed. The cyclohexyl phenoxy aldehyde derivative was chosen due to availability at the time. Several ureas were synthesized based on this principle (Figure 4.10). Regrettably, these terminal ureas possessed very little activity against MRSA and no activity against *P. aeruginosa* (Table 4.9).

#### 4.2.5 Modification of the **CZ-01-099** Scaffold

Chronologically **CZ-01-099** was the lead compound of our first and second generation CZ-series. In order to identify if any other derivations of this core structure were as potent, two additional analogs were made with different substitution patterns and limited to two side-chains (Figure 4.11). These arrangements would add support to whether a three-branched backbone was more efficient than its two-branched counterpart. The three branches of **CZ-01-099** were essential for any substantial activity of that specific series as the MICs for **CZ-01-150** and **CZ-01-151** were two- to three-fold less potent against MRSA compared to **CZ-01-099** (Table 4.10).

#### 4.2.6 Synthesis and Activity of Analogs from an Advanced Side-Chain Library

In attempts to broaden our CZ-library a number of new side-chains were synthesized. We felt that long ( $n > 4$ ) unbranched alkyl chains could be another reason for enhanced cytotoxicity. To alleviate this, we made several hydrophobic branched side-chain norspermidines including, isoamyl, 2-ethyl butyl, 2-methyl-1-butyl, and 2-ethyl-1-hexyl. The large clogp of octyl-norspermidine also led us to synthesize 4-*tert*-butyl-benzyl-norspermidine (Figure 4.12).

We recognized these substituted derivatives as useful leads to investigate the relationship between hydrophobicity and potency (Figure 4.13). **CZ-01-163** was again the most potent of the four compounds synthesized from this series with an MIC of 0.75  $\mu\text{g/mL}$  against MRSA and an MIC of 10  $\mu\text{g/mL}$  against *P. aeruginosa* (Table 4.11). Despite the unique side chain **CZ-01-163** was also cytotoxic failing at 12.5  $\mu\text{g/mL}$ .

The tris-aldehyde precursor used to construct **CZ-01-099** was chosen as another viable substrate for potency analysis for the above alkylated-norspermidine combinations. Furthermore, if the new tris-substituted norspermidine analogs were active, cytotoxicity testing would follow. In parallel with **CZ-01-099** the following compounds, **CZ-01-168**, **CZ-01-169**, **CZ-01-170** and **CZ-01-172** (Figure 4.14) were all relatively potent against MRSA (values ranging from 2 - 5  $\mu\text{g/mL}$ ) but lacked potency against *P. aeruginosa* (values ranging from 20 - >50) (Table 4.12).

#### 4.2.7 Use of $\alpha$ -helix Mimetics as a Source for CZ-Compound

##### Structural Diversity

During the above syntheses we encountered a unique antimicrobial in the literature, brilacidin **21** (Figure 4.15). This guandino pyrimidine was highly active against Gram-positive (0.5-1  $\mu\text{g/mL}$  against MRSA) and Gram-negative (1-2  $\mu\text{g/mL}$  against *E. coli*) strains and had been approved for phase IIb testing. Brilacidin mimics the action of the cationic antimicrobial peptides with two polar guanidine tails bridged by a hydrophobic triaryl core.<sup>4</sup>

Furthermore, with the knowledge we had of cationic antimicrobial peptides we desired to construct a number of  $\alpha$ -helices mimics. Andy Hamilton's lab at Yale University has pioneered this research with compounds like **22** and **23** (Figure 4.16), used to inhibit protein-protein interactions. In this regard, we began to prepare compounds with the terphenyl system constructed from a number di-brominated aromatics (Scheme 4.9).<sup>5</sup>

Drawing from Hamilton's research we envisaged a series of terphenyl systems (**26**, **27**, and **28**), representative of both brilacidin and the  $\alpha$ -helix of cationic antimicrobial peptides which could help increase compound potency. To achieve this goal, we started with both 1,2- and 1,3-dibromobenzene **24** and **25**, respectively. In a modular fashion, a series of terphenyl aldehydes were assembled with the requisite boronic acid (Scheme 4.8). Under standard conditions we were able to synthesize the CZ-series shown below. **CZ-01-161** and **CZ-01-166** have both shown promising preliminary results with MICs of 2 and 4  $\mu\text{g/mL}$  against *P. aeruginosa*. However, **CZ-01-161** was highly cytotoxic failing at 12.5  $\mu\text{g/mL}$ . When tested for cytotoxicity **CZ-01-164** also failed at concentrations as low as 12.5  $\mu\text{g/mL}$ . These values provide an accurate representation of the terphenyl system, and

in order to mitigate cytotoxicity amendments in the core structure are imperative (Table 4.13).

We were able to modify the Suzuki reaction to include a terphenyl trialdehyde system. Starting from 2,5-dichlorobenzaldehyde **29** the Suzuki reaction with 3-formyl-phenyl boronic acid produced the trialdehyde **30** (Scheme 4.10). The low yield was attributed to the poor solubility of this compound in organic solvent. The trialdehyde was then used under standard protocol to make **CZ-01-153** and **CZ-01-156** (Figure 4.18). We were surprised to see tris-hexyl and tris-isobutyl norserpermidine terphenyl systems with such mediocre activity, as the MICs for *P. aeruginosa* were greater than 50 and 20 µg/mL, respectively (Table 4.14). We felt that the substitution patterns on the terphenyl core have a direct impact on substrate binding and are pursuing other leads currently.

The central core of brilaciden (Figure 4.15) contains a unique pyrimidine unit which we could also exploit with our synthesis and the presence of the central pyrimidine core may alleviate cytotoxicity. We chose to analyze two different substitution patterns on the pyrimidine as they were readily available compounds. Starting from either 2,4-dichloropyrimidine **31** or 4,6-dichloropyrimidine **33** the Suzuki reaction with 4-formyl phenylboronic acid produced the desired terphenyl pyrimidines **32** and **34** (Scheme 4.11). With these in hand several CZ-analogs were synthesized (Figure 4.19). The potency of these analogs against *P. aeruginosa* was negligible with MICs ranging from 50 µg/mL to >40 µg/mL for *P. aeruginosa*. (Table 4.15). When tested for cytotoxicity **CZ-01-174**, however, passed at 12.5 µg/mL, which is far below its MIC for *P. aeruginosa* (50 µg/mL).

The core terphenyl system has the most promising activity but its therapeutic window is limited due to cytotoxicity. Amendments in the structure may lead to a more potent, yet

more therapeutically practical compound. The core was adjusted to include a branching *tert*-butyl substituent which we felt could add greater hydrophobic character but limit inherent toxicity as it was not attached to the pendant polyamine side-chains. Starting from 1,3-dibromo-5-(*tert*-butyl)benzene **35** the Suzuki reaction with either 3-formyl phenyl boronic acid or 4-formyl phenyl boronic acid yielded the desired *tert*-butyl terphenyl system **36** or **37** (Scheme 4.11 and 4.12). The new series (Figure 4.20) had favorable activity against both Gram-positive and Gram-negative bacteria (Table 4.16). The MICs of **CZ-01-177**, **CZ-01-178**, **CZ-01-179**, **CZ-01-182**, **CZ-01-183**, and **CZ-01-184** were sub  $\mu$ M for MRSA and low  $\mu$ M for *P. aeruginosa*. These adjustments, however, were detrimental to cytotoxicity. To support, our most active compounds to date (**CZ-01-178** and **CZ-01-184**) both failed cytotoxicity testing at 6.25  $\mu$ g/mL.

Unfortunately, the Gram-negative activity of a number of CZ-compounds is often met with cytotoxicity. In order to amend the problem continual adjustments must be made for further SAR studies. Nonetheless, given the MIC of **CZ-01-099** against MRSA coupled with its limited cytotoxicity and overall activity profile we felt further biological analysis was necessary.

#### 4.3 Biological Studies on CZ-01-099

In order to ascertain a more comprehensive biological profile for our CZ-series we selected **CZ-01-099** to move forward in testing, given its amenable cytotoxicity data. The preliminary testing was conducted on a topical pig wound model. In this wound model, a series of punches were made in the lower back of a pig and subsequently inoculated with planktonic MRSA. Topical administration of **CZ-01-099** then followed in order to demonstrate if our compound could be applicable for topical wound care. When cultured

however, the positive control showed lack of a bacterial lawn (Figure 4.21a). **CZ-01-099** displayed this same lack of growth (Figure 4.21c). We hypothesized the pig's immune system was robust enough to clear infection regardless of treatment variables as both experimental arms showed no bacterial growth.

In order to confirm that **CZ-01-099**, was indeed active we repressed the pig's immune response by inoculating with MRSA biofilm instead of planktonic bacteria. Biofilm positive controls display MRSA growth in red (Figure 4.21b). On the contrary, when treated with **CZ-01-099** no or almost no MRSA are observed.

These data confirm that **CZ-01-099** is topically active and possesses the ability to kill Gram-positive biofilm bacterial strains like MRSA. Furthermore, no skin structure side effects were observed when the CZ-compound was applied giving merit to the compounds usage as a commercially available topical antibiotic.

Serial passage data collected on **CZ-01-099** showed limited developed resistance. During the course of a 19-passage treatment, **CZ-01-099** retained a constant MIC of 6 µg/mL and further analysis revealed that after 15 passages the MRSA isolate grew at a reduced rate.

In order to determine more comprehensive antibiofilm activity for **CZ-01-099**, biofilms were grown on stainless steel titanium coupons and imaged by scanning electron microscopy (SEM). In comparison with glutaraldehyde and vancomycin, **CZ-01-099** cleared biofilms effectively as shown by the lack of any significant amount of grey dots (biofilms) upon magnification. In addition, comparison with the negative control shows **CZ-01-099** to appear similar confirming that **CZ-01-099** is indeed an antibiofilm antibiotic (Figure 4.22).

Concurrently with the **CZ-01-099** wound studies, we wanted to perform a good laboratory practice (GLP) scale-up of **CZ-01-099**. To this end, our synthetic method was sent to Array BioPharma (now Avista) a contract research organization (CRO). Through the work of Array, specific conditions were determined to assess purity and recrystallize material. We now possess the ability to quantify the purity of our CZ-compounds via LC-MS with a C-18 column and 0.1%-0.2% TFA H<sub>2</sub>O/0.1% TFA CH<sub>3</sub>CN mobile phase. Moreover, our collaboration with Array has enabled us to recrystallize material by using an H<sub>2</sub>O (solvent) *i*-PrOH (antisolvent) system. To date, **CZ-01-099** has been recrystallized to 99% purity (judged by LC-MS). It should be noted that not all CZ-compounds possess the same physiochemical properties as **CZ-01-099** and several, most notably the terphenyls, cannot be recrystallized by the above method.

#### 4.4 In vivo Pharmacokinetic Studies and Reselection of Lead

##### Compounds

The in vivo pharmacokinetic (PK) studies conducted on **CZ-01-099** had similar analytical problems as with initial purity analysis. As such, it proved to be difficult to quantify compound levels administered lower than 3 mg/Kg in rat models due to the multiple charged states of **CZ-01-099**. The toxicity of **CZ-01-099**, however, precluded us from administering compound at above this dosage efficaciously.

Furthermore, with pure material (>99% judged by LC-MS) in hand the MIC of **CZ-01-099** was tested ad nauseam. Unfortunately, testing revealed (not reported in Table 4.8) an increase in MIC (~12 µg/mL), most likely related to material purity. As a result, we looked toward developing a new lead compound.

A search through our biological data showed that **CZ-01-114** met our initial

requirements for a lead compound. **CZ-01-114** had a low MIC against MRSA (~1 µg/mL) and against *P. aeruginosa* (~10 µg/mL). **CZ-01-114** was synthesized, purified by recrystallization and quantified by LC-MS. With compound purity established at 98%, MICs were determined and are as follows: MRSA (1 µg/mL), *P. aeruginosa* (64 µg/mL), and CRE (16 µg/mL). Given the low MIC against MRSA, **CZ-01-114** was selected as a candidate for additional biological testing. Cytotoxicity tests revealed that **CZ-01-114** does not cause cell death below 50 µg/mL. More importantly, the promising profile of **CZ-01-114** would allow us to employ the compound in PK studies in hopes that the general toxicity of **CZ-01-114** will not preclude dosing at higher concentrations. These dosages should then enable us to observe appreciable levels in blood plasma and to obtain accurate PK data. Currently we are using **CZ-01-114** in our lead optimization process and tailoring the general structure to mitigate cytotoxicity while increase potency in both Gram-negative and Gram-positive strains.

#### 4.5 Conclusion and Future Aims

The CZ-compounds presented confirm the importance of both side-chain and backbone modulation. The promising cytotoxicity profiles of **CZ-01-099** and **CZ-01-114** indicate that minimal adjustments in structure mitigate mammalian cell toxicity while retaining bactericidal activity. In addition, we have discovered compounds that possess surfactant-like characteristics but are noncytotoxic and nonhemolytic against mammalian cells. The stigma associated with these polyamino compounds, due to their promiscuous binding, and multiple charged states is often associated with our CZ-compounds. Furthermore membrane active surfactants possess little specificity for bacterial cell membranes over mammalian cell membranes. The CZ-compounds developed in our lab however, have



displayed that through judicious SAR studies can exhibit selectivity for bacterial cell membranes and can be synthetically derived in high yield and good purity with effective techniques including distillation and recrystallization.

In our SAR profile we were restricted by available aldehydes but amended our synthesis to more modular starting materials (i.e., 5-bromo-isophthalaldehyde and 5-alkoxyisophthalaldehyde) thereby giving us the ability to adjust hydrophobicity in the backbone. In attempts to further diversify our synthesis we have also adjusted the norspermidine side-chain to again tailor hydrophobicity into our final compound. The side-chain modulation also alleviated issues with purity as the linear sequence developed prevented and/or purified unwanted alkylations. The influence of these minor impurities on MIC is evidenced by the data for **CZ-01-086** and **CZ-01-099**. To date, the synthetic method used to construct CZ-compounds is modular, scalable to the requisite quantities for animal testing, and high throughput with facile purification techniques including recrystallization which has been used to provide final compounds with up to 99% purity.

A significant portion of the data presented however, is preliminary and requires an analysis of overall purity via the described LC-MS. In addition, a number of aldehyde scaffolds were synthesized prior to their alkylated norspermidine counterparts, and in order to ascertain reasonable SAR leads a number of compounds need to be added to the **CZ-01**-series and are described below.

The substituted ether series (Figure 4.23) showed promising initial data with MIC values as low as 5 for MRSA. However, the purity of these compounds was only determined qualitatively and was not investigated by LC-MS. This series is also hampered by minimal SAR analysis (as only three side-chains were used in library design) and the

following compounds below are to be synthesized in the future by our method.

With the recently acquired data for **CZ-01-114** the same structural analysis will be applied to a number of biphenyl analogs not limited to what is hypothesized below (Figure 4.24). The basis of this series is three-fold: 1) addition of more polar side-chains to increase potency, 2) addition of more polar functionalization on the biphenyl system to increase potency, and 3) general SAR modifications based on readily available substituted phenyl boronic acids.

The advanced SAR profile of the CZ-series has revealed a number of the requirements to possess an active noncytotoxic analog. However, preliminary data indicated that compound purity and polarity is extremely important in dictating activity. Furthermore, additional studies, not limited to what is described above must be carried out in order to ascertain a full profile on our CZ-analogs.

The modularity of this synthetic method described above has allowed us to construct a diversified library of first in class antibiofilm antibiotics. Purification of the final CZ-compounds by recrystallization has ensured adequate and reliable MIC data and is further applicable to the scale required for animal testing. With the lack of available methods for construction of alkylated polyamines our synthesis further mandated the development of a linear sequence to afford our side-chain which has now been used to enhance our current library and substantiate SAR studies. The continuation of this chemistry is paramount in developing additional members of our novel compound class of selective antibiofilm antibiotics.

Table 4.1: The in vitro activity of the initial second generation CZ series as MICs against Gram-positive MRSA and Gram-negative *Pseudomonas aeruginosa*

Cmpd	MIC-MRSA ( $\mu\text{g/mL}$ )	MIC- <i>P. aeruginosa</i> ( $\mu\text{g/mL}$ )
<b>CZ-01-058</b>	7.3 (n=9)	50
<b>CZ-01-061</b>	>5	>20
<b>CZ-01-062</b>	4.64	18
<b>CZ-01-063</b>	>5	>20
<b>CZ-01-065</b>	2	14.5
<b>CZ-01-066</b>	5.1	19.3
<b>CZ-01-067</b>	NA	NA
<b>CZ-01-068</b>	NA	NA
<b>CZ-01-069</b>	>10	>20
<b>CZ-01-070</b>	>5	20
<b>CZ-01-071</b>	>10	>100
<b>CZ-01-075</b>	>5	20

Table 4.2: The in vitro activity of the substituted phenoxy second generation CZ series as MICs against Gram-positive MRSA and Gram-negative *Pseudomonas aeruginosa*

Cmpd	MIC-MRSA ( $\mu\text{g/mL}$ )	MIC- <i>P. aeruginosa</i> ( $\mu\text{g/mL}$ )
<b>CZ-01-076</b>	>10	>50
<b>CZ-01-081</b>	5	8.5
<b>CZ-01-090</b>	5	>25
<b>CZ-01-095</b>	10	>25

Table 4.3: Batch Variability Data for **CZ-01-086**

<b>CZ-01-086</b> Batch	MIC ( $\mu\text{g/mL}$ )
1	0.9
2	15
3	13
4	>15
5	<1
6	6
7	>12
8	>16
9	>25

Table 4.4: The in vitro activity of the substituted alkylated-norspermidine CZ series using [1,1'-biphenyl]-3,5-dicarbaldehyde, as MICs against Gram-positive MRSA and Gram-negative *Pseudomonas aeruginosa*

Cmpd	MIC-MRSA ( $\mu\text{g/mL}$ )	MIC- <i>P. aeruginosa</i> ( $\mu\text{g/mL}$ )
<b>CZ-01-092</b>	2	10
<b>CZ-01-096</b>	2	30
<b>CZ-01-111</b>	5	10
<b>CZ-01-112</b>	10	>30
<b>CZ-01-114</b>	1	10
<b>CZ-01-118</b>	1	10
<b>CZ-01-137</b>	NA	>25
<b>CZ-01-141</b>	NA	20
<b>CZ-01-142</b>	5	20

Table 4.5: The in vitro activity of the substituted alkylated-norspermidine CZ series using isophthalaldehyde, as MICs against Gram-positive MRSA and Gram-negative *Pseudomonas aeruginosa*

Cmpd	MIC-MRSA ( $\mu\text{g/mL}$ )	MIC- <i>P. aeruginosa</i> ( $\mu\text{g/mL}$ )
<b>CZ-01-097</b>	1	12
<b>CZ-01-100</b>	2.5	15
<b>CZ-01-108</b>	5	>40
<b>CZ-01-113</b>	5	>25
<b>CZ-01-158</b>	5	15

Table 4.6: The in vitro activity of the amino-ethereal CZ-series, as MICs against Gram-positive MRSA and Gram-negative *Pseudomonas aeruginosa*

Cmpd	MIC-MRSA ( $\mu\text{g/mL}$ )	MIC- <i>P. aeruginosa</i> ( $\mu\text{g/mL}$ )
<b>CZ-01-107</b>	>15	>50
<b>CZ-01-110</b>	2	20
<b>CZ-01-121</b>	5	30
<b>CZ-01-122</b>	5	>50

Table 4.7: The in vitro activity of the substituted norspermidine ethereal CZ-series as MICs against Gram-positive MRSA and Gram-negative *Pseudomonas aeruginosa*

Cmpd	MIC-MRSA ( $\mu\text{g/mL}$ )	MIC- <i>P. aeruginosa</i> ( $\mu\text{g/mL}$ )
<b>CZ-01-091</b>	15	>15
<b>CZ-01-103</b>	5	10
<b>CZ-01-124</b>	5	>50
<b>CZ-01-125</b>	5	>50

Table 4.8: The in vitro activity of the substituted tris norspermidine CZ-series, as MICs against Gram-positive MRSA and Gram-negative *Pseudomonas aeruginosa*

Cmpd	MIC-MRSA ( $\mu\text{g/mL}$ )	MIC- <i>P. aeruginosa</i> ( $\mu\text{g/mL}$ )
<b>CZ-01-099</b>	5.8	200
<b>CZ-01-126</b>	10	>40
<b>CZ-01-127</b>	3	18
<b>CZ-01-128</b>	2	3.5
<b>CZ-01-140</b>	2	40

Table 4.9: The in vitro activity of the substituted urea CZ-series, as MICs against Gram-positive MRSA and Gram-negative *Pseudomonas aeruginosa*

Cmpd	MIC-MRSA ( $\mu\text{g/mL}$ )	MIC- <i>P. aeruginosa</i> ( $\mu\text{g/mL}$ )
<b>CZ-01-129</b>	>15	>30
<b>CZ-01-130</b>	8	>50
<b>CZ-01-136</b>	>20	>30

Table 4.10: The in vitro activity of the modified **CZ-01-099** analogs as MICs against Gram-positive MRSA and Gram-negative *Pseudomonas aeruginosa*

Cmpd	MIC-MRSA ( $\mu\text{g/mL}$ )	MIC- <i>P. aeruginosa</i> ( $\mu\text{g/mL}$ )
<b>CZ-01-150</b>	30	NA
<b>CZ-01-151</b>	20	NA

Table 4.11: The in vitro activity of the altered norspermidine side chain CZ-series, as MICs against Gram-positive MRSA and Gram-negative *Pseudomonas aeruginosa*

Cmpd	MIC-MRSA ( $\mu\text{g/mL}$ )	MIC- <i>P. aeruginosa</i> ( $\mu\text{g/mL}$ )
<b>CZ-01-159</b>	10	15
<b>CZ-01-160</b>	10	15
<b>CZ-01-163</b>	0.75	10
<b>CZ-01-165</b>	4	>50
<b>CZ-01-167</b>	10	>20

Table 4.12: The in vitro activity of the altered norspermidine side chain CZ-series with respect to **CZ-01-099**, as MICs against Gram-positive MRSA and Gram-negative *Pseudomonas aeruginosa*

Cmpd	MIC-MRSA ( $\mu\text{g/mL}$ )	MIC- <i>P. aeruginosa</i> ( $\mu\text{g/mL}$ )
<b>CZ-01-168</b>	5	>20
<b>CZ-01-169</b>	5	>20
<b>CZ-01-170</b>	3	>50
<b>CZ-01-172</b>	2	20

Table 4.13: The in vitro activity of the dialdehyde terphenyl CZ-series, as MICs against Gram-positive MRSA and Gram-negative *Pseudomonas aeruginosa*

Cmpd	MIC-MRSA ( $\mu\text{g/mL}$ )	MIC- <i>P. aeruginosa</i> ( $\mu\text{g/mL}$ )
<b>CZ-01-152</b>	10	30
<b>CZ-01-154</b>	2.7	20
<b>CZ-01-155</b>	10	15
<b>CZ-01-157</b>	3	15
<b>CZ-01-161</b>	1	2
<b>CZ-01-164</b>	0.75	10
<b>CZ-01-166</b>	1	4
<b>CZ-01-180</b>	NA (due to solubility)	NA (due to solubility)

Table 4.14: The in vitro activity of the trialdehyde terphenyl CZ-series, as MICs against Gram-positive MRSA and Gram-negative *Pseudomonas aeruginosa*

Cmpd	MIC-MRSA ( $\mu\text{g/mL}$ )	MIC- <i>P. aeruginosa</i> ( $\mu\text{g/mL}$ )
<b>CZ-01-153</b>	10	>50
<b>CZ-01-156</b>	2	20

Table 4.15: The in vitro activity of the pyrimidine terphenyl CZ-series, as MICs against Gram-positive MRSA and Gram-negative *Pseudomonas aeruginosa*

Cmpd	MIC-MRSA ( $\mu\text{g/mL}$ )	MIC- <i>P. aeruginosa</i> ( $\mu\text{g/mL}$ )
<b>CZ-01-174</b>	7	50
<b>CZ-01-176</b>	20	>40

Table 4.16: The in vitro activity of the *tert*-butyl terphenyl CZ-series, as MICs against Gram-positive MRSA and Gram-negative *Pseudomonas aeruginosa*

Cmpd	MIC-MRSA ( $\mu\text{g/mL}$ )	MIC- <i>P. aeruginosa</i> ( $\mu\text{g/mL}$ )
<b>CZ-01-177</b>	0.75	1
<b>CZ-01-178</b>	0.75	1
<b>CZ-01-179</b>	0.5	4
<b>CZ-01-182</b>	0.25	4
<b>CZ-01-183</b>	0.5	8
<b>CZ-01-184</b>	0.5	16

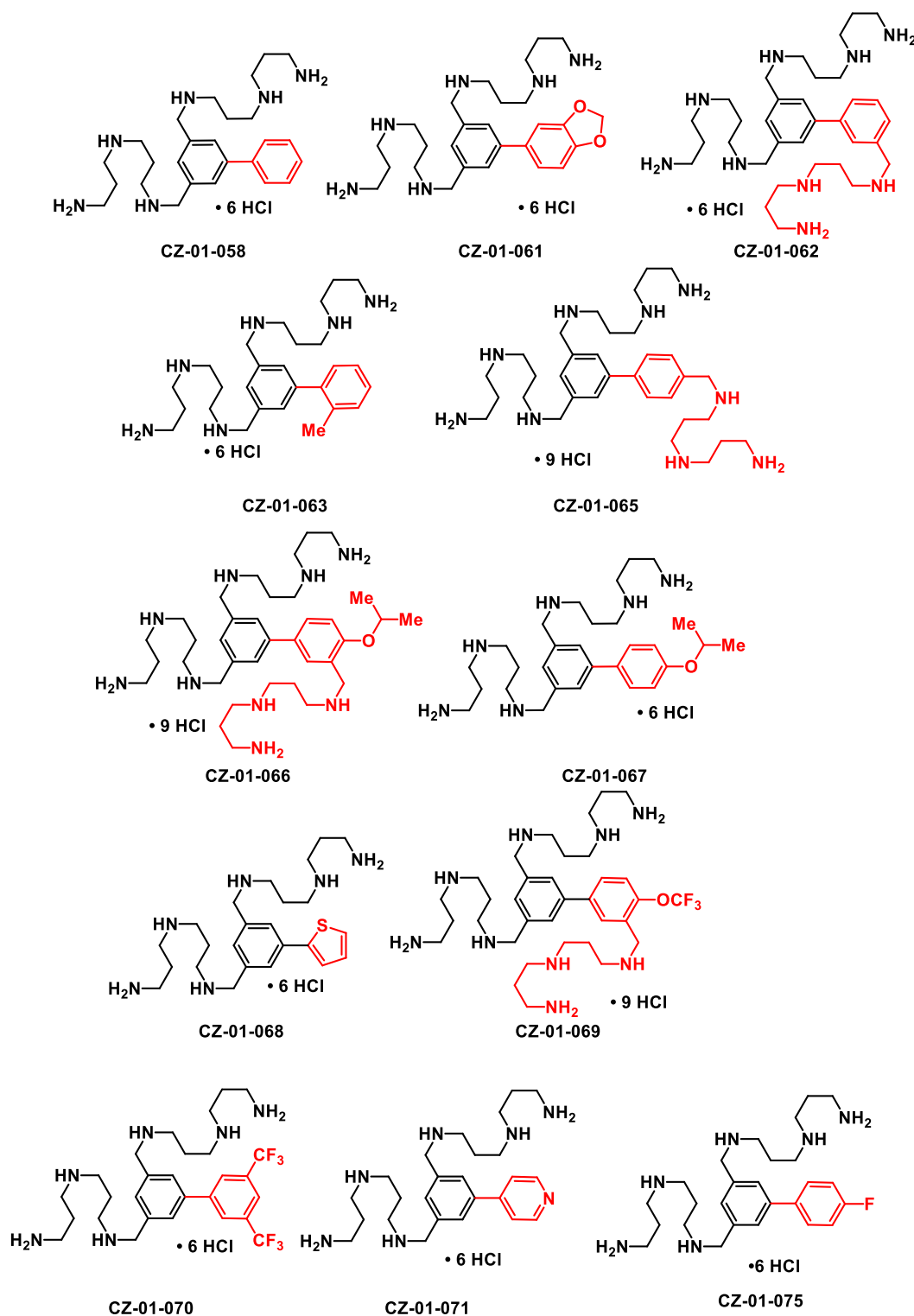


Figure 4.1: Initial second generation CZ-compounds made via the Suzuki coupling with a variety of  $sp^2$  boronic acids, followed by Boc-norspermidine reductive amination, with the pendent aryl group shown in red.



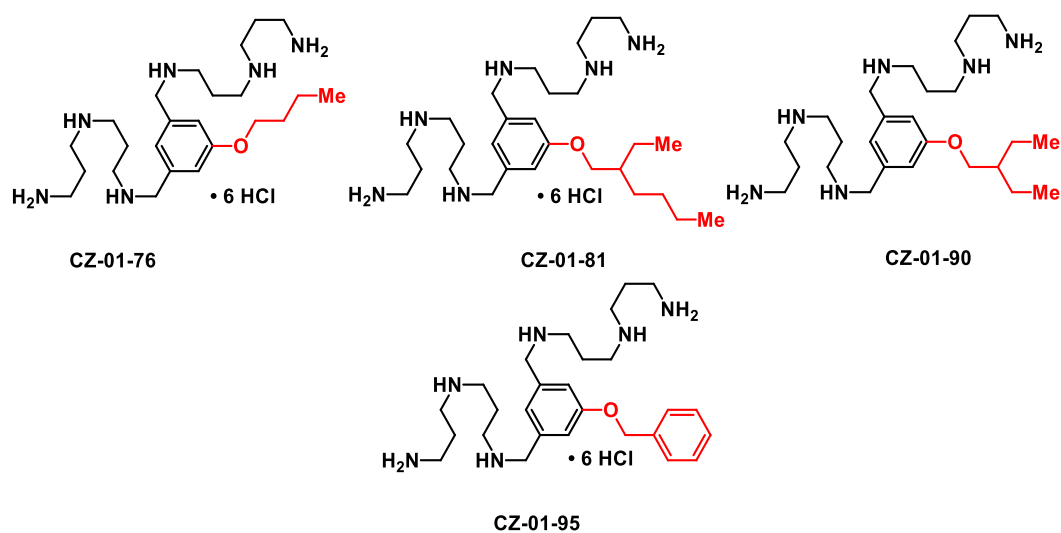


Figure 4.2: Etheral CZ compounds constructed from dimethyl 5-hydroxyisophthalate, with the pendent alkylated phenol shown in red.

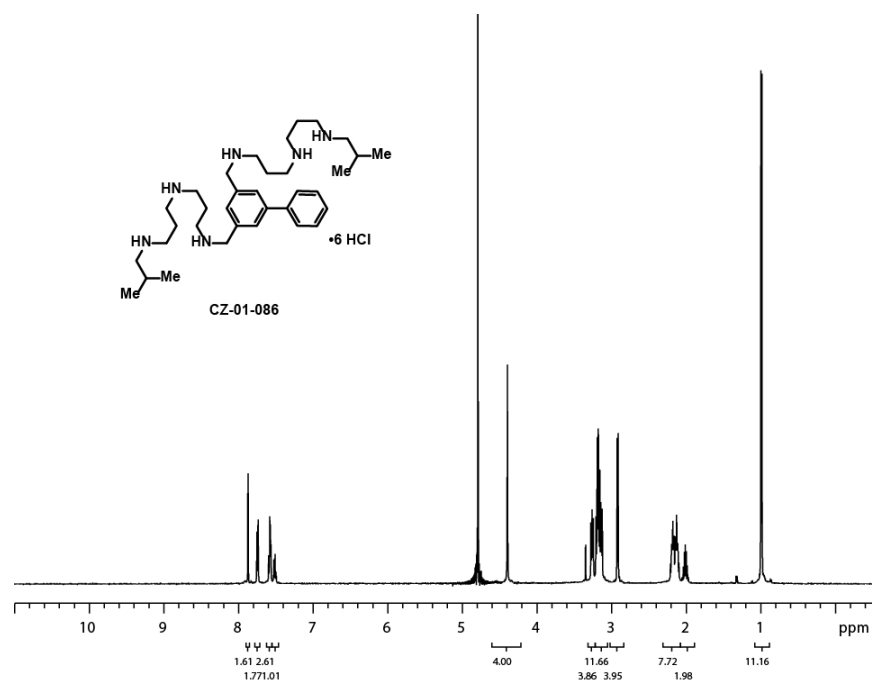


Figure 4.3: 1D  $^1\text{H}$  NMR of **CZ-01-086**

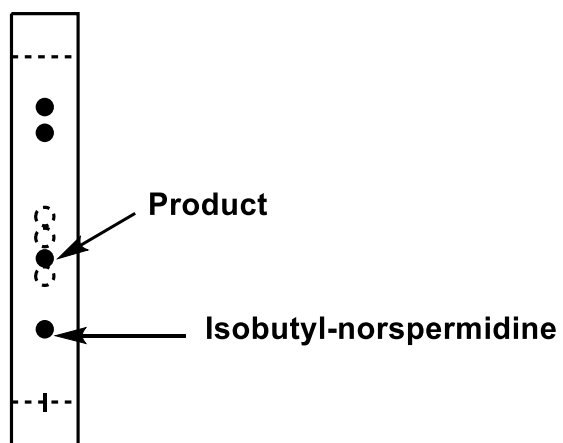


Figure 4.4: Representative TLC of **CZ-01-086**

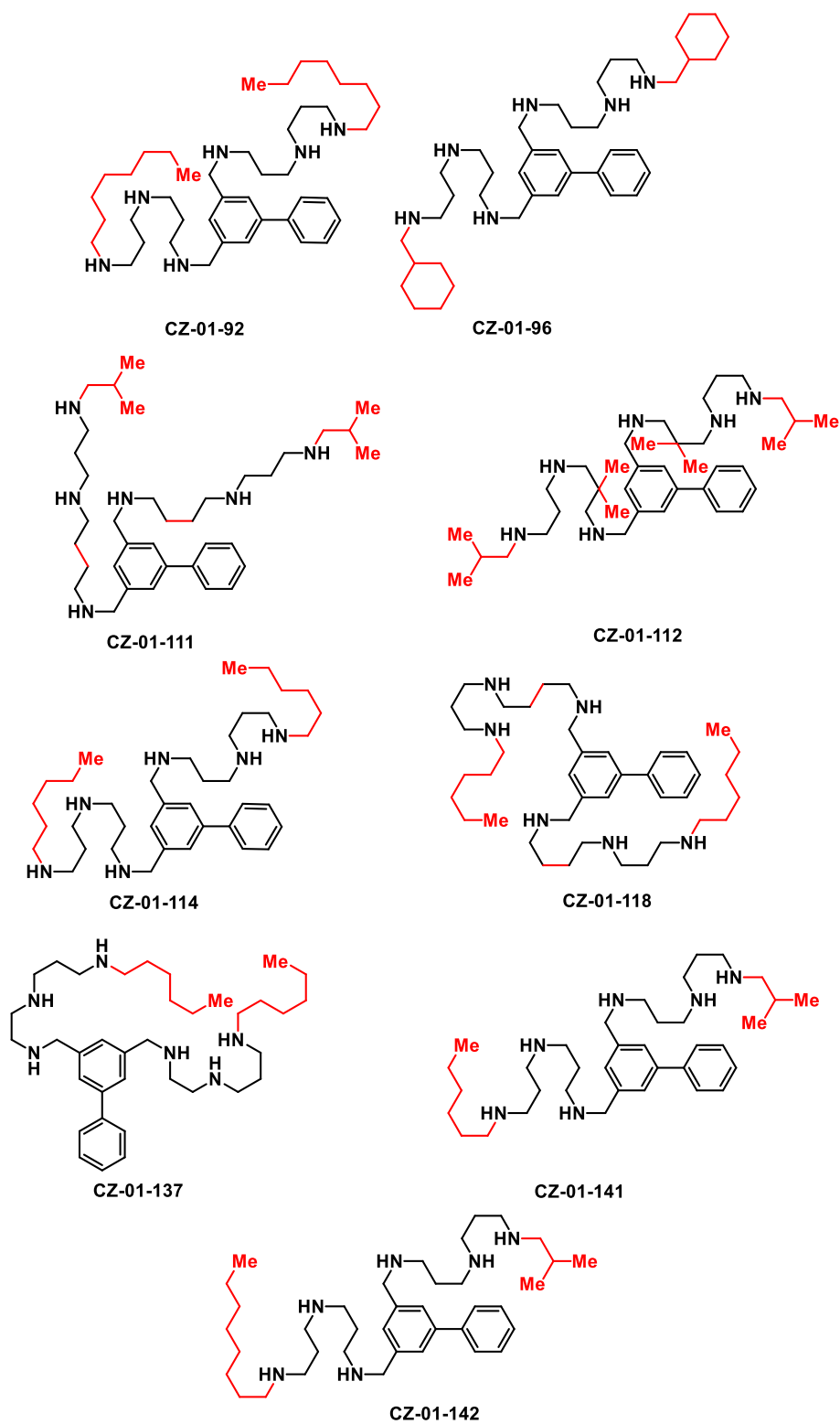


Figure 4.5: Structure profile of the initial alkylated(shown in red)-norspermidine analogs with a single phenyl ring at the 5-position

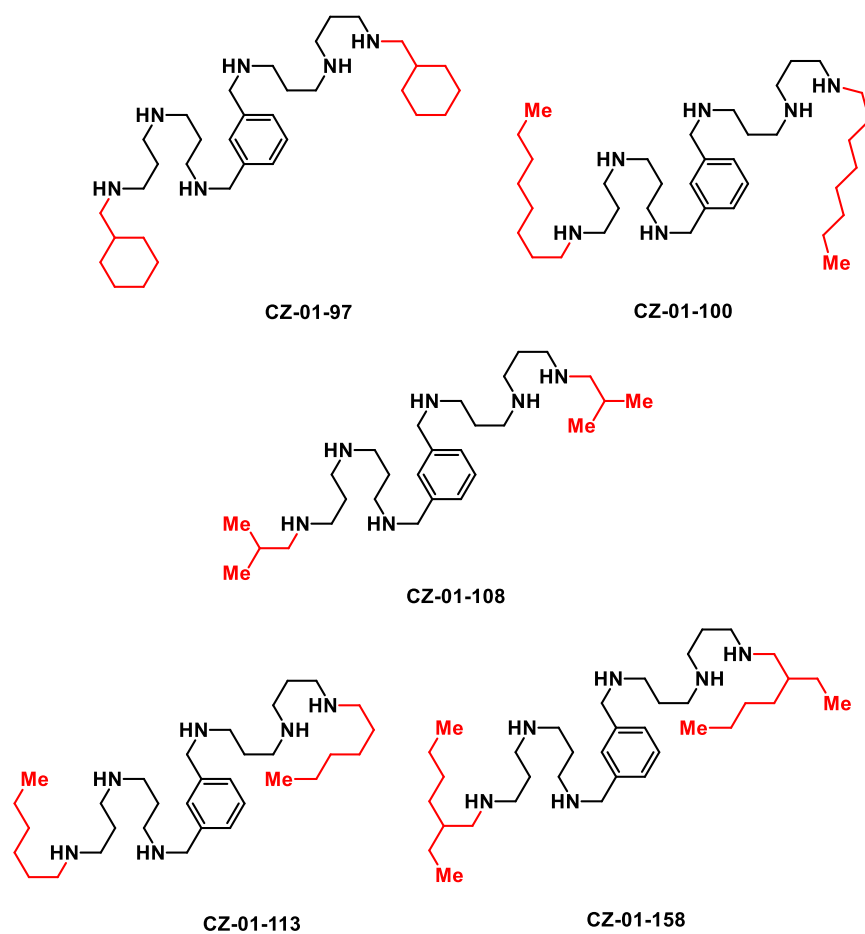


Figure 4.6: Structure profile of the initial alkylated(shown in red)-norspermidine analogs with isophthalaldehyde as the precursor

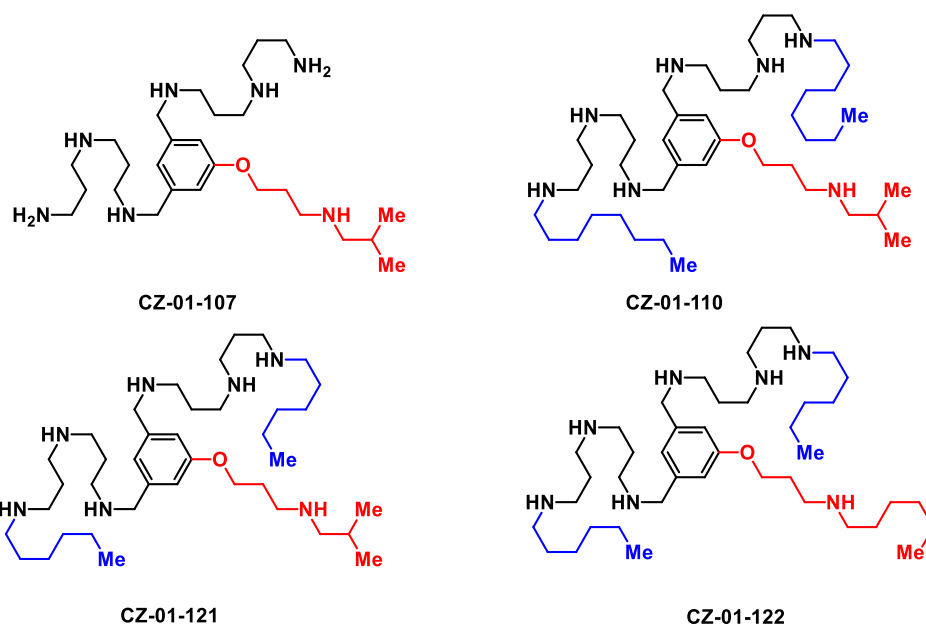


Figure 4.7: Amino-etheral derivatives with the amended 5-position in red with side-chain modifications in blue

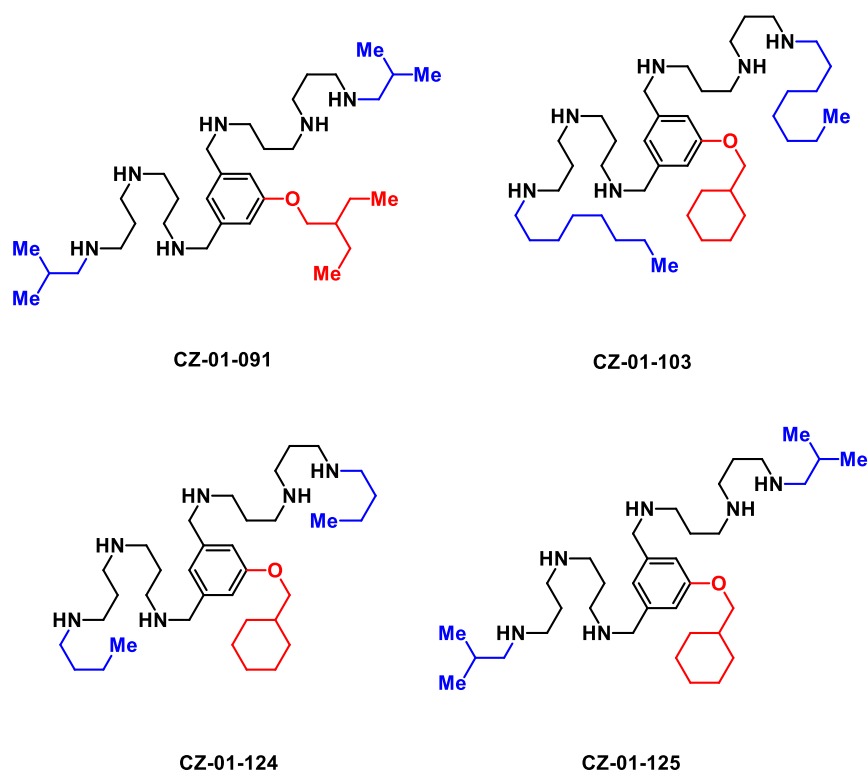


Figure 4.8: Alkylated phenoxy derivatives shown in red, with the requisite norspermidine side-chain shown in blue

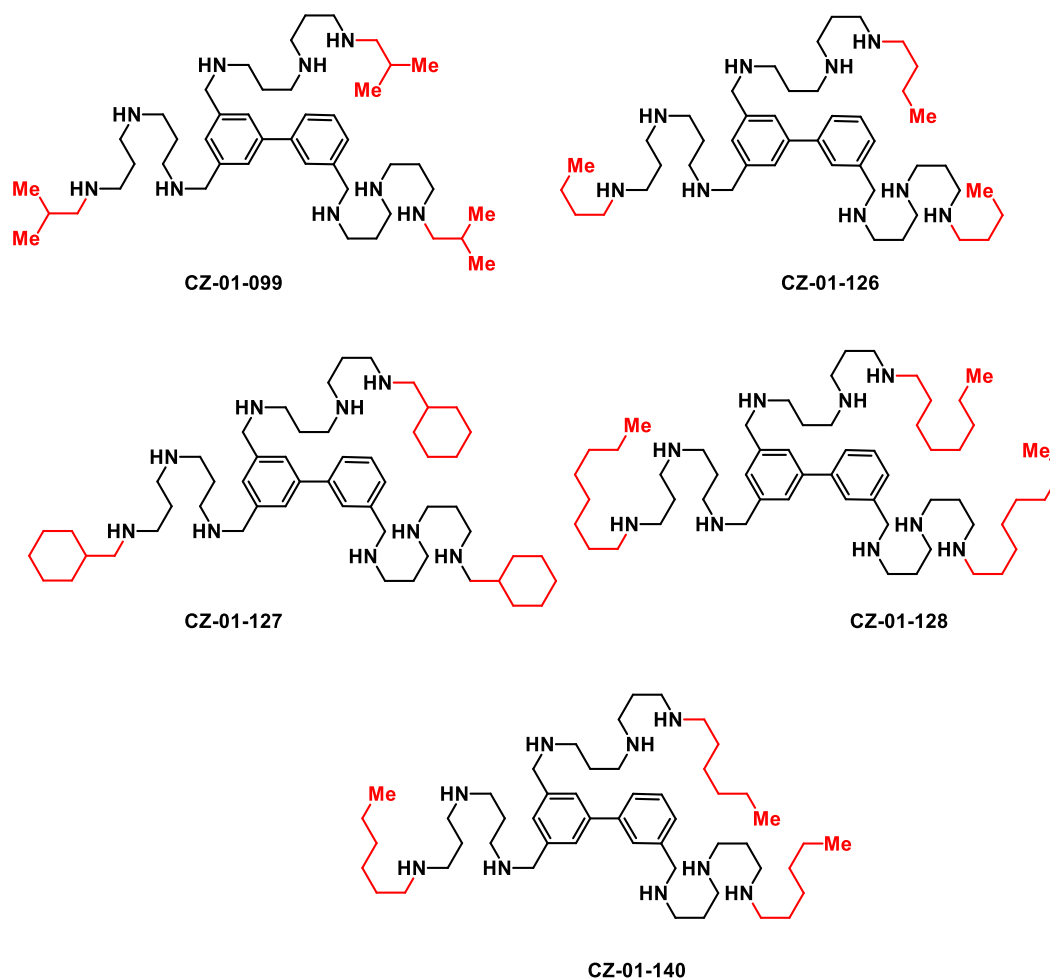


Figure 4.9: Alkylated (shown in red) tris-norspermidine analogs

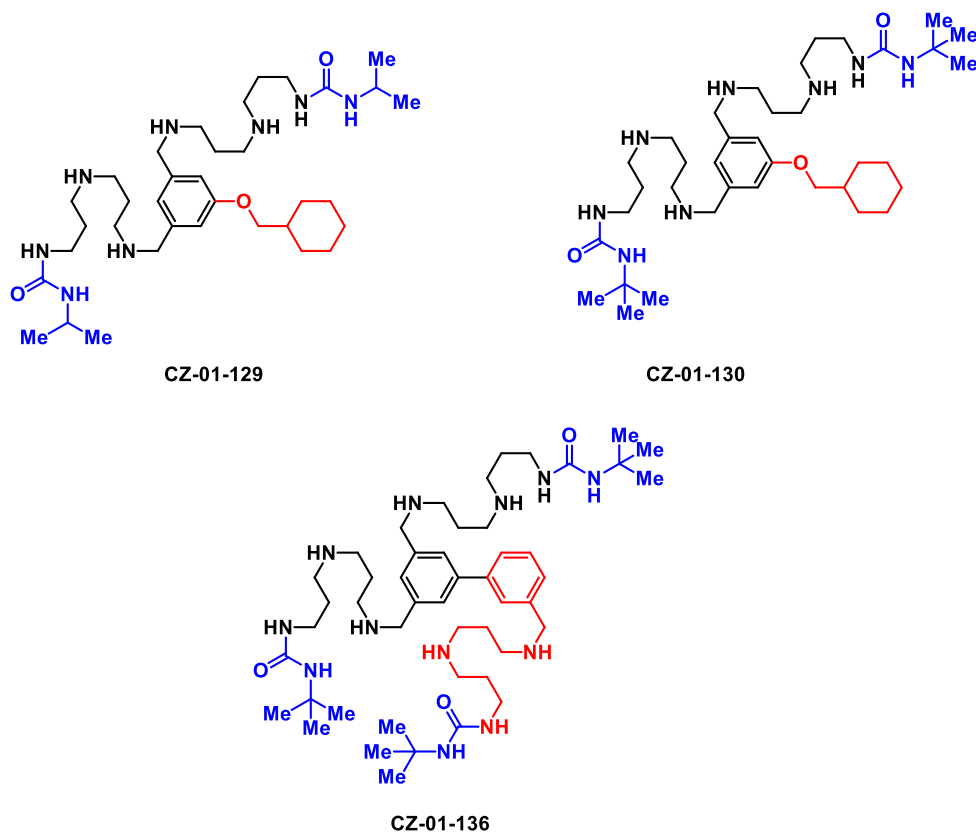


Figure 4.10: Terminally functionalized urea (shown in blue) analogs with the tris-counterpart (shown in red) or the cyclohexyl methyl ether (shown in red)

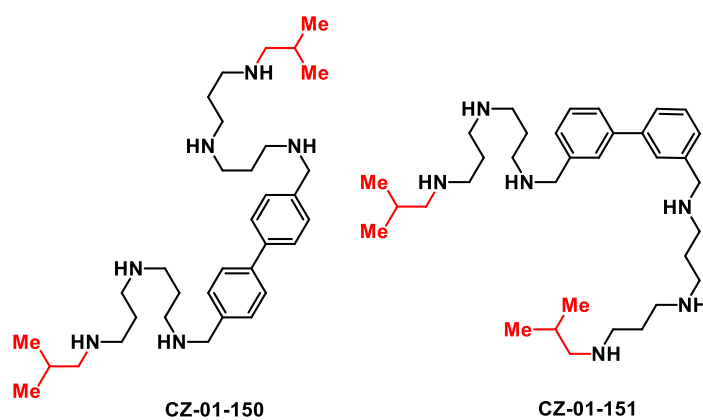


Figure 4.11: Truncated **CZ-01-099** analogs both of which contain the *i*-butyl alkylated (shown in red) side-chain

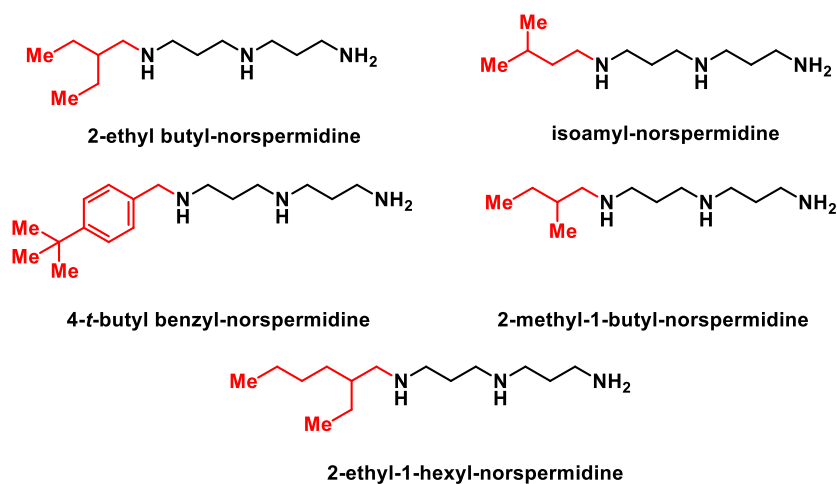


Figure 4.12: Additional alkylated (shown in red) iterations on the norspermidine side-chains

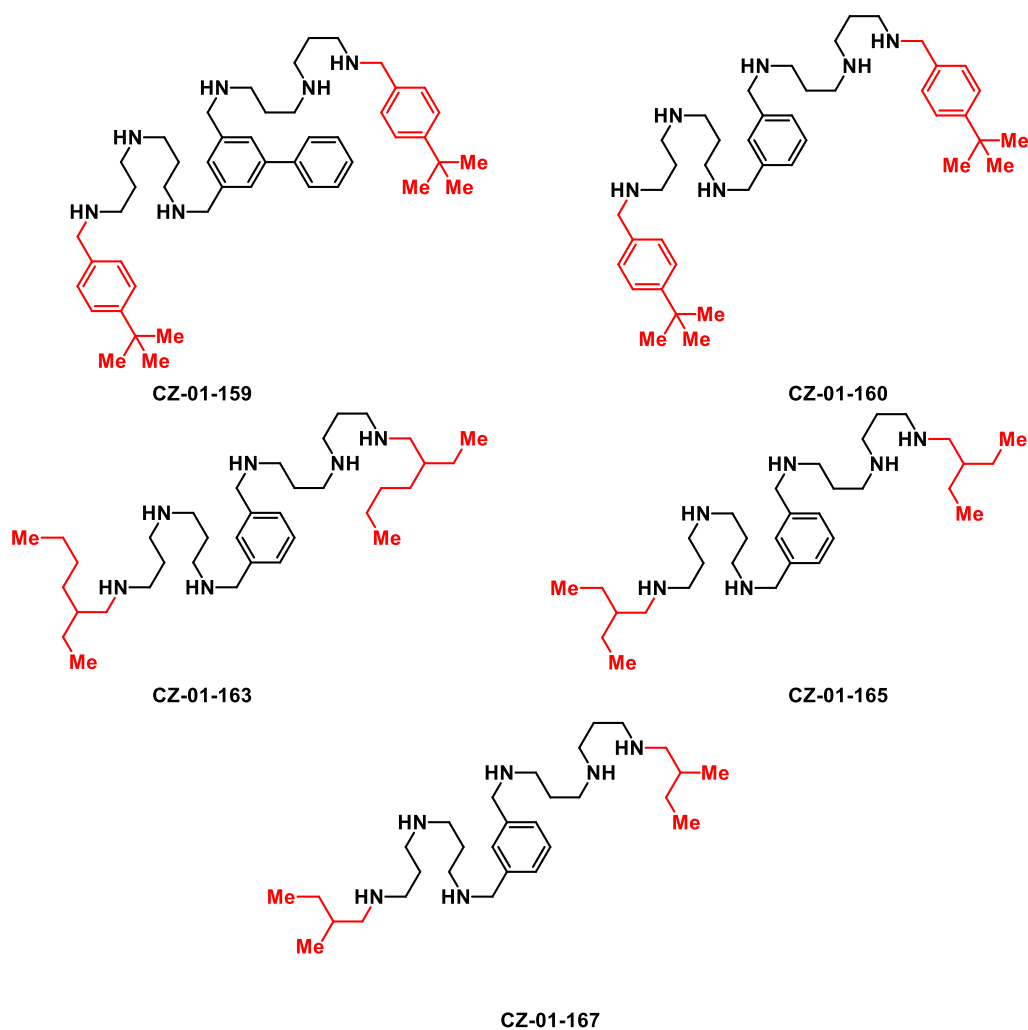


Figure 4.13: Alkylated (shown in red) norspermidine mono-phenyl and bi-phenyl analogs



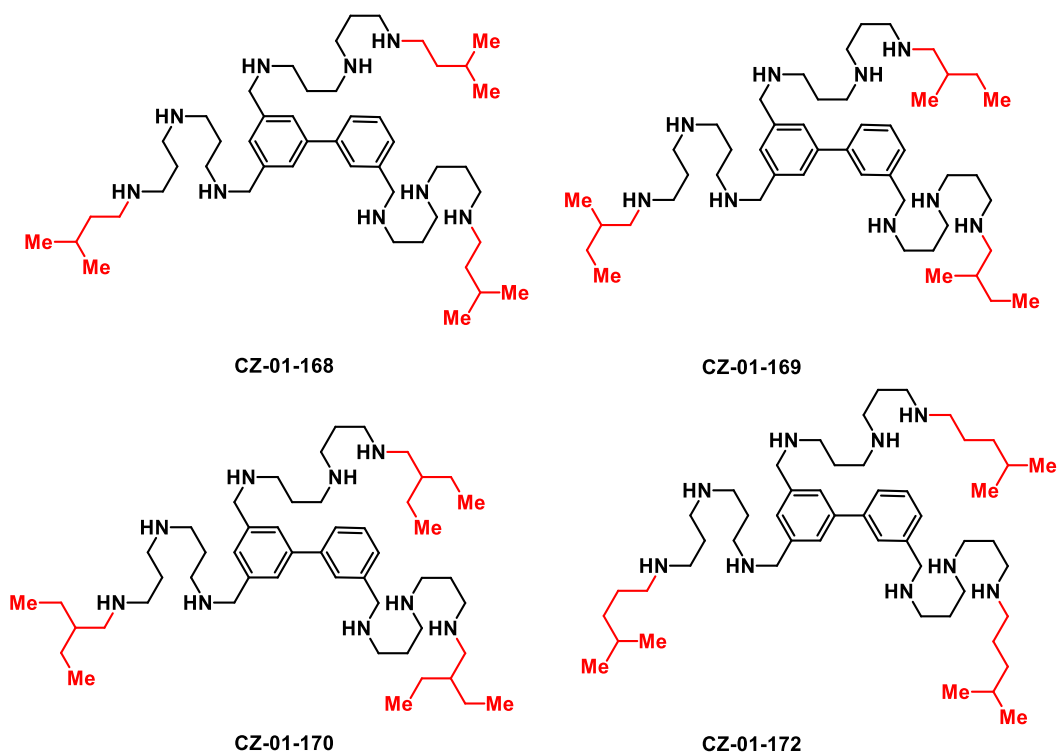


Figure 4.14: Tris-alkylated (shown in red) norspermidine bi-phenyl analogs based off of **CZ-01-099**

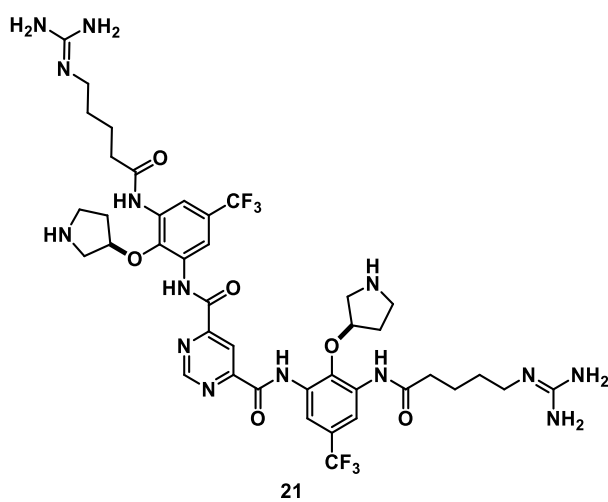


Figure 4.15: The structure of brilacidin

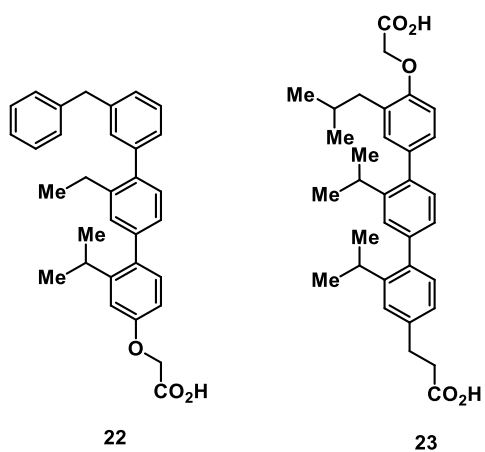


Figure 4.16: Two representative examples of Hamilton's terphenyl protein-protein inhibitors

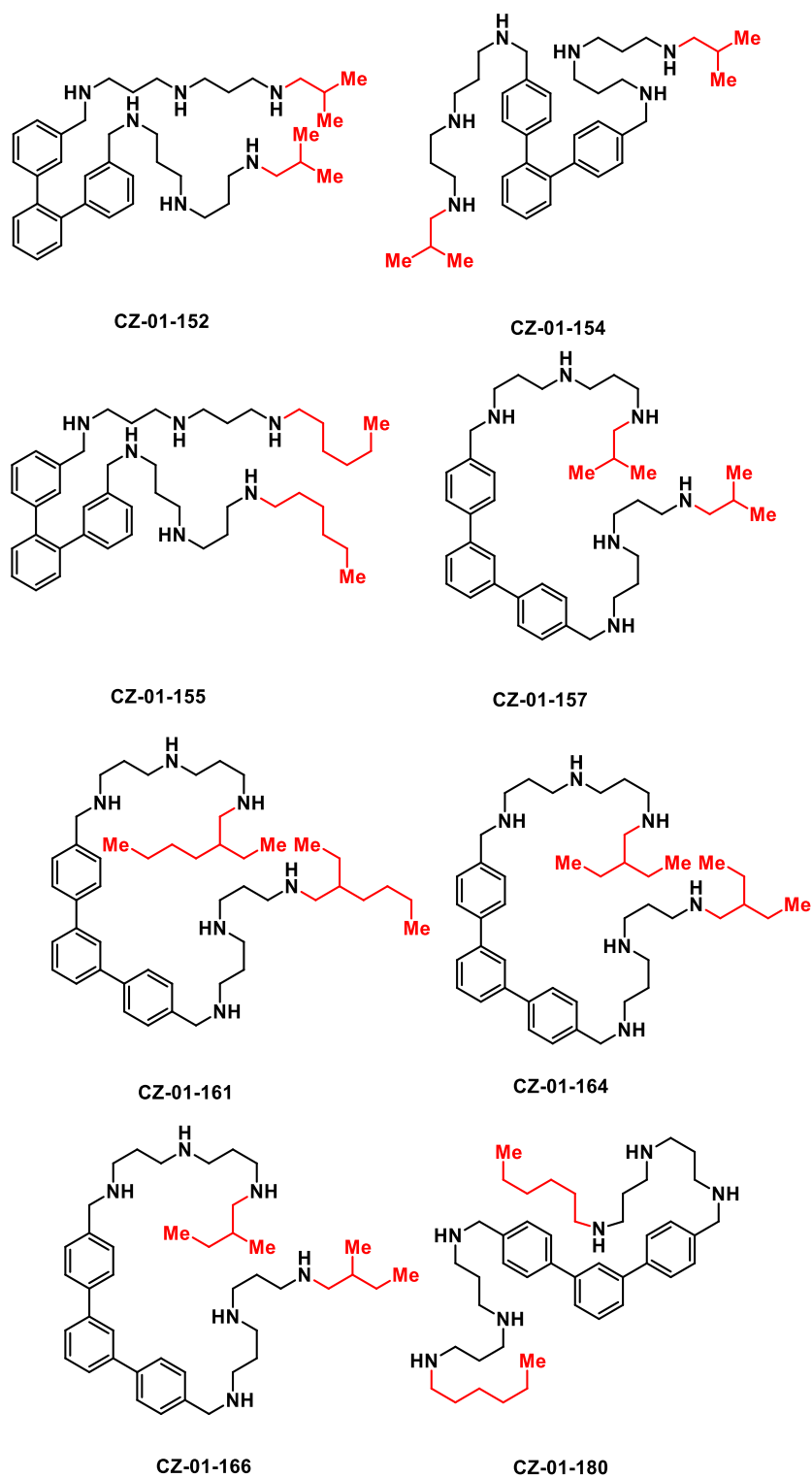


Figure 4.17: Initial terphenyl CZ-compounds with the modulated norspermidine side-chain shown in red

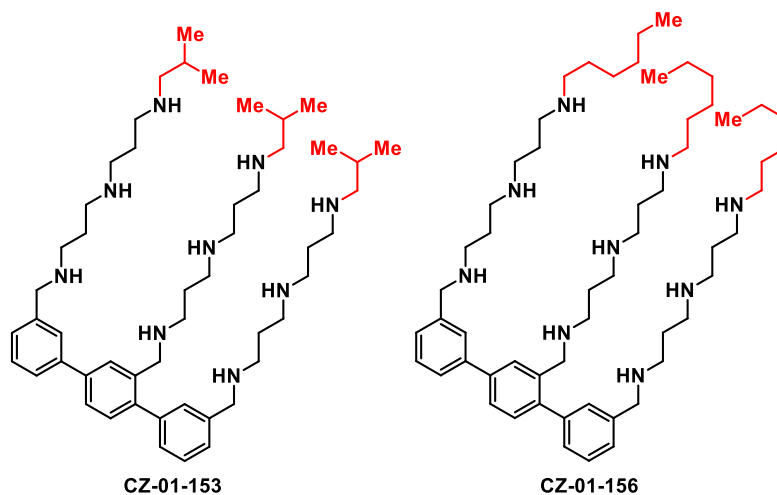


Figure 4.18: The structures of the CZ-compounds generated from the terphenyl trialdehyde with the modulated norspermidine side-chain shown in red

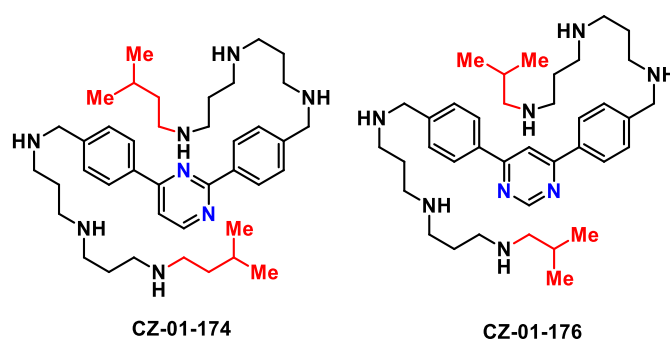


Figure 4.19: Structures of the pyrimidine analogs with the modulated norspermidine side-chain shown in red and the internal pyrimidine nitrogens shown in blue

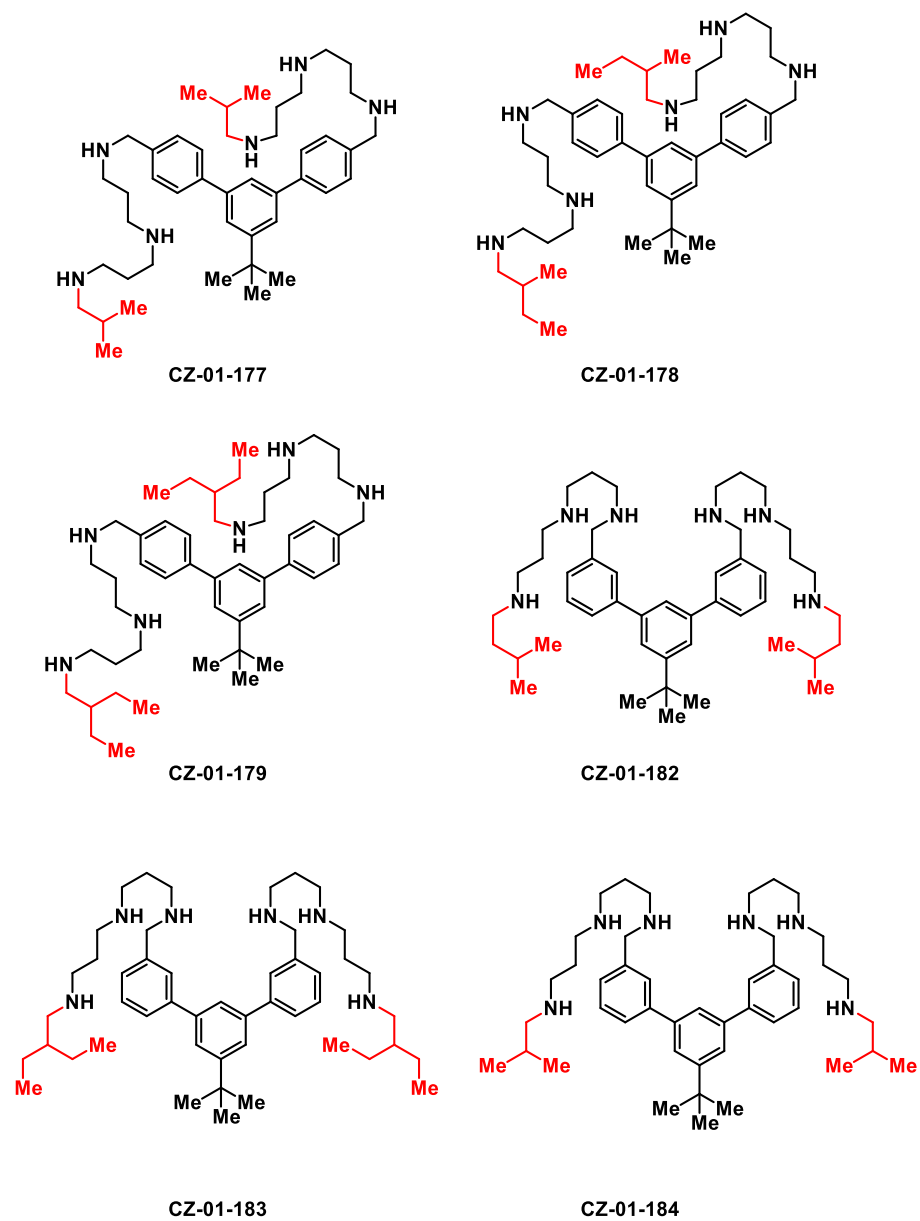


Figure 4.20: Structures of the *tert*-butyl terphenyl analogs with the modulated norspermidine side-chain shown in red

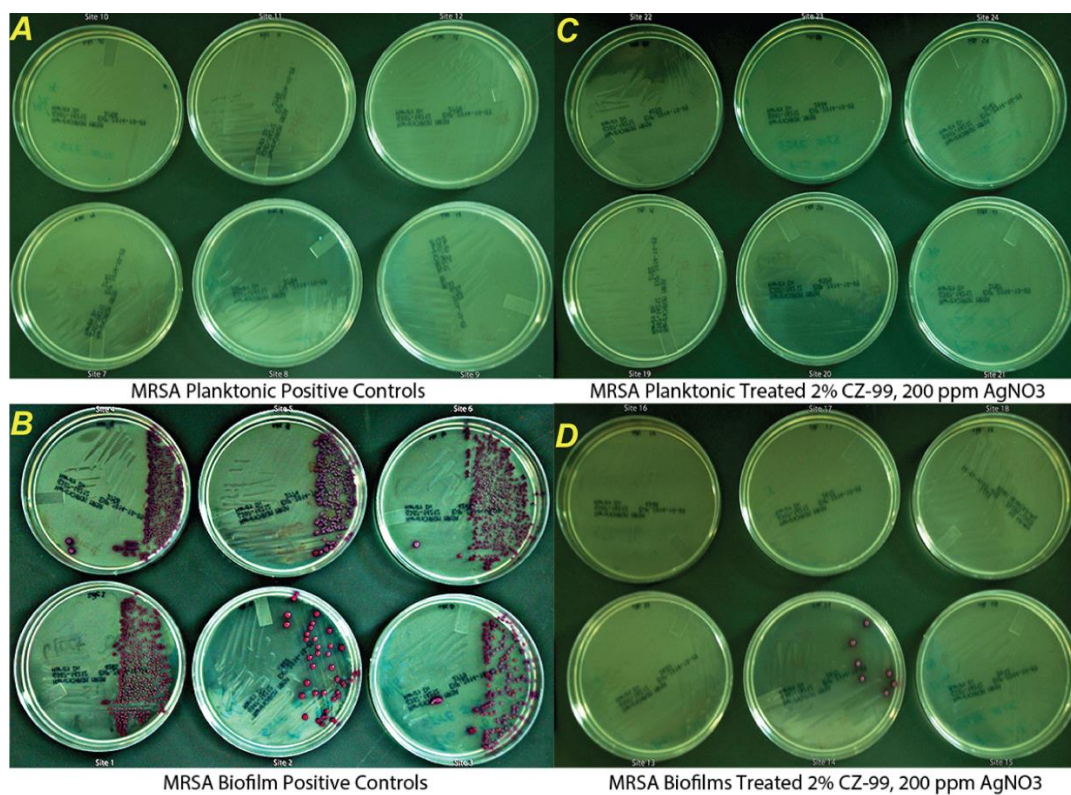


Figure 4.21: Cultured MRSA on chrome-agar plates from pig 3 of the topical wound model

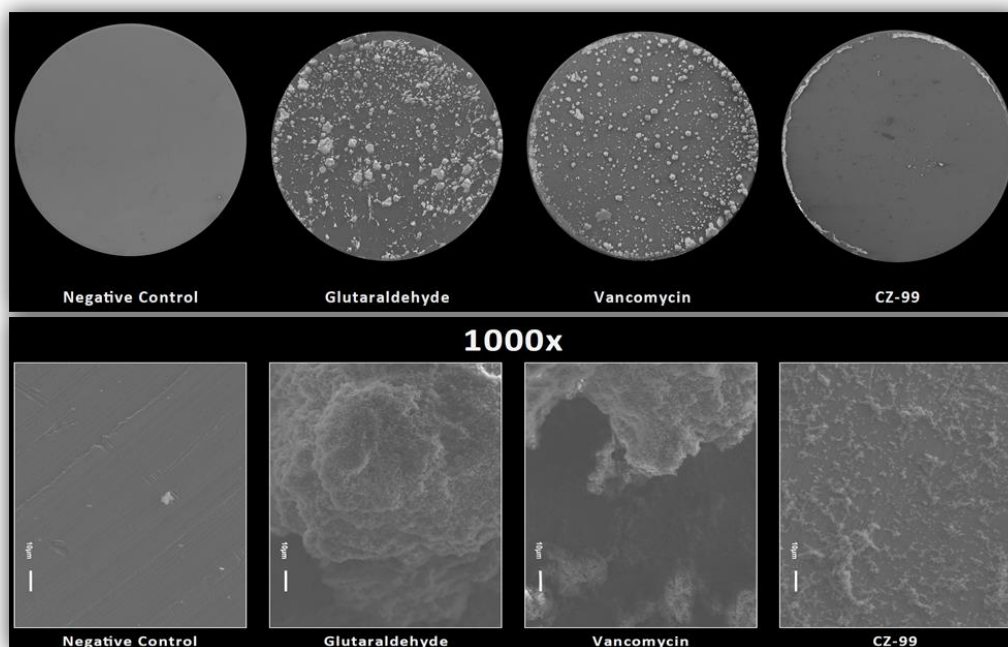


Figure 4.22: Qualitative biofilm dispersion data of **CZ-01-099** in conjunction with glutaraldehyde and vancomycin

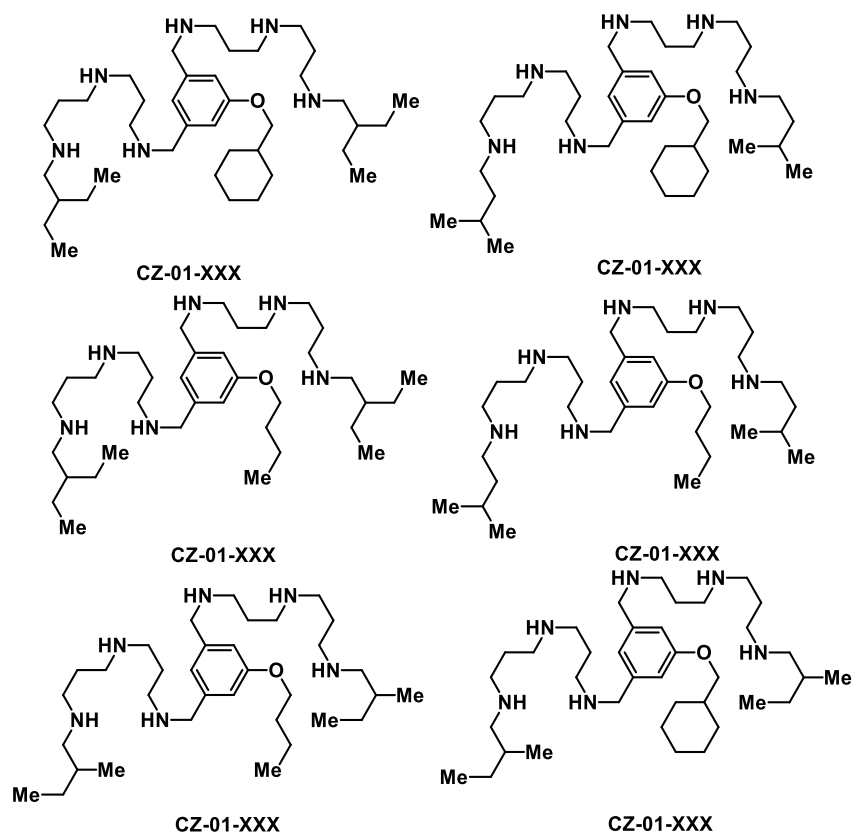


Figure 4.23: Desired structural investigation of older ether scaffolds with new norspermidine derivatives

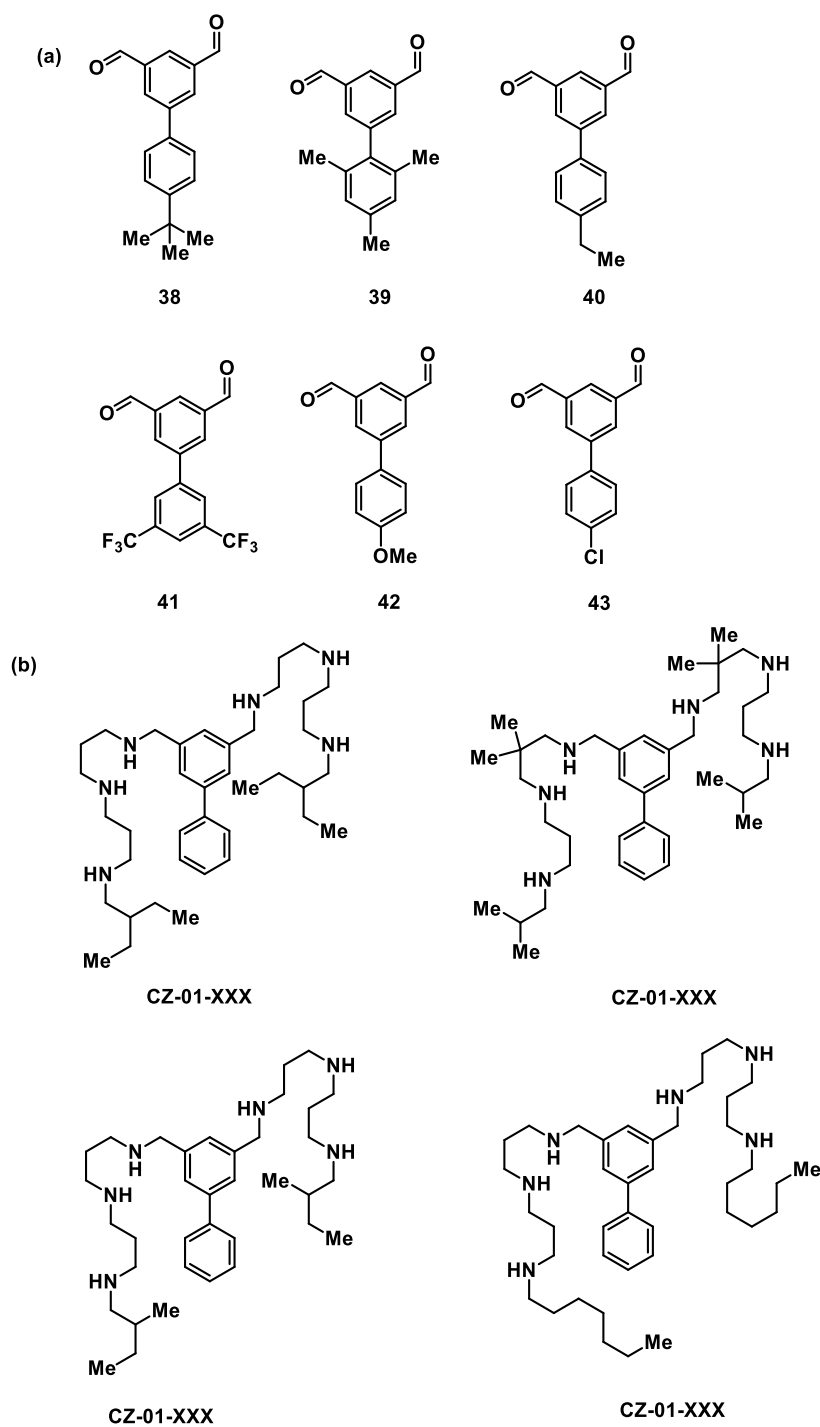
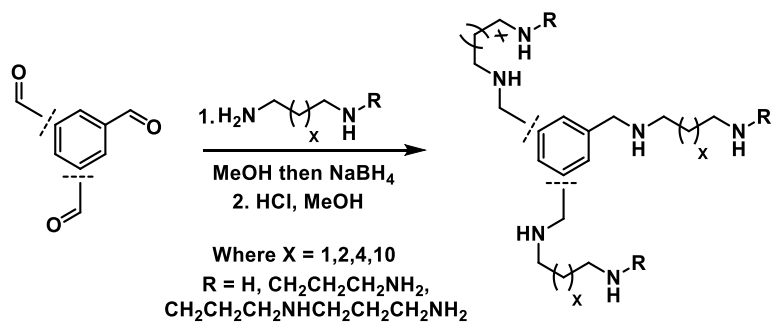
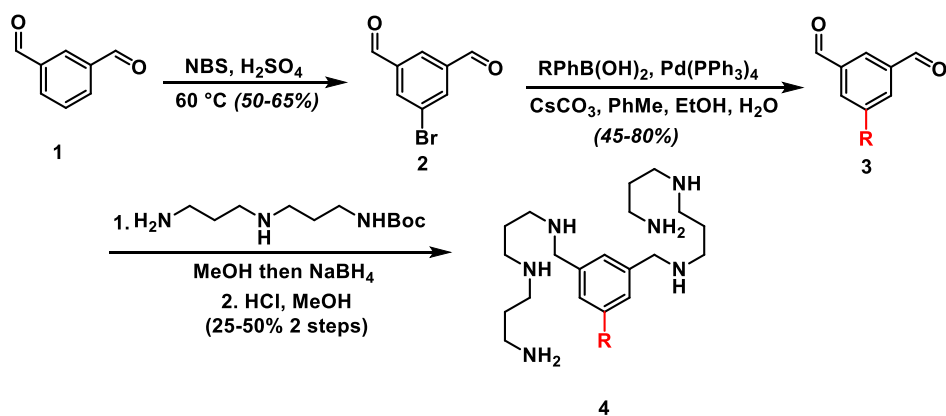


Figure 4.24: (a) Desired aldehydes used for additional SAR studies (b) Desired **CZ-01-114** analogs resultant from alternative side chains



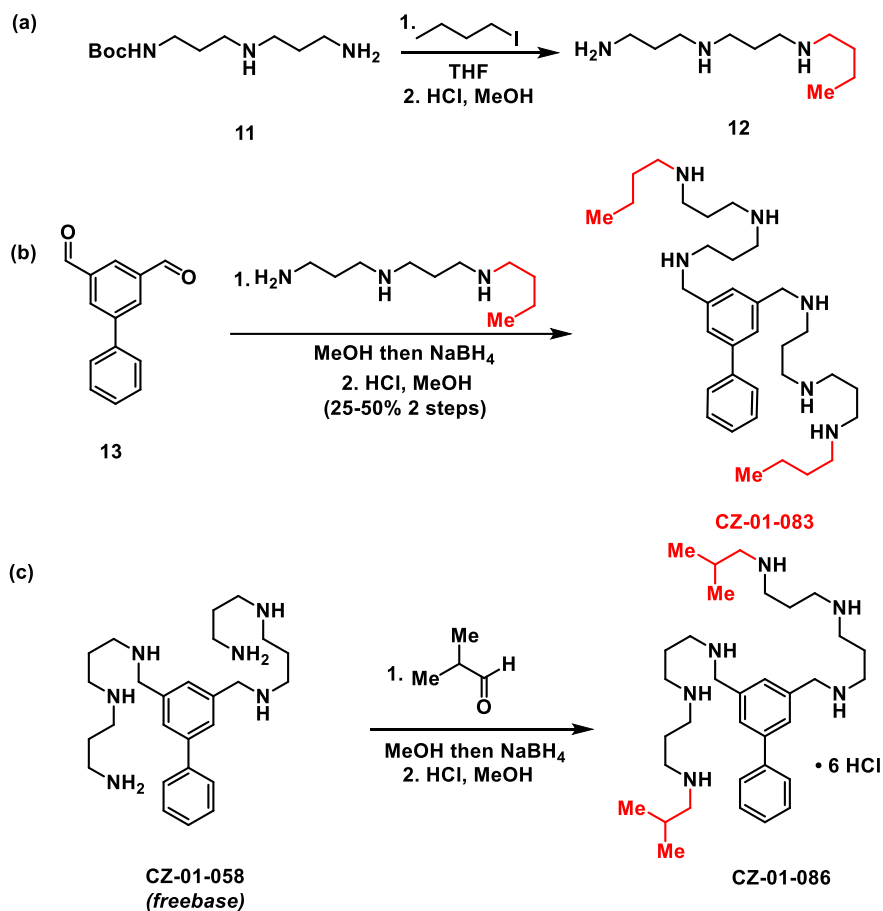


Scheme 4.1: Reiteration of the general synthesis of the first generation CZ compounds, specifically **CZ-01-01** to **CZ-01-57** (certain substituted derivatives are left out for clarity)

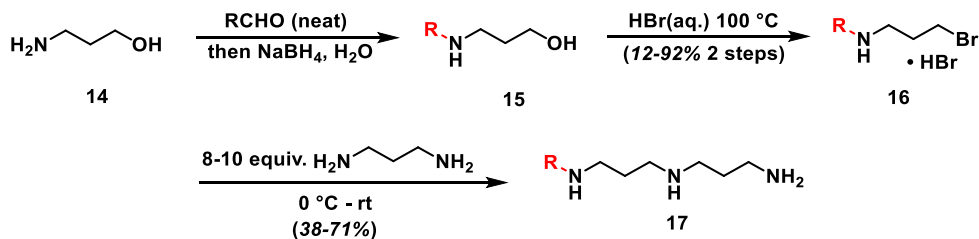


Scheme 4.2: General forward synthesis for second generation CZ compounds starting with the formation of 5-bromoisophthalaldehyde from isophthalaldehyde followed by the requisite Suzuki coupling, with the pendant R-group shown in red

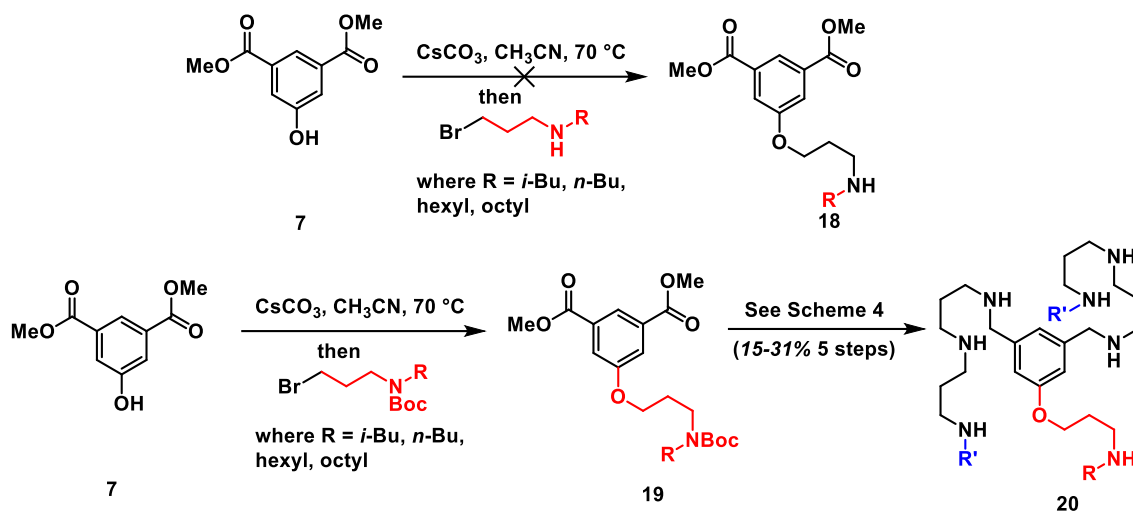
Scheme 4.4: Second generation phenoxy CZ analogs made via the substituted phenoxy diester, with the pendant alkylated phenol shown in red



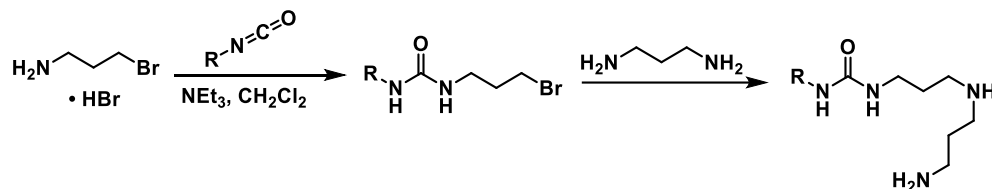
Scheme 4.5: Approach to substituted norspermidine CZ-analogs, prepared from the Boc-norspermidine (a and b) and the requisite free base (c) with the supplemental side-chain shown in red



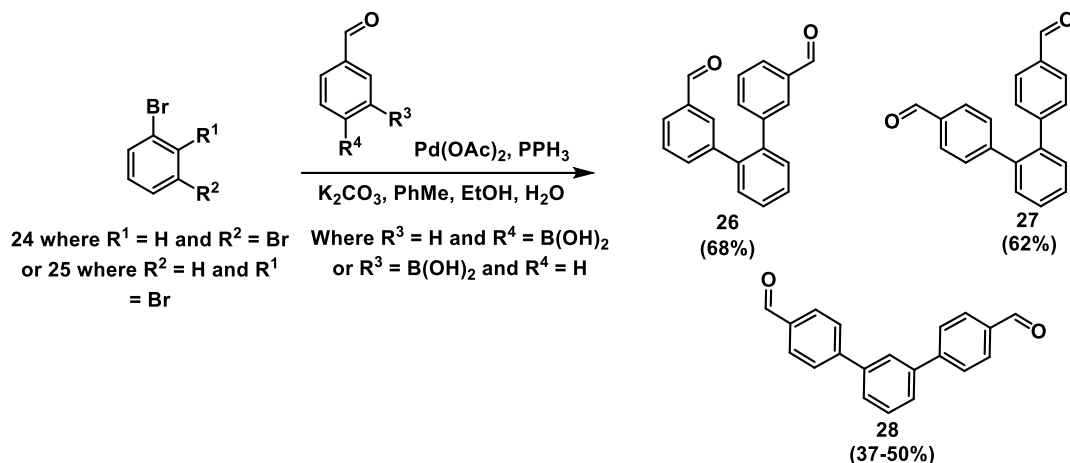
Scheme 4.6: Representative example of the construction of terminally substituted polyamines from the amino alcohol an alkylated norspermidine, with the alkyl side-chain shown in red



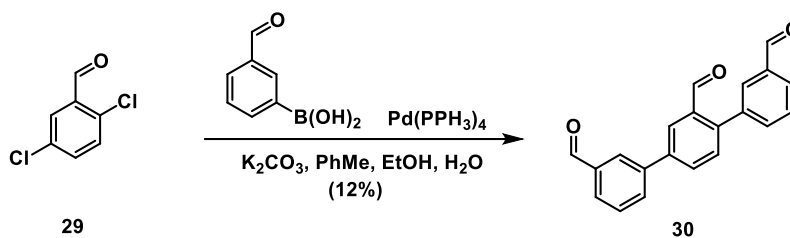
Scheme 4.7: Unsuccessful and successful use of the substituted amino bromide salts to generate novel amino etheral analogs with the amed norspermidine side-chain shown in blue and the phenolic side-chain shown in red



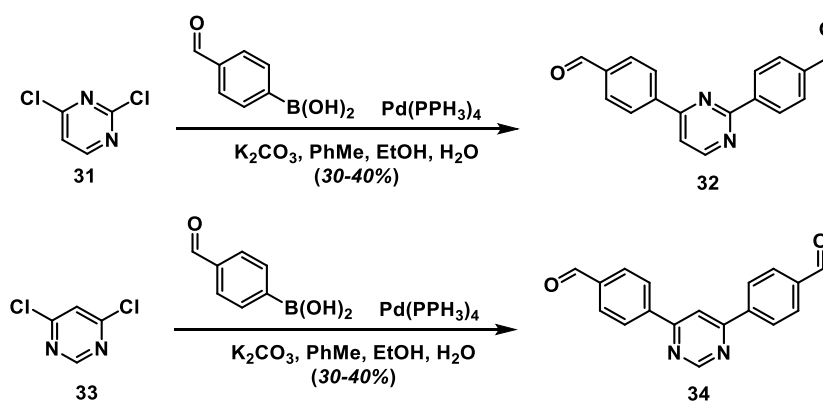
Scheme 4.8: Synthesis of the urea norspermidine side chains



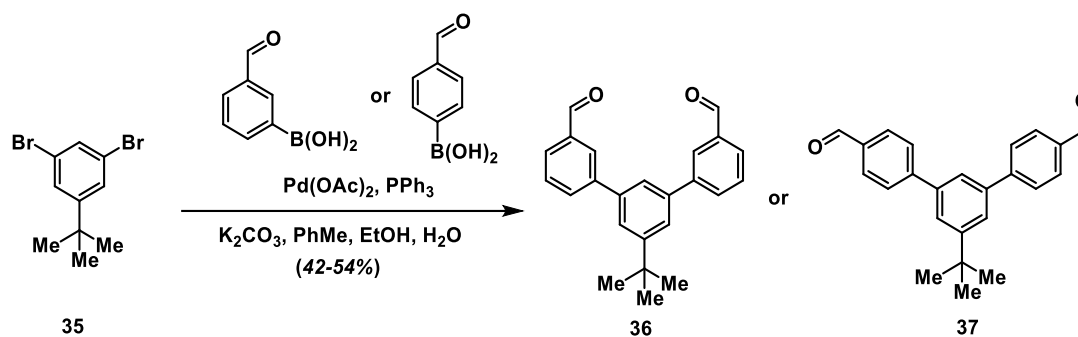
Scheme 4.9: Synthesis of the terphenyl di-aldehyde from the respective dibromo-benzene



Scheme 4.10: Synthesis of the terphenyl trialdehyde



Scheme 4.11: Synthesis of pyrimidine terphenyl aldehydes

Scheme 4.12: Synthesis of *tert*-butyl terphenyl dialdehydes

## 4.6 Supporting Information

### 4.6.1 General Experimental Conditions

Unless otherwise noted, materials were obtained from commercial sources and used without purification; otherwise, materials were purified according to Purification of Laboratory Chemicals.<sup>6</sup> All reactions requiring anhydrous conditions were performed under a positive pressure of nitrogen using flame-dried glassware. Methanol (MeOH) was distilled over magnesium prior to its usage. Diaminopropane is highly toxic and should be handled with great care. Any volatile polyamine synthesized should also be regarded as toxic and should be handled with care and always stored under N<sub>2</sub> due to reactivity with O<sub>2</sub> and CO<sub>2</sub>. Yields were calculated for material judged homogeneous by thin-layer chromatography and <sup>1</sup>H NMR. Thin-layer chromatography was performed on silica plates eluting with the solvents indicated and visualized by a 254nm UV lamp. Flash column chromatography was performed with slurry-packed silica gel with solvents indicated in glass columns. Both the solvent system used for TLC and column chromatography needs to be made fresh upon usage due to the volatile nature of NH<sub>3</sub> in H<sub>2</sub>O. <sup>1</sup>H NMR spectra were recorded at 500 or 300 MHz as indicated. The chemical shifts ( $\delta$ ) of proton resonances are reported relative to the deuterated solvent peak: 4.79 for H<sub>2</sub>O using the following format: chemical shift [multiplicity (s = singlet, bs = broad singlet, d = doublet, dd = doublet of doublets, t = triplet, tt = triplet of triplets, q = quartet, pent = pentet, hex = hextet, sept = septet, oct = octet, non = nonet m = multiplet), coupling constant(s) (J in Hz), integral]. <sup>13</sup>C NMR spectra were recorded at 125 MHz. Mass spectra were obtained by ESI/APCI for LRMS. Material purity was quantified with a Thermo scientific Ultimate 3000 LC system. Certain carbon experiments conducted with the VXR500 MHz NMR contain an artifact

peak between 170.0-174.0 ppm, which has been confirmed by the facility administrator.

Efficacy profiles of CZ-01-XXX against planktonic MRSA were determined using the microdilution minimum inhibitory concentration (MIC) and minimum bactericidal concentration (MBC) assays defined by Clinical and Laboratory Standards Institute (CLSI) in the M26-A guideline. For comparison, efficacy profiles were also determined in parallel for vancomycin. In short, to perform MIC analysis, several colonies of freshly-cultured MRSA or *P. aeruginosa* from blood agar were used to adjust a 0.5 McFarland standard (equated to  $\sim 7.5 \times 10^8$  colony forming units (CFU)/mL) in phosphate buffered saline (PBS; Fisher Scientific, catalog # BP399-1). Bacteria were diluted 1:100 in a glass test tube. In a 96-well plate, columns 2-11 were filled with cation adjusted Mueller Hinton broth (CAMHB; Fisher Scientific, catalog #B12322), antibiotic solution and MRSA as per the protocol. In order to fill the wells, liquids were poured into sterile dispensing reservoirs (Fisher Scientific, catalog #07-200-127) then pipeted using a multichannel pipet. This process gave a concentration range of antibiotic from 128  $\mu\text{g/mL}$  in column 2 to 0.25  $\mu\text{g/mL}$  in column 11. A 96-well plate was covered with a plastic plate cover and incubated at 37° C for 24 h after which time the plate was read. The lowest concentration of antibiotic with no growth (no pellet formation) of bacteria was defined as the MIC.

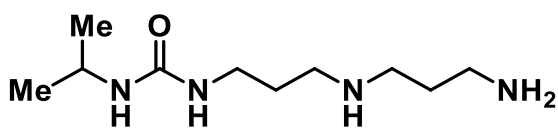
#### 4.6.2 Missing Experimental Data

Some examples included in the formal report were omitted for clarity or lack full characterization, as these compounds were synthesized only once and handed off to our biological counterpart without full compound characterization. Furthermore, we felt the biological data related to these samples did not warrant any additional pursuit.

#### 4.6.3 ISO 10993 Assay

The ISO 10993 assay is used to determine qualitative cytotoxicity against the L929 cell line. Data is given as a score of 0-4 at varying dilution levels. A score of between and including 0-2 refers to a “pass” or noncytotoxic compound, while a score of 3-4 refers to considerable cell death and is deemed cytotoxic.

#### 4.6.4 Experimental Procedures

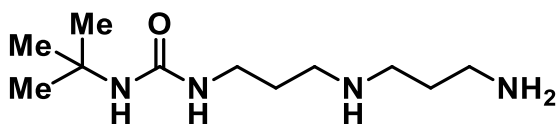


**1-(3-((3-aminopropyl)amino)propyl)-3-isopropylurea:** A flame dried flask was charged with 3-bromopropan-1-amine-hydrobromide (1.02 g, 4.66 mmol, 1.0 equiv.), NEt<sub>3</sub> (0.78 mL, 5.59 mmol, 1.2 equiv.), and CH<sub>2</sub>Cl<sub>2</sub> (20 mL) and placed under N<sub>2</sub>. To this was added isopropyl-isocyanate (0.45 mL, 4.66 mmol, 1.0 equiv.) and the reaction was left to stir for 2.5 h. The excess solvent was evaporated and the crude material was placed directly on a column and purified with EtOAc. The above purified material was added to a stirring solution of diaminopropane (7.8 mL, 93.2 mmol, 20.0 equiv.) at 0 °C over the span of 1.5 h. The reaction mixture was left to warm and stirred for 12-16 h. Excess 1,3-diaminopropane was removed under reduced pressure, and the remaining semisolid was taken up in 5% NaOH (100 mL) and extracted with 85:15 CHCl<sub>3</sub>/*i*-PrOH (5 x 20 mL), dried over Na<sub>2</sub>SO<sub>4</sub>, filtered, and concentrated under reduced pressure. Purification was accomplished by column chromatography eluting with 100:75:20 (CH<sub>2</sub>Cl<sub>2</sub>:MeOH:NH<sub>4</sub>OH) to afford the material as a pure semisolid (21%). <sup>1</sup>H NMR (500 MHz, CDCl<sub>3</sub>) δ ppm 5.38 (s, 1H), 4.99 (d, *J* = 7.5 Hz), 3.79 (oct, *J* = 6.5 Hz, 1H) 3.19(d, *J* = 6.0 Hz, 2H) 2.74 (t, *J* = 7.0 Hz, 2H), 2.63 (q, *J* = 5.0 Hz, 4H), 2.39 (bs, 4H), 1.63 (pent,

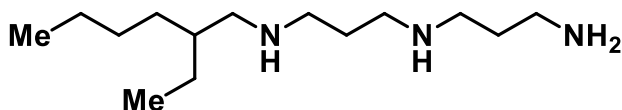


$J = 7.0$  Hz, 4H), 1.09 (d,  $J = 6.5$  Hz, 6H).  $^{13}\text{C}$  NMR (125 MHz,  $\text{CDCl}_3$ )  $\delta$  ppm 158.7, 47.9, 47.6, 42.2, 40.5, 38.7, 33.1, 30.1, 23.6.

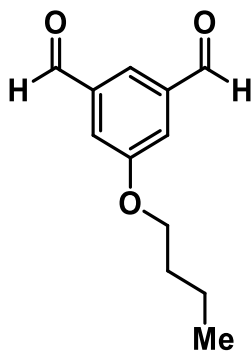
The following example was prepared similar to 1-(3-((3-aminopropyl)amino)propyl)-3-isopropylurea:



**1-(3-((3-aminopropyl)amino)propyl)-3-(tert-butyl)urea** :  $^1\text{H}$  NMR (500 MHz,  $\text{CDCl}_3$ )  $\delta$  ppm 5.54 (s, 1H), 5.22 (s, 1H), 3.07 (q,  $J = 6.0$  Hz, 2H), 2.68 (t,  $J = 7.0$  Hz, 2H), 2.55 (q,  $J = 8.0$  Hz, 4H), 1.58-1.51 (m, 4H), 1.20 (s, 9H).  $^{13}\text{C}$  NMR (125 MHz,  $\text{CDCl}_3$ )  $\delta$  ppm 158.7, 49.7, 47.7, 47.2, 40.3, 37.8, 32.7, 30.2, 29.6.



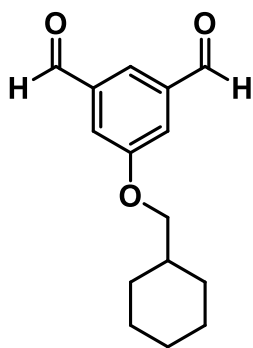
**$N^1$ -(3-aminopropyl)- $N^3$ -(2-ethylhexyl)propane-1,3-diamine**: Was prepared similar to iso-butyl norspermidine, however, during the final step column chromatography (40:8:1  $\text{CH}_2\text{Cl}_2$ :MeOH: $\text{NH}_4\text{OH}$ ) was used to afford the product as 1a yellow oil (Yield 16% 3 steps).  $^1\text{H}$  NMR (500 MHz,  $\text{CDCl}_3$ )  $\delta$  ppm 3.33-3.02 (m, 5H), 2.81-2.62 (m, 6H), 2.50-2.44 (m, 2H), 1.76-1.63 (m, 4H), 1.45-1.35 (m, 1H), 1.33-1.20 (m, 8H), 0.87-0.80 (m, 6H).  $^{13}\text{C}$  NMR (125 MHz,  $\text{CDCl}_3$ )  $\delta$  ppm 53.3, 49.1, 48.8, 48.0, 40.6, 39.2, 39.1, 31.5, 29.1, 29.0, 24.6, 23.3, 14.3, 10.9.



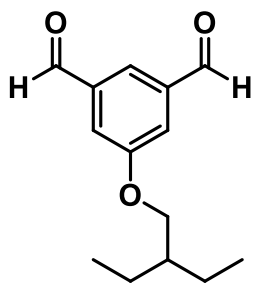
**5-butoxyisophthalaldehyde:** Dimethyl 5-hydroxyisophthalate (0.40 g, 1.90 mmol, 1.0 equiv.), cesium carbonate (1.30 g, 3.80 mmol, 2.0 equiv.) and CH<sub>3</sub>CN (12 mL) were added to a round bottom flask and stirred for 15-30 min Iodobutane (0.42 g, 2.28 mmol, 1.2 equiv.) was added and the reaction was stirred for 16 h. The solvent was concentrated under reduced pressure and the reaction mixture was partitioned between EtOAc (50 mL) and H<sub>2</sub>O (50 mL). The organic layer was separated and the aqueous layer extracted with EtOAc (50 mL). The combined organics were dried over Na<sub>2</sub>SO<sub>4</sub>, filtered, and concentrated under reduced pressure to afford the desired product which was used without further purification. To a solution of dimethyl 5-butoxyisophthalate, the product from above, (0.51 g, 1.90 mmol, 1.0 equiv.) in THF (16 mL) was slowly added LiAlH<sub>4</sub> (0.40 g, 10.5 mmol, 5.5 equiv.) and the reaction mixture was stirred for 8 h. The reaction was quenched by the addition of 2N HCl (5 mL). The mixture was extracted with Et<sub>2</sub>O (2 x 25 mL) and EtOAc (2 x 25 mL), the organics layers combined, dried over Na<sub>2</sub>SO<sub>4</sub>, filtered, and concentrated under reduced pressure to afford the desired product (0.24 g) as an oil, which was used without further purification. (5-Butoxy-1,3-phenylene)dimethanol, the product from above, (0.24 g, 1.15 mmol, 1.0 equiv.) and CH<sub>3</sub>CN (20 mL) were added to a round bottom flask. To the solution was added MnO<sub>2</sub> (1.97 g, 23.0 mmol, 20.0 equiv.) and the reaction was stirred at 60 °C for 16 h open to air. The reaction mixture was concentrated under

reduced pressure. Purification by column chromatography (90% Hexanes/EtOAc) afforded the desired product (0.18 g, 44%, 3 steps) as a white semisolid.  $^1\text{H}$  NMR (300 MHz,  $\text{CDCl}_3$ )  $\delta$  ppm 9.99 (s, 2H), 7.89 (s, 1H), 7.58 (s, 2H), 4.03 (t,  $J = 6.6$  Hz, 2H), 1.77 (quint,  $J = 6.6$  Hz, 2H), 1.47 (sext,  $J = 7.2$  Hz, 2H), 0.94 (t,  $J = 7.5$  Hz, 3H).  $^{13}\text{C}$  NMR (75 MHz,  $\text{CDCl}_3$ )  $\delta$  ppm 191.3, 160.6, 138.6, 124.2, 120.1, 68.9, 31.3, 19.4, 14.1.

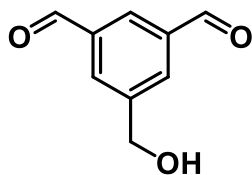
The following example were prepared similar to 5-butoxyisophthalaldehyde:



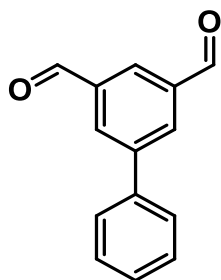
**5-(Cyclohexylmethoxy)isophthalaldehyde:**  $^1\text{H}$  NMR (300 MHz,  $\text{CDCl}_3$ )  $\delta$  ppm 10.02 (s, 2H), 7.91 (s, 1H), 7.61 (s, 2H), 3.84 (d,  $J = 6.0$  Hz, 2H), 1.87-1.67 (m, 6H), 1.31-1.03 (m, 5H).  $^{13}\text{C}$  NMR (75 MHz,  $\text{CDCl}_3$ )  $\delta$  ppm 191.4, 160.9, 138.6, 124.3, 120.2, 74.6, 37.9, 30.1, 26.7, 26.0. White solid (45%, 3 steps).



**5-(2-Ethylbutoxy)isophthalaldehyde:**  $^1\text{H}$  NMR (500 MHz,  $\text{CDCl}_3$ )  $\delta$  ppm 10.01 (s, 2H), 7.90 (s, 1H), 7.62 (s, 2H), 3.94 (d,  $J = 5.5$  Hz, 2H), 1.68 (hept,  $J = 6.5$  Hz, 1H), 1.46 (dec,  $J = 6.5$  Hz, 4H), 0.91 (t,  $J = 7.5$  Hz, 6H).  $^{13}\text{C}$  NMR (125 MHz,  $\text{CDCl}_3$ )  $\delta$  ppm 191.1, 160.7, 138.5, 124.1, 120.0, 71.1, 40.9, 23.5, 11.3. White solid (42%, 3 steps).

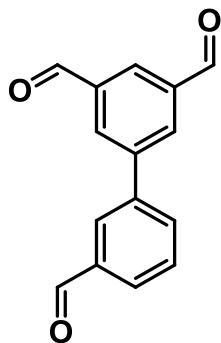


**5-(Hydroxymethyl)isophthalaldehyde:**  $^1\text{H}$  NMR (500 MHz,  $\text{CDCl}_3$ )  $\delta$  ppm 10.09 (s, 2H), 8.27 (s, 1H), 8.15 (s, 2H), 4.88 (s, 2H), 2.54 (br s, 1H).  $^{13}\text{C}$  NMR (125 MHz,  $\text{CDCl}_3$ )  $\delta$  ppm 191.4, 143.7, 137.4, 132.8, 130.3, 63.9. White solid (34%).

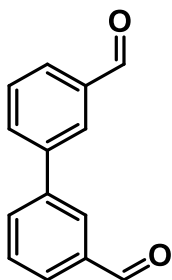


**[1,1'-biphenyl]-3,5-dicarbaldehyde:** A solution of 5-bromoisophthalaldehyde (40.0 g, 187.8 mmol, 1.0 equiv.), phenylboronic acid (22.9 g, 187.8 mmol, 1.0 equiv.) and potassium carbonate (64.8 g, 469.5 mmol, 2.5 equiv.) in DME/ $\text{H}_2\text{O}$  (5:1, 600 mL) was purged with  $\text{N}_2$  for 5 min. Tetrakis(palladium triphenylphosphine (1.1 g, 0.9 mmol) was added and the reaction mixture heated to 90  $^\circ\text{C}$  and stirred for 16 h. The reaction mixture was cooled to rt, filtered through a pad of celite and the solvent evaporated under reduced pressure. Purification by column chromatography (10% EtOAc/hexanes) afforded the desired product (74%, 29.1 g) as an off-white solid.  $^1\text{H}$  NMR (300 MHz,  $\text{CDCl}_3$ )  $\delta$  ppm 10.18 (s, 2H), 8.37 (d,  $J = 1.2$  Hz, 2H), 8.35 (t,  $J = 1.5$  Hz, 1H), 7.70-7.66 (m, 2H), 7.55-7.43 (m, 3H).  $^{13}\text{C}$  NMR (125 MHz,  $\text{CDCl}_3$ )  $\delta$  ppm 191.0, 143.2, 138.2, 137.5, 132.8, 129.6, 129.2, 128.7, 127.1.

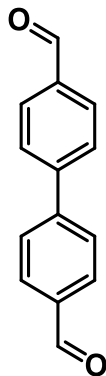
The following examples were prepared similar to [1,1'-biphenyl]-3,5-dicarbaldehyde:



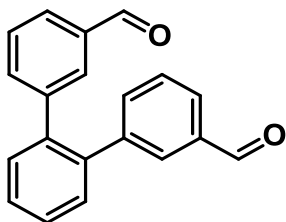
**[1,1'-biphenyl]-3,3',5-tricarbaldehyde:**  $^1\text{H}$  NMR (300 MHz,  $\text{CDCl}_3$ )  $\delta$  ppm 10.20 (s, 2H), 10.10 (s, 1H), 8.42 (s, 3H), 8.21 (s, 1H), 7.98 (t,  $J = 5.4$  Hz, 2H), 7.72 (t,  $J = 5.4$  Hz, 2H).  $^{13}\text{C}$  NMR (125 MHz,  $\text{CDCl}_3$ )  $\delta$  ppm 192.0, 191.0, 142.1, 139.6, 138.0, 137.5, 133.1, 133.0, 130.7, 130.5, 130.3, 128.1. Off-white solid (64-90%).



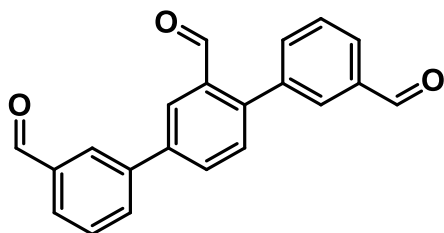
**[1,1'-biphenyl]-3,4'-dicarbaldehyde:**  $^1\text{H}$  NMR (500 MHz,  $\text{CDCl}_3$ )  $\delta$  ppm 10.10 (s, 2H), 8.13 (t,  $J = 2.0$  Hz, 2H), 7.91-7.88 (m, 4H), 7.65 (t,  $J = 7.5$  Hz, 2H).  $^{13}\text{C}$  NMR (125 MHz,  $\text{CDCl}_3$ )  $\delta$  ppm 192.2, 140.9, 137.3, 133.2, 130.0, 129.7, 128.2. Off white solid (56%)



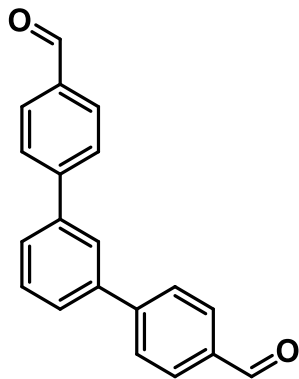
**[1,1'-biphenyl]-4,4'-dicarbaldehyde:**  $^1\text{H}$  NMR (500 MHz,  $\text{CDCl}_3$ )  $\delta$  ppm 10.06 (s, 2H), 7.97 (d,  $J = 7.5$  Hz, 4H), 7.77 (d,  $J = 8.5$  Hz, 4H).  $^{13}\text{C}$  NMR (125 MHz,  $\text{CDCl}_3$ )  $\delta$  ppm 191.8, 145.7, 136.2, 130.5, 128.2. Off white solid (67%)



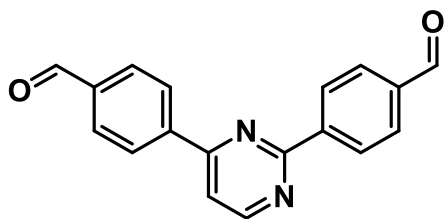
**[1,1':2',1''-terphenyl]-3,3''-dicarbaldehyde:**  $^1\text{H}$  NMR (500 MHz,  $\text{CDCl}_3$ )  $\delta$  ppm 9.90 (s, 2H), 7.73-7.70 (m, 4H), 7.50-7.46 (m, 4H), 7.36-7.31 (m, 4H).  $^{13}\text{C}$  NMR (125 MHz,  $\text{CDCl}_3$ )  $\delta$  ppm 192.2, 142.3, 139.4, 136.7, 136.2, 131.2, 130.8, 128.9, 128.6, 128.3. Yellow solid (68%)



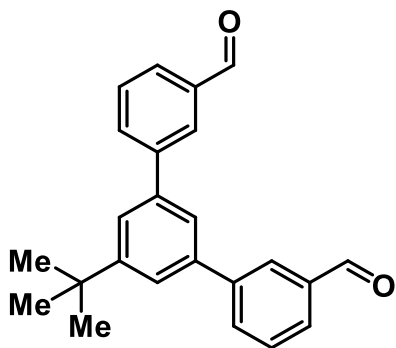
**[1,1':4',1''-terphenyl]-2',3,3''-tricarbaldehyde:**  $^1\text{H}$  NMR (500 MHz,  $\text{CDCl}_3$ )  $\delta$  ppm 10.11-10.10 (m, 2H), 9.99 (s, 1H), 8.18-8.15 (m, 1H), 8.00-7.93 (m, 2H), 7.82-7.81 (m, 1H), 7.71-7.57 (m, 6H), 7.50-7.47 (m, 1H).  $^{13}\text{C}$  NMR (125 MHz,  $\text{CDCl}_3$ )  $\delta$  ppm 192.1, 191.9, 191.2, 145.1, 140.5, 138.9, 137.3, 136.9, 136.0, 133.4, 130.8, 130.4, 130.1, 130.0, 129.8, 129.5, 129.4, 129.0, 128.9, 129.3, 127.4. White solid (12%).



**[1,1':3',1''-terphenyl]-4,4''-dicarbaldehyde:**  $^1\text{H}$  NMR (500 MHz,  $\text{CDCl}_3$ )  $\delta$  ppm 10.06 (s, 2H), 7.97 (d,  $J = 8.0$  Hz, 4H), 7.86 (t,  $J = 2.0$  Hz, 1H), 7.79 (d,  $J = 8.0$  Hz, 4H), 7.68-7.66 (m, 2H), 7.60-7.57 (m, 1H).  $^{13}\text{C}$  NMR (125 MHz,  $\text{CDCl}_3$ )  $\delta$  ppm 192.1, 146.9, 140.8, 135.7, 130.6, 130.0, 128.1, 127.7, 126.7. Off-white solid (37-50%).

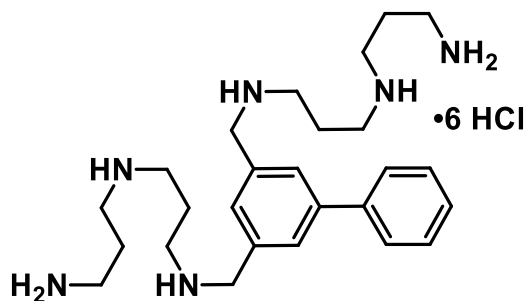


**4,4'-(pyrimidine-2,4-diyl)dibenzaldehyde:**  $^1\text{H}$  NMR (500 MHz,  $\text{CDCl}_3$ )  $\delta$  ppm 10.10 (s, 1H), 10.07 (s, 1H), 8.71 (d,  $J = 4.5$  Hz, 1H), 8.25 (d,  $J = 8.0$  Hz, 2H), 8.10 (d,  $J = 8.0$  Hz, 2H), 7.98 (d,  $J = 8.0$  Hz, 2H), 7.78 (d,  $J = 8.0$  Hz, 2H), 7.71 (d,  $J = 5.5$  Hz, 1H).  $^{13}\text{C}$  NMR (125 MHz,  $\text{CDCl}_3$ )  $\delta$  ppm 191.9, 191.7, 165.9, 160.6, 140.5, 138.6, 136.2, 130.5, 130.4, 128.3, 128.2, 116.0. Yellow solid (40%).



**5'-(*tert*-butyl)-[1,1':3',1''-terphenyl]-3,3''-dicarbaldehyde:**  $^1\text{H}$  NMR (500 MHz,  $\text{CDCl}_3$ )  $\delta$  10.12 (s, 2H), 8.16 (s, 2H), 7.94-7.89 (m, 4H), 7.67-7.65 (m, 5H), 1.46 (s, 9H).  $^{13}\text{C}$  NMR (125 MHz,  $\text{CDCl}_3$ )  $\delta$  ppm 192.5, 153.1, 142.7, 140.7, 137.2, 133.6, 129.8, 129.2, 128.5, 124.3, 123.8, 35.3, 31.7. Yellow solid (47%).

For fully characterized compounds ( $^1\text{H}$  NMR,  $^{13}\text{C}$  NMR, IR, mp, and LCMS) See: **CZ-01-086**, **CZ-01-096**, **CZ-01-097**, **CZ-01-099**, **CZ-01-100**, **CZ-01-108**, **CZ-01-114**, **CZ-01-166**, **CZ-01-168**, **CZ-01-170**, **CZ-01-179**, and **CZ-01-182**. All the respective CZ-compounds were isolated as the HCl salt as white to off-white solids unless otherwise noted.

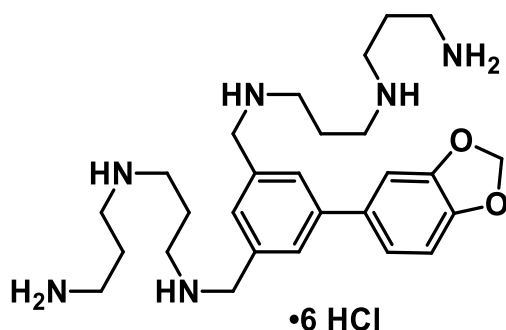


**CZ-01-058:**  $N^1,N^{1'}\text{-}([1,1'\text{-biphenyl}]\text{-}3,5\text{-diylbis(methylene)})\text{bis}(N^3\text{-(3-aminopropyl)propane-1,3-diamine})$ , **hydrochloride salt:** To a solution of [1,1'-biphenyl]-3,5-dicarbaldehyde ( ) in MeOH was added Boc-norspermidine ( ) and the reaction was left to stir for 16 h. Sodium borohydride (4 equiv.) was then added portion wise and the reaction mixture was left to stir for an additional 1 h. The excess MeOH was evaporated and the crude solid was partitioned between EtOAc (50 mL) and 10% NaOH (mL). The aqueous layer was then back extracted with EtOAc (1 x 50 mL) dried over  $\text{Na}_2\text{SO}_4$  and evaporated to afford the crude free base. If desired column chromatography can be performed using gradient conditions starting at (300:16:1  $\text{CH}_2\text{Cl}_2$ :MeOH: $\text{NH}_4\text{OH}$ ). The free base was acidified with HCl in MeOH (50 mL) and then placed at 0 °C for 1 h to



precipitate. The corresponding precipitate was filtered and dried to afford the pure HCl salt as a white solid (25-52%).  $^1\text{H}$  NMR ( $\text{D}_2\text{O}$ , 500 MHz)  $\delta$  ppm 7.85 (s, 2H), 7.74 (d,  $J = 7.5$  Hz, 2H), 7.59-7.56 (m, 3H), 7.50-7.49 (m, 1H), 4.38 (s, 4H), 3.29 (t,  $J = 8.0$  Hz, 4H), 3.23 (q,  $J = 5.0$  Hz, 8H), 3.14 (t,  $J = 8.0$  Hz, 4H), 2.25-2.19 (m, 4H), 2.17-2.11 (m, 4H).  $^{13}\text{C}$  NMR (125 MHz,  $\text{D}_2\text{O}$ ) 142.3, 138.8, 132.1, 130.0, 129.5, 129.2, 128.4, 127.0, 50.8, 44.7, 44.6, 44.2, 36.5, 23.7, 22.7. LRMS calculated for  $\text{C}_{26}\text{H}_{44}\text{N}_6$   $m/z$  441.4  $[\text{M}+\text{H}]^+$ , Obsd. 441.4.

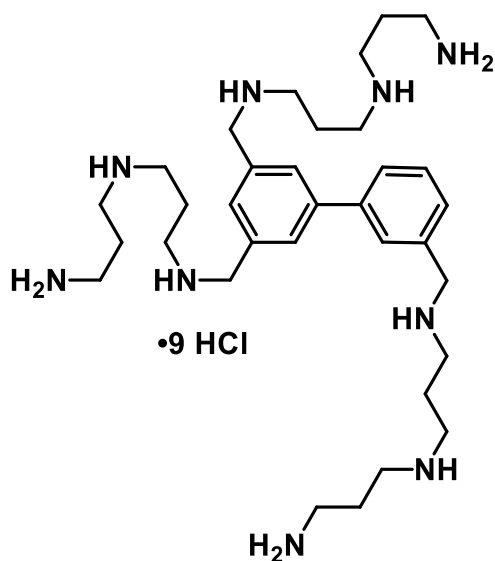
The following example were prepared similar to **CZ-01-058**, in later cases the alkylated norspermidine side-chains were used to replace Boc-norspermidine:



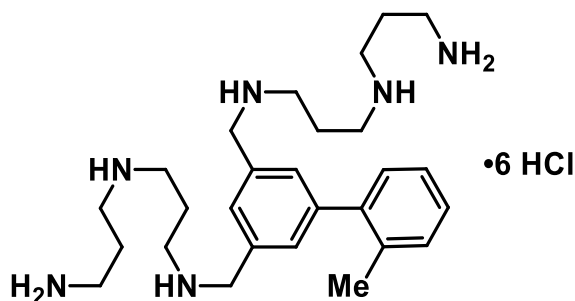
**CZ-01-061:**

*N*<sup>1</sup>,*N*<sup>1'</sup>-((5-(Benzo[d][1,3]dioxol-5-yl)-1,3-phenylene)bis(methylene))bis(*N*<sup>3</sup>-(3-ammoniopropyl)propane-1,3-diaminium)

**chloride:**  $^1\text{H}$  NMR (500 MHz,  $\text{D}_2\text{O}$ )  $\delta$  7.72 (s, 2H), 7.49 (s, 1H), 7.15 (s, 2H), 6.93 (d,  $J = 8.5$  Hz, 1H), 5.95 (s, 2H), 4.30 (s, 4H), 3.21-3.12 (m, 8H), 3.05 (t,  $J = 8.0$  Hz, 4H), 2.17-2.02 (m, 8H).  $^{13}\text{C}$  NMR (125 MHz,  $\text{D}_2\text{O}$ )  $\delta$  148.1, 147.6, 142.3, 133.3, 132.2, 130.8, 129.7, 129.6, 129.4, 121.1, 109.0, 107.5, 101.6, 51.0, 44.8, 44.8, 44.4, 36.6, 23.9, 22.8.

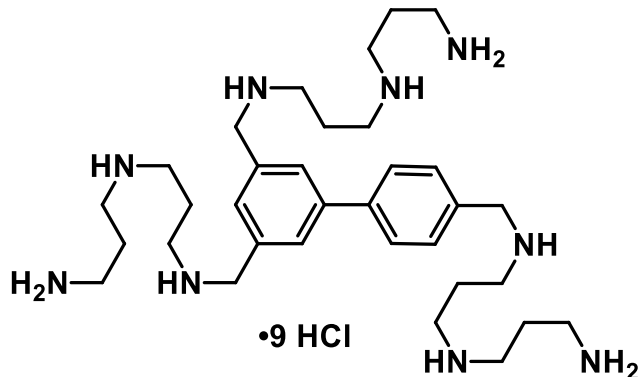


**CZ-01-062:**  $N^1,N^{1'},N^{1''}$ -([1,1'-Biphenyl]-3,3',5-triyltris(methylene))tris( $N^3$ -(3-aminopropyl)propane-1,3-diamine), hydrohydrochloride salt:  $^1\text{H}$  NMR (400 MHz,  $\text{D}_2\text{O}$ )  $\delta$  7.96 (s, 2H), 7.93-7.85 (m, 2H), 7.71-7.61 (m,  $J = 8.5$  Hz, 3H), 4.47 (s, 4H), 4.44 (s, 2H), 3.36-3.23 (m, 18H), 3.17 (t,  $J = 8.0$  Hz, 6H), 2.30-2.22 (m, 6H), 2.20-2.13 (m, 6H). LRMS calculated for  $\text{C}_{33}\text{H}_{61}\text{N}_9$   $m/z$  584.5  $[\text{M}+\text{H}]^+$ , Obsd. 584.5.

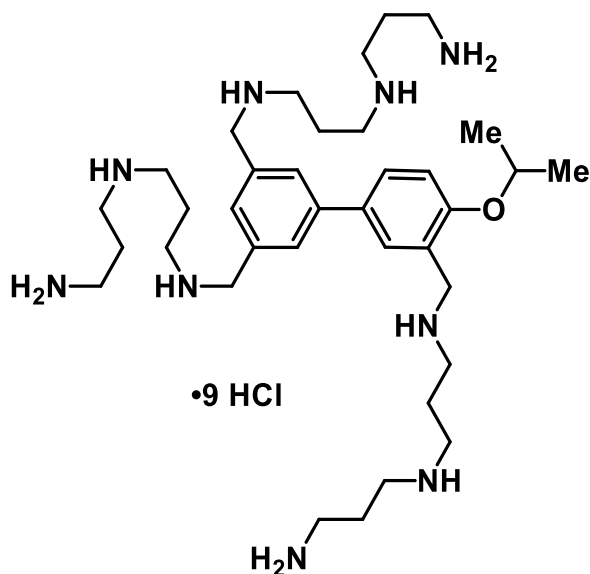


**CZ-01-063:**  $N^1,N^{1'}$ -((2'-Methyl-[1,1'-biphenyl]-3,5-diyl)bis(methylene))bis( $N^3$ -(3-aminopropyl)propane-1,3-diamine), hydrochloride salt:  $^1\text{H}$  NMR (500 MHz,  $\text{D}_2\text{O}$ )  $\delta$  7.59 (s, 1H), 7.56 (d,  $J = 1.0$  Hz, 2H), 7.41-7.40 (m, 2H), 7.38-7.35 (m, 1H), 7.32-7.31 (m, 1H), 4.38 (s, 4H), 3.25 (t,  $J = 7.5$  Hz, 4H), 3.20-3.18 (m, 8H), 3.11 (t,  $J = 8.0$  Hz, 4H), 2.25 (m, 3H), 2.20-2.15 (m, 4H), 2.14-2.07 (m, 4H).  $^{13}\text{C}$  NMR (125 MHz,  $\text{D}_2\text{O}$ )  $\delta$  143.3, 139.9, 135.6, 131.8, 131.7, 131.5, 131.0, 130.5, 129.9, 129.7, 128.2, 126.1, 50.8, 44.7, 44.6, 44.2,

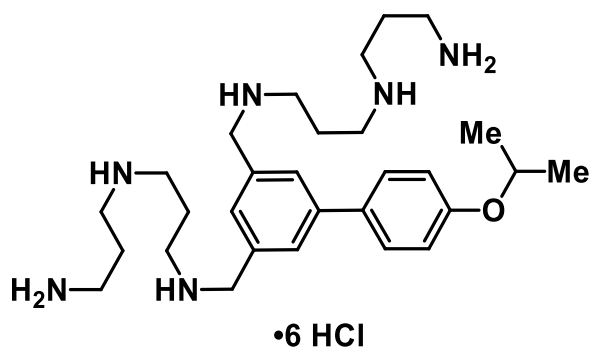
36.6, 23.7, 22.7. LRMS calculated for  $C_{27}H_{46}N_6$   $m/z$  455.4  $[M+H]^+$ , Obsd. 455.4.



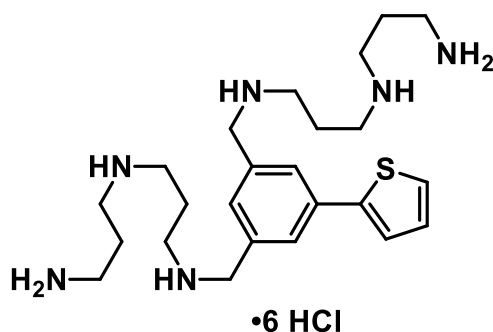
**CZ-01-065:**  $N^1,N^{1'},N^{1''}$ -([1,1'-Biphenyl]-3,4',5-triyltris(methylene))tris( $N^3$ -(3-aminopropyl)propane-1,3-diamine), hydrochloride salt:  $^1H$  NMR (500 MHz,  $D_2O$ )  $\delta$  7.92 (s, 2H), 7.84 (d,  $J = 8.5$  Hz, 2H), 7.65 (d,  $J = 8.5$  Hz, 3H), 4.43 (s, 4H), 4.37 (s, 2H), 3.31-3.28 (m, 6H), 3.26-3.20 (m, 12H), 3.14 (t,  $J = 8.0$  Hz, 6H), 2.25-2.17 (m, 6H), 2.16-2.10 (m, 6H).  $^{13}C$  NMR (125 MHz,  $D_2O$ )  $\delta$  141.6, 140.1, 132.2, 130.6, 130.6, 130.4, 129.7, 127.8, 50.8, 44.7, 44.6, 44.2, 36.5, 23.7, 22.7, 22.6. LRMS calculated for  $C_{33}H_{61}N_9$   $m/z$  584.5  $[M+H]^+$ , Obsd. 584.5.



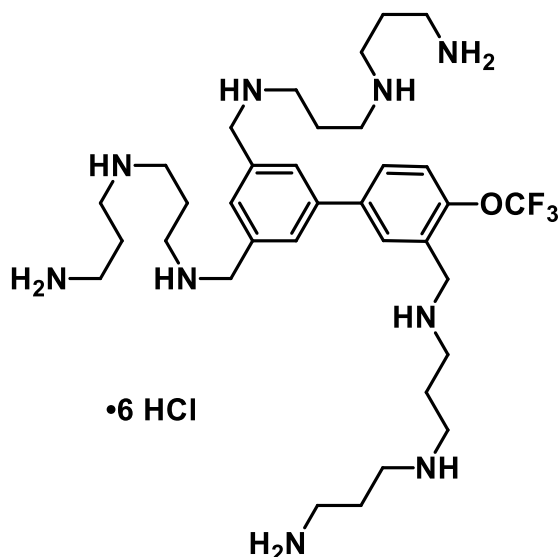
**CZ-01-066:**  $N^1,N^{1'},N^{1''}$ -((4'-Isopropoxy-[1,1'-biphenyl]-3,3',5-triyl)tris(methylene))tris( $N^3$ -(3-aminopropyl)propane-1,3-diamine), hydrochloride salt:  $^1\text{H}$  NMR (500 MHz,  $\text{D}_2\text{O}$ )  $\delta$  7.93 (s, 2H), 7.88-7.82 (m, 2H), 7.65 (s, 1H), 7.35 (d,  $J$  = 9.0 Hz, 1H), 4.94-4.87 (m, 1H), 4.47 (s, 4H), 4.43 (s, 2H), 3.39-3.28 (m, 18H), 3.22 (t,  $J$  = 8.0 Hz, 6H), 2.33-2.18 (m, 12H), 1.48 (d,  $J$  = 6.5 Hz, 6H).  $^{13}\text{C}$  NMR (125 MHz,  $\text{D}_2\text{O}$ )  $\delta$  158.9, 143.9, 134.8, 133.8, 132.9, 132.6, 132.3, 131.8, 122.7, 117.0, 84.4, 74.5, 53.5, 49.6, 47.3, 47.3, 47.0, 46.9, 46.7, 39.2, 26.3, 25.3, 25.2, 23.9. LRMS calculated for  $\text{C}_{36}\text{H}_{67}\text{N}_9\text{O}$   $m/z$  642.5  $[\text{M}+\text{H}]^+$ , Obsd. 642.5.



**CZ-01-067:**  $N^1,N^{1'}$ -((4'-Isopropoxy-[1,1'-biphenyl]-3,5-diyl)bis(methylene))bis( $N^3$ -(3-aminopropyl)propane-1,3-diamine), hydrochloride salt:  $^1\text{H}$  NMR (500 MHz,  $\text{D}_2\text{O}$ )  $\delta$  7.81 (s, 2H), 7.68 (d,  $J$  = 8.5 Hz, 2H), 7.54 (s, 1H), 7.12 (d,  $J$  = 8.5 Hz, 2H), 4.78-4.72 (m, 1H), 4.37 (s, 4H), 3.28 (t,  $J$  = 8.0 Hz, 4H), 3.24-3.19 (m, 8H), 3.13 (t,  $J$  = 8.0 Hz, 4H), 2.24-2.19 (m, 4H), 2.17-2.09 (m, 4H), 1.35 (d,  $J$  = 6.0 Hz, 6H).  $^{13}\text{C}$  NMR (125 MHz,  $\text{D}_2\text{O}$ )  $\delta$  157.0, 141.8, 132.0, 131.8, 129.4, 129.0, 128.3, 116.8, 71.6, 50.8, 44.6, 44.6, 44.1, 36.4, 23.6, 22.6, 21.0.

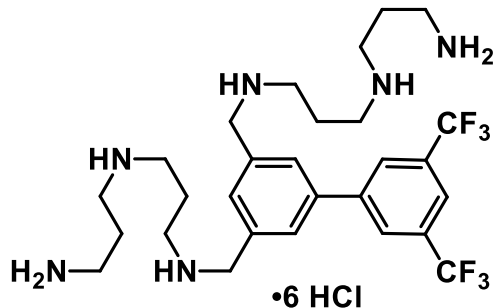


**CZ-01-068:** *N*<sup>1</sup>,*N*<sup>1'</sup>-((5-(Thiophen-2-yl)-1,3-phenylene)bis(methylene))bis(*N*<sup>3</sup>-(3-aminopropyl)propane-1,3-diamine), hydrochloride salt: <sup>1</sup>H NMR (500 MHz, D<sub>2</sub>O) δ 7.90 (s, 2H), 7.83 (t, *J* = 1.0 Hz, 1H), 7.63-7.61 (m, 1H), 7.60-7.57 (m, 1H), 7.53 (s, 1H), 4.38 (s, 4H), 3.27 (t, *J* = 8.0 Hz, 4H), 3.23-3.19 (m, 8H), 3.13 (t, *J* = 8.0 Hz, 4H), 2.23-2.17 (m, 4H), 2.15-2.09 (m, 4H). <sup>13</sup>C NMR (125 MHz, D<sub>2</sub>O) δ 139.9, 137.1, 132.2, 129.6, 128.7, 127.7, 125.9, 122.3, 50.8, 44.7, 44.6, 44.1, 36.5, 23.7, 22.6. LRMS calculated for C<sub>24</sub>H<sub>42</sub>N<sub>6</sub>S m/z 447.3 [M+H]<sup>+</sup>, Obsd. 447.3.

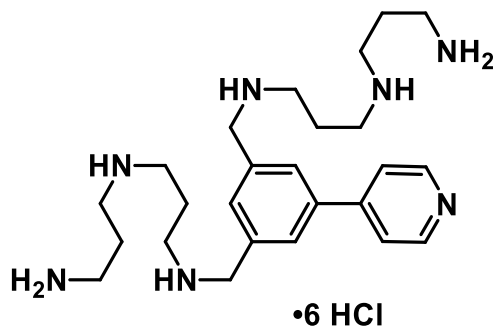


**CZ-01-069:** *N*<sup>1</sup>,*N*<sup>1'</sup>,*N*<sup>1''</sup>-((4'-(trifluoromethyl)-[1,1'-biphenyl]-3,3',5-triyl)tris(methylene))tris(*N*<sup>3</sup>-(3-aminopropyl)propane-1,3-diamine), hydrochloride salt: <sup>1</sup>H NMR (500 MHz, D<sub>2</sub>O) δ 7.93 (s, 2H), 7.87 (s, 2H), 7.61 (s, 2H), 4.45 (s, 2H), 4.38

(s, 4H), 3.27-3.14 (m, 16H), 3.10-06 (m, 8H), 2.25-2.05 (m, 12H).

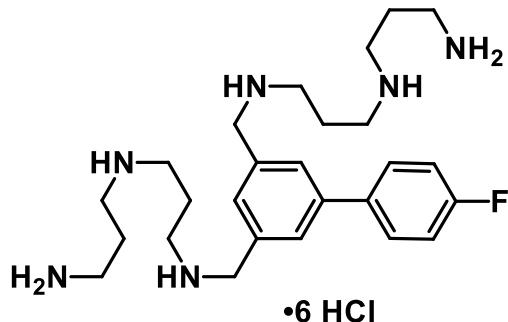


**CZ-01-070:** *N*<sup>1</sup>,*N*<sup>1'</sup>-((3',5'-Bis(trifluoromethyl)-[1,1'-biphenyl]-3,5-diyl)bis(methylene))bis(*N*<sup>3</sup>-(3-aminopropyl)propane-1,3-diamine), hydrochloride salt: <sup>1</sup>H NMR (500 MHz, D<sub>2</sub>O) δ 8.20 (s, 2H), 8.07 (s, 1H), 7.91 (s, 2H), 7.69 (s, 1H), 4.41 (s, 4H), 3.30 (t, *J* = 7.5 Hz, 4H), 3.26-3.21 (m, 8H), 3.14 (t, *J* = 8.0 Hz, 4H), 2.23-2.19 (m, 4H), 2.17-2.10 (m, 4H). <sup>13</sup>C NMR (125 MHz, D<sub>2</sub>O) δ 140.6, 139.7, 132.4, 131.5, 131.2, 129.9, 127.5, 124.4, 122.2, 50.7, 44.7, 44.6, 44.3, 36.5, 23.7, 22.6. LRMS calculated for C<sub>28</sub>H<sub>42</sub>F<sub>6</sub>N<sub>6</sub> *m/z* 577.3 [M+H]<sup>+</sup>, Obsd. 577.3.

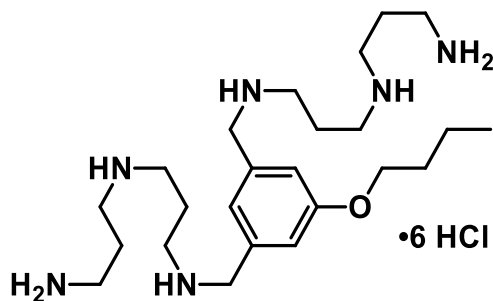


**CZ-01-071:** *N*<sup>1</sup>,*N*<sup>1'</sup>-((5-(Pyridin-4-yl)-1,3-phenylene)bis(methylene))bis(*N*<sup>3</sup>-(3-aminopropyl)propane-1,3-diamine), hydrochloride salt: <sup>1</sup>H NMR (500 MHz, D<sub>2</sub>O) δ 8.87 (d, *J* = 6.0 Hz, 2H), 8.39 (d, *J* = 6.5 Hz, 2H), 8.15 (s, 2H), 7.88 (s, 1H), 4.47 (s, 4H), 3.30 (t, *J* = 8.0 Hz, 4H), 3.24-3.19 (m, 8H), 3.12 (t, *J* = 8.0 Hz, 4H), 2.24-2.19 (m, 4H), 2.15-2.08 (m, 4H). <sup>13</sup>C NMR (125 MHz, D<sub>2</sub>O) δ 156.6, 141.6, 136.8, 134.4, 133.2, 131.0, 125.2, 50.8, 44.9, 44.8, 44.6, 36.7, 23.9, 22.9. LRMS calculated for C<sub>25</sub>H<sub>43</sub>N<sub>7</sub> *m/z* 442.4

$[M+H]^+$ , Obsd. 442.4.

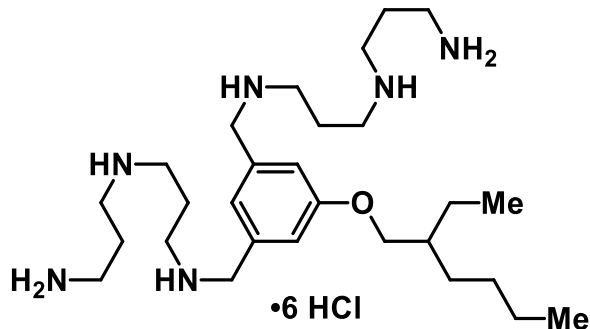


**CZ-01-075:**  $N^1,N^{1'}-((4'\text{-Fluoro-[1,1'-biphenyl]-3,5-diyl})\text{bis(methylene)})\text{bis}(N^3\text{-(3-aminopropyl)propane-1,3-diamine})$ , hydrochloride salt:  $^1\text{H}$  NMR (500 MHz,  $\text{D}_2\text{O}$ )  $\delta$  7.80 (s, 2H), 7.71-7.68 (m, 2H), 7.56 (s, 1H), 7.25 (t,  $J = 9.0$  Hz, 2H), 4.37 (s, 4H), 3.26 (t,  $J = 8.0$  Hz, 4H), 3.19 (q,  $J = 8.0$  Hz, 8H), 3.11 (t,  $J = 7.5$  Hz, 4H), 2.22-2.07 (m, 8H).  $^{13}\text{C}$  NMR (125 MHz,  $\text{D}_2\text{O}$ )  $\delta$  162.9 (d, 244 Hz), 135.3 (d, 3 Hz), 132.3, 130.1, 129.7, 129.1 (d, 8 Hz), 116.1 (d, 21 Hz), 51.1, 44.9, 44.8, 44.4, 36.7, 23.9, 22.9. LRMS calculated for  $\text{C}_{26}\text{H}_{43}\text{FN}_6$   $m/z$  459.4  $[M+H]^+$ , Obsd. 459.4.



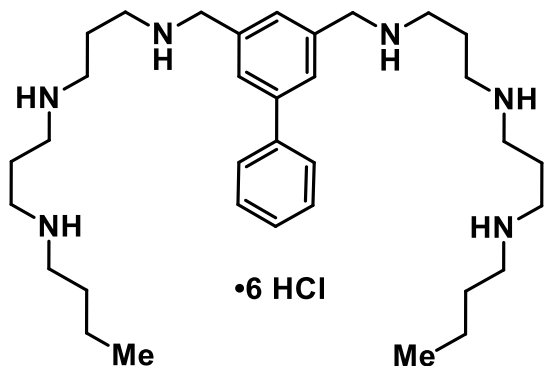
**CZ-01-076:**  $N^1,N^{1'}-((5\text{-Butoxy-1,3-phenylene})\text{bis(methylene)})\text{bis}(N^3\text{-(3-aminopropyl)propane-1,3-diamine})$ , hydrochloride salt:  $^1\text{H}$  NMR (500 MHz,  $\text{D}_2\text{O}$ )  $\delta$  ppm 7.20 (s, 3H), 4.30 (s, 4H), 4.15 (t,  $J = 6.5$  Hz, 2H), 3.26-3.20 (m, 12H), 3.14 (t,  $J = 7.5$  Hz, 4H), 2.22-2.10 (m, 8H), 1.79 (quint,  $J = 6.5$  Hz, 2H), 1.48 (sext,  $J = 7.5$  Hz, 2H), 0.96 (t,  $J = 7.0$  Hz, 3H).  $^{13}\text{C}$  NMR (125 MHz,  $\text{D}_2\text{O}$ ) 159.2, 132.9, 123.5, 117.3, 68.8, 50.8, 44.7, 44.6, 44.1, 36.5, 30.3, 23.7, 22.6, 18.5, 13.0. LRMS calculated for  $\text{C}_{24}\text{H}_{48}\text{N}_6\text{O}$   $m/z$

437.4  $[M+H]^+$ , Obsd. 437.4.



**CZ-01-081:**  $N^1, N^{1'}$ -((5-((2-Ethylhexyl)oxy)-1,3-phenylene)bis(methylene))bis( $N^3$ -(3-aminopropyl)propane-1,3-diamine), hydrochloride salt:  $^1\text{H}$  NMR (500 MHz,  $\text{D}_2\text{O}$ )  $\delta$  .

$^{13}\text{C}$  NMR (125 MHz,  $\text{D}_2\text{O}$ ) 159.9, 133.2, 123.7, 117.7, 72.0, 51.1, 44.9, 44.6, 44.4, 38.8, 36.8, 29.9, 28.5, 24.0, 23.4, 22.9, 22.7, 13.7, 10.6. LRMS calculated for  $\text{C}_{28}\text{H}_{56}\text{N}_6\text{O}$   $m/z$  493.5  $[M+H]^+$ , Obsd. 493.5.

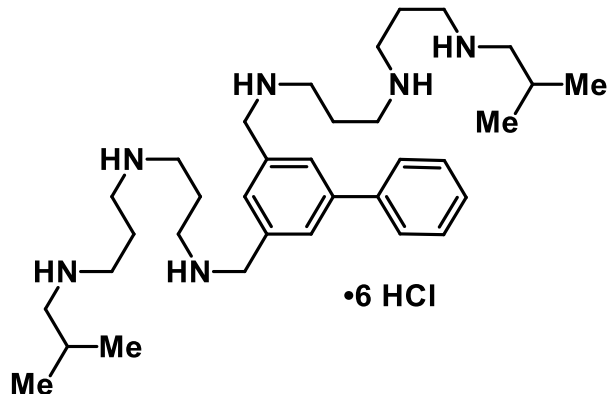


**CZ-01-083:**  $N^1, N^{1'}$ -([1,1'-biphenyl]-3,5-diylbis(methylene))bis( $N^3$ -(3-(butylamino)propyl)propane-1,3-diamine), hydrochloride salt:  $^1\text{H}$  NMR (500 MHz,  $\text{D}_2\text{O}$ )  $\delta$  7.83 (s, 2H), 7.71 (d,  $J = 7.5$  Hz, 2H), 7.55-7.52 (m, 3H), 7.49-7.45 (m, 1H), 4.35

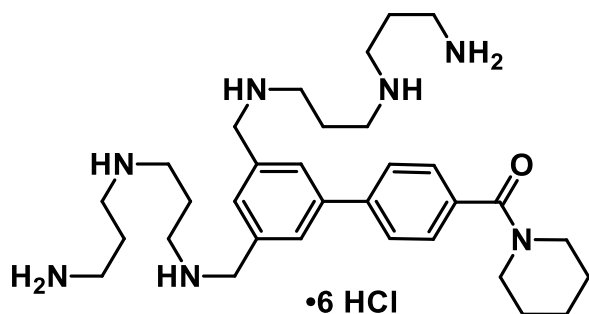
(s, 4H), 3.26 (t,  $J = 7.5$  Hz, 4H), 3.21-3.16 (m, 8H), 3.14 (t,  $J = 8.0$  Hz, 4H), 3.05 (t,  $J = 8.0$  Hz, 4H), 2.21-2.10 (m, 8H), 1.65 (quint,  $J = 7.0$  Hz, 4H), 1.37 (sext,  $J = 8.0$  Hz, 4H), 0.91 (t,  $J = 7.0$  Hz, 6H).  $^{13}\text{C}$  NMR (125 MHz,  $\text{D}_2\text{O}$ )  $\delta$  142.5, 138.9, 132.3, 130.3, 129.8, 129.5, 128.7, 127.3, 51.0, 47.8, 44.9, 44.5, 44.4, 27.7, 22.9, 22.9 19.3, 13.0. LRMS



calculated for  $C_{34}H_{60}N_6$   $m/z$  553.5  $[M+H]^+$ , Obsd. 553.5.

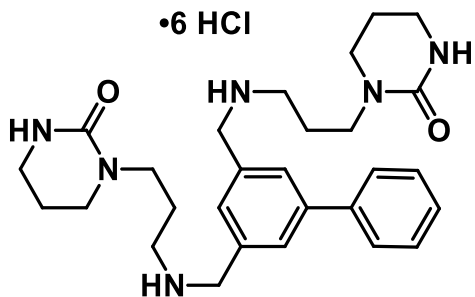


**CZ-01-086:**  $N^1,N^{1'}-([1,1'-biphenyl]-3,5-diylbis(methylene))bis(N^3-(3-(isobutylamino)propyl)propane-1,3-diamine)$ , hydrochloride salt:  $^1H$  NMR (500 MHz,  $D_2O$ )  $\delta$  7.87 (s, 2H), 7.75(d,  $J = 7.5$ , 2H), 7.59-7.48 (m, 4H), 4.39 (s, 4H), 3.26 (t,  $J = 8.0$  Hz, 4H), 3.21-3.12 (m, 12H), 2.92 (d,  $J = 7.0$  Hz, 4H), 2.21-2.10 (m, 8H), 2.01 (sept,  $J = 7.0$  Hz, 2H), 0.99 (d,  $J = 7.0$  Hz, 12H).  $^{13}C$  NMR (125 MHz,  $D_2O$ )  $\delta$  142.8, 139.1, 132.4, 130.1, 129.8, 129.5, 128.7, 127.3, 55.1, 51.1, 44.9, 44.8, 44.4, 25.8, 22.8, 22.7, 19.2. IR (neat): 3400 (bs), 2961, 2765 (all s)  $cm^{-1}$ . mp decomposition (202-204  $^{\circ}C$ ). LRMS calculated for  $C_{34}H_{60}N_6$   $m/z$  553.5  $[M+H]^+$ , Obsd. 553.5.

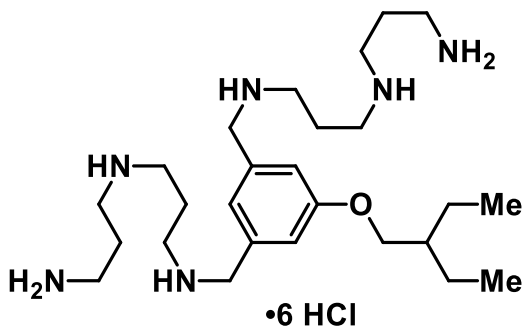


**CZ-01-088:**  $(3',5'-Bis(((3-((3-aminopropyl)amino)propyl)amino)methyl)-[1,1'-biphenyl]-4-yl)(piperidin-1-yl)methanone$ , hydrochloride salt:  $^1H$  NMR (300 MHz,  $D_2O$ )  $\delta$  7.87 (s, 2H), 7.78 (d,  $J = 8.4$  Hz, 2H), 7.58 (s, 1H), 7.54-7.49 (m, 2H), 4.37 (s, 4H), 3.68 (bs, 2H), 3.42-3.38 (m, 2H), 3.26-3.13 (m, 12H), 3.07 (t,  $J = 7.8$  Hz, 4H), 2.20-2.01

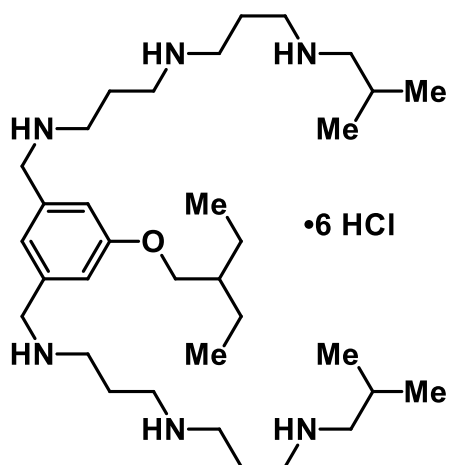
(m, 8H), 1.71-1.64 (m, 4H), 1.58-1.49 (m, 4H). LRMS calculated for  $C_{32}H_{53}N_7O$  m/z 552.4  
 $[M+H]^+$ , Obsd. 552.4.



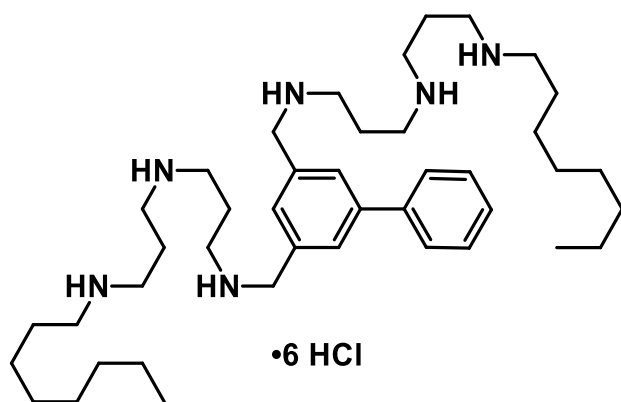
**CZ-01-089: 1,1'-(((1,1'-Biphenyl)-3,5diylbis(methylene))bis(azanediyl))bis(propane-3,1-diyl))bis(tetrahydropyrimidin-2(1H)-one), hydrochloride salt:**  $^1H$  NMR (300 MHz,  $D_2O$ )  $\delta$  7.80 (d,  $J$  = 6.5 Hz, 2H), 7.71-7.68 (m, 2H), 7.56-7.45 (m, 4H), 4.30 (s, 4H), 3.34 (t,  $J$  = 6.6 Hz, 4H), 3.21 (t,  $J$  = 6.0 Hz, 4H), 3.11 (t,  $J$  = 6.0 Hz, 4H), 3.04 (t,  $J$  = 7.2 Hz, 4H), 1.97-1.88 (m, 4H), 1.78 (p,  $J$  = 6.0 Hz, 4H). LRMS  $[M+H]^+$  493.4.



**CZ-01-090:  $N^1,N^{1'}-((5-(2\text{-Ethylbutoxy})-1,3\text{-phenylene})bis(methylene))bis(N^3-(3\text{-aminopropyl})propane-1,3\text{-diamine})$ , hydrochloride salt:**  $^1H$  NMR (500 MHz,  $D_2O$ )  $\delta$  7.23 (s, 2H), 7.22 (s, 1H), 4.32 (s, 4H), 4.06 (t,  $J$  = 7.0 Hz, 2H), 3.27-3.18 (m, 12H), 3.15 (t,  $J$  = 8.0 Hz, 4H), 2.24-2.12 (m, 8H), 1.72 (m,  $J$  = 6.0 Hz, 1H), 1.52-1.44 (m, 4H), 0.94-0.91 (m, 6H).  $^{13}C$  NMR (125 MHz,  $D_2O$ )  $\delta$  159.6, 132.9, 123.5, 117.5, 71.43, 50.8, 44.7, 44.6, 44.1, 40.1, 36.5, 23.7, 22.6, 10.3. LRMS calculated for  $C_{25}H_{52}N_6O$  m/z 465.4  
 $[M+H]^+$ , Obsd. 465.4.

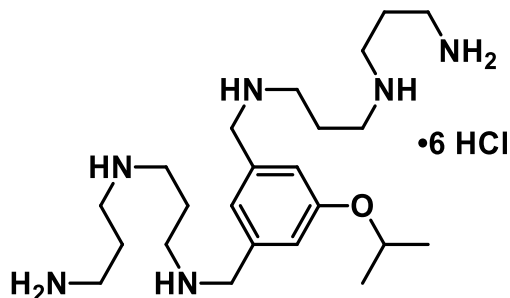


**CZ-01-091:**  $N^1,N^{1'}-((5-(2\text{-ethylbutoxy})-1,3\text{-phenylene})\text{bis(methylene)})\text{bis}(N^3-(3\text{-(isobutylamino)propyl)propane-1,3-diamine})$ , hydrochloride salt:  $^1\text{H}$  NMR (500 MHz,  $\text{D}_2\text{O}$ )  $\delta$  7.20 (s, 2H), 7.18 (s, 1H), 4.29 (s, 4H), 4.05 (d,  $J = 6.0$  Hz, 2H), 3.25-3.15 (m, 16H), 2.94 (d,  $J = 7.0$  Hz, 2H), 2.21-2.12 (m, 8H), 2.07-1.99 (m, 2H), 1.72 (quint,  $J = 6.5$  Hz, 1H), 1.50-1.43 (m, 4H), 1.00 (d,  $J = 7.0$  Hz, 12H), 0.92 (t,  $J = 6.0$  Hz, 6H).  $^{13}\text{C}$  NMR (125 MHz,  $\text{D}_2\text{O}$ )  $\delta$  159.6, 132.9, 123.4, 117.4, 71.4, 54.8, 50.8, 44.7, 44.6, 44.6, 44.1, 40.1, 25.5, 22.6, 22.5, 19.0, 10.2. LRMS calculated for  $\text{C}_{34}\text{H}_{68}\text{N}_6\text{O}$   $m/z$  577.6  $[\text{M}+\text{H}]^+$ , Obsd. 577.6.

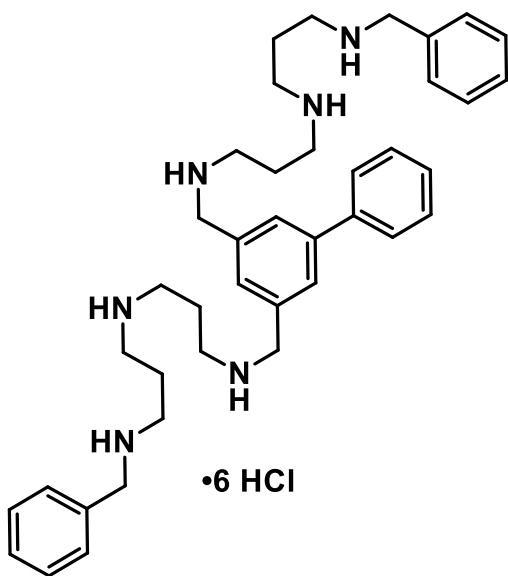


**CZ-01-092:**  $N^1,N^{1'}-([1,1'\text{-Biphenyl}]-3,5\text{-diylbis(methylene)})\text{bis}(N^3-(3\text{-(octylamino)propyl)propane-1,3-diamine})$ , hydrochloride salt:  $^1\text{H}$  NMR (500 MHz,  $\text{D}_2\text{O}$ )  $\delta$  7.88 (s, 2H), 7.75 (d,  $J = 8.0$  Hz, 2H), 7.60-7.56 (m, 3H), 7.53-7.50 (m, 1H), 4.40

(s, 4H), 3.26 (t,  $J = 8.0$  Hz, 4H), 3.21-3.16 (m, 12H), 3.14 (t,  $J = 8.0$  Hz, 4H), 3.06 (t,  $J = 8.0$  Hz, 4H), 2.21-2.09 (m, 4H), 1.69-1.65 (m, 4H), 1.38-1.28 (m, 20H), 0.86 (t,  $J = 6.0$  Hz, 6H).  $^{13}\text{C}$  NMR (125 MHz,  $\text{D}_2\text{O}$ )  $\delta$  142.5, 138.8, 132.2, 129.9, 129.5, 129.3, 128.5, 127.0, 50.8, 47.8, 44.6, 44.1, 30.9, 28.1, 28.0, 25.6, 25.4, 22.7, 22.6, 21.9, 13.3. LRMS calculated for  $\text{C}_{42}\text{H}_{76}\text{N}_6$   $m/z$  665.6  $[\text{M}+\text{H}]^+$ , Obsd. 333.3  $[\text{M}+\text{H}]/2^+$ .

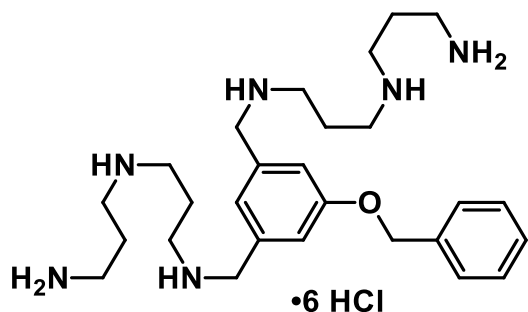


**CZ-01-093:**  $N^1,N^{1'}-((5\text{-}i\text{soPropoxy-1,3-phenylene})\text{bis(methylene)})\text{bis}(N^3\text{-(3-aminopropyl)propane-1,3-diamine})$ , hydrochloride salt:  $^1\text{H}$  NMR (300 MHz,  $\text{D}_2\text{O}$ )  $\delta$  7.13 (s, 3H), 4.78-4.72 (m, 1H), 4.23 (s, 4H), 3.27-3.18 (m, 12H), 3.13 (t,  $J = 7.8$  Hz, 4H), 2.23-2.18 (m, 4H), 2.18-2.10 (m, 4H), 1.36 (d,  $J = 10.2\text{Hz}$ , 6H).

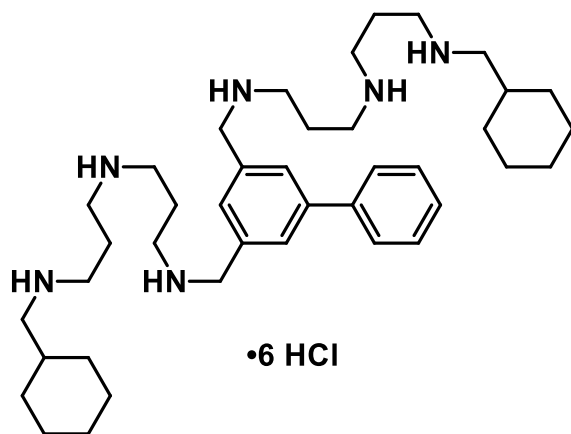


**CZ-01-094:**  $N^1,N^{1'}-([1,1'\text{-Biphenyl}]\text{-3,5-diylbis(methylene)})\text{bis}(N^3\text{-(3-(benzylamino)propyl)propane-1,3-diamine})$ , hydrochloride salt:  $^1\text{H}$  NMR (300 MHz,

D<sub>2</sub>O)  $\delta$  7.84 (s, 2H), 7.74-7.70 (m, 2H), 7.58-7.50 (m, 4H), 7.47 (s, 10H), 4.37 (s, 4H), 4.24 (s, 4H), 3.26-3.11 (m, 16H), 2.20-2.05 (m, 8H).

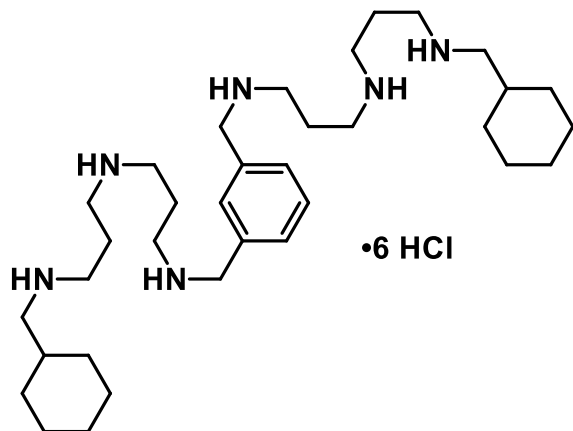


**CZ-01-095:** *N*<sup>1</sup>,*N*<sup>1'</sup>-((5-(Benzyloxy)-1,3-phenylene)bis(methylene))bis(*N*<sup>3</sup>-(3-aminopropyl)propane-1,3-diamine), hydrochloride salt: <sup>1</sup>H NMR (500 MHz, D<sub>2</sub>O)  $\delta$  7.52 (d, *J* = 7.0 Hz, 2H), 7.49-7.41 (m, 3H), 7.23 (s, 2H), 7.20 (s, 1H), 5.23 (s, 2H), 4.29 (s, 4H), 3.22-3.15 (m, 12H), 3.13 (t, *J* = 8.0 Hz, 4H), 2.20-2.09 (m, 8H). <sup>13</sup>C NMR (125 MHz, D<sub>2</sub>O)  $\delta$  158.7, 136.0, 133.0, 132.5, 128.5, 128.0, 123.9, 117.7, 70.4, 50.7, 44.3, 44.0, 36.5, 23.7, 22.6 LRMS calculated for C<sub>27</sub>H<sub>46</sub>N<sub>6</sub>O *m/z* 471.4 [M+H]<sup>+</sup>, Obsd. 471.4.

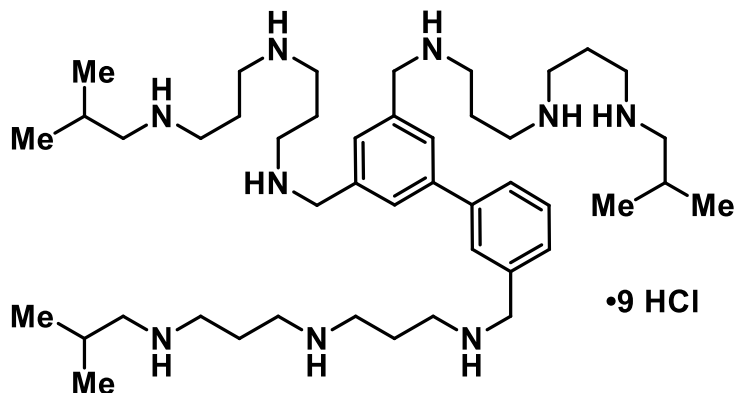


**CZ-01-096:** *N*<sup>1</sup>,*N*<sup>1'</sup>-([1,1'-Biphenyl]-3,5-diylbis(methylene))bis(*N*<sup>3</sup>-(3-((cyclohexylmethyl)amino)propyl)propane-1,3-diamine), hydrochloride salt: <sup>1</sup>H NMR (500 MHz, D<sub>2</sub>O)  $\delta$  7.87 (s, 2H), 7.75 (d, *J* = 7.5 Hz, 2H), 7.59-7.56 (m, 3H), 7.51-7.49 (m, 1H), 4.40 (s, 4H), 3.28 (t, *J* = 8.0 Hz, 4H), 3.24-3.18 (m, 8H), 3.15 (t, *J* = 8.0 Hz,

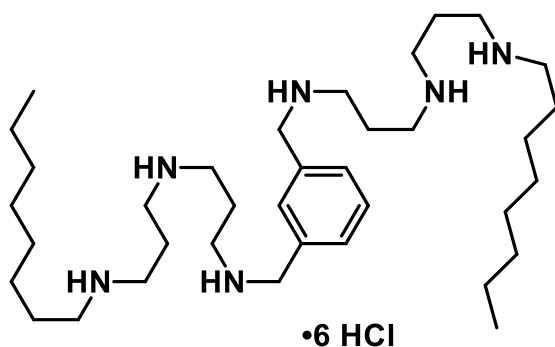
4H), 2.93 (d,  $J = 7.0$  Hz, 4H), 2.24-2.12 (m, 8H), 1.74-1.60 (m, 12H), 1.30-1.14 (m, 6H), 1.05-0.98 (m, 4H).  $^{13}\text{C}$  NMR (125 MHz,  $\text{D}_2\text{O}$ )  $\delta$  142.4, 138.8, 132.1, 130.0, 129.6, 129.3, 128.5, 127.0, 53.7, 50.8, 44.7, 44.6, 44.2, 34.5, 29.7, 25.4, 24.9, 22.6, 22.5. IR (neat): 3386 (bs), 2921, 2739, 1453 (all s)  $\text{cm}^{-1}$ . mp decomposition (235-237  $^\circ\text{C}$ ). LRMS calculated for  $\text{C}_{40}\text{H}_{68}\text{N}_6$   $m/z$  633.6  $[\text{M}+\text{H}]^+$ , Obsd. 633.5.



**CZ-01-097:**  $N^1,N^{1'}\text{-(1,3-phenylenebis(methylene))bis}(N^3\text{-(3-((cyclohexylmethyl)amino)propyl)propane-1,3-diamine})$ , hydrochloride salt:  $^1\text{H}$  NMR (500 MHz,  $\text{D}_2\text{O}$ )  $\delta$  7.57 (s, 4H), 4.30 (s, 4H), 3.22 (t,  $J = 7.5$  Hz, 4H), 3.18-3.15 (m, 8H), 3.12 (t,  $J = 8.0$  Hz, 4H), 2.91 (d,  $J = 7.0$  Hz, 4H), 2.18-2.08 (m, 8H), 1.72-1.62 (m, 12H), 1.28-1.11 (m, 6H), 1.03-0.96 (m, 4H).  $^{13}\text{C}$  NMR (125 MHz,  $\text{D}_2\text{O}$ )  $\delta$  131.4, 131.2, 131.0, 130.2, 53.7, 50.8, 48.8, 44.7, 44.6, 44.0, 34.5, 29.7, 25.3, 24.8, 22.6, 22.5. IR (neat): 3330 (bs), 2971, 2936, 2831, 1455 (all s)  $\text{cm}^{-1}$ . mp decomposition (250-251  $^\circ\text{C}$ ). LRMS calculated for  $\text{C}_{34}\text{H}_{64}\text{N}_6$   $m/z$  557.5  $[\text{M}+\text{H}]^+$ , Obsd. 557.5.

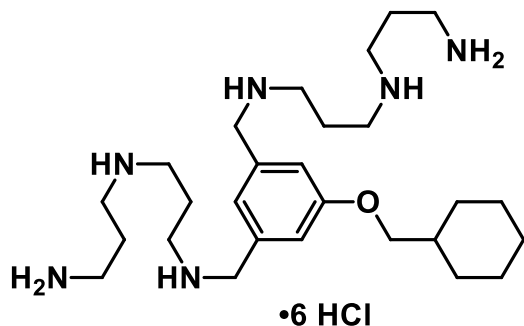


**CZ-01-099:**  $N^1, N^{1'}, N^{1''}$ -([1,1'-biphenyl]-3,3',5-triyltris(methylene))tris( $N^3$ -(3-(isobutylamino)propyl)propane-1,3-diamine), hydrochloride salt:  $^1\text{H}$  NMR (500 MHz,  $\text{D}_2\text{O}$ )  $\delta$  ppm 7.91 (s, 1H), 7.85-7.82 (m, 3H), 7.65-7.56 (m, 3H), 4.42 (s, 4H), 4.39 (s, 2H), 3.29-3.16 (m, 24H), 2.93 (d,  $J = 6.0$  Hz, 6H), 2.20-2.13 (m, 12H), 2.07-2.00 (m, 3H), 0.99 (d,  $J = 6.0$  Hz, 18H).  $^{13}\text{C}$  NMR (125 MHz,  $\text{D}_2\text{O}$ )  $\delta$  ppm 141.6, 139.8, 132.2, 131.3, 130.4, 130.3, 129.7, 129.5, 128.6, 128.4, 54.8, 54.8, 51.1, 50.8, 44.7, 44.6, 44.2, 44.0, 25.5, 22.7, 22.5, 19.0. IR (neat): 3381 (bs), 2950, 2755, 1447 (all s)  $\text{cm}^{-1}$ . mp decomposition (248-250  $^\circ\text{C}$ ). LRMS calculated for  $\text{C}_{45}\text{H}_{85}\text{N}_9$   $m/z$  752.7  $[\text{M}+\text{H}]^+$ , Obsd. 376.8  $[\text{M}+\text{H}]^+/2$ .



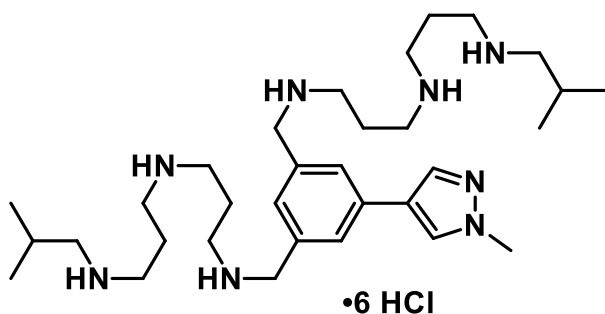
**CZ-01-100:**  $N^1, N^{1'}$ -(1,3-Phenylenebis(methylene))bis( $N^3$ -(3-(octylamino)propyl)propane-1,3-diamine), hydrochloride salt:  $^1\text{H}$  NMR (500 MHz,  $\text{D}_2\text{O}$ )  $\delta$  7.58 (s, 4H), 4.32 (s, 4H), 3.10-2.98 (m, 16H), 2.91 (t,  $J = 8.0$  Hz, 4H), 2.05-1.95 (m, 8H), 1.53 (quint,  $J = 7.0$  Hz, 4H), 1.24-1.13 (m, 20H), 0.71 (t,  $J = 7.0$  Hz, 6H).  $^{13}\text{C}$  NMR (125 MHz,  $\text{D}_2\text{O}$ )

$\delta$  131.4, 131.2, 131.1, 130.2, 50.8, 47.9, 44.6, 44.6, 44.2, 44.1, 30.9, 28.1, 28.1, 25.6, 25.4, 22.6, 21.9, 13.3. IR (neat): 3326 (bs), 2942, 2831, 1457 (all s)  $\text{cm}^{-1}$ . mp decomposition (254-255  $^{\circ}\text{C}$ ). LRMS calculated for  $\text{C}_{36}\text{H}_{72}\text{N}_6$   $m/z$  589.6  $[\text{M}+\text{H}]^+$ , Obsd. 589.5.



**CZ-01-101:**  $N^1, N^{1'}\text{-}((5\text{-(Cyclohexylmethoxy)-1,3-phenylene})\text{bis(methylene)})$

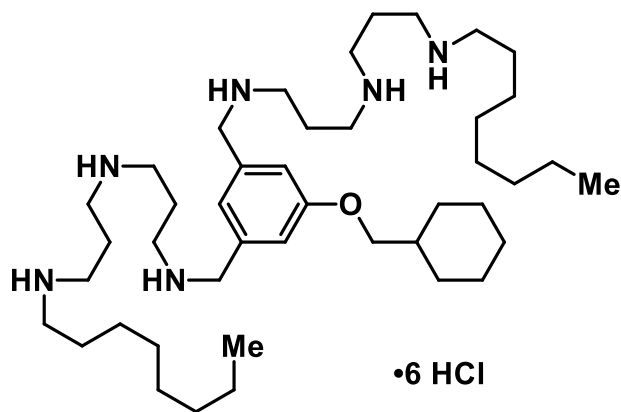
**bis( $N^3$ -(3-aminopropyl)propane-1,3-diamine), hydrochloride salt:**  $^1\text{H}$  NMR (500 MHz,  $\text{D}_2\text{O}$ )  $\delta$  7.16 (d,  $J = 7.5$  Hz 3H), 4.27 (s, 4H), 3.93 (t,  $J = 6.0$  Hz, 2H), 3.23-3.09 (m, 16H), 2.19-2.07 (m, 8H), 1.83-1.66 (m, 6H), 1.31-1.17 (m, 3H), 1.10-1.05 (m, 2H).  $^{13}\text{C}$  NMR (125 MHz,  $\text{D}_2\text{O}$ )  $\delta$  131.4, 131.2, 131.1, 130.2, 50.8, 47.9, 44.6, 44.6, 44.2, 44.1, 30.9, 28.1, 28.1, 25.6, 25.4, 22.6, 21.9, 13.3.



**CZ-01-102:**  $N^1, N^{1'}\text{-}((5\text{-(1-Methyl-1H-pyrazol-4-yl)-1,3-phenylene})\text{bis(methylene)})\text{bis}(N^3\text{-(3-(isobutylamino)propyl)propane-1,3-diamine})$ ,  
**hydrochloride salt:**  $^1\text{H}$  NMR (300 MHz,  $\text{D}_2\text{O}$ )  $\delta$  7.75-7.69 (m, 4H), 6.60 (d,  $J = 2.1$  Hz, 2H), 4.38 (s, 4H), 3.92 (s, 3H), 3.27-3.09 (m, 16H), 2.89 (d,  $J = 7.2$  Hz, 4H), 2.21-2.06 (m, 8H), 2.03-1.94 (m, 2H), 0.97 (d,  $J = 6.9$  Hz, 12H).  $^1\text{H}$  NMR (300 MHz,  $\text{D}_2\text{O}$ )  $\delta$  7.75-7.69

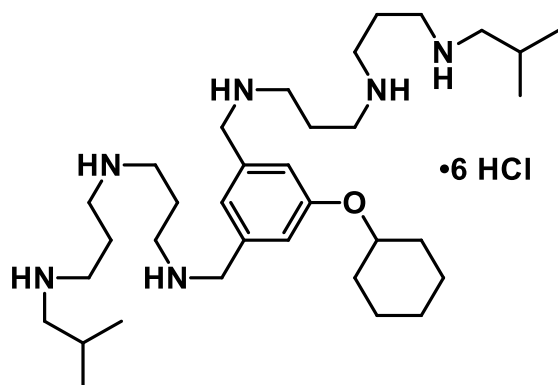


(m, 4H), 6.60 (d,  $J = 2.1$  Hz, 2H), 4.38 (s, 4H), 3.92 (s, 3H), 3.27-3.09 (m, 16H), 2.89 (d,  $J = 7.2$  Hz, 4H), 2.21-2.06 (m, 8H), 2.03-1.94 (m, 2H), 0.97 (d,  $J = 6.9$  Hz, 12H).



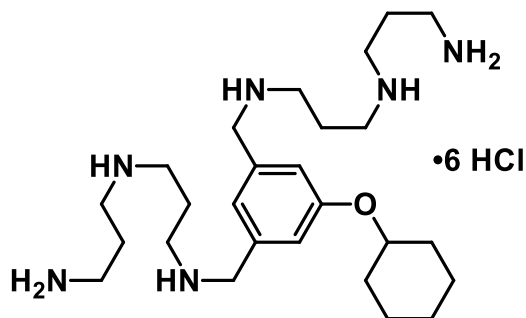
**CZ-01-103**

**CZ-01-103:**  $N^1, N^{1'}$ -((5-(Cyclohexylmethoxy)-1,3-phenylene)bis(methylene))bis( $N^3$ -(3-(octylamino)propyl)propane-1,3-diamine), hydrochloride salt:  $^1\text{H}$  NMR (500 MHz,  $\text{D}_2\text{O}$ )  $\delta$  7.18 (s, 3H), 4.28 (s, 4H), 3.95 (s, 2H) 3.20-3.14 (m, 16H), 3.06 (t,  $J = 7.5$  Hz, 4H), 2.22-2.10 (m, 8H), 1.88-1.80 (m, 3H), 1.76-1.64 (m 8H), 1.41-1.20 (m, 22H), 1.12-1.03 (m, 2H), 0.89-0.83 (m, 6H).  $^{13}\text{C}$  NMR (125 MHz,  $\text{D}_2\text{O}$ )  $\delta$  159.5, 133.0, 123.4, 117.3, 74.4, 50.8, 47.8, 44.6, 44.6, 44.2, 44.1, 36.8, 30.9, 29.1, 28.1, 28.0, 25.9, 25.6, 25.4, 25.2, 22.6, 22.6, 21.9, 13.3. LRMS calculated for  $\text{C}_{43}\text{H}_{84}\text{N}_6\text{O}$   $m/z$  701.7  $[\text{M}+\text{H}]^+$ , Obsd. 701.7.

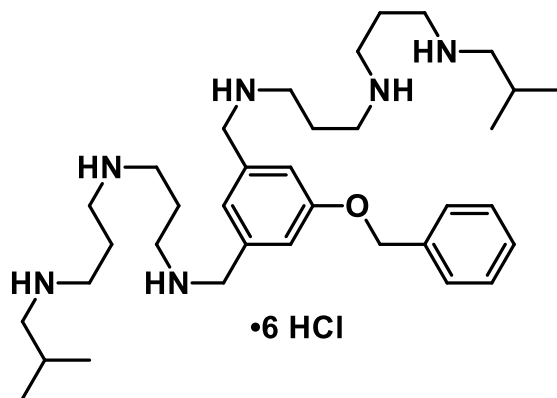


**CZ-01-104:**  $N^1, N^{1'}$ -((5-(Cyclohexyloxy)-1,3-phenylene)bis(methylene))bis( $N^3$ -(3-(isobutylamino)propyl)propane-1,3-diamine), hydrochloride salt:  $^1\text{H}$  NMR (300 MHz,

D<sub>2</sub>O)  $\delta$  7.60 (s, 2H), 7.53 (s, 1H), 4.73 (t,  $J$  = 1.2 Hz, 1H), 4.42 (s, 4H), 3.26-3.13 (m, 16H), 2.84 (d,  $J$  = 6.9 Hz, 2H), 2.23-2.08 (m, 8H), 2.06-1.96 (m, 2H), 1.87-1.78 (m, 4H), 1.65-1.36 (m, 6H), 0.99 (d,  $J$  = 6.6 Hz, 12H). LRMS calculated for C<sub>34</sub>H<sub>66</sub>N<sub>6</sub>O  $m/z$  575.5 [M+H]<sup>+</sup>, Obsd. 575.5.

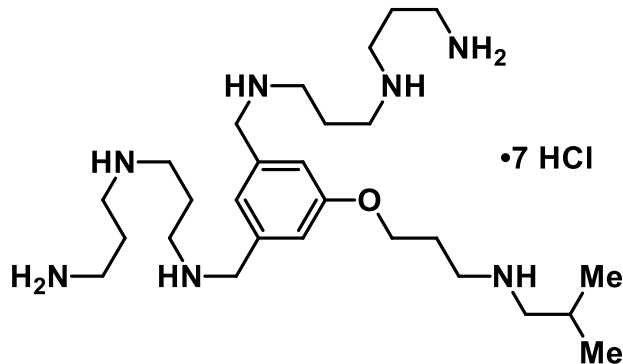


**CZ-01-105:** *N*<sup>1</sup>,*N*<sup>1'</sup>-((5-(cyclohexyloxy)-1,3-phenylene)bis(methylene))bis(*N*<sup>3</sup>-(3-aminopropyl)propane-1,3-diamine), hydrochloride salt: <sup>1</sup>H NMR (300 MHz, D<sub>2</sub>O)  $\delta$  7.22 (s, 2H), 7.18 (s, 1H), 4.68 (t,  $J$  = 1.2 Hz, 1H), 4.30 (s, 4H), 3.28-3.18 (m, 12H), 3.14 (t,  $J$  = 7.8 Hz, 4H), 2.21-2.06 (m, 8H), 1.84-1.75 (m, 4H), 1.63-1.34 (m, 6H). LRMS calculated for C<sub>26</sub>H<sub>50</sub>N<sub>6</sub>O  $m/z$  463.4 [M+H]<sup>+</sup>, Obsd. 463.5.



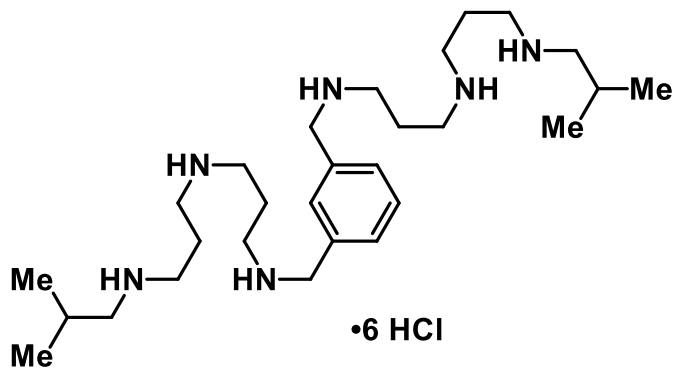
**CZ-01-106:** *N*<sup>1</sup>,*N*<sup>1'</sup>-((5-(benzyloxy)-1,3-phenylene)bis(methylene))bis(*N*<sup>3</sup>-(3-(isobutylamino)propyl)propane-1,3-diamine), hydrochloride salt: <sup>1</sup>H NMR (400 MHz, D<sub>2</sub>O)  $\delta$  7.55 (s, 1H), 7.52 (d,  $J$  = 2.1 Hz, 2H), 7.49 (s, 2H), 7.26 (s, 3H), 5.29 (s, 2H), 4.31 (s, 4H), 3.26-3.13 (m, 16H), 2.95 (d,  $J$  = 7.2 Hz, 4H), 2.25-2.09 (m, 8H), 2.07-2.01 (m,

2H), 1.03 (d,  $J = 6.6$  Hz, 12H).



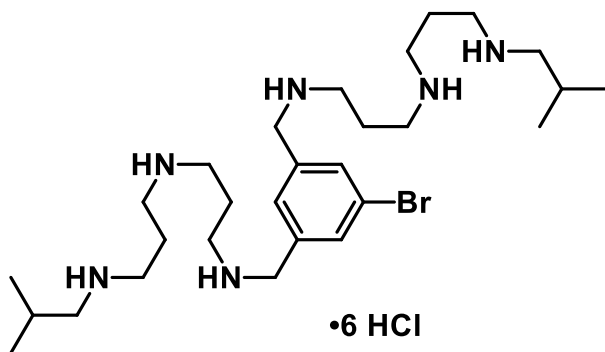
**CZ-01-107:**  $N^1,N^{1'}-((5-(3-(\text{isobutylamino})\text{propoxy})-1,3\text{-phenylene})\text{bis(methylene)})\text{bis}(N^3-(3\text{-aminopropyl})\text{propane-1,3-diamine}),$

**hydrochloride salt:**  $^1\text{H}$  NMR (500 MHz,  $\text{D}_2\text{O}$ )  $\delta$  ppm 7.21 (s, 1H), 7.19 (s, 2H), 4.30 (s, 4H), 4.23 (t,  $J = 5.5$  Hz, 2H), 3.29 (t,  $J = 7.0$  Hz, 2H), 3.25-3.19 (m, 12H), 3.12 (t,  $J = 7.5$  Hz, 4H), 2.95 (d,  $J = 7.0$  Hz, 2H), 2.25-2.03 (m, 13H), 1.01 (d,  $J = 7.5$  Hz, 6H).  $^{13}\text{C}$  NMR (125 MHz,  $\text{D}_2\text{O}$ ) 158.9, 133.0, 123.7, 117.1, 65.8, 54.8, 50.7, 45.7, 44.7, 44.6, 44.2, 36.7, 25.5, 25.2, 23.7, 22.6, 19.1. LRMS calculated for  $\text{C}_{27}\text{H}_{55}\text{N}_7\text{O}$   $m/z$  494.4  $[\text{M}+\text{H}]^+$ , Obsd. 494.4.

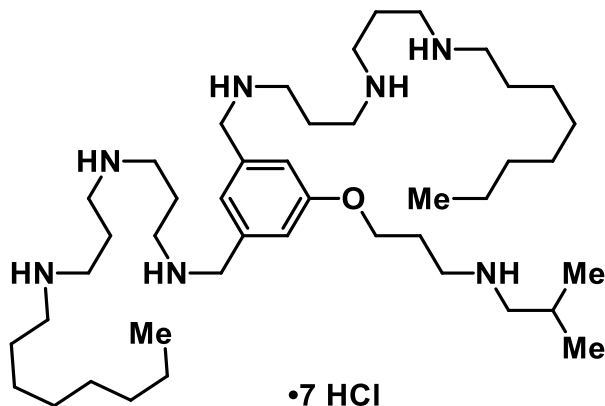


**CZ-01-108:**  $N^1,N^{1'}-(1,3\text{-Phenylenebis(methylene)})\text{bis}(N^3-(3-(\text{isobutylamino})\text{propyl})\text{propane-1,3-diamine}),$  **hydrochloride salt:**  $^1\text{H}$  NMR (300 MHz,  $\text{D}_2\text{O}$ )  $\delta$  7.54 (s, 4H), 4.28 (s, 4H), 3.19-3.08 (m, 16H), 2.88 (d,  $J = 7.5$  Hz, 4H), 2.15-2.05 (m, 8H), 2.02-1.90 (m,

2H), 0.95 (d,  $J = 6.9$  Hz, 12H).  $^{13}\text{C}$  NMR (125 MHz,  $\text{D}_2\text{O}$ )  $\delta$  131.6, 131.5, 131.3, 130.4, 55.1, 51.1, 45.0, 44.9, 44.8, 44.3, 25.8, 22.8, 22.7, 19.3. IR (neat): 3451 (bs), 2763, 1457 (all s)  $\text{cm}^{-1}$ . mp decomposition (250-251  $^\circ\text{C}$ ). LRMS calculated for  $\text{C}_{28}\text{H}_{56}\text{N}_6$   $m/z$  477.5  $[\text{M}+\text{H}]^+$ , Obsd. 477.4.

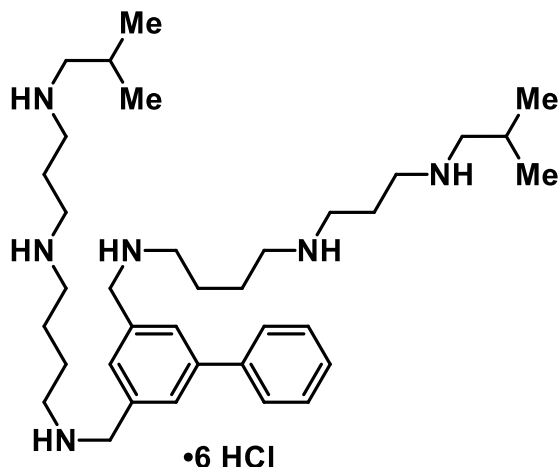


**CZ-01-109:**  $N^1,N^{1'}-((5\text{-Bromo-1,3-phenylene})\text{bis(methylene)})\text{bis}(N^3\text{-(3-(isobutylamino)propyl)propane-1,3-diamine})$ , hydrochloride salt:  $^1\text{H}$  NMR (300 MHz,  $\text{D}_2\text{O}$ )  $\delta$  7.76 (s, 2H), 7.51 (s, 1H), 4.27 (s, 4H), 3.21-3.08 (m, 16H), 2.88 (d,  $J = 7.5$  Hz, 4H), 2.16-2.06 (m, 8H), 2.02-1.93 (m, 2H), 0.96 (d,  $J = 6.6$  Hz, 12H). . LRMS calculated for  $\text{C}_{28}\text{H}_{55}\text{BrN}_6$   $m/z$  555.4  $[\text{M}+\text{H}]^+$ , Obsd. 555.4.

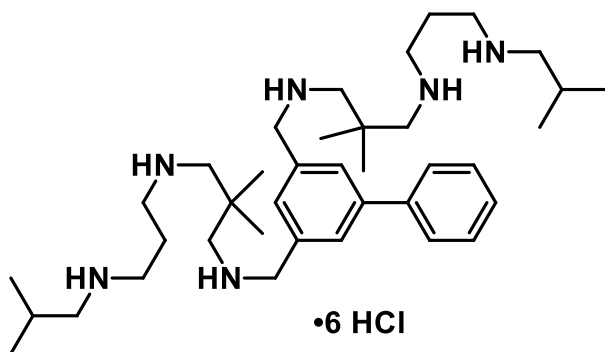


**CZ-01-110:**  $N^1,N^{1'}-((5\text{-(3-(isobutylamino)propoxy)-1,3-phenylene})\text{bis(methylene)})\text{bis}(N^3\text{-(3-(octylamino)propyl)propane-1,3-diamine})$ , hydrochloride salt:  $^1\text{H}$  NMR (500 MHz,  $\text{D}_2\text{O}$ )  $\delta$  7.21 (s, 1H), 7.20 (s 2H), 4.30 (s, 4H),

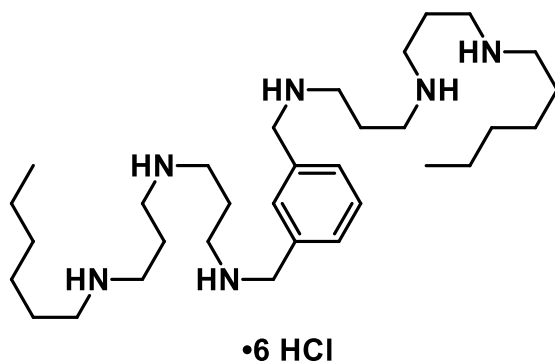
4.24 (t,  $J = 5.0$  Hz, 2H), 3.30 (t,  $J = 7.0$  Hz, 2H), 3.26-3.14 (m, 16H), 3.07 (t,  $J = 7.0$  Hz, 4H), 2.96 (d,  $J = 7.5$  Hz, 2H), 2.26-2.03 (m, 11H), 1.69 (quint,  $J = 6.5$  Hz, 4H), 1.38-1.28 (m, 20H), 1.02 (d,  $J = 6.5$  Hz, 6H), 0.87 (t,  $J = 5.5$  Hz, 6H).  $^{13}\text{C}$  NMR (125 MHz,  $\text{D}_2\text{O}$ )  $\delta$  158.9, 133.0, 123.7, 117.1, 65.8, 54.8, 50.8, 47.9, 45.7, 44.6, 44.6, 44.2, 44.1, 30.9, 28.1, 28.1, 25.6, 25.5, 25.4, 25.2, 22.6, 22.6, 19.1, 13.4.



**CZ-01-111:**  $N^1, N^{1'}\text{-}([1,1'\text{-Biphenyl}]\text{-}3,5\text{-diylbis(methylene))bis}(N^4\text{-(3-(isobutylamino)propyl)butane-1,4-diamine})$ , hydrochloride salt:  $^1\text{H}$  NMR (500 MHz,  $\text{D}_2\text{O}$ )  $\delta$  7.86 (s, 2H), 7.75 (d,  $J = 7.5$  Hz, 2H), 7.58 (t,  $J = 8.0$  Hz, 3H), 7.50 (t,  $J = 7.5$  Hz, 1H), 4.37 (s, 4H), 3.20-3.11 (m, 16H), 2.92 (d,  $J = 7.5$  Hz, 4H), 2.16-2.10 (m, 4H), 2.06-1.97 (m, 2H), 1.88-1.80 (m, 8H), 0.99 (d,  $J = 6.5$  Hz, 12H).  $^{13}\text{C}$  NMR (125 MHz,  $\text{D}_2\text{O}$ )  $\delta$  142.7, 139.1, 132.6, 130.1, 129.7, 129.5, 128.7, 127.7, 55.1, 50.9, 47.2, 46.7, 44.5, 44.7, 25.8, 23.0, 22.9, 22.7, 19.2. LRMS calculated for  $\text{C}_{36}\text{H}_{64}\text{N}_6$   $m/z$  581.5  $[\text{M}+\text{H}]^+$ , Obsd. 581.5.

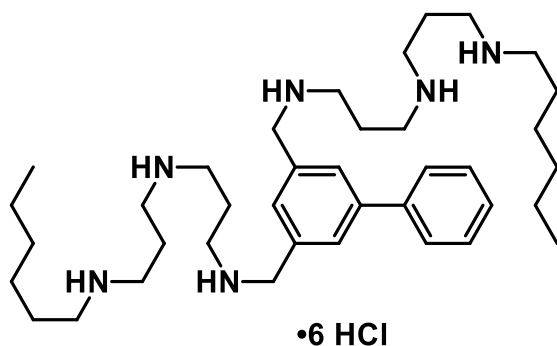


**CZ-01-112:**  $N^1,N^{1'}-([1,1'\text{-Biphenyl}]\text{-3,5-diylbis(methylene)})\text{bis}(N^3\text{-(3-(isobutylamino)propyl)-2,2-dimethylpropane-1,3-diamine})$ , hydrochloride salt:  $^1\text{H}$  NMR (500 MHz,  $\text{D}_2\text{O}$ )  $\delta$  7.89 (s, 2H), 7.71 (d,  $J = 7.5$  Hz, 2H), 7.62 (s, 1H), 7.52 (t,  $J = 7.5$  Hz, 2H), 7.44 (t,  $J = 7.5$  Hz, 1H), 4.39 (s, 4H), 3.19-3.01 (m, 16H), 2.89 (d,  $J = 7.5$  Hz, 4H), 2.21-2.15 (m, 4H), 2.03-1.96 (m, 2H), 1.18 (s, 12H), 0.97 (d,  $J = 6.5$  Hz, 12H).  $^{13}\text{C}$  NMR (125 MHz,  $\text{D}_2\text{O}$ )  $\delta$  142.2, 138.8, 131.7, 131.4, 130.2, 129.5, 128.7, 127.2, 55.6, 55.1, 52.1, 46.3, 45.0, 33.2, 25.8, 22.5, 22.4, 21.9, 19.3. LRMS calculated for  $\text{C}_{38}\text{H}_{68}\text{N}_6$   $m/z$  609.6  $[\text{M}+\text{H}]^+$ , Obsd. 609.5.

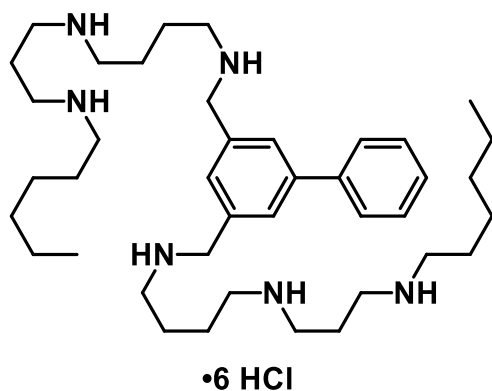


**CZ-01-113:**  $N^1,N^{1'}\text{-(1,3-Phenylenebis(methylene))bis}(N^3\text{-(3-(hexylamino)propyl)propane-1,3-diamine})$ , hydrochloride salt:  $^1\text{H}$  NMR (500 MHz,  $\text{D}_2\text{O}$ )  $\delta$  7.58 (s, 4H), 4.32 (s, 4H), 3.24-3.13 (m, 16H), 3.05 (t,  $J = 8.0$  Hz, 4H), 2.20-2.09 (m, 8H), 1.68-1.63 (m, 4H), 1.38-1.33 (m, 4H), 1.32-1.26 (m, 8H), 0.85 (t,  $J = 7.5$  Hz, 6H).  $^{13}\text{C}$  NMR (125 MHz,  $\text{D}_2\text{O}$ )  $\delta$  131.6, 131.5, 131.4, 130.4, 51.1, 48.1, 44.9, 44.8, 44.5, 44.3,

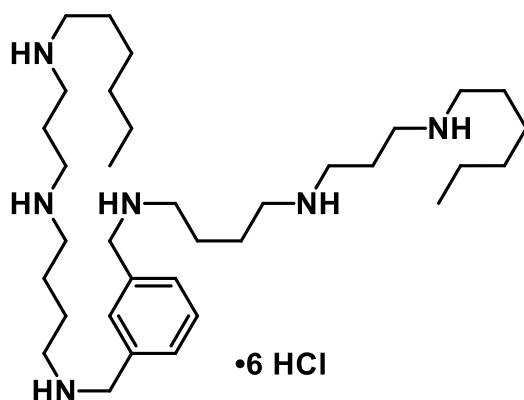
30.6, 25.6, 25.5, 22.8, 21.9, 13.5. LRMS calculated for  $C_{32}H_{64}N_6$   $m/z$  533.5  $[M+H]^+$ , Obsd. 533.6.



**CZ-01-114:**  $N^1,N^{1'}-([1,1'-\text{Biphenyl}]-3,5\text{-diylbis(methylene)})\text{bis}(N^3\text{-(3-(hexylamino)propyl)propane-1,3-diamine})$ , hydrochloride salt:  $^1\text{H}$  NMR (500 MHz,  $D_2O$ )  $\delta$  7.83 (s, 2H), 7.71 (d,  $J = 7.5$  Hz, 2H), 7.55-7.53 (m, 3H), 7.47 (t,  $J = 6.5$  Hz, 1H), 4.34 (s, 4H), 3.25 (t,  $J = 8.0$  Hz, 4H), 3.19 (q,  $J = 8.0$  Hz, 8H), 3.13 (t,  $J = 8.0$  Hz, 4H), 3.04 (t,  $J = 8.5$  Hz, 4H), 2.22-2.09 (m, 8H), 1.66 (quint,  $J = 7.5$  Hz, 4H), 1.36-1.31 (m, 4H), 1.28-1.27 (m, 8H), 0.85 (t,  $J = 7$  Hz, 6H).  $^{13}\text{C}$  NMR (125 MHz,  $D_2O$ )  $\delta$  142.5, 139.0, 132.3, 130.3, 129.8, 129.5, 128.7, 127.3, 51.0, 48.1, 44.9, 44.4, 44.4, 30.6, 25.6, 25.5, 22.9, 22.8, 21.9, 13.5. IR (neat): 3404 (bs), 2947, 2762, 1738, 1712 (all s)  $\text{cm}^{-1}$ . mp decomposition (226-228  $^{\circ}\text{C}$ ). LRMS calculated for  $C_{38}H_{68}N_6$   $m/z$  609.6  $[M+H]^+$ , Obsd. 609.5

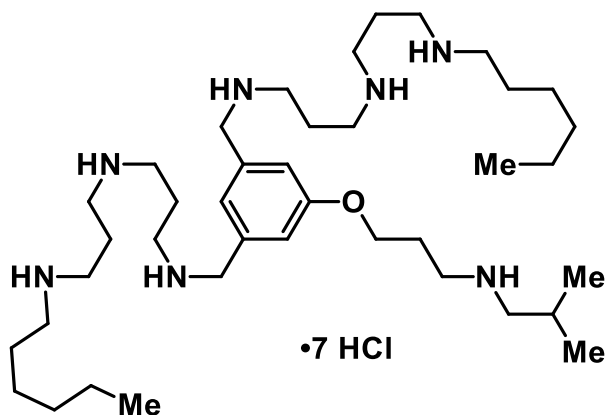


**CZ-01-118:**  $N^1,N^{1'}\text{-}([1,1'\text{-Biphenyl-3,5-diylbis(methylene))bis}(N^4\text{-(3-(hexylamino)propyl)butane-1,4-diamine})$ , hydrochloride salt:  $^1\text{H}$  NMR (500 MHz,  $\text{D}_2\text{O}$ )  $\delta$  7.87 (s, 2H), 7.76 (d,  $J = 7.5$  Hz, 2H), 7.58 (t,  $J = 8.0$  Hz, 3H), 7.51 (t,  $J = 7.5$  Hz, 1H), 4.37 (s, 4H), 3.21-3.14 (m, 12H), 3.07 (t,  $J = 7.0$  Hz, 4H), 2.16-2.09 (m, 4H), 1.90-1.77 (m, 10H), 1.69 (quint,  $J = 7.0$  Hz, 4H), 1.39-1.37 (m, 4H), 1.32-1.31 (m, 10H), 0.86 (t,  $J = 7.0$  Hz, 6H).  $^{13}\text{C}$  NMR (125 MHz,  $\text{D}_2\text{O}$ )  $\delta$  142.6, 139.1, 132.6, 130.2, 129.7, 129.5, 128.7, 127.3, 50.9, 48.1, 47.2, 46.7, 44.7, 44.5, 30.6, 25.6, 25.5, 23.0, 23.0, 22.8, 21.9, 13.4. LRMS calculated for  $\text{C}_{40}\text{H}_{72}\text{N}_6$   $m/z$  637.6  $[\text{M}+\text{H}]^+$ , Obsd. 637.6.



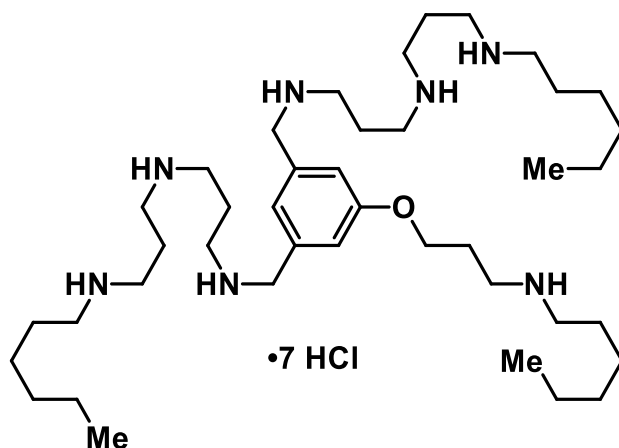
**CZ-01-119:**  $N^1,N^{1'}\text{-(1,3-Phenylenebis(methylene))bis}(N^4\text{-(3-(hexylamino)propyl)butane-1,4-diamine})$ , hydrochloride salt:  $^1\text{H}$  NMR (500 MHz,  $\text{D}_2\text{O}$ )  $\delta$  7.65 (s, 4H), 4.37 (s, 4H), 3.26-3.19 (m, 16H), 3.14 (t,  $J = 7.5$  Hz, 4H), 2.20 (quint,  $J = 8.0$  Hz, 4H), 1.88 (br s, 8H), 1.75 (quint,  $J = 8.0$  Hz, 4H), 1.46-1.42 (m, 4H), 1.39-1.36 (m, 8H), 0.94 (t,  $J = 6.5$  Hz, 6H).  $^{13}\text{C}$  NMR (125 MHz,  $\text{D}_2\text{O}$ )  $\delta$  134.2, 133.7, 133.5, 132.7, 53.3, 50.4, 49.6, 49.1, 47.1, 46.8, 32.9, 27.9, 27.8, 25.4, 25.3, 25.2, 24.2, 15.8. LRMS calculated for  $\text{C}_{34}\text{H}_{68}\text{N}_6$   $m/z$  561.6  $[\text{M}+\text{H}]^+$ , Obsd. 561.5.





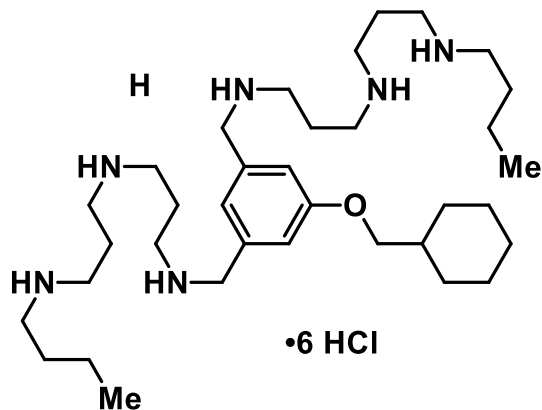
**CZ-01-121:** *N*<sup>1</sup>,*N*<sup>1'</sup>-((5-(3-(isobutylamino)propoxy)-1,3-phenylene)bis(methylene))bis(*N*<sup>3</sup>-(3-(hexylamino)propyl)propane-1,3-diamine),

**hydrochloride salt:** <sup>1</sup>H NMR (500 MHz, D<sub>2</sub>O) δ ppm 7.05 (s, 1H), 7.03 (s, 2H), 4.13 (s, 4H), 4.07 (t, *J* = 6.0 Hz, 2H), 3.15-2.97 (m, 18H), 2.90 (t, *J* = 8.0 Hz, 4H), 2.78 (d, *J* = 6.5 Hz, 2H), 2.09-1.94 (m, 10H), 1.88 (sept, *J* = 7.0 Hz, 1H), 1.51 (pent, *J* = 7.5 Hz, 4H), 1.23-1.08 (m, 12H), 0.84 (d, *J* = 6.0 Hz, 6H), 0.70 (t, *J* = 7.0 Hz, 6H). <sup>13</sup>C NMR (125 MHz, D<sub>2</sub>O) δ 159.0, 133.1, 124.0, 117.4, 66.1, 55.0, 50.9, 49.0, 48.0, 45.9, 44.8, 44.4, 44.3, 30.5, 25.7, 25.5, 25.4, 25.4, 22.8, 21.8, 19.3, 13.4. LRMS calculated for C<sub>39</sub>H<sub>79</sub>N<sub>7</sub>O *m/z* 662.6 [M+H]<sup>+</sup>, Obsd. 662.4.

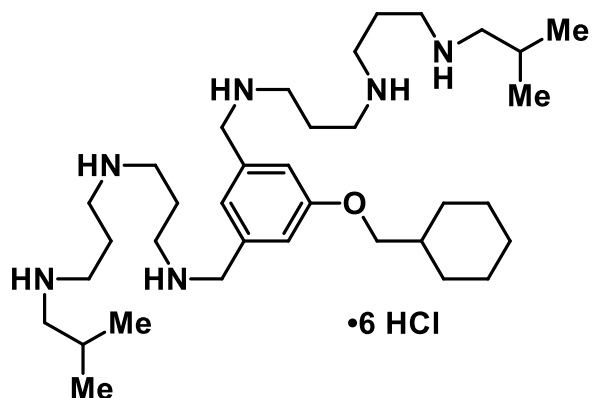


**CZ-122:** *N*<sup>1</sup>,*N*<sup>1'</sup>-((5-(3-(hexylamino)propoxy)-1,3-phenylene)bis(methylene))bis(*N*<sup>3</sup>-(3-(hexylamino)propyl)propane-1,3-diamine), **hydrochloride salt:** <sup>1</sup>H NMR (500 MHz,

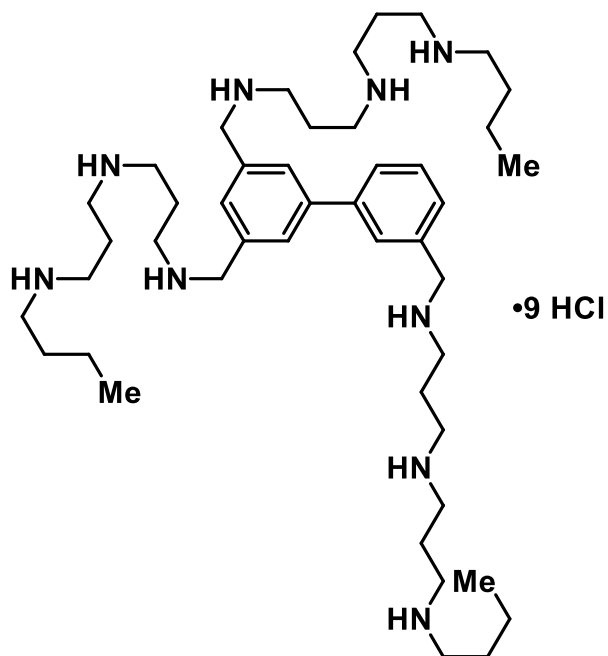
D<sub>2</sub>O)  $\delta$  ppm 7.20 (s, 1H), 7.18 (s, 2H), 4.28 (s, 4H), 4.21 (t,  $J = 5.5$  Hz, 2H), 3.28-3.12 (m, 18H), 3.08-3.03 (m, 6H), 2.22-2.09 (m, 10H), 1.72-1.63 (m, 6H), 1.38-1.24 (m, 18H), 0.85 (t,  $J = 6.0$  Hz, 9H). <sup>13</sup>C NMR (125 MHz, D<sub>2</sub>O)  $\delta$  159.1, 133.2, 124.0, 117.4, 66.0, 51.0, 48.1, 45.4, 44.9, 44.8, 44.4, 44.4, 30.6, 30.6, 25.6, 25.6, 25.6, 25.5, 25.5, 22.8, 21.9, 21.9, 13.4, 13.4.



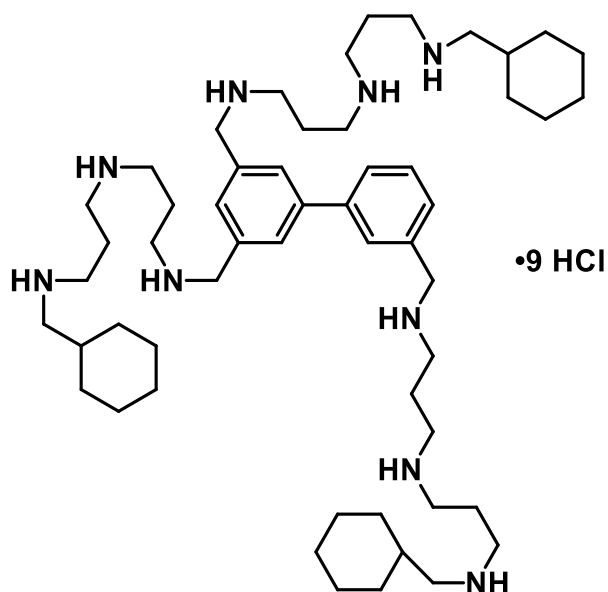
**CZ-01-124: *N*<sup>1</sup>,*N*<sup>1'</sup>-((5-(cyclohexylmethoxy)-1,3-phenylene)bis(methylene))bis(*N*<sup>3</sup>-(3-(butylamino)propyl)propane-1,3-diamine), hydrochloride salt:** <sup>1</sup>H NMR (500 MHz, D<sub>2</sub>O)  $\delta$  ppm 7.16 (s, 3H), 4.27 (s, 4H), 3.93 (d,  $J = 6.0$  Hz, 2H), 3.22-3.12 (m, 16H), 3.05 (t,  $J = 8.0$  Hz, 4H), 2.18-2.07 (m, 8H), 1.82-1.71 (m, 5H), 1.65 (pent,  $J = 7.5$  Hz, 4H), 1.37 (hex,  $J = 7.5$  Hz, 4H), 1.30-1.01 (m, 6H), 0.91 (t,  $J = 7.0$  Hz, 6H). <sup>13</sup>C NMR (125 MHz, D<sub>2</sub>O)  $\delta$  159.7, 133.2, 123.6, 117.6, 74.6, 51.0, 47.8, 44.8, 44.4, 44.3, 37.1, 29.4, 27.7, 26.2, 25.5, 22.8, 19.3, 12.9. LRMS calculated for C<sub>35</sub>H<sub>68</sub>N<sub>6</sub>O  $m/z$  589.5 [M+H]<sup>+</sup>, Obsd. 589.4.



**CZ-01-125:**  $N^1, N^{1'}$ -((5-(cyclohexylmethoxy)-1,3-phenylene)bis(methylene))bis( $N^3$ -(3-(isobutylamino)propyl)propane-1,3-diamine), hydrochloride salt:  $^1\text{H}$  NMR (500 MHz,  $\text{D}_2\text{O}$ )  $\delta$  ppm 7.16 (s, 3H), 4.27 (s, 4H), 3.93 (d,  $J = 6.0$  Hz, 2H), 3.22-3.12 (m, 16H), 2.91 (d,  $J = 7.5$  Hz, 4H), 2.18-2.09 (m, 8H), 2.00 (sept,  $J = 6.5$  Hz, 2H), 1.82-1.64 (m, 5H), 1.32-1.01 (m, 6H), 0.98 (d,  $J = 6.5$  Hz, 12H).  $^{13}\text{C}$  NMR (125 MHz,  $\text{D}_2\text{O}$ )  $\delta$  159.7, 133.2, 123.6, 117.6, 74.6, 55.1, 51.0, 45.0, 44.9, 44.3, 37.1, 29.4, 26.2, 25.8, 25.4, 22.8, 22.7, 19.2. LRMS calculated for  $\text{C}_{35}\text{H}_{68}\text{N}_6\text{O}$   $m/z$  589.5  $[\text{M}+\text{H}]^+$ , Obsd. 589.3.

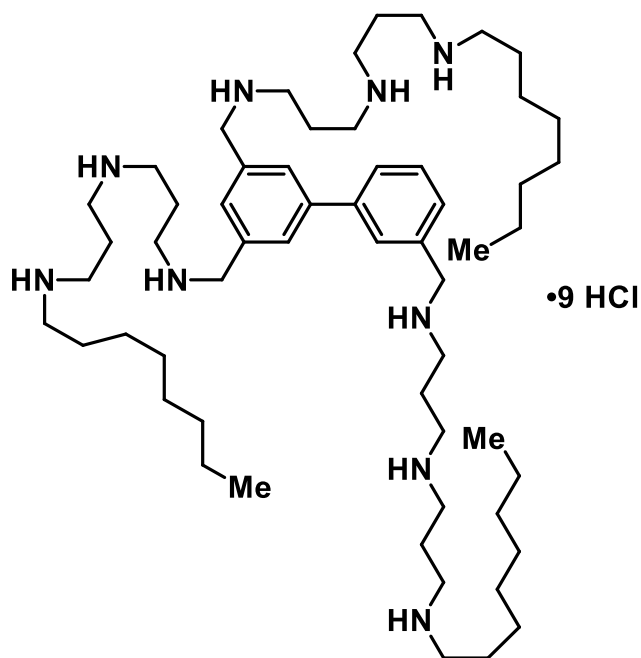


**CZ-01-126:** *N*<sup>1</sup>,*N*<sup>1'</sup>,*N*<sup>1''</sup>-([1,1'-biphenyl]-3,3',5-triyltris(methylene))tris(*N*<sup>3</sup>-(3-(butylamino)propyl)propane-1,3-diamine), hydrochloride salt: <sup>1</sup>H NMR (500 MHz, D<sub>2</sub>O) δ ppm 7.91 (s, 2H), 7.85-7.82 (m, 2H), 7.65-7.62 (m, 2H), 7.57-7.56 (m, 1H), 4.42 (s, 4H), 4.39 (s, 2H), 3.30-3.14 (m, 24H), 3.07 (t, *J* = 7.5 Hz, 6H), 2.24-2.10 (m, 12H), 1.66 (t, *J* = 7.5 Hz, 6H), 1.39 (hex, *J* = 8.0 Hz, 6H), 0.92 (t, *J* = 7.5 Hz, 9H). <sup>13</sup>C NMR (125 MHz, D<sub>2</sub>O) δ 141.9, 140.0, 132.4, 131.5, 130.6, 130.3, 130.0, 129.8, 128.8, 128.6, 51.4, 51.1, 47.8, 44.9, 44.4, 44.3, 27.7, 22.9, 22.8, 19.3, 12.9. LRMS calculated for C<sub>45</sub>H<sub>85</sub>N<sub>9</sub> m/z 753.2 [M+H]<sup>+</sup>, Obsd. 376.7 [M+H]<sup>+</sup>/2.

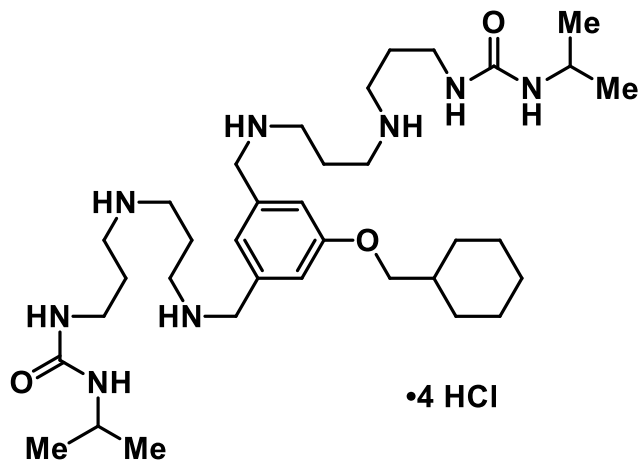


**CZ-01-127:** *N*<sup>1</sup>,*N*<sup>1'</sup>,*N*<sup>1''</sup>-([1,1'-biphenyl]-3,3',5-triyltris(methylene))tris(*N*<sup>3</sup>-(3-((cyclohexylmethyl)amino)propyl)propane-1,3-diamine), hydrochloride salt: <sup>1</sup>H NMR (500 MHz, D<sub>2</sub>O) δ 7.92 (s, 2H), 7.86-7.83 (m, 2H), 7.67-7.64 (m, 2H), 7.58-7.57 (m, 1H), 4.43 (s, 4H), 4.40 (s, 2H), 3.31-3.14 (m, 24H), 2.94 (d, *J* = 7.0 Hz, 6H), 2.25-2.12 (m, 12H), 1.73-1.64 (m, 17H), 1.31-0.98 (m, 16H). <sup>13</sup>C NMR (125 MHz, D<sub>2</sub>O) δ 141.9, 140.0, 133.4, 131.5, 130.6, 130.3, 130.0, 129.8, 128.8, 128.6, 53.9, 51.4, 51.1, 44.9, 44.9, 44.5, 44.3, 34.8, 30.0, 25.6, 25.1, 22.9, 22.7. LRMS calculated for C<sub>54</sub>H<sub>97</sub>N<sub>9</sub> m/z 872.8 [M+H]<sup>+</sup>,

Obsd. 436.8  $[M+H]^+/2$ .

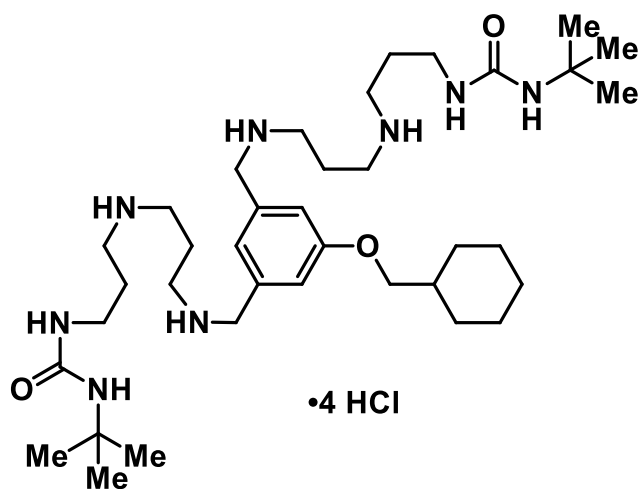


**CZ-01-128:**  $N^1, N^{1'}, N^{1''}$ -([1,1'-biphenyl]-3,3',5-triyltris(methylene))tris( $N^3$ -(3-(octylamino)propyl)propane-1,3-diamine):  $^1\text{H}$  NMR (500 MHz,  $\text{D}_2\text{O}$ )  $\delta$  7.91 (s, 2H), 7.85-7.82 (m, 2H), 7.66-7.63 (m, 2H), 7.58 (t,  $J = 7.5$  Hz, 1H), 4.42 (s, 4H), 4.39 (s, 2H), 3.30-3.13 (m, 24H), 3.06 (t,  $J = 7.5$  Hz, 6H), 2.24-2.10 (m, 12H), 1.68 (pent,  $J = 7.0$  Hz, 6H), 1.38-1.27 (m, 30H), 0.86 (t,  $J = 7.0$  Hz, 9H)  $^{13}\text{C}$  NMR (125 MHz,  $\text{D}_2\text{O}$ )  $\delta$  141.9, 140.0, 132.5, 131.5, 130.6, 130.3, 130.0, 129.8, 128.8, 128.6, 51.4, 51.1, 48.1, 44.9, 44.5, 44.4, 44.3, 31.2, 28.3, 28.3, 25.8, 25.6, 22.9, 22.8, 22.1, 13.6. LRMS calculated for  $\text{C}_{57}\text{H}_{109}\text{N}_9$   $m/z$  920.9  $[M+H]^+$ , Obsd. 460.9  $[M+H]^+/2$ .



**CZ-01-129:** **1,1'-((((((5-(cyclohexylmethoxy)-1,3-phenylene)bis(methylene))bis(azanediyloxy))bis(propane-3,1-diyl))bis(azanediyloxy))bis(propane-3,1-diyl))bis(3-isopropylurea), hydrochloride salt:**

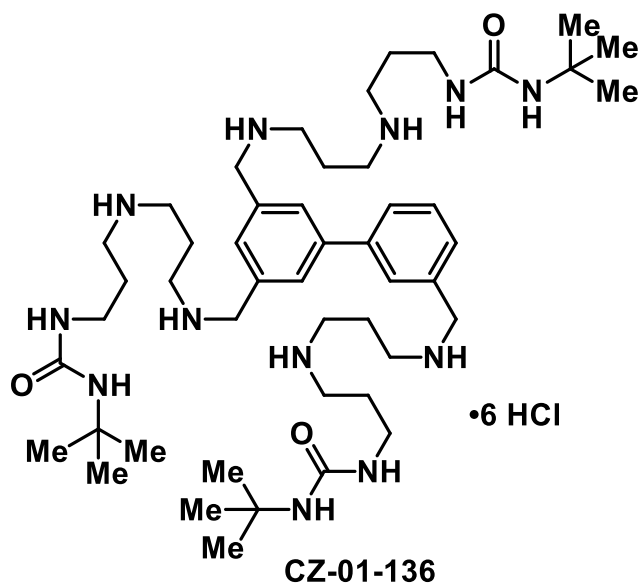
$^1\text{H}$  NMR (500 MHz,  $\text{D}_2\text{O}$ )  $\delta$  ppm 7.16 (s, 2H), 7.15 (s, 1H), 4.26 (s, 4H), 3.93 (d,  $J = 6.0$  Hz, 2H), 3.68 (pent,  $J = 6.5$  Hz, 2H), 3.22-3.18 (m, 8H), 3.13 (t,  $J = 7.5$  Hz, 4H), 3.07 (t,  $J = 7.5$  Hz, 4H), 2.17-2.10 (m, 4H), 1.87-1.65 (m, 11H), 1.32-1.15 (m, 4H), 1.09 (d,  $J = 6.5$  Hz, 12H).  $^{13}\text{C}$  NMR (125 MHz,  $\text{D}_2\text{O}$ )  $\delta$  160.2, 159.6, 133.2, 123.6, 117.5, 74.6, 50.9, 45.3, 44.5, 44.3, 42.4, 37.0, 36.3, 29.4, 26.7, 26.2, 25.4, 22.8, 22.3, 22.3.



**CZ-01-130**

**CZ-01-130:****1,1'-((((((5-(cyclohexylmethoxy)-1,3-****phenylene)bis(methylene))bis(azanediy))bis(propane-3,1-****diyl))bis(azanediy))bis(propane-3,1-diyl))bis(3-(*tert*-butyl)urea), hydrochloride salt:**

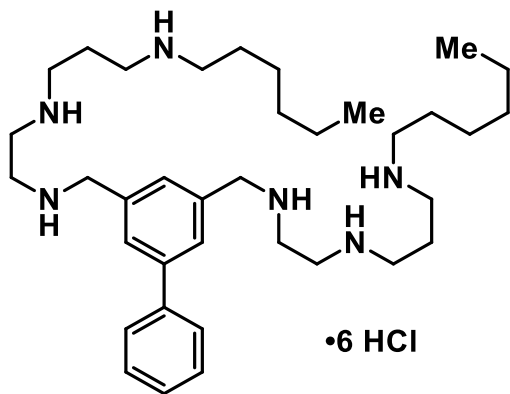
$^1\text{H}$  NMR (500 MHz,  $\text{D}_2\text{O}$ )  $\delta$  ppm 7.13 (s, 3H), 4.24 (s, 4H), 3.90 (d,  $J = 6.5$  Hz, 2H), 3.19-3.09 (m, 12H), 3.03 (t,  $J = 7.5$  Hz, 4H), 2.13-2.10 (m, 4H), 1.82-1.61 (m, 11H), 1.22 (s, 18H) 1.15-0.97 (m, 4H).  $^{13}\text{C}$  NMR (125 MHz,  $\text{D}_2\text{O}$ )  $\delta$  160.4, 159.7, 133.2, 123.6, 117.6, 74.6, 50.9, 50.3, 45.4, 44.6, 44.3, 37.1, 36.1, 29.4, 28.8, 26.7, 26.2, 25.5, 22.9. LRMS calculated for  $\text{C}_{39}\text{H}_{70}\text{N}_8\text{O}_3$   $m/z$  675.6  $[\text{M}+\text{H}]^+$ , Obsd. 675.4.



**CZ-01-136: 1-(3-((3-((3'-(3,5-bis(13,13-dimethyl-11-oxo-2,6,10,12-tetraazatetradecyl)-[1,1'-biphenyl]-3-yl)methyl)amino)propyl)amino)propyl)-3-(*tert*-butyl)urea,**

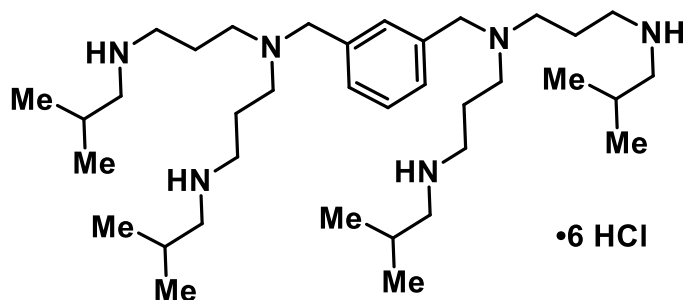
**hydrochloride salt:**  $^1\text{H}$  NMR (500 MHz,  $\text{D}_2\text{O}$ )  $\delta$  ppm 7.89 (s, 2H), 7.84-7.79 (m, 2H), 7.60 (t,  $J = 8.0$  Hz, 2H), 7.54-7.52 (m, 1H), 4.38 (s, 4H), 4.35 (s, 2H), 3.27-3.04 (m, 24H), 2.21-2.14 (m, 6H), 1.82 (pent,  $J = 7.0$  Hz, 6H), 1.23 (s, 27H).  $^{13}\text{C}$  NMR (125 MHz,  $\text{D}_2\text{O}$ )  $\delta$  ppm 160.3, 141.8, 140.0, 132.4, 131.5, 130.7, 130.3, 130.0, 129.8, 128.9, 128.6, 51.3, 51.0, 50.4, 45.5, 44.7, 44.4, 44.3, 36.2, 28.9, 26.7, 22.9. LRMS calculated for  $\text{C}_{48}\text{H}_{88}\text{N}_{12}\text{O}_3$

$m/z$  881.7  $[M+H]^+$ , Obsd. 881.7.



**CZ-01-137**

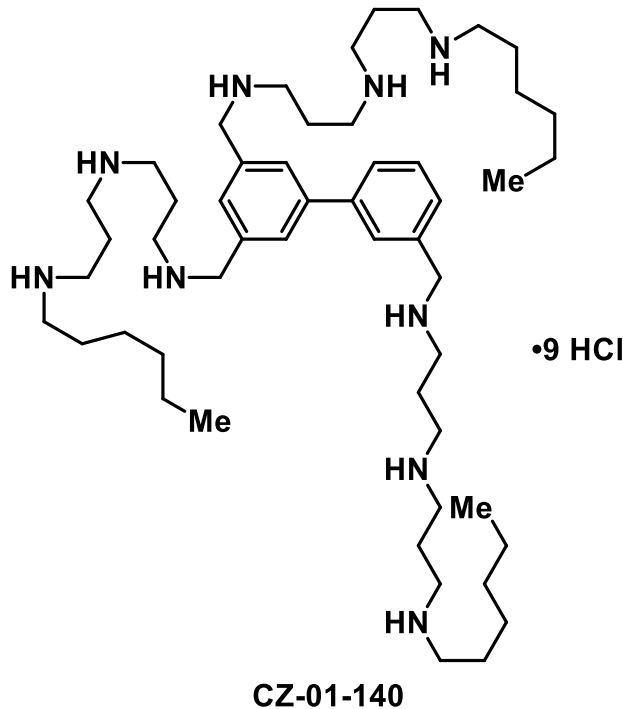
**CZ-01-137:**  $N^1,N^{1'}-(((1,1'-biphenyl)-3,5-diylbis(methylene))bis(azanediy))bis(ethane-2,1-diyl))bis(N^3-hexylpropane-1,3-diamine)$ , hydrochloride salt:  $^1H$  NMR (500 MHz,  $D_2O$ )  $\delta$  ppm 7.88 (s, 2H), 7.74-7.72 (m, 2H), 7.60 (s, 1H), 7.56 (t,  $J = 8.0$  Hz, 2H), 7.50-7.47 (m, 1H), 4.43 (s, 4H), 3.62-3.56 (m, 8H), 3.28 (t,  $J = 8.0$  Hz, 4H), 3.17 (t,  $J = 8.5$  Hz, 4H), 3.06 (t,  $J = 7.5$  Hz, 4H), 2.20-2.14 (m, 4H), 1.68 (pent,  $J = 8.0$  Hz, 4H), 1.41-1.26 (m, 12H), 0.88-0.85 (m, 6H).  $^{13}C$  NMR (125 MHz,  $D_2O$ )  $\delta$  ppm 142.6, 138.8, 132.0, 130.3, 130.0, 129.5, 128.7, 127.3, 51.4, 48.1, 45.3, 44.4, 43.5, 43.0, 30.6, 25.6, 25.5, 22.9, 21.9, 13.5. LRMS calculated for  $C_{36}H_{64}N_6$   $m/z$  581.5  $[M+H]^+$ , Obsd. 581.3.



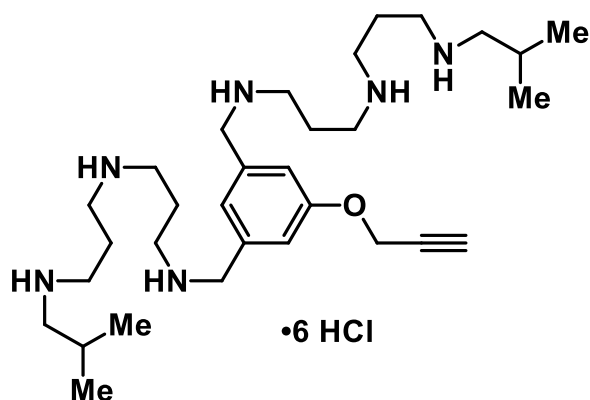
**CZ-01-138:**  $N^1,N^{1'}-(1,3-phenylenebis(methylene))bis(N^3-isobutyl-N1-(3-(isobutylamino)propyl)propane-1,3-diamine)$ , hydrochloride salt: LRMS calculated



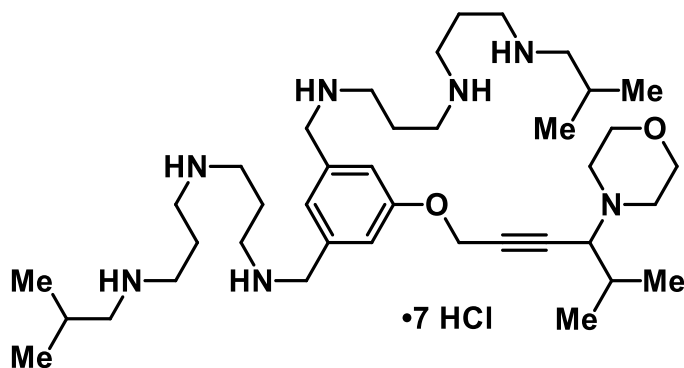
for  $C_{36}H_{72}N_6$   $m/z$  589.6  $[M+H]^+$ , Obsd. 589.4.



**CZ-01-140:**  $N^1, N^{1'}, N^{1''}$ -([1,1'-biphenyl]-3,3',5-triyltris(methylene))tris( $N^3$ -(3-(hexylamino)propyl)propane-1,3-diamine), hydrochloride salt:  $^1\text{H}$  NMR (500 MHz,  $\text{D}_2\text{O}$ )  $\delta$  ppm 7.90 (s, 2H), 7.86-7.81 (m, 2H), 7.65-7.62 (m, 2H), 7.56-7.55 (m, 1H), 4.41 (s, 4H), 4.38 (s, 2H), 3.29-3.12 (m, 24H), 3.05 (t,  $J = 8.0$  Hz, 6H), 2.23-2.09 (m, 12H), 1.67 (t,  $J = 7.5$  Hz, 6H), 1.38-1.29 (m, 18H), 0.86 (t,  $J = 7.0$  Hz, 9H).  $^{13}\text{C}$  NMR (125 MHz,  $\text{D}_2\text{O}$ )  $\delta$  ppm 141.7, 139.9, 132.4, 131.4, 130.6, 130.2, 130.0, 129.8, 128.8, 128.5, 51.4, 51.0, 48.1, 44.8, 44.4, 44.2, 30.5, 25.6, 25.4, 22.8, 21.8, 13.4. LRMS calculated for  $C_{51}H_{97}N_9$   $m/z$  836.8  $[M+H]^+$ , Obsd. 418.8  $[M+H]^+/2$ .

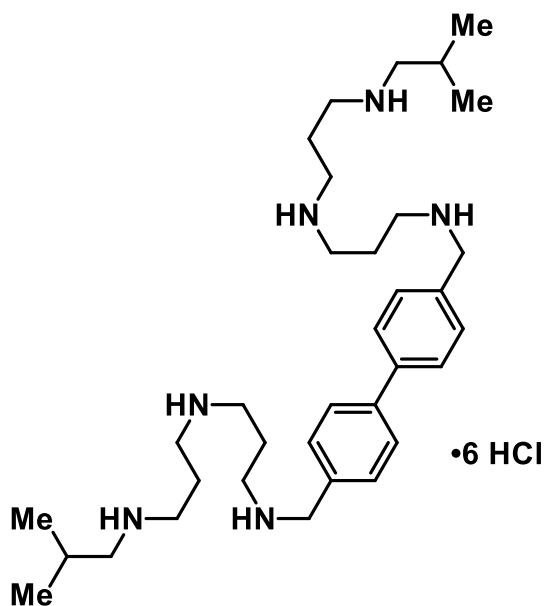


**CZ-01-144:**  $N^1, N^{1'}-((5-(\text{prop-2-yn-1-yloxy})-1,3\text{-phenylene})\text{bis}(\text{methylene}))\text{bis}(N^3\text{-(3-(isobutylamino)propyl)propane-1,3-diamine})$ , hydrochloride salt:  $^1\text{H}$  NMR (500 MHz,  $\text{D}_2\text{O}$ )  $\delta$  ppm 7.33 (s, 1H), 7.31 (s, 2H), 4.93 (d,  $J = 1.5$  Hz, 2H), 4.38 (s, 4H), 3.32-3.22 (m, 16H), 3.08 (t,  $J = 2.0$  Hz, 1H), 3.00 (d,  $J = 7.5$  Hz, 4H), 2.28-2.19 (m, 8H), 2.10 (sept,  $J = 7.0$  Hz, 2H), 1.06 (d,  $J = 7.0$  Hz, 12H).  $^{13}\text{C}$  NMR (125 MHz,  $\text{D}_2\text{O}$ )  $\delta$  ppm 157.7, 133.1, 124.5, 117.7, 78.4, 77.2, 56.4, 54.9, 50.7, 44.8, 44.7, 44.7, 44.2, 25.6, 22.7, 22.6, 19.2.

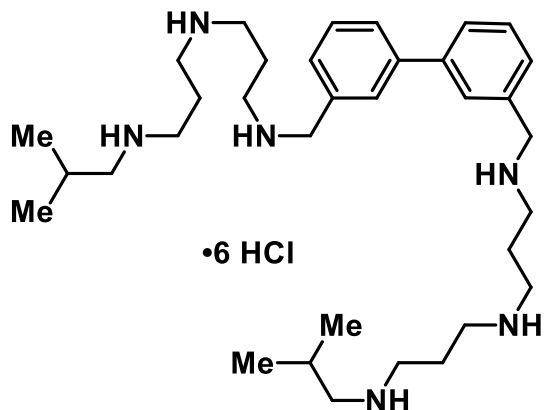


**CZ-01-148:**  $N^1, N^{1'}-((5-((5\text{-methyl-4-morpholinohex-2-yn-1-yl)oxy})-1,3\text{-phenylene})\text{bis}(\text{methylene}))\text{bis}(N^3\text{-(3-(isobutylamino)propyl)propane-1,3-diamine})$ , hydrochloride salt:  $^1\text{H}$  NMR (500 MHz,  $\text{D}_2\text{O}$ )  $\delta$  ppm 7.34 (s, 2H), 7.32 (s, 1H), 5.08 (s, 2H), 4.36 (s, 4H), 4.23 (d,  $J = 6.0$  Hz, 1H), 4.14-3.83 (m, 4H), 3.69-3.46 (m, 4H), 3.32-3.20 (m, 16H), 2.98 (d,  $J = 7.5$  Hz, 4H), 2.41 (oct,  $J = 6.0$  Hz, 1H), 2.27-2.17 (m, 8H), 2.09 (sept,  $J = 6.5$  Hz, 2H), 1.07-1.04 (m, 18H).  $^{13}\text{C}$  NMR (125 MHz,  $\text{D}_2\text{O}$ )  $\delta$  ppm 157.6, 133.3,

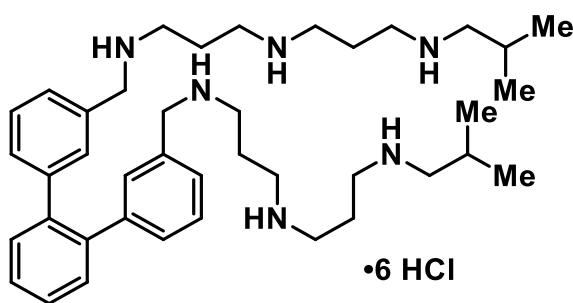
124.5, 117.9, 86.8, 77.3, 65.2, 63.5, 56.2, 54.9, 50.7, 44.8, 44.7, 44.6, 44.3, 27.3, 25.6, 22.6, 22.5, 19.0, 19.0, 16.4.



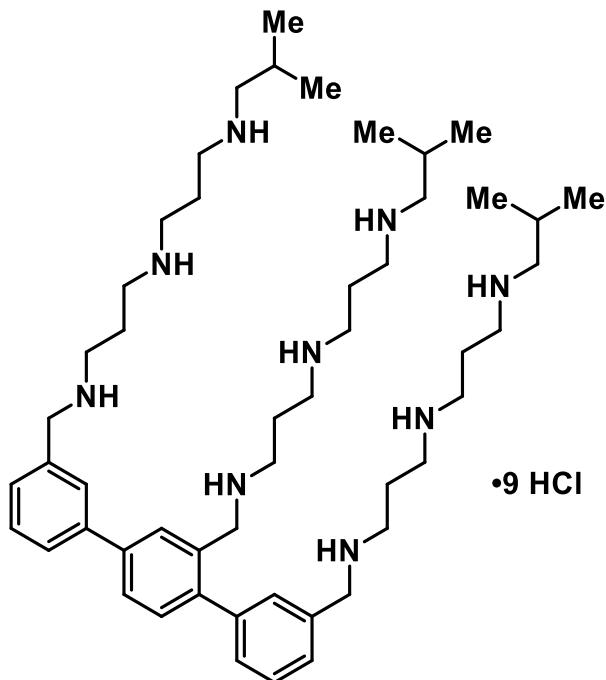
**CZ-01-150:**  $N^1,N^{1'}\text{-}([1,1'\text{-biphenyl}]\text{-}4,4'\text{-diylbis(methylene)})\text{bis}(N^3\text{-(3-(isobutylamino)propyl)propane-1,3-diamine})$ :  $^1\text{H}$  NMR (500 MHz,  $\text{D}_2\text{O}$ )  $\delta$  ppm 7.87 (d,  $J = 7.5$  Hz, 4H), 7.67 (d,  $J = 8.0$  Hz, 4H), 4.40 (s, 4H), 3.32-3.19 (m, 16H), 2.98 (d,  $J = 7.5$  Hz, 4H), 2.28-2.16 (m, 8H), 2.07 (sept,  $J = 7.0$  Hz, 2H), 1.05 (d,  $J = 6.5$  Hz, 12H).  $^{13}\text{C}$  NMR (125 MHz,  $\text{D}_2\text{O}$ )  $\delta$  ppm 140.9, 130.5, 130.1, 127.7, 54.9, 50.9, 44.7, 44.6, 44.0, 25.6, 22.6, 22.5, 19.0. LRMS calculated for  $\text{C}_{34}\text{H}_{60}\text{N}_6$   $m/z$  553.5  $[\text{M}+\text{H}]^+$ , Obsd. 553.3.



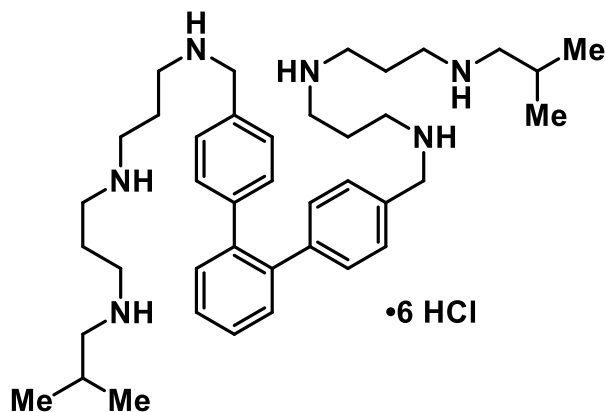
**CZ-01-151:**  $N^1,N^{1'}\text{-}([1,1'\text{-biphenyl}]\text{-}3,3'\text{-diylbis(methylene))bis}(N^3\text{-}(3\text{-(isobutylamino)propyl)propane-1,3-diamine})$ , hydrochloride salt:  $^1\text{H}$  NMR (500 MHz,  $\text{D}_2\text{O}$ )  $\delta$  ppm 7.87-7.85 (m, 4H), 7.67 (t,  $J = 7.0$  Hz, 2H), 7.59-7.58 (m, 2H), 4.42 (s, 4H), 3.32-3.19 (m, 16H), 2.98 (d,  $J = 7.5$  Hz, 4H), 2.28-2.17 (m, 8H), 2.07 (sept,  $J = 7.0$  Hz, 2H), 1.05 (d,  $J = 6.5$  Hz, 12H).  $^{13}\text{C}$  NMR (125 MHz,  $\text{D}_2\text{O}$ )  $\delta$  ppm 140.6, 131.2, 130.0, 129.2, 128.5, 128.3, 54.9, 51.2, 44.8, 44.7, 44.0, 25.6, 22.6, 22.5, 19.1. LRMS calculated for  $\text{C}_{34}\text{H}_{60}\text{N}_6$   $m/z$  553.5  $[\text{M}+\text{H}]^+$ , Obsd. 553.4.



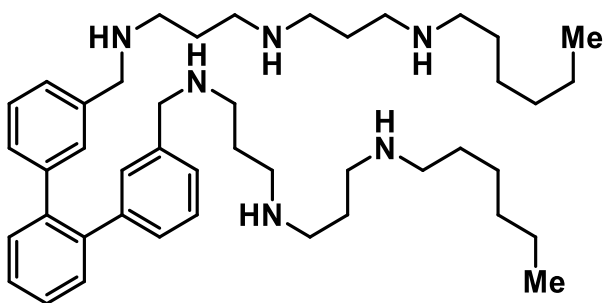
**CZ-01-152:**  $N^1,N^{1'}\text{-}([1,1':2',1''\text{-terphenyl}]\text{-}3,3''\text{-diylbis(methylene))bis}(N^3\text{-}(3\text{-(isobutylamino)propyl)propane-1,3-diamine})$ , hydrochloride salt:  $^1\text{H}$  NMR (500 MHz,  $\text{D}_2\text{O}$ )  $\delta$  ppm 7.64-7.58 (m, 4H), 7.43-7.38 (m, 6H), 7.30-7.28 (m, 2H), 4.23 (s, 4H), 3.24-3.13 (m, 16H), 2.97 (d,  $J = 7.5$  Hz, 4H), 2.22-2.14 (m, 8H), 2.06 (sept,  $J = 6.5$  Hz, 2H), 1.04 (d,  $J = 7.0$  Hz, 12H).  $^{13}\text{C}$  NMR (125 MHz,  $\text{D}_2\text{O}$ )  $\delta$  ppm 142.0, 139.4, 131.2, 131.1, 130.5, 130.4, 128.9, 128.4, 128.1, 54.9, 51.0, 48.9, 44.7, 44.6, 43.8, 25.6, 22.6, 22.5, 19.0. LRMS calculated for  $\text{C}_{40}\text{H}_{64}\text{N}_6$   $m/z$  629.5  $[\text{M}+\text{H}]^+$ , Obsd. 315.2  $[\text{M}+\text{H}]^+/2$ .



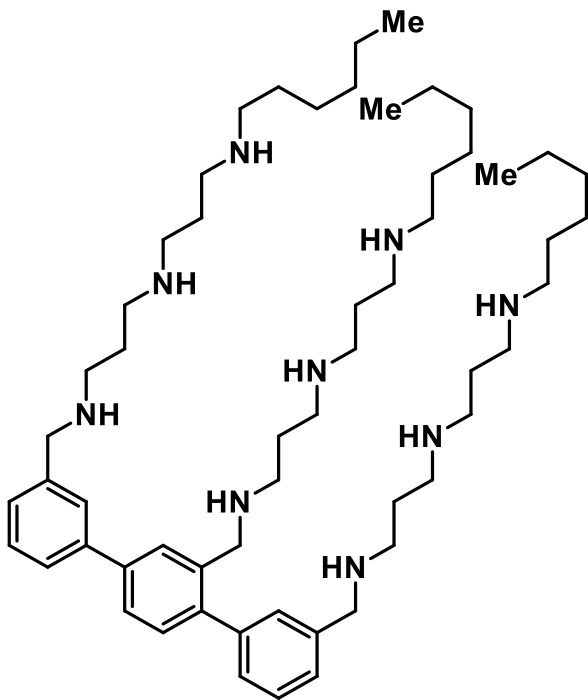
**CZ-01-153:**  $N^1,N^{1'},N^{1''}$ -([1,1':4',1'':2',3,3'']-terphenyl)-2',3,3''-trilyltris(methylene))tris( $N^3$ -(3-(isobutylamino)propyl)propane-1,3-diamine), hydrochloride salt:  $^1\text{H}$  NMR (500 MHz,  $\text{D}_2\text{O}$ )  $\delta$  ppm 7.94-7.90 (m, 3H), 7.81-7.80 (m, 2H), 7.75-7.60 (m, 6H), 4.44-4.43 (m, 6H), 3.36-3.06 (m, 24H), 2.98-2.97 (m, 6H), 2.29-2.03 (m, 15H), 1.05 (d,  $J = 6.5$  Hz, 18H).  $^{13}\text{C}$  NMR (125 MHz,  $\text{D}_2\text{O}$ )  $\delta$  ppm 142.5, 140.9, 140.2, 140.1, 131.3, 131.2, 130.7, 130.3, 130.0, 129.4, 128.5, 128.4, 127.7, 127.1, 54.9, 51.2, 48.0, 44.8, 44.6, 44.7, 44.5, 44.3, 44.2, 44.1, 25.6, 22.6, 22.5, 19.0. LRMS calculated for  $\text{C}_{51}\text{H}_{89}\text{N}_9$   $m/z$  828.7  $[\text{M}+\text{H}]^+$ , Obsd. 414.8  $[\text{M}+\text{H}]^+/2$ .



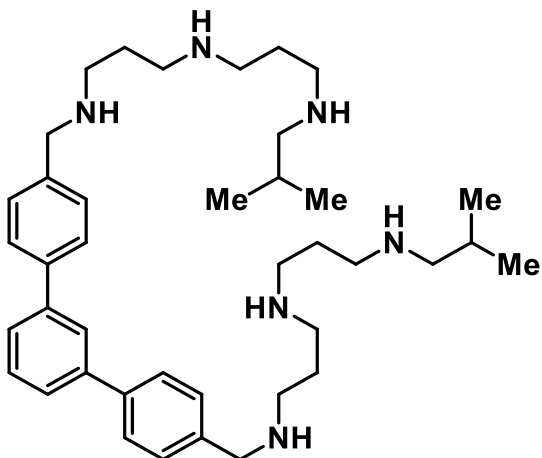
**CZ-01-154:** *N*<sup>1</sup>,*N*<sup>1'</sup>-([1,1':2',1''-terphenyl]-4,4''-diylbis(methylene))bis(*N*<sup>3</sup>-(3-(isobutylamino)propyl)propane-1,3-diamine), hydrochloride salt: <sup>1</sup>H NMR (500 MHz, D<sub>2</sub>O) δ ppm 7.63-7.58 (m, 4H), 7.41 (d, *J* = 8.0 Hz, 4H), 7.33 (d, *J* = 8.5 Hz, 4H), 4.29 (s, 4H), 3.26-3.18 (m, 16H), 2.97 (d, *J* = 7.5 Hz, 4H), 2.23-2.13 (m, 8H), 2.08 (sept, *J* = 7.0 Hz, 2H), 1.05 (d, *J* = 7.0 Hz, 12H). <sup>13</sup>C NMR (125 MHz, D<sub>2</sub>O) δ ppm 142.5, 139.4, 130.6, 130.5, 129.5, 128.9, 128.3, 54.9, 50.9, 44.8, 44.6, 43.9, 25.6, 22.6, 22.5, 19.0. LRMS calculated for C<sub>40</sub>H<sub>64</sub>N<sub>6</sub> m/z 629.6 [M+H]<sup>+</sup>, Obsd. 629.5.



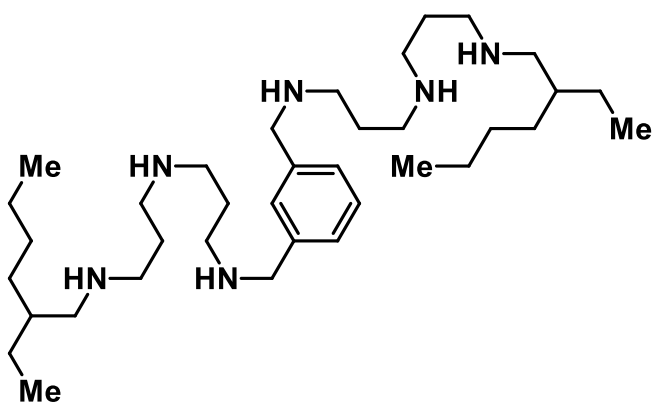
**CZ-01-155:** *N*<sup>1</sup>,*N*<sup>1'</sup>-([1,1':2',1''-terphenyl]-3,3''-diylbis(methylene))bis(*N*<sup>3</sup>-(3-(hexylamino)propyl)propane-1,3-diamine), hydrochloride salt: <sup>1</sup>H NMR (500 MHz, D<sub>2</sub>O) δ ppm 7.63-7.58 (m, 4H), 7.44-7.38 (m, 6H), 7.29 (d, *J* = 7.0 Hz, 2H), 4.24 (s, 4H), 3.27-3.11 (m, 20H), 2.22-2.16 (m, 8H), 1.74 (pent, *J* = 7.0 Hz, 4H), 1.45-1.36 (m, 12H), 0.93 (t, *J* = 6.0 Hz, 6H). <sup>13</sup>C NMR (125 MHz, D<sub>2</sub>O) δ ppm 142.0, 139.4, 131.2, 131.1, 130.6, 130.4, 128.9, 128.4, 128.1, 51.0, 47.9, 44.7, 44.6, 44.2, 43.8, 30.4, 25.4, 25.3, 22.6, 22.6, 21.7, 13.2. LRMS calculated for C<sub>44</sub>H<sub>72</sub>N<sub>6</sub> m/z 685.6 [M+H]<sup>+</sup>, Obsd. 685.4.



**CZ-01-156:**  $N^1, N^{1'}, N^{1''}$ -([1,1':4',1''-terphenyl]-2',3,3''-trilyltris(methylene))tris( $N^3$ -(3-(hexylamino)propyl)propane-1,3-diamine), hydrochloride salt:  $^1\text{H}$  NMR (500 MHz,  $\text{D}_2\text{O}$ )  $\delta$  ppm 7.92-7.88 (m, 3H), 7.81-7.78 (m, 2H), 7.74-7.66 (m, 3H), 7.63-7.60 (m, 3H), 4.45-4.43 (m, 6H), 3.37-3.06 (m, 30H), 2.31-2.06 (m, 12H), 1.76-1.71 (m, 6H), 1.44-1.34 (m, 18H), 0.92 (t,  $J = 6.5$  Hz, 9H).  $^{13}\text{C}$  NMR (125 MHz,  $\text{D}_2\text{O}$ )  $\delta$  ppm 142.5, 140.9, 140.2, 140.0, 131.3, 131.2, 130.8, 130.7, 130.4, 130.0, 129.8, 129.4, 129.3, 128.5, 128.3, 127.6, 127.1, 51.2, 51.2, 48.0, 47.9, 44.7, 44.7, 44.5, 44.3, 44.2, 44.2, 44.1, 30.4, 25.4, 25.3, 22.7, 22.6, 22.5, 21.7, 13.2. LRMS calculated for  $\text{C}_{57}\text{H}_{101}\text{N}_9$   $m/z$  912.8  $[\text{M}+\text{H}]^+$ , Obsd. 456.8  $[\text{M}+\text{H}]^+/2$ .



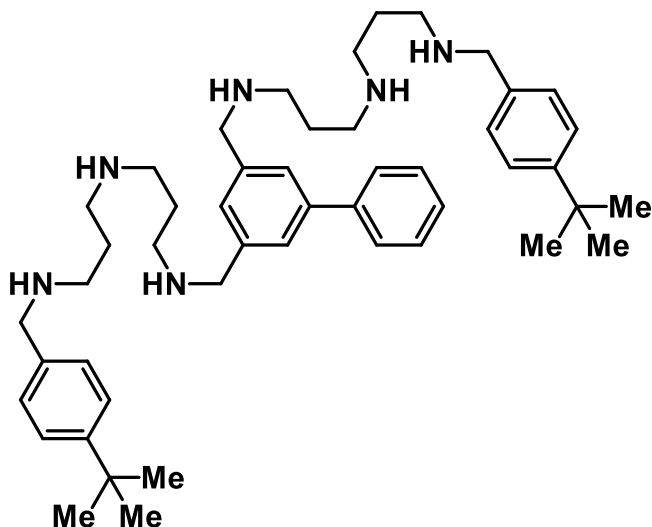
**CZ-01-157:** *N*<sup>1</sup>,*N*<sup>1'</sup>-([1,1':3',1''-terphenyl]-4,4''-diylbis(methylene))bis(*N*<sup>3</sup>-(3-(isobutylamino)propyl)propane-1,3-diamine), hydrochloride salt: <sup>1</sup>H NMR (500 MHz, D<sub>2</sub>O) δ ppm 7.97 (s, 1H), 7.86 (d, *J* = 8.0 Hz, 4H), 7.77 (d, *J* = 7.5 Hz, 2H), 7.68-7.64 (m, 5H), 4.38 (s, 4H), 3.31-3.17 (m, 16H), 2.96 (d, *J* = 7.5 Hz, 4H), 2.25-2.15 (m, 8H), 2.06 (sept, *J* = 7.0 Hz, 2H), 1.03 (d, *J* = 6.5 Hz, 12H). <sup>13</sup>C NMR (125 MHz, D<sub>2</sub>O) δ ppm 141.5, 140.4, 130.5, 129.9, 129.8, 127.7, 126.6, 125.4, 54.9, 50.9, 44.8, 44.6, 43.9, 25.6, 22.6, 22.5, 19.0. LRMS calculated for C<sub>40</sub>H<sub>64</sub>N<sub>6</sub> *m/z* 629.5 [M+H]<sup>+</sup>, Obsd. 629.4.



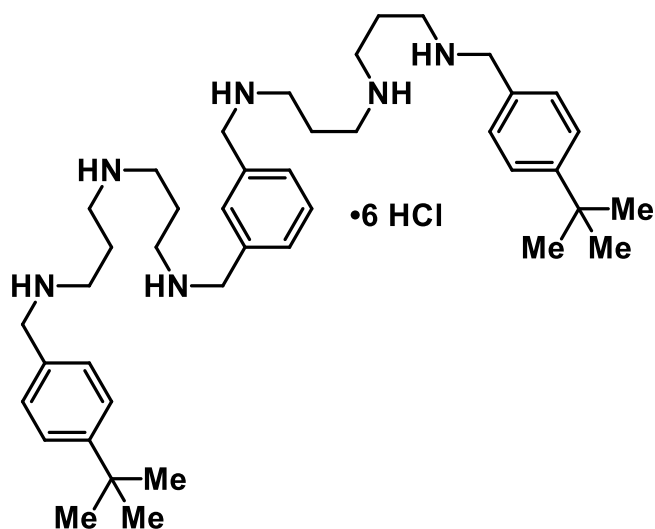
**CZ-01-158:** *N*<sup>1</sup>,*N*<sup>1'</sup>-(1,3-phenylenebis(methylene))bis(*N*<sup>3</sup>-(3-((2-ethylhexyl)amino)propyl)propane-1,3-diamine), hydrochloride salt: <sup>1</sup>H NMR (500 MHz, D<sub>2</sub>O) δ ppm 7.65 (s, 4H), 4.39 (s, 4H), 3.31-3.16 (m, 16H), 3.07 (d, *J* = 7.0 Hz, 4H), 2.26-2.16 (m, 8H), 1.78 (pent, *J* = 6.5 Hz, 2H), 1.48-1.33 (m, 16H), 0.94 (t, *J* = 7.5 Hz,



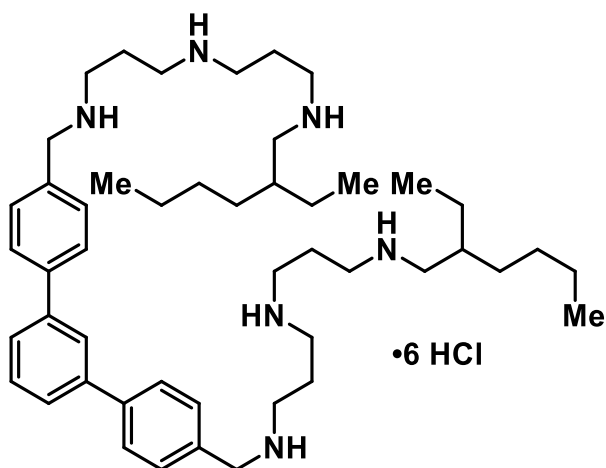
12H).  $^{13}\text{C}$  NMR (125 MHz,  $\text{D}_2\text{O}$ )  $\delta$  ppm 131.5, 131.3, 131.1, 130.2, 51.4, 50.9, 44.9, 44.7, 44.7, 44.1, 36.2, 29.5, 27.6, 22.9, 22.6, 22.5, 22.1, 13.3, 9.4. LRMS calculated for  $\text{C}_{36}\text{H}_{72}\text{N}_6$   $m/z$  589.6  $[\text{M}+\text{H}]^+$ , Obsd. 589.3.



**CZ-01-159:**  $N^1,N^{1'}\text{-}([1,1'\text{-biphenyl}]\text{-}3,5\text{-diylbis(methylene)})\text{bis}(N^3\text{-}((4\text{-}(tert\text{-butyl)benzyl)amino)propyl)propane\text{-}1,3\text{-diamine})$ , hydrochloride salt:  $^1\text{H}$  NMR (500 MHz,  $\text{D}_2\text{O}$ )  $\delta$  ppm 7.92 (s, 2H), 7.80 (d,  $J = 7.5$  Hz, 2H), 7.66-7.62 (m, 7H), 7.56 (t,  $J = 7.0$  Hz, 1H), 7.50 (d,  $J = 8.5$  Hz, 4H), 4.45 (s, 4H), 4.30 (s, 4H), 3.33-3.15 (m, 16H), 2.77-2.12 (m, 8H), 1.37 (m, 18H).  $^{13}\text{C}$  NMR (125 MHz,  $\text{D}_2\text{O}$ )  $\delta$  ppm 153.6, 142.6, 138.9, 132.2, 130.0, 129.8, 129.6, 129.3, 128.5, 127.4, 127.1, 126.3, 50.8, 50.8, 44.6, 44.3, 43.6, 36.6, 34.1, 30.4, 23.7, 22.6. LRMS calculated for  $\text{C}_{48}\text{H}_{72}\text{N}_6$   $m/z$  733.6  $[\text{M}+\text{H}]^+$ , Obsd. 733.4.



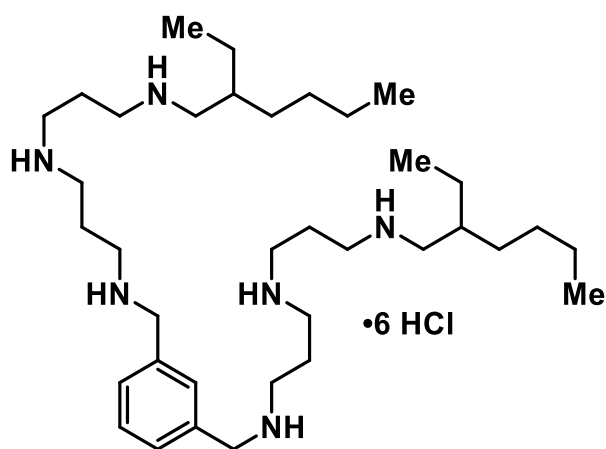
**CZ-01-160:** ***N*<sup>1</sup>,*N*<sup>1'</sup>-(1,3-phenylenebis(methylene))bis(*N*<sup>3</sup>-(3-((4-(*tert*-butyl)benzyl)amino)propyl)propane-1,3-diamine), hydrochloride salt:** <sup>1</sup>H NMR (500 MHz, D<sub>2</sub>O) δ ppm 7.63-7.61 (m, 8H), 7.49-7.48 (m, 4H), 4.35 (s, 4H), 4.28 (s, 4H), 3.28-3.14 (m, 16H), 2.33-2.11 (m, 8H), 1.35 (s, 18H). <sup>13</sup>C NMR (125 MHz, D<sub>2</sub>O) δ ppm 153.5, 131.6, 131.2, 131.1, 129.8, 127.5, 126.3, 50.9, 50.7, 44.6, 44.1, 43.7, 34.1, 30.4, 22.6, 22.6. LRMS calculated for C<sub>42</sub>H<sub>68</sub>N<sub>6</sub> m/z 657.6 [M+H]<sup>+</sup>, Obsd. 657.4.



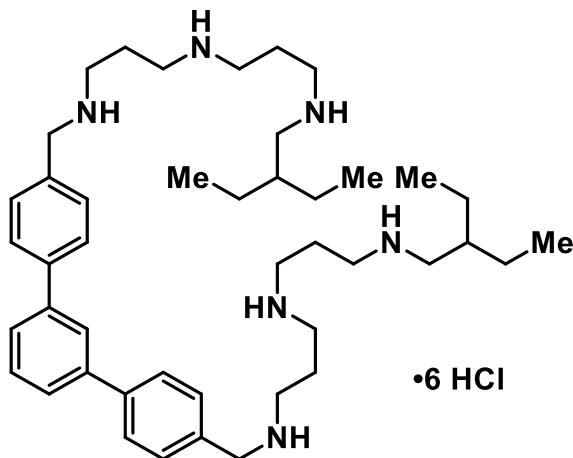
**CZ-01-161**

**CZ-01-161:** ***N*<sup>1</sup>,*N*<sup>1'</sup>-([1,1':3',1''-terphenyl]-4,4''-diylbis(methylene))bis(*N*<sup>3</sup>-(3-((2-ethylhexyl)amino)propyl)propane-1,3-diamine), hydrochloride salt:** <sup>1</sup>H NMR (500

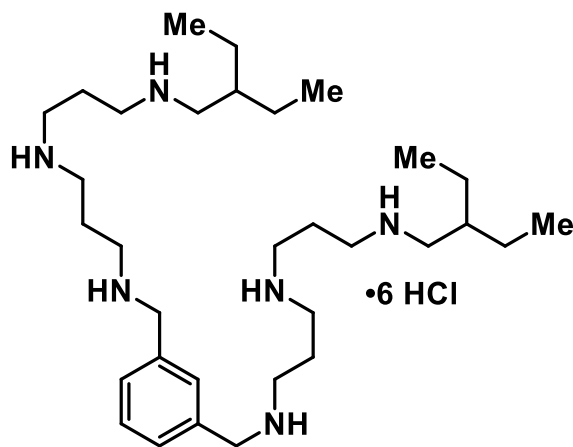
MHz, D<sub>2</sub>O)  $\delta$  ppm 8.06 (t,  $J$  = 1.5 Hz, 1H), 7.91 (d,  $J$  = 8.0 Hz, 4H), 7.84-7.82 (m, 2H), 7.72 (t,  $J$  = 7.5 Hz, 1H), 7.68 (d,  $J$  = 8.0 Hz, 4H), 4.41 (s, 4H), 3.30 (t,  $J$  = 8.0 Hz, 4H), 3.26-3.17 (m, 12H), 3.04 (d,  $J$  = 7.0 Hz, 4H), 2.25-2.18 (m, 8H), 1.76 (sept,  $J$  = 6.0 Hz, 2H), 1.48-1.33 (m, 16H), 0.94-0.91 (m, 12H). <sup>13</sup>C NMR (125 MHz, D<sub>2</sub>O)  $\delta$  ppm 141.4, 140.3, 130.5, 129.8, 129.7, 127.7, 126.6, 125.4, 51.3, 50.8, 44.8, 44.5, 43.8, 36.1, 29.4, 27.5, 22.8, 22.5, 22.4, 22.1, 13.2, 9.3. LRMS calculated for C<sub>48</sub>H<sub>80</sub>N<sub>6</sub>  $m/z$  741.6 [M+H]<sup>+</sup>, Obsd. 371.3. [M+H]<sup>+</sup>/2.



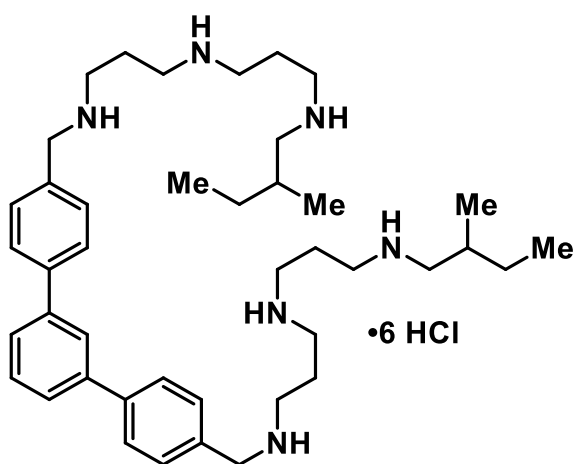
**CZ-01-163:** *N*<sup>1</sup>,*N*<sup>1'</sup>-(1,3-phenylenebis(methylene))bis(*N*<sup>3</sup>-(3-((2-ethylhexyl)amino)propyl)propane-1,3-diamine), hydrochloride salt: <sup>1</sup>H NMR (500 MHz, D<sub>2</sub>O)  $\delta$  ppm 7.57 (s, 4H), 4.30 (s, 4H), 3.23-3.12 (m, 16H), 2.99 (d,  $J$  = 7.0 Hz, 4H), 2.18-2.09 (m, 8H), 1.71(sept,  $J$  = 6.0 Hz, 2H), 1.41-1.25 (m, 16H), 0.86 (t,  $J$  = 7.5 Hz, 12H). <sup>13</sup>C NMR (125 MHz, D<sub>2</sub>O)  $\delta$  ppm 131.4, 131.2, 131.0, 130.1, 51.3, 50.8, 44.8, 44.6, 44.6, 44.0, 36.1, 29.4, 27.5, 22.8, 22.4, 22.1, 13.2, 9.3. LRMS calculated for C<sub>36</sub>H<sub>72</sub>N<sub>6</sub>  $m/z$  589.6 [M+H]<sup>+</sup>, Obsd. 589.4.



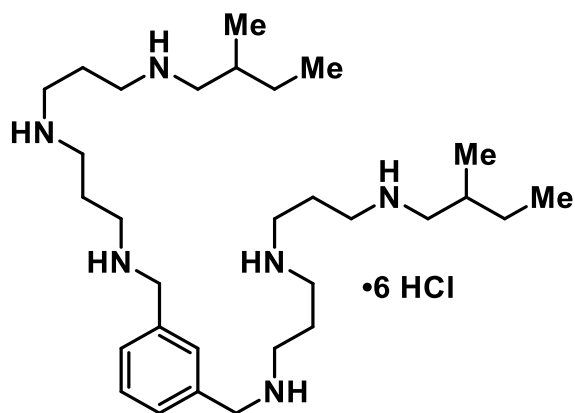
**CZ-01-164:**  $N^1,N^{1'}-([1,1':3',1''\text{-terphenyl}]-4,4''\text{-diylbis(methylene)})\text{bis}(N^3\text{-}((2\text{-ethylbutyl)amino})\text{propyl})\text{propane-1,3-diamine}$ ), hydrochloride salt:  $^1\text{H}$  NMR (500 MHz,  $\text{D}_2\text{O}$ )  $\delta$  ppm 7.97 (t,  $J = 1.5$  Hz, 1H), 7.83 (d,  $J = 8.0$  Hz, 4H), 7.75-7.73 (m, 2H), 7.64 (t,  $J = 7.0$  Hz, 1H), 7.60 (d,  $J = 8.0$  Hz, 4H), 4.33 (s, 4H), 3.23 (t,  $J = 8.0$  Hz, 4H), 3.19-3.10 (m, 12H), 2.97 (d,  $J = 7.0$  Hz, 4H), 2.19-2.08 (m, 8H), 1.64 (sept,  $J = 6.5$  Hz, 2H), 1.37 (p,  $J = 7.0$  Hz, 8H), 0.85 (t,  $J = 7.5$  Hz, 12H).  $^{13}\text{C}$  NMR (125 MHz,  $\text{D}_2\text{O}$ )  $\delta$  ppm 141.5, 140.4, 130.4, 129.8, 129.7, 127.7, 126.6, 125.5, 50.9, 50.8, 44.8, 44.5, 43.8, 37.6, 22.6, 22.3, 22.4, 9.3. LRMS calculated for  $\text{C}_{44}\text{H}_{72}\text{N}_6$   $m/z$  685.6  $[\text{M}+\text{H}]^+$ , Obsd. 343.1  $[\text{M}+\text{H}]^+/2$ .



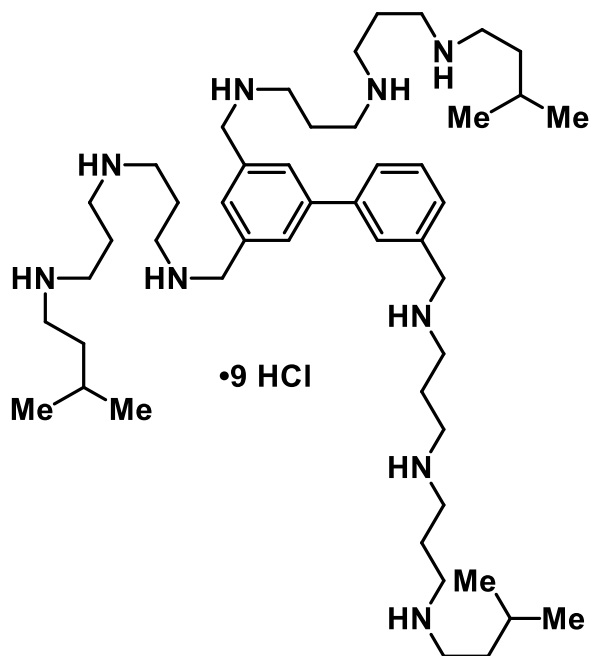
**CZ-01-165:** *N*<sup>1</sup>,*N*<sup>1'</sup>-(1,3-phenylenebis(methylene))bis(*N*<sup>3</sup>-(3-((2-ethylbutyl)amino)propyl)propane-1,3-diamine), hydrochloride salt: <sup>1</sup>H NMR (500 MHz, D<sub>2</sub>O) δ ppm 7.59 (s, 4H), 4.33 (s, 4H), 3.25-3.16 (m, 16H), 3.01 (d, *J* = 7.0 Hz, 4H), 2.20-2.11 (m, 8H), 1.67 (sept, *J* = 7.0 Hz, 2H), 1.40 (p, *J* = 7.5 Hz, 8H), 0.87 (t, *J* = 7.0 Hz, 12H). <sup>13</sup>C NMR (125 MHz, D<sub>2</sub>O) δ ppm 131.6, 131.5, 131.3, 130.4, 51.2, 51.1, 45.1, 44.8, 44.8, 44.3, 37.8, 22.9, 22.7, 22.6, 9.7. LRMS calculated for C<sub>32</sub>H<sub>64</sub>N<sub>6</sub> *m/z* 533.5 [M+H]<sup>+</sup>, Obsd. 533.4 [M+H]<sup>+</sup>.



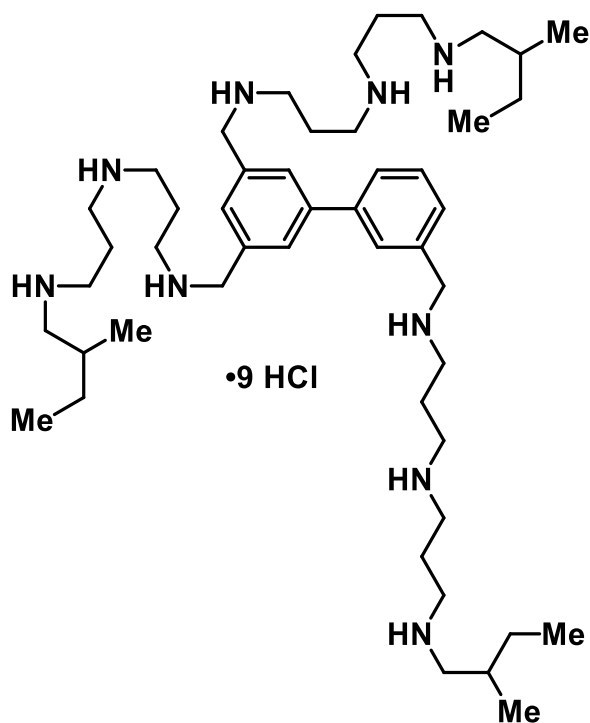
**CZ-01-166:** *N*<sup>1</sup>,*N*<sup>1'</sup>-([1,1':3',1''-terphenyl]-4,4''-diylbis(methylene))bis(*N*<sup>3</sup>-(3-((2-methylbutyl)amino)propyl)propane-1,3-diamine), hydrochloride salt: <sup>1</sup>H NMR (500 MHz, D<sub>2</sub>O) δ ppm 7.86 (t, *J* = 1.5 Hz, 1H), 7.78 (d, *J* = 8.5 Hz, 4H), 7.71-7.67 (m, 2H), 7.63-7.58 (m, 6H), 4.36 (s, 4H), 3.31-3.18 (m, 16H), 3.07 (dd, *J* = 6.0, 12 Hz, 2H), 2.93 (dd, *J* = 8.5, 12.5 Hz, 2H), 2.26-2.17 (m, 8H), 1.89-1.82 (m, 2H), 1.52-1.44 (m, 2H), 1.34-1.25 (m, 2H), 1.03 (d, *J* = 6.5 Hz, 6H), 0.95 (t, *J* = 8.0 Hz, 6H). <sup>13</sup>C NMR (125 MHz, D<sub>2</sub>O) δ ppm 141.4, 140.3, 130.5, 129.8, 129.7, 127.7, 126.6, 125.4, 53.5, 50.9, 44.8, 44.6, 43.9, 31.8, 26.2, 22.6, 22.5, 16.0, 10.1. IR (neat): 3342 (bs), 2963, 2766, 1457 (all s) cm<sup>-1</sup>. mp decomposition (232-234 °C). LRMS calculated for C<sub>42</sub>H<sub>68</sub>N<sub>6</sub> *m/z* 657.6 [M+H]<sup>+</sup>, Obsd. 657.4.



**CZ-01-167:** *N*<sup>1</sup>,*N*<sup>1'</sup>-(1,3-phenylenebis(methylene))bis(*N*<sup>3</sup>-(3-((2-methylbutyl)amino)propyl)propane-1,3-diamine), hydrochloride salt: <sup>1</sup>H NMR (500 MHz, D<sub>2</sub>O)  $\delta$  ppm 7.66 (s, 4H), 4.39 (s, 4H), 3.32-3.21 (m, 16H), 3.10 (dd, *J* = 6.0, 12.0 Hz, 2H), 2.96 (dd, *J* = 8.0, 12.0 Hz, 2H), 2.27-2.18 (m, 8H), 1.88 (oct, *J* = 7.0 Hz, 2H), 1.50 (sept, *J* = 8.0 Hz, 2H), 1.31 (sept, *J* = 7.5 Hz, 2H), 1.05 (d, *J* = 7.0 Hz, 6H), 0.96 (t, *J* = 7.5 Hz, 6H). <sup>13</sup>C NMR (125 MHz, D<sub>2</sub>O)  $\delta$  ppm 131.5, 131.3, 131.1, 130.2, 53.5, 50.9, 44.9, 44.7, 44.7, 44.1, 31.8, 26.2, 22.6, 22.5, 16.0, 10.1. LRMS calculated for C<sub>30</sub>H<sub>60</sub>N<sub>6</sub> *m/z* 505.5 [M+H]<sup>+</sup>, Obsd. 505.4 [M+H]<sup>+</sup>.

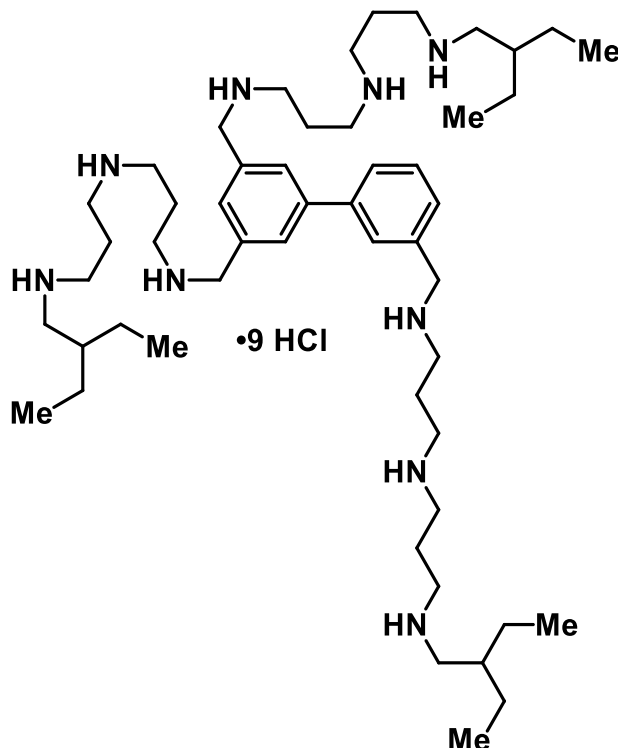


**CZ-01-168:**  $N^1,N^{1'},N^{1''}-([1,1'\text{-biphenyl}]\text{-}3,3',5\text{-triyltris(methylene)})\text{tris}(N^3\text{-(3-(isopentylamino)propyl)propane-1,3-diamine})$ , hydrochloride salt:  $^1\text{H}$  NMR (500 MHz,  $\text{D}_2\text{O}$ )  $\delta$  ppm 7.97 (s, 2H), 7.91-7.88 (m, 2H), 7.72-7.69 (m, 2H), 7.64-7.62 (m, 1H), 4.48 (s, 4H), 4.45 (s, 2H), 3.37-3.20 (m, 24H), 3.15 (t,  $J = 8.5$  Hz, 8H), 2.30-2.17 (m, 14H), 1.72 (sept,  $J = 6.5$  Hz, 3H), 1.66-1.61 (m, 7H), 0.98 (d,  $J = 6.5$  Hz, 18H).  $^{13}\text{C}$  NMR (125 MHz,  $\text{D}_2\text{O}$ )  $\delta$  ppm 141.7, 139.9, 132.3, 131.4, 130.5, 130.1, 129.8, 129.6, 128.6, 128.5, 51.2, 50.9, 46.4, 44.7, 44.3, 34.2, 25.2, 22.7, 22.7, 21.4. IR (neat): 3390 (bs), 2951, 2742, 1450 (all s)  $\text{cm}^{-1}$ . mp decomposition (256-257  $^\circ\text{C}$ ). LRMS calculated for  $\text{C}_{48}\text{H}_{91}\text{N}_9$   $m/z$  794.7  $[\text{M}+\text{H}]^+$ , Obsd. 397.8  $[\text{M}+\text{H}]^+/2$ .



**CZ-01-169:**  $N^1,N^1',N^1''$ -([1,1'-biphenyl]-3,3',5-triyltris(methylene))tris( $N^3$ -(3-((2-methylbutyl)amino)propyl)propane-1,3-diamine), hydrochloride salt:  $^1\text{H}$  NMR (500 MHz,  $\text{D}_2\text{O}$ )  $\delta$  ppm 7.97 (s, 2H), 7.91-7.87 (m, 2H), 7.71-7.69 (m, 2H), 7.63-7.62 (m, 1H), 4.47 (s, 4H), 4.45 (s, 2H), 3.36-3.20 (m, 24H), 3.09 (dd,  $J = 6.0, 12.5$  Hz, 3H), 2.95 (dd,  $J$

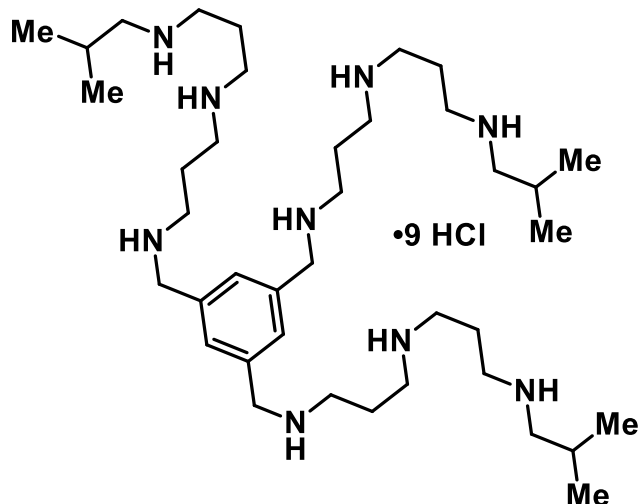
= 7.5, 12.0 Hz, 3H), 2.30-2.18 (m, 12H), 1.87 (oct,  $J = 6.5$  Hz, 3H), 1.49 (sept,  $J = 6.0$  Hz, 3H), 1.32 (sept,  $J = 6.5$  Hz, 3H), 1.04 (d,  $J = 7.0$  Hz, 9H), 0.95 (t,  $J = 7.5$  Hz, 9H).  $^{13}\text{C}$  NMR (125 MHz,  $\text{D}_2\text{O}$ )  $\delta$  ppm 141.7, 139.8, 132.3, 131.3, 130.4, 130.1, 129.8, 129.6, 128.6, 128.4, 53.5, 51.2, 50.9, 44.9, 44.7, 44.3, 44.1, 31.8, 26.2, 22.7, 22.5, 16.0, 10.1. LRMS calculated for  $\text{C}_{48}\text{H}_{91}\text{N}_9$   $m/z$  794.7  $[\text{M}+\text{H}]^+$ , Obsd. 397.8  $[\text{M}+\text{H}]^+/2$ .



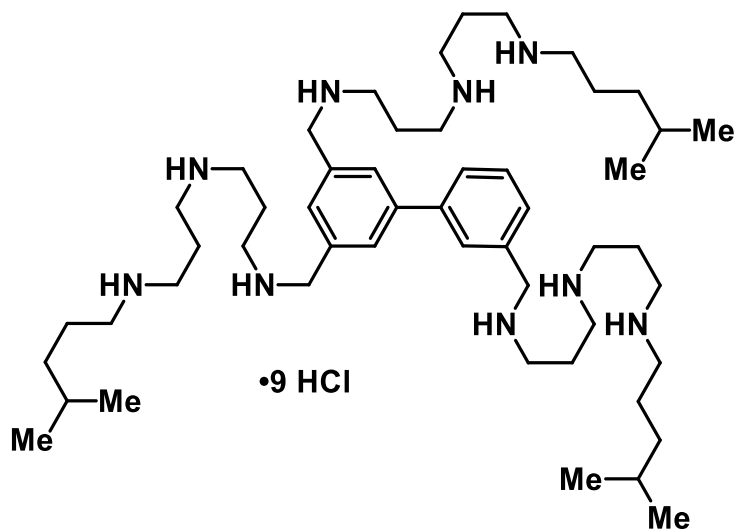
**CZ-01-170:**  $N^1, N^{1'}, N^{1''}$ -([1,1'-biphenyl]-3,3',5-triyltris(methylene))tris( $N^3$ -(3-((2-ethylbutyl)amino)propyl)propane-1,3-diamine), hydrochloride salt:  $^1\text{H}$  NMR (500 MHz,  $\text{D}_2\text{O}$ )  $\delta$  ppm 7.97 (s, 2H), 7.91-7.88 (m, 2H), 7.72-7.69 (m, 2H), 7.64-7.62 (m, 1H), 4.48 (s, 4H), 4.45 (s, 2H), 3.36-3.21 (m, 24H), 3.07 (d,  $J = 7.0$  Hz, 6H), 2.30-2.18 (m, 12H), 1.73 (p,  $J = 6.5$  Hz, 3H), 1.46 (p,  $J = 7.0$  Hz, 12H), 0.94 (t,  $J = 7.5$  Hz, 18H).  $^{13}\text{C}$  NMR (125 MHz,  $\text{D}_2\text{O}$ )  $\delta$  ppm 141.7, 139.9, 132.3, 131.4, 130.4, 130.1, 129.8, 129.6, 128.6, 128.4, 51.0, 44.9, 44.7, 44.7, 44.3, 44.1, 37.6, 22.7, 22.5, 22.5, 9.5. IR (neat): 3457 (bs), 2840, 1468 (all s)  $\text{cm}^{-1}$ . mp decomposition (223-225  $^\circ\text{C}$ ). LRMS calculated for  $\text{C}_{51}\text{H}_{97}\text{N}_9$



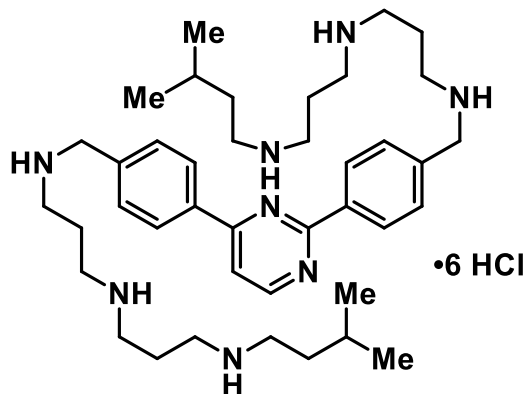
$m/z$  836.8  $[M+H]^+$ , Obsd. 418.8  $[M+H]^+/2$ .



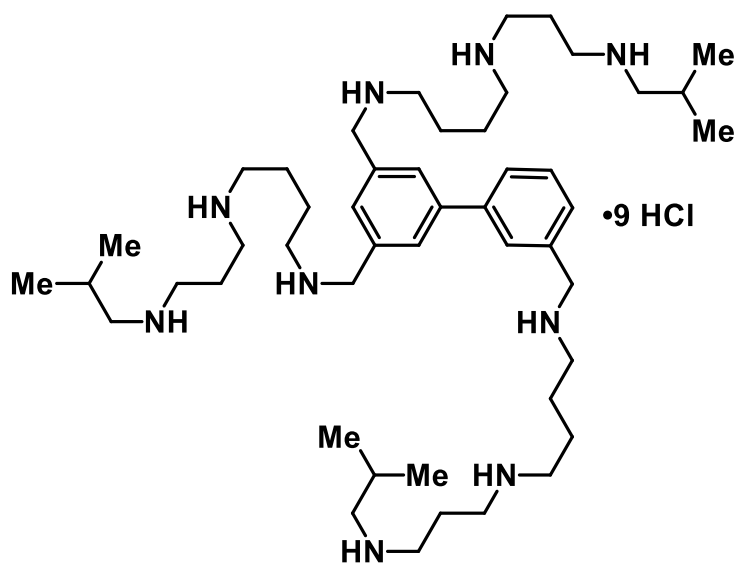
**CZ-01-171:** *N*<sup>1</sup>,*N*<sup>1'</sup>,*N*<sup>1''</sup>-(benzene-1,3,5-triyltris(methylene))tris(*N*<sup>3</sup>-(3-(isobutylamino)propyl)propane-1,3-diamine), hydrochloride salt: <sup>1</sup>H NMR (500 MHz, D<sub>2</sub>O)  $\delta$  ppm 7.77 (s, 3H), 4.44 (s, 6H), 3.34-3.20 (m, 24H), 2.99 (d,  $J$  = 7.5 Hz, 6H), 2.28-2.18 (m, 12H), 2.08 (sept,  $J$  = 7.0 Hz, 3H), 1.05 (d,  $J$  = 6.5 Hz, 18H). <sup>13</sup>C NMR (125 MHz, D<sub>2</sub>O)  $\delta$  ppm 132.6, 54.9, 50.5, 44.8, 44.7, 44.7, 44.4, 25.6, 22.7, 22.5, 19.1. LRMS calculated for C<sub>39</sub>H<sub>81</sub>N<sub>9</sub>  $m/z$  675.7  $[M+H]^+$ , Obsd. 676.5  $[M+H]^+$ .



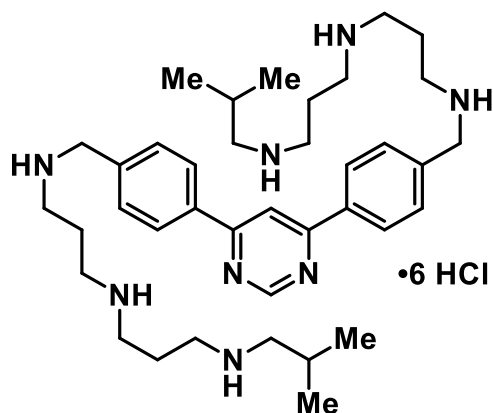
**CZ-01-172:**  $N^1,N^{1'},N^{1''}$ -([1,1'-biphenyl]-3,3',5-triyltris(methylene))tris( $N^3$ -(3-((4-methylpentyl)amino)propyl)propane-1,3-diamine), hydrochloride salt:  $^1\text{H}$  NMR (500 MHz,  $\text{D}_2\text{O}$ )  $\delta$  ppm 7.90-7.52 (m, 8H), 4.38 (s, 4H), 4.36 (s, 2H), 3.27-3.06 (m, 24H), 3.02 (t,  $J = 7.5$  Hz, 6H), 2.20-2.06 (m, 12H), 1.66 (t,  $J = 7.5$  Hz, 6H), 1.55 (sept,  $J = 6.5$  Hz, 3H), 1.22 (q,  $J = 8.5$  Hz, 6H), 1.15 (tt,  $J = 1.0, 7.0$  Hz, 6H), 0.85 (d,  $J = 6.5$  Hz, 18H).



**CZ-01-174:**  $N^1,N^1$ -((pyrimidine-2,4-diylbis(4,1-phenylene))bis(methylene))bis( $N^3$ -(3-(isopentylamino)propyl)propane-1,3-diamine), hydrochloride salt:  $^1\text{H}$  NMR (500 MHz,  $\text{D}_2\text{O}$ )  $\delta$  ppm 8.91 (d,  $J = 5.5$  Hz, 1H), 8.36 (d,  $J = 8.0$  Hz, 2H), 8.27 (d,  $J = 7.5$  Hz, 2H), 7.96 (d,  $J = 5.5$  Hz, 1H), 7.72 (d,  $J = 7.0$  Hz, 4H), 4.43 (s, 2H), 4.42 (s, 2H), 3.35-3.20 (m, 16H), 3.14 (t,  $J = 8.0$  Hz, 4H), 2.28-2.16 (m, 8H), 1.72 (sept,  $J = 6.5$  Hz, 2H), 1.65-1.60 (m, 4H), 0.97 (d,  $J = 6.5$  Hz, 12H).  $^{13}\text{C}$  NMR (125 MHz,  $\text{D}_2\text{O}$ )  $\delta$  ppm 164.5, 163.4, 157.7, 137.6, 136.9, 133.8, 133.4, 130.5, 130.4, 129.0, 128.4, 116.4, 50.8, 50.8, 46.4, 44.7, 44.6, 44.2, 44.2, 44.1, 34.1, 25.2, 22.6, 21.3. LRMS calculated for  $\text{C}_{40}\text{H}_{66}\text{N}_8$   $m/z$  659.5  $[\text{M}+\text{H}]^+$ , Obsd. 659.4.

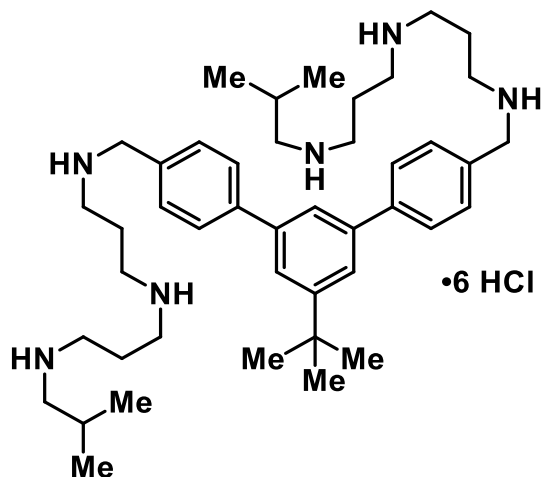


**CZ-01-175:**  $N^1, N^{1'}, N^{1''}$ -([1,1'-biphenyl]-3,3',5-triyltris(methylene))tris( $N^4$ -(3-(isobutylamino)propyl)butane-1,4-diamine), hydrochloride salt:  $^1\text{H}$  NMR (500 MHz,  $\text{D}_2\text{O}$ )  $\delta$  ppm 7.89 (s, 2H), 7.84-7.80 (m, 2H), 7.65-7.55 (m, 3H), 4.38 (s, 4H), 4.36 (s, 2H), 3.22-3.14 (m, 24H), 2.93 (d,  $J = 7.5$  Hz, 6H), 2.16-2.13 (m, 6H), 2.02 (sept,  $J = 6.5$  Hz, 3H), 1.89-1.76 (m, 12H), 0.99 (d,  $J = 7.0$  Hz, 18H). LRMS calculated for  $\text{C}_{48}\text{H}_{91}\text{N}_9$   $m/z$  794.7  $[\text{M}+\text{H}]^+$ , Obsd. 397.9  $[\text{M}+\text{H}]^+/2$ .

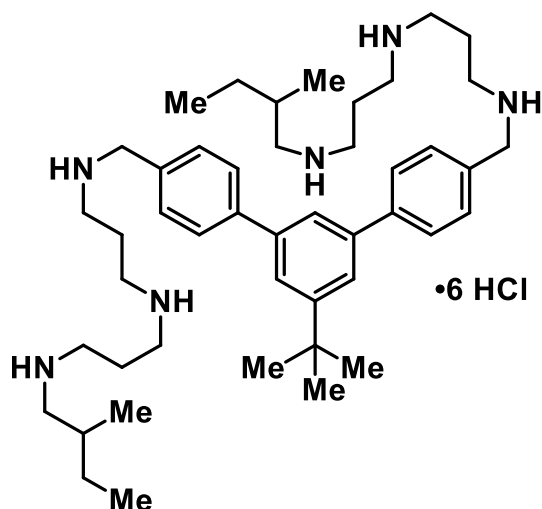


**CZ-01-176:**  $N^1, N^{1'}$ -((pyrimidine-4,6-diylbis(4,1-phenylene))bis(methylene))bis( $N^3$ -(3-(isobutylamino)propyl)propane-1,3-diamine), hydrochloride salt:  $^1\text{H}$  NMR (500 MHz,  $\text{D}_2\text{O}$ )  $\delta$  ppm 9.22 (s, 1H), 8.37 (s, 1H), 8.16 (d,  $J = 8.5$  Hz, 4H), 7.71 (d,  $J = 8.0$  Hz, 4H),

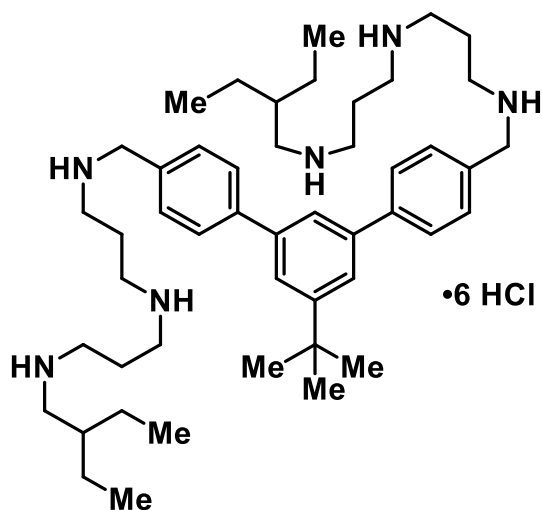
4.39 (s, 4H), 3.28 (t,  $J = 8.5$  Hz, 4H), 3.23-3.15 (m, 12H), 2.93 (d,  $J = 7.0$  Hz, 4H), 2.23-2.12 (m, 8H), 2.02 (sept,  $J = 7.0$  Hz, 2H), 1.00 (d,  $J = 6.5$  Hz, 12H).  $^{13}\text{C}$  NMR (125 MHz,  $\text{D}_2\text{O}$ )  $\delta$  ppm 164.6, 157.6, 136.9, 133.7, 130.6, 128.4, 115.6, 54.8, 50.7, 44.7, 44.6, 44.6, 44.1, 25.5, 22.6, 22.5, 19.0. LRMS calculated for  $\text{C}_{38}\text{H}_{62}\text{N}_8$   $m/z$  631.5  $[\text{M}+\text{H}]^+$ , Obsd. 631.9.



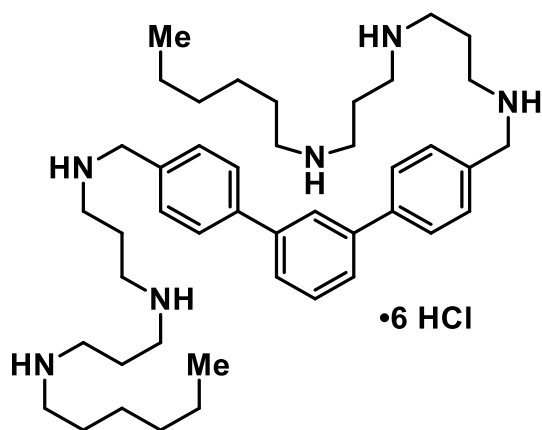
**CZ-01-177:**  $N^1, N^{1'}\text{-}((5'\text{-}(tert\text{-butyl})\text{-}[1,1':3',1''\text{-terphenyl}] \text{-}4,4''\text{-diyl})\text{bis(methylene)})\text{bis}(N^3\text{-}(3\text{-(isobutylamino)propyl)propane-1,3-diamine})$ ,  
**hydrochloride salt:**  $^1\text{H}$  NMR (500 MHz,  $\text{D}_2\text{O}$ )  $\delta$  ppm 7.78 (d,  $J = 7.5$  Hz, 4H), 7.74 (d, 2H), 7.71 (s, 1H), 7.60 (d,  $J = 8.0$  Hz, 4H), 4.34 (s, 4H), 3.28-3.14 (m, 16H), 2.93 (d,  $J = 7.0$  Hz, 4H), 2.22-2.12 (m, 8H), 2.02 (sept,  $J = 7.0$  Hz, 2H), 1.39 (s, 9H), 1.00 (d,  $J = 6.5$  Hz, 12H).  $^{13}\text{C}$  NMR (125 MHz,  $\text{D}_2\text{O}$ )  $\delta$  ppm 153.4, 141.8, 140.5, 130.4, 129.7, 127.8, 123.8, 122.9, 54.9, 50.9, 44.7, 44.6, 43.9, 34.5, 30.5, 25.5, 22.6, 22.5, 19.0. LRMS calculated for  $\text{C}_{44}\text{H}_{72}\text{N}_6$   $m/z$  685.6  $[\text{M}+\text{H}]^+$ , Obsd. 343.3  $[\text{M}+\text{H}]^+/2$



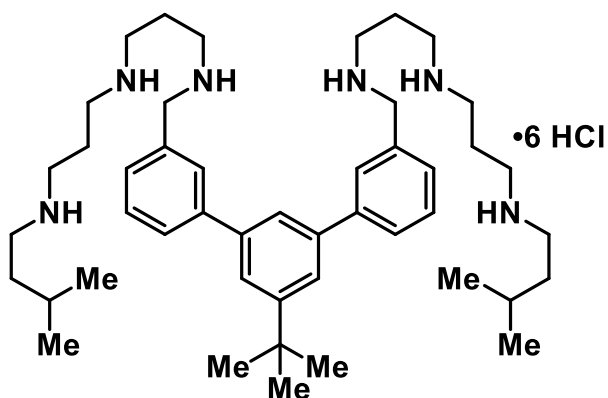
**CZ-01-178:**  $N^1,N^{1'}-((5'-(tert\text{-}butyl)\text{-}[1,1':3',1''\text{-}terphenyl]\text{-}4,4''\text{-}diyl)bis(methylene))bis(N^3\text{-}(3\text{-}((2\text{-}methylbutyl)amino)propyl)propane\text{-}1,3\text{-}diamine)$  ,  
**hydrochloride salt:**  $^1\text{H}$  NMR (500 MHz,  $\text{D}_2\text{O}$ )  $\delta$  ppm 7.65 (d,  $J = 7.5$  Hz, 4H), 7.59 (s, 2H), 7.57-7.52 (m, 5H), 4.27 (s, 4H), 3.22-3.09 (m, 16H), 2.98 (dd,  $J = 6.0, 12.0$  Hz, 2H), 2.84 (dd,  $J = 8.5, 12.0$  Hz, 2H), 2.18-2.09 (m, 8H), 1.77 (hex,  $J = 6.0$  Hz, 2H), 1.39 (sept,  $J = 7.0$  Hz, 2H), 1.27 (s, 9H), 1.23-1.19 (m, 2H), 0.94 (d,  $J = 6.0$  Hz, 6H), 0.86 (t,  $J = 7.5$  Hz, 6H).  $^{13}\text{C}$  NMR (125 MHz,  $\text{D}_2\text{O}$ )  $\delta$  ppm 153.2, 141.7, 140.2, 130.4, 129.6, 127.7, 123.6, 122.8, 53.4, 50.9, 48.8, 44.8, 44.6, 43.9, 34.4, 31.7, 30.5, 26.2, 22.6, 22.5, 15.9, 10.0.  
 LRMS calculated for  $\text{C}_{46}\text{H}_{76}\text{N}_6$   $m/z$  713.6  $[\text{M}+\text{H}]^+$ , Obsd. 356.6  $[\text{M}+\text{H}]^+/2$ .



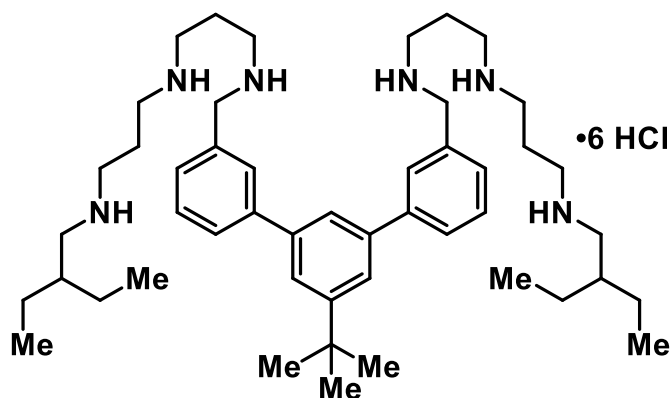
**CZ-01-179:** *N*<sup>1</sup>,*N*<sup>1'</sup>-((5'-(*tert*-butyl)-[1,1':3',1''-terphenyl]-4,4''-diyl)bis(methylene))bis(*N*<sup>3</sup>-(3-((2-ethylbutyl)amino)propyl)propane-1,3-diamine), hydrochloride salt: <sup>1</sup>H NMR (500 MHz, D<sub>2</sub>O) δ ppm 7.78-7.69 (m, 7H), 7.61 (bs, 4H), 4.38 (s, 4H), 3.26-3.20 (m, 16H), 3.01 (s, 4H), 2.17 (bs, 8H), 1.67 (bs, 2H), 1.38 (bs, 17H), 0.88 (s, 12H). <sup>13</sup>C NMR (125 MHz, D<sub>2</sub>O) δ ppm 153.4, 141.8, 140.4, 130.4, 129.7, 127.8, 123.8, 122.9, 50.9, 50.9, 44.9, 44.6, 43.9, 37.6, 34.4, 30.5, 22.6, 22.4, 22.4, 9.4. IR (neat): 3334 (bs), 2963, 2766, 1457 (all s) cm<sup>-1</sup>. mp decomposition (180-184 °C). LRMS calculated for C<sub>48</sub>H<sub>80</sub>N<sub>6</sub> m/z 741.6 [M+H]<sup>+</sup>, Obsd. 370.7 [M+H]<sup>+</sup>/2.



**CZ-01-180:** *N*<sup>1</sup>,*N*<sup>1'</sup>-([1,1':3',1''-terphenyl]-4,4''-diylbis(methylene))bis(*N*<sup>3</sup>-(3-(hexylamino)propyl)propane-1,3-diamine), hydrochloride salt: <sup>1</sup>H NMR (500 MHz, D<sub>2</sub>O) δ ppm 8.62-8.55 (m, 1H), 8.50 (d, *J* = 8.5 Hz, 4H), 8.39 (d, *J* = 7.5 Hz, 2H), 8.34-8.29 (m, 5H), 4.87 (s, 4H), 3.77 (t, *J* = 7.5 Hz, 4H), 3.72-3.64 (m, 12H), 3.57 (t, *J* = 7.5 Hz, 4H), 2.75-2.62 (m, 8H), 2.28-2.22 (m, 4H), 1.99-1.88 (m, 12H), 1.53 (t, *J* = 6.5 Hz, 6H). LRMS calculated for C<sub>44</sub>H<sub>72</sub>N<sub>6</sub> m/z 685.6 [M+H]<sup>+</sup>, Obsd. 342.5 [M+H]<sup>+</sup>/2.

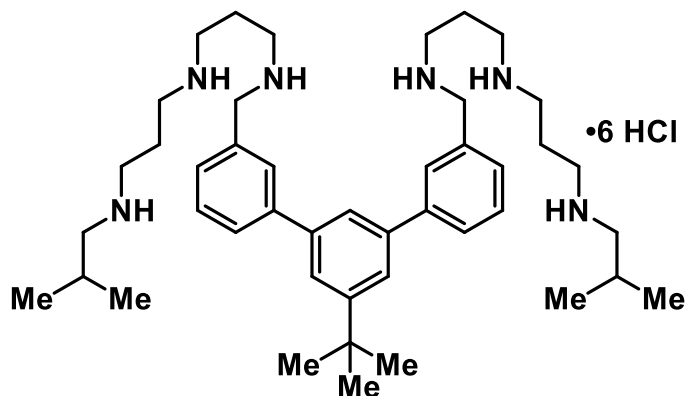


**CZ-01-182:**  $N^1, N^{1'}-((5'-(tert\text{-butyl})-[1,1':3',1'']\text{-terphenyl})-3,3''\text{-diyl})\text{bis(methylene))bis}(N^3\text{-}(3\text{-}(\text{isopentylamino})\text{propyl})\text{propane-1,3-diamine})$ , hydrochloride salt:  $^1\text{H}$  NMR (500 MHz,  $\text{D}_2\text{O}$ )  $\delta$  ppm 7.86-7.82 (m, 6H), 7.63 (t,  $J = 7.5$  Hz, 2H), 7.53 (d,  $J = 7.5$  Hz, 2H), 4.37 (s, 4H), 3.26-3.05 (m, 20H), 2.20-2.07 (m, 8H), 1.65 (sept,  $J = 6.5$  Hz, 2H), 1.57-1.53 (m, 4H), 1.43 (s, 9H), 0.90 (d,  $J = 7.0$  Hz, 12H).  $^{13}\text{C}$  NMR (125 MHz,  $\text{D}_2\text{O}$ )  $\delta$  ppm 153.6, 141.5, 140.8, 131.1, 129.8, 128.9, 128.6, 128.5, 123.8, 123.1, 51.2, 46.3, 44.5, 44.1, 43.9, 34.5, 34.1, 30.5, 25.1, 22.6, 22.6, 21.2. IR (neat): 3367 (bs), 2957, 1457 (all s)  $\text{cm}^{-1}$ . mp decomposition (218-220  $^{\circ}\text{C}$ ). LRMS calculated for  $\text{C}_{46}\text{H}_{76}\text{N}_6$   $m/z$  713.6  $[\text{M}+\text{H}]^+$ , Obsd. 713.5  $[\text{M}+\text{H}]^+$ .



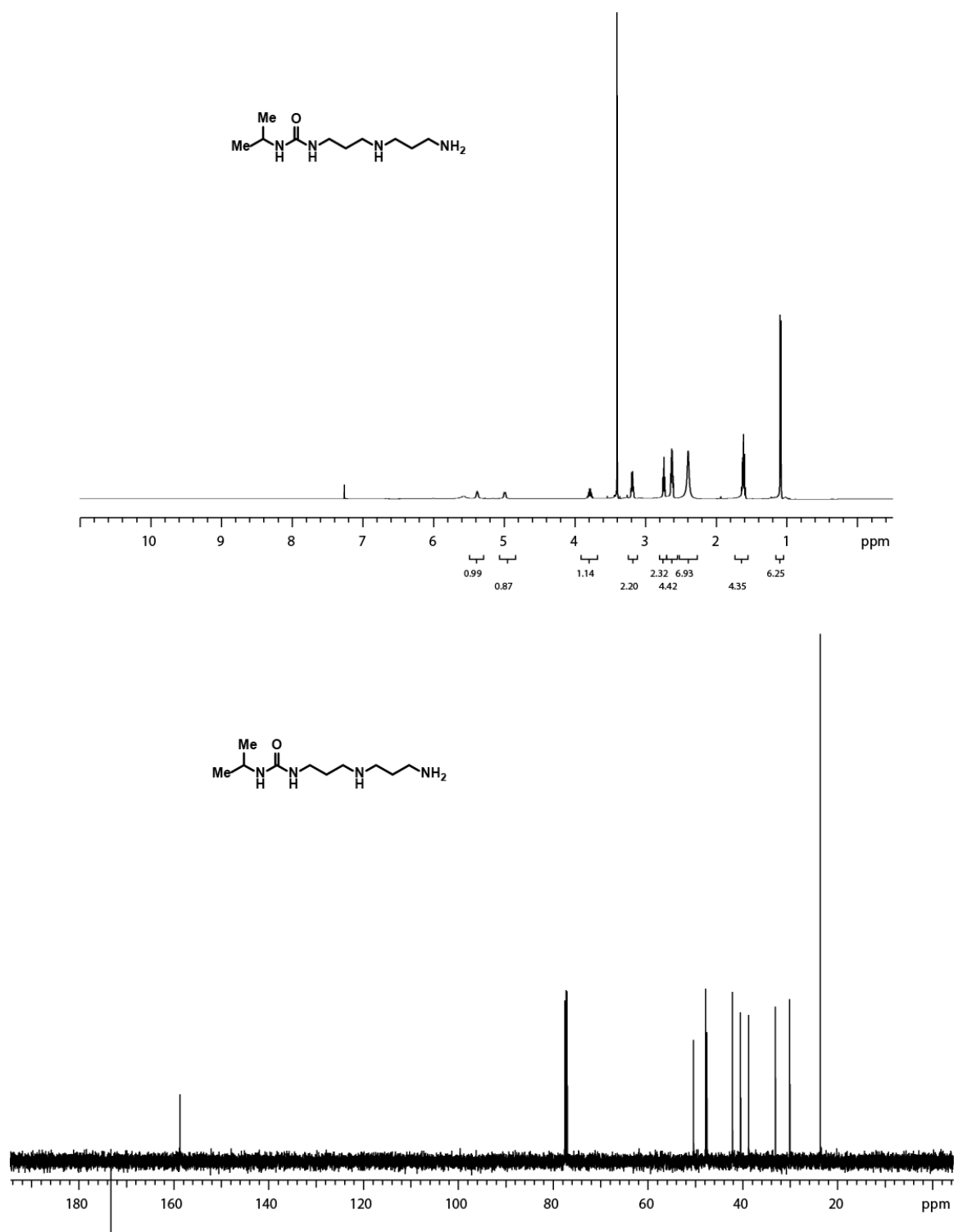
**CZ-01-183:**  $N^1, N^{1'}-((5'-(tert\text{-butyl})-[1,1':3',1'']\text{-terphenyl})-3,3''\text{-diyl})\text{bis(methylene))bis}(N^3\text{-}(3\text{-}((2\text{-ethylbutyl})\text{amino})\text{propyl})\text{propane-1,3-diamine})$ , hydrochloride salt:  $^1\text{H}$  NMR (500 MHz,  $\text{D}_2\text{O}$ )  $\delta$  ppm 7.80-7.68 (m, 7H), 7.59-7.50 (m,

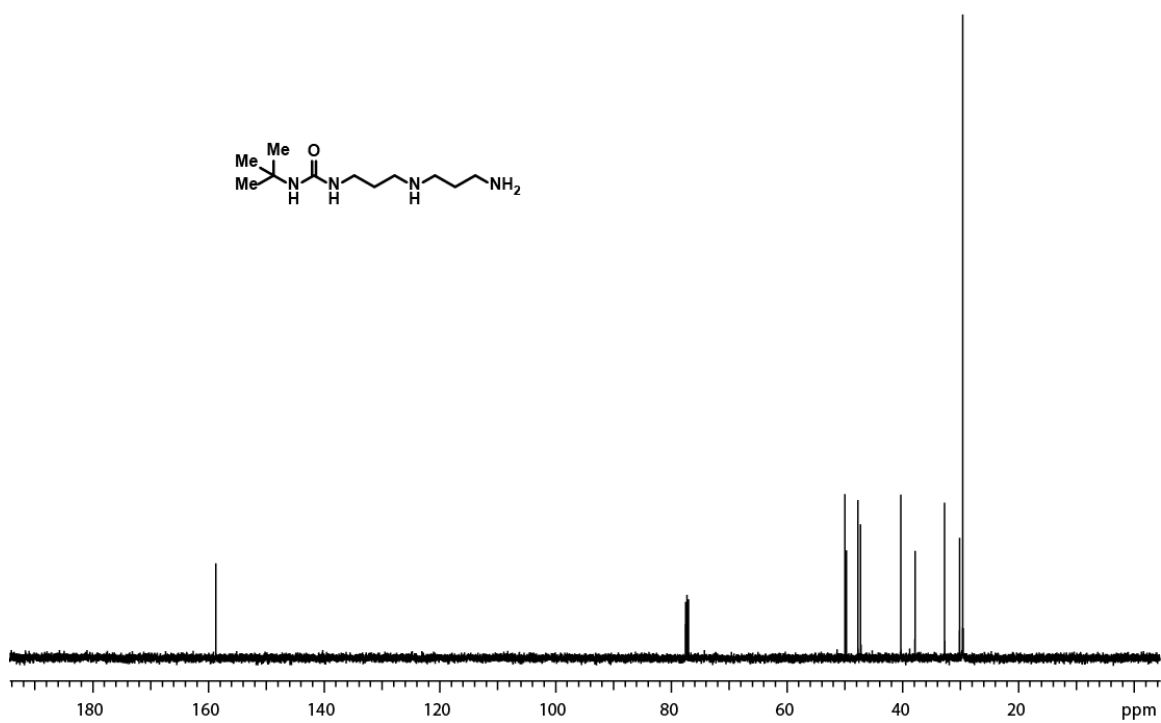
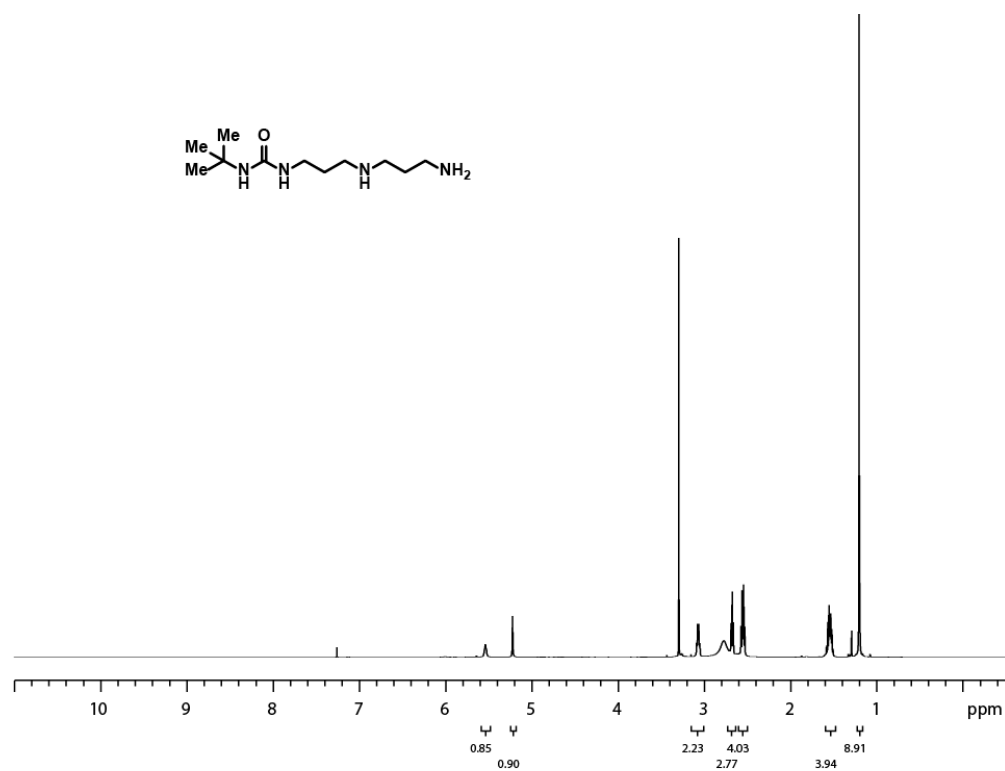
4H), 4.32 (s, 4H), 3.24-3.13 (m, 16H), 2.99 (d,  $J = 6.5$  Hz, 4H), 2.18-2.14 (m, 8H), 1.66 (pent,  $J = 5.5$  Hz, 2H), 1.38 (s, 17H), 0.87 (t,  $J = 6.5$  Hz, 12H).  $^{13}\text{C}$  NMR (125 MHz,  $\text{D}_2\text{O}$ )  $\delta$  ppm 153.4, 141.4, 140.5, 131.0, 129.8, 128.9, 128.5, 128.3, 123.6, 122.9, 51.2, 50.9, 44.8, 44.6, 43.9, 37.6, 34.5, 30.5, 22.6, 22.4, 22.4, 9.4. LRMS calculated for  $\text{C}_{48}\text{H}_{80}\text{N}_6$   $m/z$  741.6  $[\text{M}+\text{H}]^+$ , Obsd. 741.6  $[\text{M}+\text{H}]^+$ .

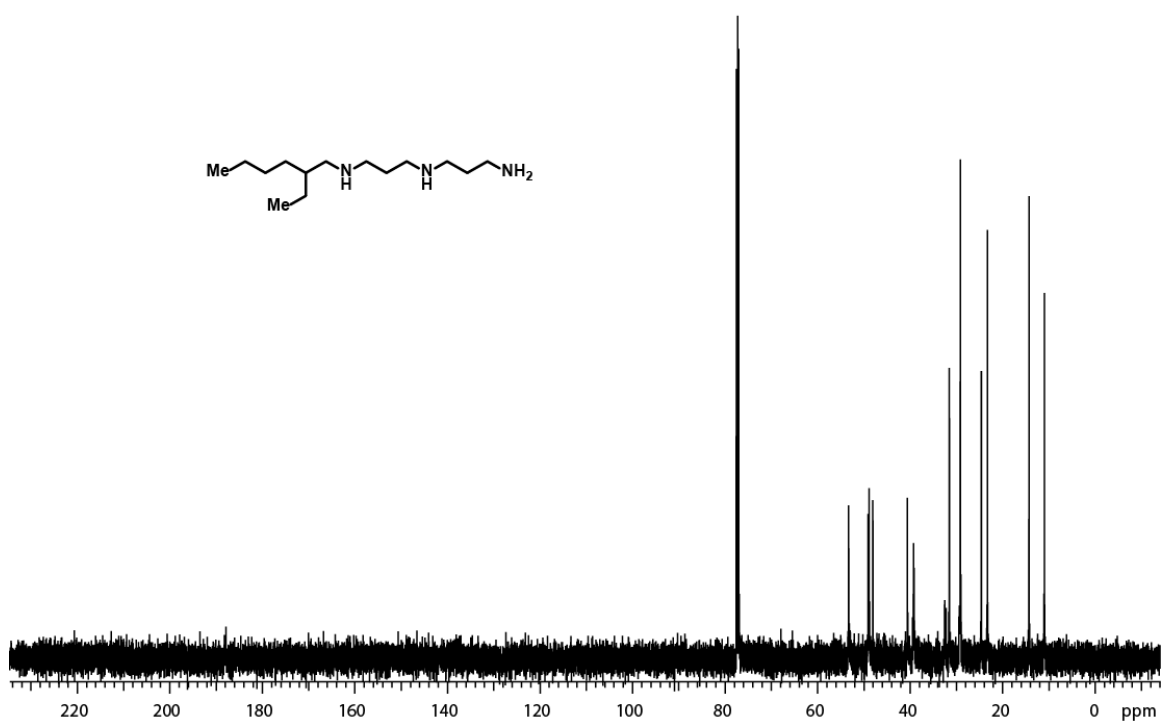
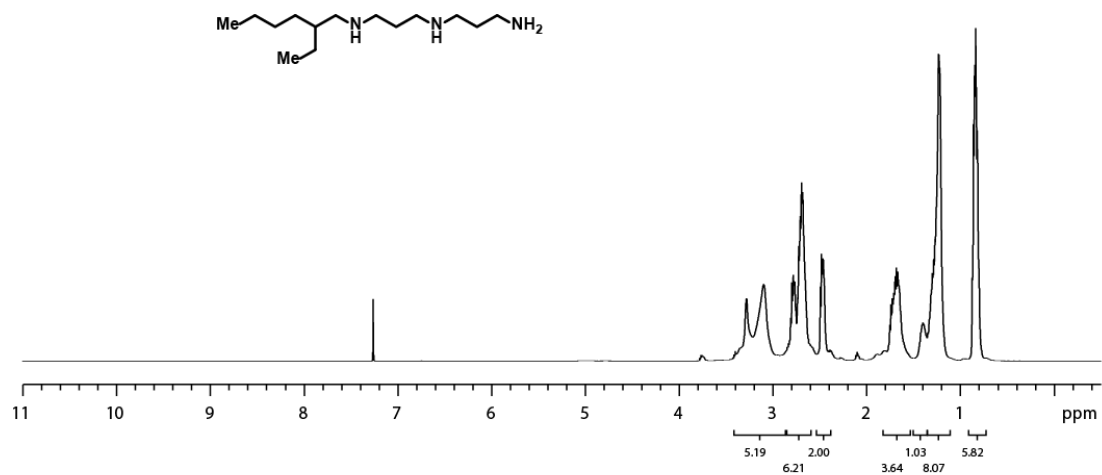


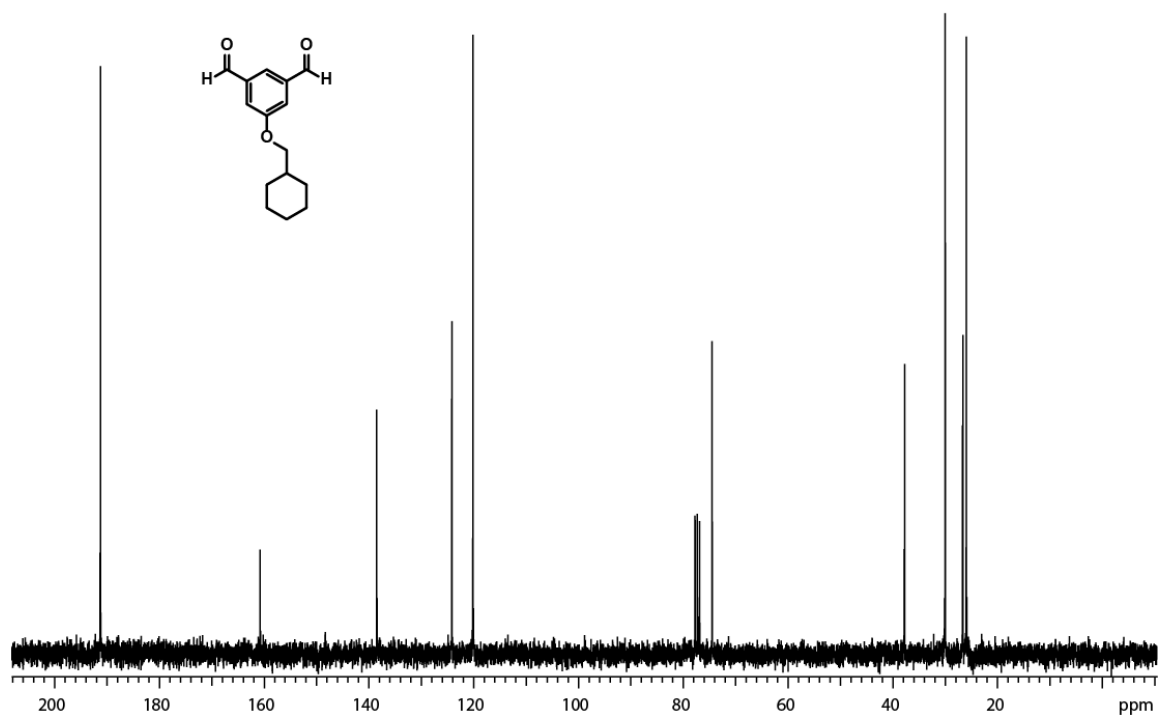
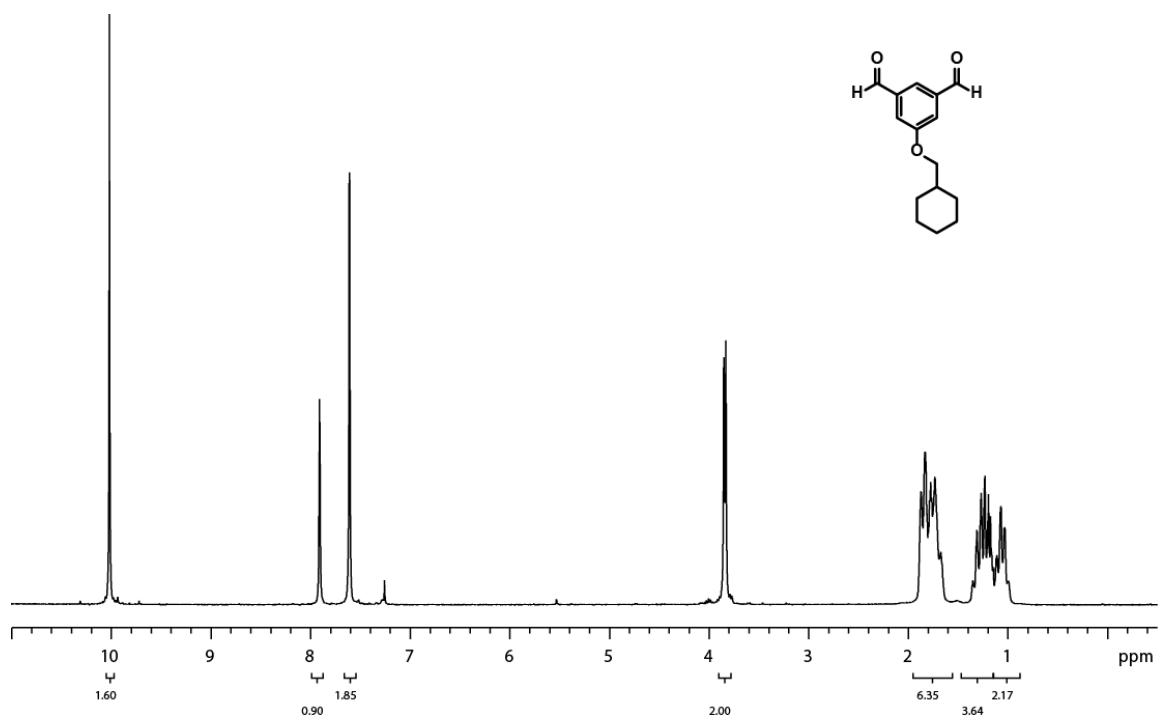
**CZ-01-184:**  $N^1,N^{1'}-((5'-(tert\text{-butyl})-[1,1':3',1'']\text{-terphenyl})-3,3''\text{-diyl})\text{bis(methylene))bis}(N^3\text{-(3-(isobutylamino)propyl)propane-1,3-diamine})$ ,  
**hydrochloride salt:**  $^1\text{H}$  NMR (500 MHz,  $\text{D}_2\text{O}$ )  $\delta$  ppm 7.75 (s, 2H), 7.71-7.67 (m, 4H), 7.63 (s, 1H), 7.54 (t,  $J = 8.0$  Hz, 2H), 7.46 (d,  $J = 6.5$  Hz, 2H), 4.28 (s, 4H), 3.23-3.10 (m, 16H), 2.89 (d,  $J = 7.0$  Hz, 4H), 2.19-2.08 (m, 8H), 1.98 (sept,  $J = 6.5$  Hz, 2H), 1.34 (s, 9H), 0.96 (d,  $J = 7.0$  Hz, 12H). LRMS calculated for  $\text{C}_{44}\text{H}_{72}\text{N}_6$   $m/z$  685.6  $[\text{M}+\text{H}]^+$ , Obsd. 685.4  $[\text{M}+\text{H}]^+$ .

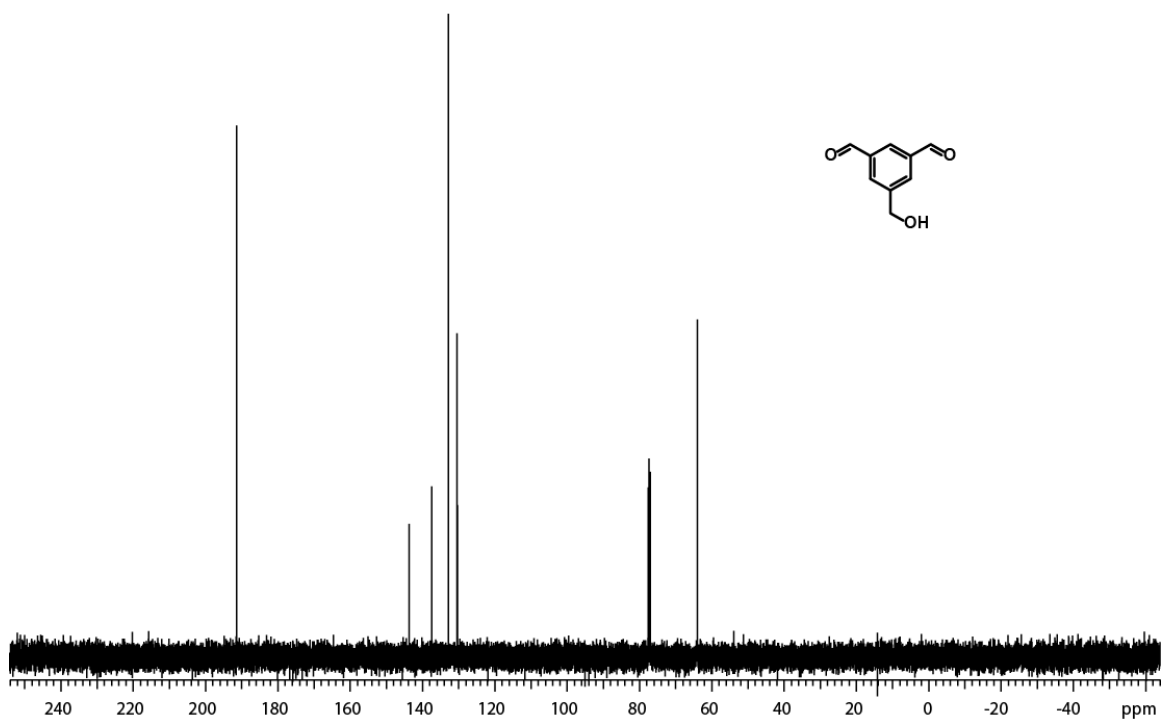
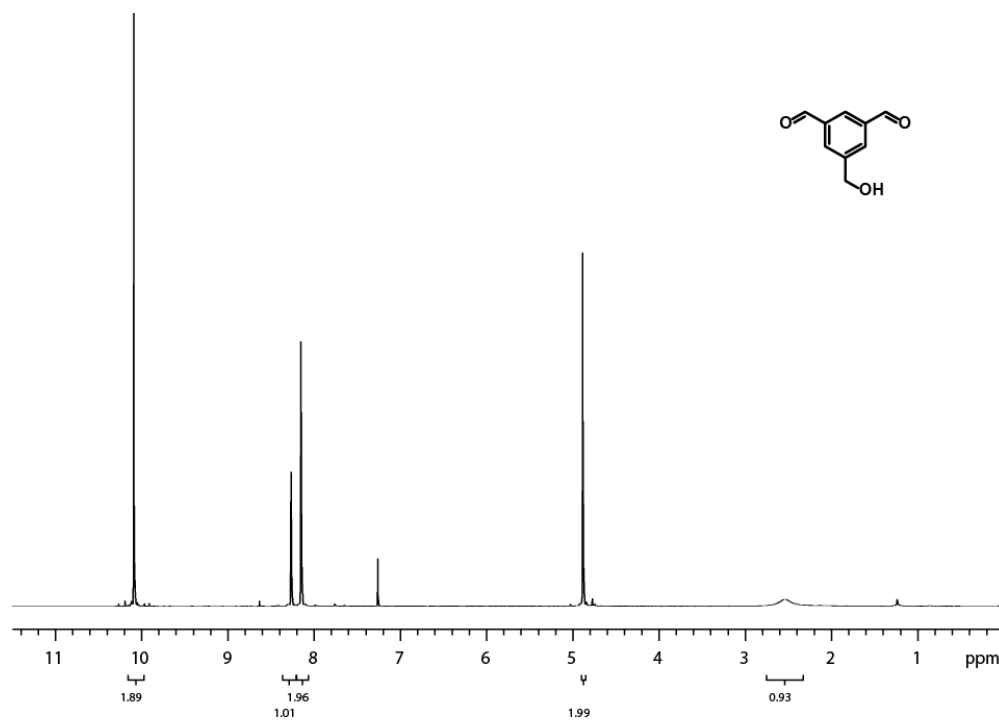


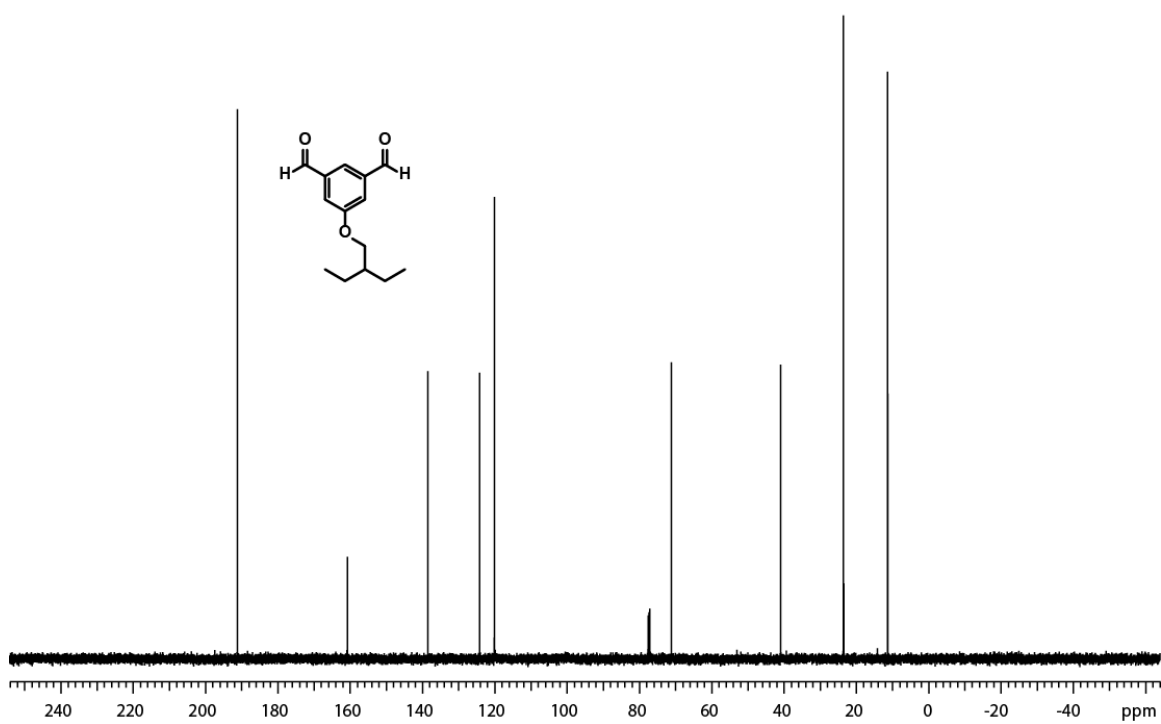
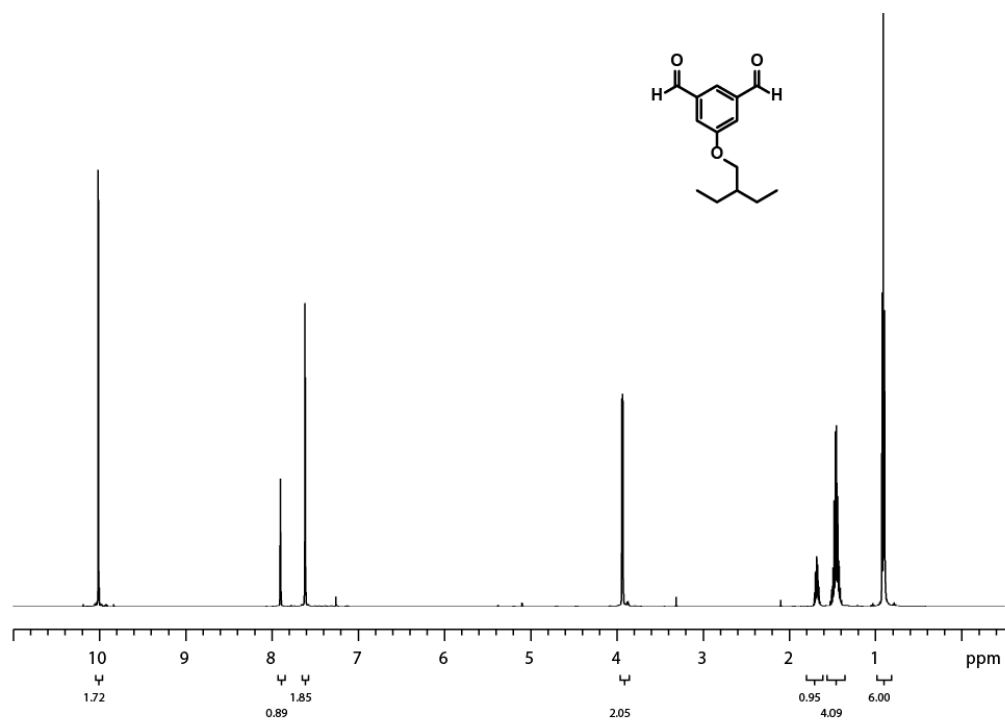
4.6.5 Representative  $^1\text{H}$  NMR and  $^{13}\text{C}$  NMR

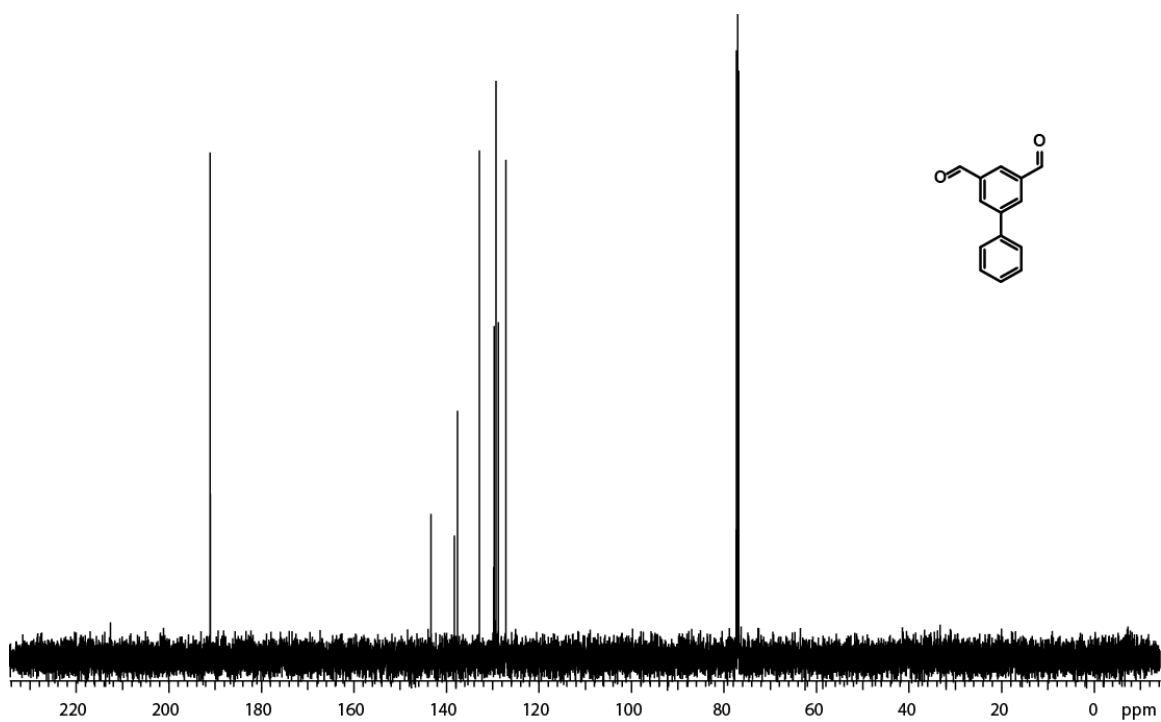
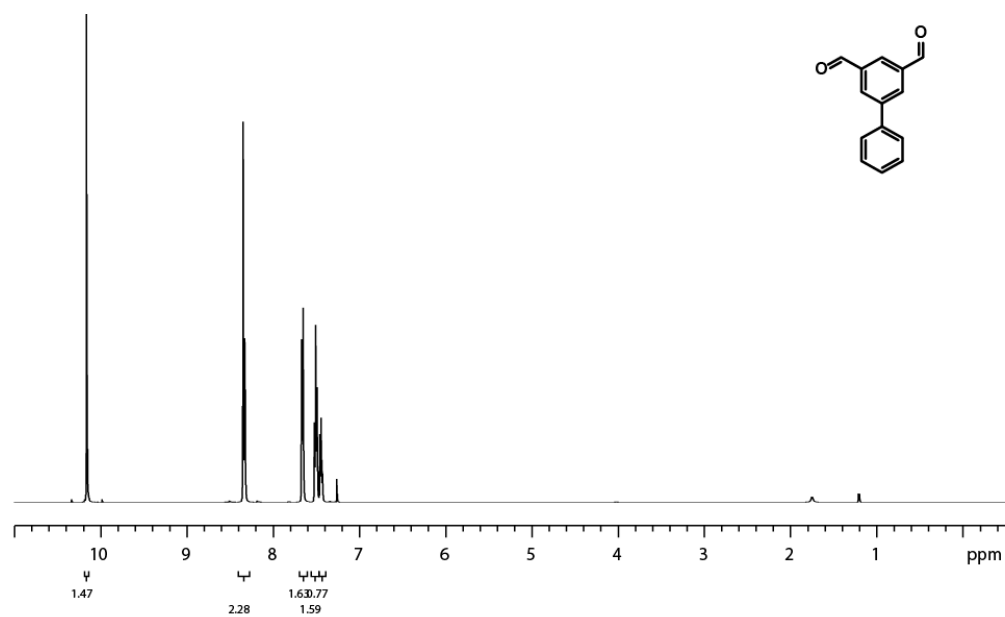


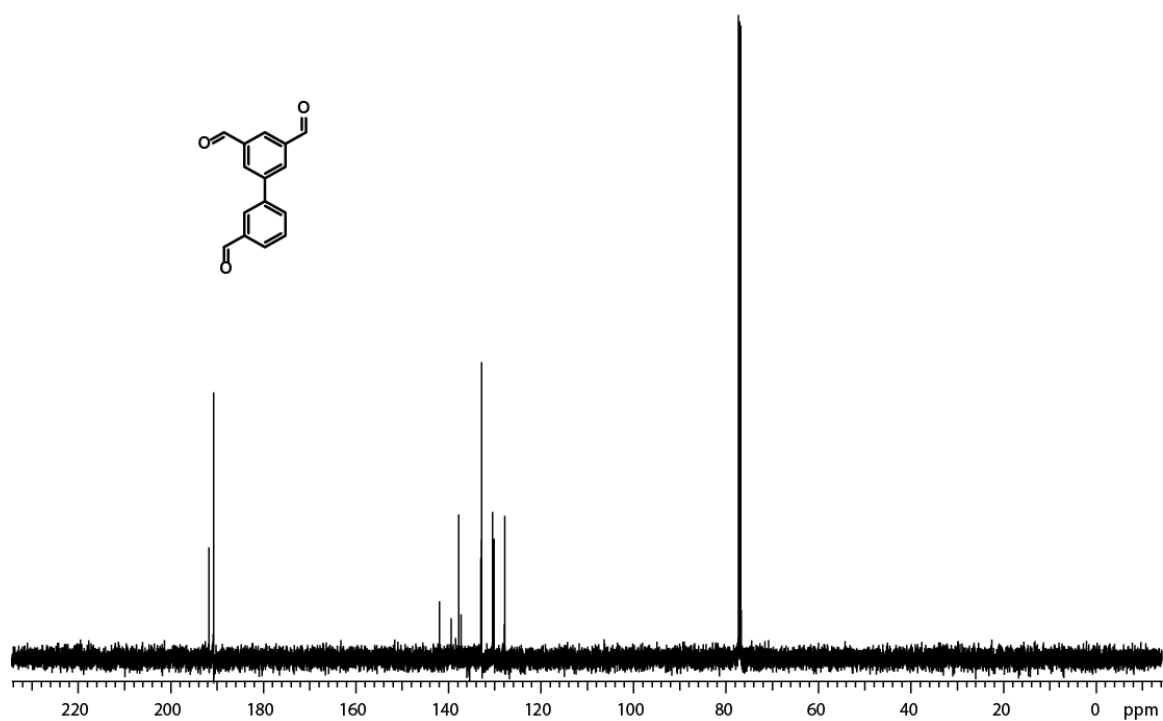
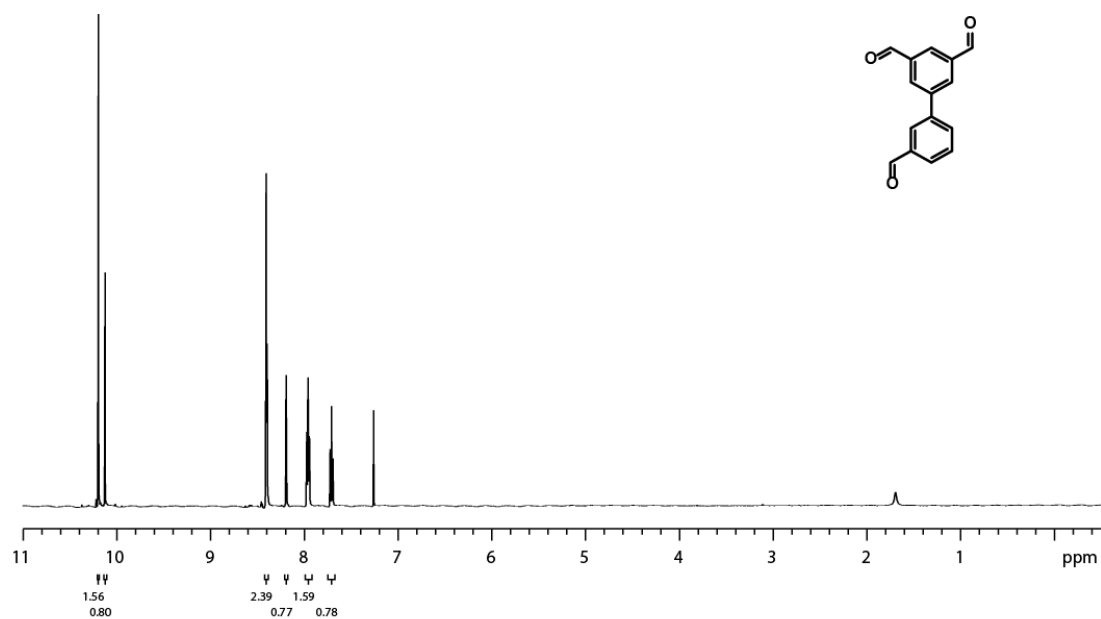




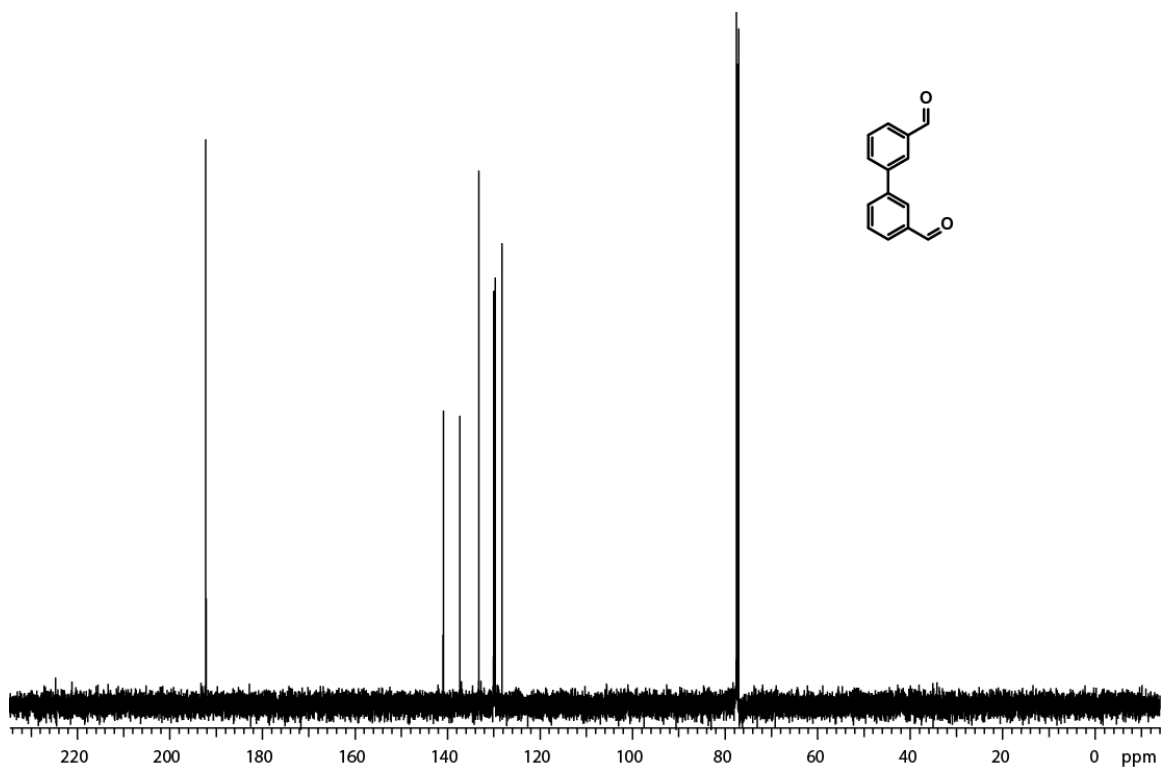
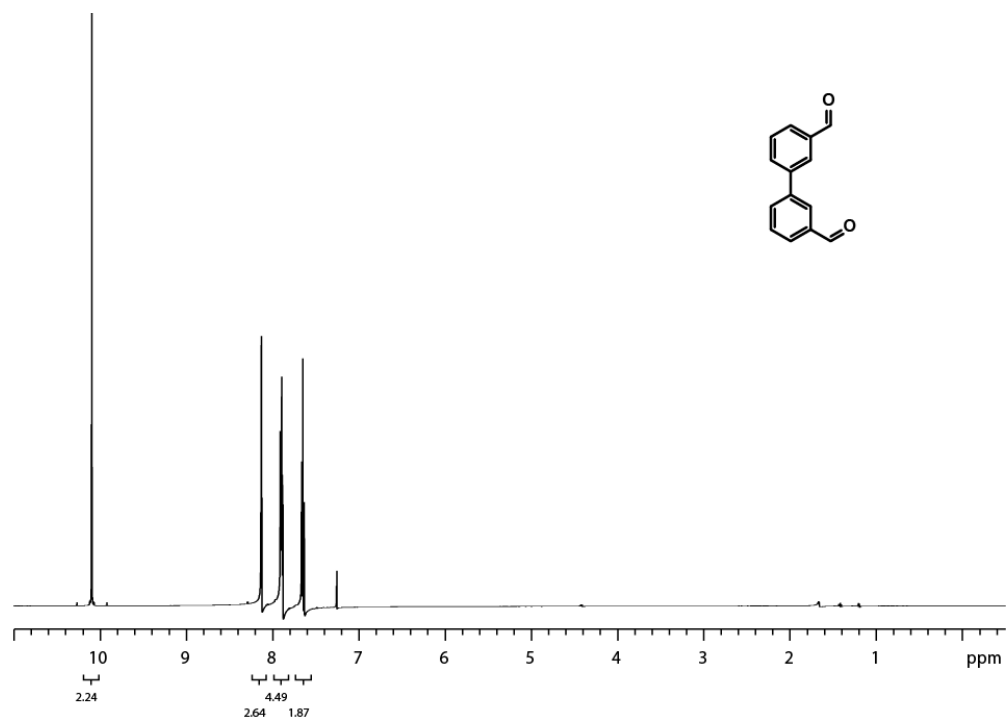


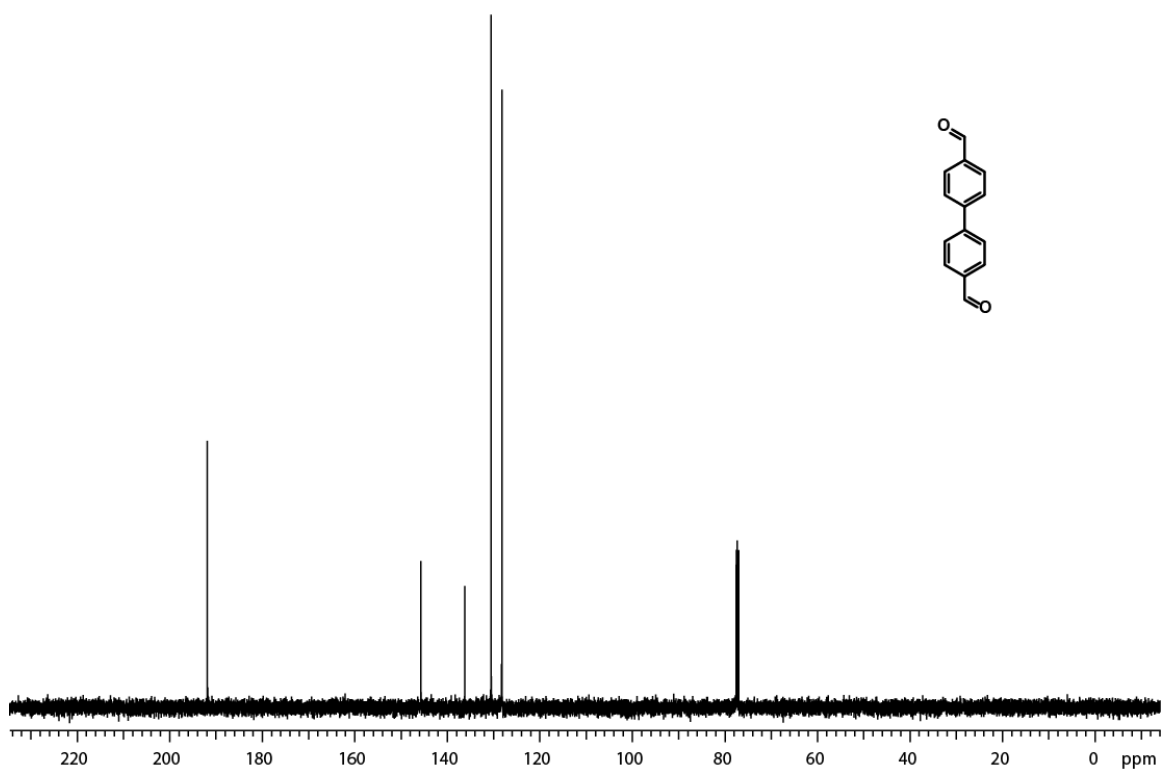
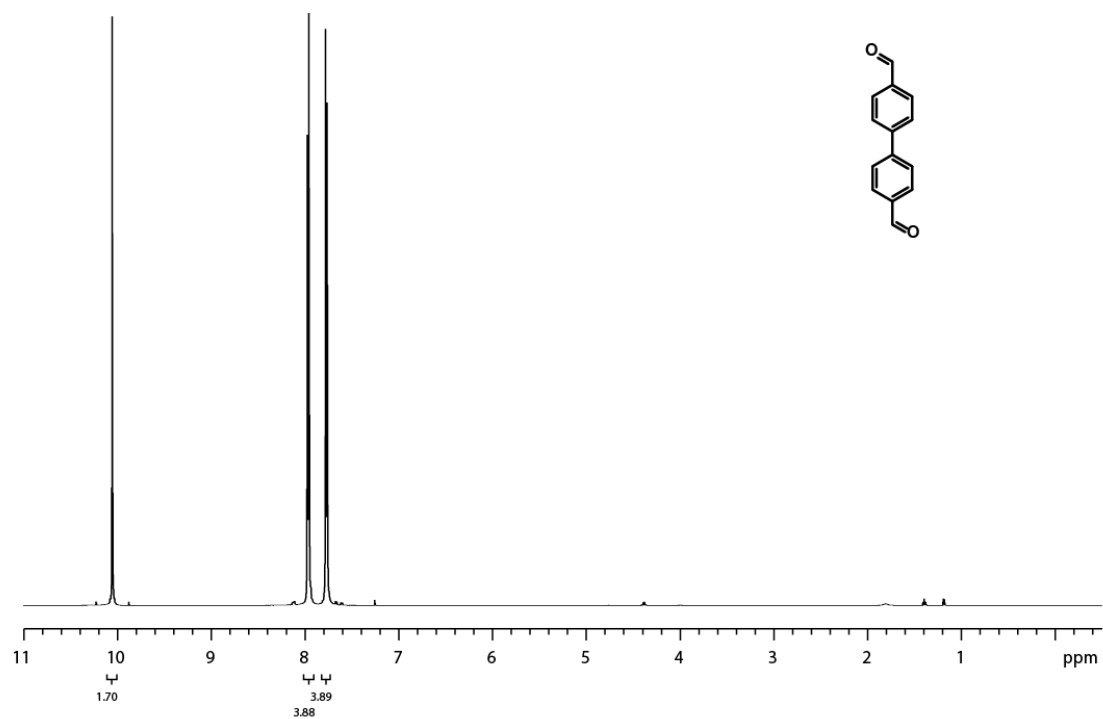


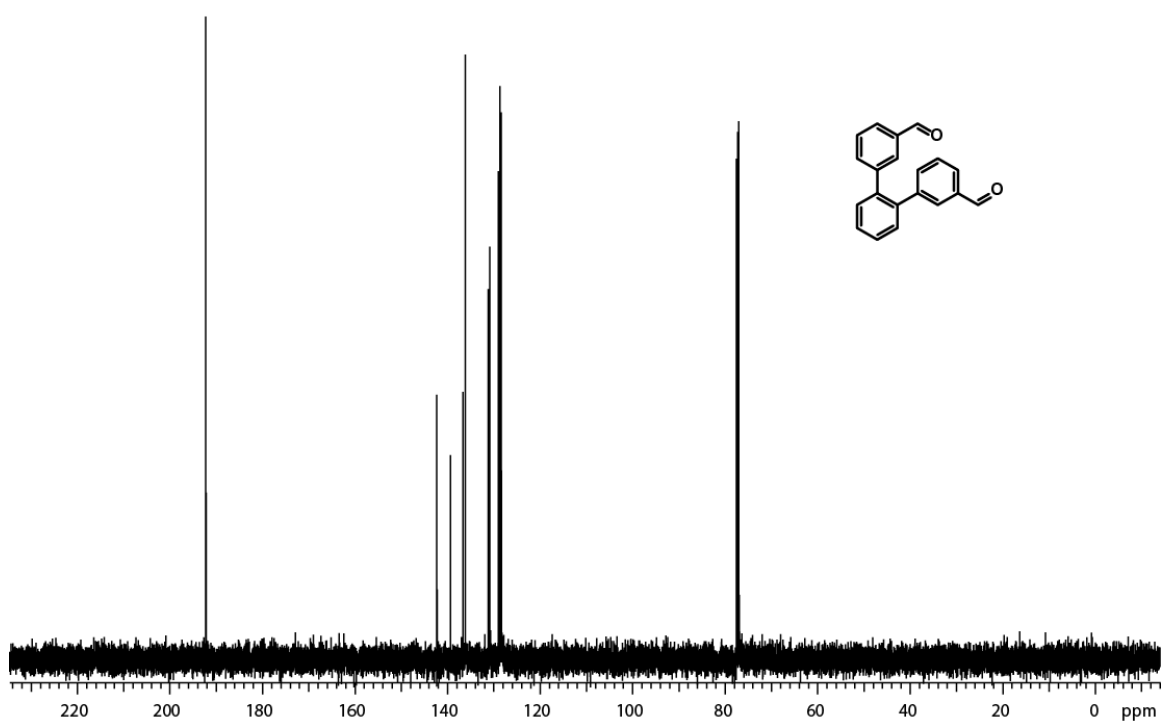
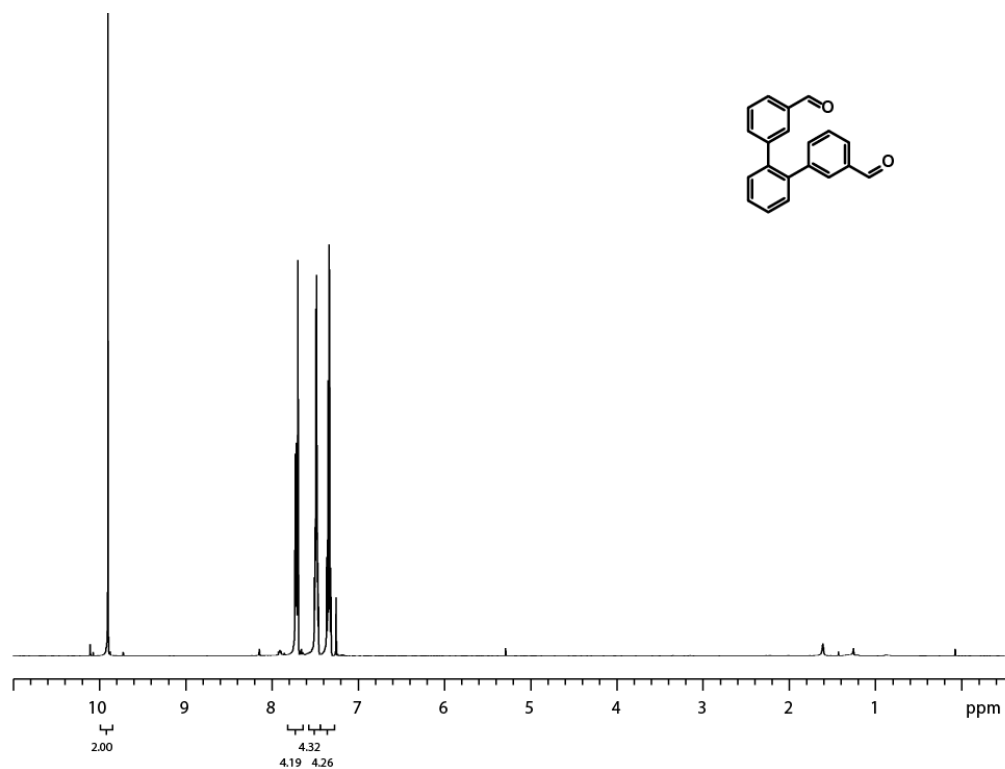


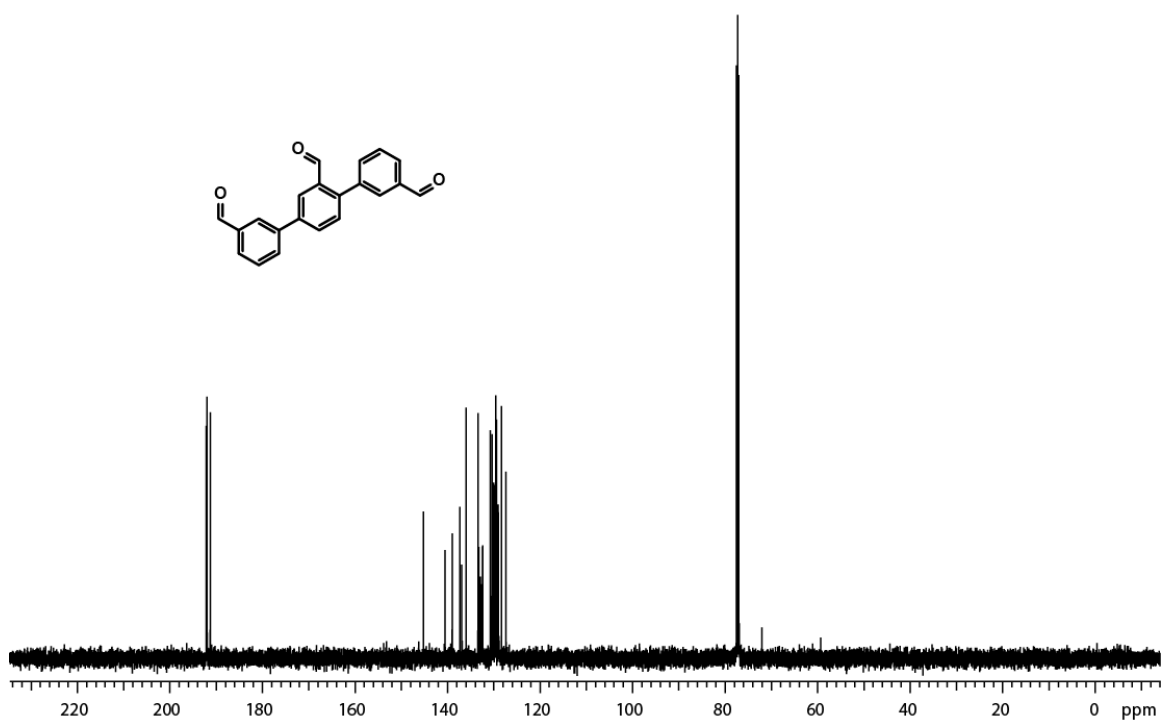
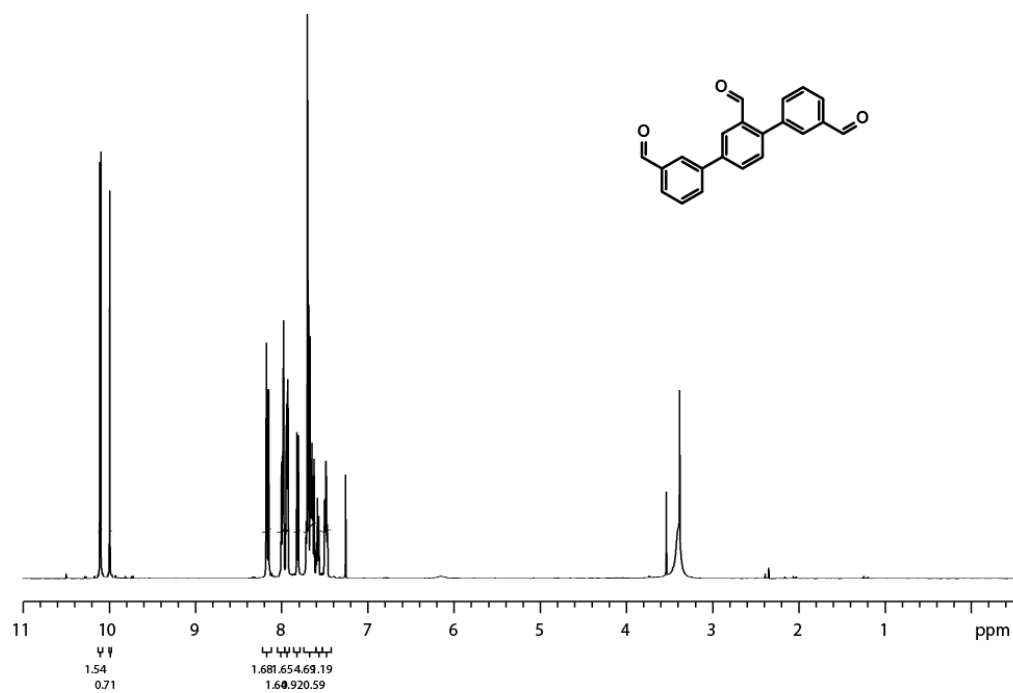


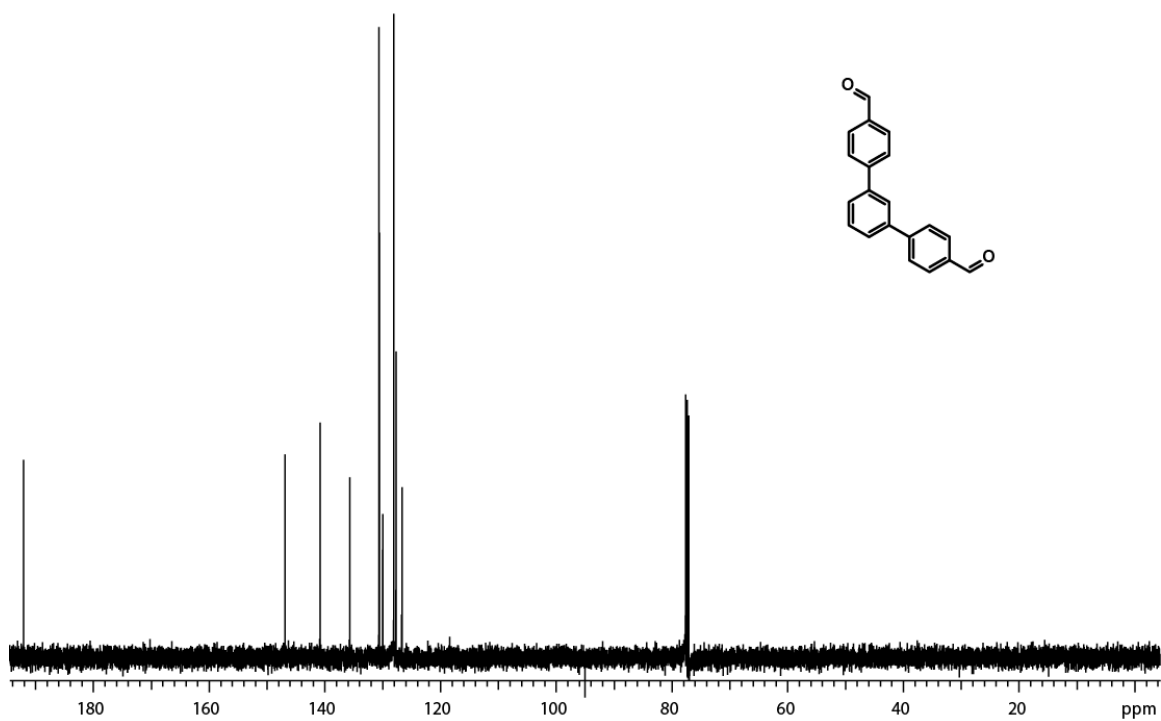
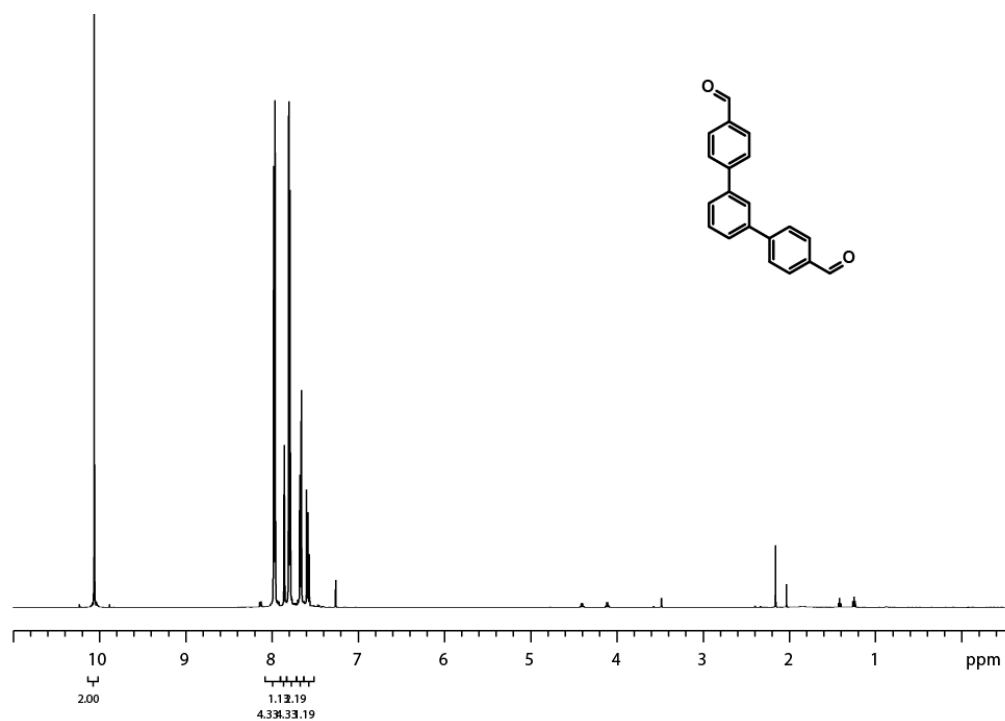


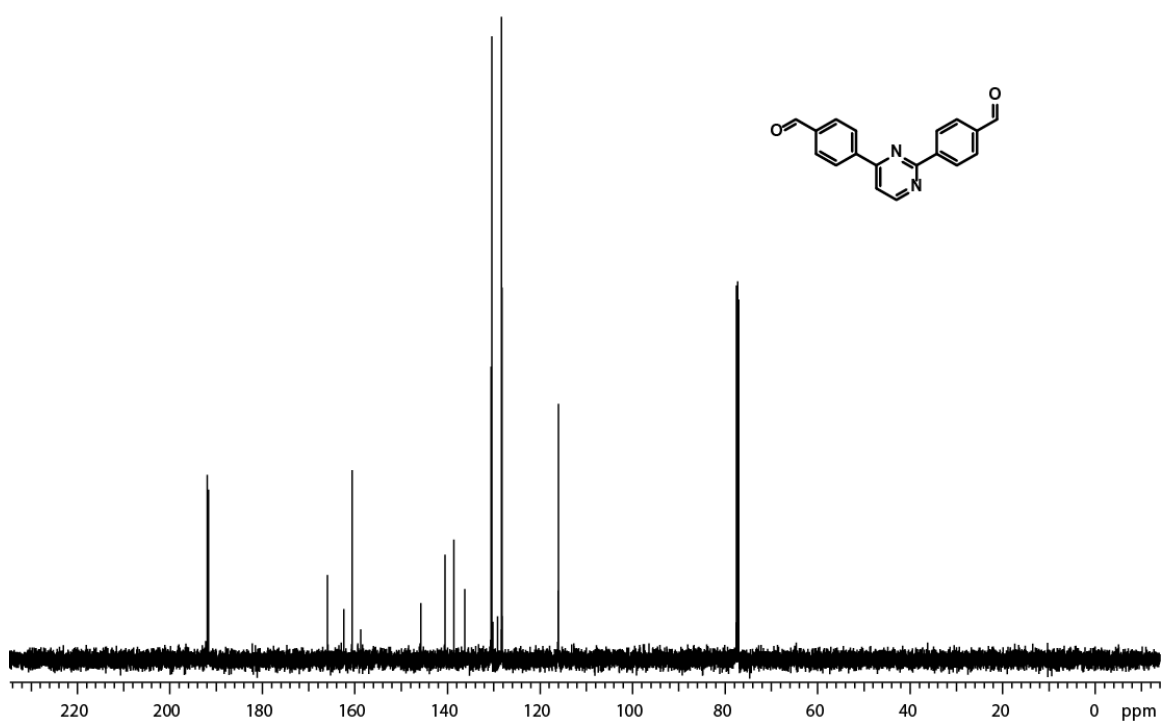
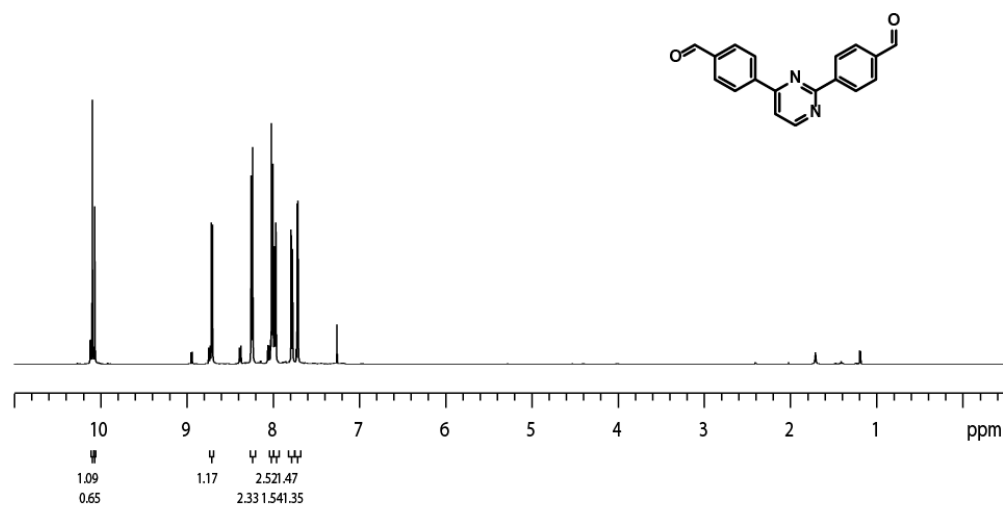


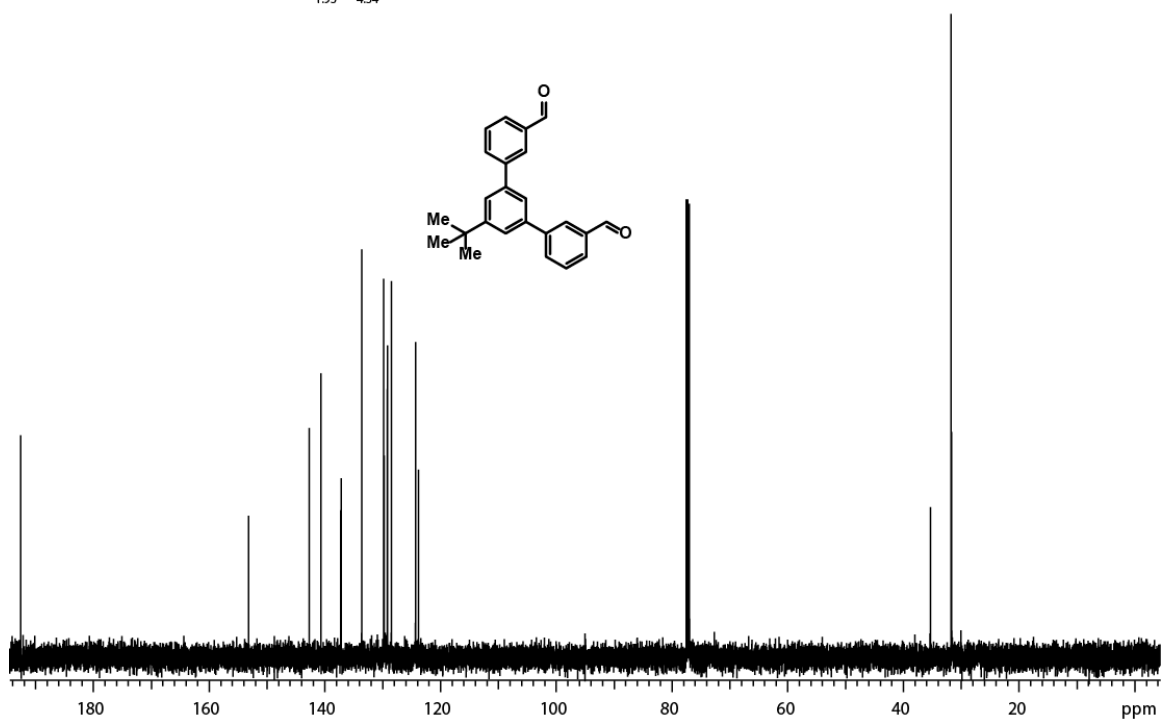
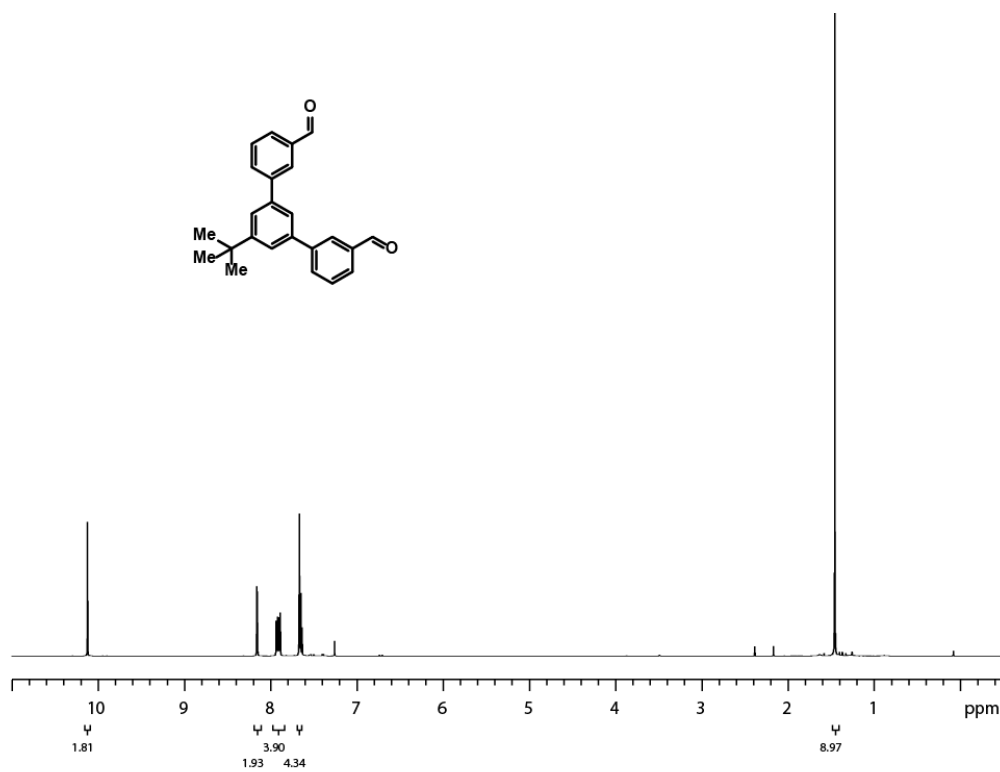


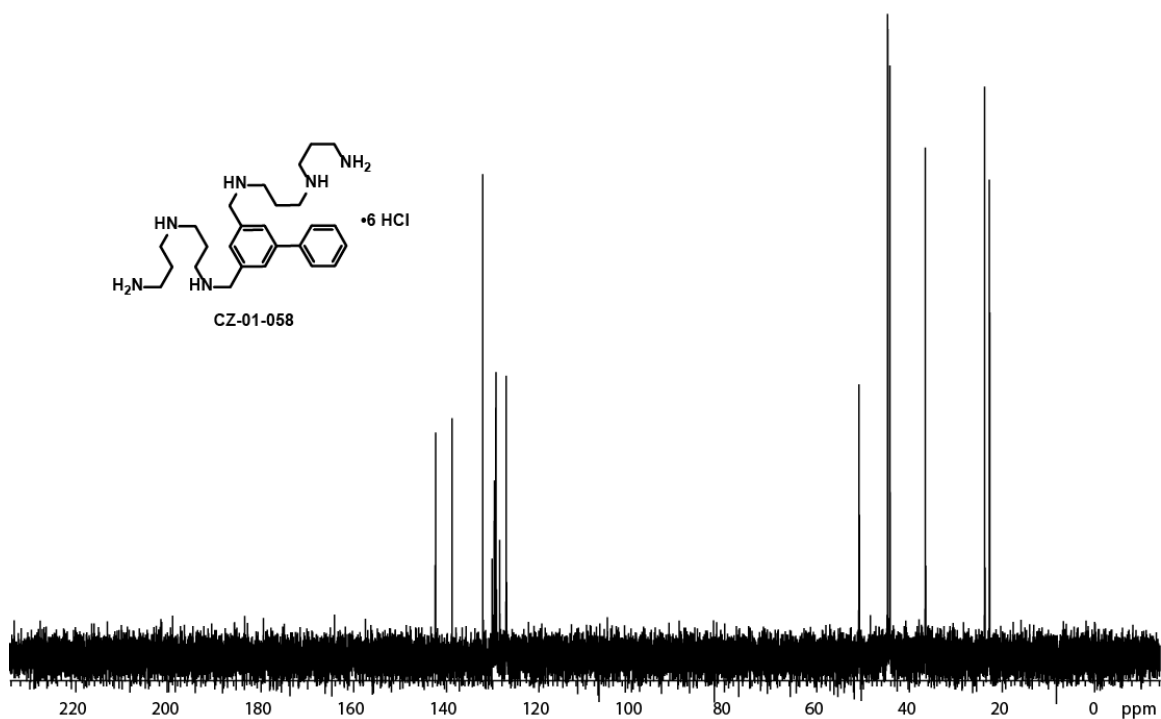
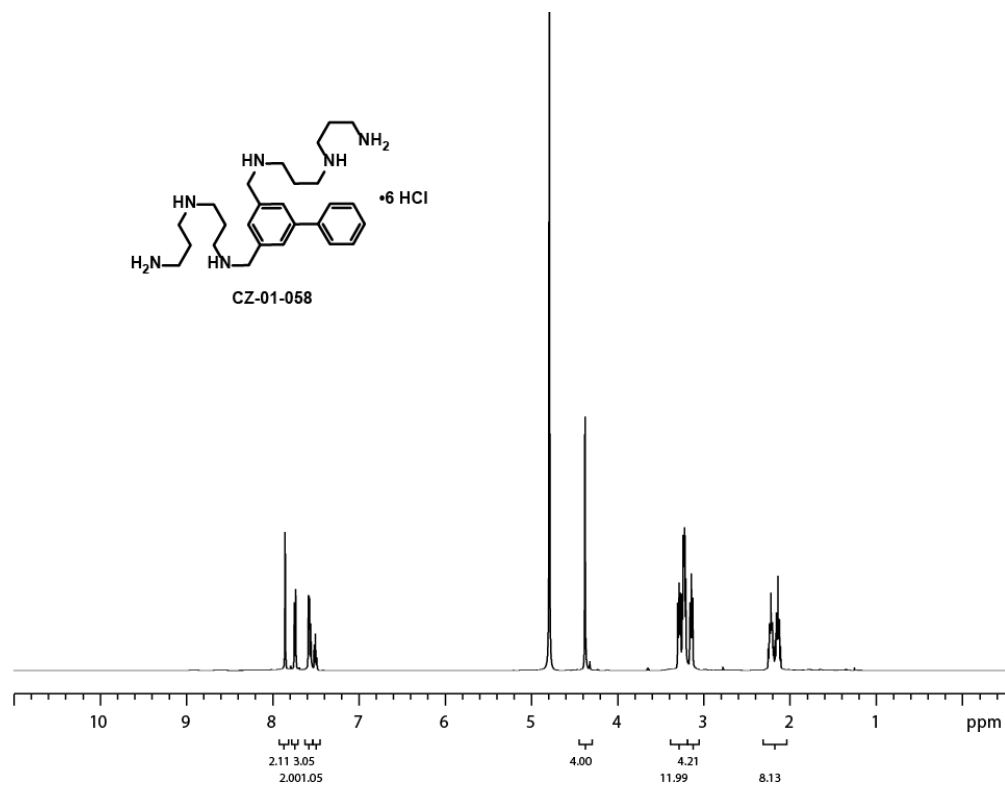




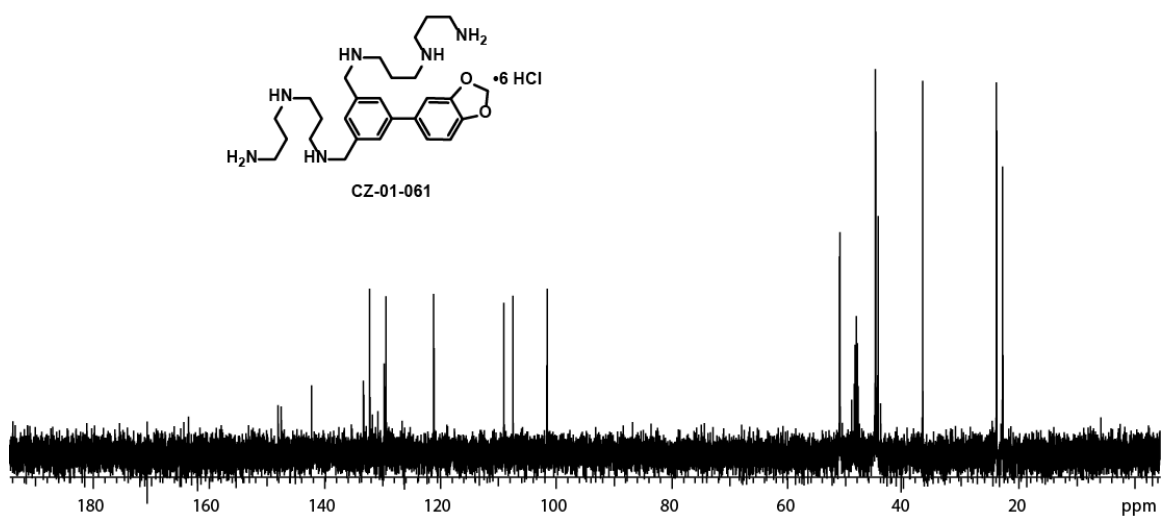
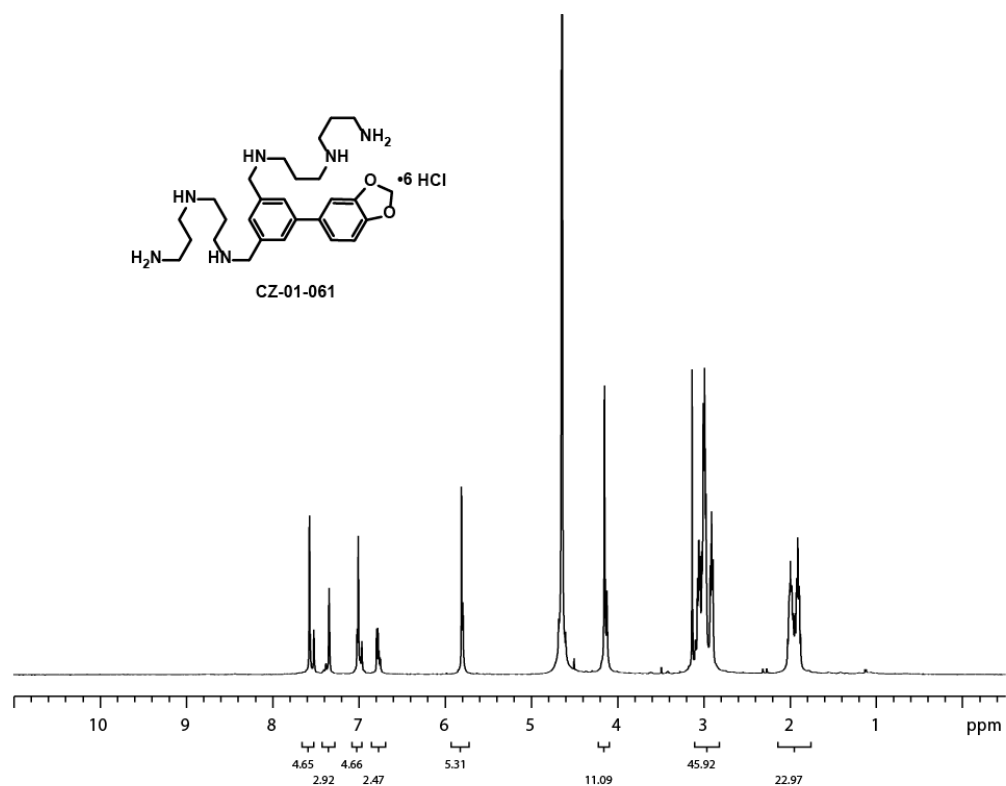


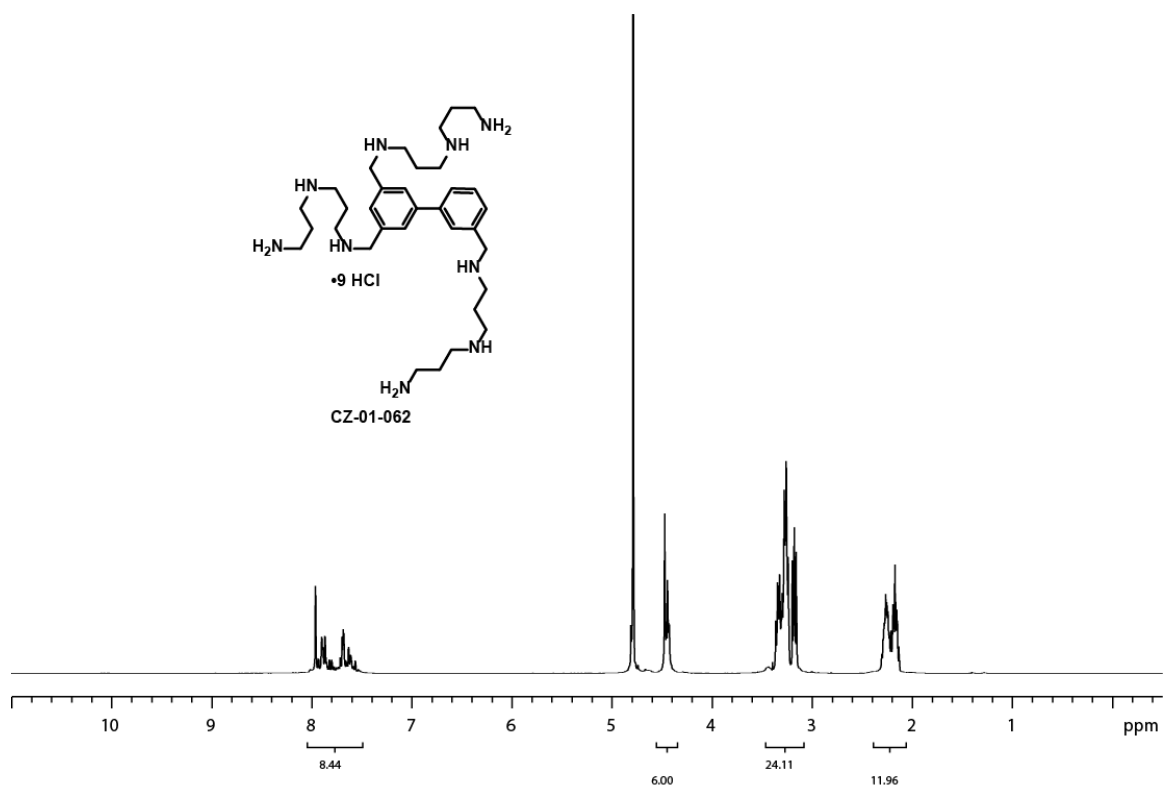


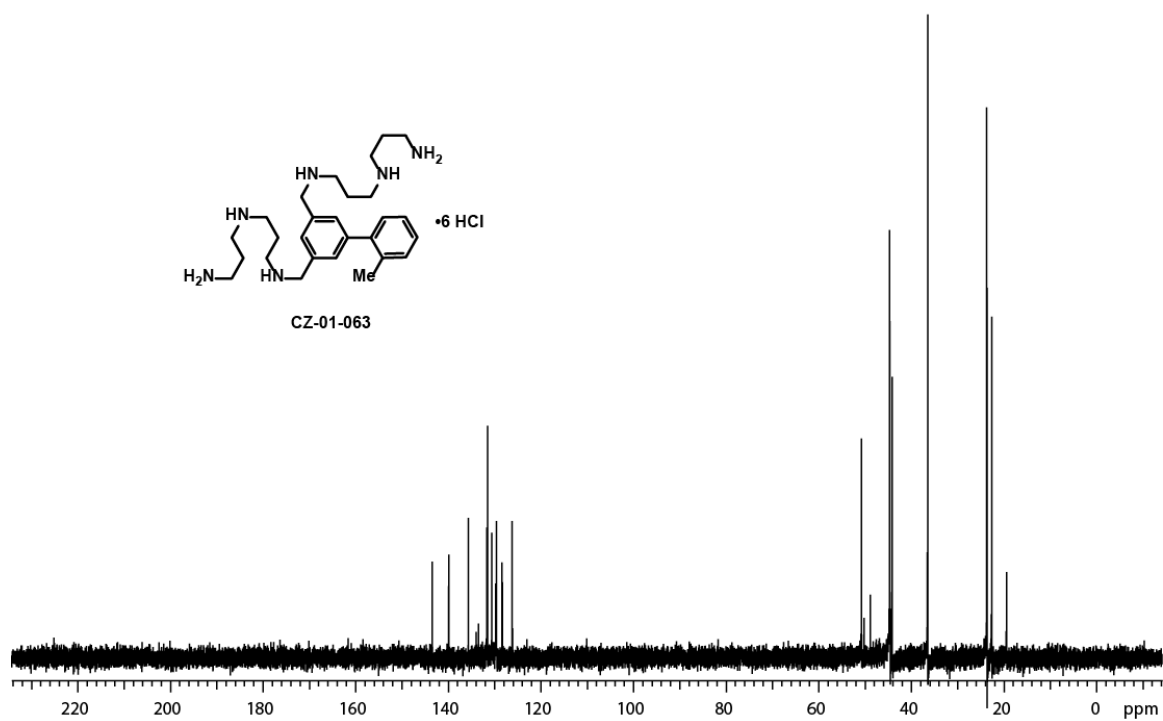
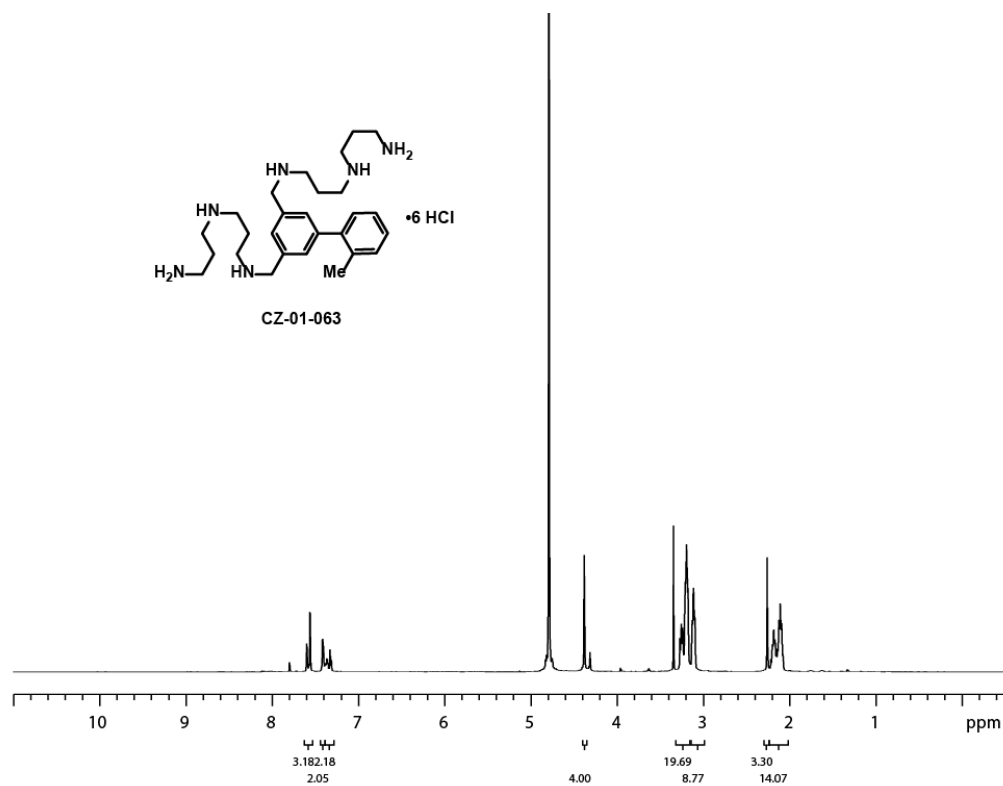


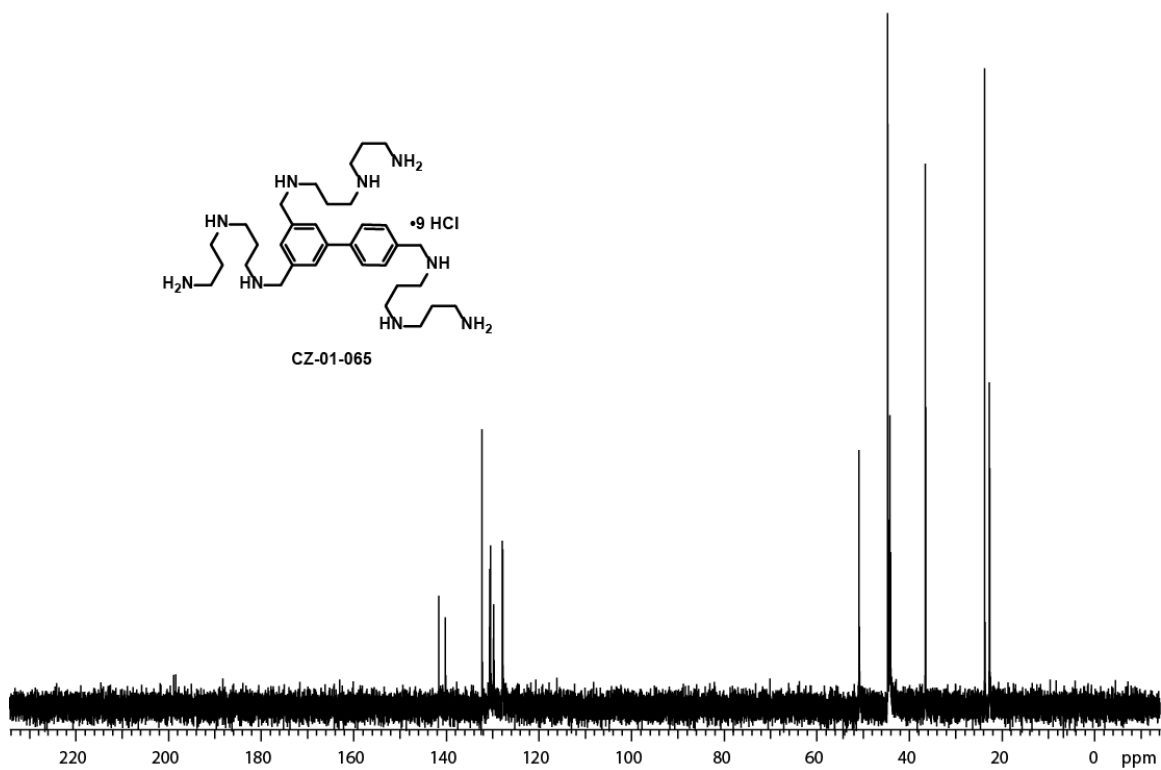
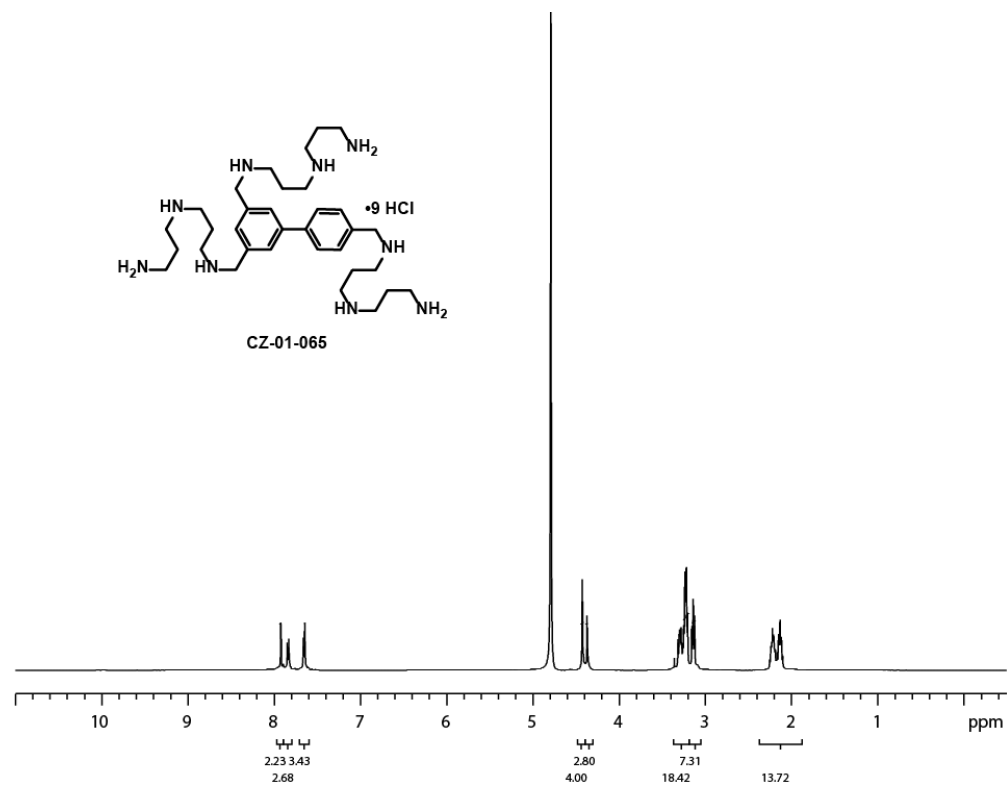


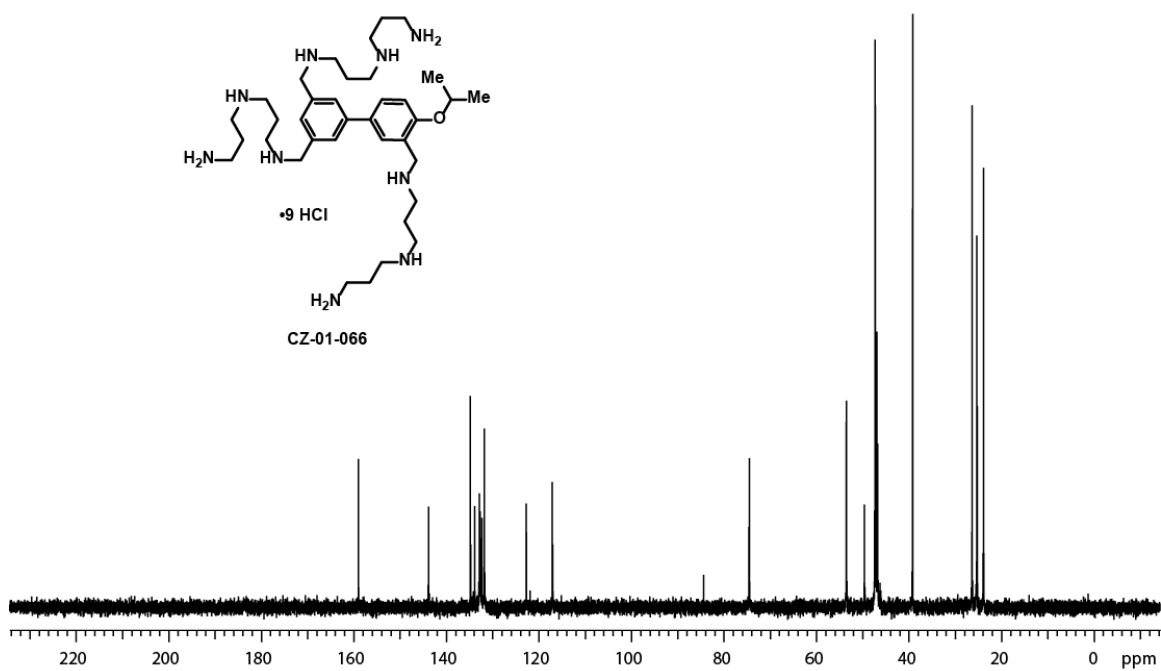
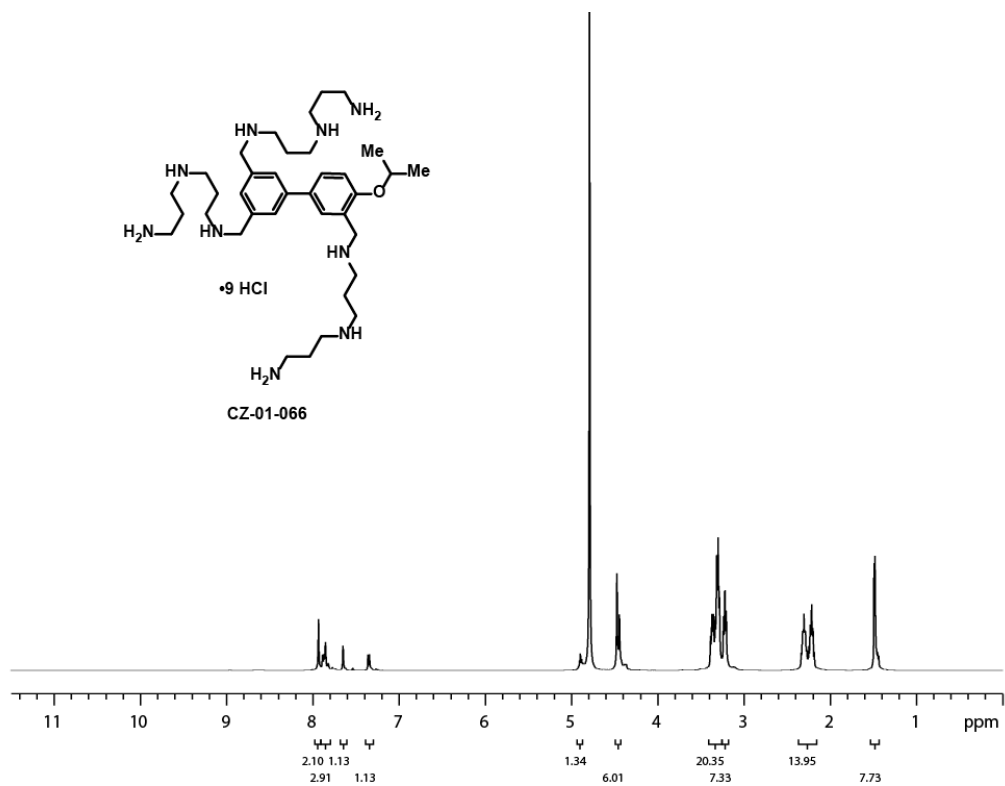




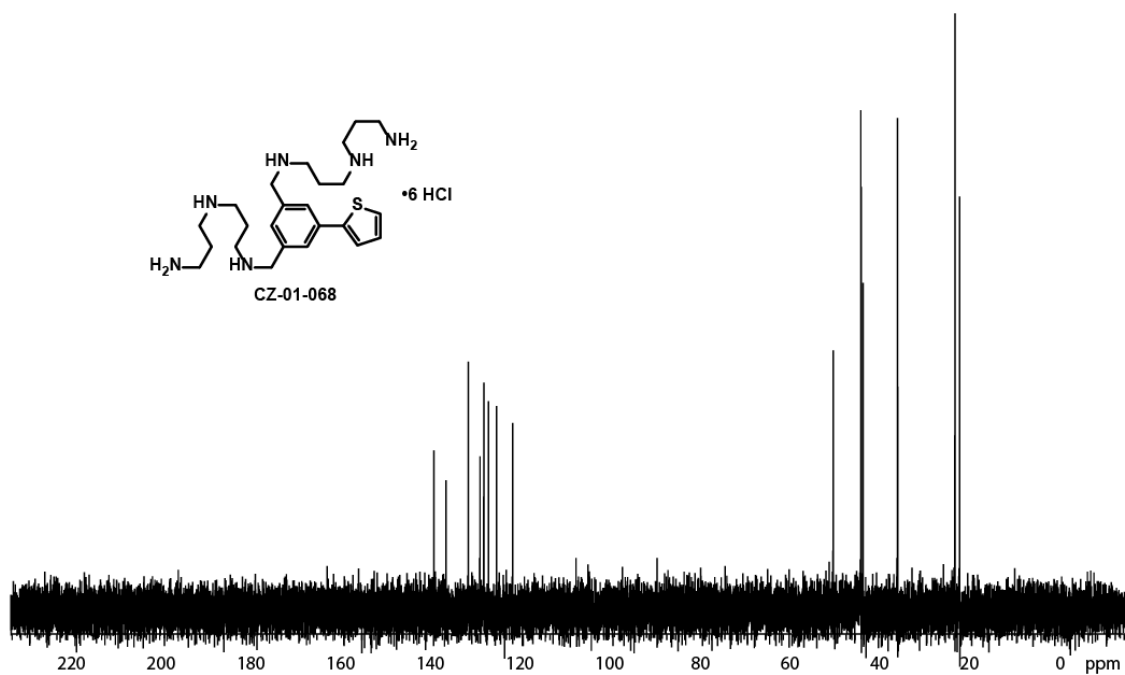
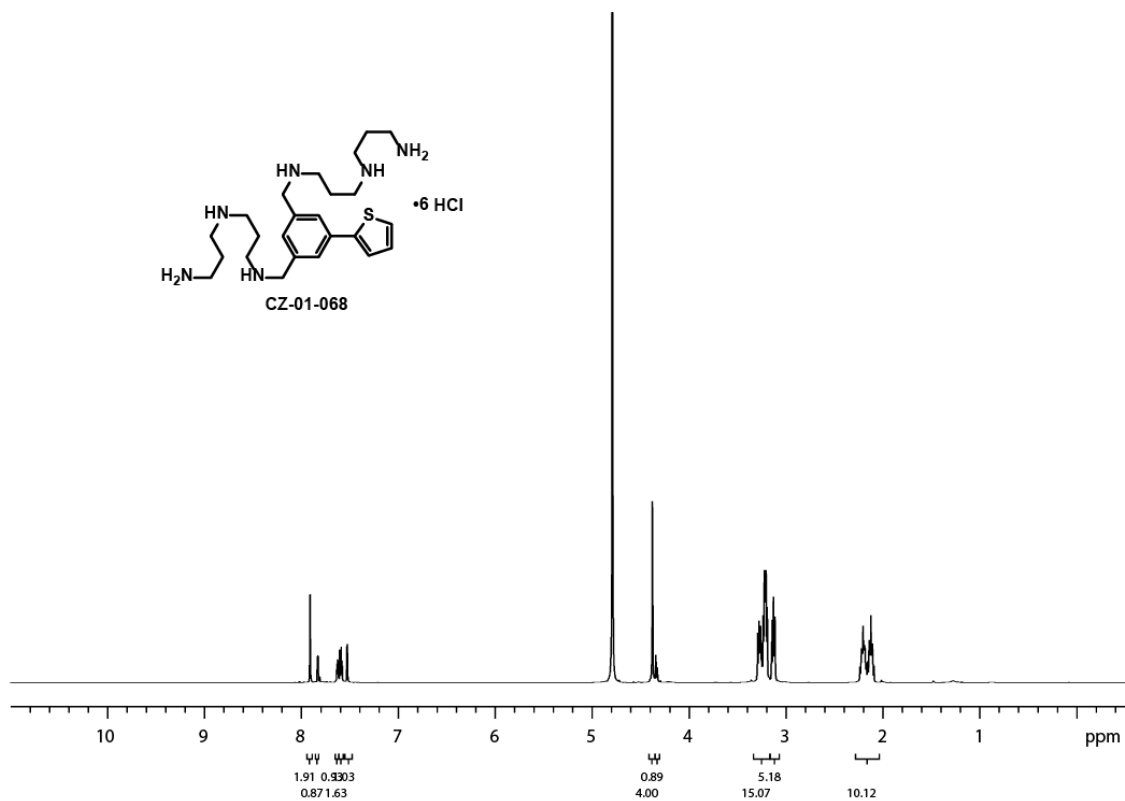


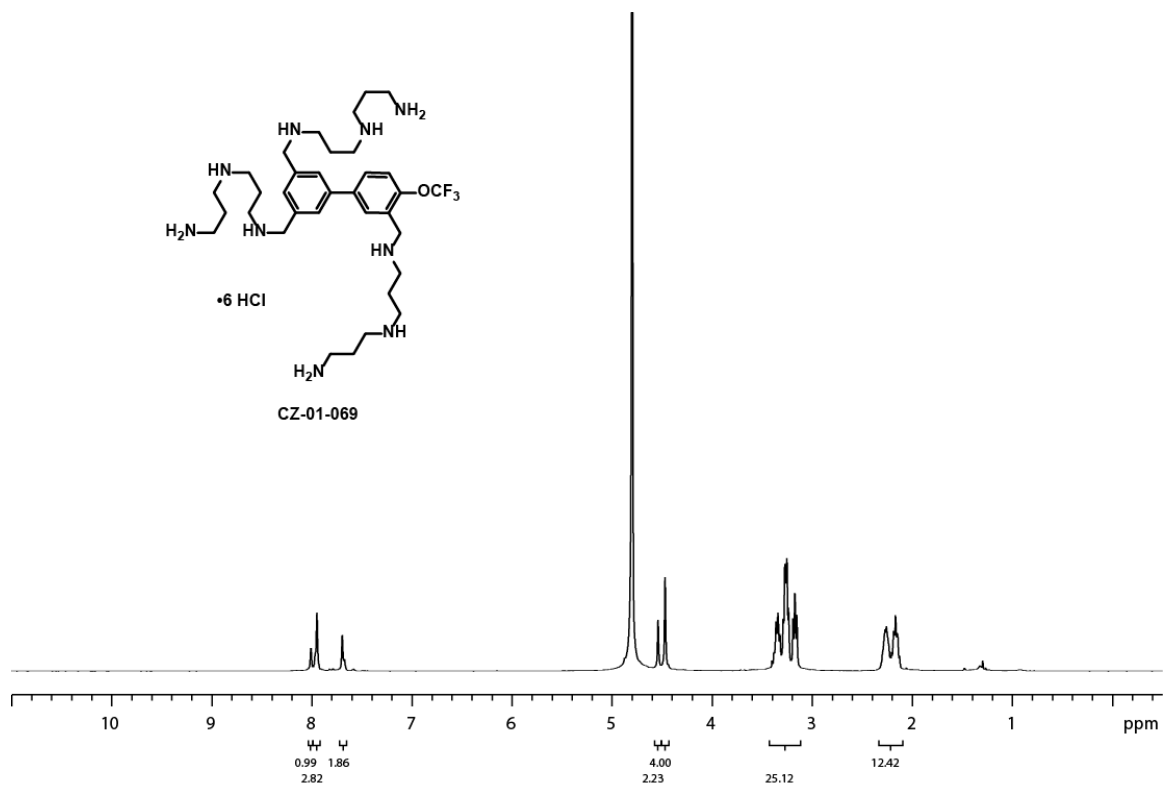
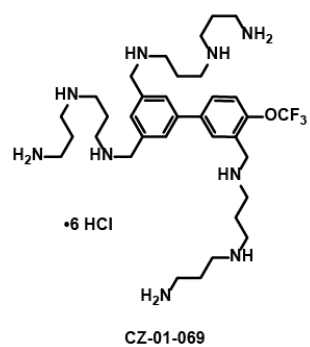




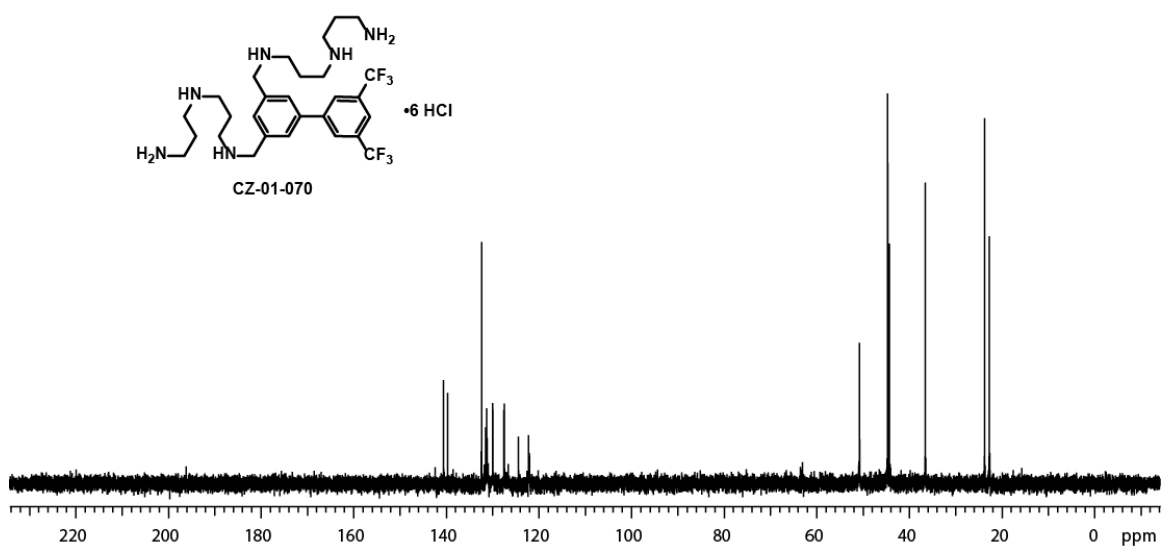
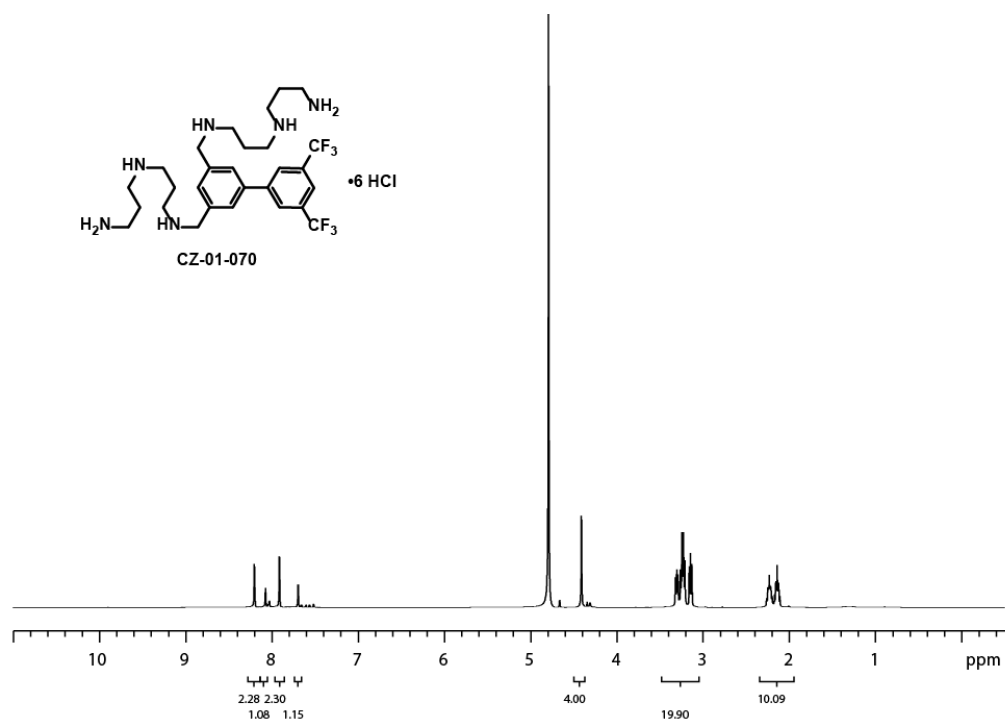


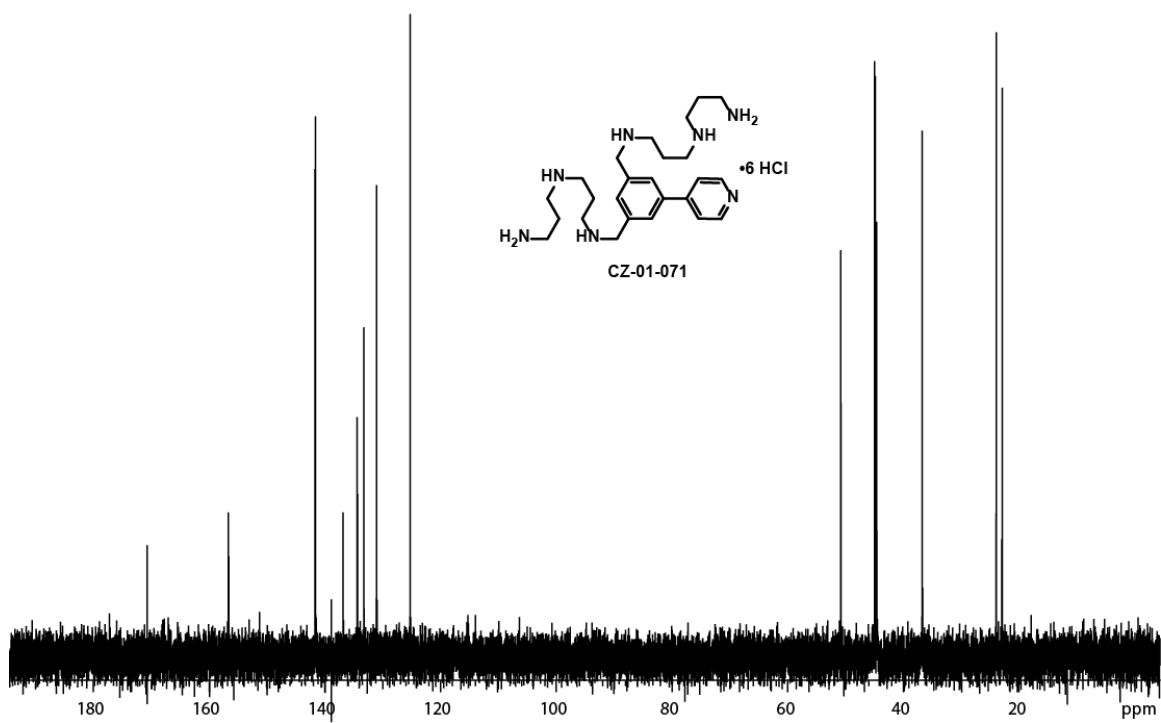
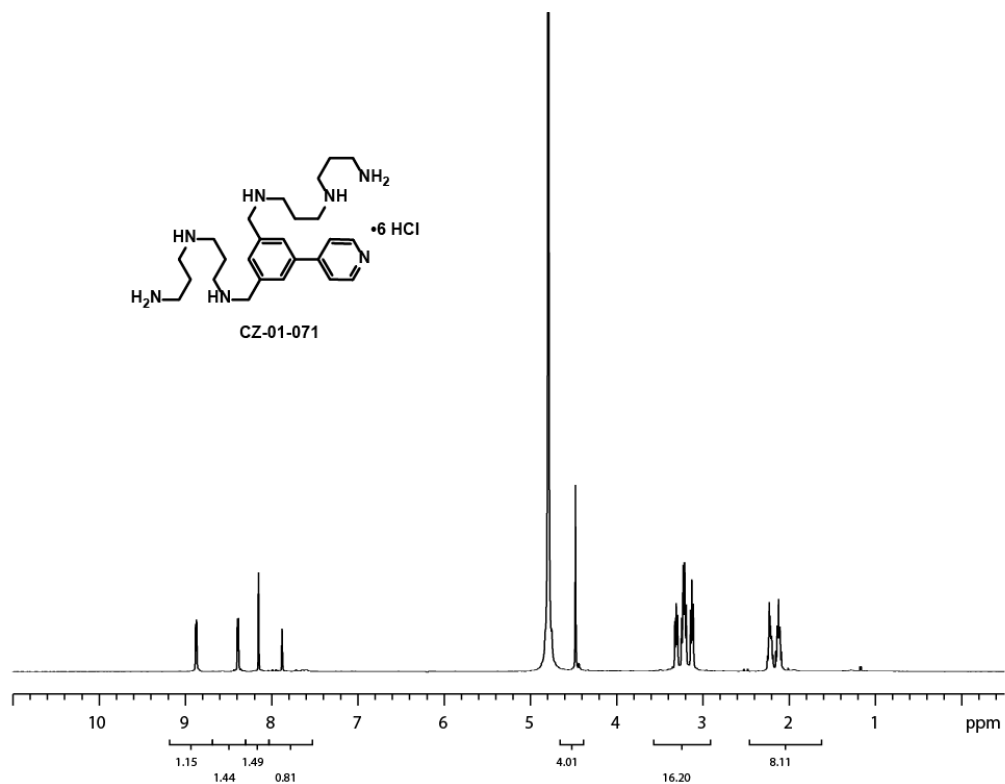


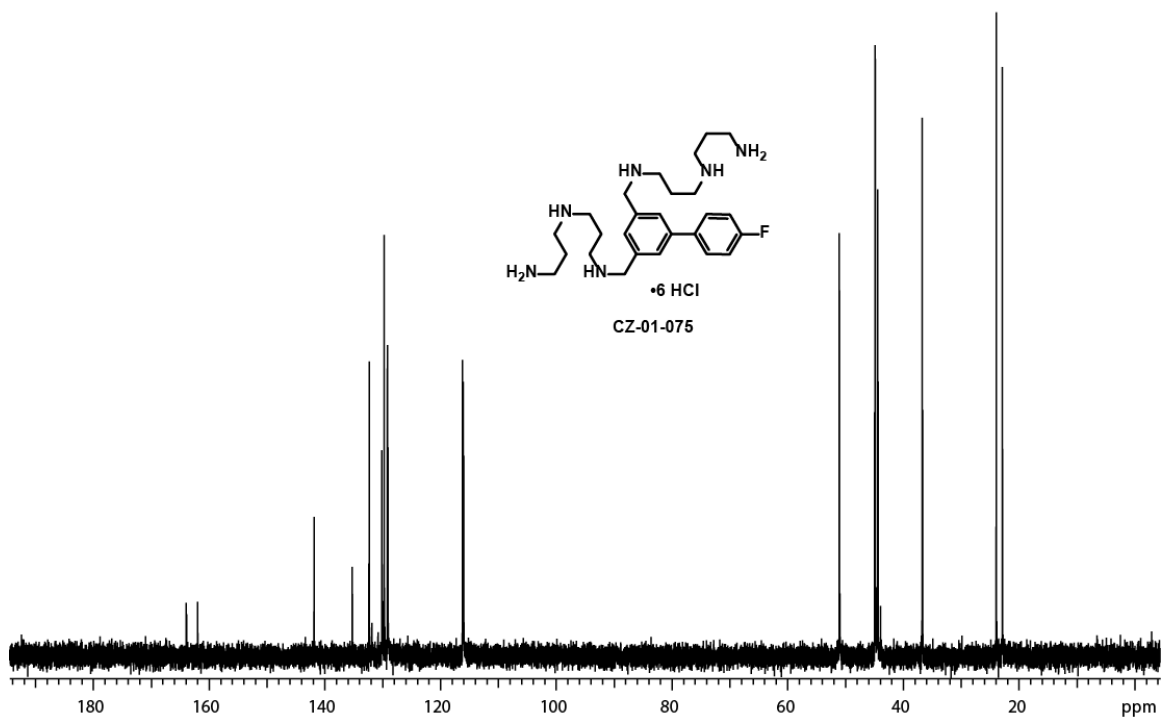
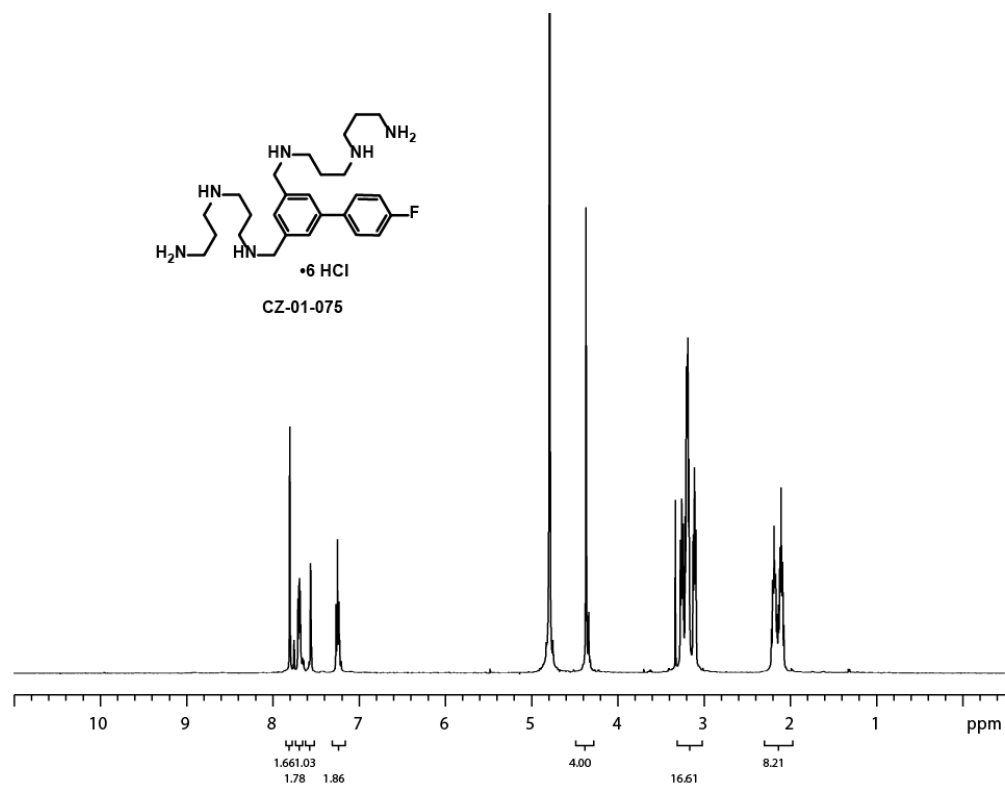


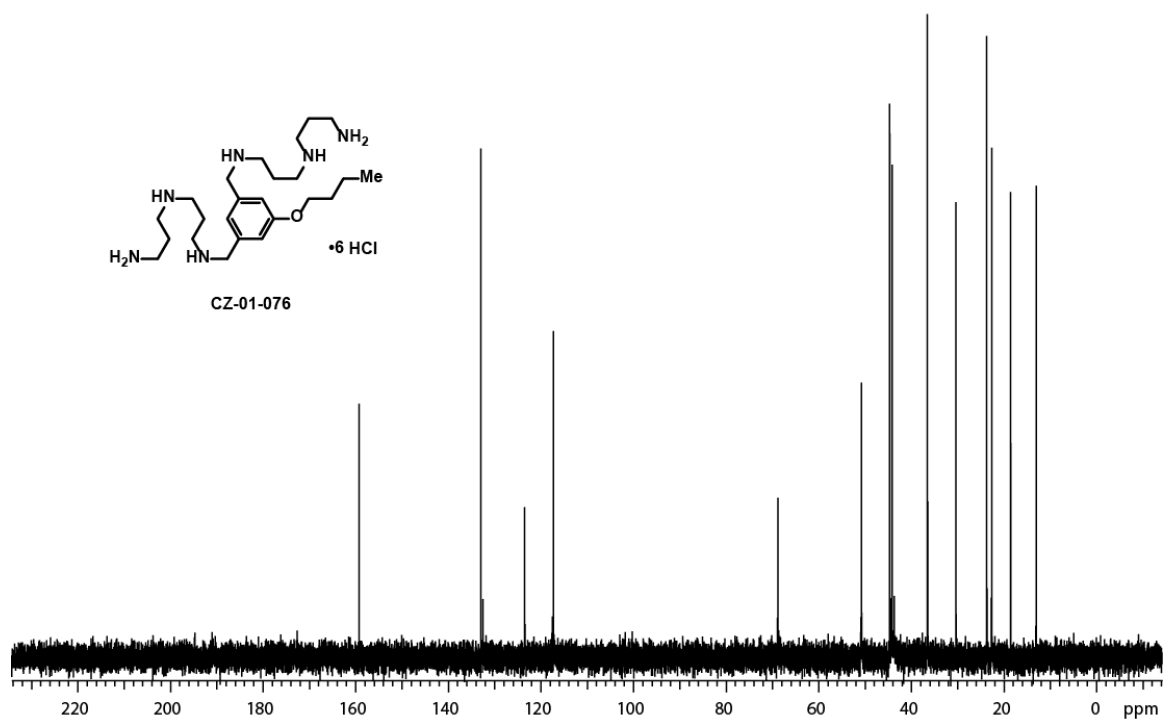
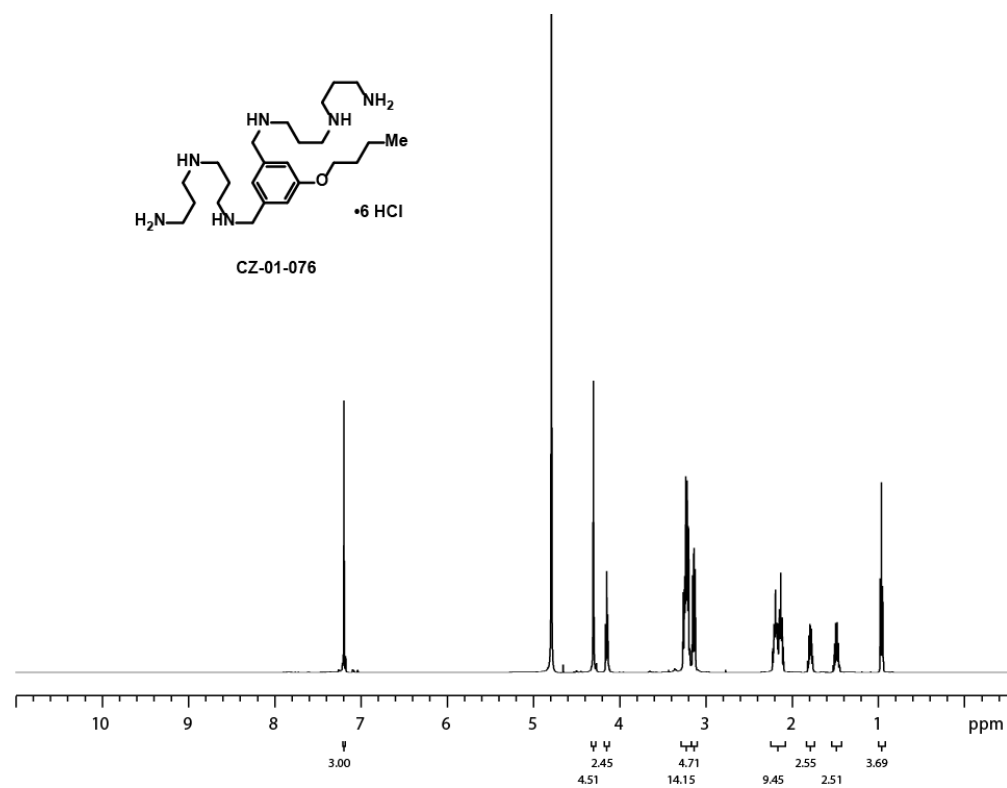




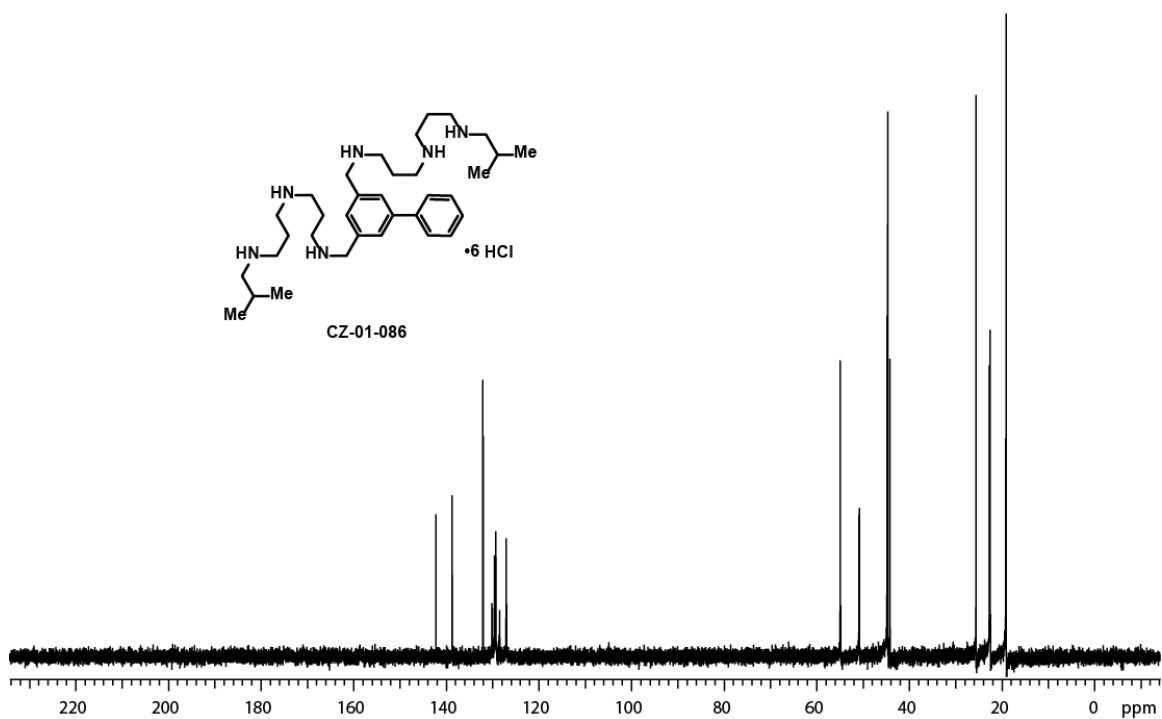
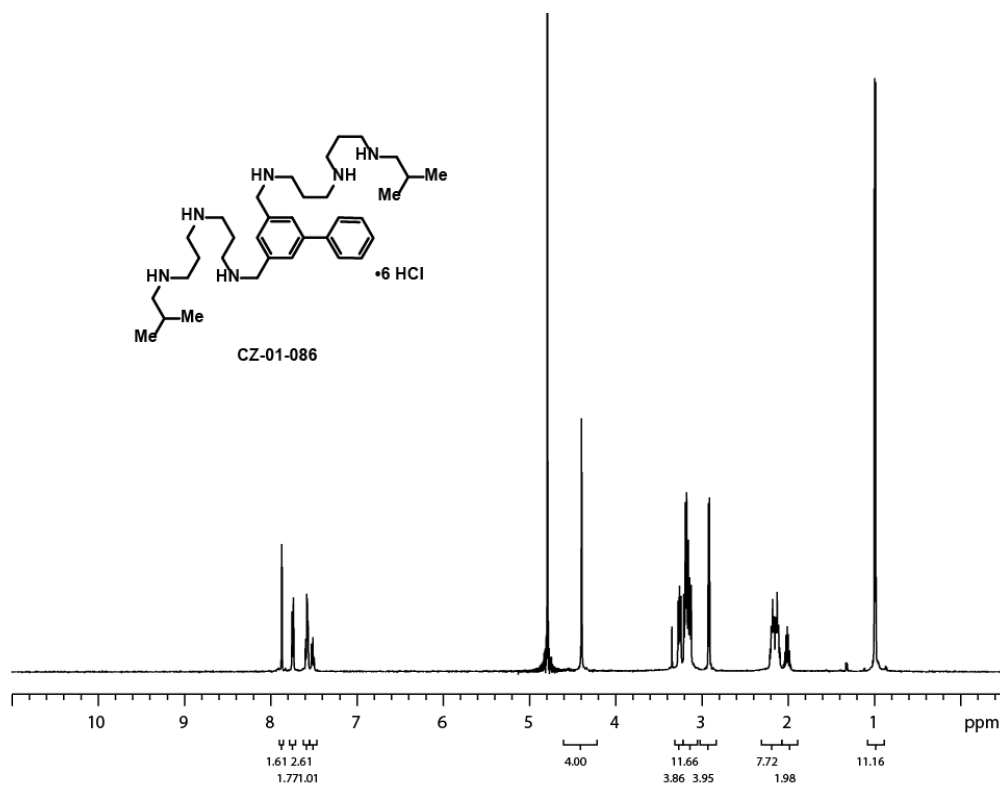


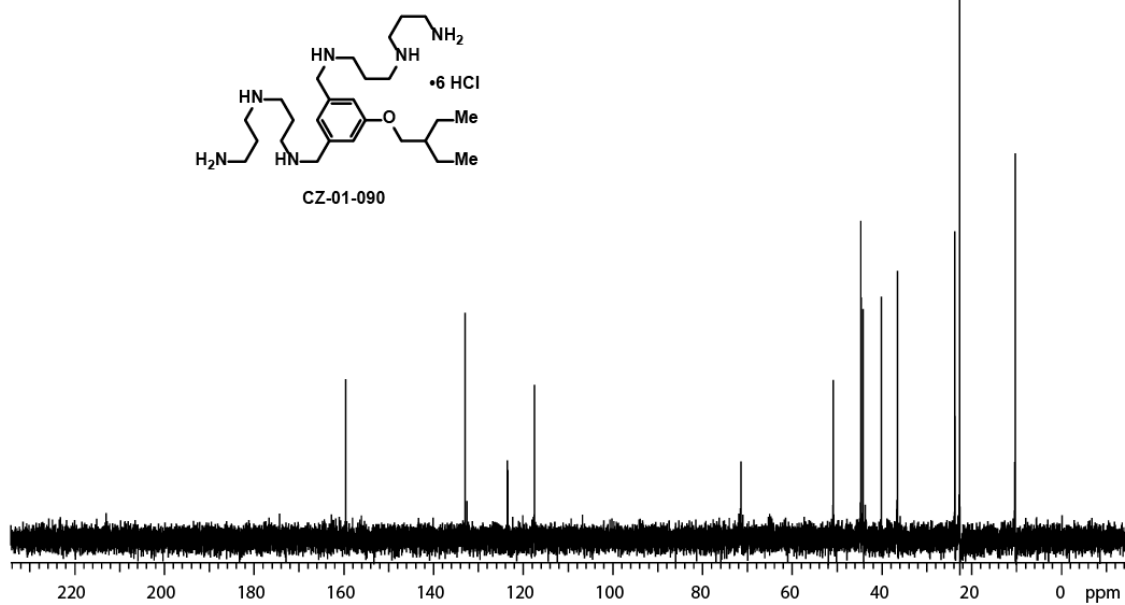
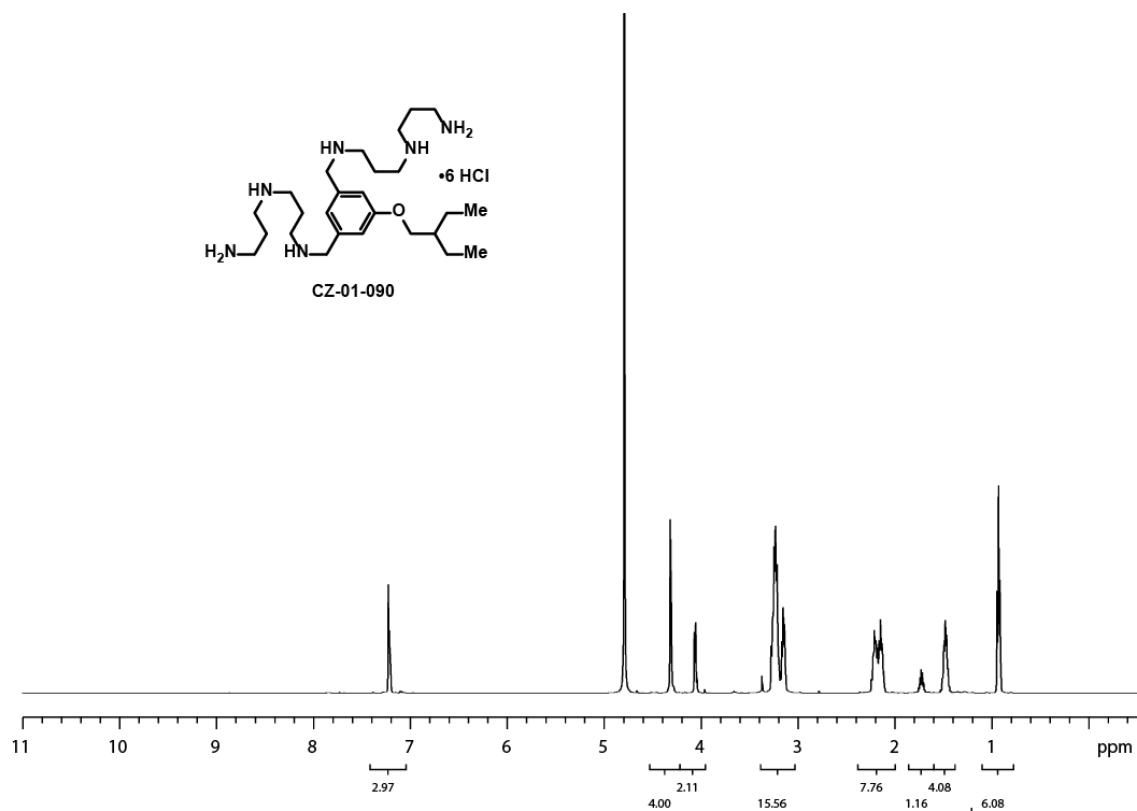


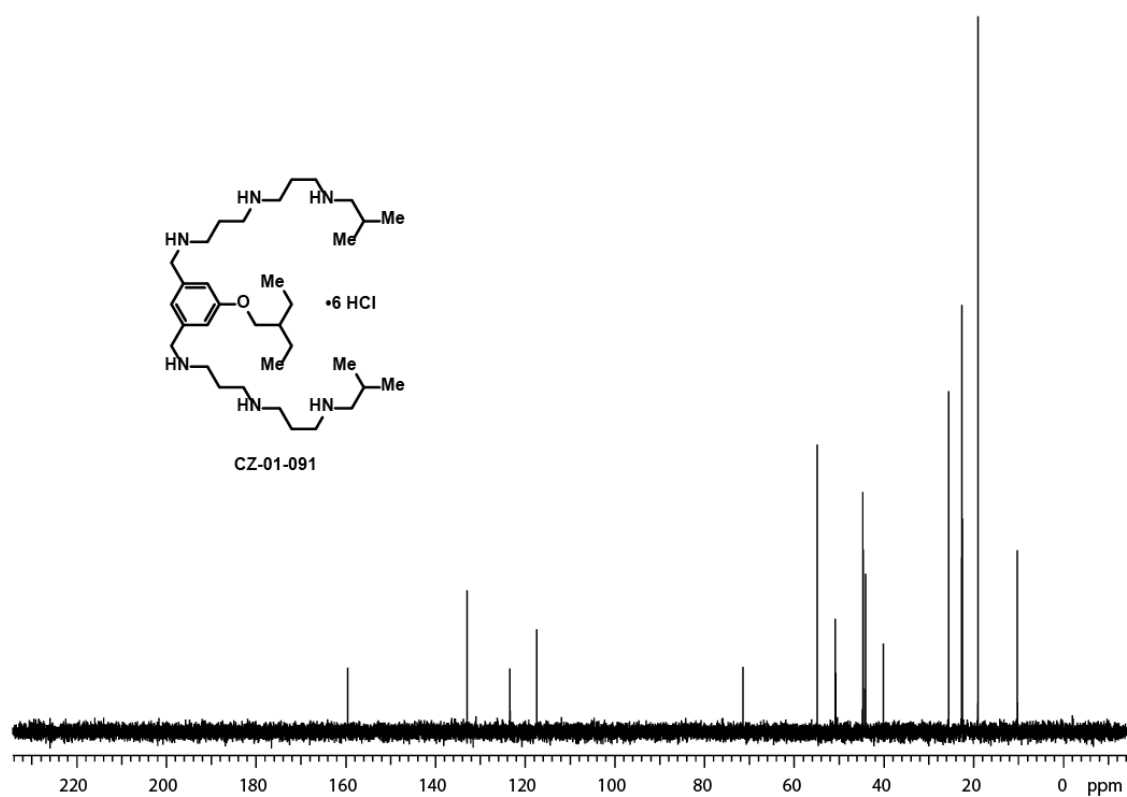
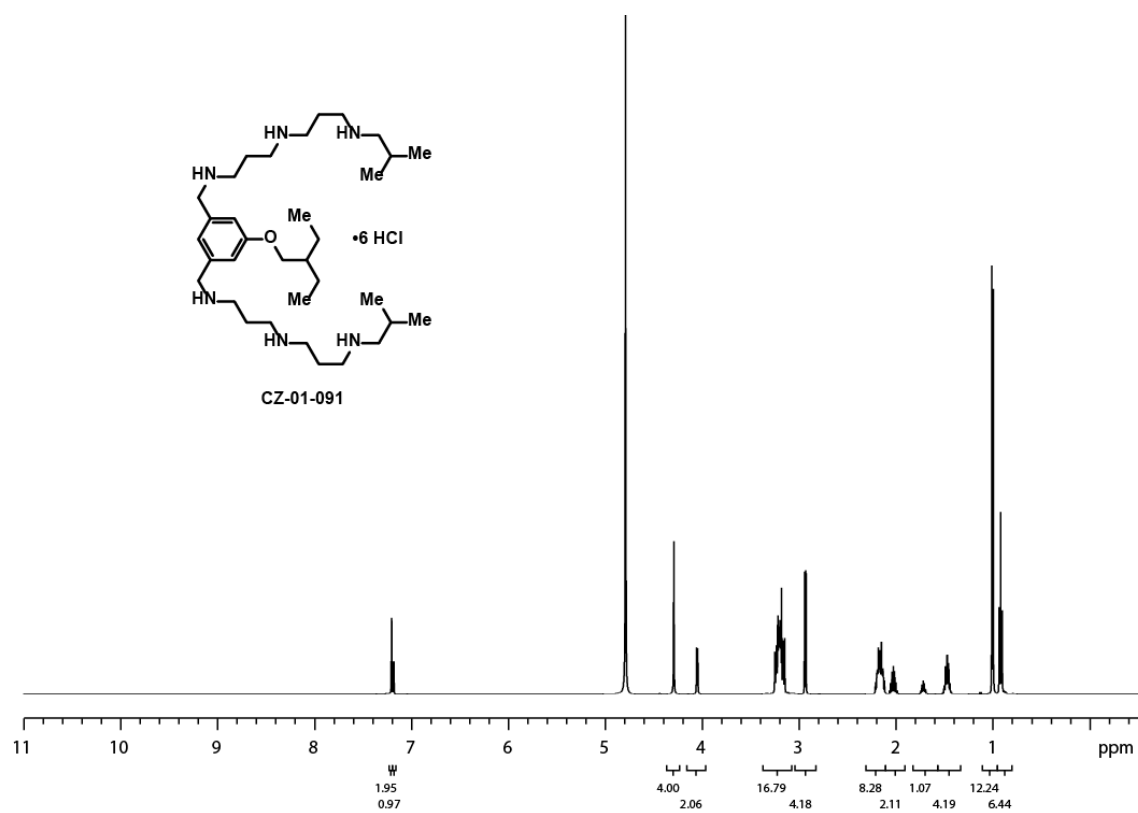




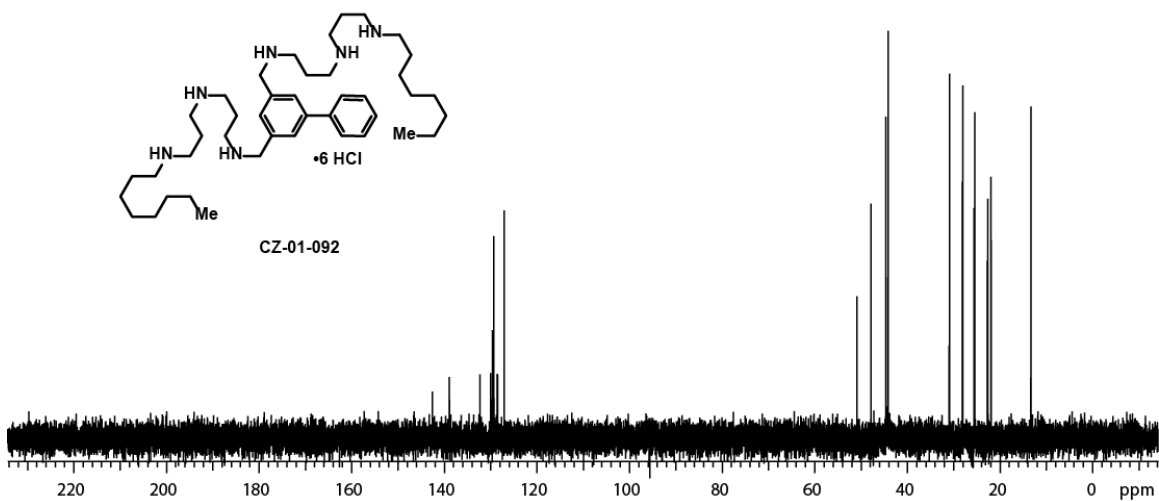
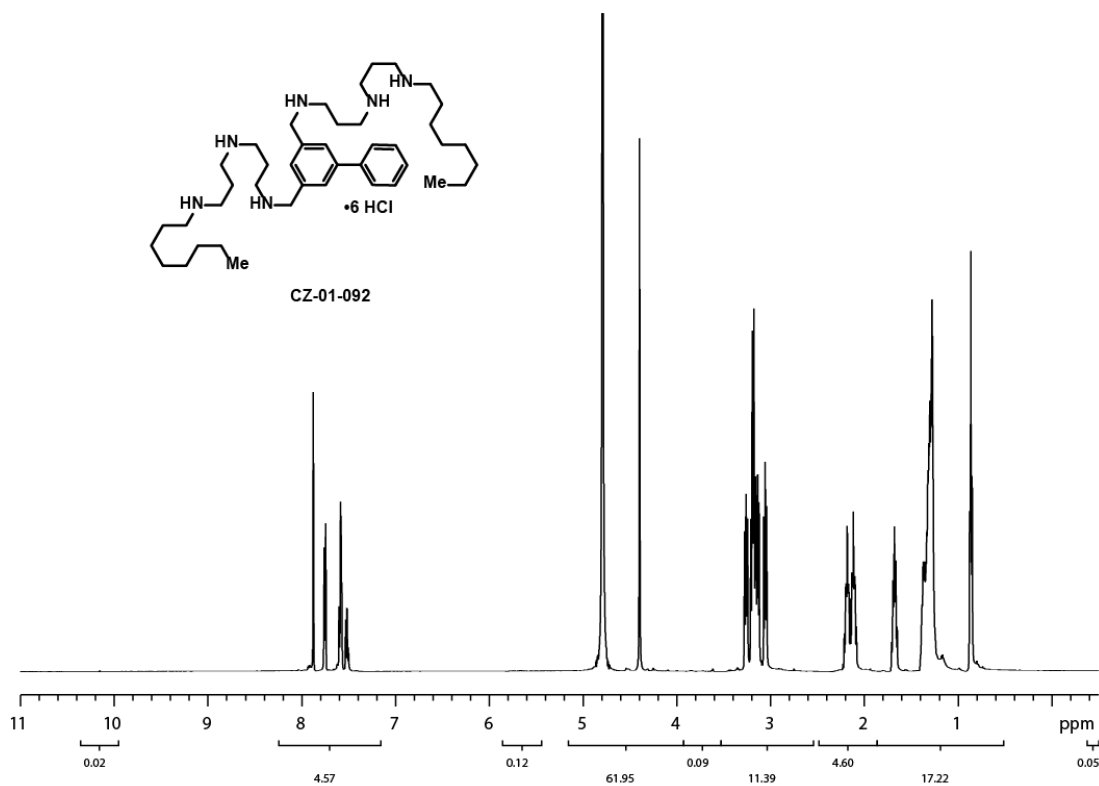


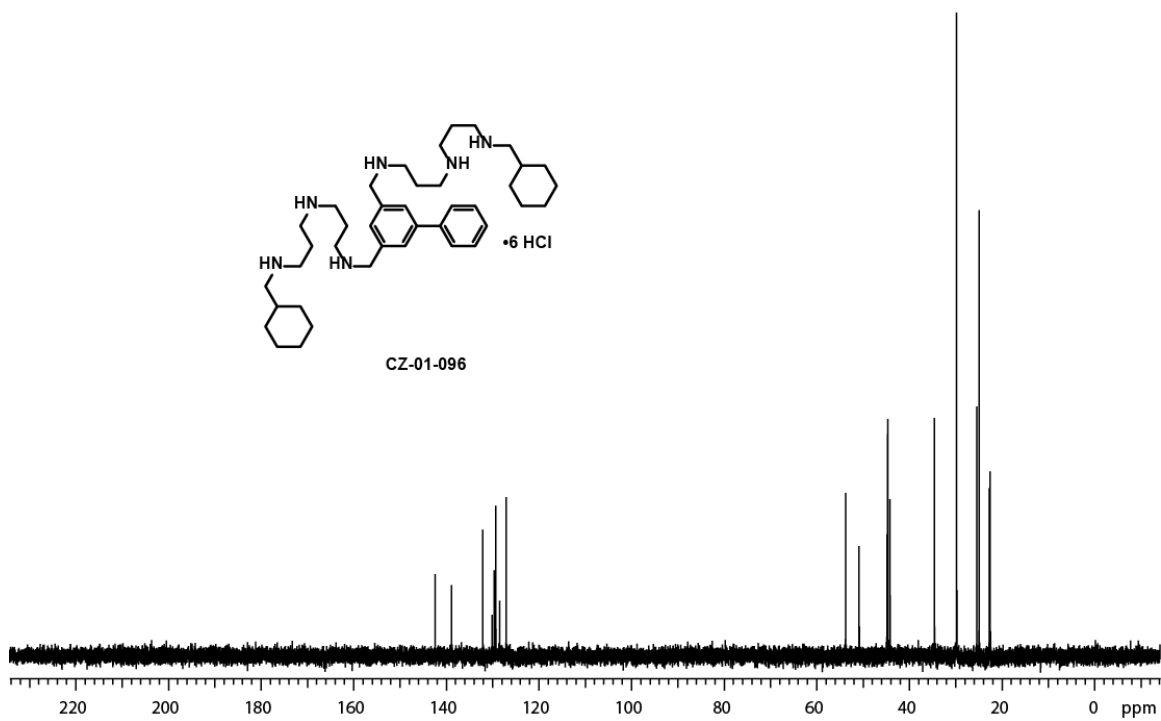
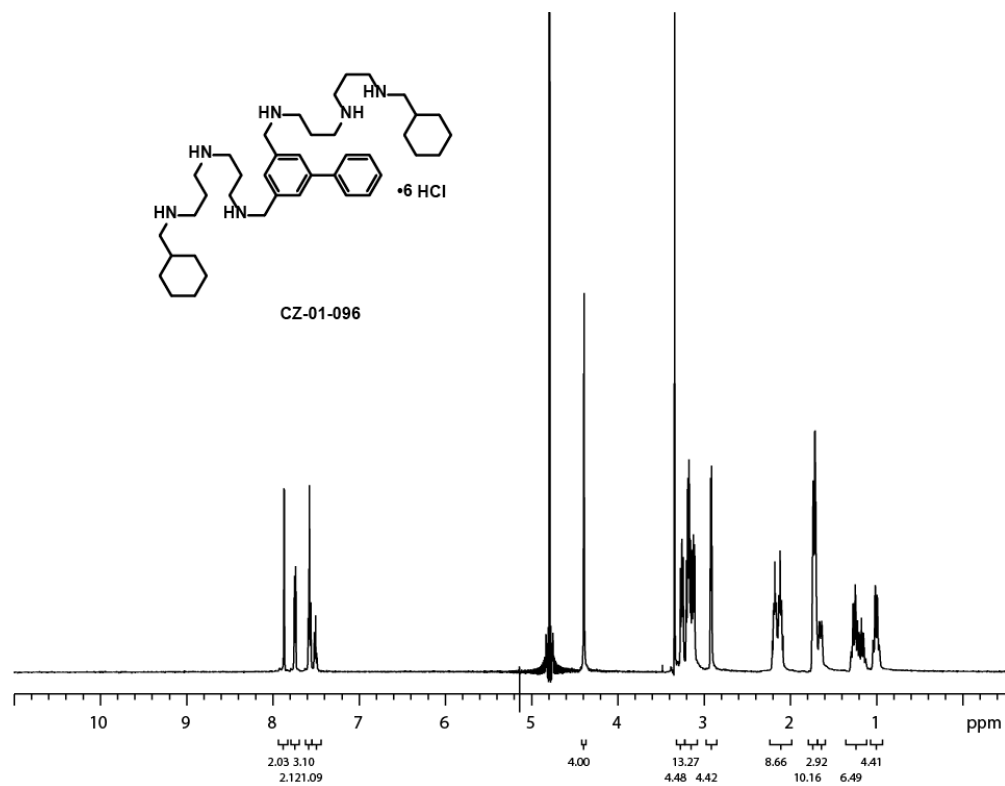


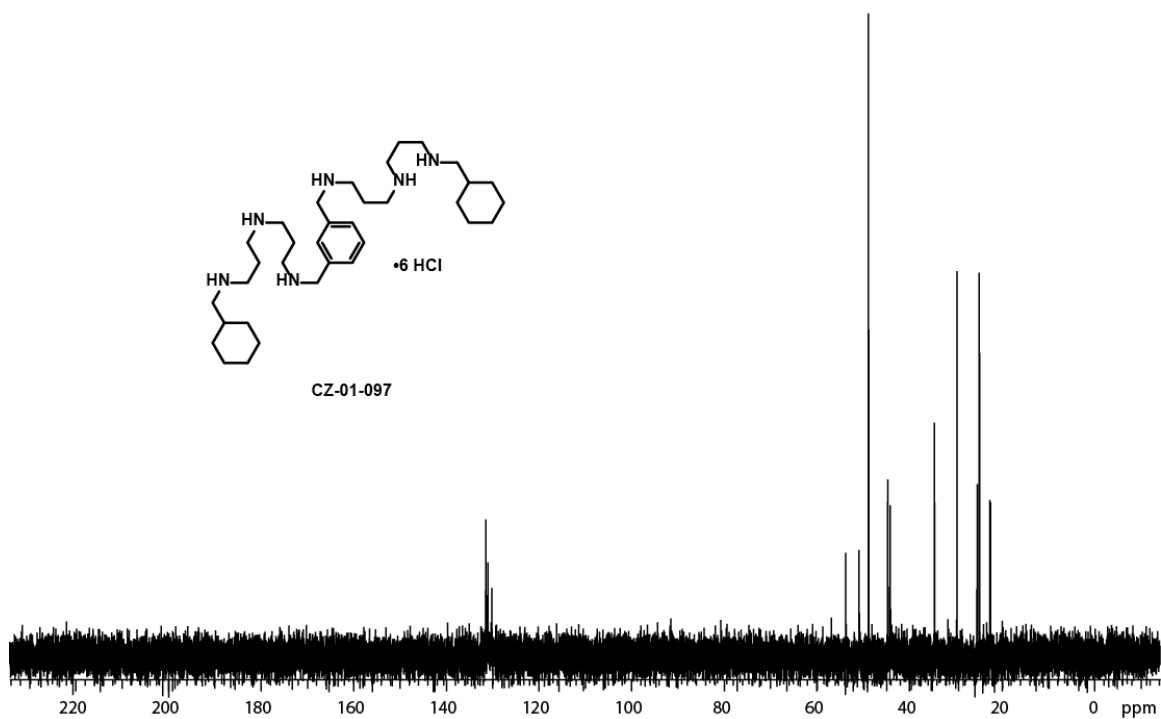
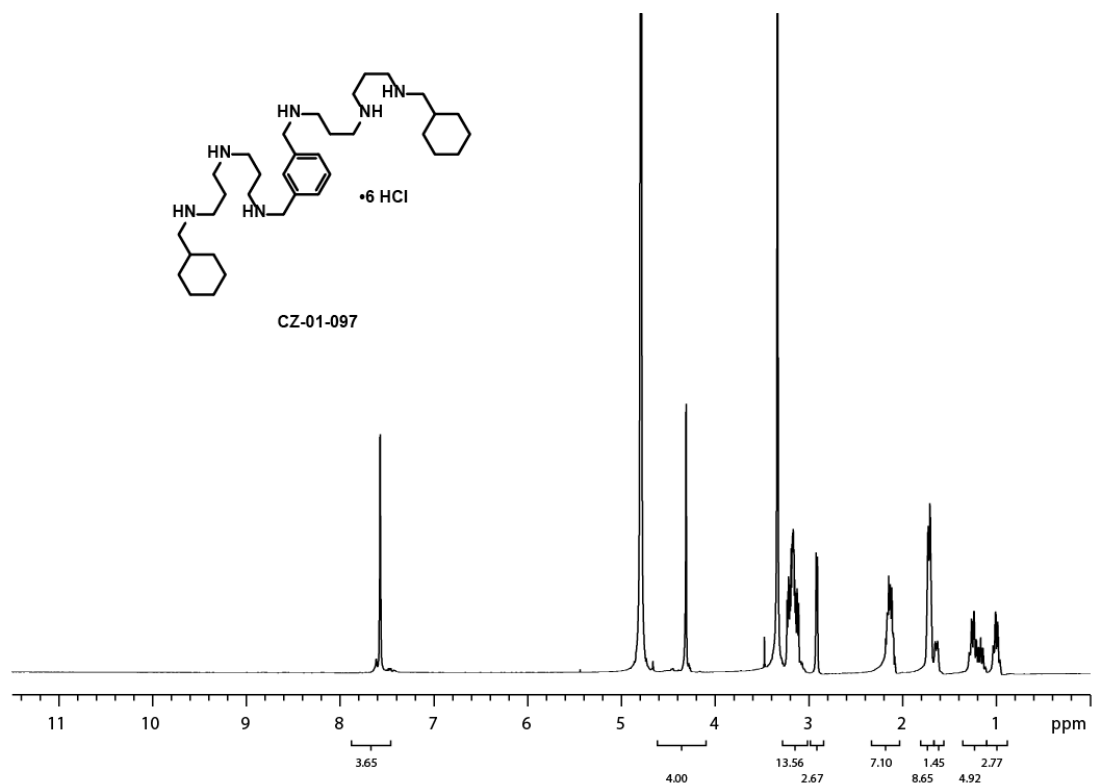


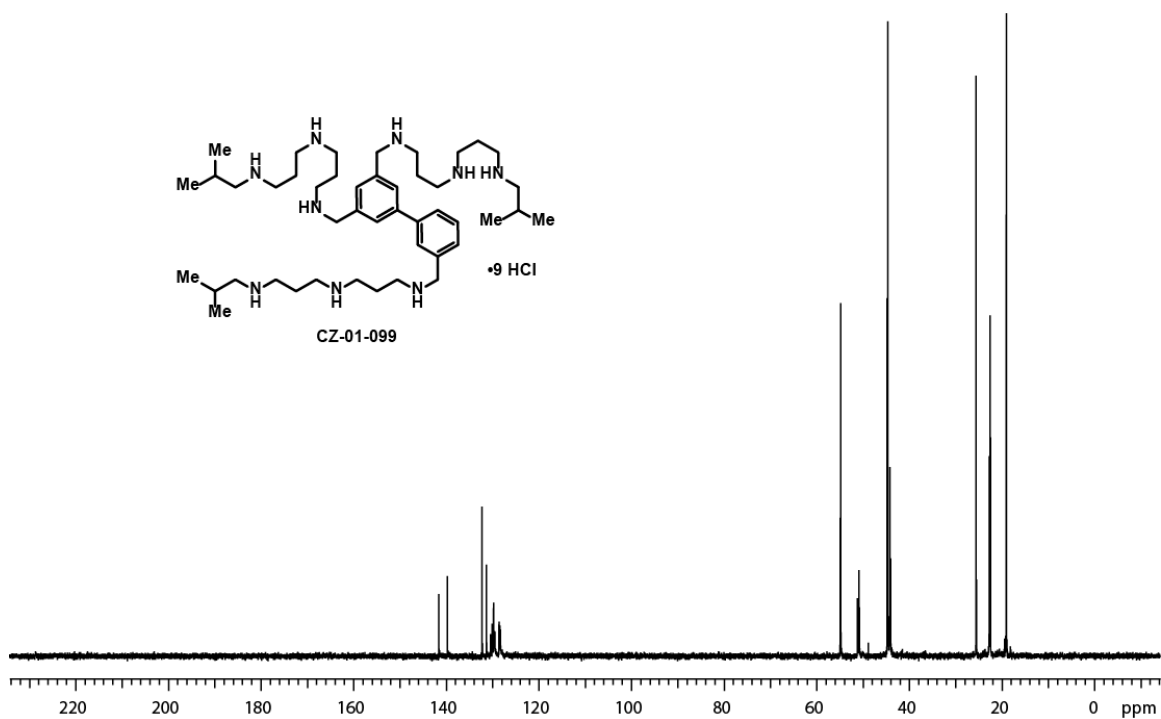
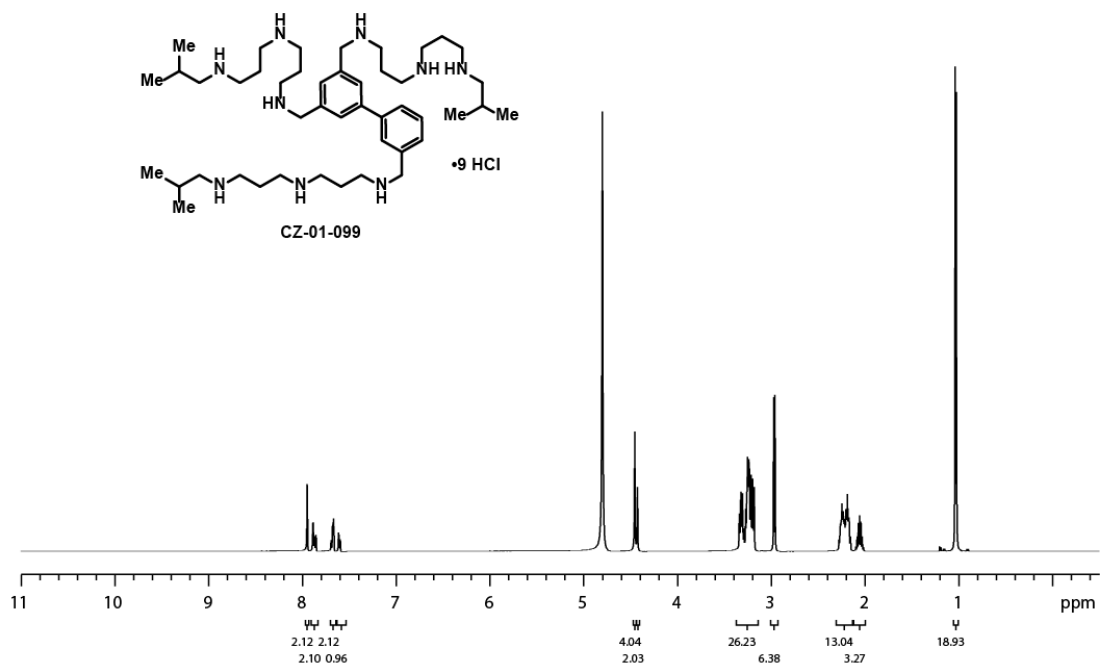


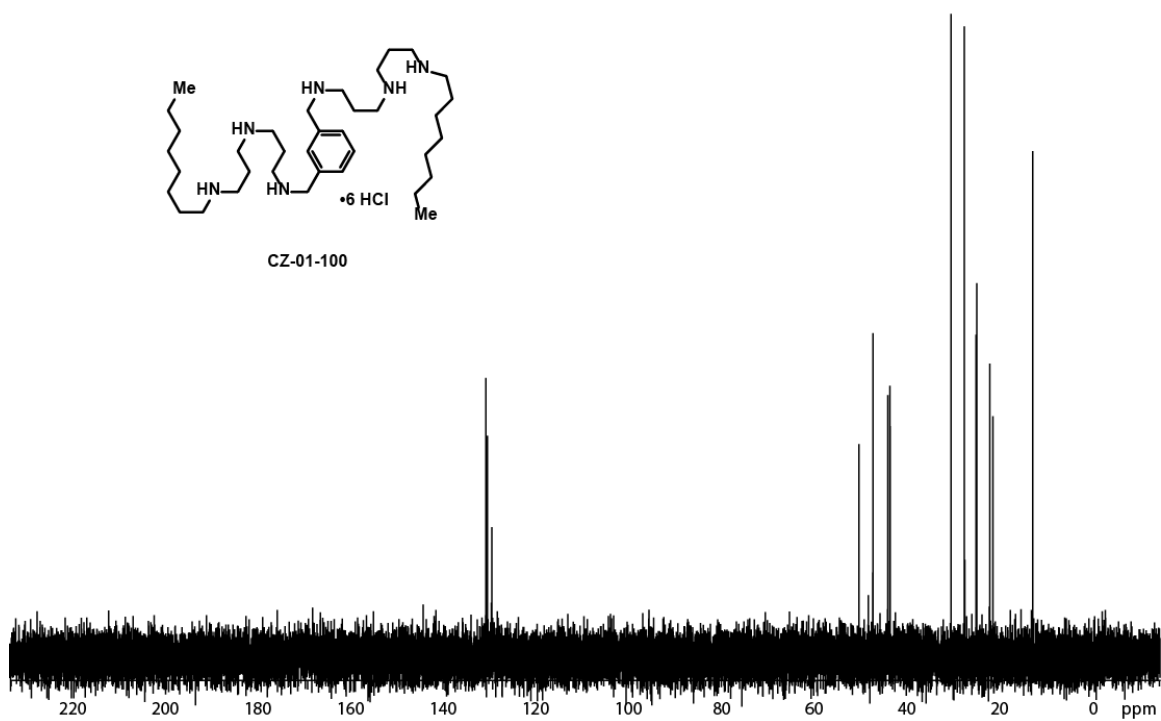
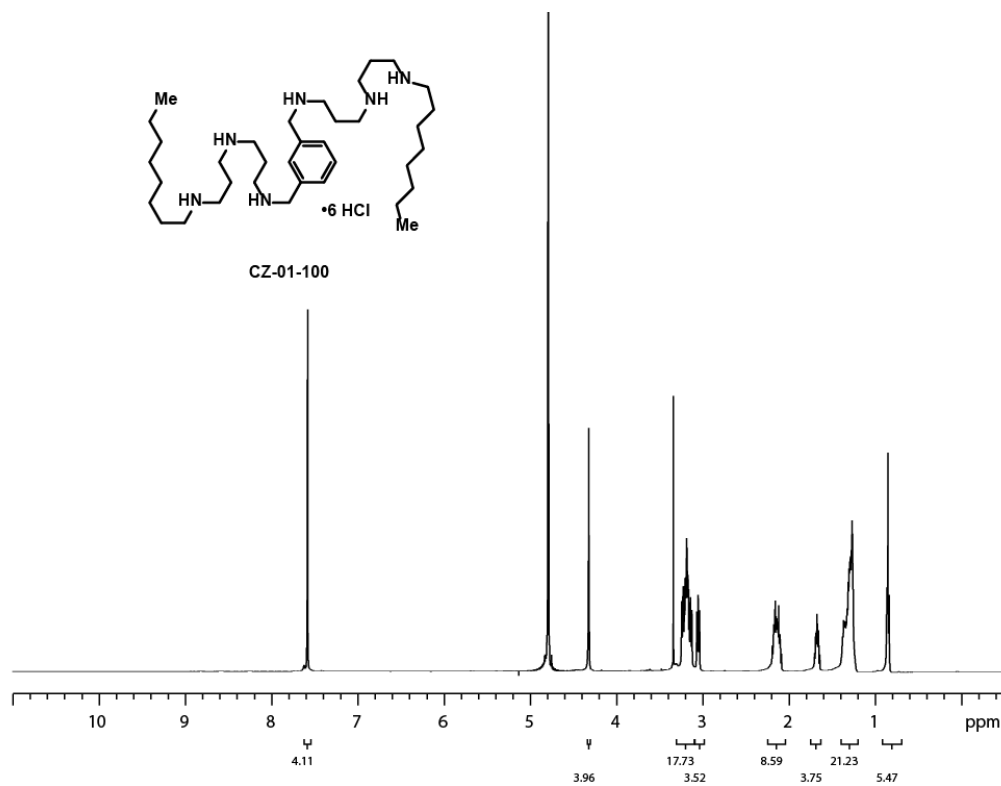


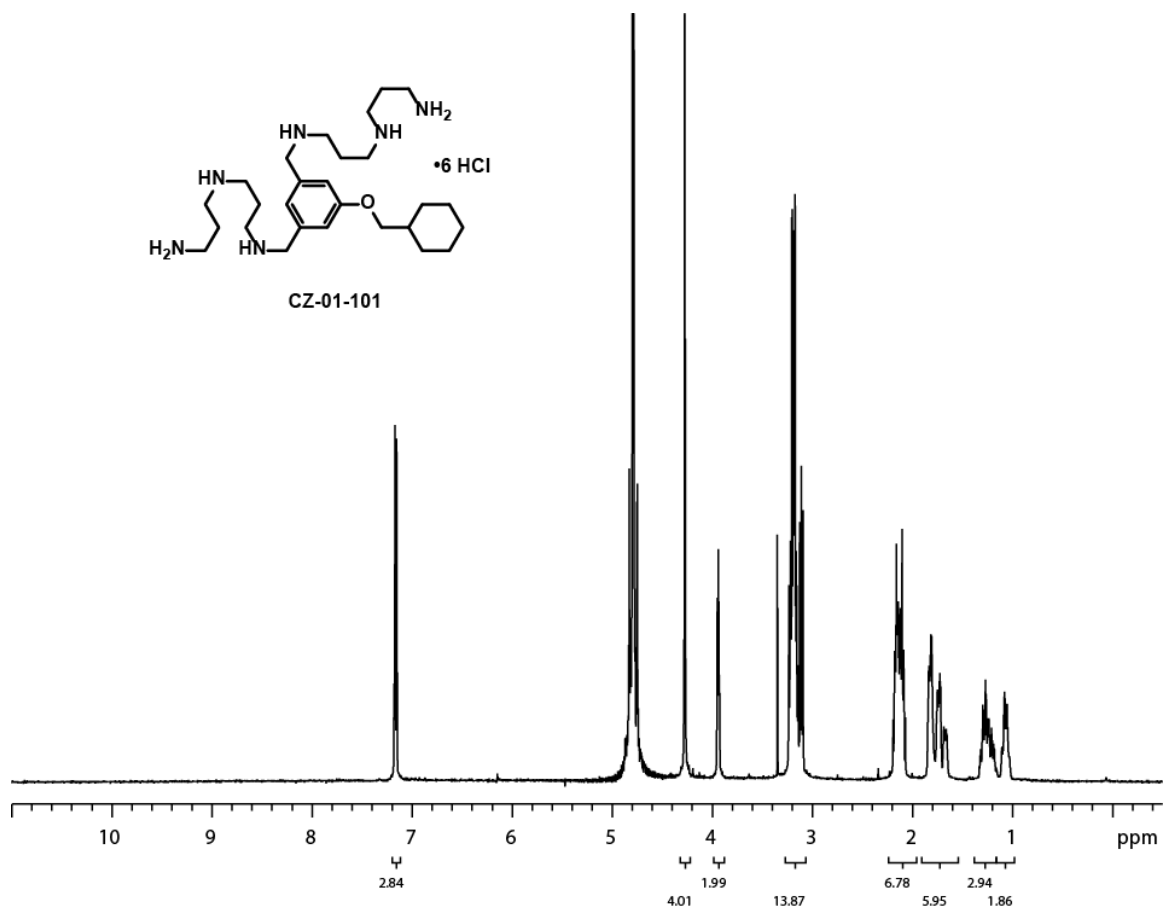
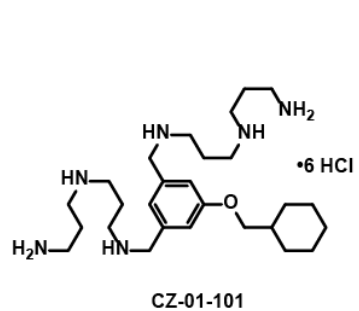


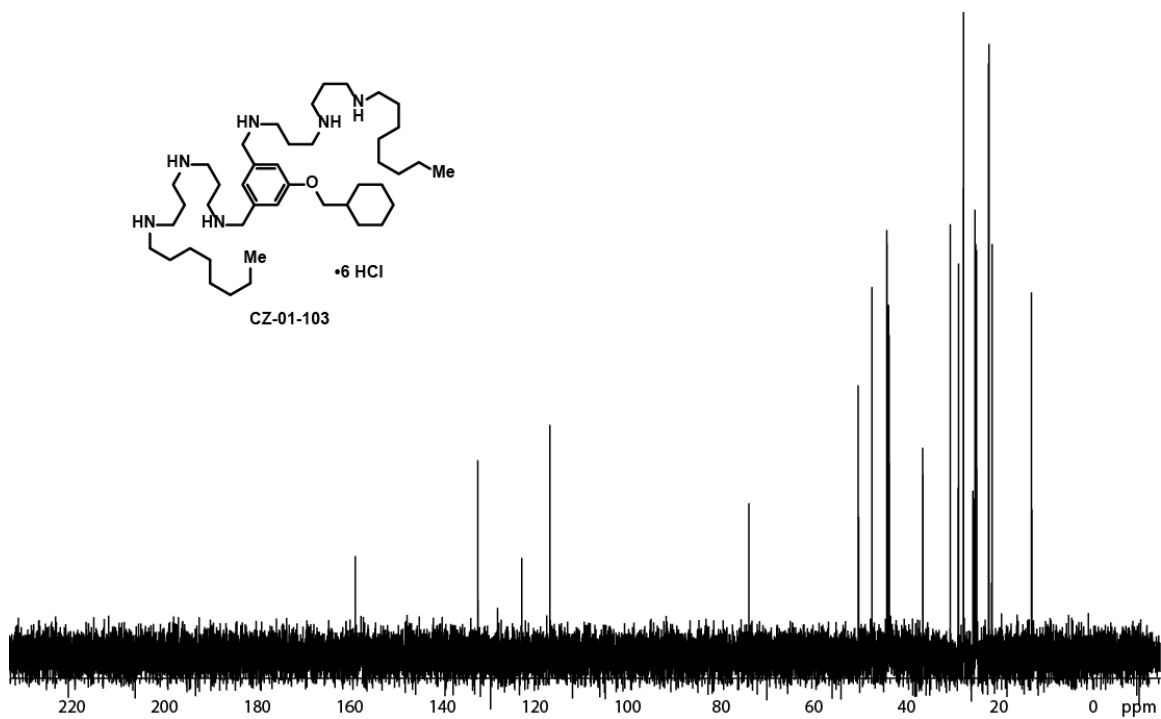
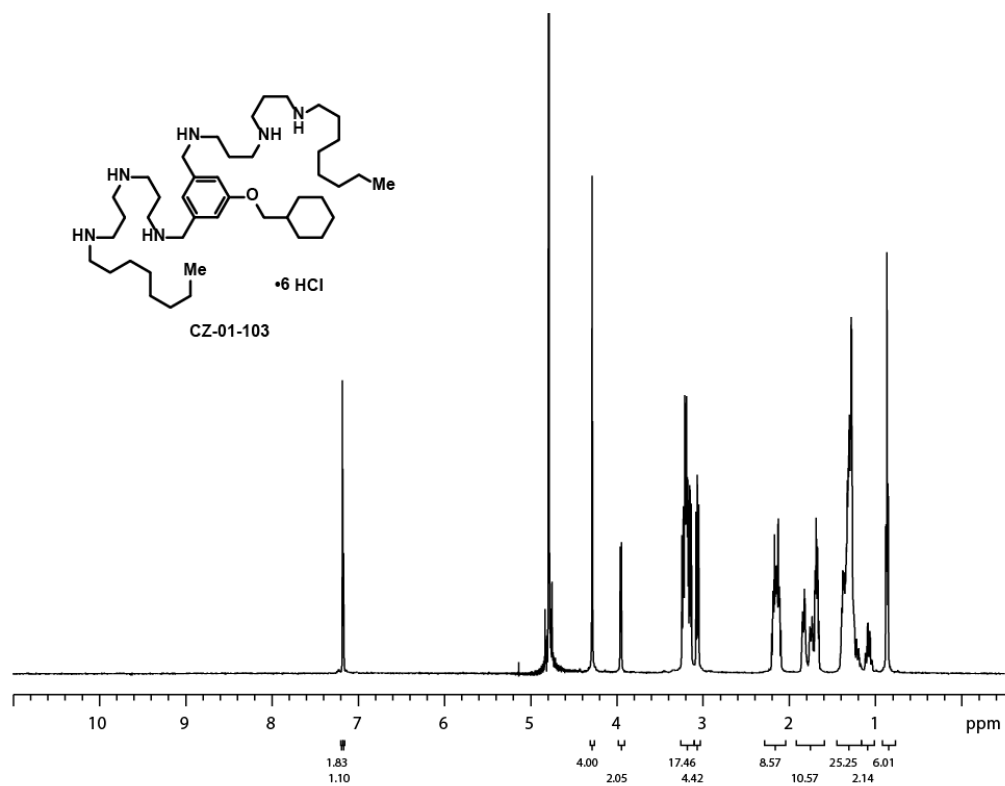


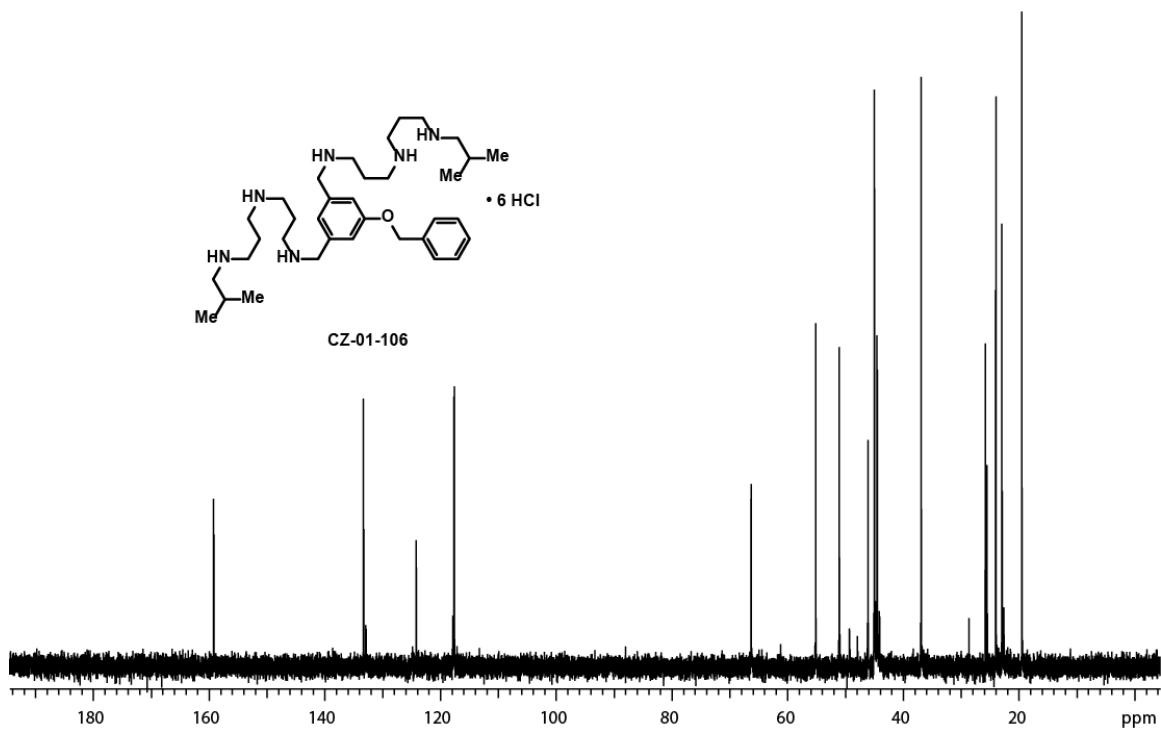
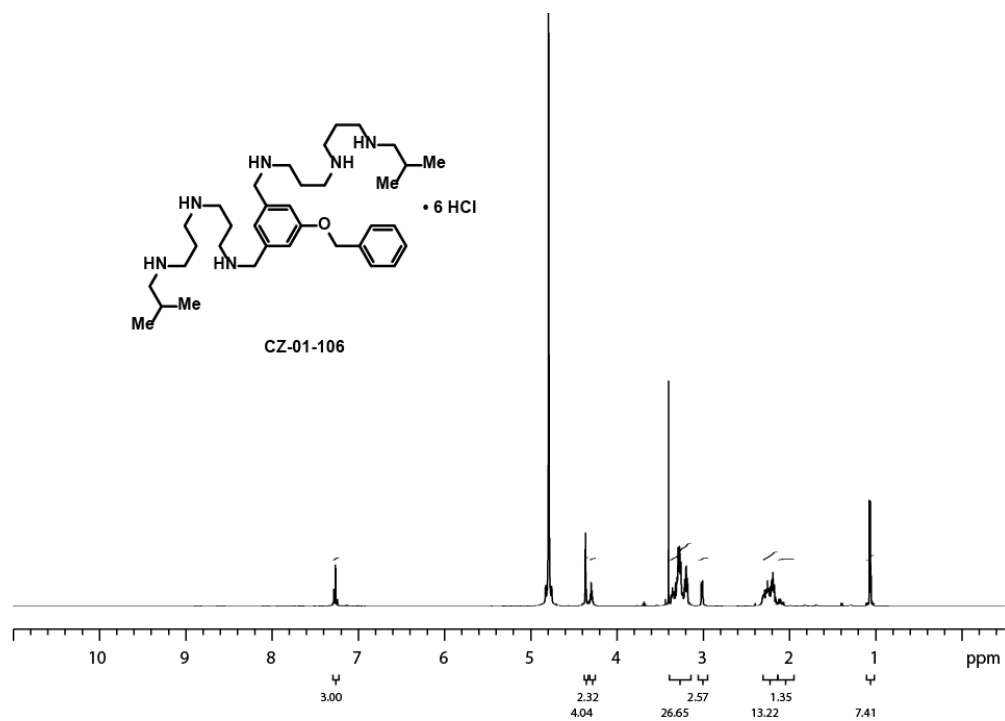




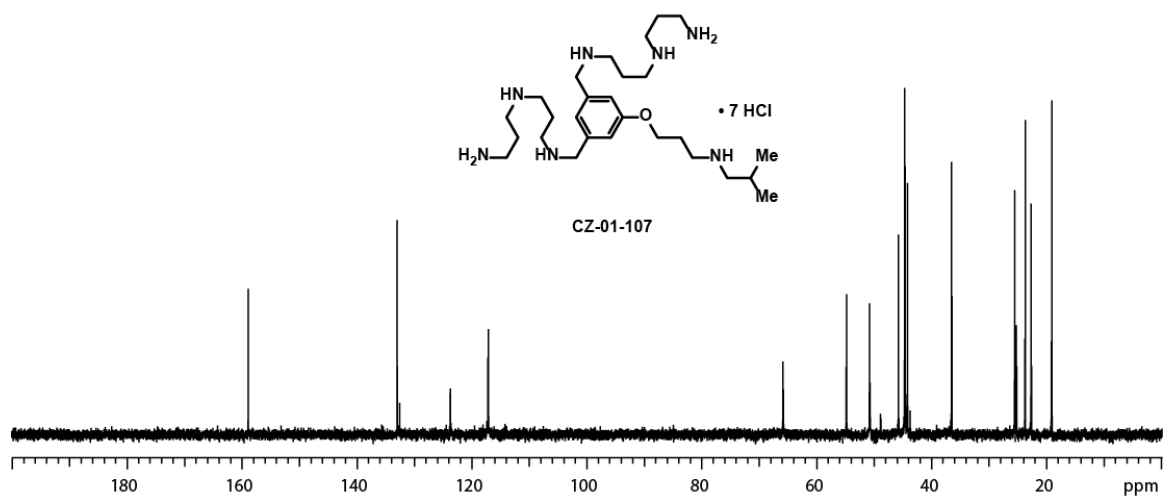
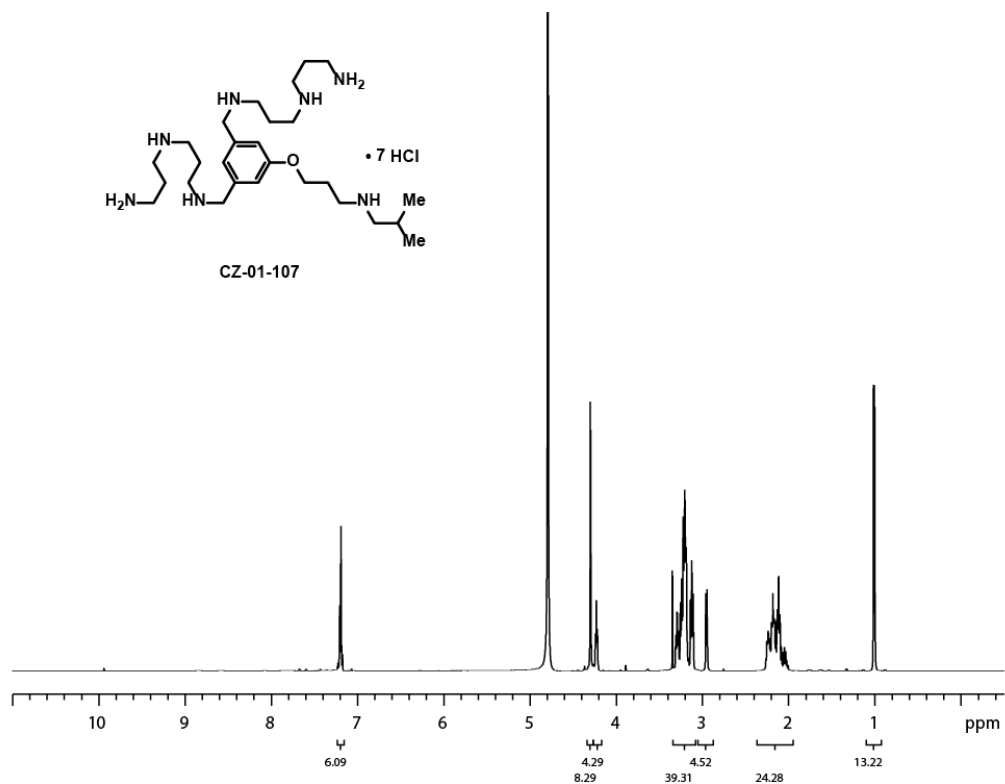


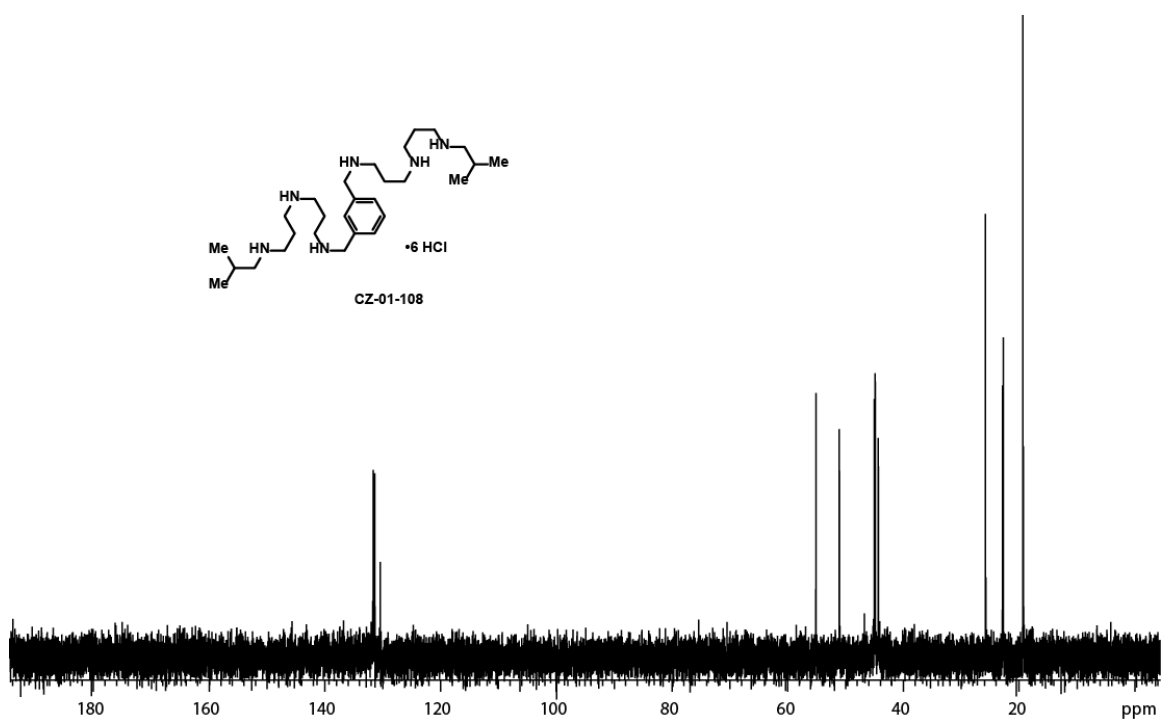


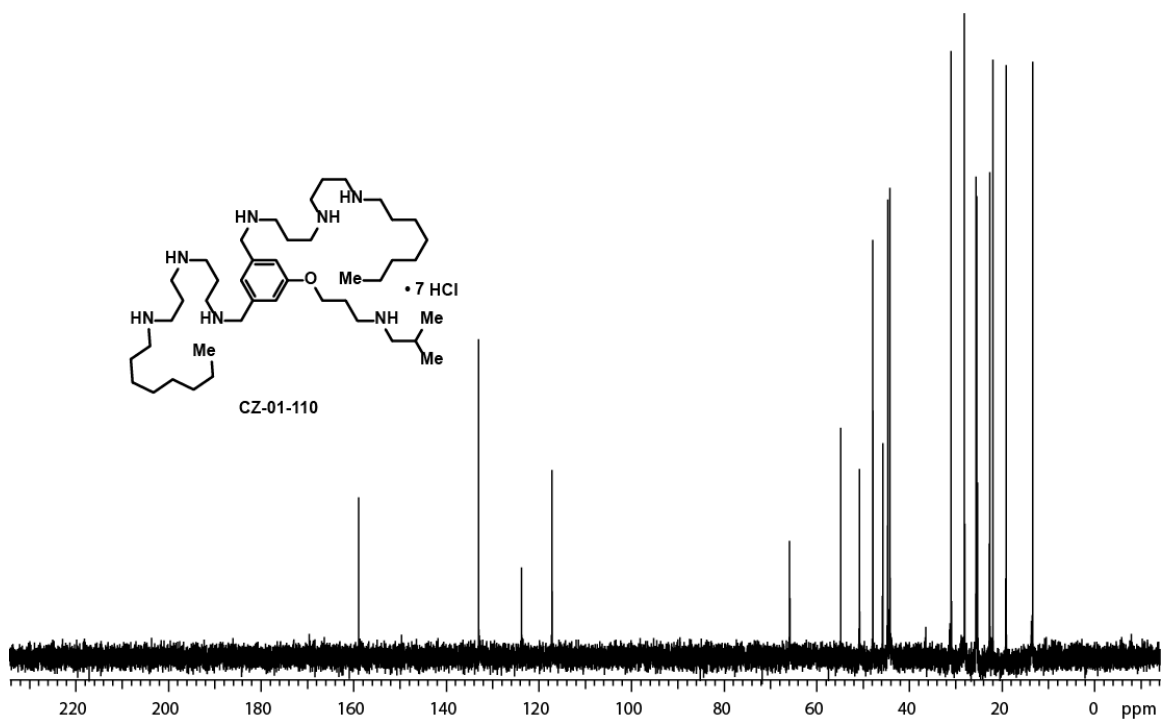
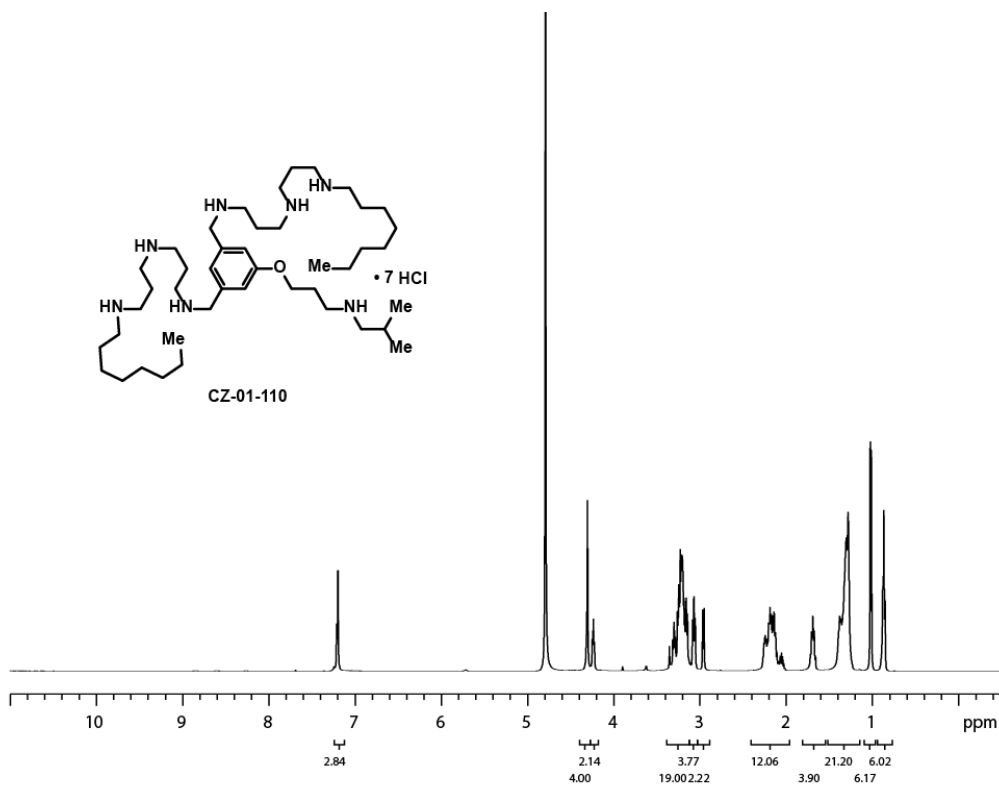


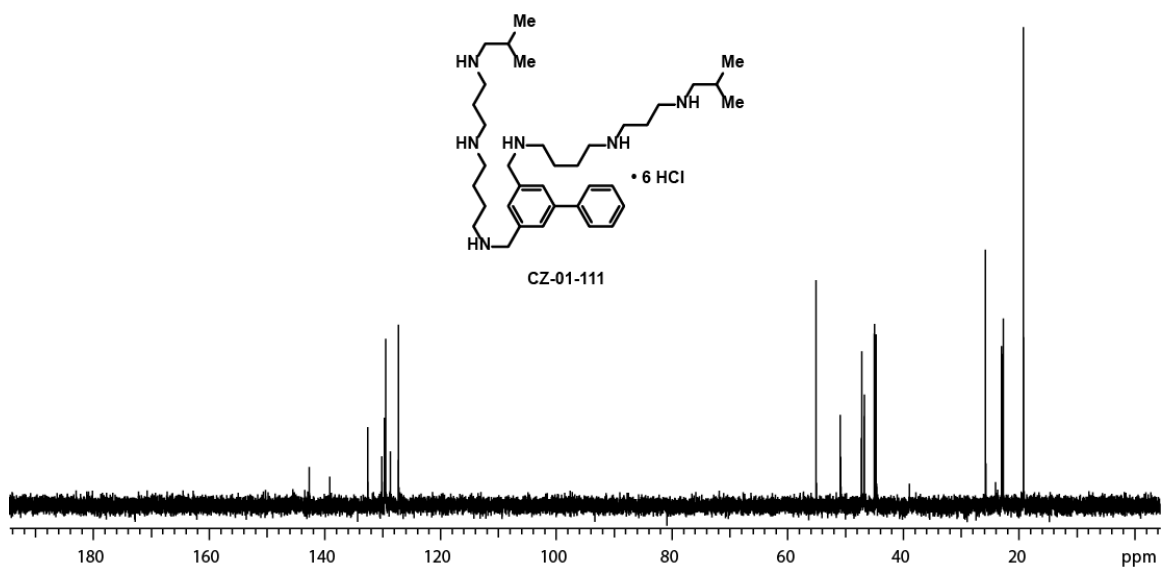
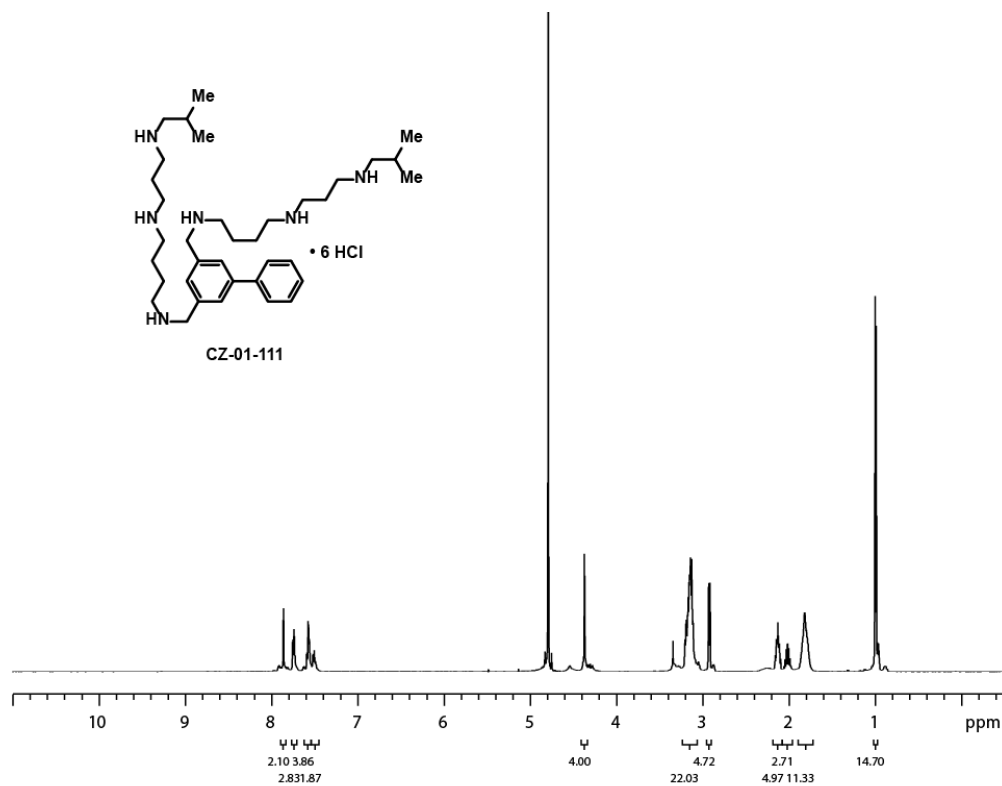


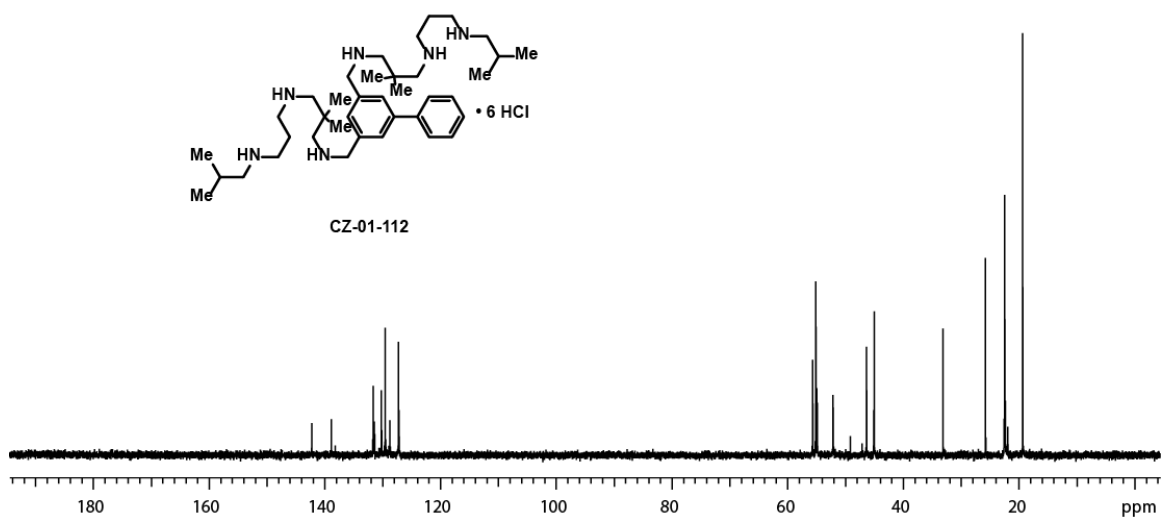
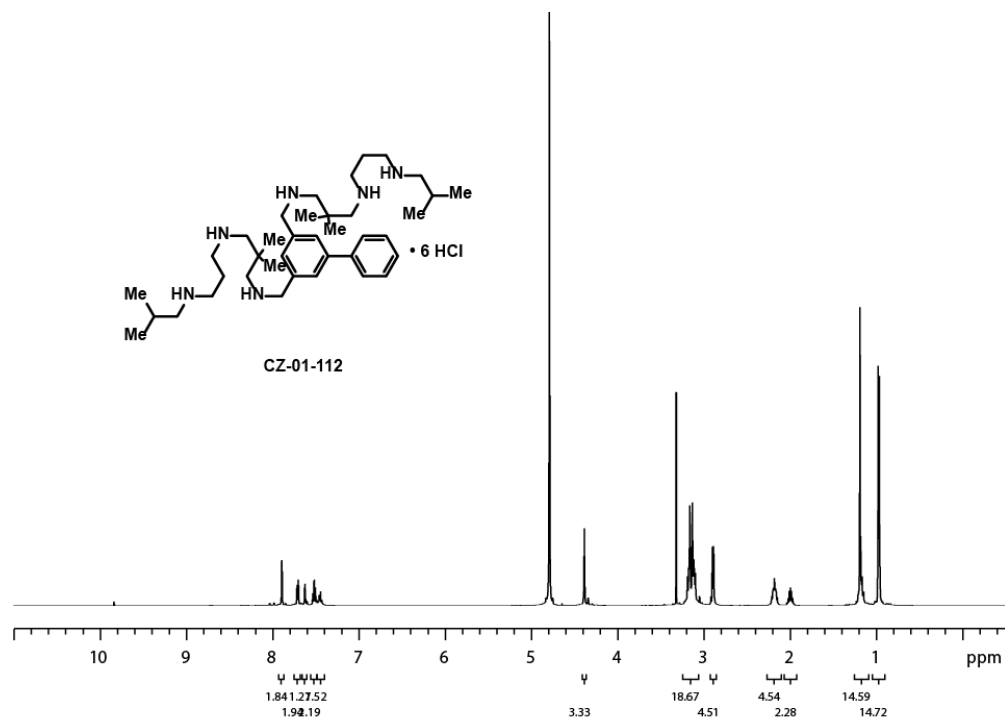


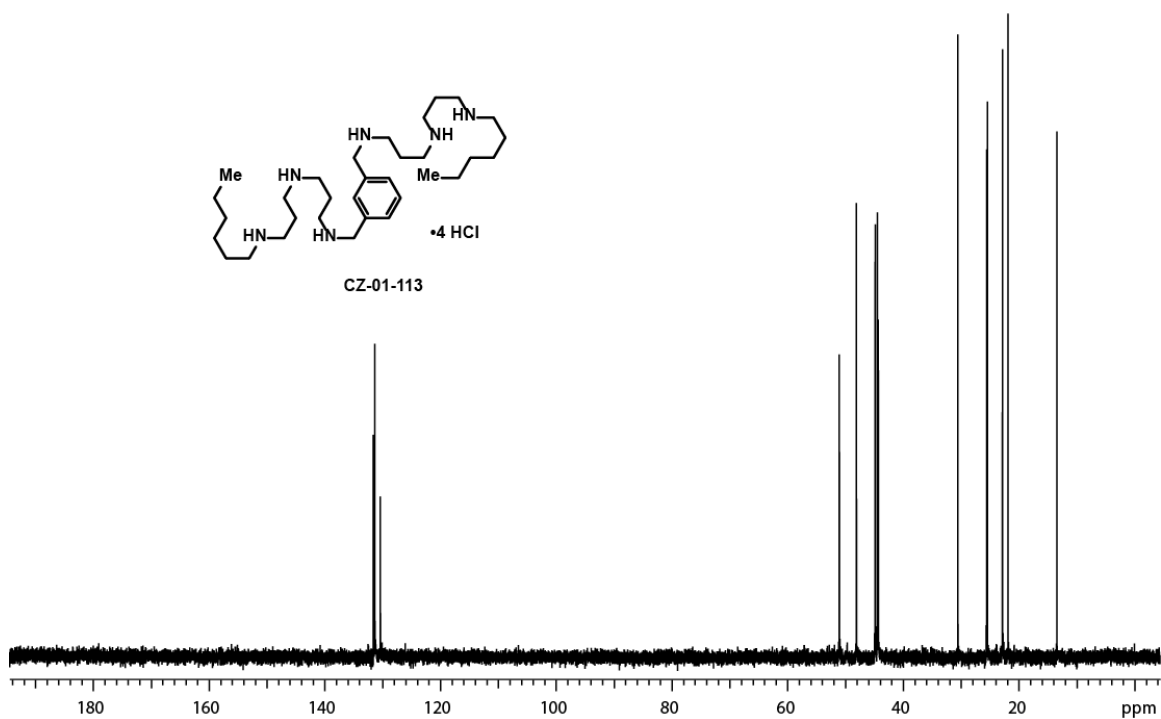
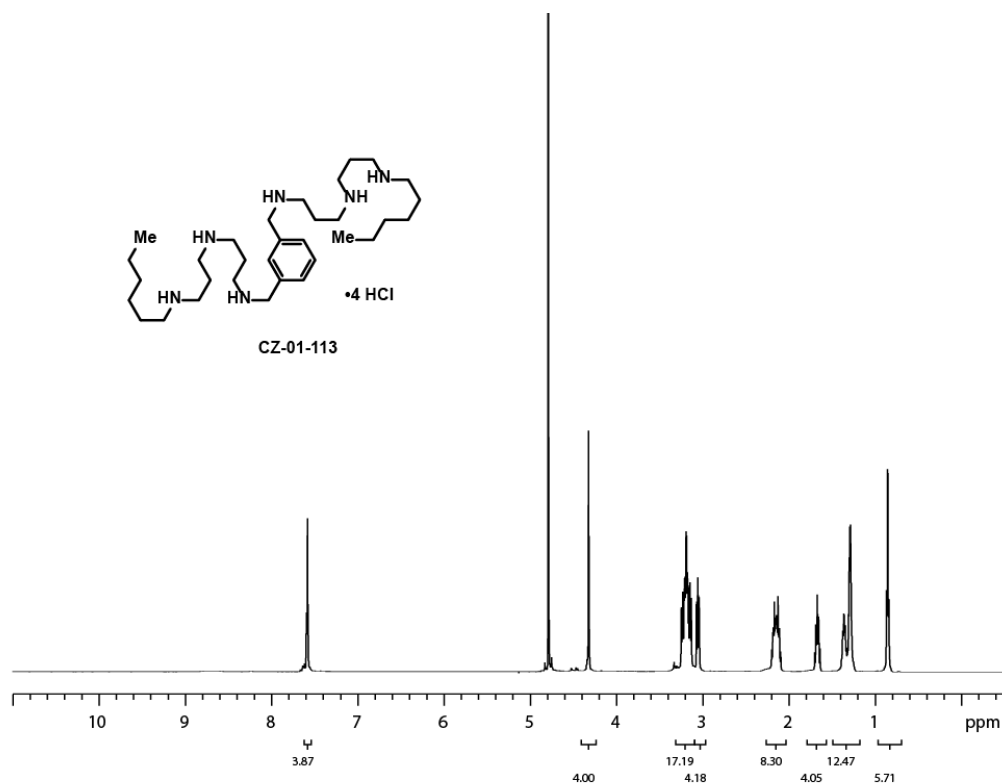


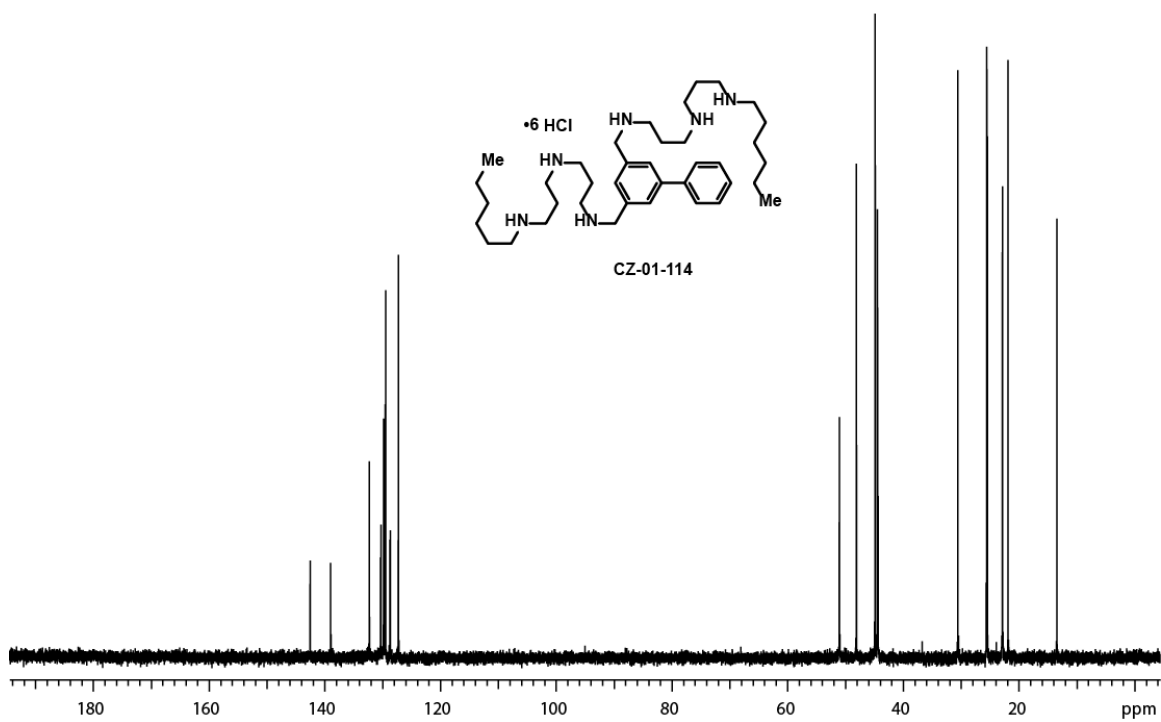
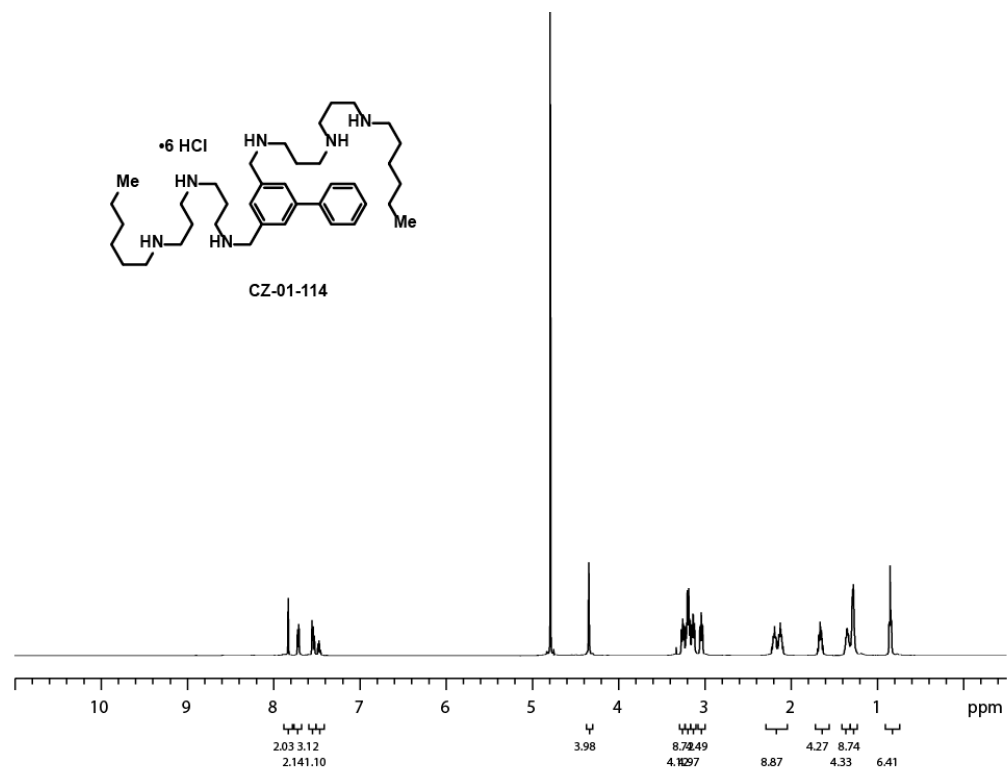


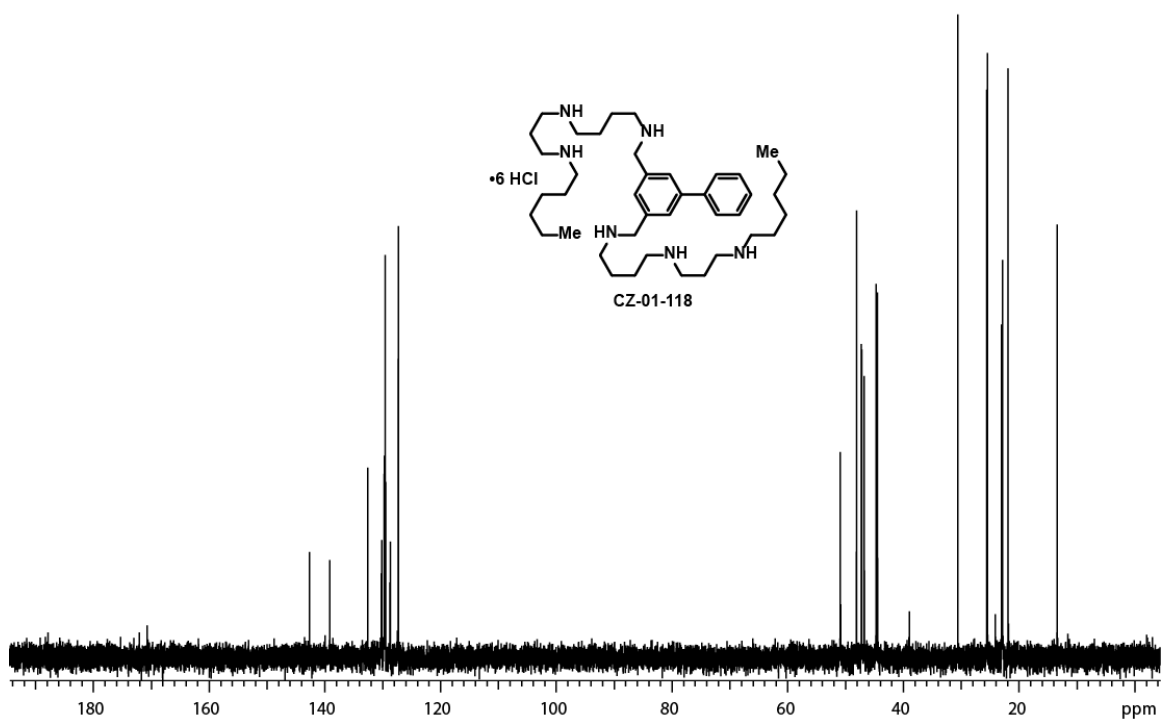
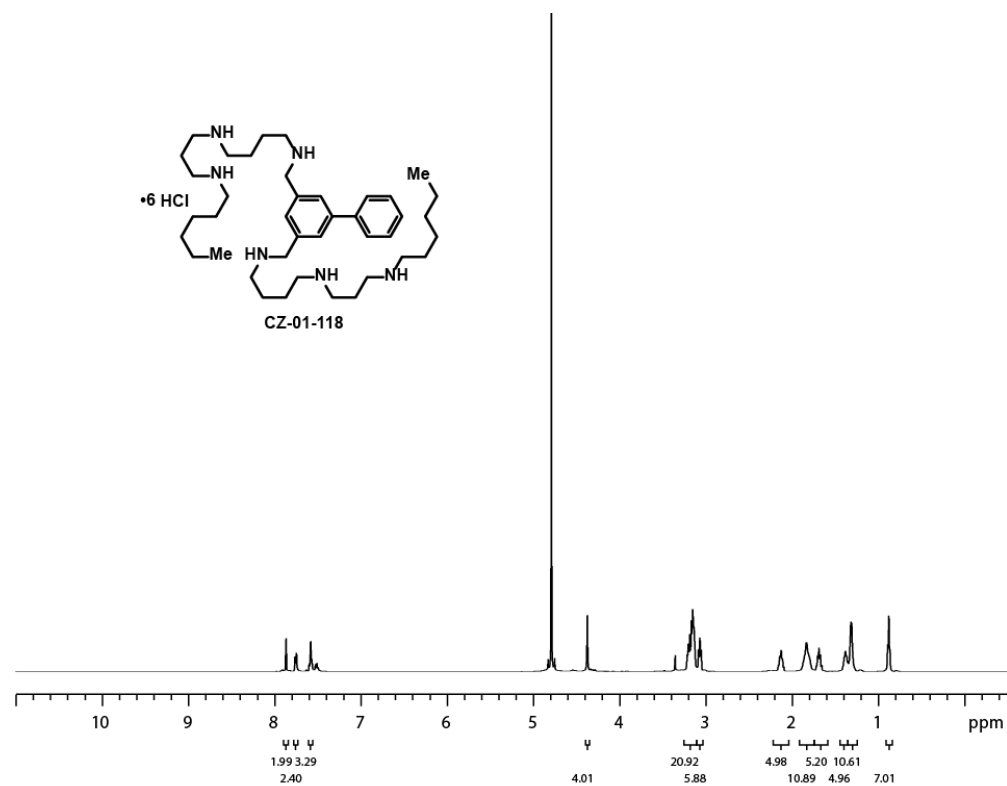






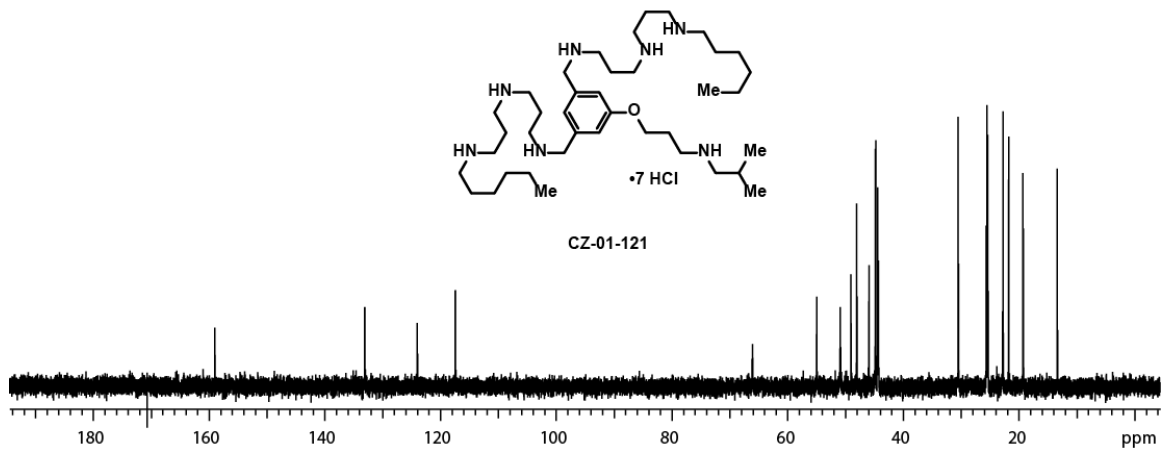
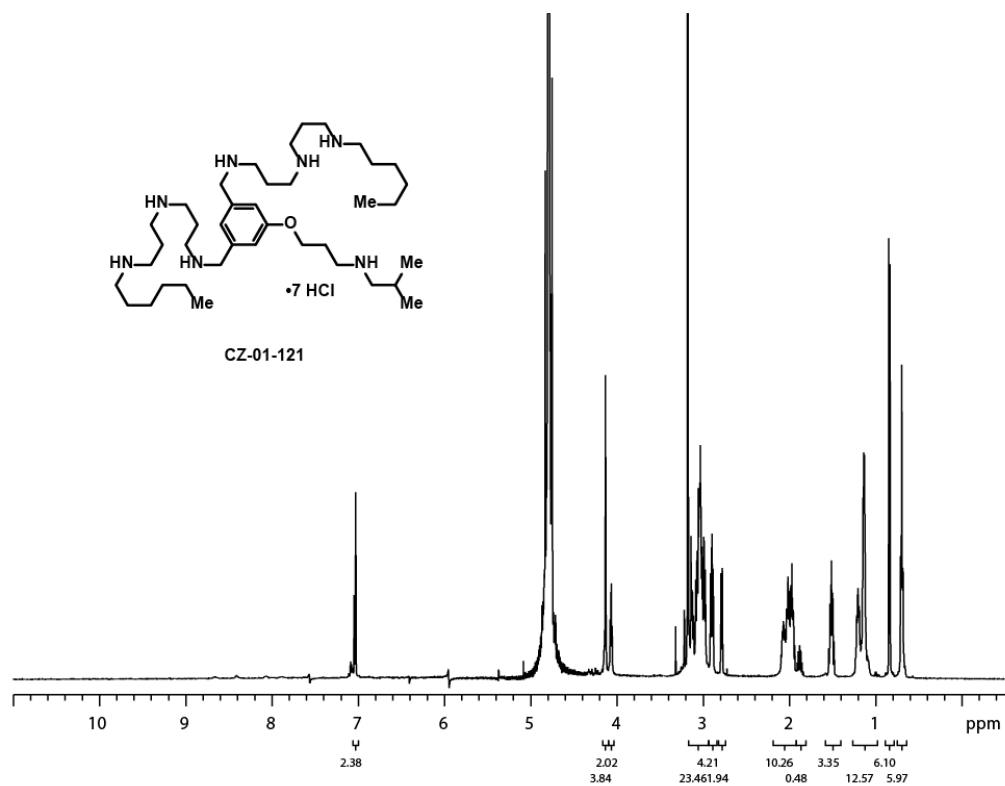


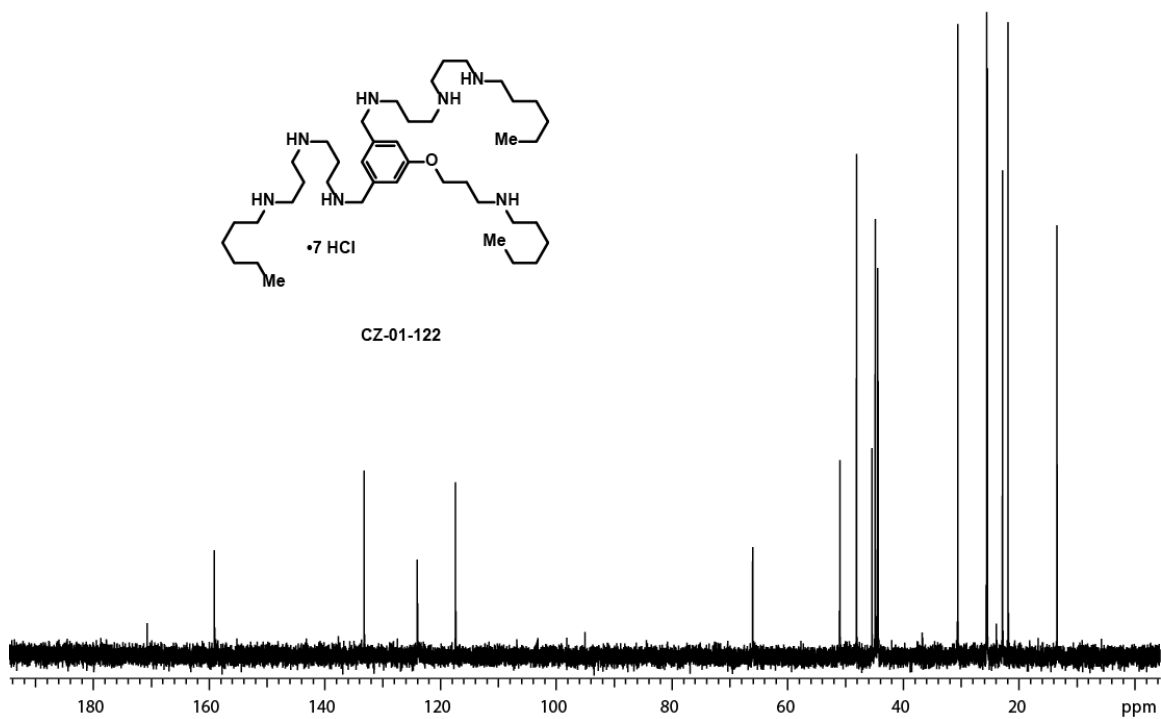
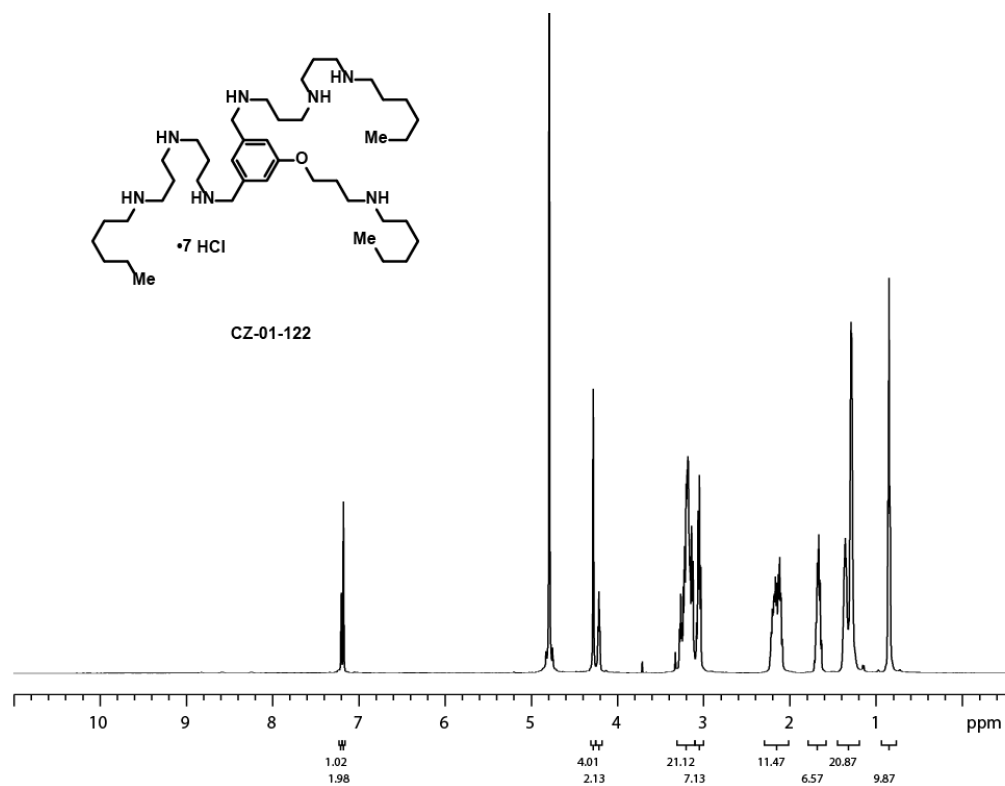


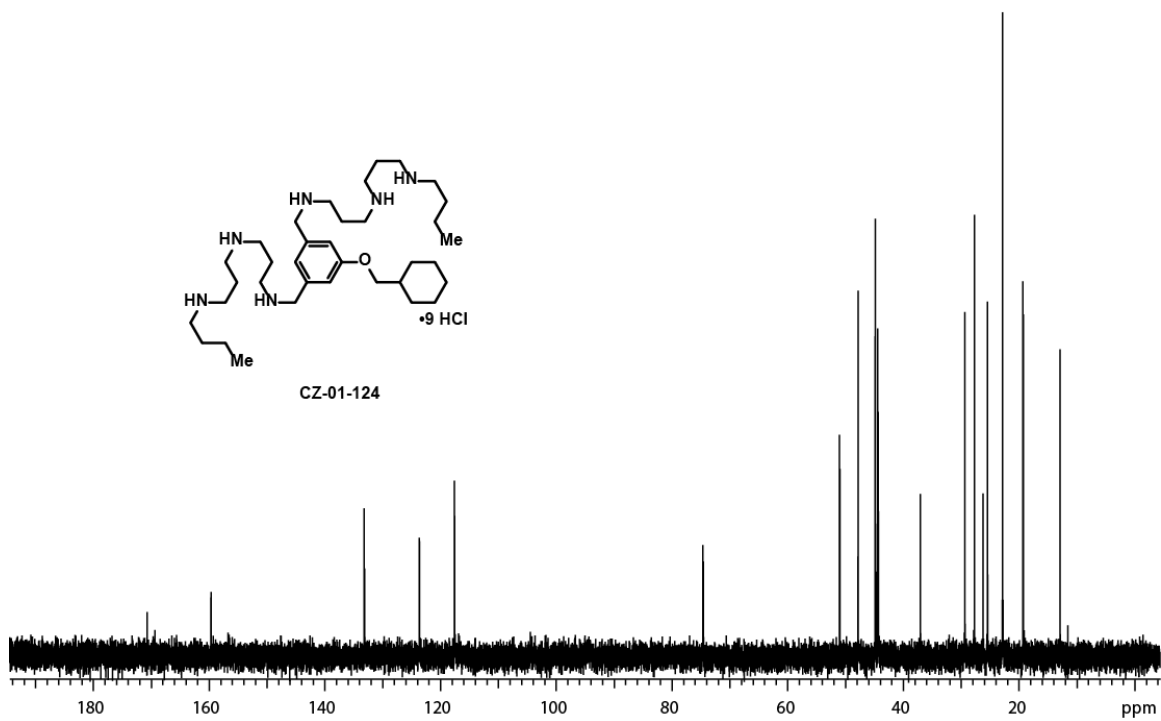
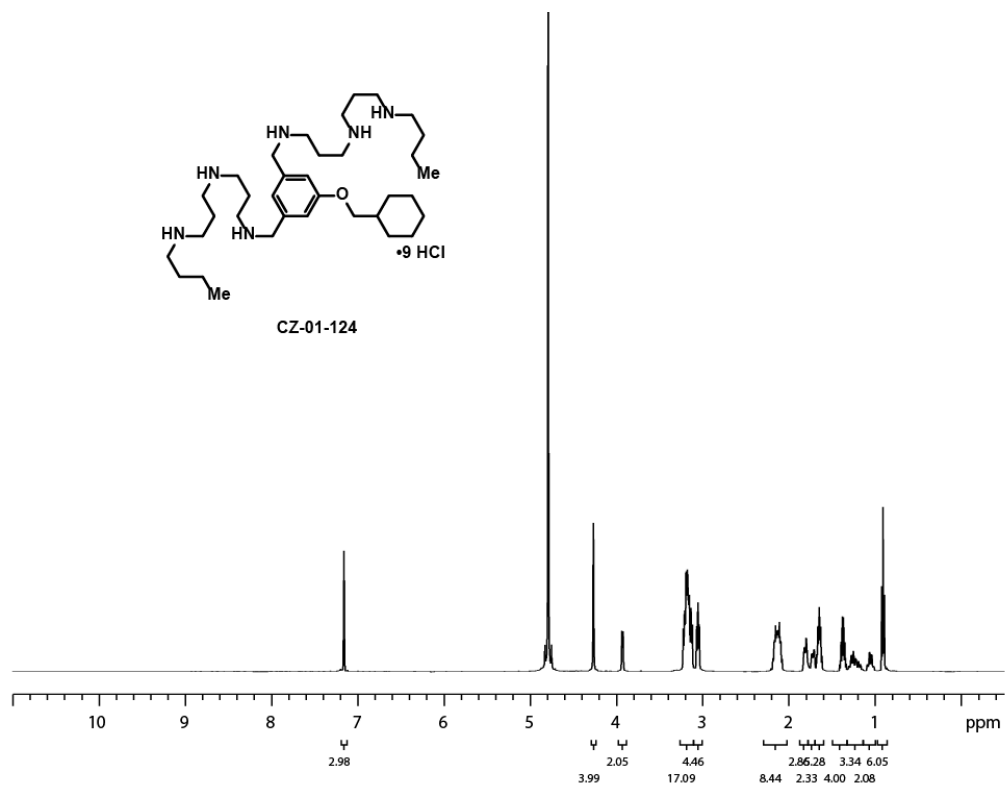


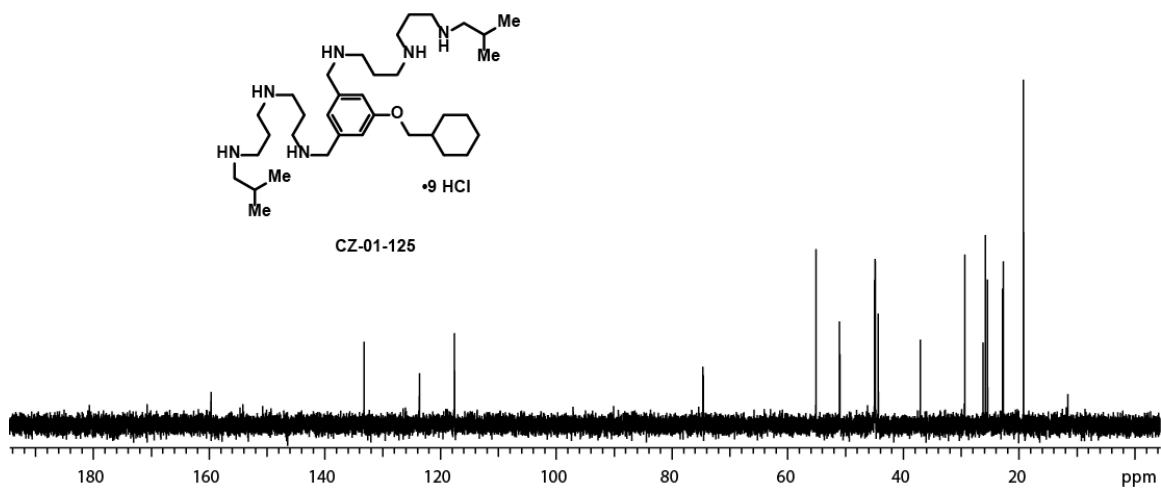
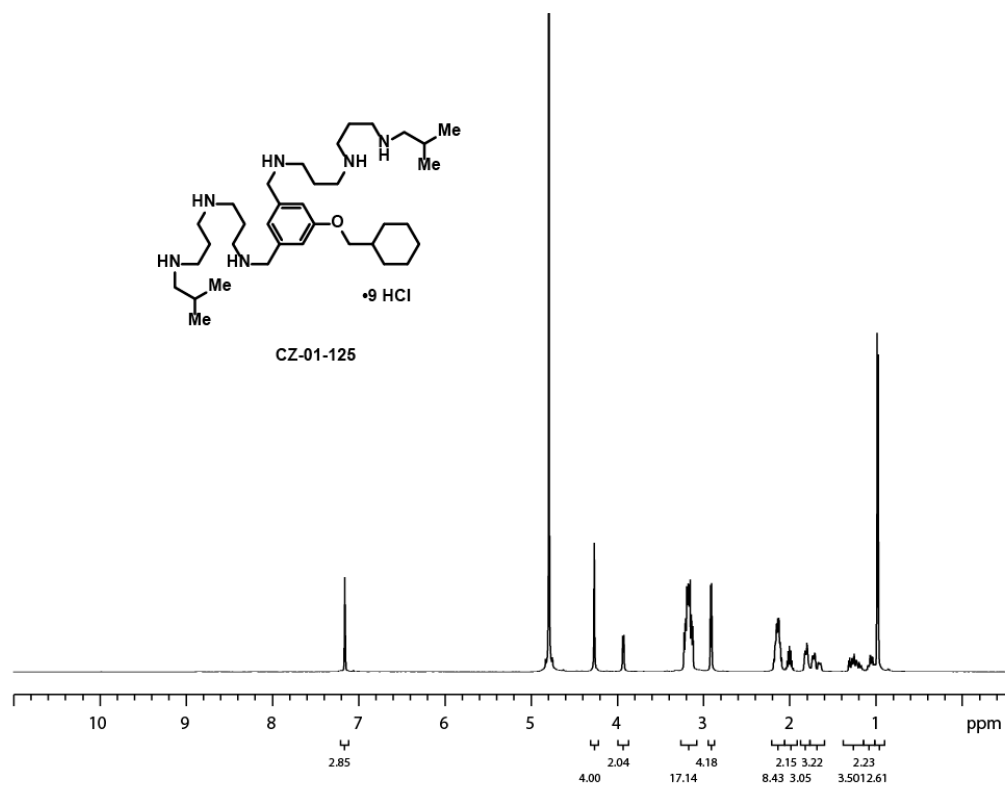


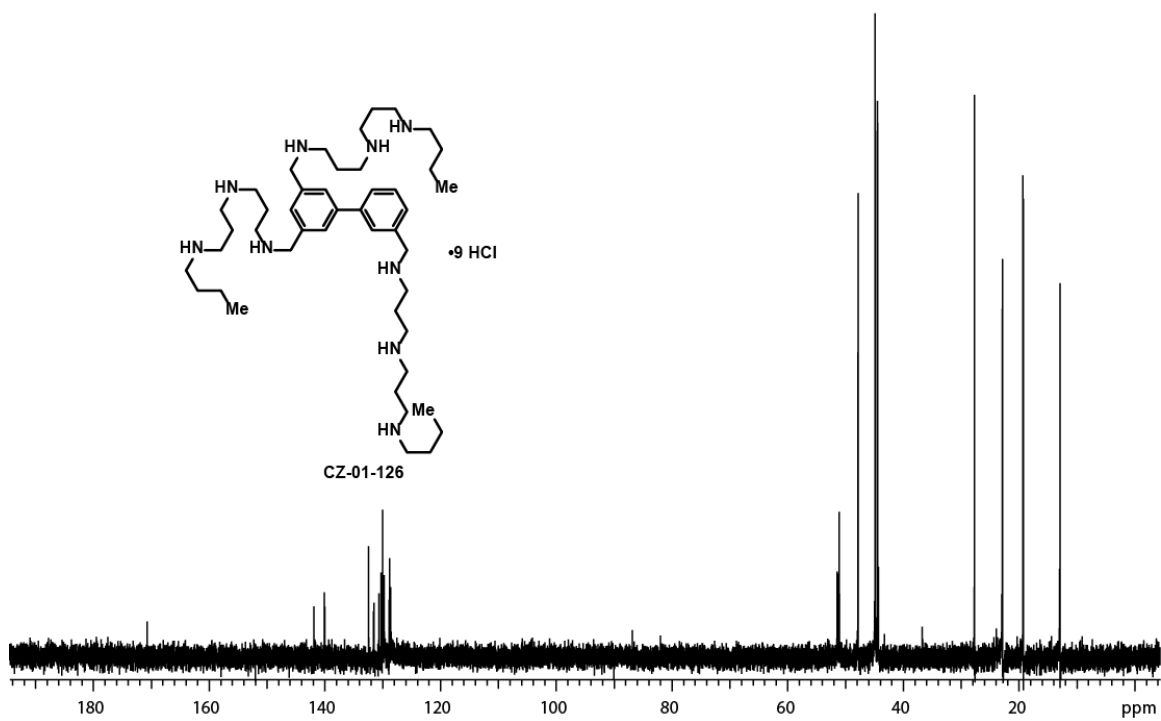
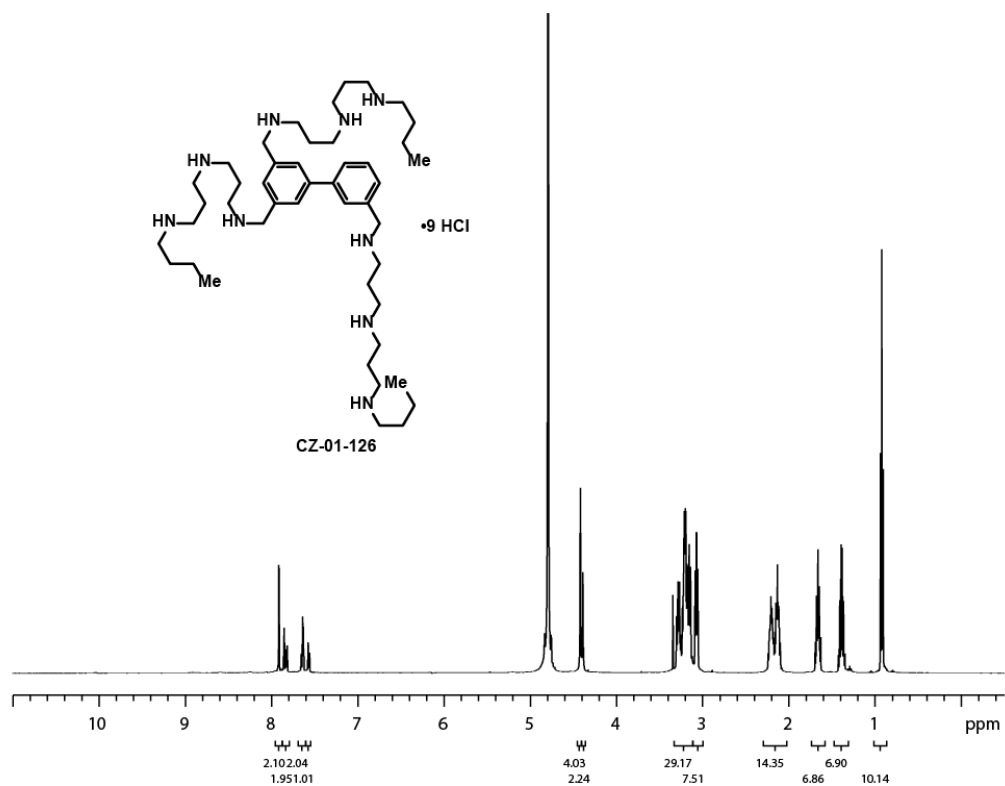


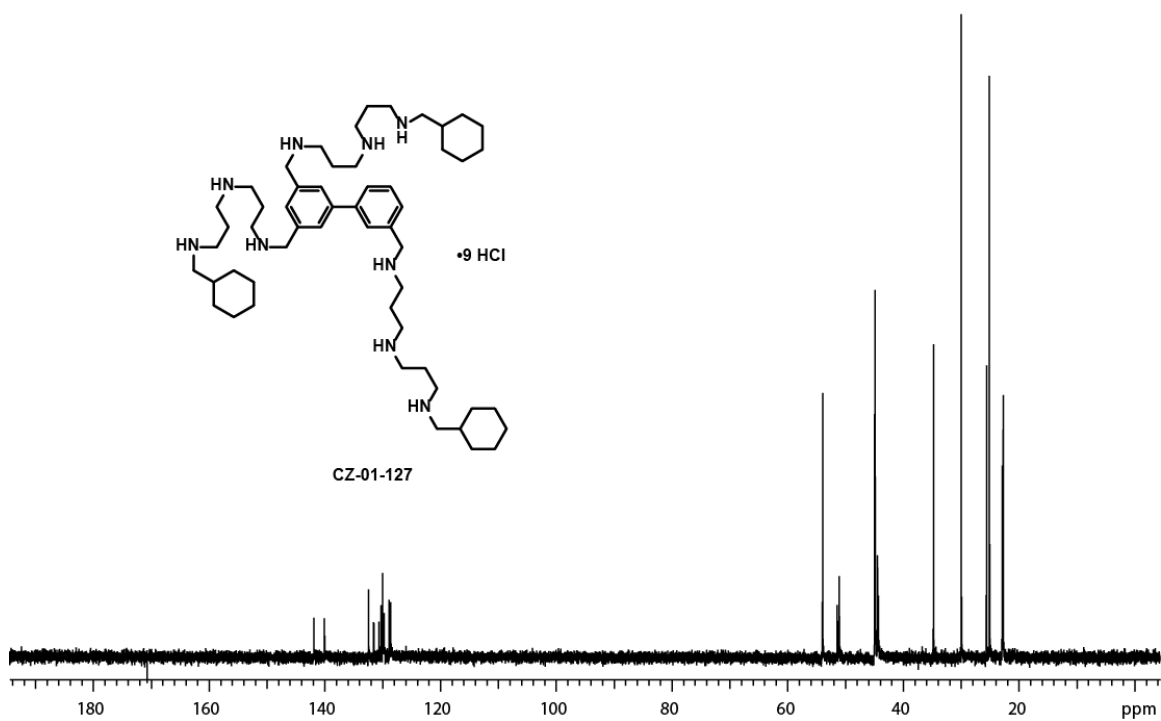
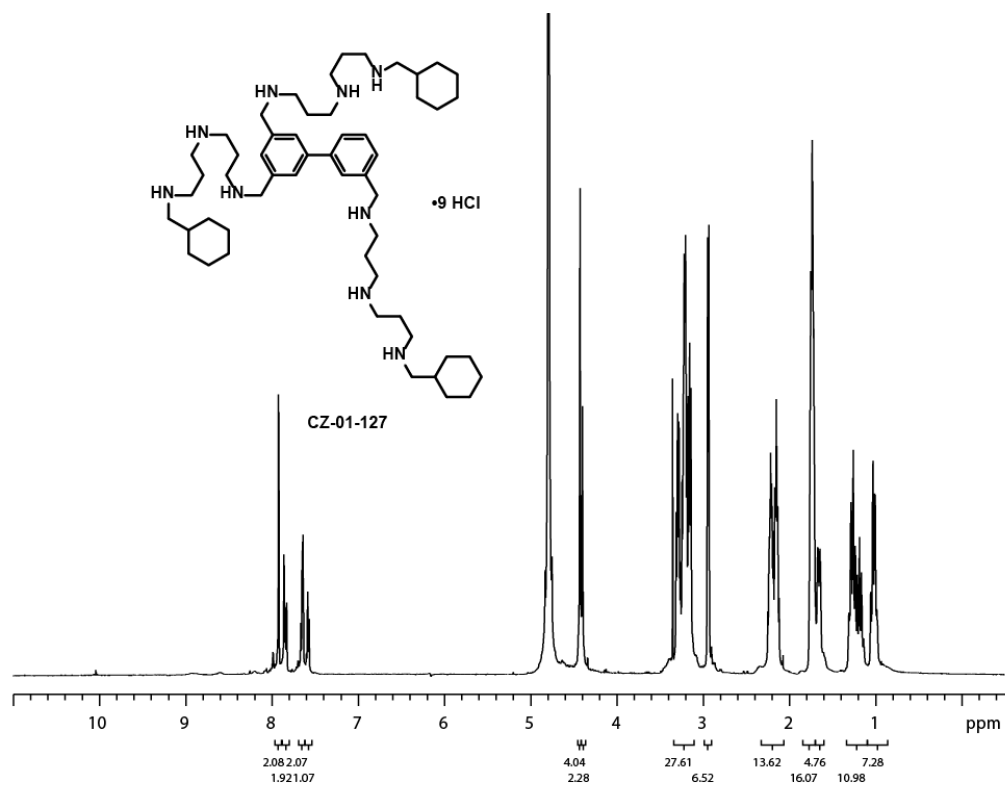


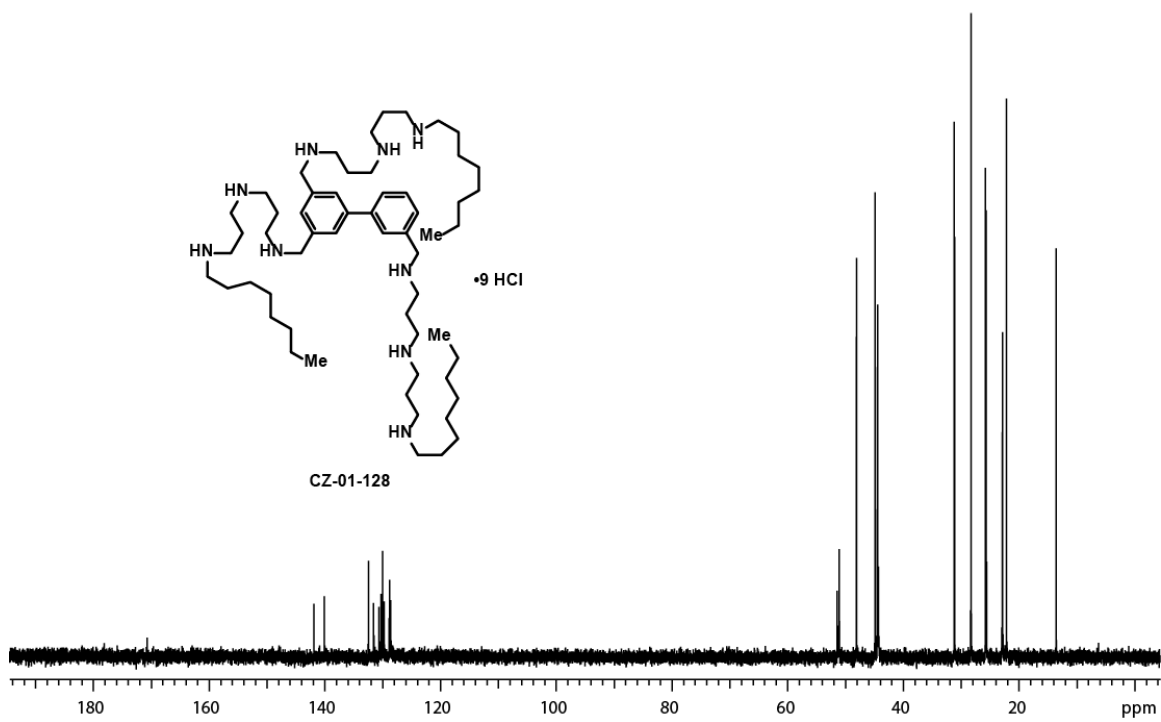
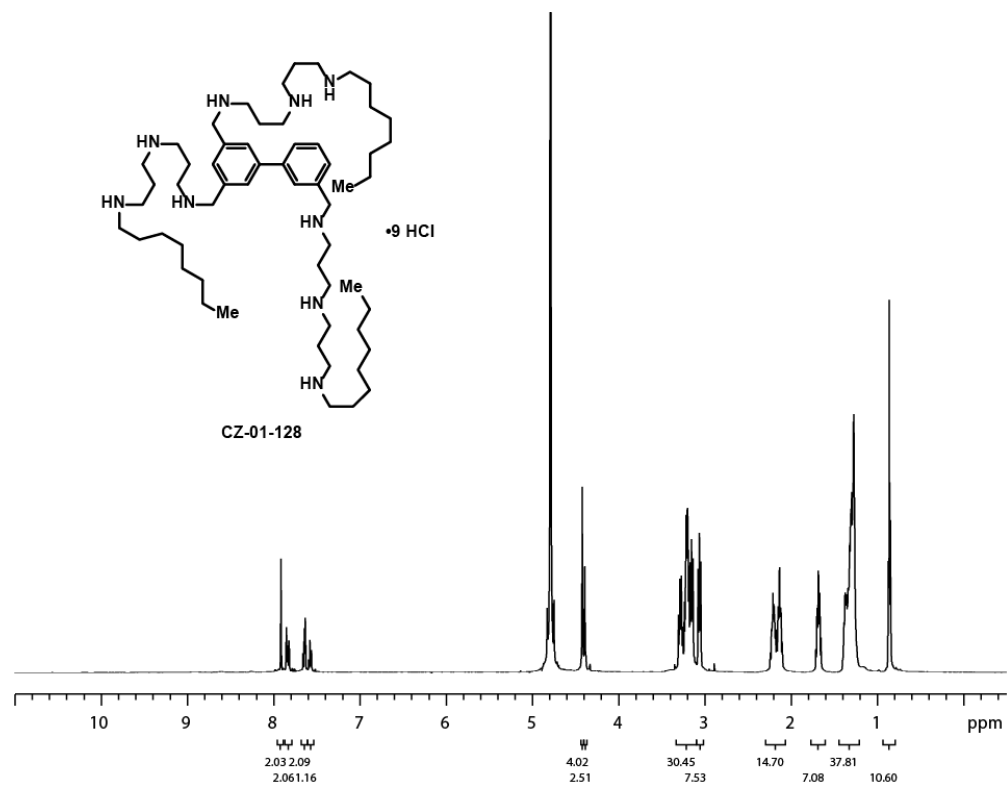




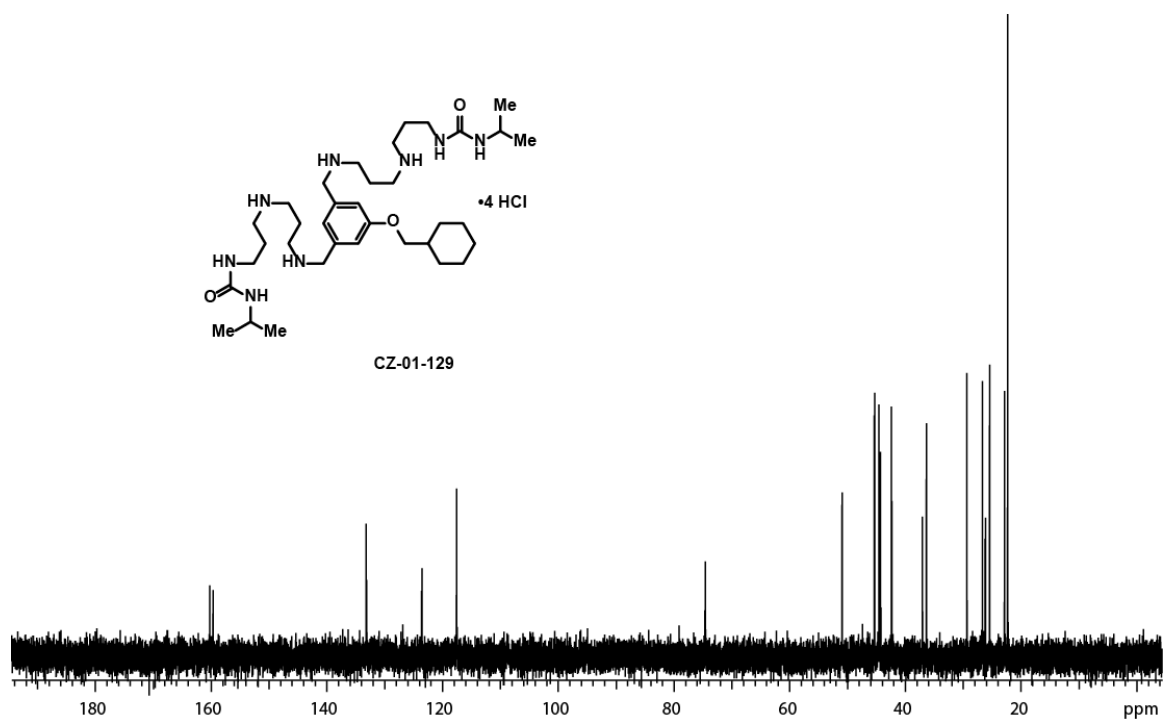


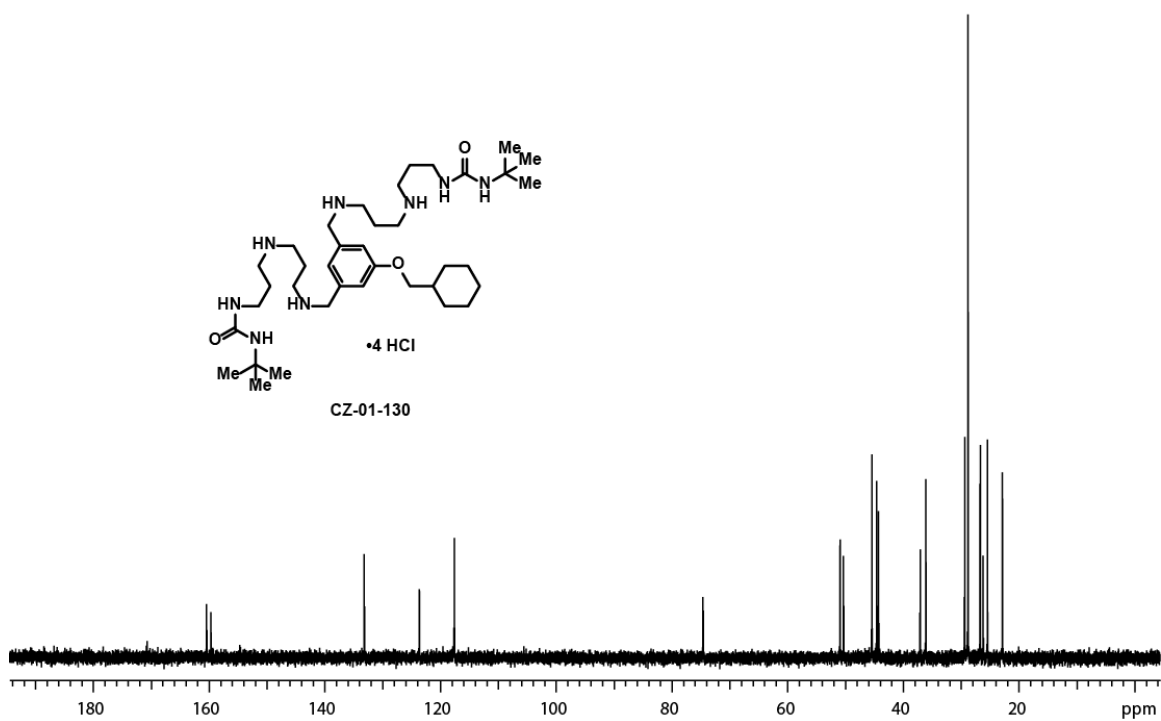
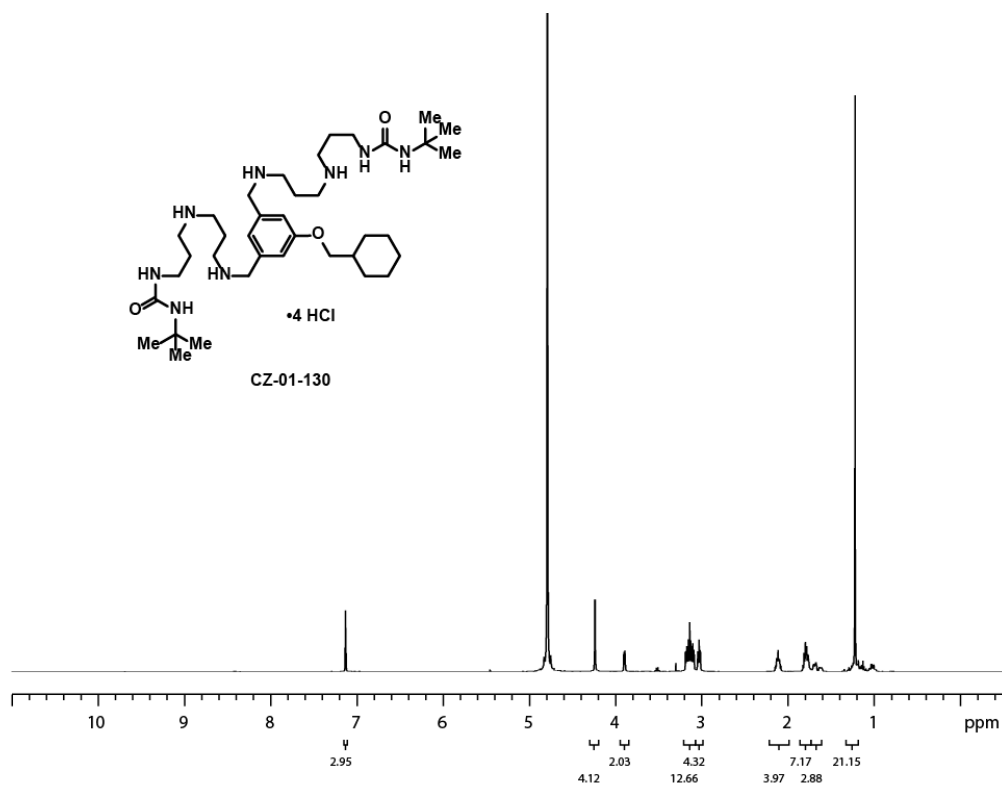


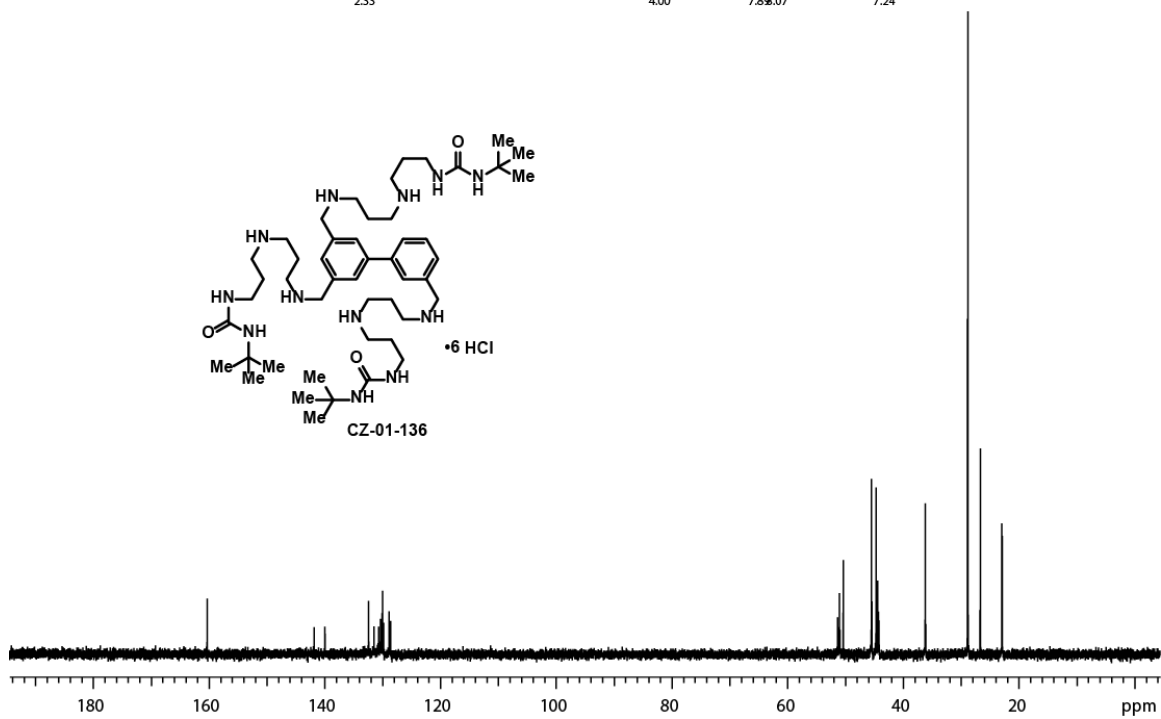
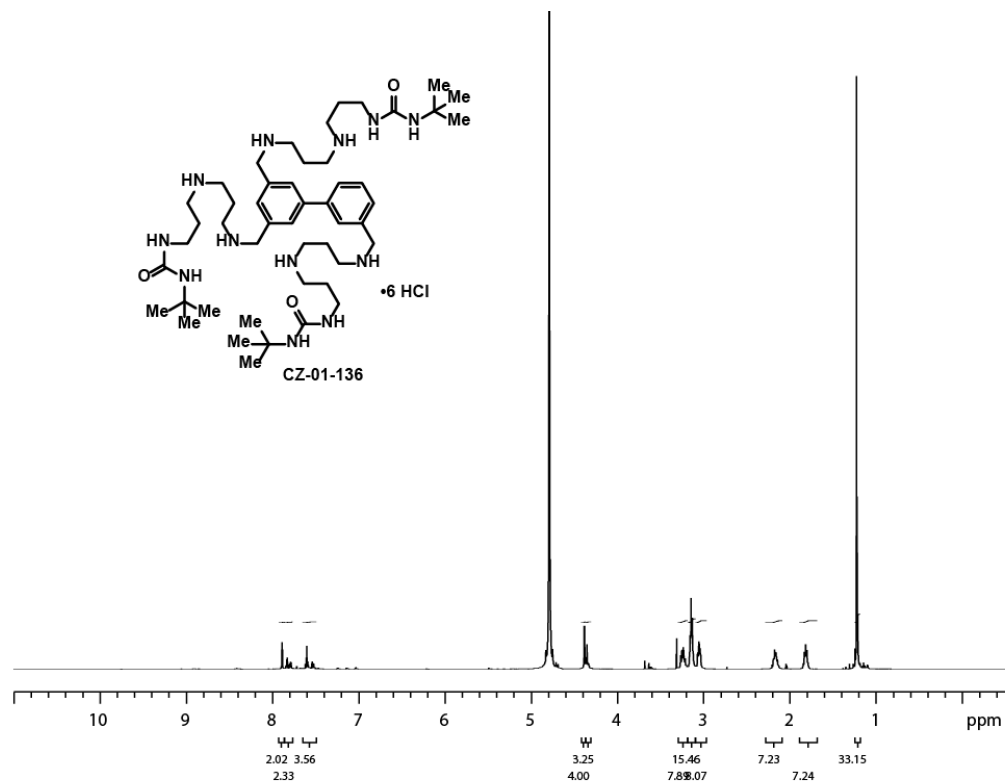


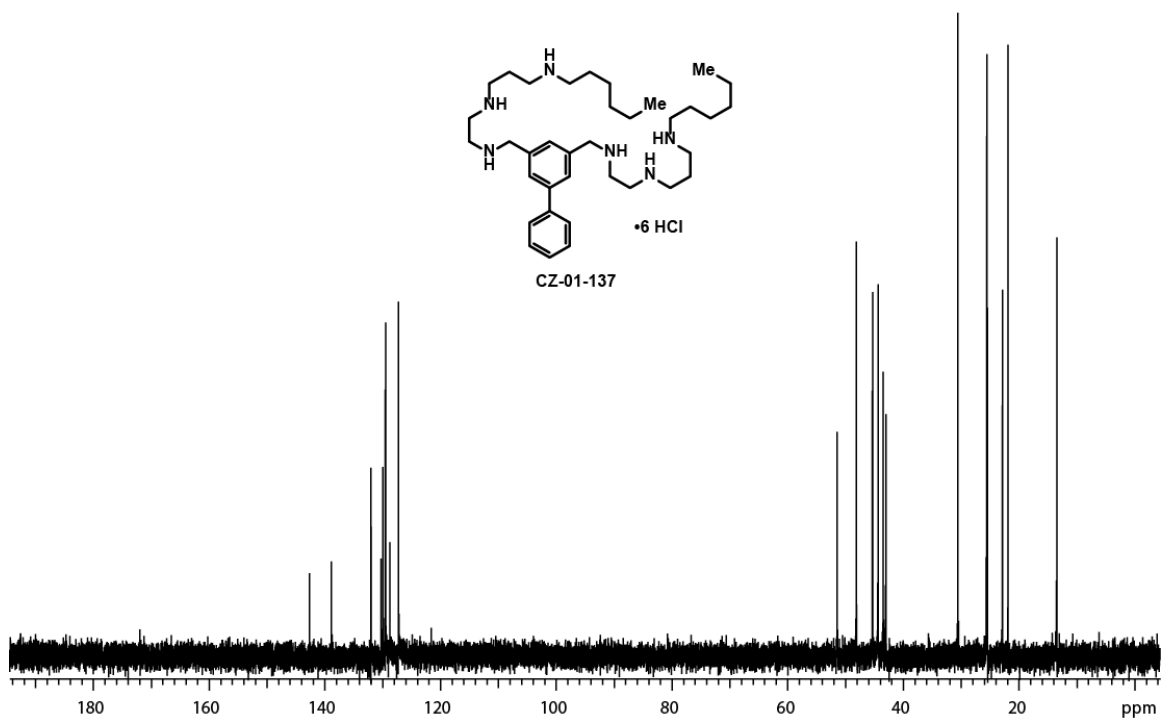
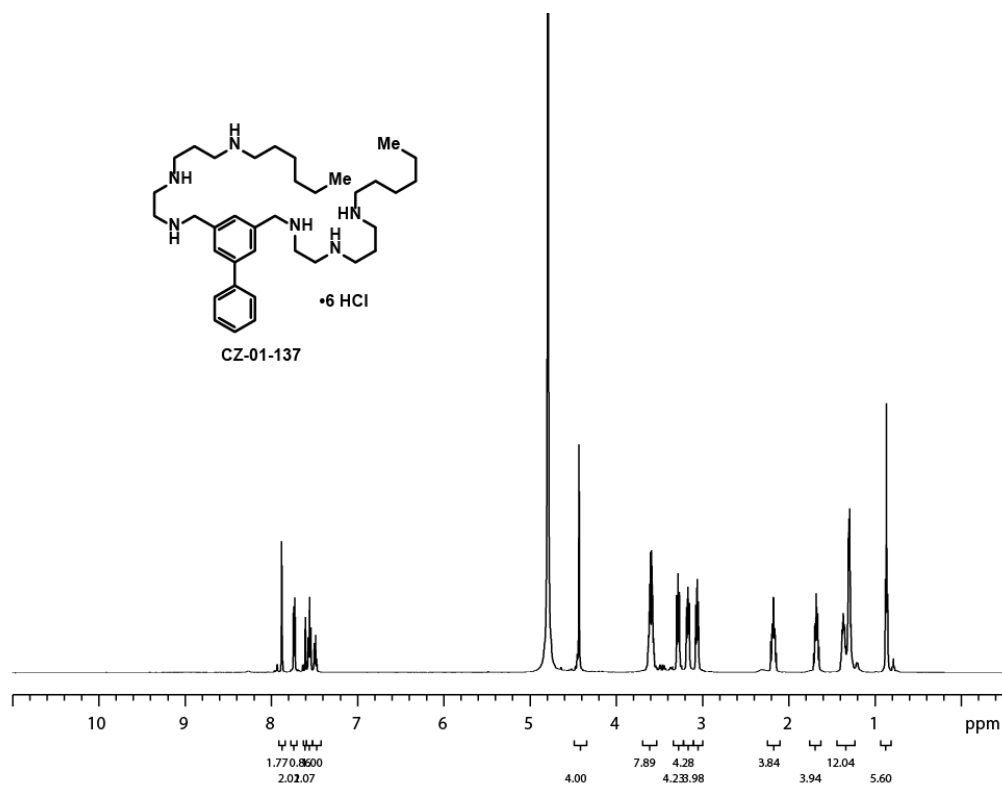


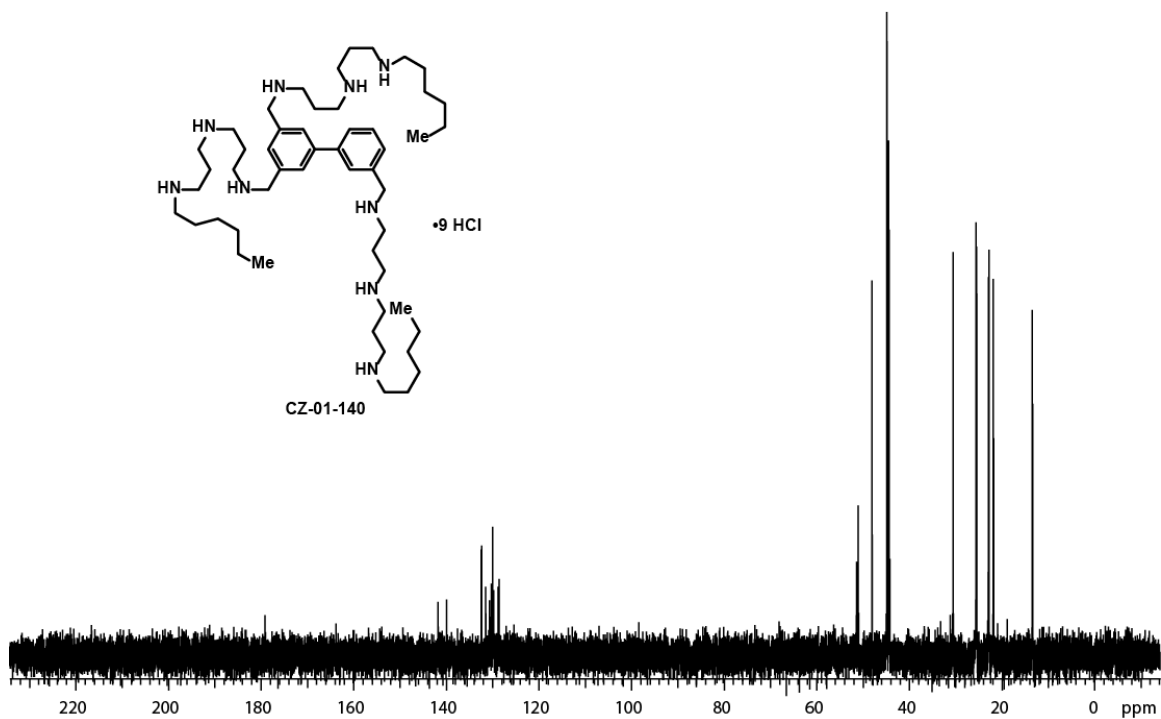
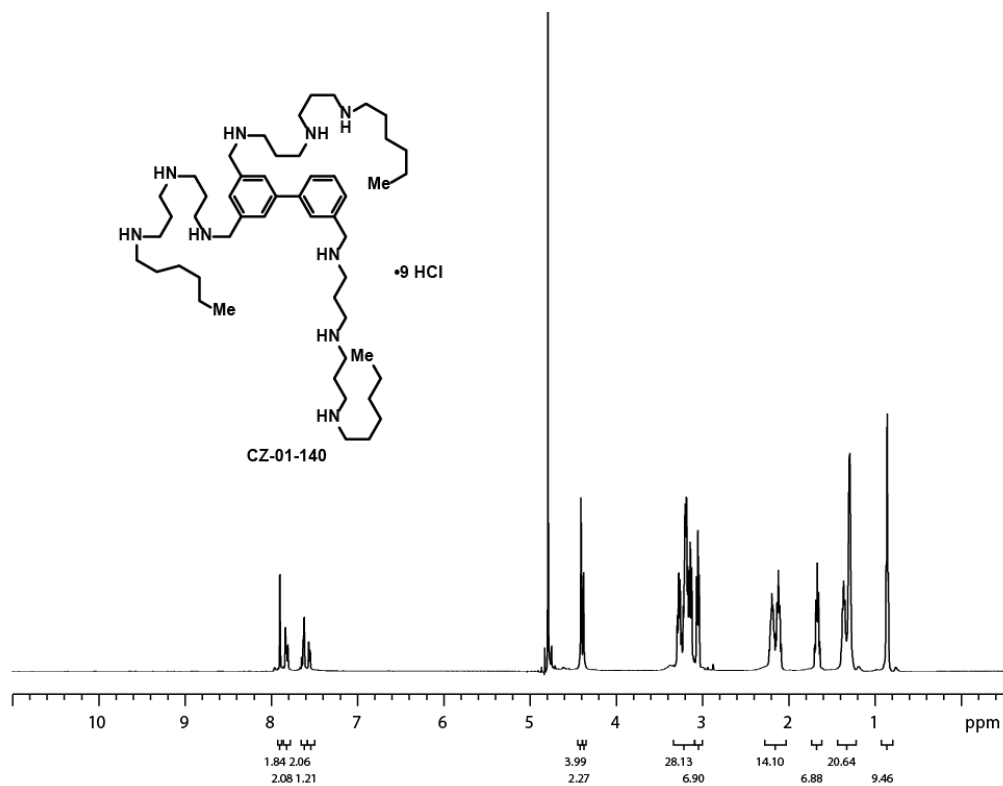


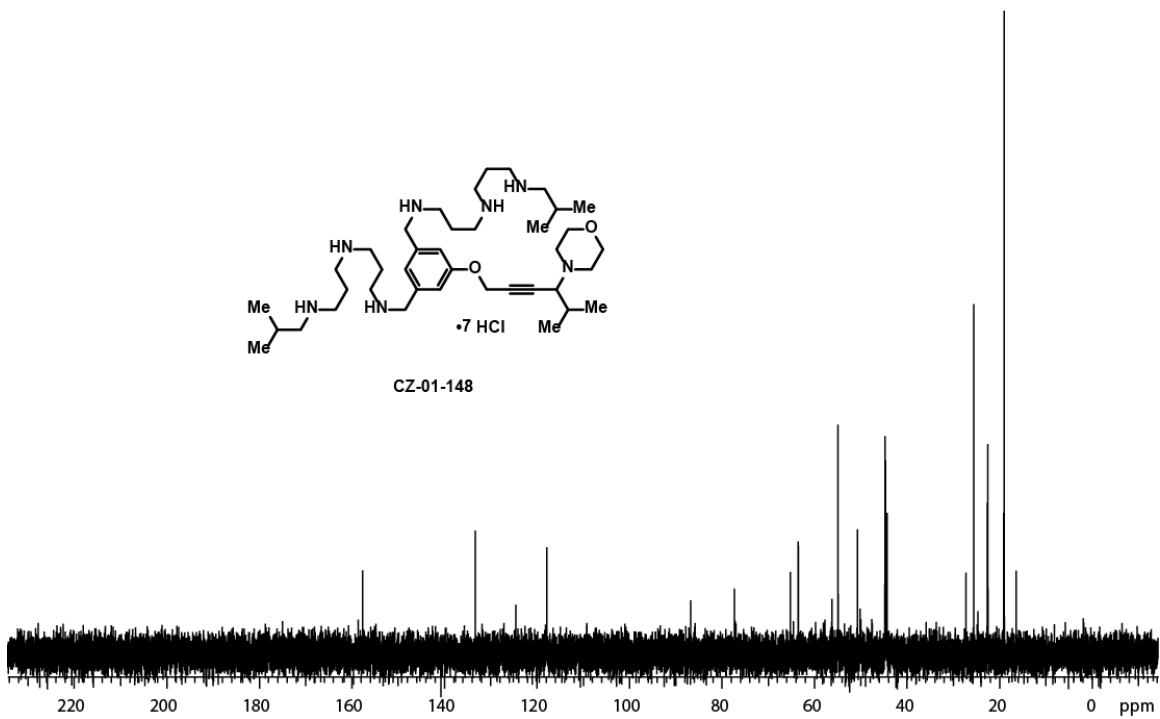
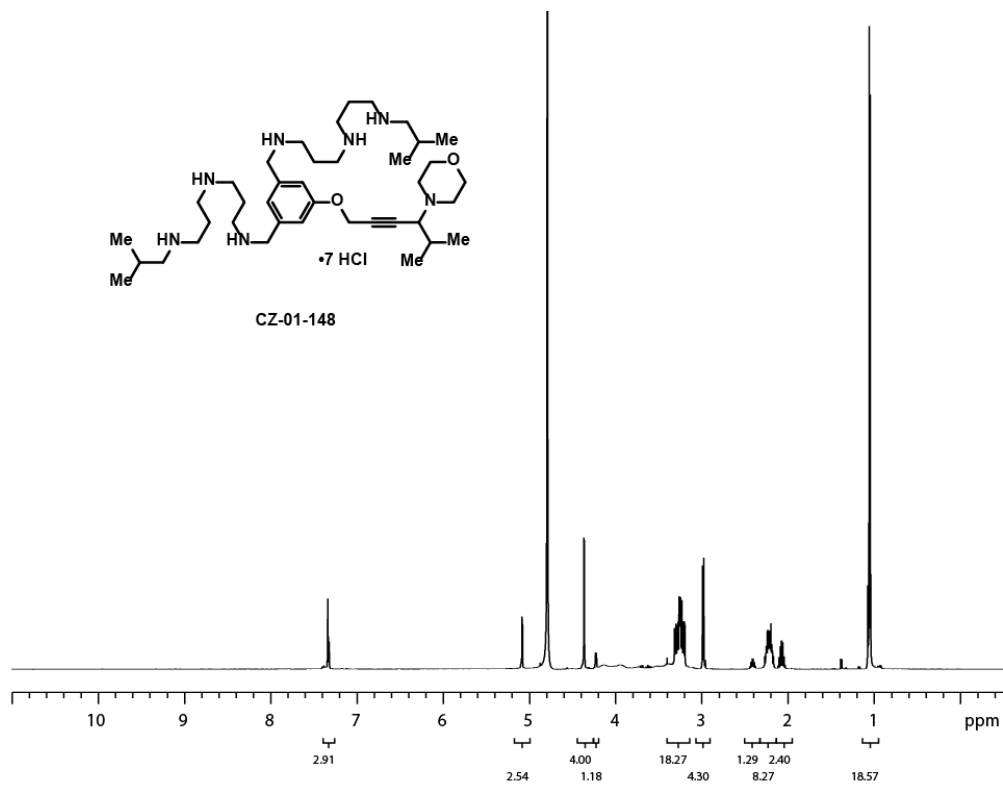


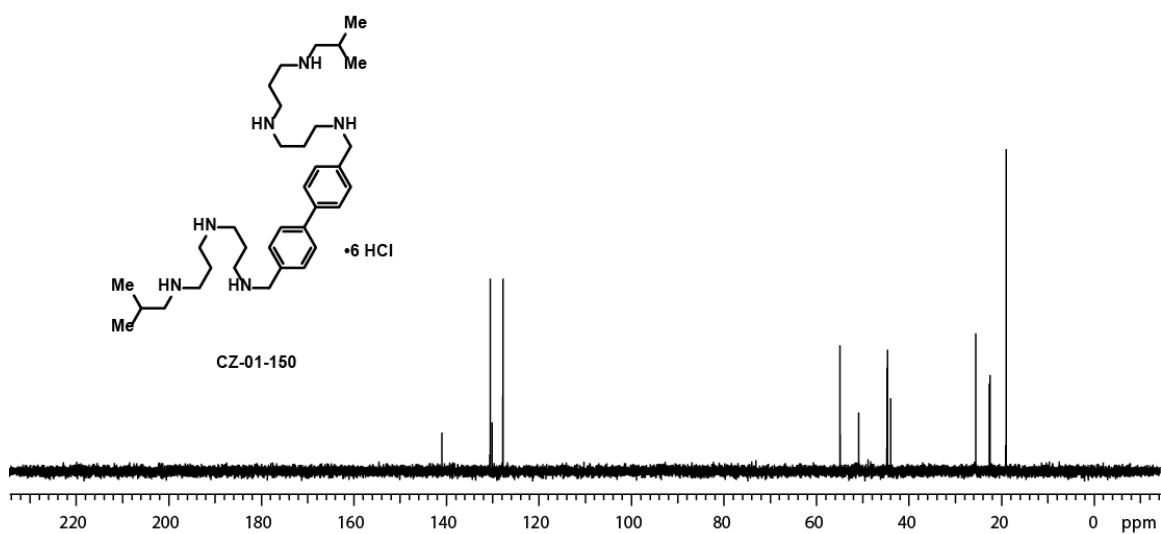
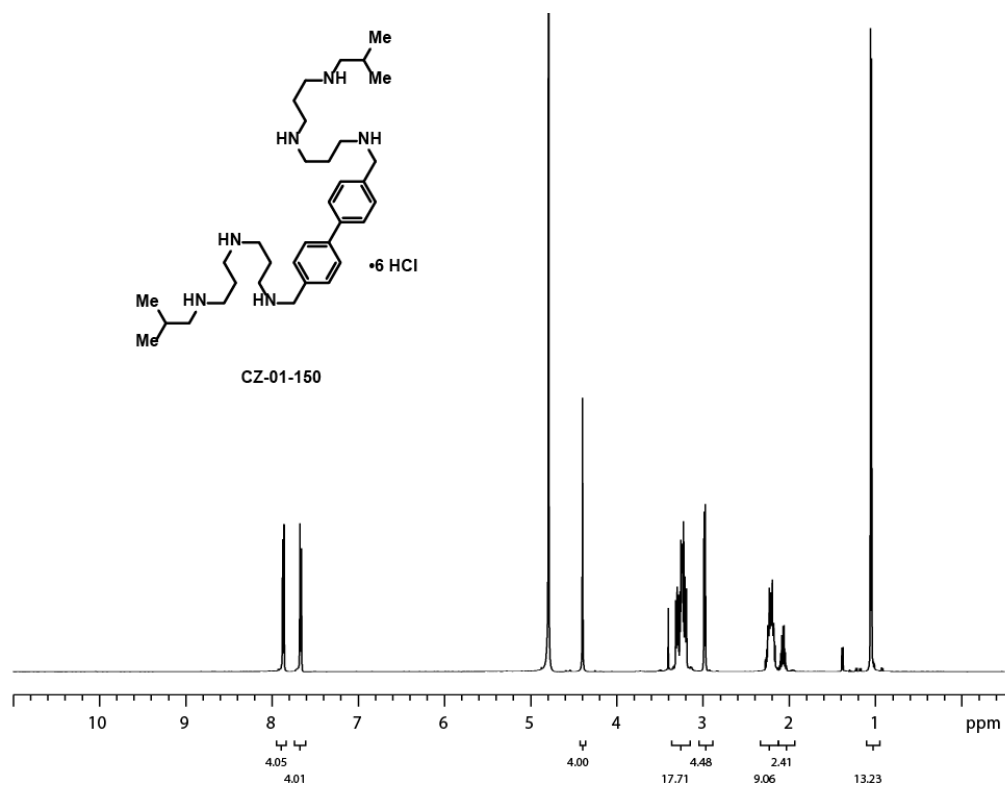


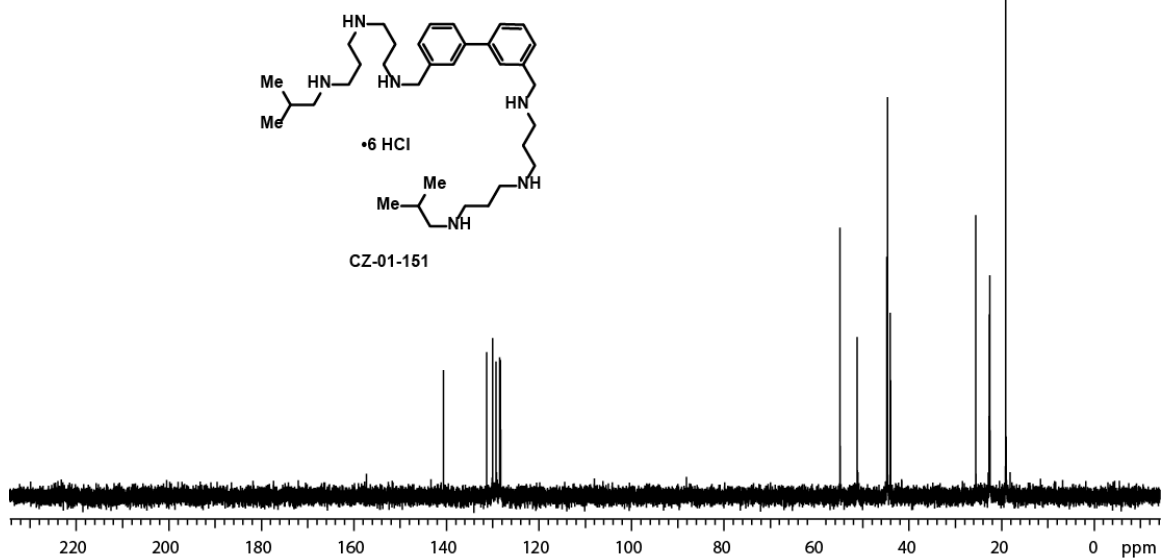
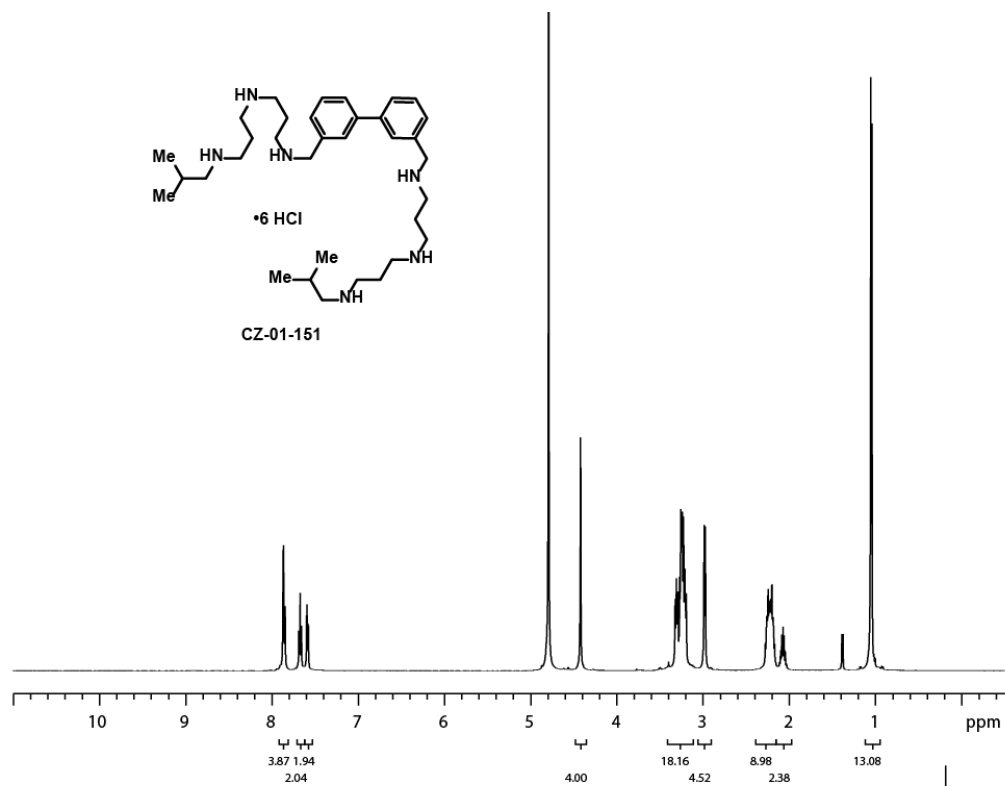




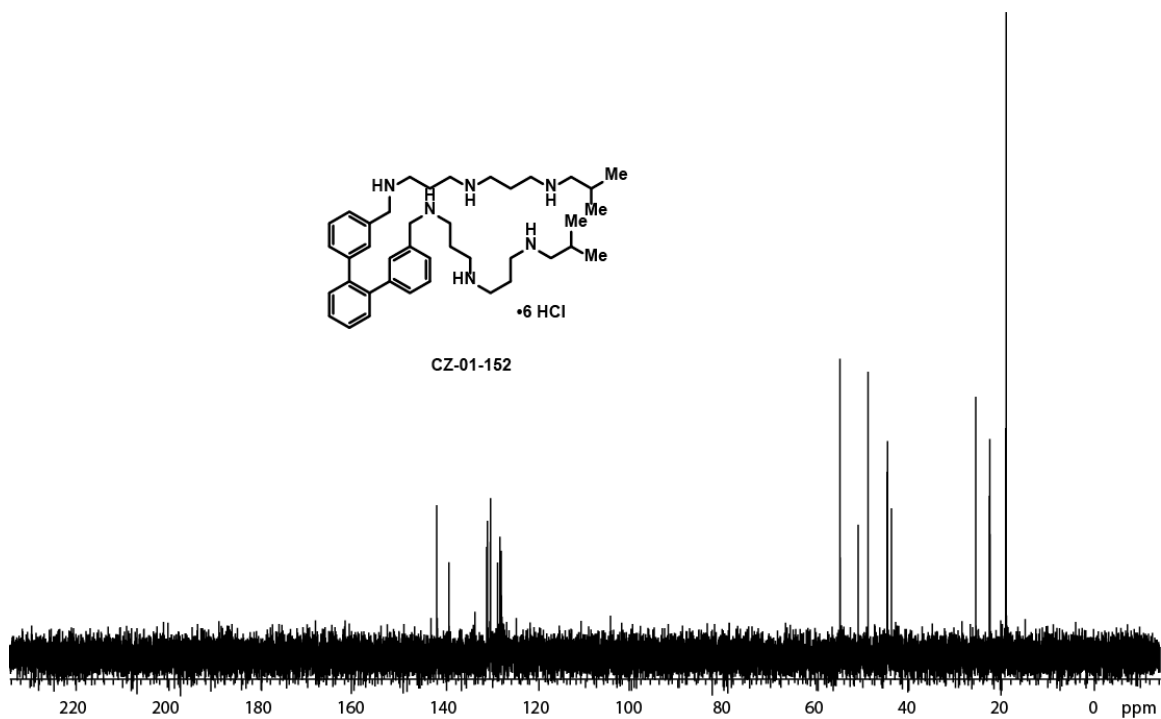
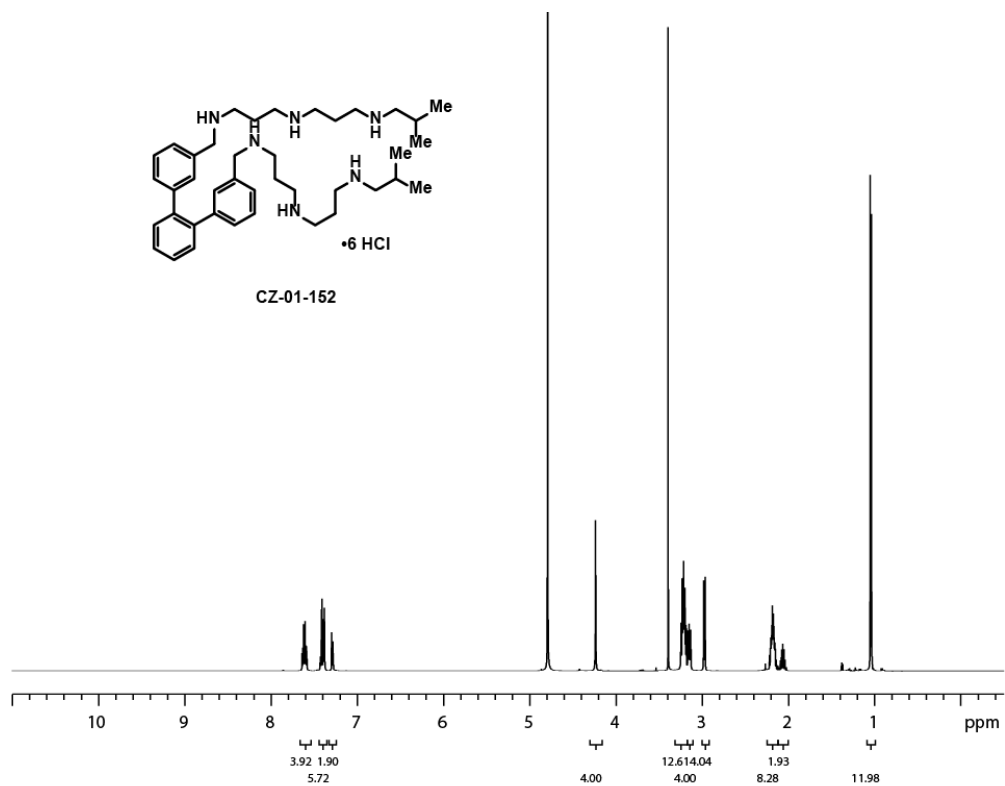


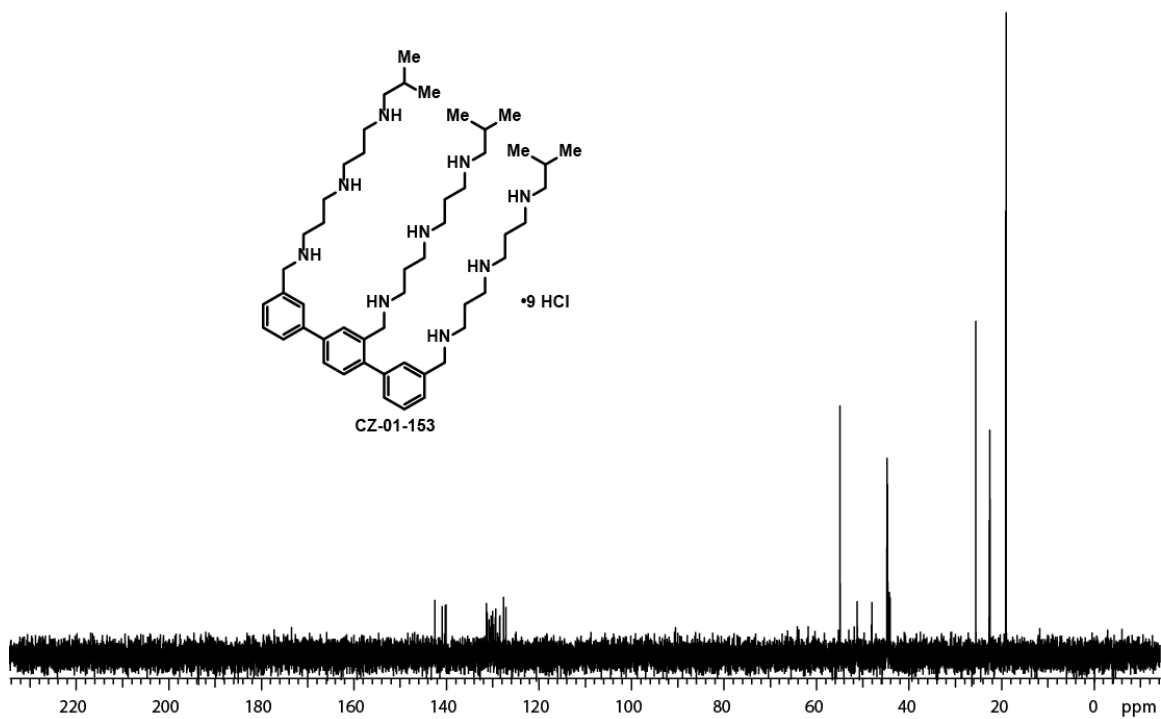
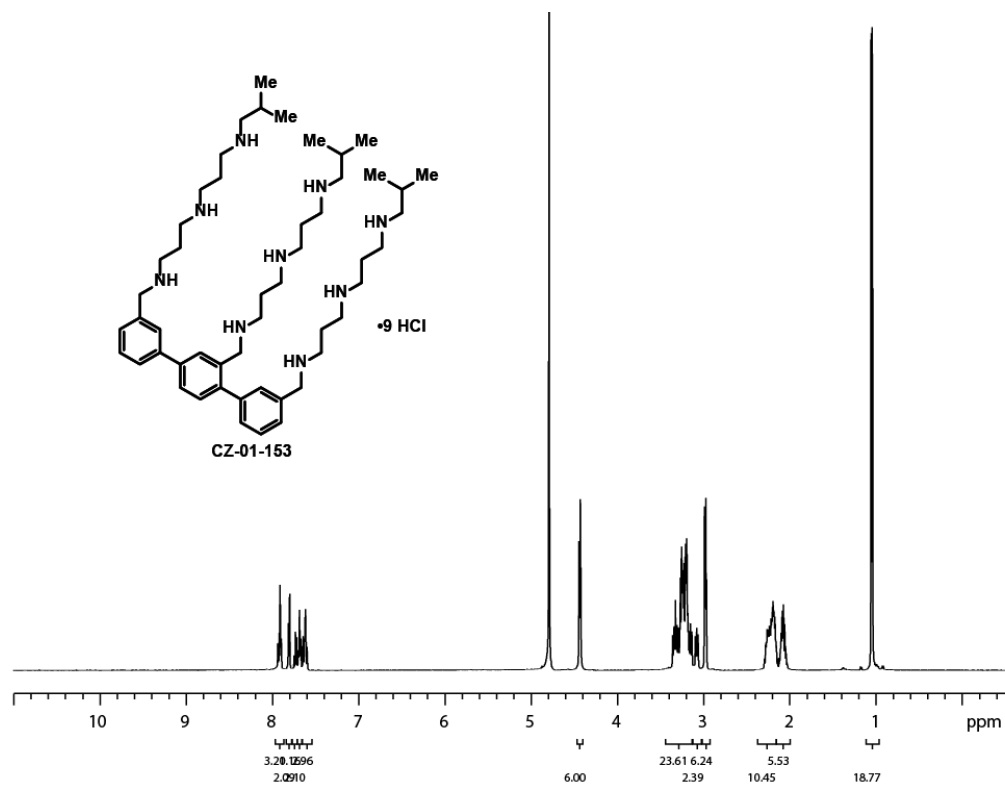


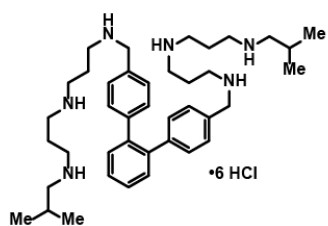




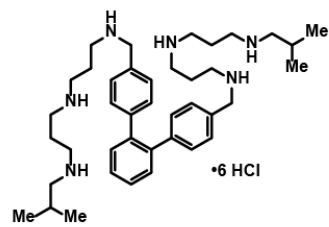
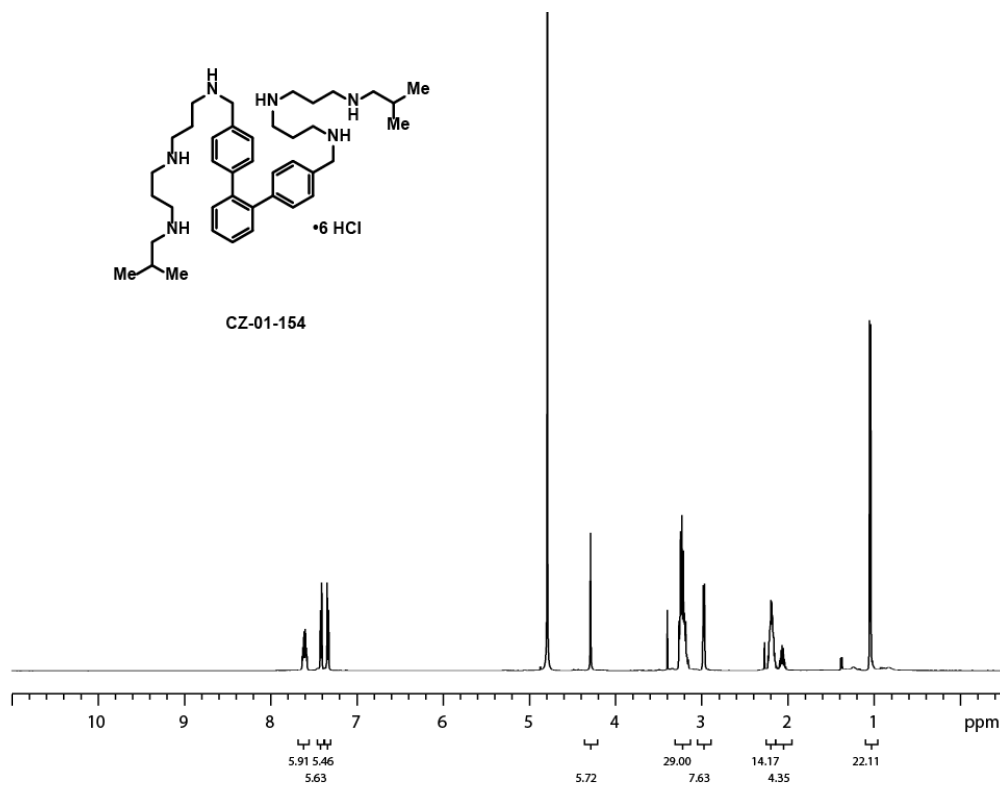




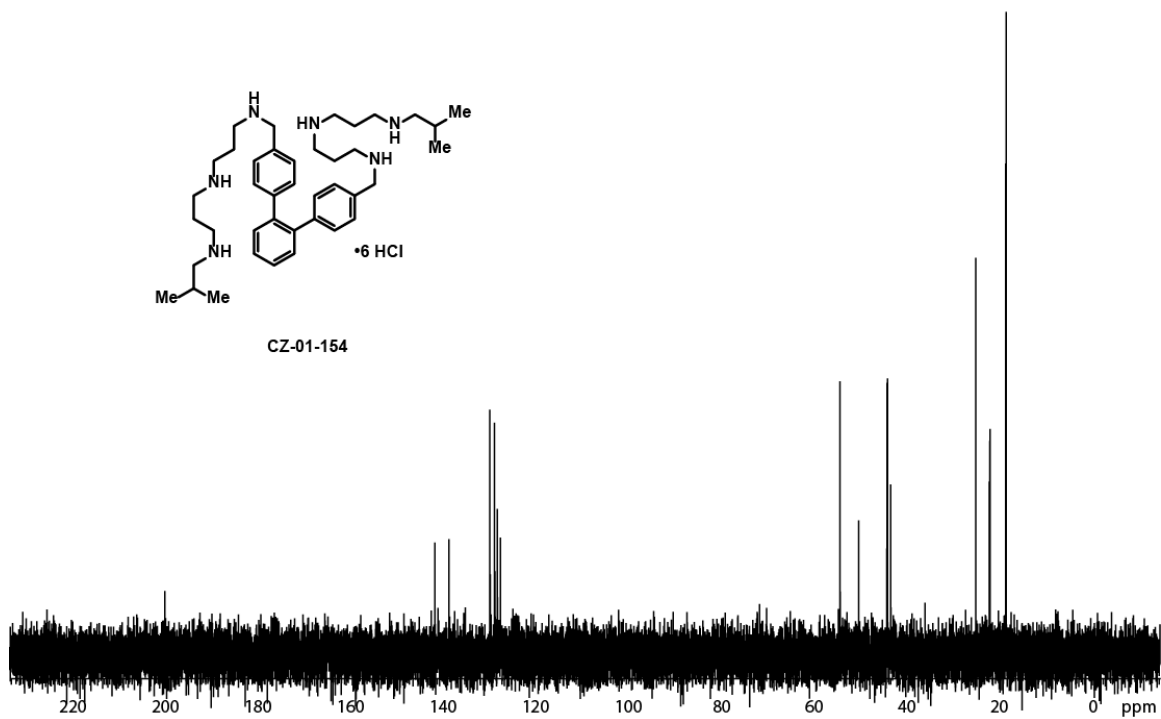


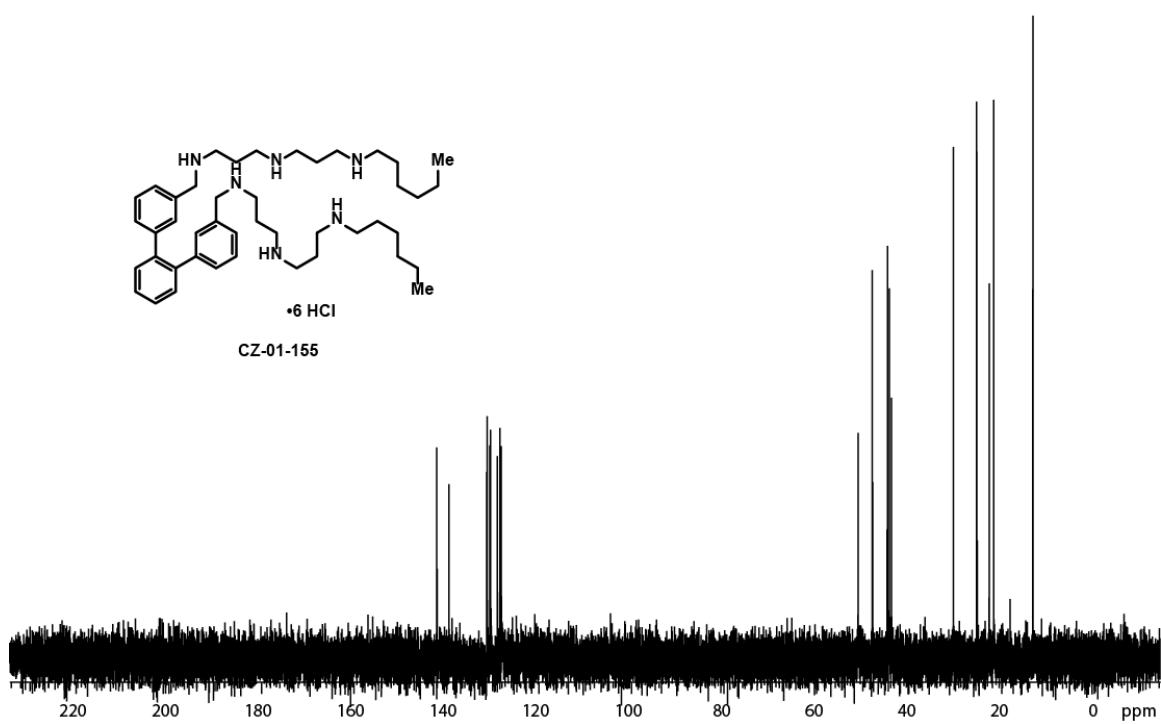
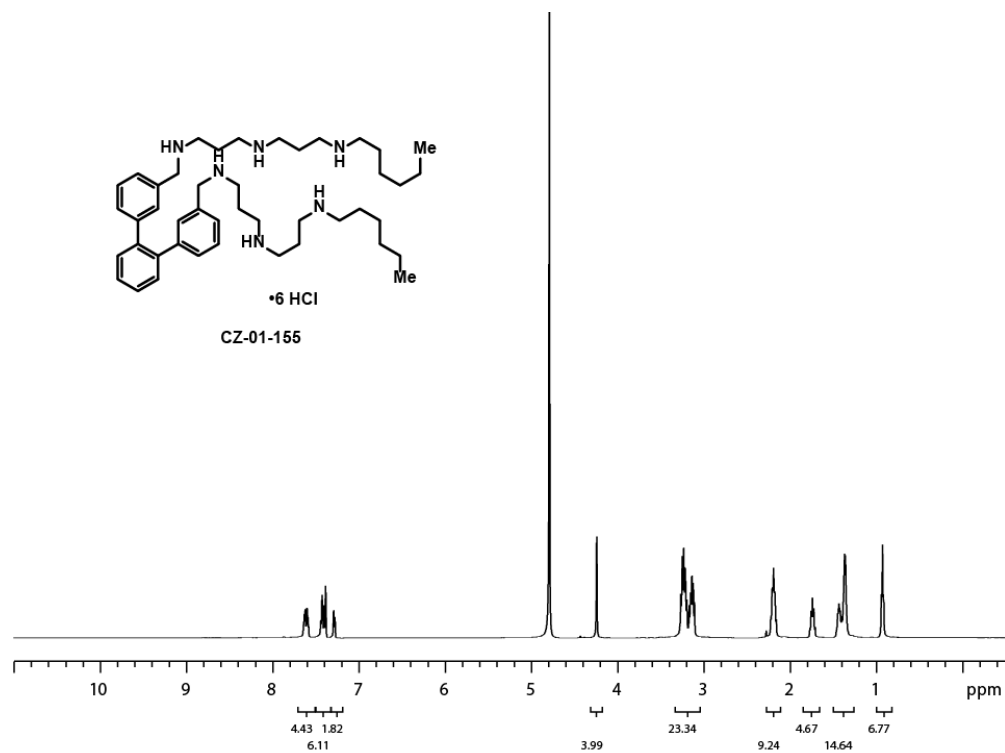


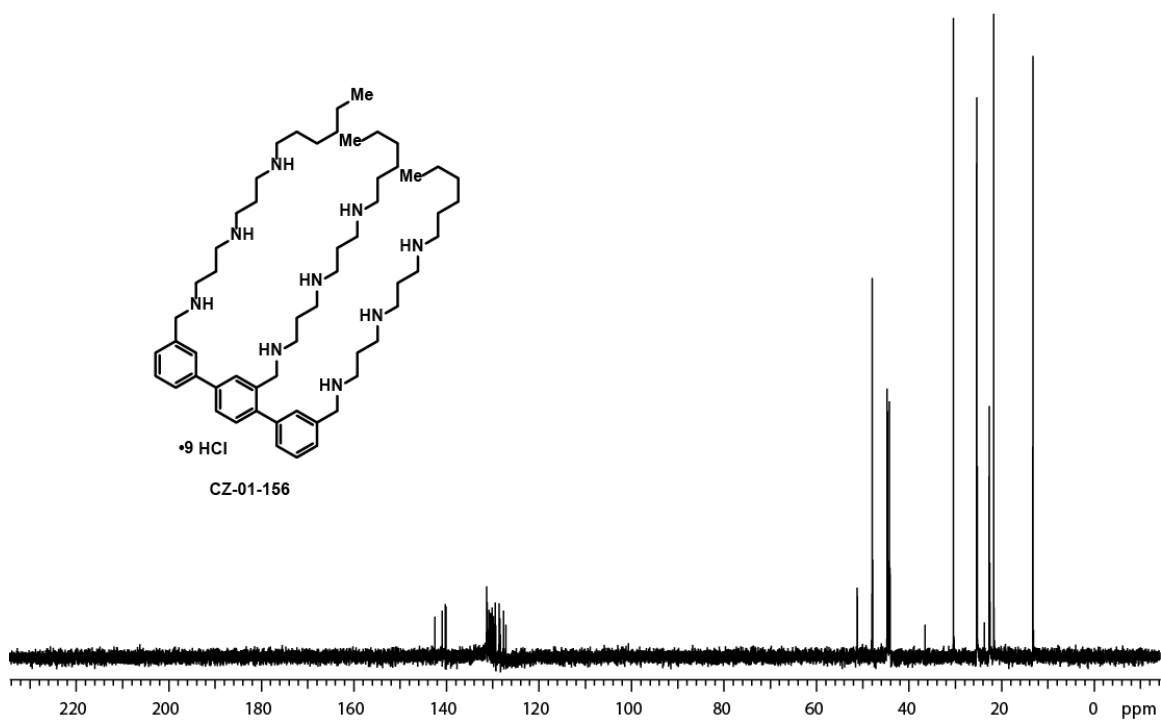
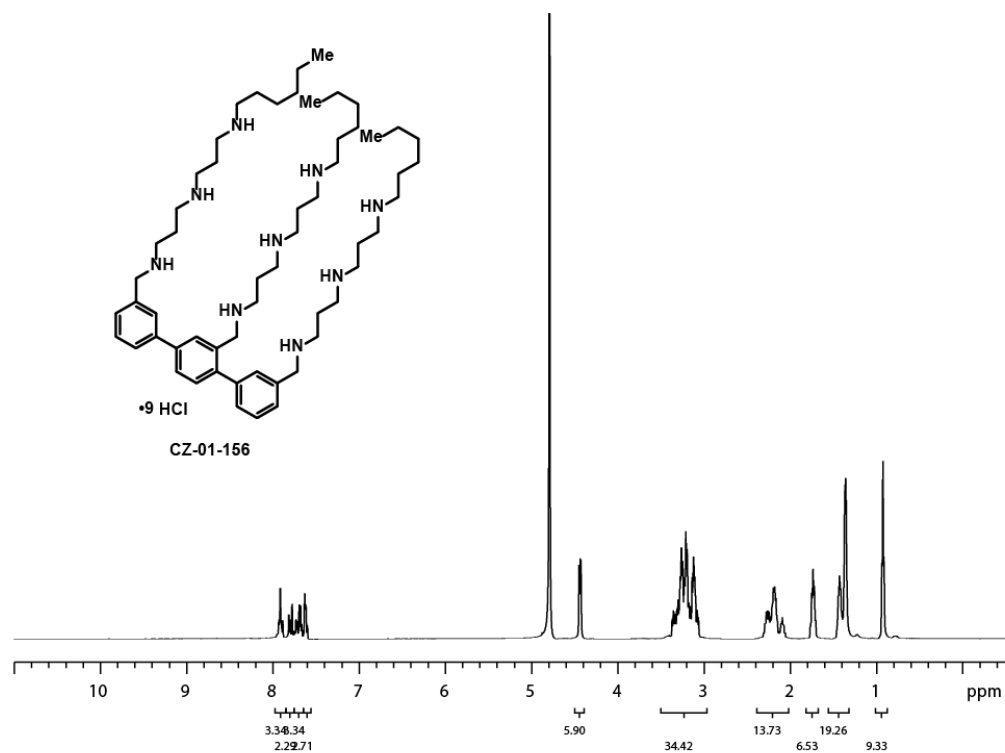
CZ-01-154

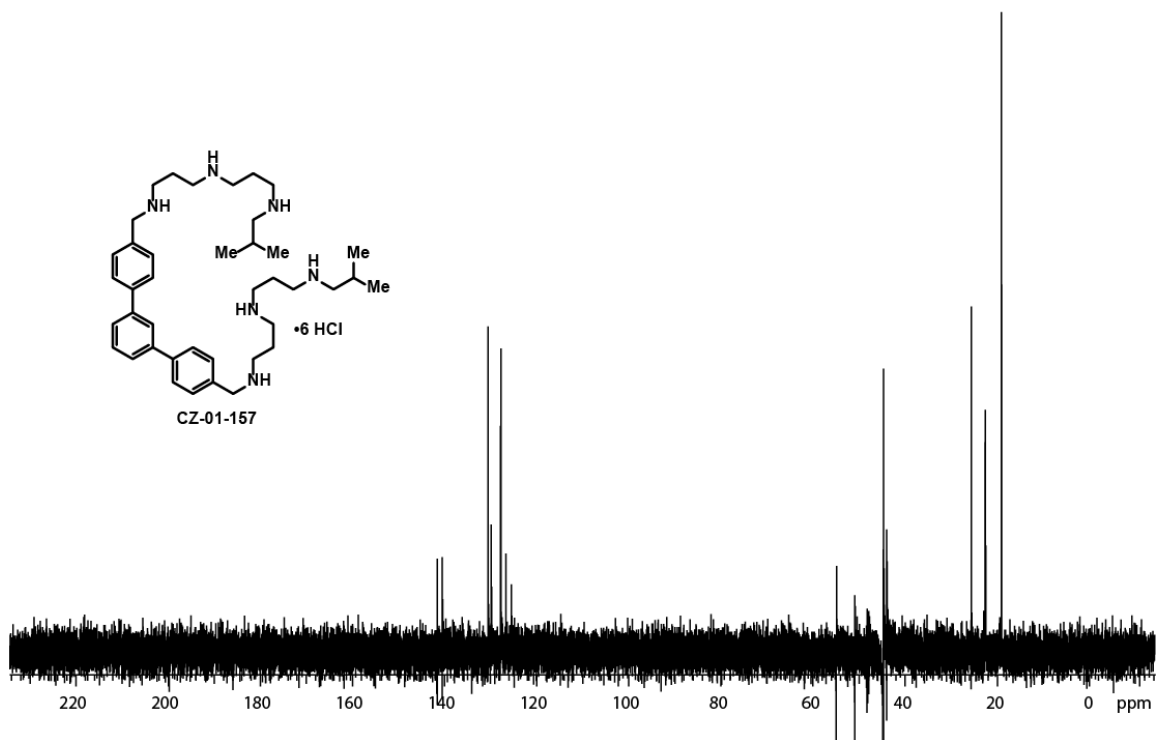
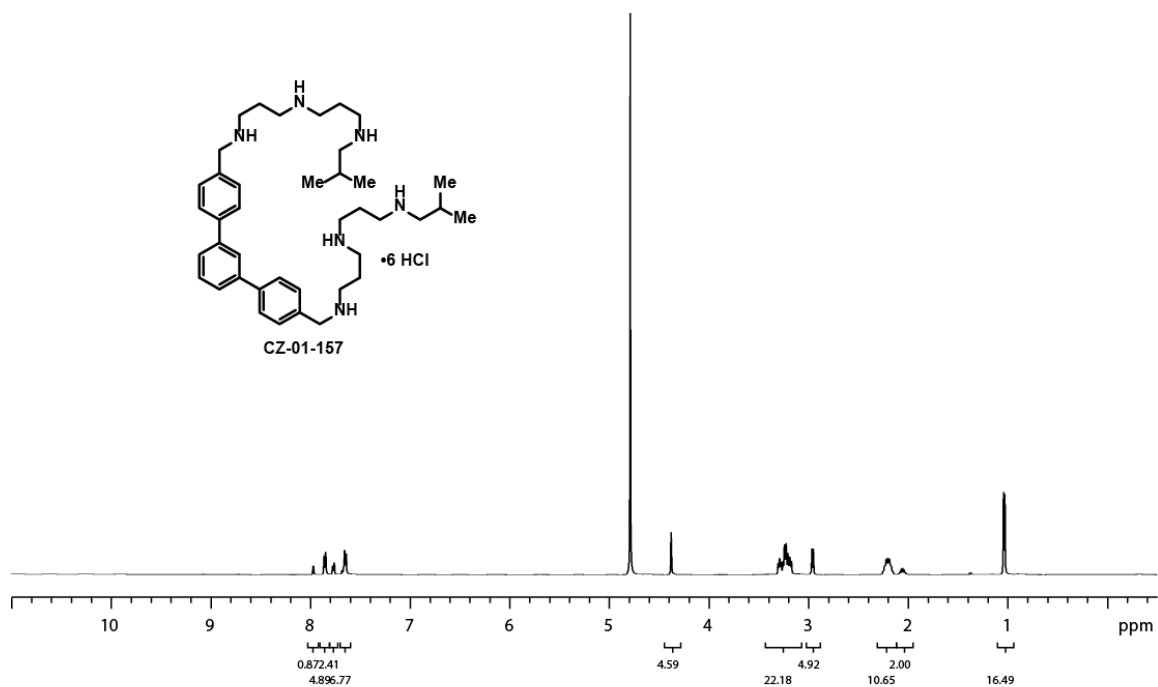


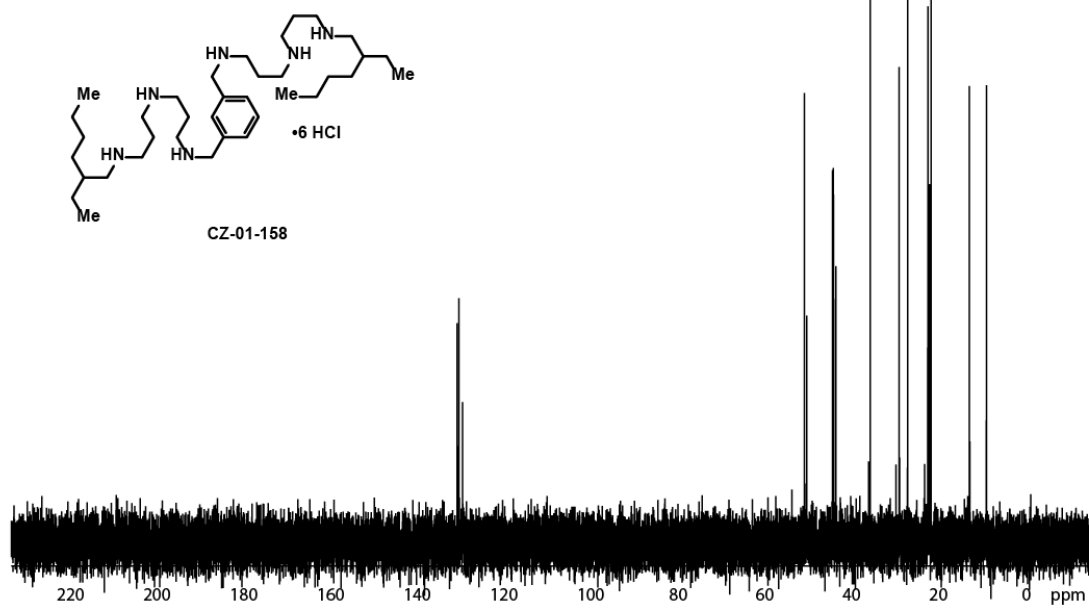
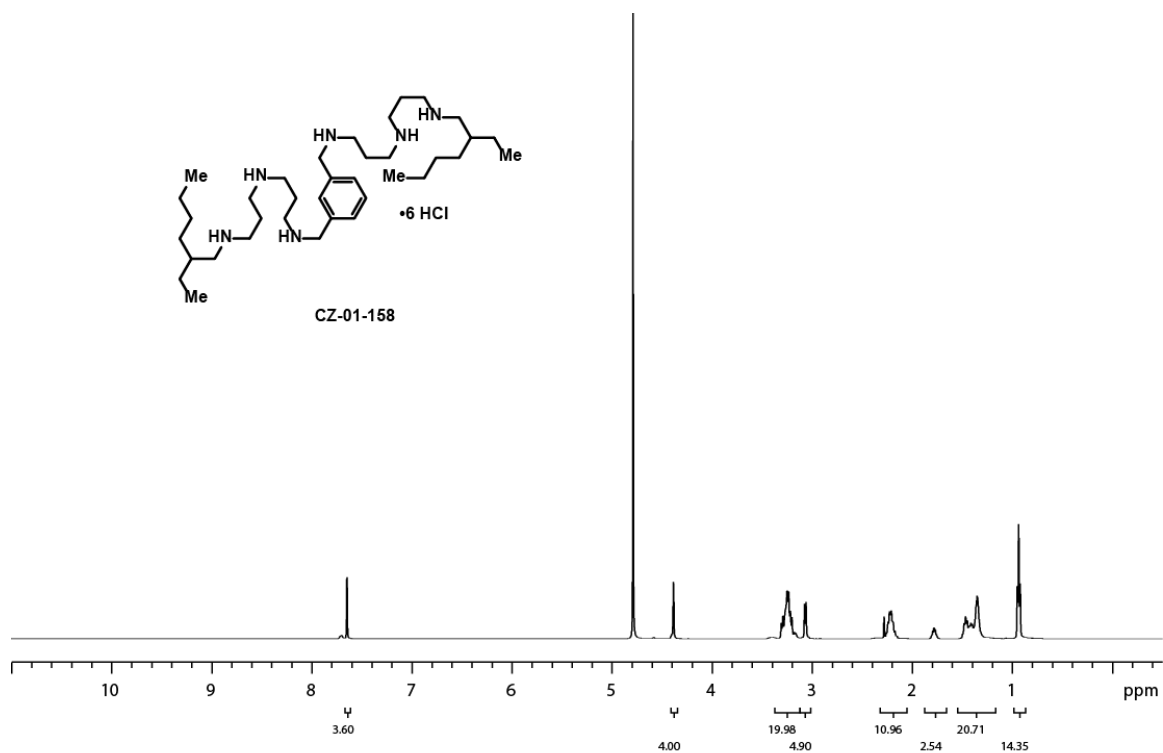
CZ-01-154

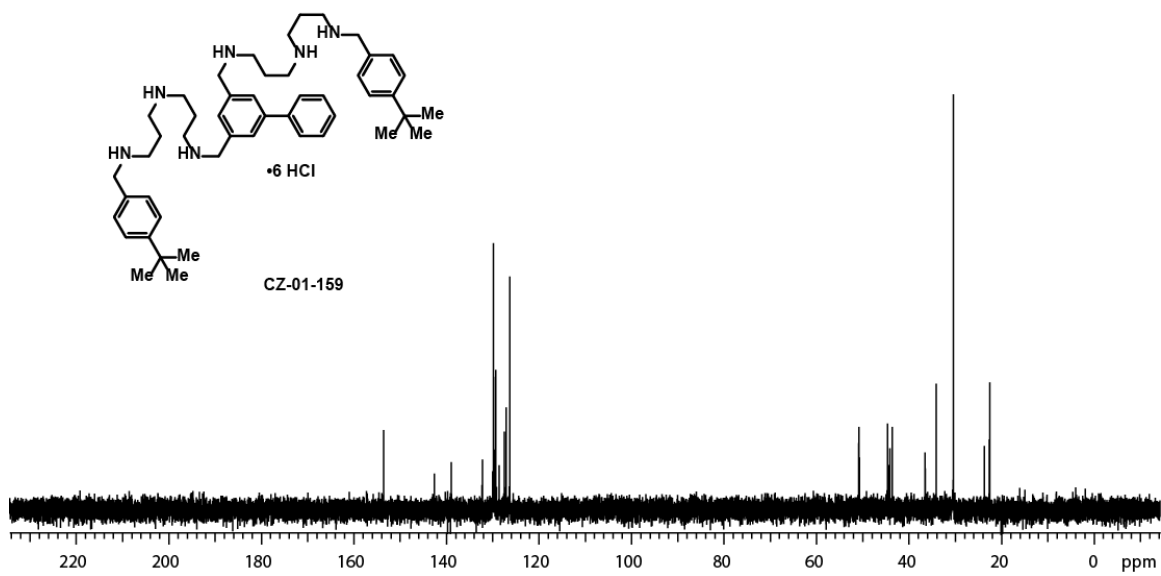
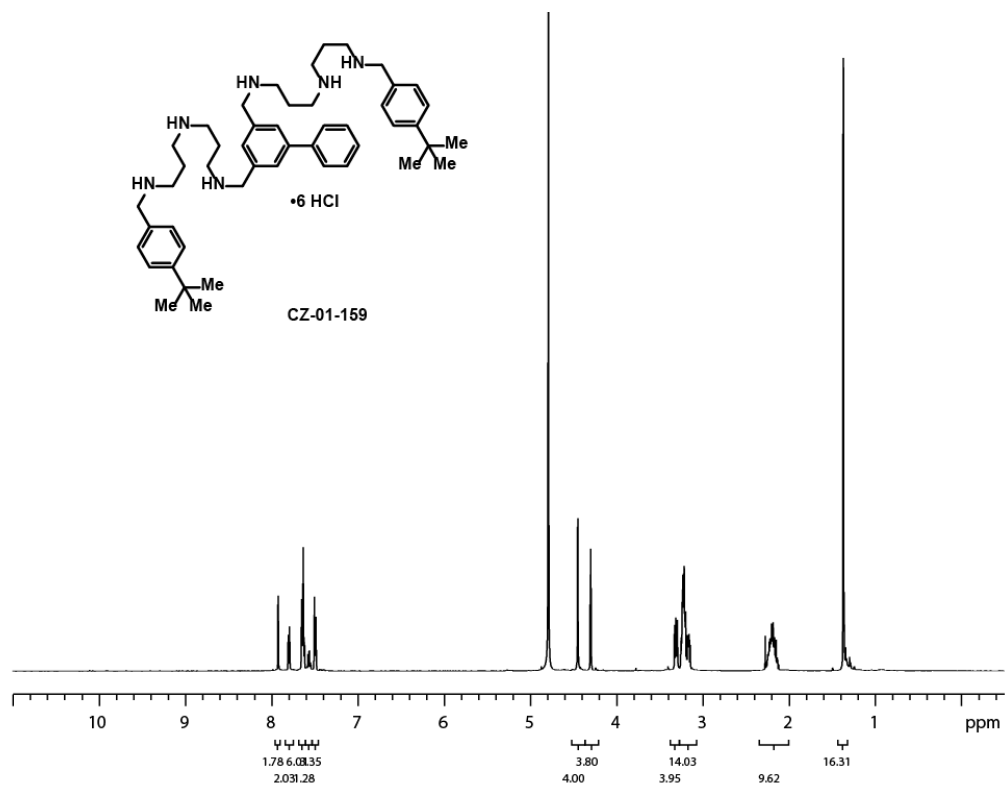




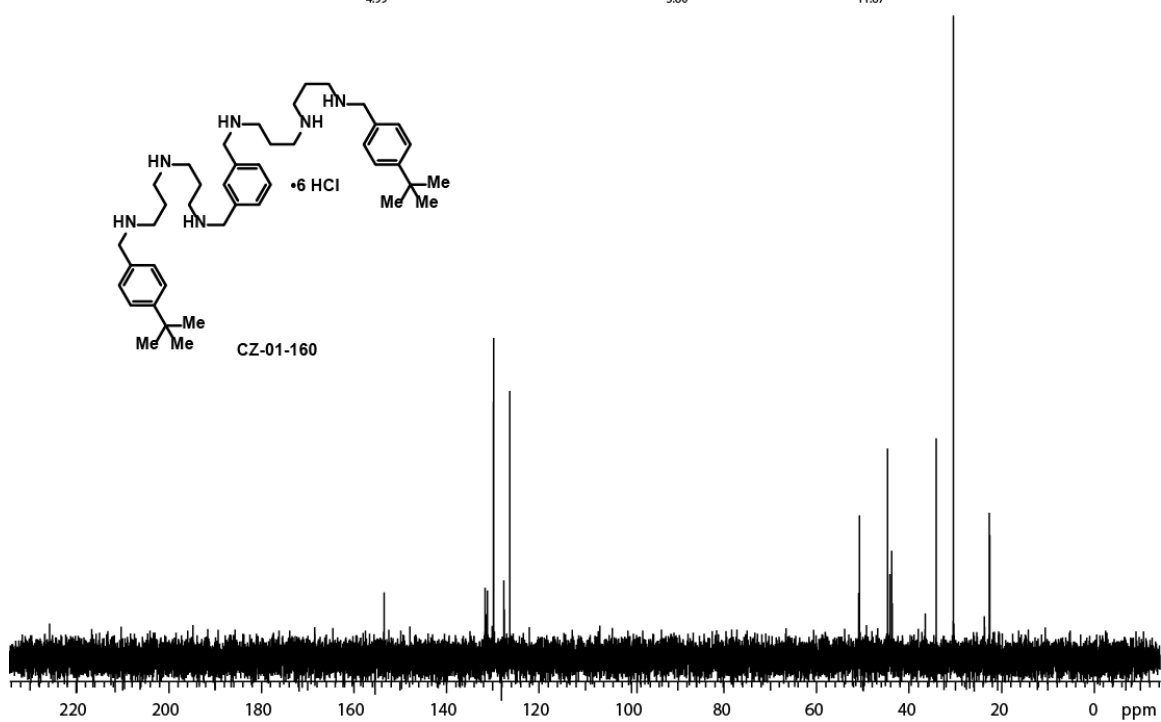
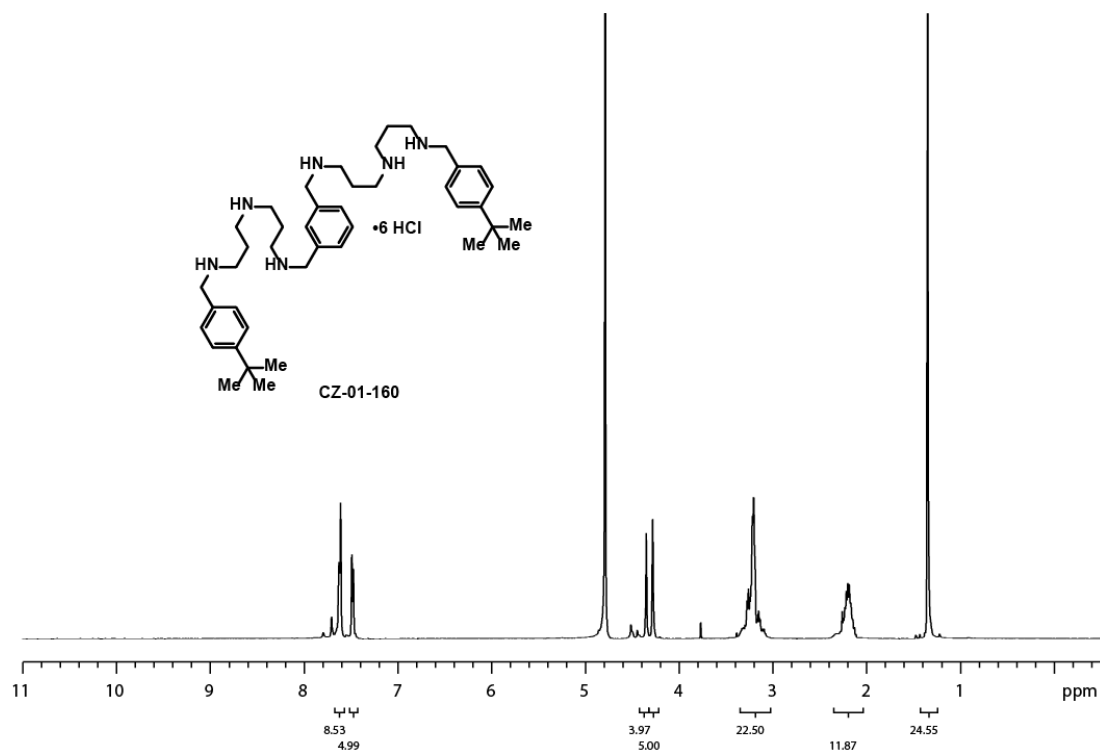


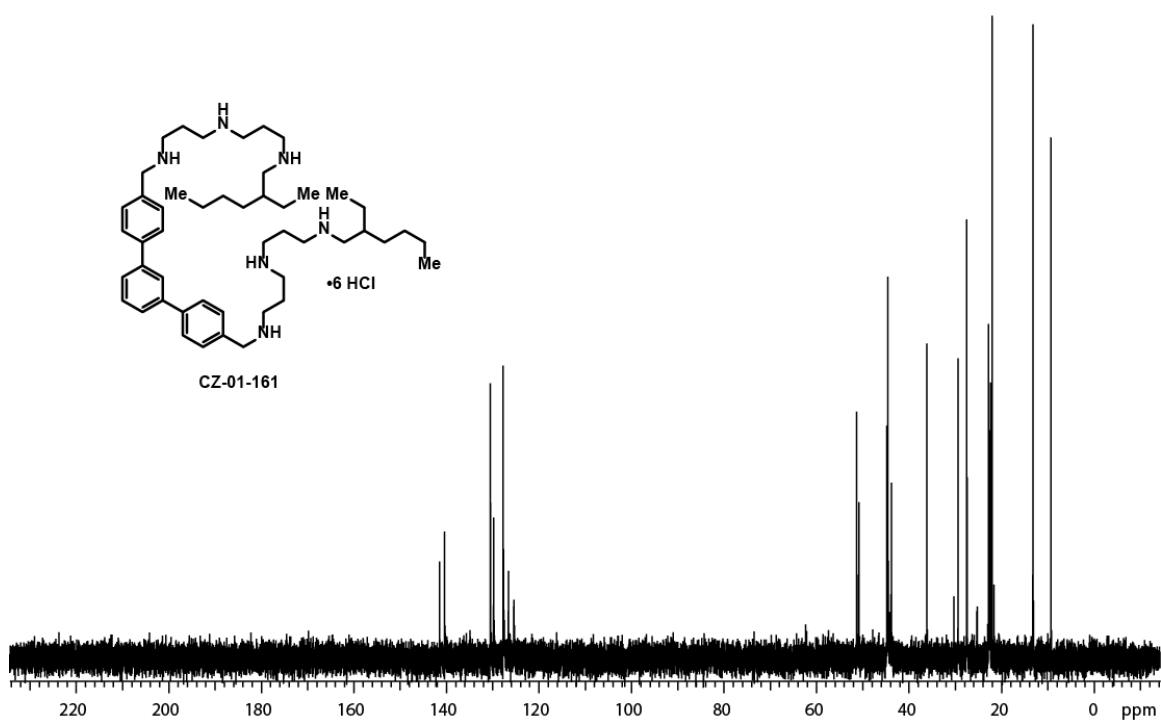
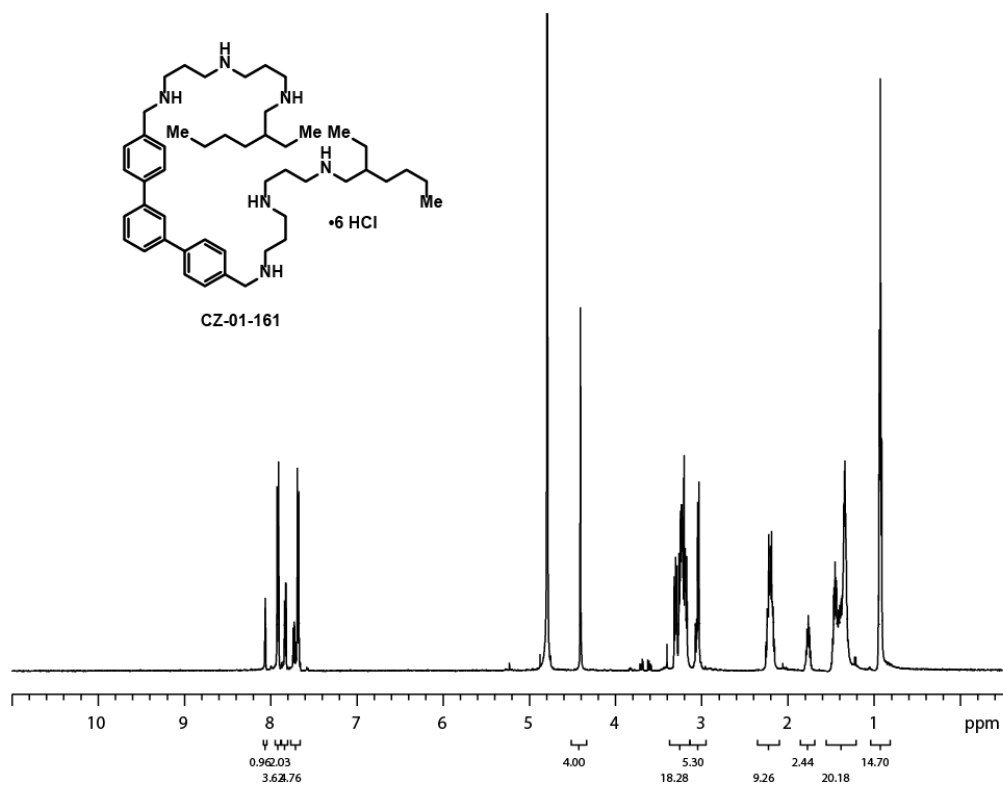


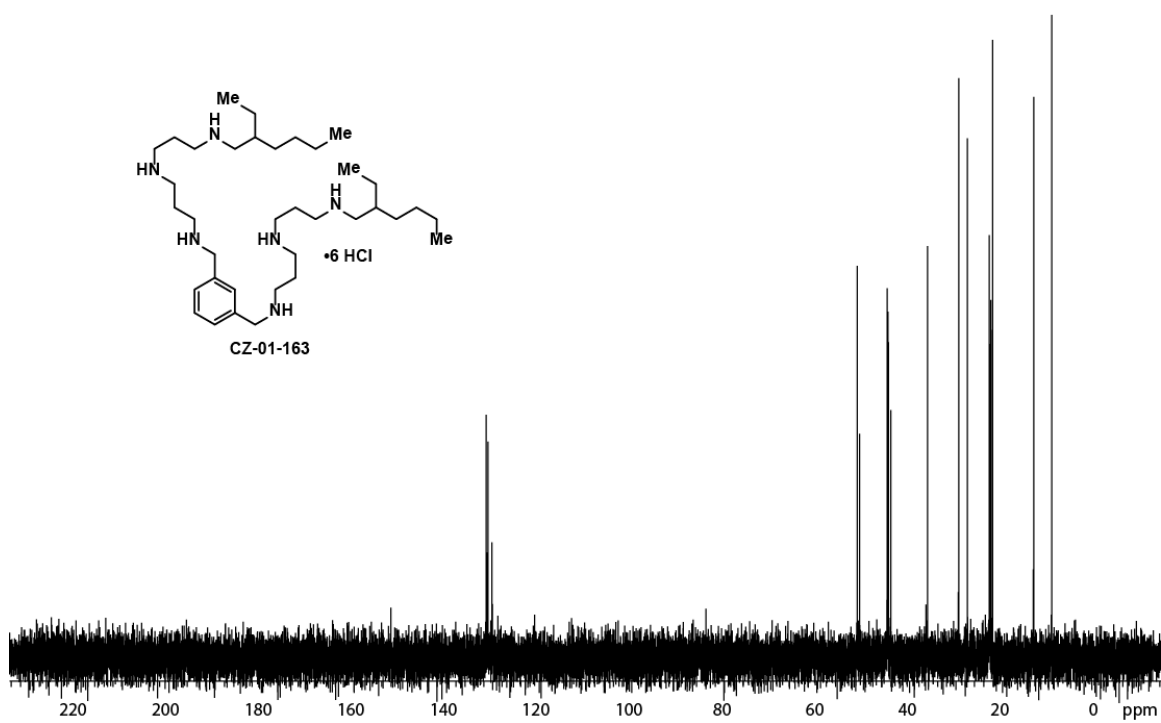
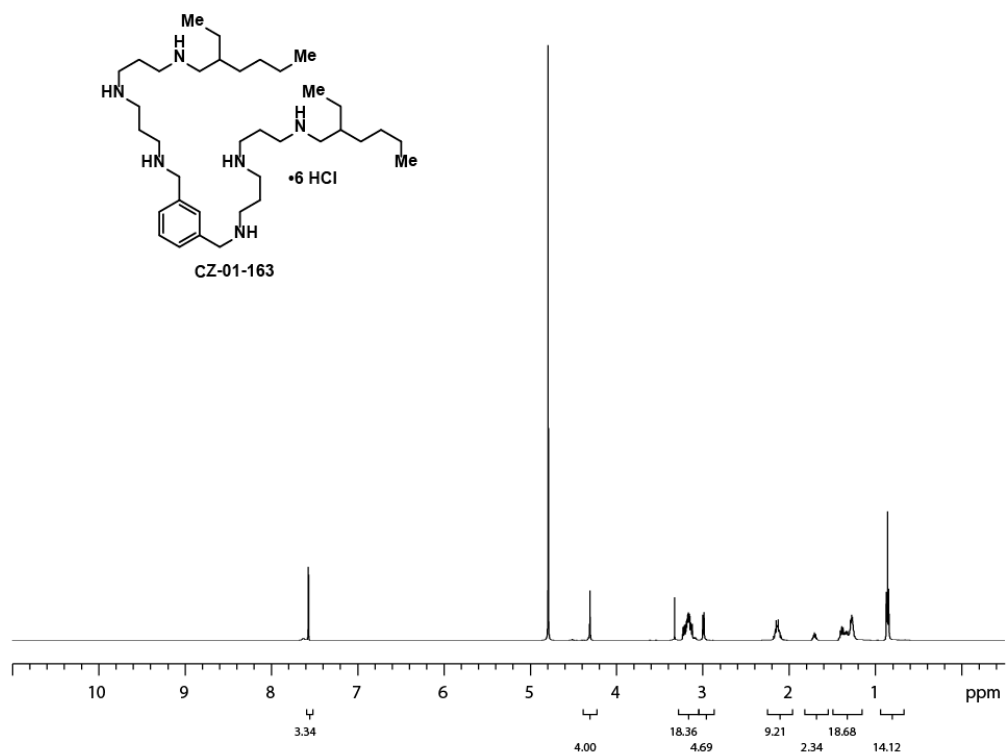


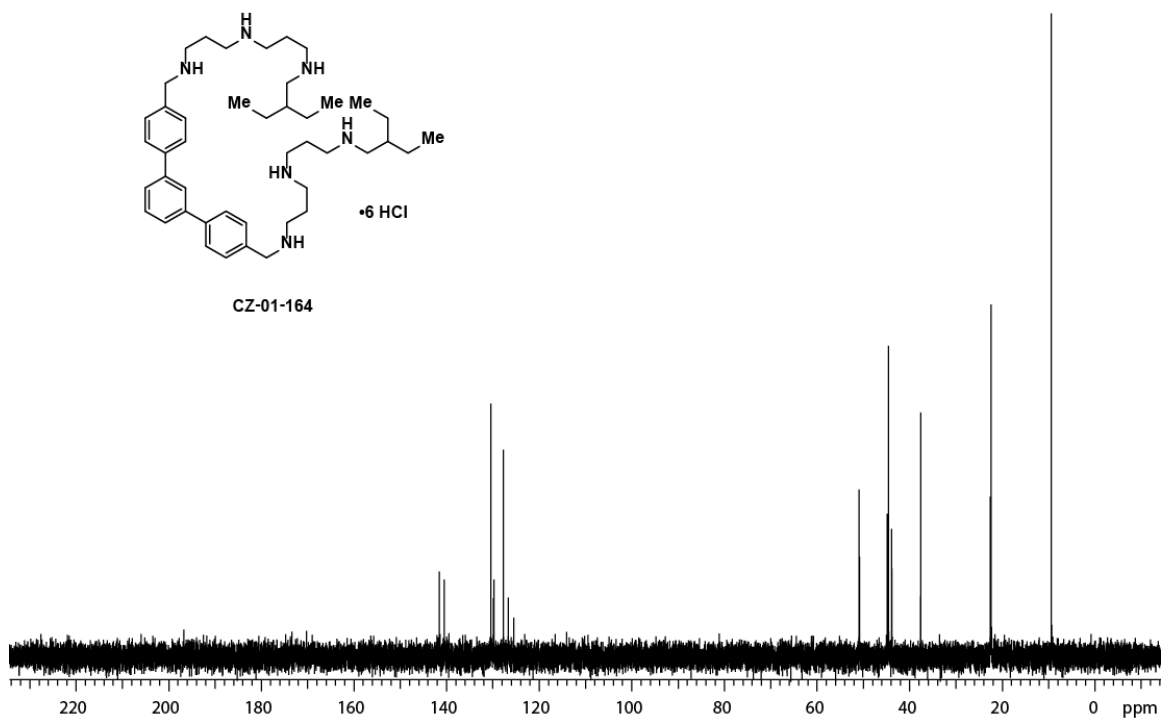
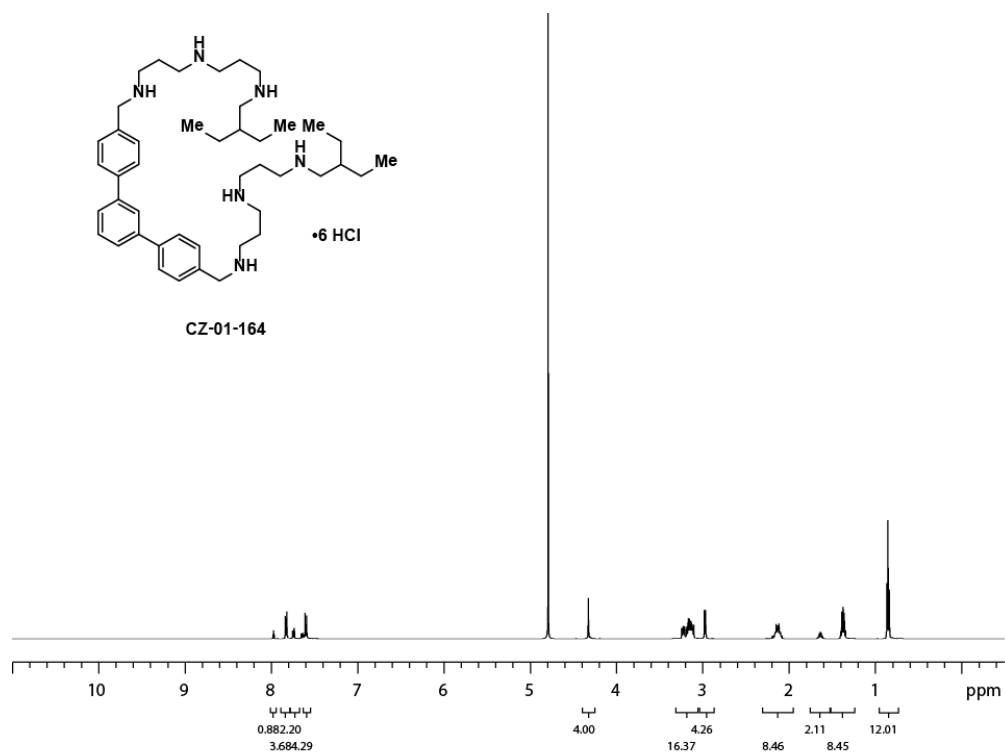


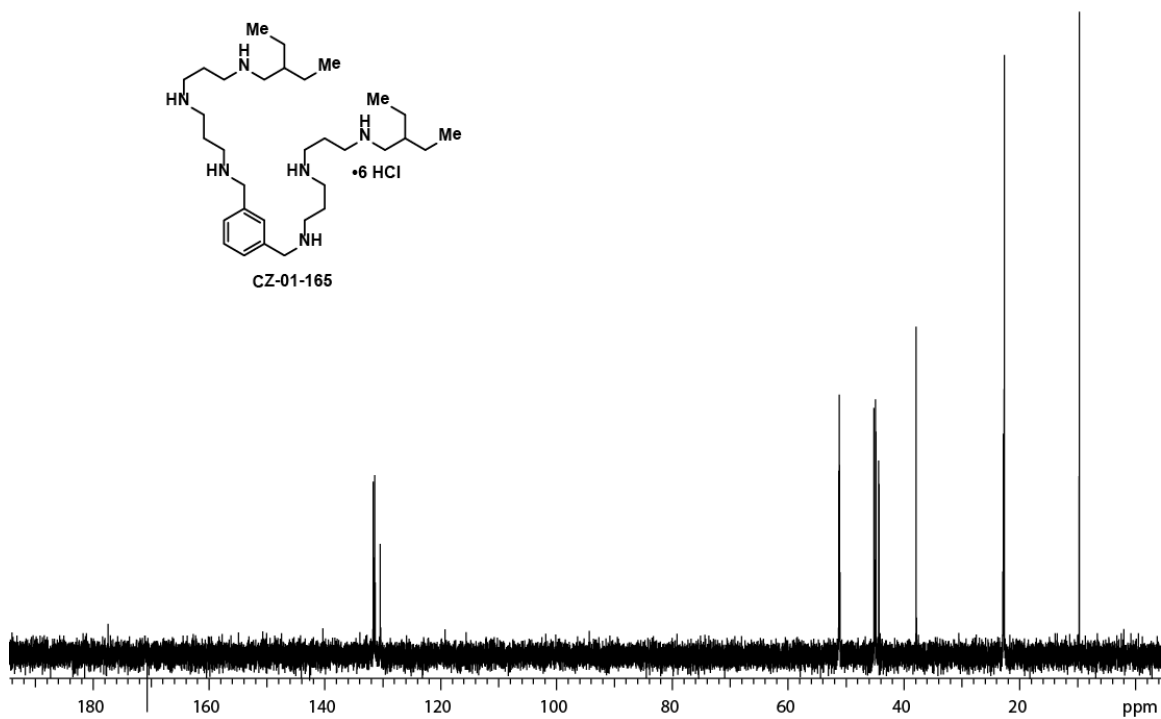
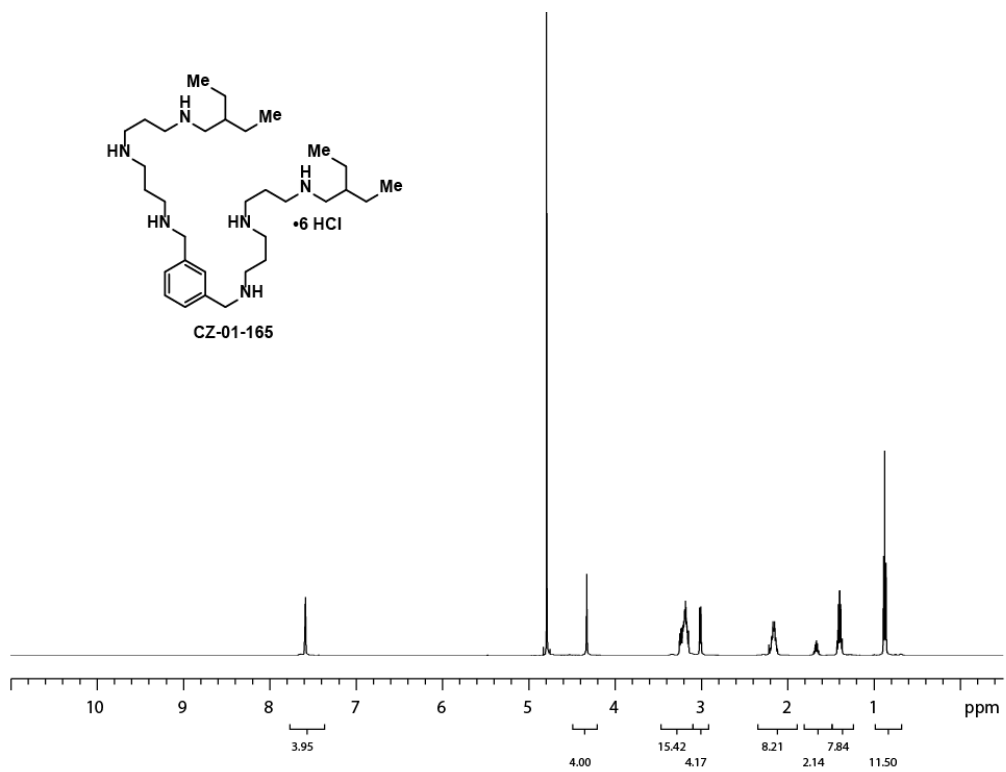


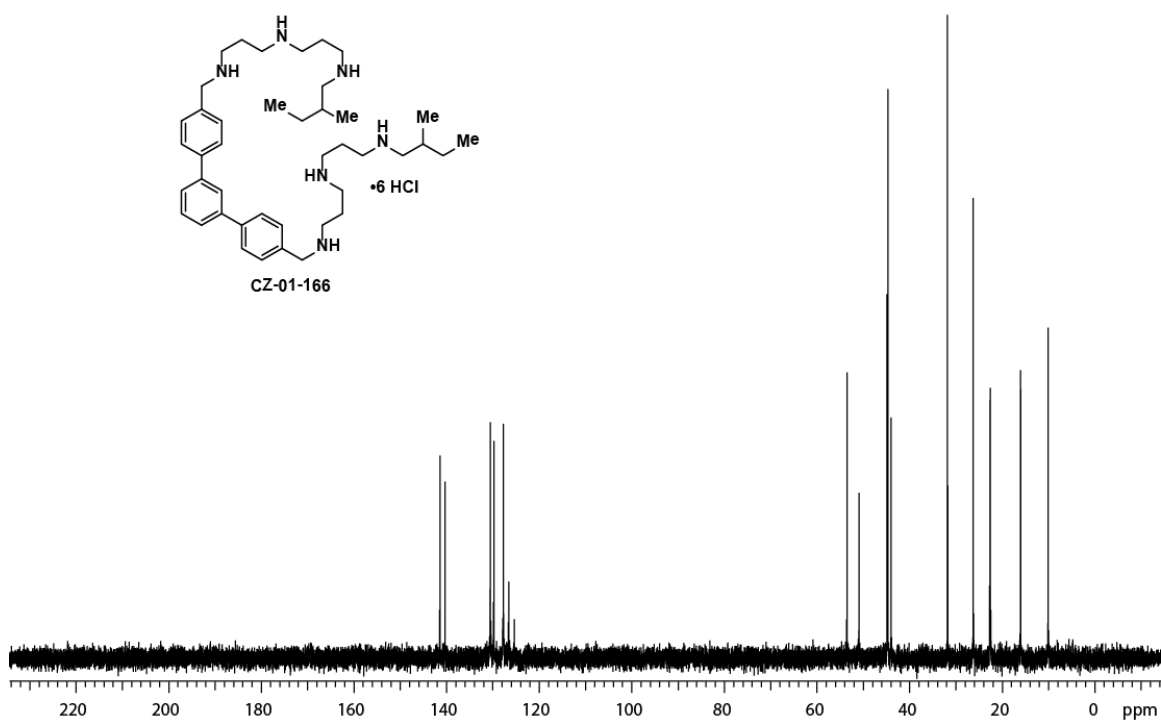
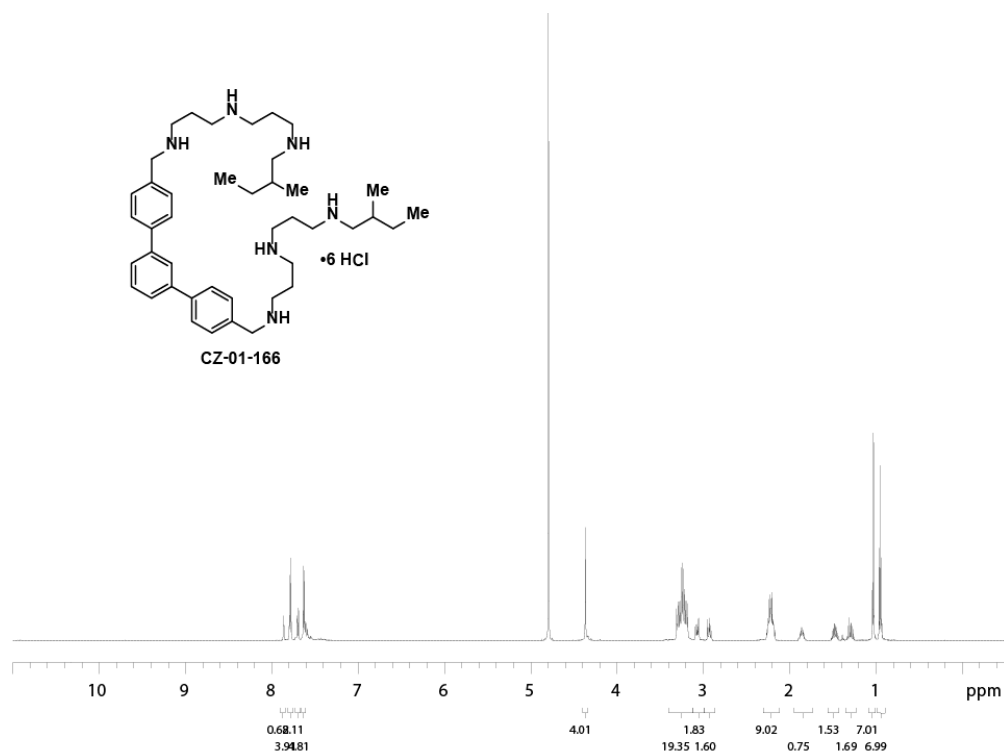


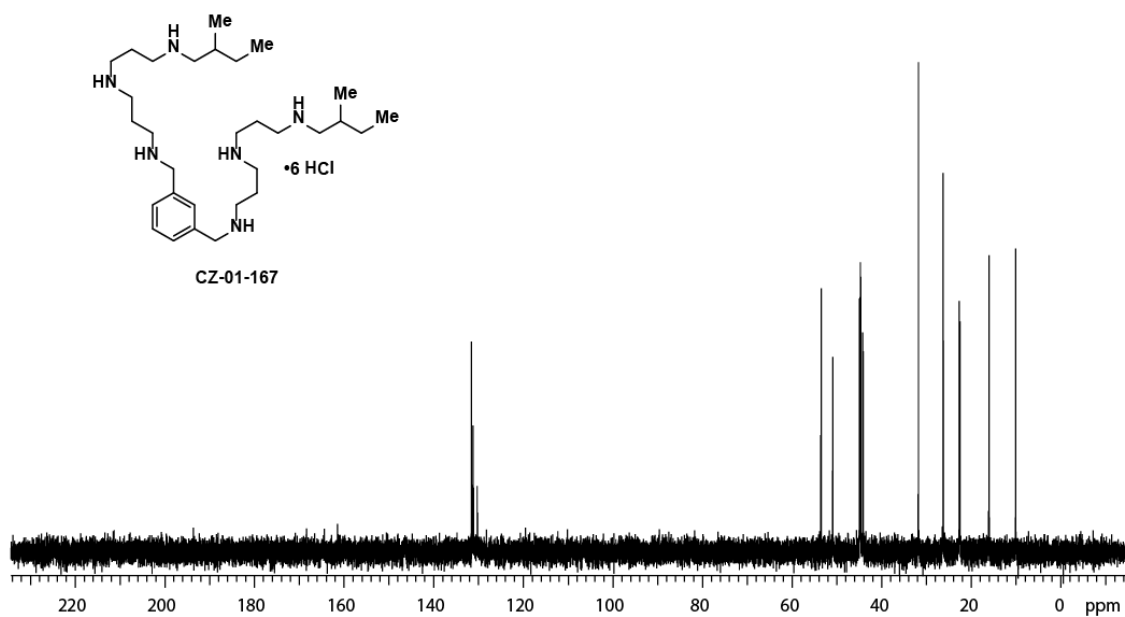
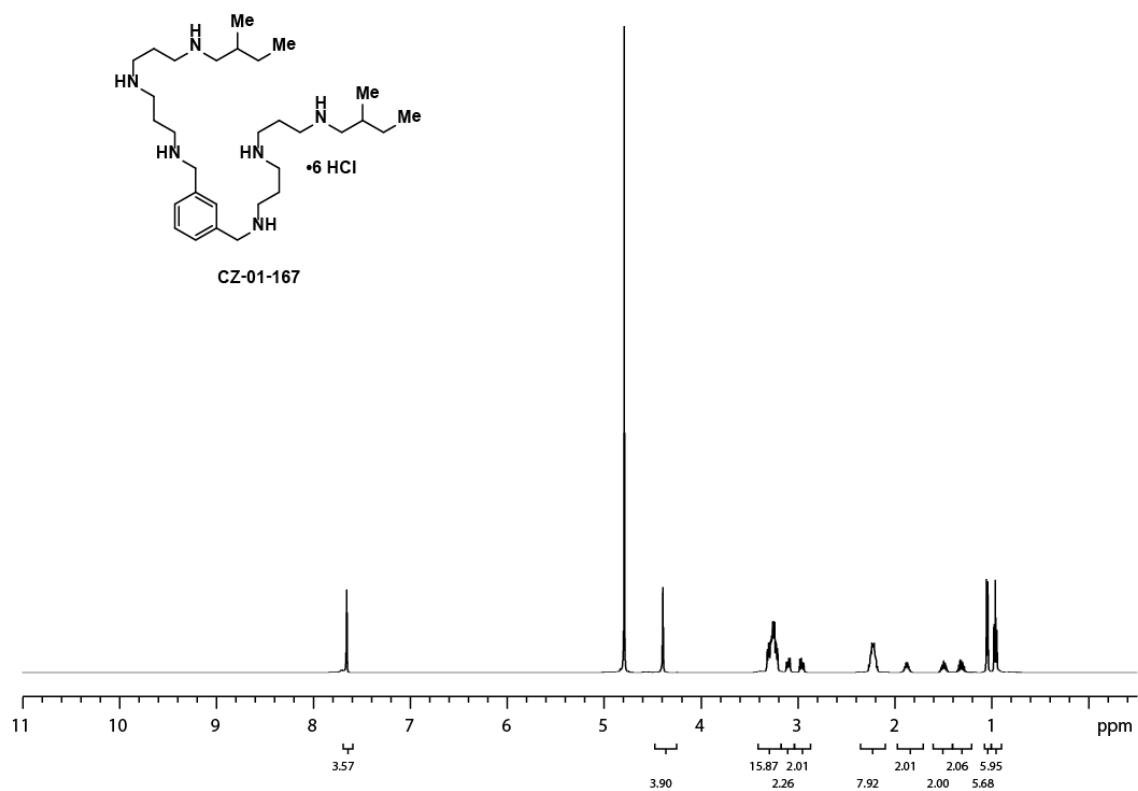


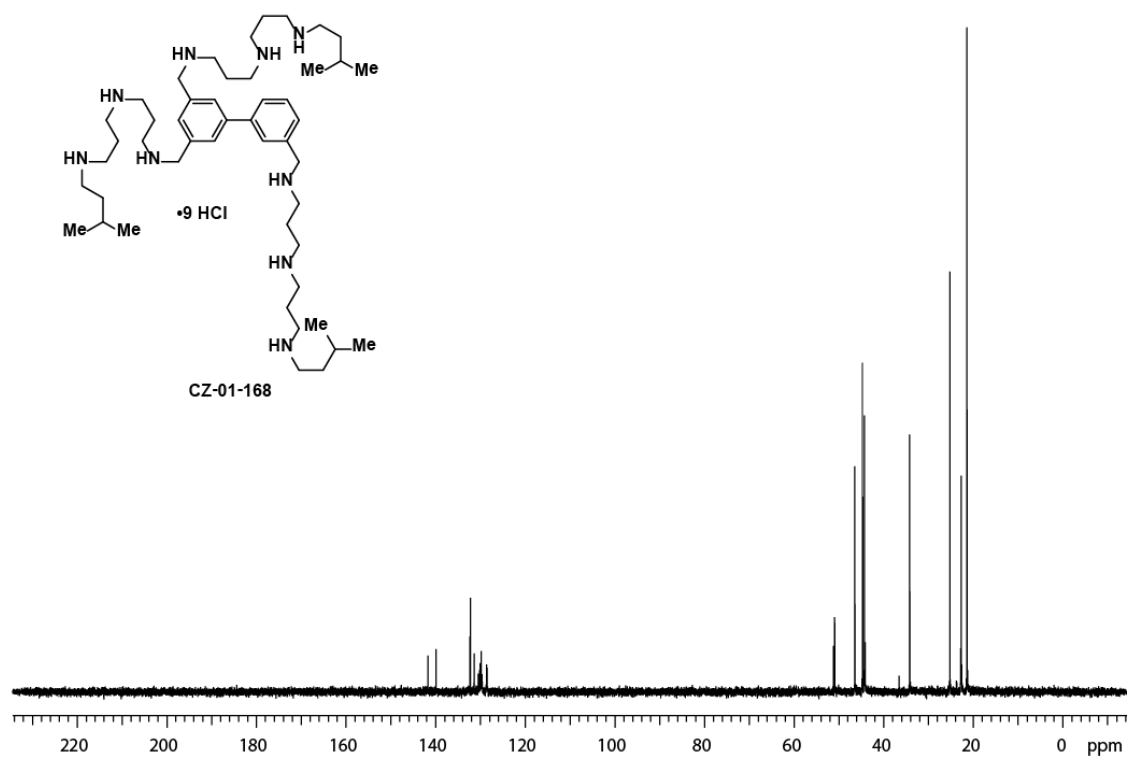
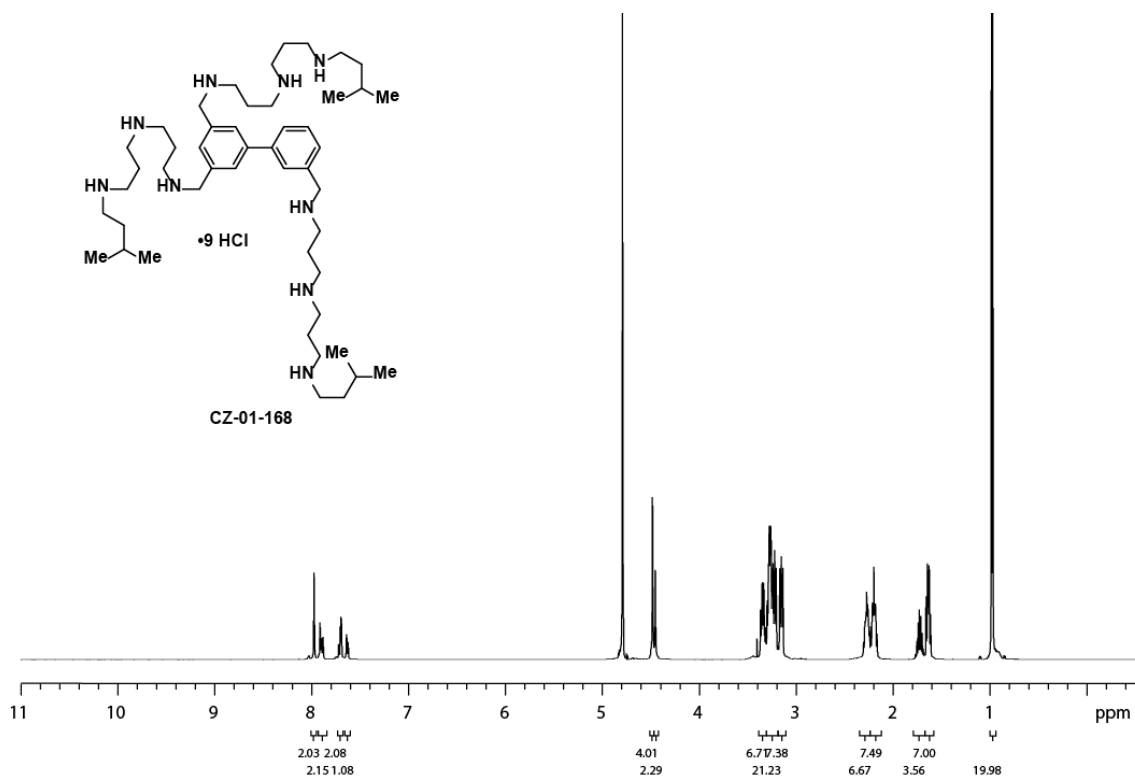




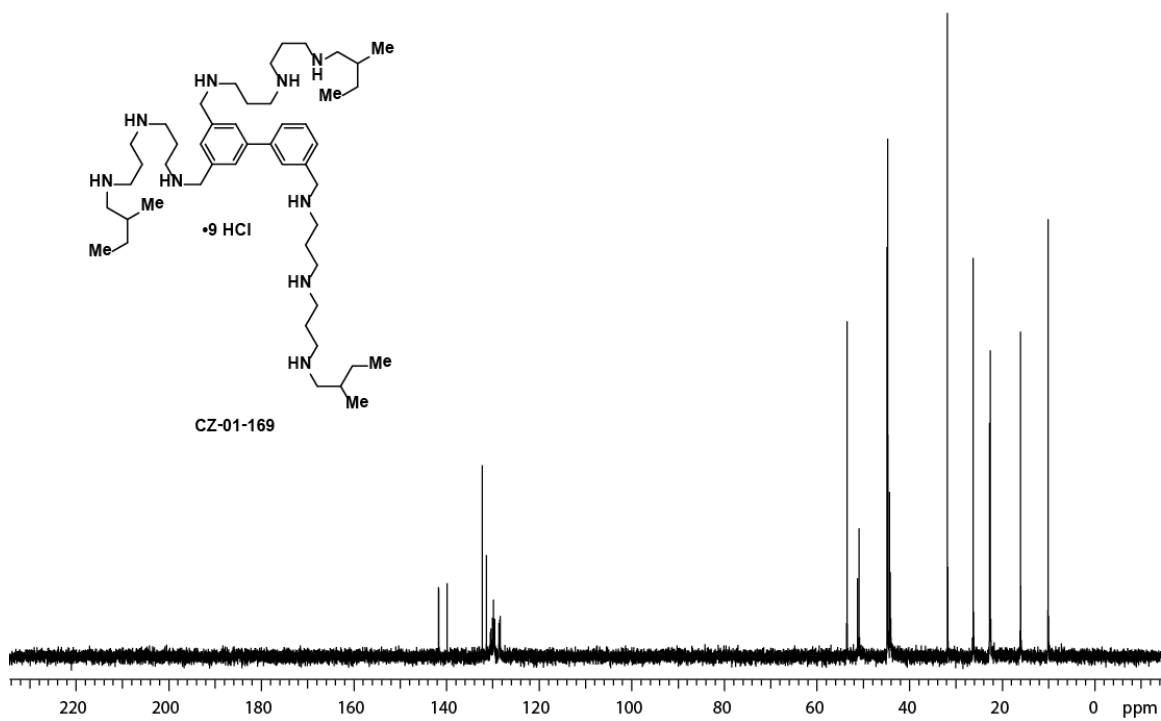
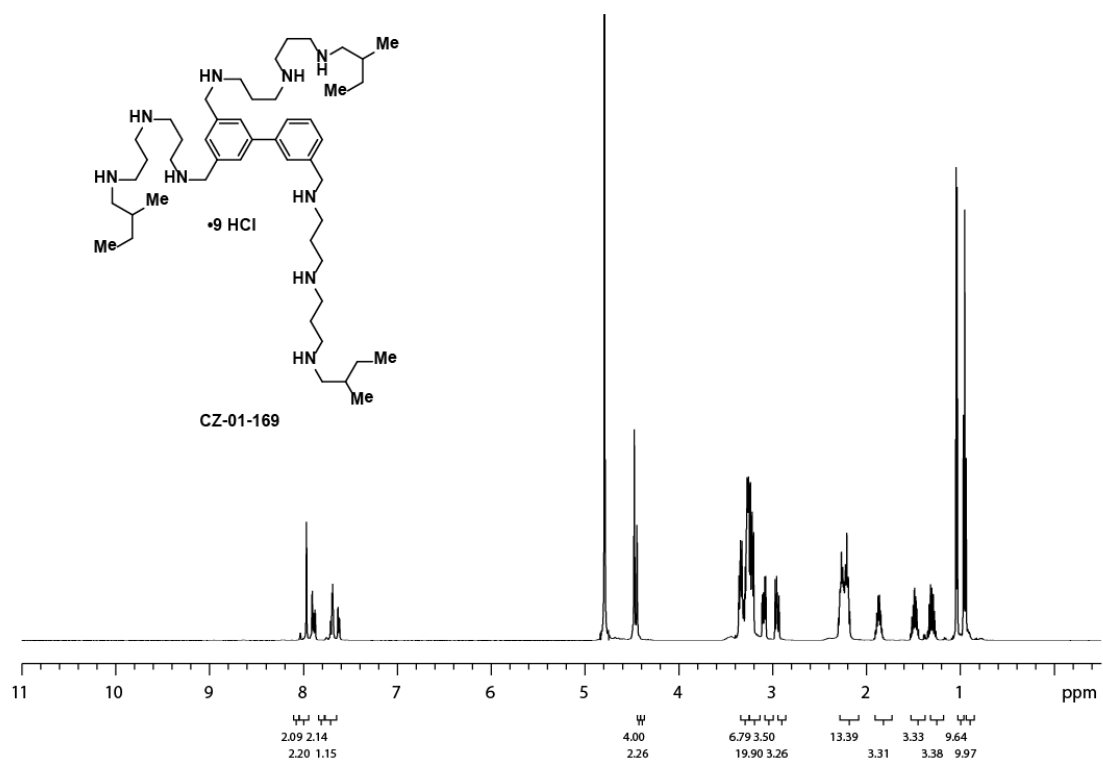


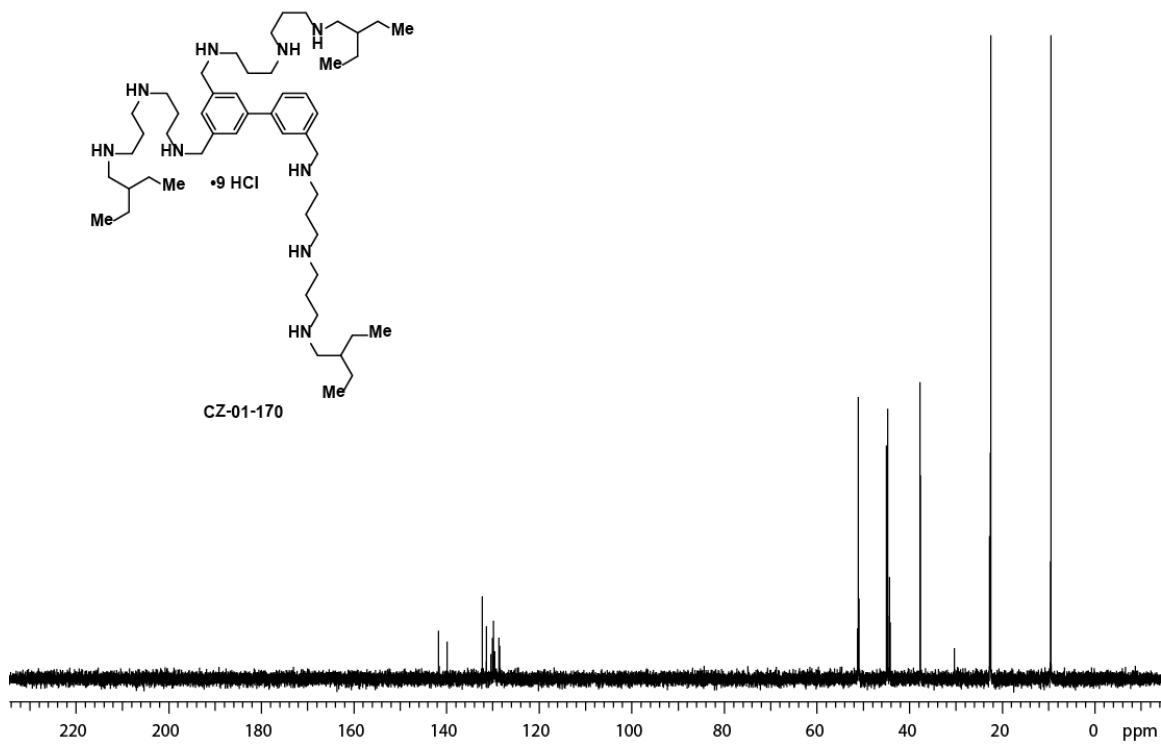
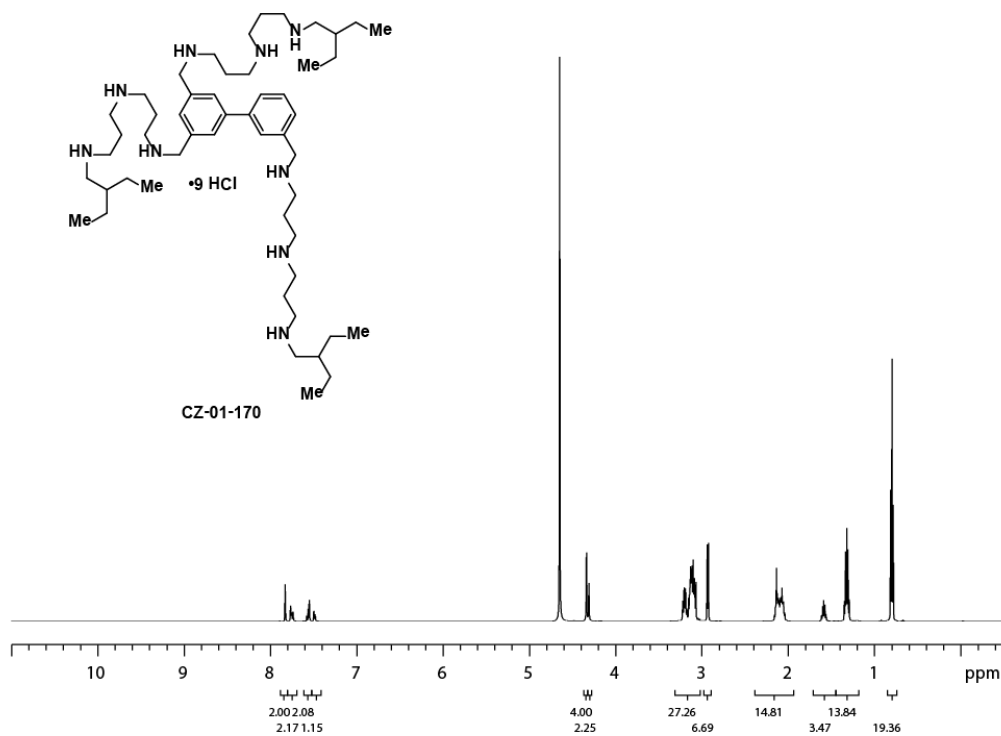


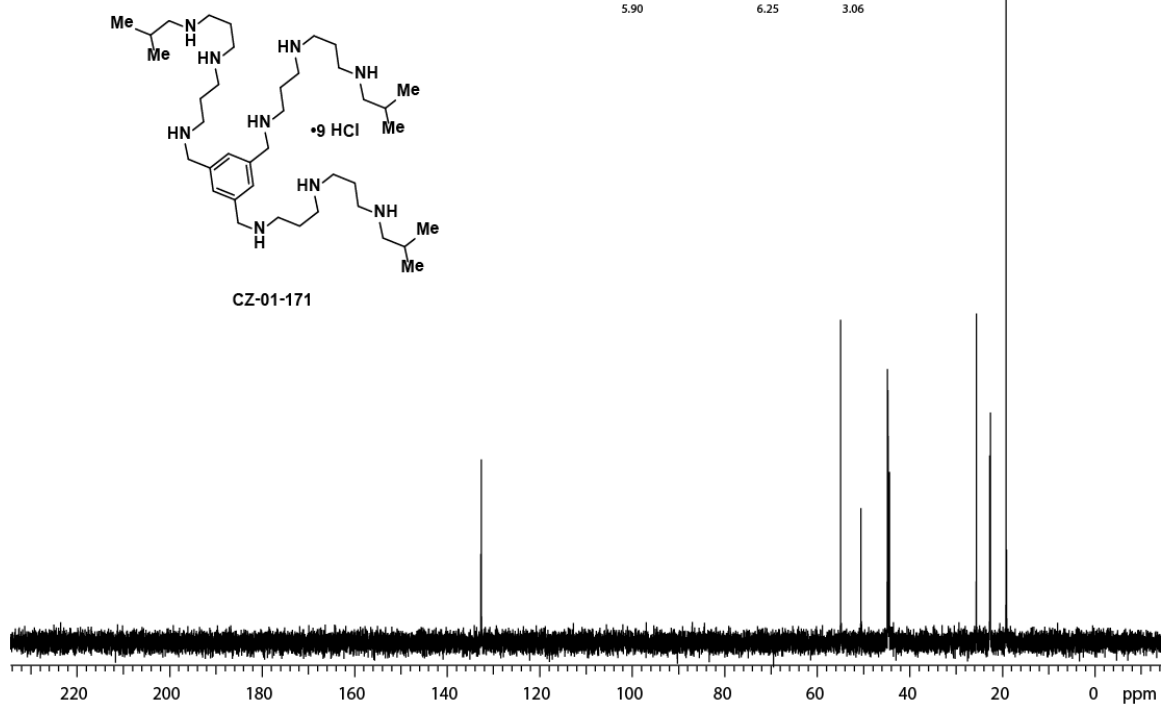
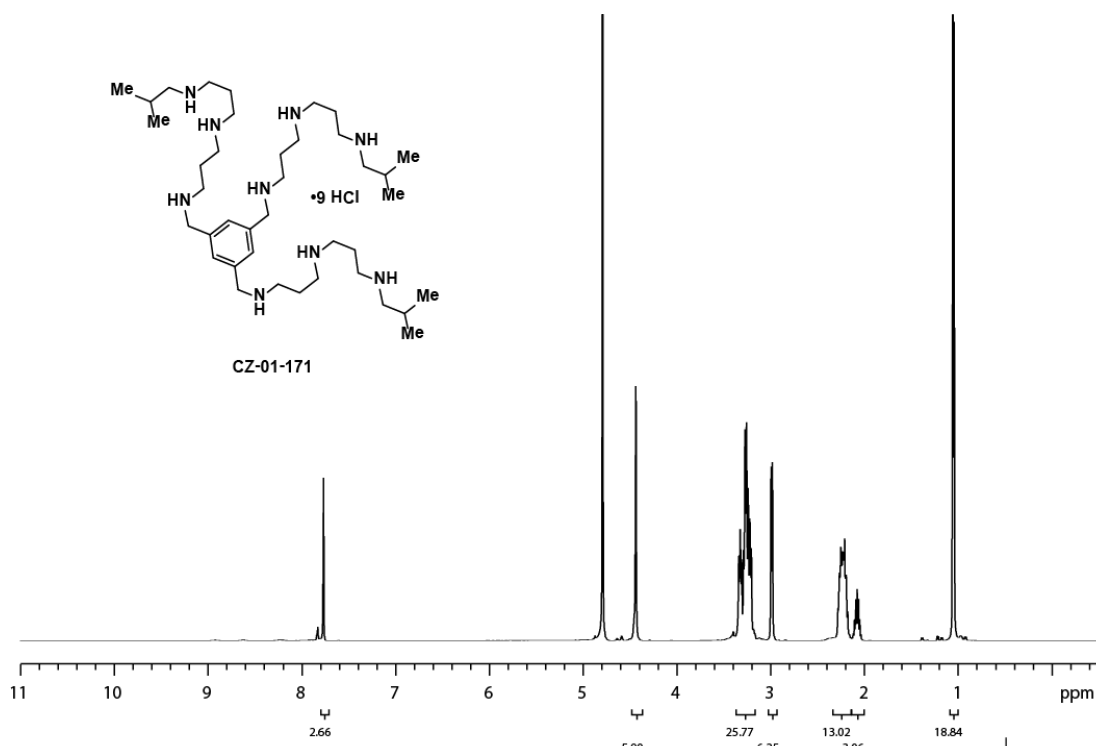


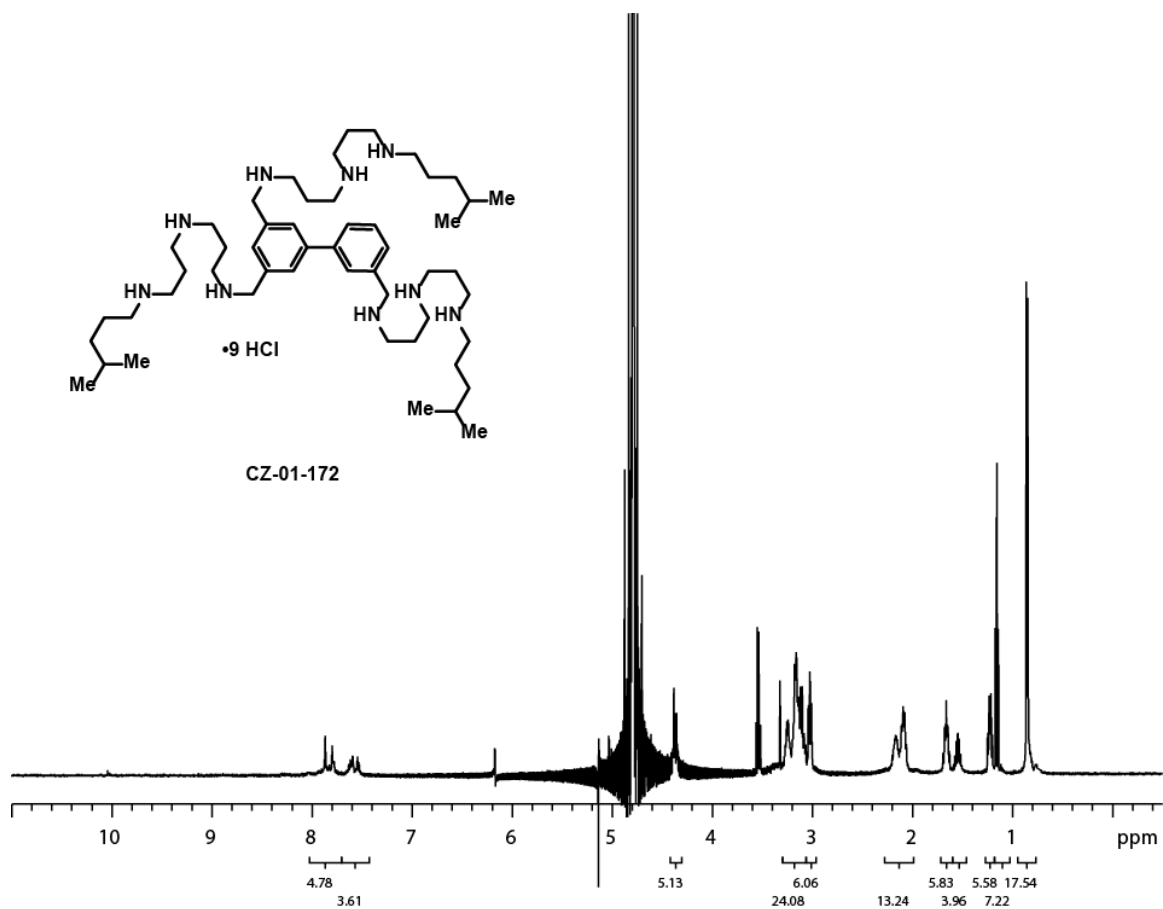


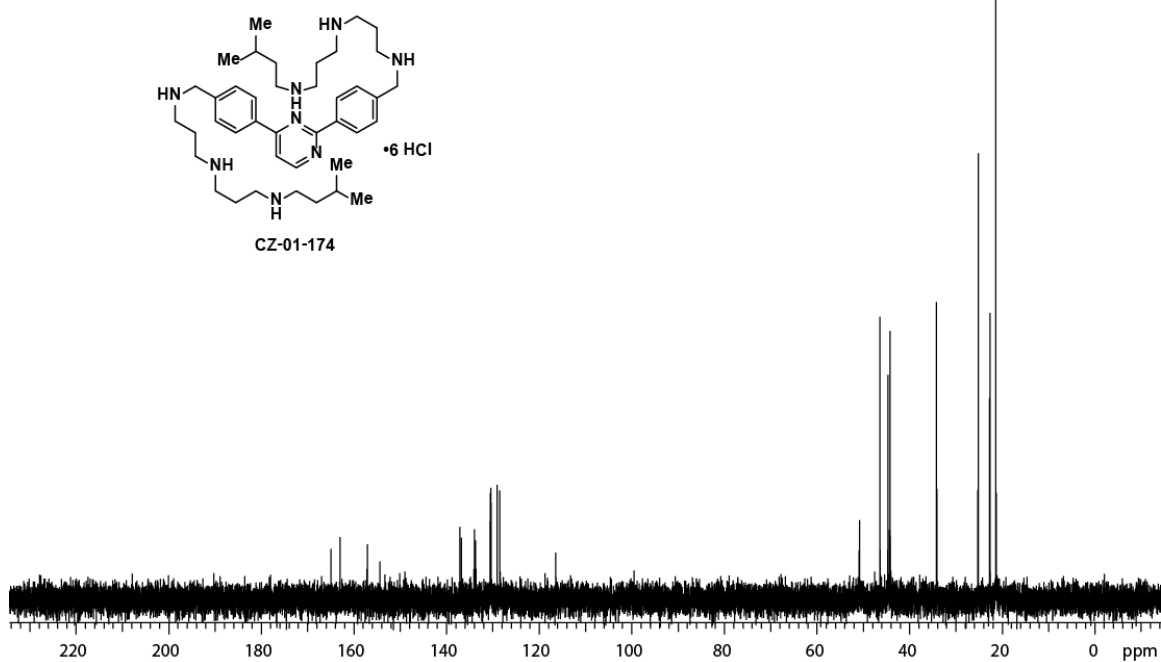
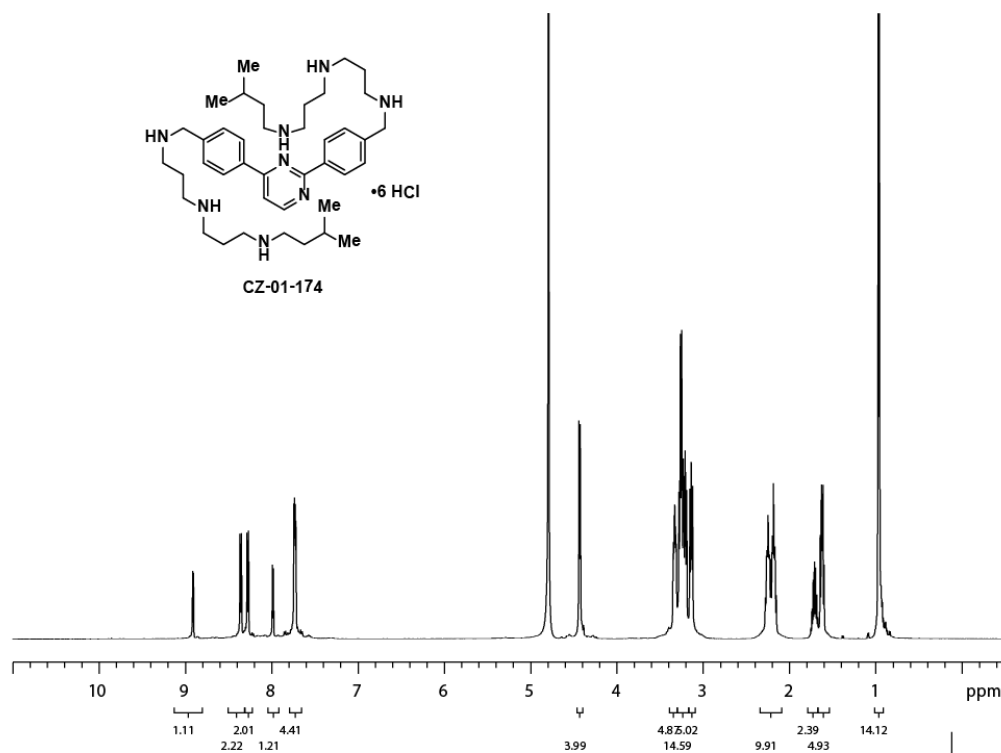


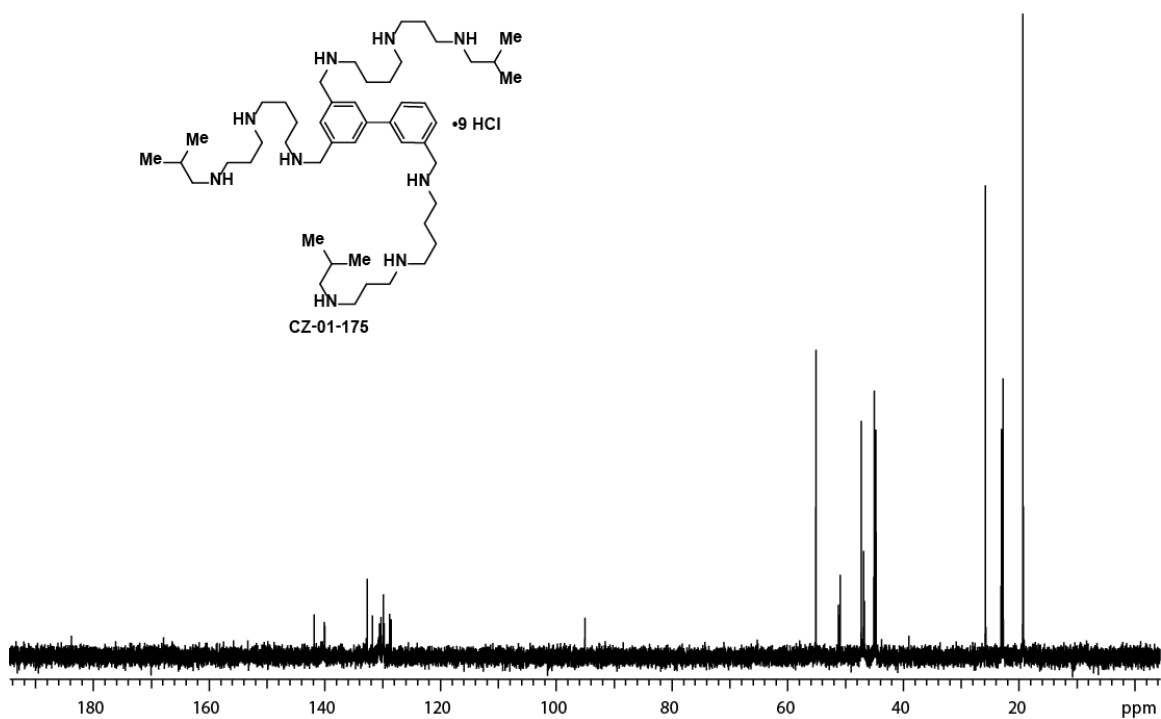


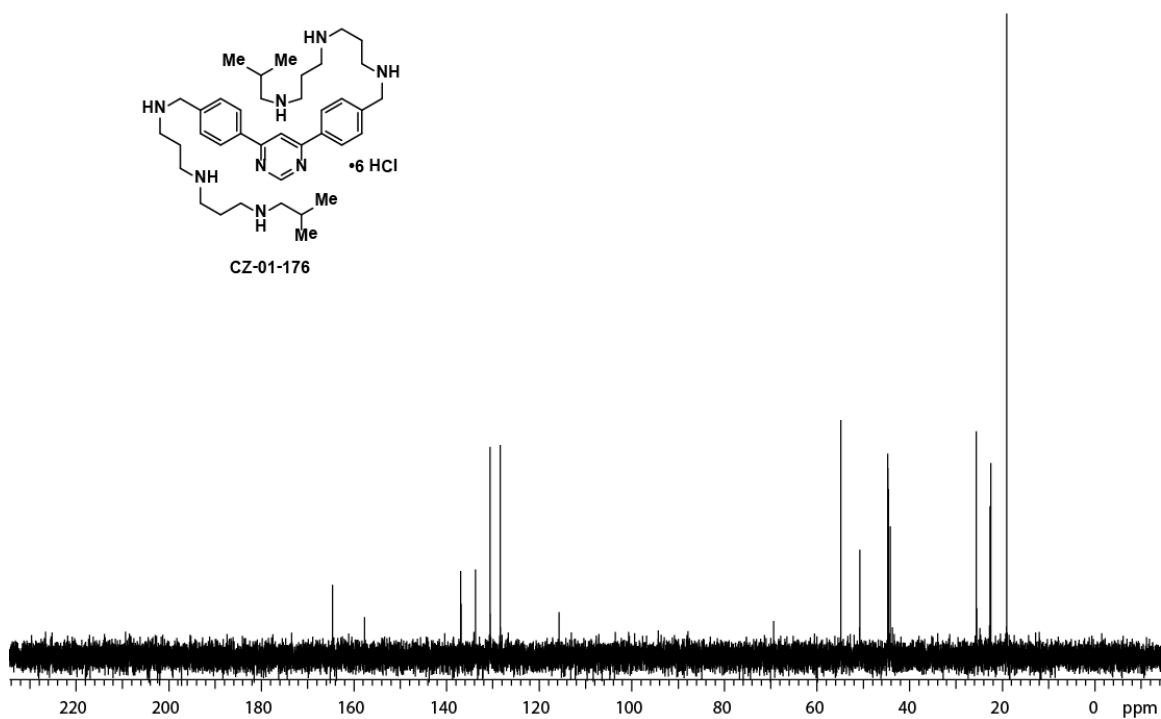
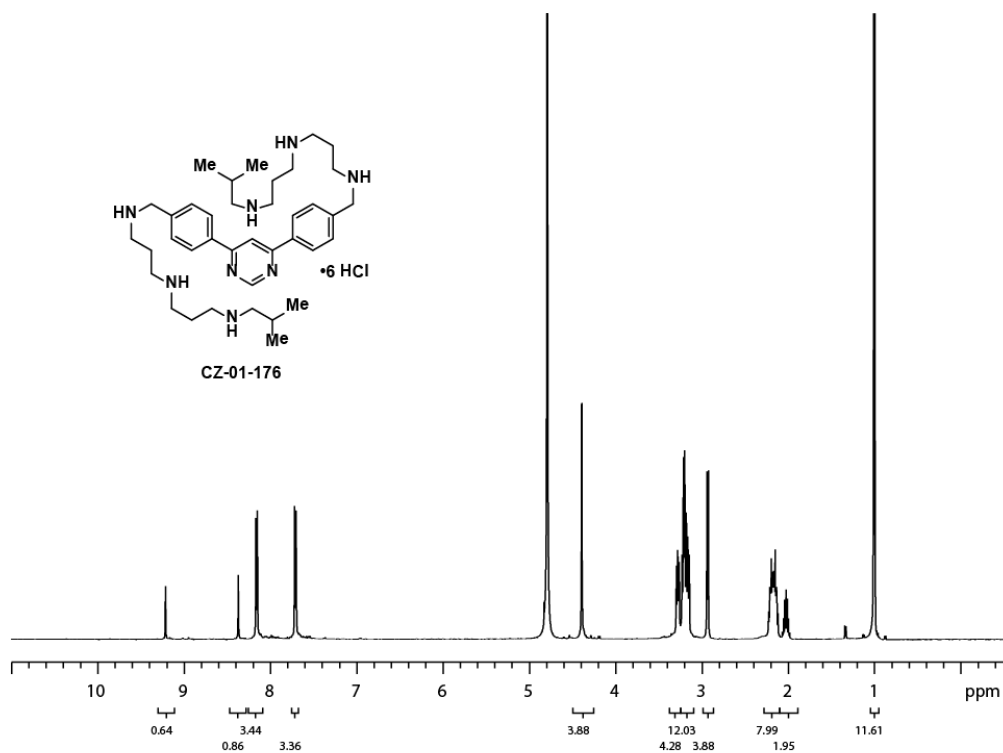


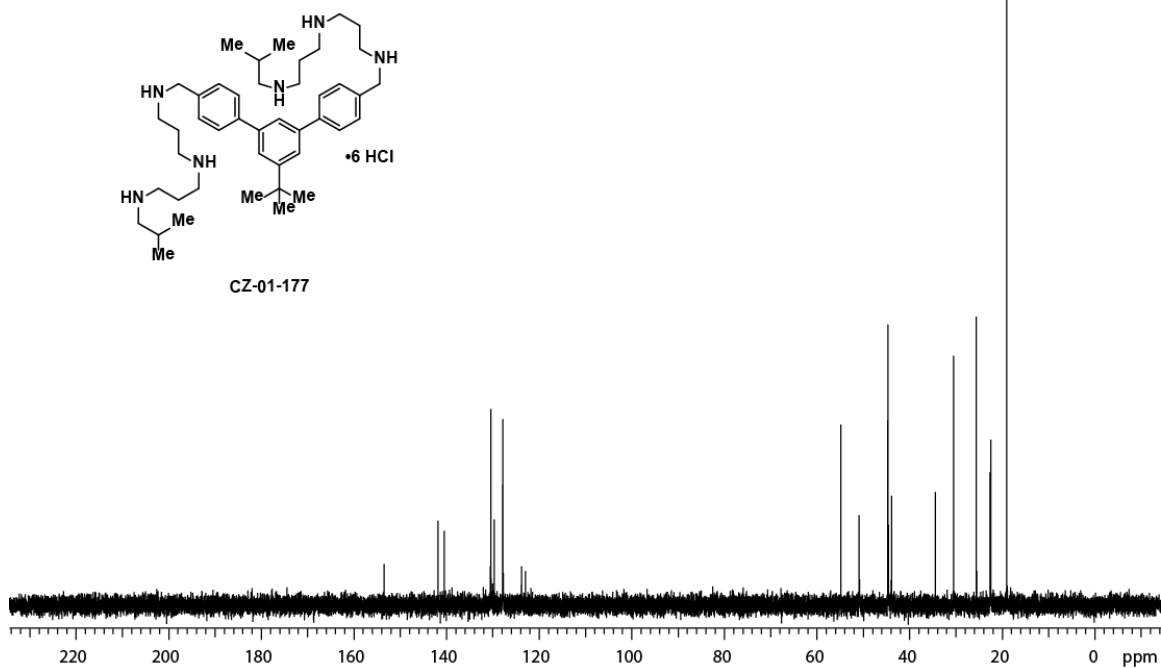
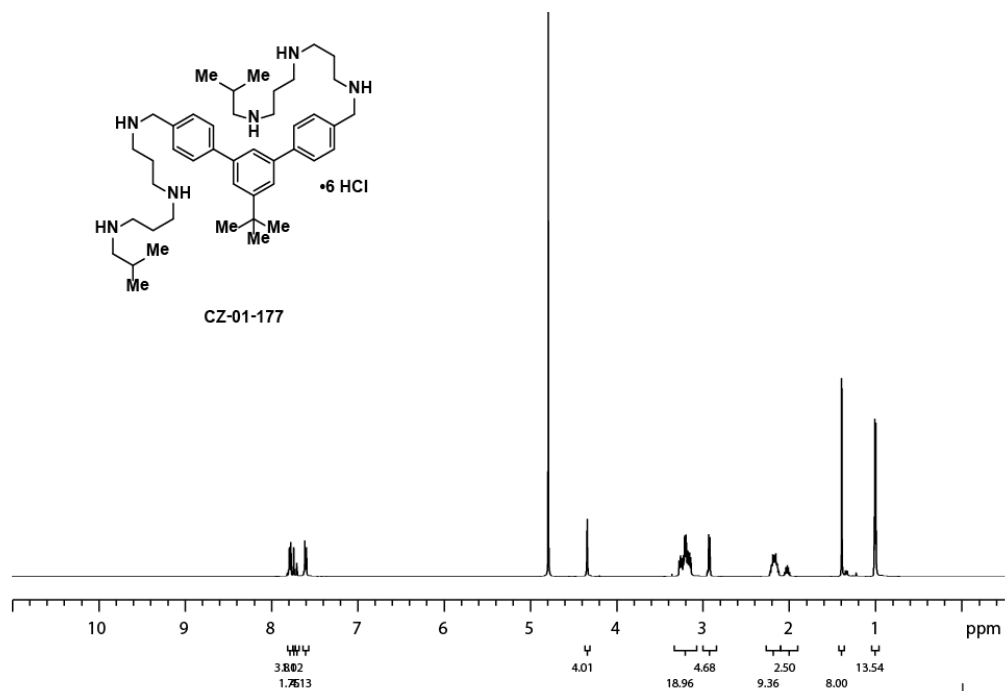




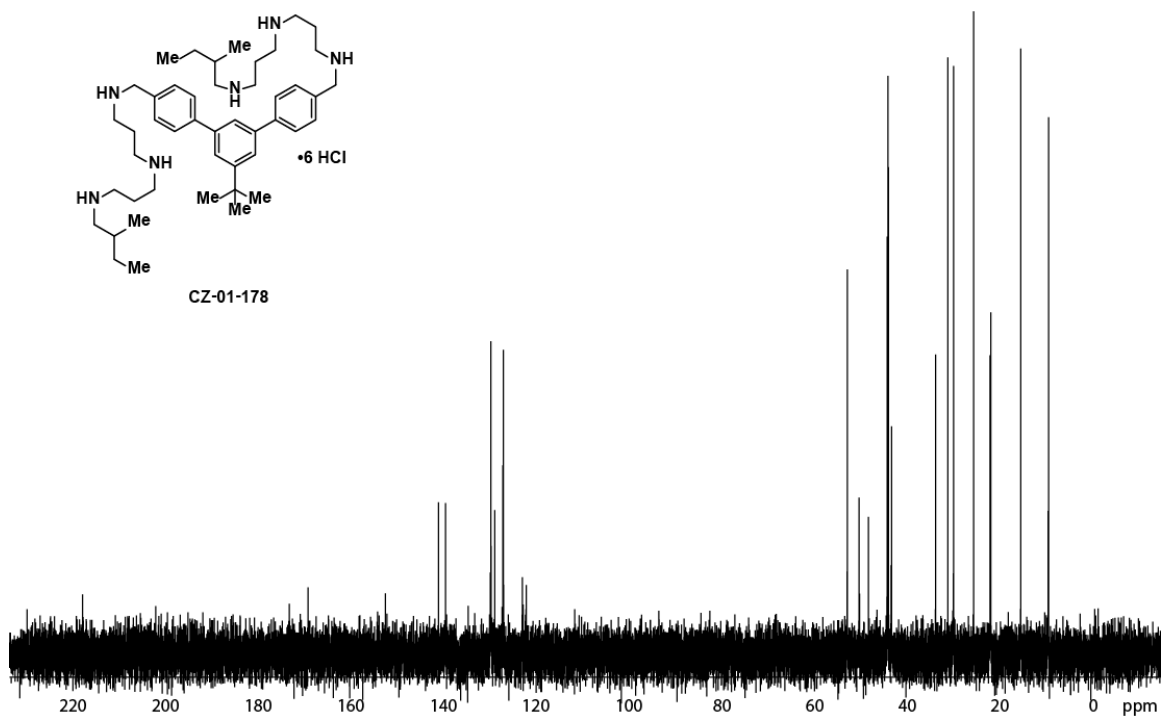
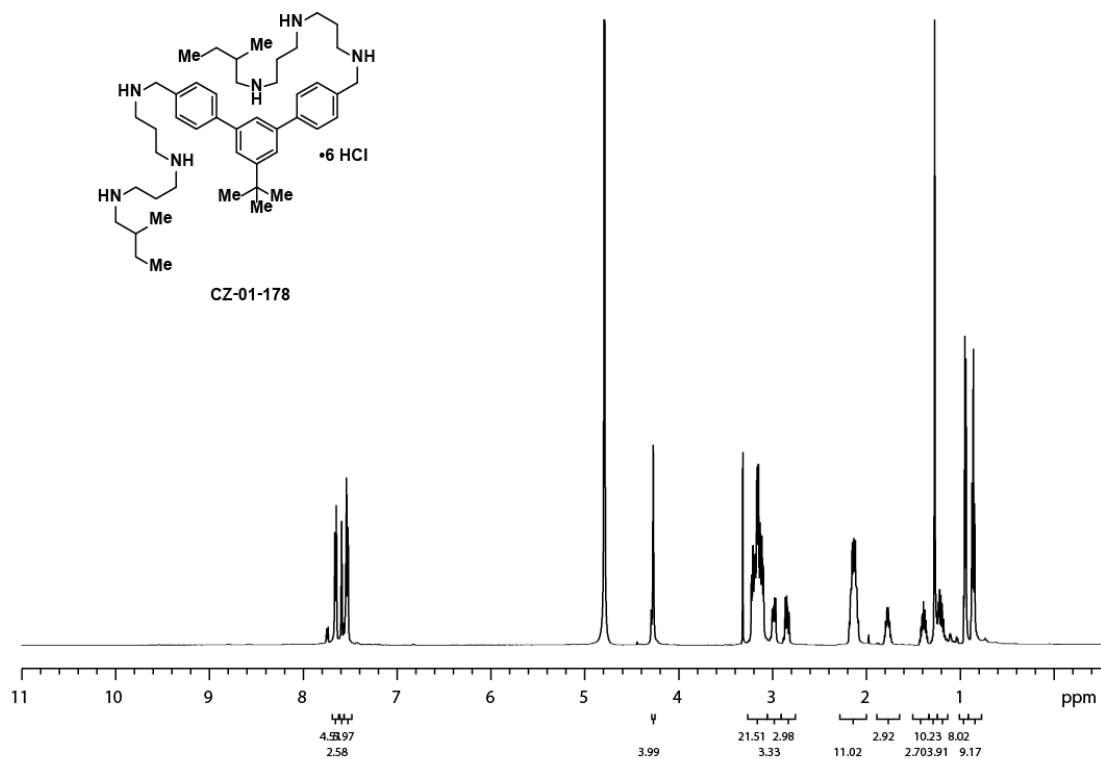


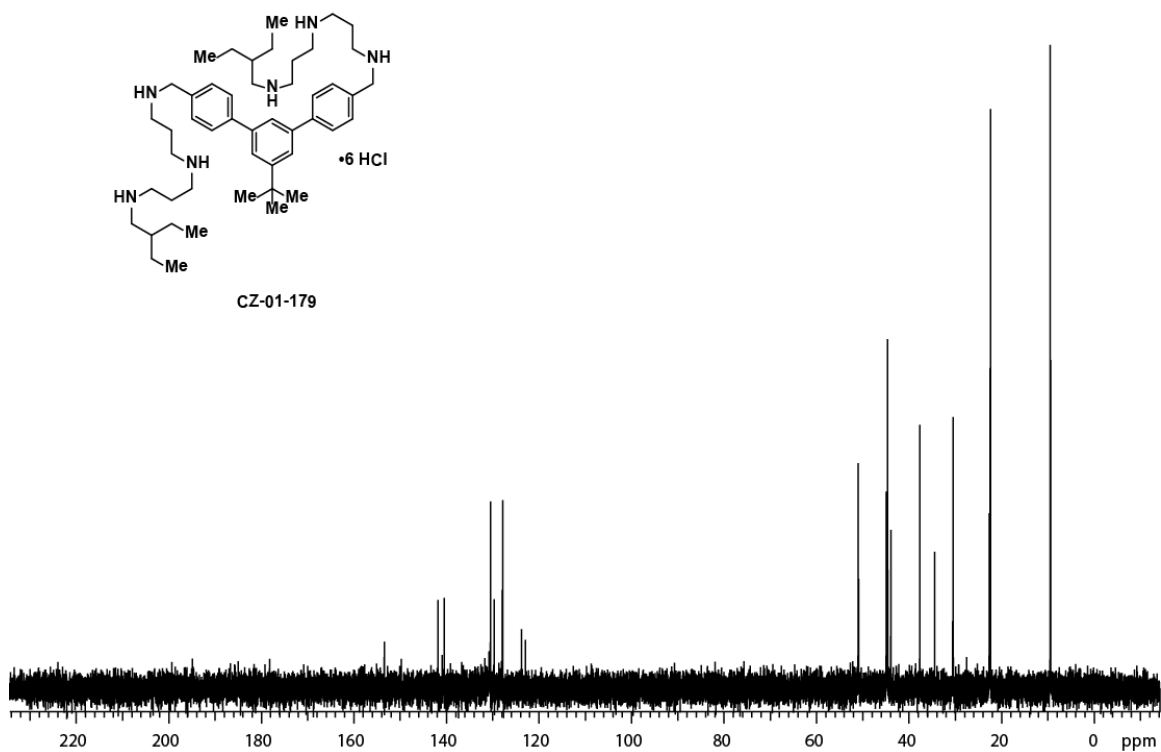
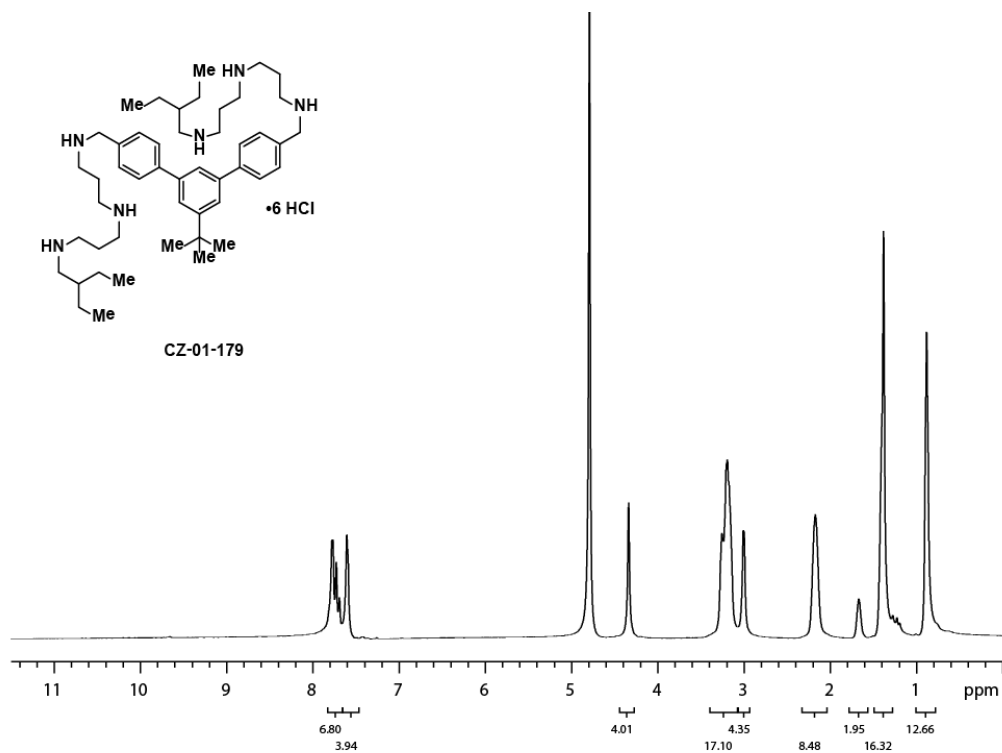








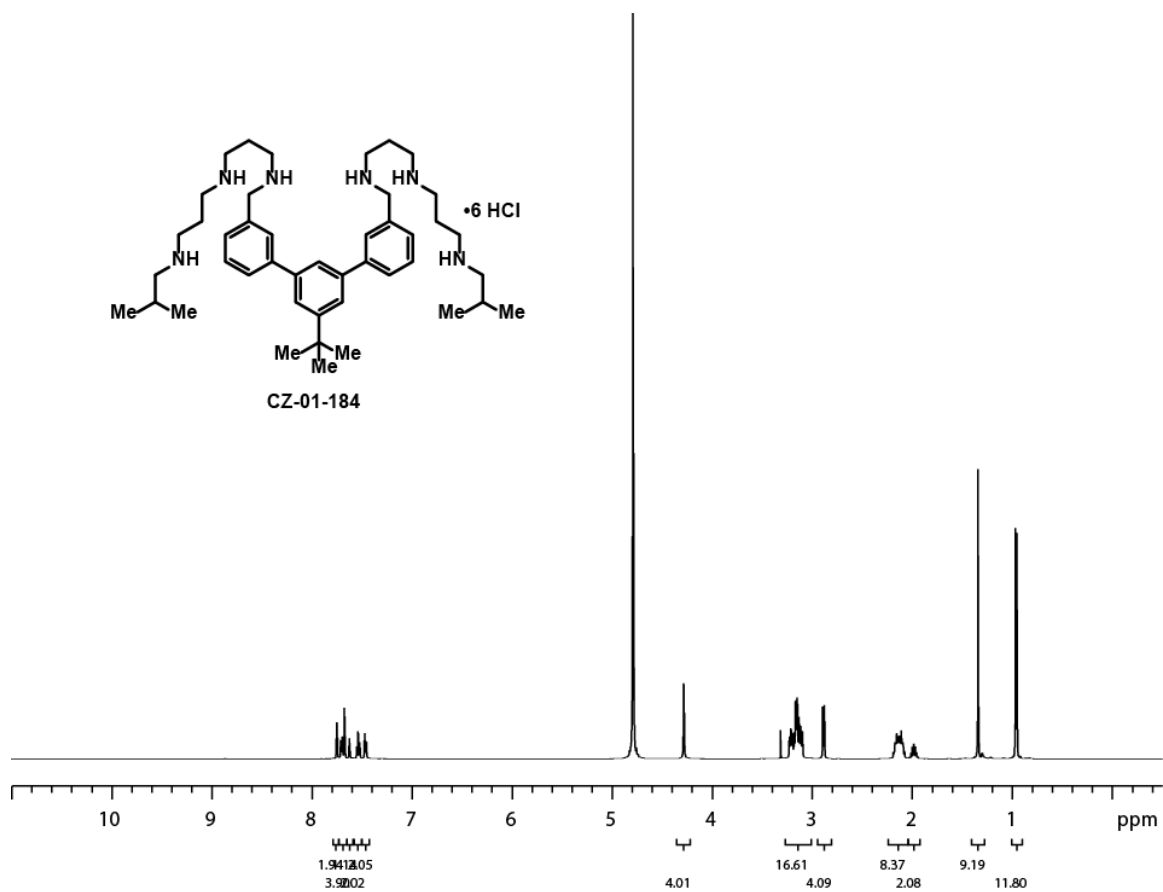












## 4.7 References

1. For the synthesis of 5-bromoisophthalaldehyde see: Drewry, J. A.; Burger, S.; Mazouchi, A.; Duodu, E.; Ayers, P.; Gradinaru, C. C.; Gunning, P. T. Src Homology 2 Domain Proteomimetics: Developing Phosphopeptide Selective Receptors. *Med. Chem. Comm.* **2012**, *3*, 763-770.
2. For a comprehensive review on the Buchwald-Hartwig reaction see: Muci, A. R.; Buchwald, S. L. Practical Palladium Catalysts for C-N and C-O Bond Formation. *Top. Curr. Chem.* **2002**, *219*, 131-209.
3. For a comprehensive review on the Suzuki-Miyaura reaction see: Miyaura, N.; Suzuki, A. Palladium-Catalyzed Cross-Coupling Reactions of Organoboron Compounds. *Chem. Rev.* **1995**, *95*, 2457-2483.
4. For comprehensive studies on brilacidin see: (a) DeGrado, W. F.; Lui, D.; Scott, R. W.; Xu, Y.; Tang, H.; Korczak, B. Synthetic Mimetics of Host Defense and uses thereof. U.S. Patent WO 2010/062573A1, June 3, 2010. (b) Scott, R. W.; Sonis, S. T.; Korczak, B.; Freeman, K. B.; DeGrado, W. F.; Kumar, A.; Brennan, D. P.; Holden, S. A.; Chafai-Fadela, K.; Ram, S.; Menon, K. Brilacidin, Host Defense Peptide Mimetic, One of a New Class of Immunomodulatory Agents that can Target Multiple Disease Indications. Presented at the 2015 ECCMID Conference, Copenhagen, Denmark, April 25-28, 2015. <http://cellceutix.com/wp-content/uploads/2013/11/ECCMID-2015-OM-poster.pdf> (accessed June 12, 2015).
5. For a comprehensive review on helix mimics see: Yin, H.; Lee, G.; Hamilton, A. D. Alpha-Helix Mimetics in Drug Discovery. In *Drug Discovery Research: New Frontiers in the Post-Genomic Era*; Huang, E., Ed.; John Wiley and Sons, Inc.: Hoboken, NJ, 2007, 280-298.
6. Amarego, W. L. F.; Chai, C. L. L. *Purification of Laboratory Chemicals*. 6th ed.; Elsevier Inc.: Burlington, MA, 2009.